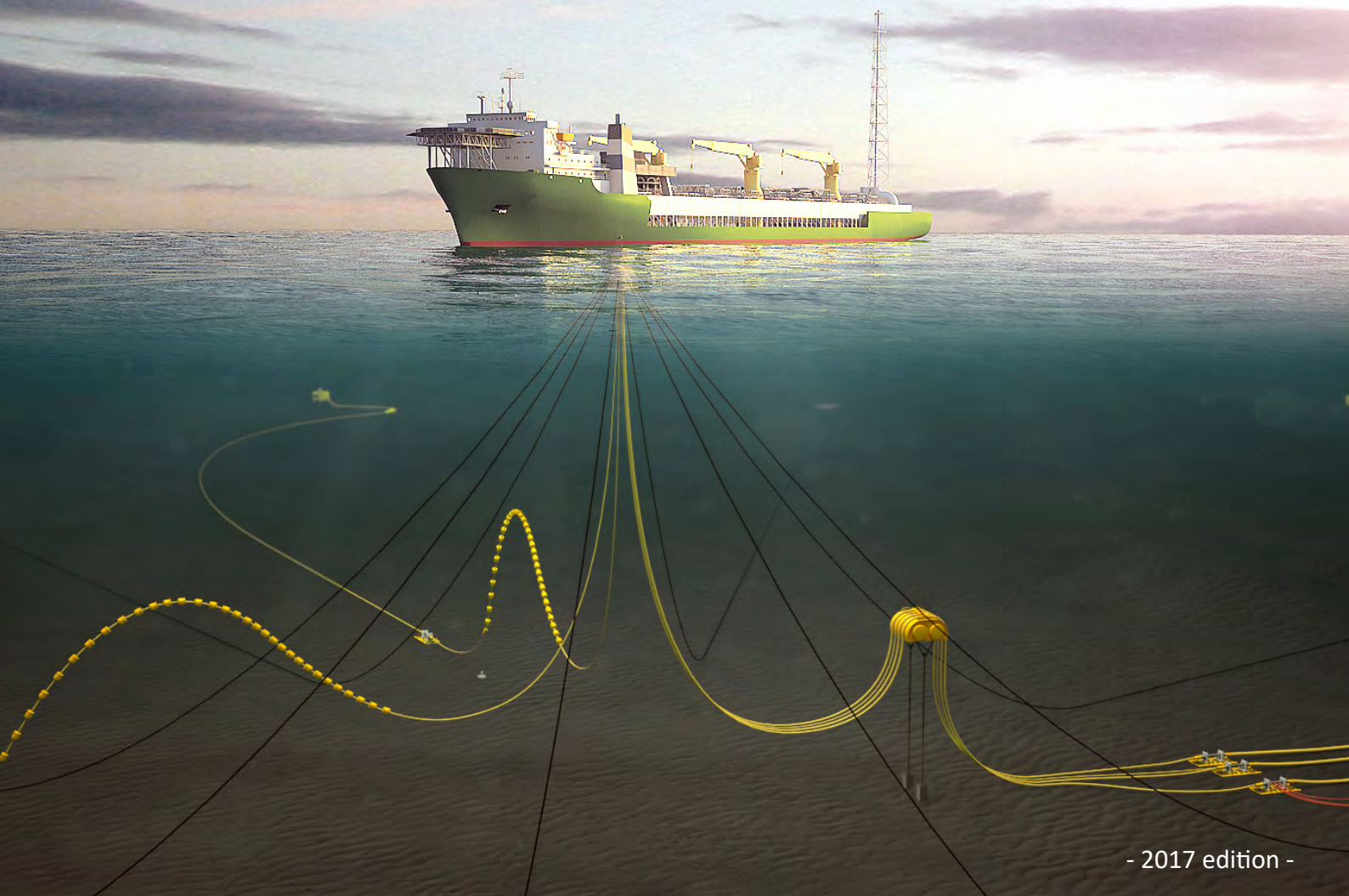


Handbook on

# Design and operation of flexible pipes

Joint Industry Project: "Safe and Cost Effective Operation of Flexible Pipes"



- 2017 edition -



# **HANDBOOK**

## **on DESIGN and OPERATION of FLEXIBLE PIPES**

**Editors:** Dag Fergestad SINTEF Ocean  
Svein Are Løtveit 4Subsea

Development of this Handbook is made possible through the Joint Industry Project (JIP): **"Safe and Cost Effective Operation of Flexible Pipes"**. 2011 - 2013.

This HANDBOOK is sponsored by:

ConocoPhillips  
Dong Energy  
ExxonMobil  
Lundin  
Maersk Oil  
Shell Norge  
Talisman Energy

This HANDBOOK is an extended revision of the Handbook issued in 1992 (FPS2000 project):  
Berge S. and Olufsen A. (eds.): "Handbook on Design and Operation of Flexible Pipes",  
Sintef Report STF70 A92006, 1992-02-07.

All changes to this document should be coordinated with Dag Fergestad: [Dag.Fergestad@sintef.no](mailto:Dag.Fergestad@sintef.no)

©2017: NTNU / 4Subsea / SINTEF Ocean  
ISBN 978-82-7174-285-0  
Issued June 6<sup>th</sup>  
Last revised 06.06.2017

SINTEF Ocean  
*Visiting address:*  
Otto Nielsens veg 10,  
NO-7052 Trondheim Norway

*Postal address:*  
P.O. Box 4762 Torgard,  
NO-7465 Trondheim Norway

Telephone: +47 464 15 000  
Email: ocean@sintef.no

Cover photo: ©4Subsea AS

## Document history

### 0.0.0.1 STF70 A92006 - 07.02.1992

- First edition Handbook on Design and Operation of Flexible Pipes, FPS2000 "Flexible Risers and Pipes" NTNF Research Programme, [Berge et al., 1992]

### 0.0.0.2 MT2014 A-001 15.04.2014

- Handbook on Design and Operation of Flexible Pipes, Vol.1 and Vol.2 (confidential), JIP – Safe and Cost Effective operation of Flexible Pipes, 2011-2014 [Fergestad et al., 2014]

### 0.0.0.3 OC2017 A-001 06.06.2017

- Handbook on Design and Operation of Flexible Pipes, Vol.1 and Vol.2 merged and edited. Confidential period expired. Some corrections and minor additions.

## PREFACE

High pressure flexible pipes are increasingly being used in the offshore production of oil and gas. Early experience with flexible pipes was gained since the late 1970s in relatively benign environments. A breakthrough for flexible pipes as dynamic risers in the harsh environments of the North Sea came in 1983/84 when it was decided to use a flexible dynamic riser system on the Balmoral field.

For flexible pipes the initial challenges for field developments on the Norwegian Continental Shelf were:

- Combination of severe environment and (at that time) deep water
- Fields with high temperature and pressure, combined with large quantities of gas
- Permanent installations with many risers, large investments and long field lives
- Stringent requirements with regard to safety documentation

In order to help meet the challenges related to floating production systems for oil and gas the Royal Norwegian Council for Scientific and Technical Research (NTNF) launched a three year research program, Floating Production Systems (FPS2000), in 1989. One objective of the program was to qualify flexible risers and pipes for use on the Norwegian Continental Shelf. The first edition of the "Handbook on Design and Operation of Flexible Pipes", [Berge et al., 1992] was also a deliverable from FPS2000. The effort was motivated by the need for cost reduction of future field developments, both facing the shortcomings of fixed platform technology available at that time, and the need for more economic robustness with respect to experienced variations in the oil price.

With the increase in floater developments offshore Norway from 1993 to 2001, the number of flexible risers increased from about 50 to more than 250. In 2013 there were 326 flexible risers in service offshore Norway. The CODAM database administered by Petroleum Safety Authority Norway (PSA Norway) reported 85 flexible riser incidents from 1995 to October 2013 including 60 "Major Incidents" with loss of containment or significant probability of such loss, and incidents with high personnel risk. Most of the risers that have experienced a major incident as well as other risers with confirmed unacceptable risk have been replaced after risk assessments. More than 25% of the flexible risers offshore Norway has not met their design service life [4Subsea, 2013].

In order to improve reliability related to operation of flexible risers there is need for cooperation, improvements and systematic work. The starting point should be an industry consensus of what is the current status and secondly promote and obtain standardization. With this as the background the JIP - Safe and Cost Effective Operation of Flexible Pipes was established in 2011 as a combined effort between Marintek / NTNU and 4Subsea AS. A key project delivery is a revised and extended version of the Handbook on Design and Operation of Flexible Pipes from 1992. The activities for the work-scope for the JIP are in short listed as:

- Repair methods for flexible pipes.
- Supporting tools for assessing the integrity of flexible pipe cross-section due to corrosion damage of tensile armour wires.
- Supporting tools for tensile armour buckling of flexible pipes.
- Life time assessment of flexible pipes.

- Reliability methods for integrity assessment of flexible pipes.
- Small scale fatigue testing of tensile armour wires from (sweet service) flexible risers taken out of service after many years in operation.
- Characterization of surfaces of corroded tensile armour wires from flexible risers taken out of service in relation to fatigue properties.
- Description and assessment of annulus environments for different segments of risers under relevant operational scenarios including corrosion issues.
- Update of Handbook on Design and Operation of Flexible Pipes based on the 1992-edition, the JIP project work and the JIP group experience.

The flexible risers from the Balmoral field were decommissioned after 23 years in service. Samples of used and stored tensile armour wires were made available for fatigue testing to the JIP through cooperation with the JIP "Riser End of Life" run by Flexlife. Along with additional material from a decommissioned riser after 11 years in service (riser named North Sea riser in this Handbook), fatigue properties of tensile armour wires subjected to annulus corrosion have been tested and specimen surfaces have been examined and characterized.

The recommendations and guidelines given in this text are not intended to serve as regulations, and there has been no attempt to write the Handbook in the style of a "recommended practice". However, it is a hope that the Handbook may be useful for experienced and new users of flexible pipes and to serve as reference literature for a new generation of flexible riser engineers.

## ACKNOWLEDGEMENTS

This Handbook has been prepared as a joint effort by Marintek, NTNU and 4Subsea, within the Joint Industry Project - "Safe and Cost Effective Operation of Flexible Pipes". The participating companies were:

ConocoPhillips  
Dong Energy  
ExxonMobil  
Lundin  
Maersk Oil North Sea  
Shell Norge  
Talisman Energy

The project was executed within a three year period from 2011 throughout 2013, with a budget of NOK 10 500 000. The participating companies have played an important role in this project, both through the Steering Committee and in technical terms through active participation as an advisory group. Hence, the scope of work and project plans has been worked out in close cooperation between the participants and the project group of Marintek, NTNU and 4Subsea.

In order to meet the challenges related to floating production systems for oil and gas in the North Sea the Royal Norwegian Council for Scientific and Technical Research (NTNF) launched a three year research program, Floating Production Systems (FPS2000), in 1989. One overall aim of the FPS2000 program was to qualify flexible risers and pipes for the Norwegian Continental Shelf, and one deliverable was the first version of the Handbook on Design and Operation of Flexible Pipes (1992 edition). We are grateful to be able to use the 1992 edition as a basis for this Handbook, which is now extended to include experience from the operation of flexible pipes as well as updates on methods and technology since the early 1990-ties.

## INTRODUCTION

The intention of this section is to give a summary of the content and the organization of the Handbook. The content is organized in chapters that are assembled in four main parts following the life cycle of the flexible pipe.

The first part - **Part A -Flexible Systems** - describes the application of flexible pipe along with the design process and some design considerations with emphasis on flexible risers and flowlines (Chapter [A1, Flexible pipe systems](#)). Components are described (in Chapter [A2, Flexible Pipe Properties and Materials](#)) by a layer by layer approach. Additional description is provided on polymers for liners. Finally the number of experienced [Failure modes](#) (separate chapter) has increased considerably since the original version of this Handbook in 1992. A layer by layer failure mode description is given with reference to [[API 17B, 2008](#)] along with detailed evaluations of selected flexible pipe layer failure.

The second part - **Part B - Design and Analysis Tools** - put emphasis on necessary tools for evaluating flexible pipe systems during operation. Flexible pipe is a complex structure. A chapter on [Design analysis](#) includes [Cross section analysis tools](#) which have developed considerably during the past twenty years, along with a textbook section on [Global analysis](#) focusing on flexible pipe systems, predominantly flexible risers, as outlined by Part [A, Flexible systems](#). Additional tools are [Risk analysis methodology](#) and [Reliability analysis](#), forming a basis for decision making for operational activities such as integrity management, assessment of (remaining) lifetime and repair. The tools also contain awareness and guidance on how the chemical environment within the complex pipe wall (Chapter [B4, Annulus environment and Corrosion](#)) may develop over time and represent a threat to the pipe integrity by [Corrosion](#) of the steel armour. Finally an overview of a large number of specified tests to be carried out during the flexible pipe lifetime is given (Chapter [B5, Test methods](#)). The test specifications are given by API documents; [[API 17B, 2008](#)] and [[API 17J, 2008](#)], an overview is given here for completeness.

The third part is devoted to flexible pipe in operation - **Part C - Operations**. The part starts out with a chapter on guidance, recommendations and activities for practical [Integrity management](#) for flexible pipes which complies with and supplements existing rules and regulations. The need to document operational conditions and monitor the flexible pipe during the entire lifetime has become more of an accepted practice. Whenever an unacceptable integrity level is detected or operation goes beyond the design limit, [Lifetime assessment](#) (separate chapter) needs to be performed. Guidance and practical advice for performing a lifetime assessment is given here, with main emphasis on describing a systematic and practical approach towards a decision on continued safe operation after damage, anomalies, change of operational conditions or exceeding of original service- or design life. A layer by layer approach is adopted as well. A decision might be to perform a repair of the pipe. Possible [Repair methods](#) (separate chapter) are finally described along with activities to be performed in relation to a repair process. A connection between failure modes, inspection methods and repair is made and accompanied by recommendations and experiences.

The last part is **Part D - Case Study**. A representative flexible riser concept subjected to typical North Sea conditions, is used to illustrate the following purposes:

- Actions taken should corrosion damage occur during operation of the riser
- Evaluations made should corrosion damage occur during operation of the riser

- Highlight the implementation of methodologies described in the Handbook sections from Chapter A2 to Chapter C3
- Document the underlying studies and evaluations made for the selected riser during the course of the JIP

The Case Study part does not illustrate all sections of the Handbook, but should serve as a good starting point for making decisions and also provides some examples. The following chapters are included: Data basis, Small scale fatigue testing, Evaluation of specimen surfaces, Integrity assessment of damaged flexible pipe cross-sections, Integrity management, Lifetime assessment and Reliability analysis.

The Case Study is based on the flexible riser concept denoted "North Sea Riser", with a riser annulus that has been flooded during a significant period of its 11 years of service. For the small scale fatigue testing and sample inspections of tensile armour wire, additional information was obtained from samples of a 4" (ID) riser from the Balmoral field (23 years of service, flooded).

Some additional description of the objectives and purposes of the different chapters within the Parts of the Handbook is given in the following:

## PART A: FLEXIBLE SYSTEMS

### ***Chapter A1 "Flexible Pipe Systems"***

The primary objectives of the chapter are to present:

- State of the art overview of flexible pipe systems in use today
- Flexible pipe design aspects
- Flexible riser system experience and guidance
- Flexible flowline experience and guidance
- Installation considerations and experience

The goal of this Chapter is to provide a background for understanding the specific design challenges for flexible pipe systems. The scope is mainly related to submerged systems (systems above water - such as topside jumpers - are not discussed in detail).

### ***Chapter A2 "Flexible Pipe Properties and Materials"***

The characteristic properties of a non-bonded flexible pipe are described. The basic components of the pipe construction are discussed, layer by layer with respect to functionality and characteristics. Some specifics concerning flowlines and smooth bore pipes as well as bend stiffeners are discussed briefly. Polymers used for liner application in flexible pipes are described in more depth.

### ***Chapter A3 "Failure Modes"***

A comprehensive understanding of failure modes is essential for both the design phase and operational phases:

- Design phase: ensure that pipes are designed with adequate consideration and measures to resist relevant failure modes
- Operational phase: ensure that all relevant failure modes can be identified and assessed in terms of remaining service life, safety margins and quantification of risks as part of integrity management and lifetime assessment

This chapter of the handbook has been developed with the following purposes:

- Define concepts and terminology relating to failure modes
- Define a framework for assessment of failures in flexible pipes
- Present state of the art for relevant failure modes with description of failure and degradation mechanisms, consequences and mitigations
- Present available and relevant failure statistics
- Provide guidance on how to address important failure mechanisms for evaluation of the integrity of flexible pipes

The primary scope of this chapter is to provide basis for systematic Integrity Management and Lifetime assessment of flexible pipes, where an understanding of flexible pipe degradation and failure mechanisms is essential.

## **PART B: DESIGN AND ANALYSIS TOOLS**

### ***Chapter B1 "Design Analysis"***

This chapter concerns tools and procedures for performing cross-section and global analysis of flexible pipes. References are made to the API-specifications for criteria and requirements to the design of flexible pipes.

The description of cross section analysis focuses on methods for analysis and design of non-bonded flexible pipes with respect to known metallic layer failure modes that can be described by analytical or numerical methods and are part of the design requirements reflected in [API 17J, 2008]. The failure modes addressed are:

- Overload, i.e. excessive yielding in the metallic layers
- Collapse of the cross-section due to external pressure
- Buckling of tensile armour
- Metal fatigue
- The effect of corrosion on metal fatigue and tensile armour buckling

Analytical formulas are included for assessment of mechanical properties and structural capacities for specific cases. These formulae are primarily given for verification purposes,

enabling capacity and performance parameters to be calculated in a simple way and under specific conditions.

The global analysis section is an up to date textbook section for the methods on global analysis of the flexible pipe, predominantly flexible risers. The use of global analysis along with simplified methods for evaluation of preliminary design is described. Prediction of global response due to internal and external forces induced by waves and current is given. Guidelines are given concerning the modelling of riser systems and forces. Furthermore, various response analysis methods are described and compared both with respect to each other and with reference to experimental results. Finally, different procedures for design analysis are described.

### ***Chapter B2, "Risk Analysis Methodology"***

The objective of the chapter is to give an overview of the methods required for risk analysis of flexible pipes.

The main steps associated with quantitative risk assessment (QRA) can be summarized as follows:

1. Definition of system boundaries and identification of hazards
2. Development of fault trees and event trees
3. Evaluation of failure probabilities and consequences (risk matrix)
4. Development of decision networks (decision trees)
5. Definition of acceptance criteria
6. Risk reduction and/or risk mitigation

These topics are highlighted in relation to flexible pipe systems. Furthermore, evaluation of probability of mechanical failure modes and the methods for risk-based riser integrity management are elaborated.

The risk concept is first briefly discussed. The main steps of quantitative risk assessment are next described in some more detail. Subsequently, methods and sources for evaluation of the probability of failure for relevant critical events are reviewed. Consequence analysis, acceptance criteria and decision making are also addressed.

### ***Chapter B3, "Reliability Analysis"***

In order to perform a risk assessment for a given flexible riser or flowline system, the potential failure modes need to be identified. For some of the failure modes a certain amount of relevant historical/empirical data may be available such that failure rates can be estimated. However, in many cases such data are missing or they can be rather irrelevant due to technological developments and improved production methods.

In many cases a mechanical model may be established corresponding to a given failure criterion. Such a model is generally referred to as a *limit state*, which is typically defined in terms of loads (or load effects) versus capacity terms. For some cases (such as for assessment

of fatigue and wear) the accumulated load effect is relevant rather than its instantaneous value.

Both the load effects and capacity associated with a particular limit state will frequently depend on a number of parameters for which inherent variability is present. This implies that they are more adequately represented as random variables than deterministic quantities, which is accommodated within the framework of structural reliability analysis.

Another application of such analysis methods is represented by cases which are not directly covered by existing design documents. Examples are life extension of flexible pipes beyond the intended service life as well as requalification and reuse of pipes. Integrity management is another example. Other examples of application are situations where additional information is to be taken into account in a systematic and consistent manner, such as monitoring of operation parameters, metocean characteristics, pipe damage, accident scenarios as well as pipe annulus conditions.

### ***Chapter B4 "Annulus Environment and Corrosion"***

The annular space in flexible pipes contains the steel armours that provide the structural support for containment of fluid and gas in the bore and the structural capacity required to sustain pressure and carry axial, bending and torsion loads. The integrity of these armours is essential. They are arranged within a confined annular space that makes it challenging to model corrosion. The annulus conditions vary significantly between pipes in service and also along a given pipe.

The purposes of this chapter are to:

- Define the span of possible conditions in flexible pipe annuli
- Identify to what extent relevant conditions in flexible pipe annuli can cause corrosion
- Review literature to identify knowledge and models that can be used to predict corrosion under identified annulus conditions
- Develop guidance relating to corrosion caused by damage to the outer sheath in terms of:
  - Detection of damage of outer sheath
  - Susceptibility for corrosion as a function of the location of cover damage
  - Risk assessment and possible mitigation

The industry needs:

- Models and procedures to assess the susceptibility and probability for corrosion of armours in flexible pipe annuli for relevant scenarios
- Solutions for monitoring, detection and predictions
- Guidance for how to deal with damage or other incidents

***Chapter B5 "Test Methods"***

Testing is an important part of the design verification for a particular pipe design. Due to the complex structure of flexible pipe and the multitude of possible failure modes, test methods and procedures should be evaluated on a case-by-case basis. An overview of methods for mechanical testing of flexible pipes are given, with details on test specification given in [API 17B, 2008], [API 17J, 2008] and referenced testing standards.

**PART C: OPERATIONS*****Chapter C1 "Integrity Management"***

The purpose of this chapter is to provide guidance and recommendations for practical in-service integrity management (IM) for flexible pipes. The intention is to comply with and provide guidance that is supplementary to the framework for integrity management in [API 17B, 2008], [DNV-RP-206, 2008] and [DNV-RP-F116, 2009]. Recommendations on the development and execution of Integrity Management Programs and on the evaluation of the activities performed are presented.

The IM-program shall provide documentation of the flexible pipe's integrity status, and verify and document acceptable integrity throughout the pipe's (design) lifetime. Unacceptable integrity level or operation outside the original design specifications requires a lifetime assessment to be performed to determine conditions for continued operation of the pipe. Details are given in [C1, Lifetime Assessment](#).

Integrity management strategies adopted in today's standards and guidelines are in general risk based. The need for follow-up and monitoring of the pipe over its entire lifetime is acknowledged and becoming universally accepted.

The main motivation for a comprehensive integrity management of flexible pipes is to ensure safe and cost effective operation of flexible pipes. Replacement of a pipe is costly, and failure of a flexible pipe may potentially be catastrophic with large economic impact.

***Chapter C2 "Lifetime Assessment"***

The scope of this chapter is to provide guidance and practical advice for performing a lifetime assessment of flexible pipe systems. Main emphasis is to describe a systematic and practical approach to determine if a flexible pipe can safely operate after sustained damages, anomalies, change of operational conditions or exceeding the original service- or design life.

A work process for performing a lifetime assessment in a systematic manner is presented, a process which is largely based on the information in [NORSOK Y-002, 2010] (Life Extension of Transportation Systems). For lifetime assessment tasks other than expiry of service or design life, relevant modifications are performed. A questionnaire based format to support the engineer performing the lifetime assessment is presented. The questions are relatively general and may be expanded on a case by case basis. Additional information sources may be required depending on the nature of the lifetime assessment being performed.

Relevant industry references and experiences are presented. This is to illustrate typical key issues, concerns and limitations during a lifetime assessment process. Two examples are

presented more in detail; one related to lifetime extension and one to re-qualification of a riser system.

### ***Chapter C3 "Repair Methods"***

This chapter addresses repair methods for flexible pipes including end-fittings. Ancillary devices to flexible pipes such as bend stiffeners, buoyancy modules and friction clamps are not discussed.

An overview of flexible pipe failure modes with evaluation of service experience, available inspection methods and repair methods is presented. The overview shows that methods for inspection and repair are available for only a limited number of the failure modes. The failure statistics and available inspection and repair methods advocate the importance of repair methods for the failure modes reviewed in this report:

- Outer sheath damage
- Restricted annulus vent flow

Re-termination of end fitting is applicable as a repair method for damages located near the pipe ends. Re-termination of flexible risers normally requires that flexible manufacturer provides new end-fittings and is responsible for the repair. A flowchart of the repair process from detection of damage to continued operation (if proven viable) of the flexible pipe after repair is given.

## **PART D: CASE STUDY**

The Case Study illustrates some steps to be taken and evaluations to be made should corrosion damage occur during operation of a given riser for a given situation. The damage described and the operational scenario selected is believed to be typical in order to serve as a representative example. For the JIP "Safe and Cost Effective Operation of Flexible Pipes", the scenario of tensile armour with corrosion damage was selected. It is a hope that this Case Study will highlight the implementation of methods and methodologies described in the Handbook sections from Chapter A2 to Chapter C3. The underlying studies and evaluations made for the selected riser during the course of the JIP are compiled in this Part.

The Case Study is generally based on the riser case "North Sea Riser". However, during the JIP some studies were performed using the 4" (ID) riser from the Balmoral field as a case: fatigue testing of armour wire in air, evaluation of corroded armour wire surfaces by microscopy and application of in-air SN-curve for reliability evaluation. The results from the studies based on the Balmoral riser are included where relevant in supplementing the results from the North Sea Riser.

After describing the riser structures, necessary aspects of operational life are defined - along with selected alternative scenario, Chapter D2.

Chapter D3 describes the fatigue testing performed for the corroded armour wire samples. The testing performed is not sufficient to obtain SN-curves to be used in a reassessment process, but provide valuable information on the effect of corrosion on the armour wires.

The study of the corroded armour wire samples continue in Chapter D4 by investigating the corroded surfaces with the aim of obtaining yet more helpful data in understanding the effect

of corrosion damage and how to measure the corrosion damage.

In Chapter [D5](#) some structural aspects of tensile armour wires are studied; a) tension armour wire failure due to corrosion; numerical analysis and methodology on how to account for wire failures in the integrity assessment analysis, and b) lateral buckling analysis of tensile wires and the effect of lay angle of the anti-buckling tape.

In Chapter [D6](#) - Integrity management - a working methodology is described for transforming the information tools from Handbook Chapter [B2](#) - Risk Analysis Methodology, [A3](#) - Failure Modes and Chapter [C1](#) - Integrity Management into an actual integrity management plan for the case study riser.

Chapter [D7](#) - Lifetime assessment presents an example of a lifetime assessment process for the North Sea riser according to the work flow described in the Handbook Chapter [C2](#) - Lifetime Assessment and Chapter [A3](#) - Failure Modes.

In Chapter [D8](#) the basis for reliability analysis related to fatigue lifetime of specific flexible riser configurations is elaborated. Initial reliability calculations are also performed with a focus on the tensile armour. Fatigue damage due to the combination of wave action and dynamic floater motion is considered along with different scenarios with respect to repair as well as tensile wire failures.



# Contents

<b>A Flexible Systems</b>	<b>1</b>
<b>A1 Flexible Pipe Systems</b>	<b>3</b>
A1.1 Introduction . . . . .	4
A1.2 Flexible Pipe Systems . . . . .	4
A1.3 Flexible Pipe Design . . . . .	8
A1.3.1 Design stages . . . . .	8
A1.3.2 Standards and Recommended Practices . . . . .	10
A1.3.3 Flexible Pipe Cross-Section Components . . . . .	10
A1.3.4 Flexible Pipe Design Considerations . . . . .	12
A1.4 Flexible Risers . . . . .	18
A1.4.1 Introduction . . . . .	18
A1.4.2 Riser configurations . . . . .	19
A1.4.3 In-service experience overview . . . . .	32
A1.5 Flowlines and tie-ins . . . . .	35
A1.5.1 General . . . . .	35
A1.5.2 Selection of Flexible pipe (alternatives) . . . . .	36
A1.5.3 Flowline restraint and tie-in flexibility . . . . .	37
A1.5.4 Crossings . . . . .	38
A1.5.5 Installation . . . . .	38
A1.5.6 Design and Analysis . . . . .	42
A1.6 Other flexible pipe systems . . . . .	53
A1.6.1 Offloading . . . . .	53
A1.7 Installation . . . . .	54
A1.7.1 Introduction . . . . .	54
A1.7.2 Vessels . . . . .	55
A1.7.3 Installation Operations . . . . .	57
A1.7.4 Post-Installation Procedure . . . . .	63
A1.7.5 Documentation . . . . .	63
<b>A2 Flexible Pipe Properties and Materials</b>	<b>65</b>
A2.1 General remarks . . . . .	66
A2.2 Pipe wall structure and materials . . . . .	68
A2.2.1 Pipe wall structure . . . . .	69
A2.2.2 Carcass . . . . .	69
A2.2.3 Liner . . . . .	71
A2.2.4 Pressure armour . . . . .	73
A2.2.5 Intermediate sheath . . . . .	74
A2.2.6 Tensile armour . . . . .	74

A2.2.7 Composite armour . . . . .	75
A2.2.8 Anti-wear tape . . . . .	75
A2.2.9 Anti-buckling tape . . . . .	76
A2.2.10 Thermal insulation . . . . .	76
A2.2.11 Outer sheath . . . . .	76
A2.2.12 Bend stiffener . . . . .	76
A2.2.13 Smooth bore pipe . . . . .	77
A2.2.14 Flowlines . . . . .	77
A2.3 Polymers for liner applications . . . . .	77
A2.3.1 Introduction . . . . .	77
A2.3.2 Relevant Aspects of Polymer Performance . . . . .	79
A2.3.3 Polymers used in Flexible Pipes . . . . .	87
<b>A3 Failure Modes</b>	<b>99</b>
A3.1 Purpose . . . . .	100
A3.1.1 Description of document objective . . . . .	100
A3.1.2 Scope of document . . . . .	100
A3.2 Definitions of concepts and terminology . . . . .	101
A3.2.1 General concepts . . . . .	101
A3.2.2 Definitions . . . . .	102
A3.2.3 Probability of Failure (PoF) . . . . .	103
A3.2.4 Format for Description of Failure Causes . . . . .	104
A3.3 Flexible Pipe Failures . . . . .	105
A3.3.1 Overview of layer failures and failure causes . . . . .	105
A3.3.2 Detailed evaluation of selected flexible pipe layer failure causes . . . . .	109
A3.3.3 Examples of Ancillary devices failure causes . . . . .	144
A3.4 Failure Statistics . . . . .	151
<b>B Design and Analysis Tools</b>	<b>153</b>
<b>B1 Design Analysis</b>	<b>155</b>
B1.1 Introduction . . . . .	156
B1.2 Design Criteria . . . . .	157
B1.3 Cross Section Analysis . . . . .	158
B1.3.1 General remarks . . . . .	158
B1.3.2 Governing stress components . . . . .	159
B1.3.3 Wire geometries . . . . .	161
B1.3.4 Behaviour due to axisymmetric loads . . . . .	163
B1.3.5 Behaviour in bending . . . . .	173
B1.3.6 Buckling . . . . .	185
B1.3.7 Fatigue . . . . .	193
B1.3.8 Computational methods . . . . .	200
B1.4 Global Analysis . . . . .	205
B1.4.1 Use of global analyses . . . . .	205
B1.4.2 Weight and buoyancy; the effective weight concept . . . . .	208
B1.4.3 Simplified analysis for preliminary design . . . . .	212
B1.4.4 Loads from internal fluid flow . . . . .	221
B1.4.5 External loads . . . . .	226
B1.4.6 Finite Element Models . . . . .	238

B1.4.7 Coupled Analysis Models . . . . .	254
B1.4.8 Stochastic analysis . . . . .	258
B1.4.9 Vortex induced vibrations . . . . .	284
B1.4.10 Use of results from global analyses . . . . .	284
B1.4.11 Quality assurance and quality control . . . . .	287
<b>B2 Risk Analysis Methodology</b>	<b>291</b>
B2.1 Introduction . . . . .	292
B2.2 Risk-based approach: risk definition, classification and quantification . . . . .	293
B2.2.1 General . . . . .	293
B2.2.2 Definition of risk . . . . .	293
B2.2.3 Risk categories . . . . .	293
B2.2.4 Derived risk measures . . . . .	294
B2.3 Building blocks of quantitative risk assessment (QRA) . . . . .	294
B2.3.1 General . . . . .	294
B2.3.2 Definition of system boundaries and identification of hazards . . . . .	295
B2.3.3 FMEA/FMECA . . . . .	295
B2.3.4 HAZOP . . . . .	296
B2.3.5 Event tree analysis . . . . .	296
B2.3.6 Fault tree analysis . . . . .	297
B2.3.7 Risk Matrix: Evaluation of failure probabilities and consequences . . . . .	298
B2.3.8 Decision trees . . . . .	299
B2.3.9 Acceptance criteria . . . . .	299
B2.3.10 Risk reduction . . . . .	301
B2.4 Quantification of mechanical failure probability . . . . .	302
B2.4.1 General . . . . .	302
B2.4.2 Flexible pipe failure data based on test results . . . . .	302
B2.4.3 Probabilistic evaluation of mechanical limit states, including time-variation of loads and resistance . . . . .	303
B2.5 Risk-based Riser Integrity Management . . . . .	304
B2.6 Historical failure mechanisms and qualification of new technology . . . . .	306
B2.6.1 Historical failure mechanisms . . . . .	306
B2.6.2 Qualification of new technology . . . . .	307
B2.7 Concluding remarks . . . . .	307
<b>B3 Reliability Methods</b>	<b>309</b>
B3.1 Introduction . . . . .	310
B3.2 Mechanical Limit States . . . . .	310
B3.2.1 Limit states and levels of reliability analysis . . . . .	310
B3.2.2 A basic limit state formulation: Failure function and probability of failure . . . . .	311
B3.2.3 Time-varying characteristics of load-effects and capacity . . . . .	314
B3.3 Data Basis and Input Modeling Relevant for Mechanical Limit States . . . . .	315
B3.4 Acceptance criteria . . . . .	316
B3.5 Analysis procedures . . . . .	318
B3.6 Reliability Analysis for the Fatigue Limit State . . . . .	320
B3.6.1 General . . . . .	320
B3.6.2 Example of application to fatigue assessment of a flexible riser . . . . .	321
B3.7 Reliability Analysis for the Ultimate Limit State . . . . .	329
B3.7.1 General . . . . .	329

B3.7.2 A Simplified Example of Application to a Flexible Riser Configuration	330
B3.8 Effect of Monitoring/inspection/repair on reliability level	331
B3.9 Concluding remarks	333
<b>B4 Annulus environment and corrosion</b>	<b>335</b>
B4.1 Introduction	336
B4.2 Annulus environment and conditions	337
B4.2.1 Definition of the annulus	337
B4.2.2 Permeation into the annulus	338
B4.2.3 Annuli environment evolvement	339
B4.2.4 Conditions affecting corrosion of armour wires	344
B4.2.5 Some relevant quantities	347
B4.2.6 Summary of Scenarios	347
B4.3 Corrosion issues in flexible pipe annuli	349
B4.3.1 Potential Consequences of Corrosion	349
B4.3.2 The role of the steel	349
B4.3.3 Corrosion mechanisms	350
B4.3.4 Hole in the outside cover	356
B4.3.5 Effects on fatigue resistance from corrosion processes	359
B4.4 Field experience	362
B4.4.1 Cases with severe corrosion	362
B4.4.2 Other field experience	363
B4.5 Summary and recommendations	365
B4.5.1 Summary of field experience:	365
B4.5.2 Key findings relating to CO <sub>2</sub> corrosion	365
B4.5.3 Issues for concern	366
B4.5.4 Mitigation:	366
B4.5.5 Future challenges	368
<b>B5 Test Methods</b>	<b>369</b>
B5.1 Introduction	370
B5.2	370
B5.2.1 Prototype testing	370
B5.2.2 End termination tests	371
B5.2.3 Vacuum tests	371
B5.2.4 Factory acceptance tests	371
B5.2.5 On-board structural integrity test	372
B5.2.6 Offshore structural integrity test	372
B5.2.7 Materials testing	372
B5.3 Corrosion fatigue testing	373
B5.3.1 Test protocol	373
B5.3.2 Specifications for the environment	373
B5.3.3 Specimen preparation and fatigue loading	376
B5.3.4 Assessment of design criteria from SN-data	377
B5.4 Fatigue testing of pressure armour	377
<b>C Operation</b>	<b>379</b>
<b>C1 Integrity Management</b>	<b>381</b>

C1.1 Introduction . . . . .	382
C1.2 Key aspects of integrity management . . . . .	383
C1.2.1 Standards and Guidelines for Integrity Management . . . . .	383
C1.2.2 Governmental requirements and Company specific requirements . . . . .	384
C1.2.3 Information Handling . . . . .	384
C1.3 Risk Based Integrity Management for Flexible Pipes . . . . .	384
C1.3.1 Pipe system boundaries and system components definition . . . . .	384
C1.3.2 Classification and grouping of pipes . . . . .	385
C1.3.3 Hazard identification and probability of pipe failure . . . . .	385
C1.3.4 Consequence of pipe failure . . . . .	387
C1.3.5 Risk assessment . . . . .	388
C1.3.6 Risk mitigation and development of an Integrity Management Program	389
C1.4 Practical Integrity Management . . . . .	390
C1.4.1 Introduction . . . . .	390
C1.4.2 Inspections . . . . .	392
C1.4.3 Testing . . . . .	397
C1.4.4 Monitoring and monitoring data review . . . . .	405
C1.4.5 Integrity Review and Reporting . . . . .	413
C1.4.6 When is repair advisable? . . . . .	413
C1.4.7 Learning and improvement . . . . .	413
<b>C2 Lifetime Assessment</b>	<b>415</b>
C2.1 Introduction . . . . .	416
C2.1.1 Objective and Scope . . . . .	416
C2.1.2 General . . . . .	416
C2.1.3 Limitations . . . . .	416
C2.1.4 Contents . . . . .	417
C2.2 Principles of lifetime assessment . . . . .	417
C2.2.1 General . . . . .	417
C2.2.2 Process overview and Methodology . . . . .	419
C2.2.3 Initiators . . . . .	420
C2.2.4 Assessment Premise . . . . .	425
C2.2.5 Lifetime Assessment . . . . .	426
C2.2.6 Improved Condition Control, Mitigations and Modifications . . . . .	429
C2.2.7 Documentation and Implementation . . . . .	431
C2.3 Standards and Guidelines for Lifetime Assessment . . . . .	433
C2.3.1 Overview . . . . .	433
C2.3.2 Process Guidance . . . . .	434
C2.3.3 Detail Engineering Guidance . . . . .	434
C2.4 Lifetime Assessment Questionnaire . . . . .	437
C2.4.1 General . . . . .	437
C2.4.2 System Screening . . . . .	437
C2.4.3 Condition Control Basis . . . . .	440
C2.4.4 Layer Assessment . . . . .	443
C2.4.5 Ancillary Components . . . . .	459
C2.5 Industry References and Experiences . . . . .	461
C2.5.1 General . . . . .	461
C2.5.2 Flowlines Life Extension Example . . . . .	463

C2.5.3 Re-qualification example after outer sheath damage and annulus flooding . . . . .	468
<b>C3 Repair Methods</b>	<b>471</b>
C3.1 Introduction . . . . .	472
C3.2 Repair method status . . . . .	473
C3.2.1 Overview of failure modes . . . . .	473
C3.2.2 Market screening . . . . .	478
C3.2.3 Evaluation of repair methods and general guidance on repair possibilities	479
C3.2.4 Qualification of new inspection methods and repair methods . . . . .	479
C3.3 Planning for repair . . . . .	481
C3.3.1 Damage assessment . . . . .	481
C3.3.2 Design and qualification of repair method . . . . .	482
C3.3.3 Execution of repair and verification of pipe integrity . . . . .	483
C3.4 Repair methods for outer sheath damages . . . . .	485
C3.4.1 Injection of inhibitor liquid in annulus . . . . .	485
C3.4.2 Soft repair clamp . . . . .	487
C3.4.3 Rigid clamp . . . . .	490
C3.4.4 Structural repair clamp . . . . .	492
C3.4.5 Design aspects . . . . .	495
C3.4.6 Casting repair . . . . .	496
C3.4.7 Polymer welding of outer sheath . . . . .	499
C3.4.8 Examples of commercially available products for outer sheath repair . . . . .	500
C3.5 Repair methods to re-establish annulus vent . . . . .	503
C3.5.1 Installation of annulus vent clamp and drilling through outer sheath . . . . .	503
C3.5.2 Establish new vent ports for a pipe located inside a guide tube . . . . .	506
C3.5.3 Cyclic vacuum and nitrogen pressure . . . . .	509
C3.5.4 Hydraulic pressurization of vent port . . . . .	510
C3.5.5 Drilling a new vent port through the end-fitting . . . . .	512
C3.6 Re-termination of end-fitting as a repair method . . . . .	513
C3.6.1 Objective and application . . . . .	513
C3.6.2 Re-termination . . . . .	513
C3.6.3 Subsequent inspection and maintenance . . . . .	514
C3.6.4 Advantages and drawbacks . . . . .	514
C3.7 Summary . . . . .	515
C3.7.1 Track record for repair methods . . . . .	518
<b>D Case Study</b>	<b>519</b>
<b>D1 Introduction</b>	<b>521</b>
D1.1 Introduction . . . . .	522
D1.2 Case Description . . . . .	522
D1.2.1 North Sea Riser . . . . .	522
D1.2.2 Balmoral Riser . . . . .	524
<b>D2 Data Basis</b>	<b>527</b>
D2.1 Introduction . . . . .	528
D2.2 Temperature and pressure records (operation pressure) . . . . .	528
D2.3 Annulus pressure tests . . . . .	528

D2.3.1 Annulus gas sampling . . . . .	528
D2.4 Stress cycle distribution . . . . .	528
D2.5 Sheath and corrosion damage . . . . .	529
D2.6 SN-curves . . . . .	530
D2.7 Parameter variations . . . . .	531
D2.8 Available floater motion and position data . . . . .	532
<b>D3 Testing . . . . .</b>	<b>533</b>
D3.1 Introduction . . . . .	534
D3.2 Data provided by testing . . . . .	534
D3.3 Small scale testing in air . . . . .	534
D3.3.1 Fatigue testing - general . . . . .	534
D3.3.2 Test procedure . . . . .	535
D3.3.3 Armour wire from North Sea riser tested in air . . . . .	536
D3.3.4 Armour Wire from Balmoral riser tested in air . . . . .	540
D3.4 Concluding remarks . . . . .	545
<b>D4 Evaluation of specimen surface of tension armour samples from two different risers . . . . .</b>	<b>547</b>
D4.1 Introduction . . . . .	548
D4.1.1 Balmoral riser . . . . .	548
D4.1.2 North Sea riser . . . . .	548
D4.1.3 Material samples . . . . .	549
D4.2 Surface characterization of fatigue specimens . . . . .	550
D4.2.1 Microscopy . . . . .	550
D4.2.2 Procedure for investigation . . . . .	550
D4.2.3 North Sea Riser . . . . .	551
D4.2.4 Discussion and summary . . . . .	555
D4.3 Scanning electron microscopy of fatigue fracture surfaces of tensile armour . . . . .	556
D4.3.1 Microscopy . . . . .	556
D4.3.2 Specimen description . . . . .	556
D4.3.3 Discussion and summary . . . . .	558
<b>D5 Numerical evaluation of some integrity problems for flexible pipe cross-sections . . . . .</b>	<b>561</b>
D5.1 Introduction . . . . .	562
D5.2 Integrity assessment of damaged flexible pipe cross-sections . . . . .	562
D5.2.1 Introduction . . . . .	562
D5.2.2 Stresses and stress component . . . . .	562
D5.2.3 FE analysis procedure . . . . .	564
D5.2.4 FE analysis of North Sea Riser section . . . . .	567
D5.2.5 FE analysis results . . . . .	574
D5.3 Lateral buckling analysis of flexible riser tensile armour wire . . . . .	587
D5.3.1 Background . . . . .	587
D5.3.2 Introduction . . . . .	587
D5.3.3 Theoretical background . . . . .	589
D5.3.4 Analysis tools . . . . .	592
D5.3.5 Model description . . . . .	592
D5.3.6 Analysis and results . . . . .	595
D5.3.7 Effect of anti-buckling tape . . . . .	600
D5.3.8 Conclusions . . . . .	603

<b>D6 Integrity Management of North Sea Riser</b>	<b>605</b>
D6.1 Introduction . . . . .	606
D6.2 Methodology . . . . .	606
D6.3 Review of Selected Failure Modes . . . . .	607
D6.3.1 Carcass Collapse . . . . .	607
D6.3.2 Carcass Axial Overloading . . . . .	609
D6.3.3 Pressure Sheath Embrittlement (Ageing of Polyamides) . . . . .	612
D6.3.4 Tensile Armour Wire Fatigue . . . . .	614
D6.3.5 Outer Sheath: hole in the outer sheath . . . . .	616
D6.4 Summary . . . . .	620
D6.4.1 Failure Event Tree . . . . .	620
D6.4.2 Unmitigated Risk Level . . . . .	621
D6.4.3 Mitigated Risk Level . . . . .	622
D6.4.4 Control Mechanisms . . . . .	622
D6.4.5 Implementation . . . . .	624
<b>D7 Lifetime Assessment of North Sea Riser</b>	<b>625</b>
D7.1 Introduction . . . . .	626
D7.2 Lifetime Assessment - North Sea Riser Case Study . . . . .	627
D7.2.1 Lifetime Assessment Initiator . . . . .	627
D7.2.2 Lifetime Assessment Premise . . . . .	627
D7.2.3 Lifetime Assessment . . . . .	628
D7.2.4 Lifetime Assessment Conclusion . . . . .	634
<b>D8 Reliability</b>	<b>637</b>
D8.1 Probabilistic Models and Reliability analysis . . . . .	638
D8.1.1 Introduction . . . . .	638
D8.1.2 Relevant failure functions . . . . .	638
D8.1.3 Random variables and probabilistic models . . . . .	639
D8.1.4 Analysis method . . . . .	640
D8.1.5 Acceptance criteria . . . . .	640
D8.2 Assessment of remaining SN-lifetime . . . . .	640
D8.2.1 Introduction . . . . .	640
D8.2.2 Scenario A: Initial assessment: In-air one-slope SN-curve . . . . .	641
D8.2.3 Scenario B: Initial assessment: SN-curve for corrosive environment with full operation pressure . . . . .	643
D8.2.4 Scenario C: Lifetime estimation based on monitored data (i.e.pressure reduction) . . . . .	644
D8.2.5 Comparison of results for cases without sheath damage - Scenario A - C . . . . .	645
D8.2.6 Scenario D: Sheath damage with repair . . . . .	646
D8.2.7 Scenario E: Sheath damage without repair . . . . .	647
D8.2.8 Comparison of base case results for all scenarios A - E . . . . .	648
D8.2.9 Scenario F: Carbon dioxide with reduced pressure: Multiple sources of variability . . . . .	649
D8.2.10 Scenario G: Sheath damage with repair: Multiple sources of variability . . . . .	651
D8.2.11 Scenario H: Sheath damage without repair: Multiple sources of variability . . . . .	652
D8.3 Consideration of successive wire failures . . . . .	654
D8.3.1 General . . . . .	654

D8.3.2 Correlation properties between pairs of failure events . . . . .	654
D8.3.3 Consideration of possible failure sequences . . . . .	655
D8.3.4 Failure of first wire . . . . .	656
D8.3.5 Failure of second wire . . . . .	657
D8.3.6 Failure of third wire . . . . .	658
D8.3.7 Failure of fourth wire . . . . .	659
D8.3.8 Failure of fifth wire . . . . .	661
D8.3.9 Failure of sixth wire . . . . .	662
D8.3.10 Summary of results for sequential wire failure . . . . .	664
D8.4 Concluding remarks . . . . .	665
<b>E Abbreviations, Units and Constants</b>	<b>667</b>
<b>E1 Abbreviations</b>	<b>669</b>
<b>E2 Units and Constants</b>	<b>673</b>

## **Part A**

# **Flexible Systems**



## **Chapter A1**

# **Flexible Pipe Systems**

*Author: 4Subsea*

## A1.1 Introduction

The primary objectives of this Chapter are to present:

- State of the art overview of flexible pipe systems in use today
- Flexible pipe design aspects
- Flexible riser system experience and guidance
- Flexible flowline experience and guidance
- Installation considerations and experience

Items and recommendations addressed in [API 17B, 2008] and [API 17J, 2008] are not covered in any detail in this document, where it is relevant, supplementary information and cross references are given.

## A1.2 Flexible Pipe Systems

The chapter will provide the background for understanding the design challenges that are specific to the flexible pipe systems. The scope of the present discussion is mainly related to systems in water. Above water applications like topside jumpers are not discussed in detail.

A flexible pipe is constructed using a polymeric sealing material that contains the bore fluid, multiple helical armoring layers that provide the required strength, and a polymer outer sheath that prevents seawater from interacting with the armor wires. The construction enables design of pipes with a lower allowable bending radius compared to homogeneous pipes with the same pressure capacity (steel pipes typically require 25 times higher bend radius).

There are two basic reasons for using flexible pipes instead of steel pipes:

1. The compliant structure allows for permanent connection between a floating support vessel with large motions and subsea installations
2. Transport and installation is significantly simplified due to the possibility for prefabrication in long lengths stored on limited sized reels and ease of handling

Reeling is also possible with steel pipes. However, the reeling process involves plastic yielding and ovalization of the pipe, and the requirements to the handling equipment are high. Flexible riser systems have become a standard solution for permanent connection of subsea systems to floating vessels. Alternatives such as Steel Catenary Risers (SCR) may replace flexibles in some applications like deep water riser systems for TLPs and Spar buoys, and floaters with particularly favorable motions in deep waters.

In addition to dynamic flexible risers used to connect subsea installation with top side facilities, flexible pipe are used as flowlines and jumpers connecting subsea equipment. Use of flexible pipes subsea enables routing in crowded subsea layouts and reduces the installation cost. This is covered in more detail in Section A1.4. Some illustrations and short descriptions of the components included in a flexible pipe system are shown in Figure A1.1 , Figure A1.2, Table A1.1 and A1.2.

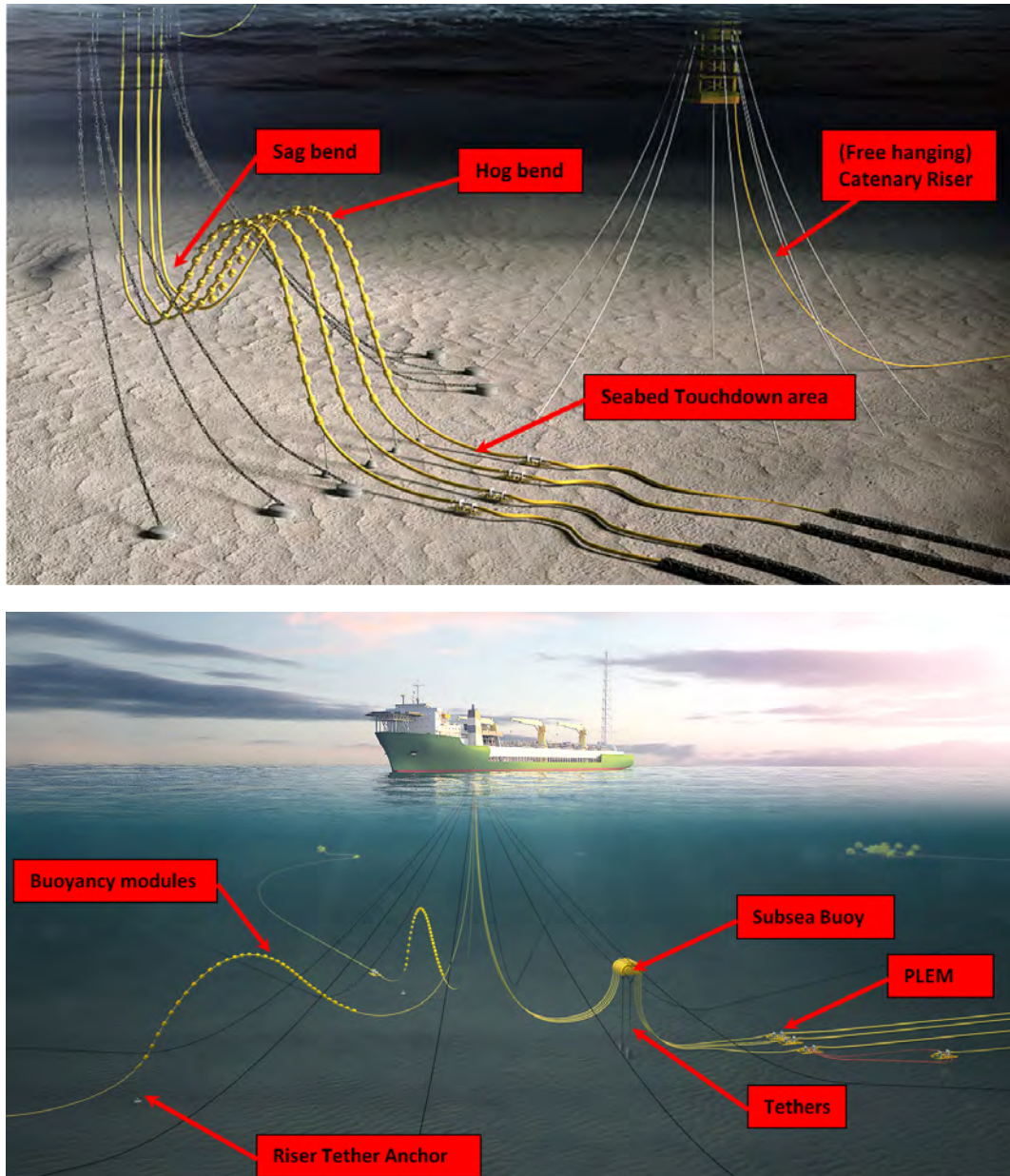


Figure A1.1: Typical flexible riser system and definitions, courtesy of 4subsea

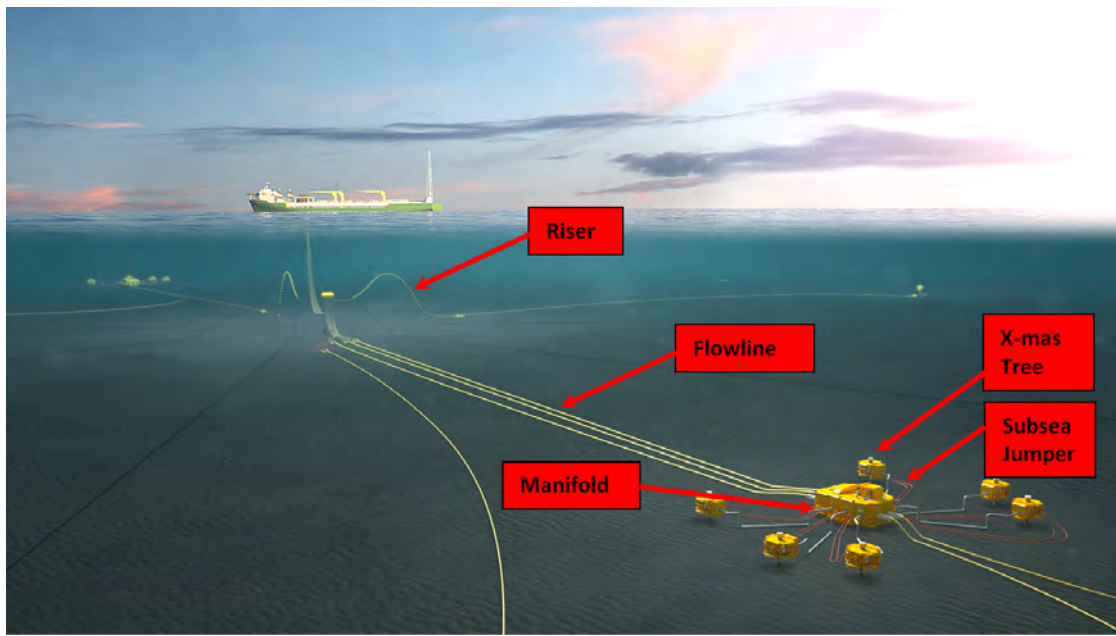


Figure A1.2: Flexible pipe flowline and riser system examples, courtesy of 4subsea

Table A1.1: Common flexible pipe distinctions

Name	Description
Flowline	Pipe transporting fluid over large distances, that is primarily subject to static loads
Jumper	Short length of flexible pipe transporting fluid subsea or topside
Riser	Pipe transporting fluid between subsea structure and topside structure, that is primarily subject to dynamic loads

Table A1.2: Flexible pipe system components

Component	Function
Annulus Ventilation System	<b>To ventilate annulus gases.</b> Gas will permeate slowly from the bore of the pipe into the annulus between the inner pressure sheath and the outer sheath. Unless the gas is ventilated, the pressure will build up in the annulus until the outer sheath bursts and exposes the armor wires to the external environment.
Bellmouth	A cylindrical section with increasing radius used at the exit of I/J-tubes. Used to support the pipe and avoid over-bending.
Bend restrictors	Metal or polymer interlocking rings that restrict minimum bending radius over a small length section. Normally only used in static applications, commonly used subsea.
Bend stiffeners	Tapered external polymer structure that gradually increases in radius and bending stiffness over a small length section. Common at pipe ends in dynamic applications.
Buoyancy modules and ballast modules	Polymer foam modules that are clamped to the riser to provide buoyancy or ballast. Used to set up riser configuration to absorb floater movements and lower topside hang-off tension.
Connectors	Connector systems are fastened to the pipe ends and are used to lock the pipe to topside and subsea structures.
I/J-tube	Large diameter steel pipe fixed to the platform that shields the flexible riser from waves and current.
I/J-tube seals	Seals around the flexible riser at the I/J-tube exit to avoid sea water circulation inside I/J-tube.
Instrumentation	Sensors and measurements used for the system. E.g. flow rate, pressure and temperature which are normally monitored both topside and subsea. Subsea instrumentation signals are normally sent via an umbilical to the main control room topside.
Subsea Manifolds	A large subsea structure that combines the flow from multiple pipes into one. Often used to gather the flow from separate wells into one flowline that leads to the platform.
Mechanical protection and fire protection	Extra outer sheath on risers close to topside and external structure covering end fitting.
Mid-Water Arch (MWA)	Large subsea structure used to control riser hog bend positions. The hog bend of several risers are clamped to the top of the MWA which allows a large number of risers to pass in a narrow sector without high-energy interference problems.
Piggy back clamps	Clamps that connect a small diameter riser to a larger diameter riser at regular intervals to align riser configuration to each other.
PLEM/ PLET	Pipe Line End Manifold/Termination are subsea structures used as connection points between pipes or pipe and structures.
Pull-in heads/installation aids	Tools/items that are used to provide connection points for winches/ROVs/Cranes or to manipulate the shape of the flexible pipe during installation.
Repair clamps	Used to seal off outer sheath defects that allow oxygen or seawater to come into contact with armor wires.
Riser base	Subsea structure that connects the riser to a subsea structure e.g. flowline.
Rock dumps	Rock that has been dumped over a flexible pipe to provide trawl protection and prevent upheaval buckling.

Component	Function
SSIV	The SubSea Isolation Valve is a subsea structure that allows for shutting down a part of the flow circuit. The valves are operated via umbilicals.
Subsea buoys	Large subsea buoy anchored by tethers. The hog bend of several risers are clamped to the top of the buoy which allows a large number of risers to pass in a narrow sector without high-energy interference problems.
Tether Anchor Base	Subsea structure that anchors tethers used in riser configurations.
Tether Anchor System	A tether connecting a clamp on the riser to a tether anchor base Used to limit the riser movement.
Tethers	Fiber or steel wire rope used to hold clamps or buoys in place.
Trawl protection covers	Subsea protection covers that are placed over flowlines to protect them from being damaged by fishing trawls or dropped objects.
Trenches	Trenches are used to lower the pipe below the seabed, usually as a measure to provide trawl protection.
Turret	Structure on weather-waning floating production units (FPSO) that remains fixed when the vessel rotates. All risers on weather-waning FPSOs are connected through a turret. Some turrets can be disconnected and will remain floating at a certain depth until they are retrieved and re-connected.
Umbilical	A flexible pipe consisting of several smaller hydraulics and/or electric signal lines. Umbilicals are used to operate subsea valves, compressors and other subsea functions. Umbilicals transmit the pressure and temperature instrument data.
X-mas tree	A subsea structure that is placed on top of each well to control the flow through a set of valves and instruments.

## A1.3 Flexible Pipe Design

As a minimum, the flexible pipe consists of a flexible pipe section and two end fittings. Bending stiffeners or bend restrictors are often used at the end fitting to protect the pipe from excessive bending in the transition between the pipe and the stiff end fitting. The key considerations for designing a flexible pipe are outlined in the following sections.

### A1.3.1 Design stages

The main design stages for flexible pipe systems are as follows, [API 17B, 2008]:

- Stage 1 – Material selection
- Stage 2 – Cross-section configuration design
- Stage 3 – System configuration design
- Stage 4 – Dynamic analysis and design
- Stage 5 – Detail and service life design
- Stage 6 – Installation design

In Stage 1, the pipe material selection is made based on internal environment (transported fluid), functional requirements, and material options. [API 17B, 2008] (Clause 6) contains guidelines for material selection. Note, only a limited number of materials are covered by the

design standards used for flexible pipes. Use of new materials requires qualification. The purchaser must be aware of the limitations for flexible pipes and the need for qualification if the planned operation is outside the envelope of qualified products, e.g. very high temperature.

In Stage 2, the cross-section configuration and dimensions are selected based on the pipe's functional requirements. Pipe dimensions are often specified by the purchaser. Cross-section design calculations and checks are typically carried out by the manufacturer using proprietary software. In order for the manufacturer to supply pipes according to [API 17J, 2008] or [API 17K, 2005] the design methodology including software validation shall be verified by an independent third party.

Stage 3 involves selection of the system configuration, and is often partly or fully performed by the purchaser.

For all flexible pipe systems the field layout will give boundaries for the system configuration, e.g. spacing between mooring lines will limit the number of risers and flowlines in each mooring sector, drill rig mooring pattern will limit flowline routing, flexible risers are normally placed inside a zone with restricted access etc.

Interface description is of crucial importance and interface requirements should be agreed on as early as possible.

For flowlines stage 3 involves protection design, e.g. no protection, trenching or rock dump, routing, subsea interfaces including tie-ins etc.

For riser stage 3 typically involve selection of configuration, definition of riser base position, definition of riser hang off and platform interface etc.

Stage 4 involves the more detailed design of the system. Stage 4 is normally performed by the manufacturer.

For risers this task typically considers the dynamic response of the riser, subject to a series of imposed loading conditions derived from the functional, environmental, and accidental loads on the system. Issues to be addressed include possible interference with other system components, riser tension and/or compression loads throughout the riser, minimum bending radius (MBR), the top departure angle and interface loads (described by tension-angle or moment and shear force).

For flowlines this stage includes preliminary analyses of installation, thermal insulation, upheaval buckling, seabed stability, tie in, system behavior during hydrotesting, etc.

Stage 5 includes service life analysis as it applies to the pipe and components.

Stage 6 completes the design process and involves the selection and design of the installation system, including vessel, equipment, methodology, and environment conditions. Stage 6 requires detailed global and local analyses to confirm the feasibility of the selected installation system. This stage is in many cases critical for the pipe design, and it is therefore recommended that preliminary installation analyses be performed at an early stage in the design process. Installation is important for both risers and flowlines e.g. weather limitation, vessel selection, type of lay spread, crushing loads are a potential issue for both risers and flowlines from caterpillars etc.

Further details and recommendations for riser and flowline systems are included in section 4 and 5, respectively.

### A1.3.2 Standards and Recommended Practices

All aspects of flexible pipe design and technology, from functional definition to installation, are addressed in the standards and recommended practices

- [API 17J, 2008] (Non-bonded flexible pipe), equivalent to [ISO 13628-2, 2006]
- [API 17K, 2005] (Bonded flexible pipe), equivalent to [ISO 13628-10, 2005]
- [API 17B, 2008] (Recommended practice for flexible pipe), equivalent to [ISO 13628-11, 2007]

Ancillary components for flexible pipe systems are described in detail in [API 17L1, 2013] and [API 17L2, 2013]. For more information on any design topic, refer to these standards for details.

Supplementary standards for definition of hydrodynamic loads, sour service qualification, integrity management etc. is required when designing a flexible pipe system, typically from sources like:

- DNV
- NORSO
- ASME
- NACE
- Company specific standards.

Use of supplementary standards is to some extent covered in other sections of this handbook.

### A1.3.3 Flexible Pipe Cross-Section Components

Each layer of the flexible pipe has a specific design function as shown in Table A1.4. The table shows the key components of a flexible pipe wall structure. The area between the internal pressure sheath and the outer sheath is defined as the annulus of a flexible pipe. Depending on whether the pipe is built with or without carcass, the pipe is classified as a rough or smooth bore pipe. Pipes without carcass usually have an intermediate sheath layer extruded onto the pressure armor to withstand external seawater pressure in case of outer sheath breaches.

Table A1.3: Smooth and rough bore definitions

Definition	Description
Smooth bore	Flexible pipe without carcass, usually designed with a sealed intermediate sheath.
Rough bore	Flexible pipe with carcass. No sealed intermediate sheath required.

Table A1.4: Flexible pipe Components

Layer	Function
Carcass	Provides Internal Pressure Sheath with collapse resistance.
Internal Pressure Sheath	Contains process fluid within pipe bore.
Pressure Armor Wire	Provides radial compression resistance. Partially supports internal sheath and contains internal pressure loads.

Intermediate sheath	Provides Internal Pressure Sheath with collapse resistance in case of outer sheath breach for smooth-bore pipes.
Tensile Armor Wires	Provides tensile strength and contain end-cap loads. Partially supports containment of internal pressure loads.
Anti-friction layers	Tape or thin extruded polymer that prevents metal-metal contact.
Anti-buckling layer	High strength fiber composite that prevents radial or lateral buckling.
Insulation	Provides thermal insulation for bore fluid if necessary.
Outer Sheath	Prevents ingress of seawater and oxygen to the annulus.

### A1.3.4 Flexible Pipe Design Considerations

#### A1.3.4.1 Bonded and non-bonded structures

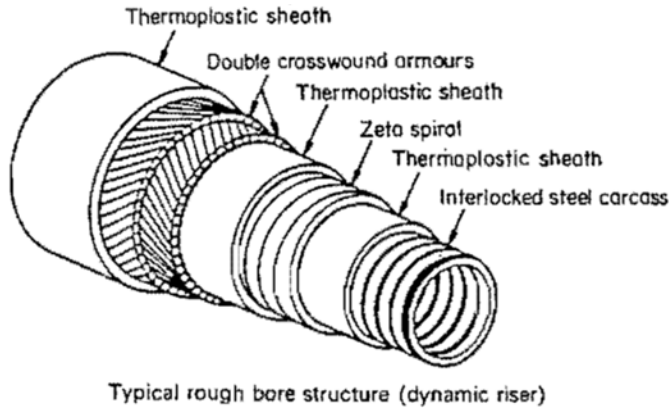
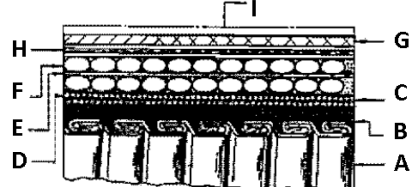


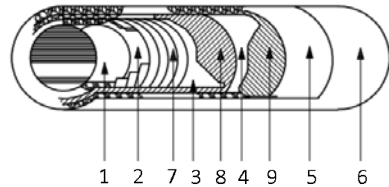
Figure A1.3: Typical non-bonded flexible pipe cross-section

Cross section of armalink - armaline



- A. Stainless steel, strip wound, interlock tube
- B. Duralon elastomeric liner
- C. Textile, anti-extrusion layer
- D. Hydrodraulic transfer layer
- E. Clad steel reinforcement
- F. Anti-chaffing layer
- G. Abrasion resistance cover
- H. Fire resisting layer (optional)
- I. Armouring

(1) Cross section of Dunlop pipe



Sketch of a typical PAGUAG flexible offshore pipe cutaway showing a typical composition.

Especially developed elastomer compounds (NBR and CR based) are used for the inner liner (1), the adhesion layers (2, 3, 4, 5) and the cover (6). The main functions of these layers are to make the pipe leakproof, corrosion, abrasion and fatigue resistant and still maintaining high flexibility by cushioning and bonding all reinforcement materials to form a high-integrity unit.

A helically-wound wire (7) is normally applied mainly to increase both the hydrostatic pressure resistance (for sub-sea installations) and/or the tensile strength capacity of the pipe. Brass coated steel cord wires (8, 9) provide the internal pressure capability of the flexibles.

(2) Cross section of Pag-O-Flex pipe

Figure A1.4: Bonded flexible pipe cross-sections (Illustration is old and cover design proposed for high pressure applications. For bonded flexibles in other applications, see [PSA Norway, 2009]).

Two different types of pipe construction are available as shown in Figure A1.3 and Figure A1.4:

- Non-bonded structures where each component makes up a cylindrical layer that is able to slide relative to the other layers
- Bonded structures where the armor elements and the pressure containing components are molded into a single structure. All components are glued together as an elastic composite material

The bonded structure is primarily used for short length jumpers in high dynamic applications. Non-bonded structures are used in most applications, as shown tabulated in Table A1.5 and

Table A1.6.

Table A1.5: Typical limitations

Item	Bonded flexible pipes [API 17K, 2005]	Non-bonded flexible pipes [API 17J, 2008]	Comment
Length	12 - 100m	Up to several kilometers	Manuli is the only supplier capable of making long length bonded hose for some specific services.
Transported fluid	Normally not used for high pressure gas service or high temperature service	High Pressures Temperature up to 120°C	Non-bonded pipes are normally preferred for service with gas, unstable crude or high temperature fluids
Internal Diameter	Up to 24 inches	Up to 19 inches	Large bore bonded pipes normally delivered in 12m lengths.
Bending flexibility	Excellent	Good	Bonded hoses are often preferred for applications requiring high bending.

Table A1.6: Typical applications for bonded and non-bonded flexible pipes

Application	Bonded flexible pipe	Non-bonded flexible pipes	Examples
Flowline	Normally not	Yes	Subsea line from satellite wells to manifold or riser base
Subsea jumper	Normally not	Yes	Short line connecting subsea units, e.g. test and service lines between individual wells
Flexible riser	In some cases	Yes	Lines from a subsea installation to a floating platform.  Flexible risers may in addition be used inside guide tubes to ease installation, in this case the application may be considered static.
Oil offloading	Yes, both reel systems and stationary systems	Only in stationary system like loading buoys	For oil offloading it is often required with dimensions exceeding the diameter limit for non-bonded pipes.  Reeling based offloading systems are normally designed with bonded hose due to the low bending stiffness and the small permissible bending radius for bonded hoses
Jumpers	Yes	Yes	Drilling applications (not included in [API 17K, 2005] and [API 17J, 2008])  Turret jumpers on FPSO Topside jumpers on TLPs Long jumpers connection platforms

#### A1.3.4.2 Static or Dynamic Applications

Flowlines and subsea jumpers are static configurations that will normally experience the largest loads during testing, reeling and installation. Non-bonded flexible risers are designed to be fatigue resistant by use of anti-friction tape layers and fatigue resistant materials.

Bonded offloading hoses and other short jumpers are designed to withstand large dynamic forces from frequent handling operations.

A set of design load cases are defined in the standards for a flexible riser system that covers all events which may influence the component design or system operation, including installation, operation, extreme and accidental events. Further details may be found in [API 17B, 2008].

#### A1.3.4.3 Transported fluid

The fluid that is to be transported influences the design and must be taken into consideration at a very early stage. The key considerations that have to be made are listed in Table A1.7.

Table A1.7: Transported fluid considerations

Issue	Comment
Corrosive elements	The carcass of the flexible pipe is directly exposed to the fluid and the material must be selected accordingly. AISI 304, AISI 316 or Super Duplex materials are commonly used for flexibles. Use of other materials is often limited by the manufacturing process which involves cold forming.
Fluid Density	The design of flexible pipe systems should consider the effect of variations in internal fluid density over the life of the project, particularly for riser systems where a change in fluid density can change the shape of the riser configuration.
Gas diffusion	<p>Transported fluids containing gas, e.g. oil production and gas injection service will give gas diffusion through the polymeric pressure barrier. For non-bonded flexible pipes it is required to vent the annulus in the pipe wall to avoid pressure build up and to consider the diffused gas when selecting armour wire material. Due to the pressure build up in the pipe wall a rough bore design with carcass to prevent collapse of the liner is normally used.</p> <p>For bonded hose the elastomeric material must have sufficient blistering resistance during rapid decompression of the pipe. This is challenging and bonded flexible pipes with elastomeric liner are seldom used in gas applications.</p> <p>See also Section A1.3.4.5</p>

Issue	Comment
Gas Flow Induced Vibrations	<p>Gas flow in rough bore pipes has resulted in high frequency vibrations. Presently the main challenge has been for gas export systems where export limitations, unacceptable noise and unacceptable vibration level has been experienced. Similar noise in other rough bore flexibles transporting gas, e.g. gas injection, has also been observed but generally speaking with less critical vibrations</p> <p>Experience is that mitigation of gas induced vibrations may be challenging, typical mitigating actions to be considered are:</p> <ul style="list-style-type: none"> <li>▪ Replace rough bore riser with smooth bore riser</li> <li>▪ Limit gas flow</li> <li>▪ Introduce silencers (dampening of acoustic noise)</li> </ul>
Internal Friction	The friction parameter varies significantly between smooth and rough bore pipes because of the carcass construction in a rough bore pipe. The friction is strongly influenced by the carcass characteristics, such as ID and profile dimensions
Design and Operating pressure	The armour wire dimensions are normally selected primarily based on pressure requirements. Design pressure conditions are normally governing for max stress in wires and operating pressure has major influence on fatigue as the interlayer contact pressure increase with pressure
Design and Operating temperature	<p>The design and operating temperature is normally the governing criterion for selection of polymer material. There are in addition other parameters which must be considered when selecting polymer, e.g. pH, gas, depressurisation rate etc. The polymer liner materials considered in [API 17J, 2008] are:</p> <ul style="list-style-type: none"> <li>▪ PE (including XLPE)</li> <li>▪ PA 11</li> <li>▪ PVDF</li> </ul> <p>Use of other materials requires qualification</p>
Sand Production	The fluid velocity is important, particularly if abrasive materials such as sand are present in the produced fluids this can result in wear of the pipe's internal layer
Slug Flow	In the case of two phase flow, the effect of slug induced vibration should be considered
Sour or sweet service	This is normally governing for selection of steel material

#### A1.3.4.4 Thermal insulation

Thermal insulation may be required to retain the desired temperature profile. Rock-dumping and trenching of flowlines influence the thermal insulation of the pipe and must be included in design considerations.

#### A1.3.4.5 Gas venting – non-bonded pipe

Gas will permeate through the internal pressure sheath and into the annulus space between the armour wires. Unless the gas is allowed to ventilate, the pressure will build up and eventually the outer sheath will burst. The outer sheath is supported by the external hydrostatic pressure from the seawater, thus most of such outer sheath damages occur above, or close

Table A1.8: Amount of gas permeation normally seen for typical transported fluids

Transported fluid	Gas permeation rates	Comment
Water	None	
Reinjection of Produced Water	Low	May contain gas and may have high temperature
Gas (Export, Injection, Lift)	High	Dry gas at high temperatures leads to the highest permeation rates
Crude Oil (export)	None/low	Exported oil that has been gas scrubbed usually has very low gas permeation
Production Oil (from wells)	None-Moderate	Depends on temperature and amount of gas in the well

to the waterline. The outer sheath burst can also appear in areas of the outer sheath that have been weakened during fabrication, installation or by cuts during operation.

Outer sheath bursts have been seen from pressure build ups of 5-10 bar in the annulus, up to 20 bar for cross-sections with double outer sheaths. Most flexible pipe systems have either a Gas Relief Valve (GRV) that opens at set differential pressure, or a gas ventilation system topside, neither of which should be blocked. Flowlines and subsea jumpers are usually equipped with GRVs at both end fittings, while risers should have a topside gas ventilation system.

The transported fluid influences the rate of gas permeation, and a general overview of the permeation rates are shown in Table A1.8.

#### A1.3.4.6 Fire resistance

Extra fire resistance covers may be required, which is usually added as an extra protective cover on the outer sheath of the pipe and end fitting.

#### A1.3.4.7 Pigging and Through Flowline (TFL) requirements

Flexible pipes can be designed to be pigged with some restrictions on pigging types. Scraper pigs are not suitable for flexible pipes and brush pigs are not suitable for smooth bore pipes. If pigging is desirable, the pipe system should be designed with either a return loop or a subsea pig receiver.

Table A1.9: Pigging restrictions for flexible pipes

Riser type	Pigging equipment
Rough bore	Brush, foam, polyurethane
Smooth bore	Foam, polyurethane

If TFL service is required, the innermost layer should be constructed such that it will not impede or be damaged by the passage of TFL tools. Reference is given to [API 17C, 2010] for further description and design codes.

#### A1.3.4.8 Corrosion protection

The flexible pipe system must be designed to protect the system components to corrosion, and the common protection methods are listed below: Be aware of protection limitations due to shielding.

1. coating
2. application of corrosion inhibitors
3. application of special metallic materials or cladding
4. specification of corrosion allowance
5. cathodic protection

The flexible pipe components are protected by the outer sheath and cathodic protection through anodes placed on the end fitting. The anodes will start to protect the armor wires in case of outer sheath breaches.

Splash zone requires extra attention due to limited protection of exposed steel in areas that are not permanent submerged. With regards to armor wire corrosion, any hole in the outer sheath within the splash zone is generally regarded as the worst case scenario due to lack of continuous protection and high access to moisture and oxygen.

#### A1.3.4.9 Piggy back lines

A flexible line is a piggy back line if it is clamped to another flexible or steel pipe. The line should be protected from steel scuffing and potentially high temperature transfers from the line that it is clamped to. Several design parameters must be considered:

1. Hydrodynamic interaction, including shielding, solidification, hydroelastic vibrations, lift, and marine growth
2. Seabed interaction, particular attention to touch down area for risers and expansion and tie in areas for flowlines
3. Relative motion between the lines
4. Relative changes in length between the two lines (particularly due to different pressure and/or thermal expansion coefficients and axial stiffness between flexible and steel lines)
5. Clamp loads
6. Loads and wear of the flexible pipe
7. Creep and long-term degradation of pipe and clamp materials
8. Internal pressure, tension, external pressure, bending and torsion-induced change in cross-section geometry of the pipe
9. Trenching and flowline protection
10. Installation
11. Interface design, important for both riser systems and flowline systems

Table A1.10: Umbilicals, ISU, IPB, Multibore

Product	Description
Umbilical	Several function bundled into one line, typically hydraulic hoses, service hoses, signal cables, fiber optic cables. External armouring layers are often used to protect the umbilical core. Umbilicals are normally not manufactured by flexible pipe suppliers
Steel tube umbilicals	Umbilical with hoses replaced with steel tubes. Steel tubes give better performance than hoses in some applications. External armouring layers are only used when required, e.g. riser sections Steel tube umbilicals are normally not manufactured by flexible pipe suppliers
ISU	Integrated Service Umbilical. A flexible pipe used for service function in the center, typically 2". Umbilical functions surrounding the flexible pipe and armoring outside this. Manufactured by flexible pipe suppliers.
IPB	Integrated Production Bundle. A flexible pipe used for production fluid in the center, typically 6". Umbilical functions surrounding the flexible pipe and armoring outside this. Manufactured by flexible pipe suppliers.
Multibore	Several flexible pipes bundles together. External armouring normally used to protect and control the bundle.

#### A1.3.4.10 Umbilicals, ISU, IPB, Multibore, etc.

Flexible pipes, hydraulic hoses, steel tubes, electrical cables and fiber optic cables may be bundled. Several products are described in Table [A1.10](#)

Items to consider when designing a flexible pipe system including such lines are:

- More frequent maintenance and replacement may be required for such lines. Use of experienced manufacturers is hence normally preferred
- Umbilicals requirements, in particular steel tube umbilicals may influence the entire system design and should be addressed in the initial phases of system design
- Use of special bundled construction may have only one supplier

## A1.4 Flexible Risers

### A1.4.1 Introduction

The section of a flexible pipe system that connects the production unit to the first subsea structure is called the riser section. This section experiences dynamic loading from the vessel (production unit) motions and environmental loads, and must be designed considering loads on all components. The riser system may include connectors, end fitting flanges, buoyancy modules, subsea buoys, tethers, PLEMs and other components described in Section [A1.2](#).

The choice of what components are required relies on the selection of the riser configuration, environmental conditions and relevant standards.

## A1.4.2 Riser configurations

### A1.4.2.1 General

This section addresses flexible riser configurations presently in use and describes pros and cons associated with the various alternatives. Several of the configurations include a seabed resting part. This part of the flexible riser system may have similar challenges as flexible flowlines, ref. Section A1.5.2.

The selection of riser system configuration is based on water depth, vessel movements, environmental conditions, number of risers and interference issues. The simplest and cheapest configuration is a free hanging catenary configuration consisting of a flexible pipe only and where the subsea part of the flexible pipe is laying on the seabed and the upper end is connected to the vessel. This riser configuration is sensitive to compression loads and fatigue at the Touchdown Point (TDP) and is only feasible in some applications. Measures to compensate for the limitations in free hanging configuration by e.g. inclusion of a buoyant section are adding complexity to the flexible riser system. The most complex solutions involve large structures on the seabed and challenging installation.

Table A1.11: Riser Configuration Summary

Configuration	Complexity	Typical Applications
Dynamic Jumper	Low	- Connections between platforms/vessels/subsea tower/buoys
Free hanging catenary	Low	- Commonly used offshore Brazil and whenever feasible - Fixed platforms (often with J-tube) - TLPs and Floaters with low/moderate motions - Benign wave climate - Deep water.
Lazy Wave	Moderate	- Used in harsh environment and in systems where top tension and TDP compression must be reduced - Moderate and deep water - Configuration may be used for floater with moderate to large motions - Few seabed area restrictions - Riser motion is relatively large such that interference with neighbor structures like mooring lines may be challenging - Large riser movements on the seabed require spacing to subsea equipment and wide riser corridor - Configuration is sensitive to change in weight due to density variation of internal fluid, marine growth, water absorption in buoyancy material etc.

Configuration	Complexity	Typical Applications
Tethered wave	Moderate	<ul style="list-style-type: none"> <li>- Moderate/large motions</li> <li>- Frequently used on Norwegian sector, in particular where individual risers are preferred in a relatively crowded subsea layout</li> <li>- Shallow to deep water</li> <li>- Configuration may be used for floater with moderate to large motion</li> <li>- Riser motion is relatively large such that interference with neighbour structures like mooring lines may be challenging</li> <li>- Moderate riser motion on seabed which enable narrow corridors</li> <li>- Riser anchor with tether in the touch down area require detail attention to avoid over bending of riser and reliable long term performance</li> <li>- Configuration has moderate sensitivity to change in internal contents density</li> </ul>
Steep Wave	Moderate	<ul style="list-style-type: none"> <li>- Moderate / large motions</li> <li>- Similar to tethered wave but seabed termination is directly on a subsea structure, typically with a bend stiffener</li> </ul>
Chinese lantern	High	<ul style="list-style-type: none"> <li>- Offloading buoys</li> <li>- Configuration is unstable and reliable long term performance is difficult to achieve</li> <li>- Not common</li> </ul>
Lazy S	High	<ul style="list-style-type: none"> <li>- Used instead of lazy wave configurations when several risers shall be installed in the same corridor or whenever buoyancy element are not preferred</li> </ul>
Steep S	High	<ul style="list-style-type: none"> <li>- Moderate/large motions</li> <li>- Interference anticipated</li> <li>- Few number of risers</li> <li>- TDP compression expected</li> <li>- Large variation in riser size and content</li> <li>- Limited seabed area available</li> </ul>
Vertical tower and jumper	Very High	<ul style="list-style-type: none"> <li>- Deep water projects</li> <li>- conditions</li> <li>- High thermal insulation requirements</li> </ul>
Subsea Support	Very High	<ul style="list-style-type: none"> <li>- Moderate/large motions</li> <li>- Interference anticipated</li> <li>- High number of risers</li> <li>- Large variation in riser size and content</li> </ul>

#### A1.4.2.2 Free hanging catenary

A free hanging catenary (see Figure A1.5) is the simplest configuration for a flexible riser. It requires minimal subsea infrastructure, is relatively straight-forward and is the cheapest to install. It is commonly used on floaters and TLPs in areas with low to moderate dynamic vessel motion and on fixed platforms. The dynamic motion of the vessel is transferred to the TDP, which may result in pipe compression for the downwards movements of the vessel. This compression may lead to buckling and 'bird caging' of the armour wires.

For fixed platforms, the flexible riser may be pulled through a J-tube to shield the pipe from environmental loads.

Advantages include:

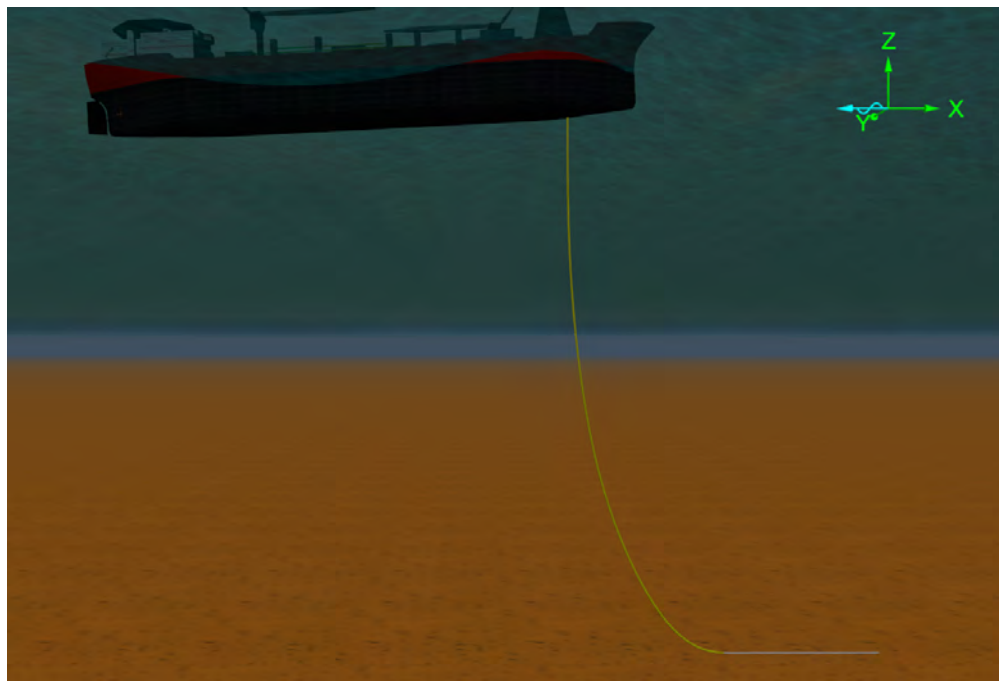


Figure A1.5: Free hanging riser configuration, courtesy of Orcina Ltd

- Simple configuration
- Simple installation
- Limited sensitivity to fluid density (apart from hang-off load variation)

Table A1.12: Free hanging catenary design challenges

Water depth	Challenges	Comment
Shallow	Over bending near TDP Motions Compression near TDP Over bending near hang-off	TDP experiences compression for low to moderate vessel motion.
Moderate	Over bending near TDP Motions Compression near TDP	
Deep	Hang-off tension (static and dynamic) Over bending near TDP Compression near TDP	High hang-off tension.

#### A1.4.2.3 Lazy wave

The lazy wave configuration Figure A1.6 consists of a flexible riser fitted with buoyancy and optionally also weight modules along parts of the length. The configuration is designed to decouple the TDP motions from the vessel motion by introducing a hog bend, thus allowing larger vessel motion and the use of floaters in harsher climates. A horizontal hold-back arrangement may optionally be installed to restrain riser movement and reduce the effective tension in the seabed part of the riser.

The 'near' and 'far' position is often used to screen for suitable configurations. The 'near'

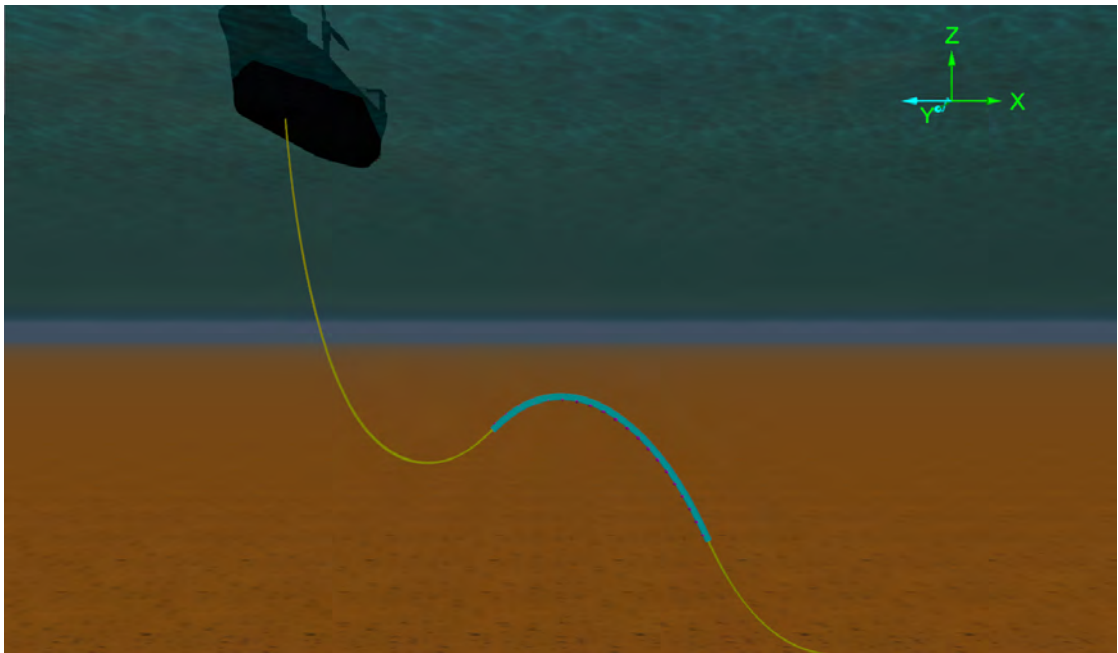


Figure A1.6: Lazy wave riser configuration, courtesy of Orcina Ltd

position refers to the minimum horizontal distance between riser ends, while the 'far' position refers to the maximum horizontal distance between riser ends. In the 'far' position, the riser hog and sag bends will straighten, and the riser length must be long enough to avoid a fully stretched configuration. In the 'near' position, the sag bend will lower towards the seabed and hog bend will rise towards the surface. The riser length must be sufficiently low to avoid excessive bending, hog bend contact vs. ship and sag bend contact vs. seabed.

The hog bend is also influenced by current and waves, thus interference challenges for these configurations are not uncommon. No interference is allowed between buoyancy module sections on neighbouring risers, and clashing energy has to be evaluated for any pipe-on-pipe collisions.

The hog bend movements are also affected by the level of marine growth, content density, water ingress in the buoyancy modules and loss of buoyancy modules. Risers placed next to each other will move more similarly if the OD/weight ratios are approximately the same, however, the riser stiffness will also affect the riser motions. Neighbouring risers with large outer diameter difference and content density variations are prone to experience interference in the upper catenary or buoyancy sections. Interference vs. anchor chains must also be checked. The configurations are likely to move significantly based on current alone.

Interference in the upper catenary is common for crowded hang offs such as for turrets. Shallow water applications in harsh environments are particularly challenging since the vessel motions are large compared to the water depth available for setting up a robust riser configuration. If the hang-off has large heave motions, the risers may in some instances be unable to move through the water at the same speed as the vessel, buckle out to the sides below the bend stiffener and over-bend. High hang-off angles will increase the likelihood of such buckling during large vessel motions. Typical hang-off angles are in the range 3-7 degrees for deep water applications and up to 17 degrees for shallow water applications.

Table A1.13: Lazy Wave design challenges

Water depth	Challenges	Comment
Shallow	Interference Over bending near hang-off Over bending near TDP Hog bend clashing into vessel in near conditions Over-pull in the far condition Sag bend interference with seabed Content density variation Loss of buoyancy	Designing a configuration with sufficient length to allow the vessel movements for the far conditions while not clashing with vessel or have seabed interference with sag bend in the near condition
Moderate	Interference Over bending near hang-off Over bending near TDP Content density variation Loss of buoyancy	
Deep	Interference Hang-off tension Over bending near hang-off Over bending near TDP Loss of buoyancy	

Advantages include:

- High floater offset tolerance
- Reduced top tension
- Reduced TDP loads
- Simple-moderate installation complexity

#### A1.4.2.4 Steep wave

The steep wave is a variation of the lazy wave configuration, where the riser is connected vertically to a riser base on the seabed. This allows for a more compact configuration with less interference problems, but puts a large upwards tension on the riser base, both during installation and operation. The installation process is more complex with either a vertical tie-in of the riser to the riser base or with deployment of the entire riser base. See Section [A1.5.5](#) for more details on installation.

Advantages include:

- High floater offset tolerance
- Moderate hog bend movement
- Reduced top tension
- Reduced TDP loads
- Moderately sensitive to content density variation

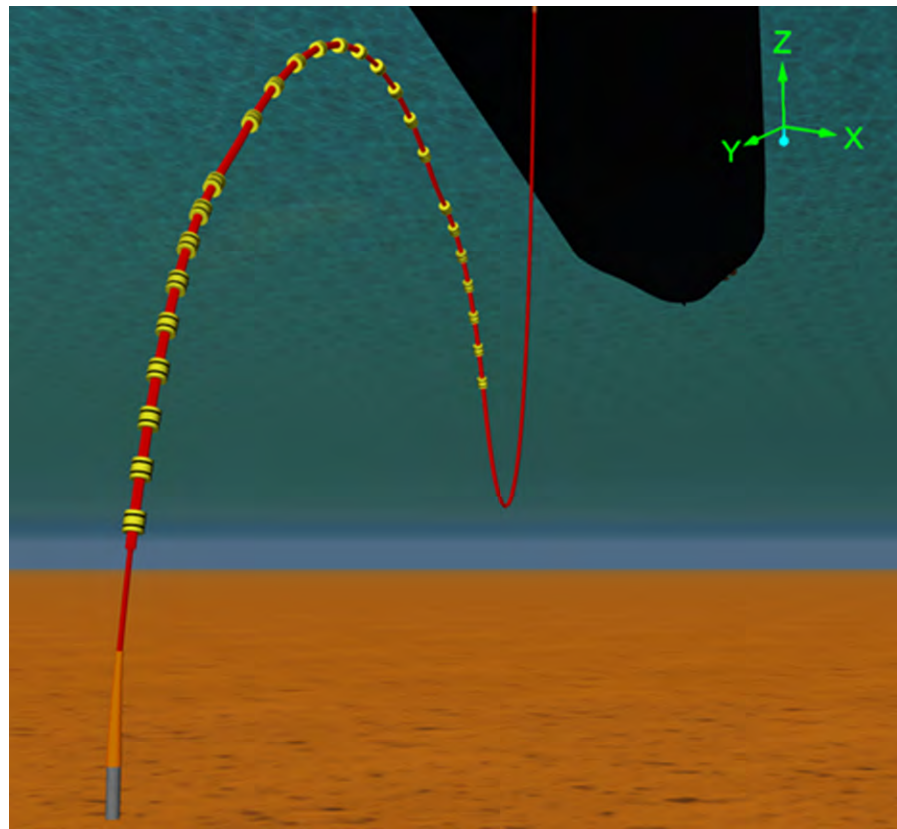


Figure A1.7: Steep wave configuration, courtesy of 4Subsea

Table A1.14: Steep wave design challenges

Water depth	Challenges	Comment
Shallow	Interference Over bending near hang-off Over bending near riser base Hog bend clashing into vessel in near conditions Over-pull in the far condition Loss of buoyancy High riser base uprooting tension High dynamic moments on riser base	The high upwards tension on the riser base requires a robust design of the subsea structure to avoid movement of the structure
Moderate	Interference Over bending near hang-off Over bending near riser base Loss of buoyancy High riser base uprooting tension	More complex than required in moderate environment
Deep	Interference Hang-off tension Over bending near hang-off Over bending near riser base High riser base uprooting tension	More complex than required in moderate environment

#### A1.4.2.5 Pliant and reverse pliant wave

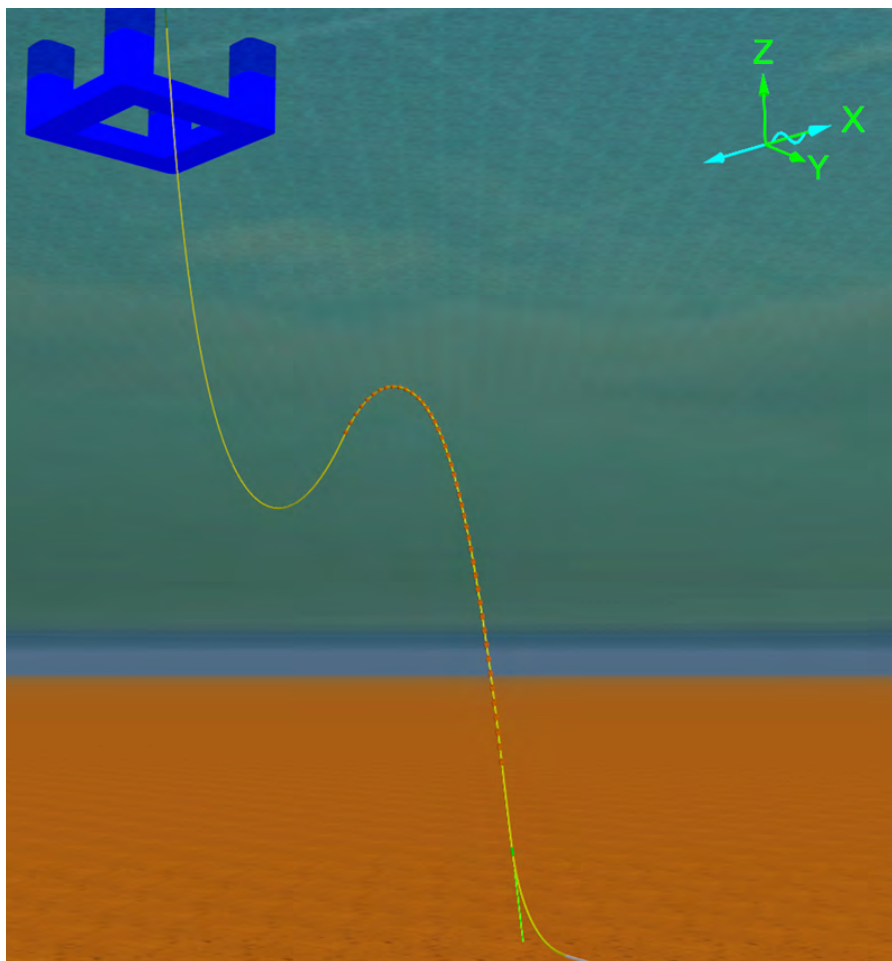


Figure A1.8: Reverse Pliant wave, courtesy of 4Subsea

The Pliant wave configuration is also a variation of the lazy wave, where the movements and tension in the TDP are controlled by a tether anchor connected to the riser above the TDP. The seabed section of a Pliant wave is tied back towards the platform, while the reverse pliant wave is routed away from the platform as for the lazy wave configuration. The pliant wave is used where the wells are located below the platform.

The configurations are also known as Tethered wave configurations.

Advantages include:

- High floater offset tolerance
- Moderate hog bend movement
- Reduced top tension
- Reduced TDP loads
- Moderately sensitive to content density variation

Table A1.15: Tethered Wave design challenges

Water depth	Challenges	Comment
Shallow	Interference Over bending near hang-off Over bending near TDP and clamp Hog bend clashing into vessel in near conditions Over-pull in the far conditions Content density variation Marine growth Loss of buoyancy Outer sheath abrasion in TDP Slack in tether	A slack tether may cause snatch tension loads in the riser when the tether is re-tensioned
Moderate	Interference Over bending near hang-off Over bending near riser base Content density variation Marine growth Loss of buoyancy High riser base uprooting tension	
Deep	Interference Hang-off tension Over bending near hang-off Over bending near riser base High riser base uprooting tension	More complex than required in moderate environment

#### A1.4.2.6 Lazy and Steep S - Subsea Buoy

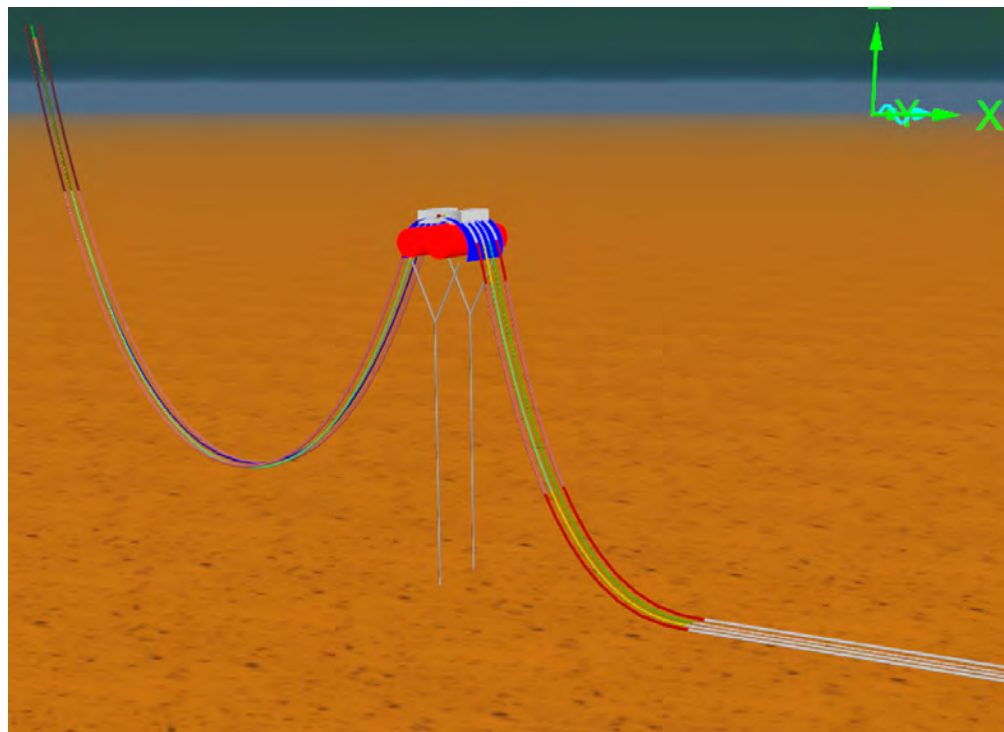


Figure A1.9: Lazy-S configuration, courtesy of 4Subsea.

Table A1.16: Lazy S design challenges

Water depth	Challenges	Comment
Shallow / moderate	Content variation for large bore risers Marine Growth Buoyancy loss Seabed contact Over-bending near hang-off Over-bending near buoy/MWA MWA clamp design Installation	Buoy stability and hydrodynamics.
Deep	As for Shallow and Moderate depths Hang-off tension	Buoy stability and hydrodynamics.

The anchored subsea buoy also known as a Mid Water Arch (MWA) is used to obtain the S-configurations. The advantage is that many risers can be run over the same subsea buoy with little or no interference. The interference that occurs is usually low energy clashing in the upper catenary section. Main challenges include buoy instability from the riser's weight and flooded buoyancy compartments which influence the hog bend height and potentially the stability. Adding new risers will significantly alter the buoy hydrodynamics.

The riser can be terminated vertically into a riser structure to create a Steep S or with weights or tethers to create the Lazy S configuration.

Advantages include:

- High floater offset tolerance.
- Compact layout.
- Allows a large number of risers in same sector.
- Large reduction in TDP dynamics.

#### A1.4.2.7 Lazy and Steep S - Riser Subsea Support (RSS)

The Riser Subsea Support (RSS) is a fixed subsea structure used to obtain the hog-sag sections in the same manner as the Subsea Buoy. The interference against the structure can be an issue, but there are no stability issues or variation in hog bend height.

Advantages include:

- High floater offset tolerance
- Compact layout
- Allows a large number of risers in same sector
- No instability issues
- Not sensitive to riser content variation

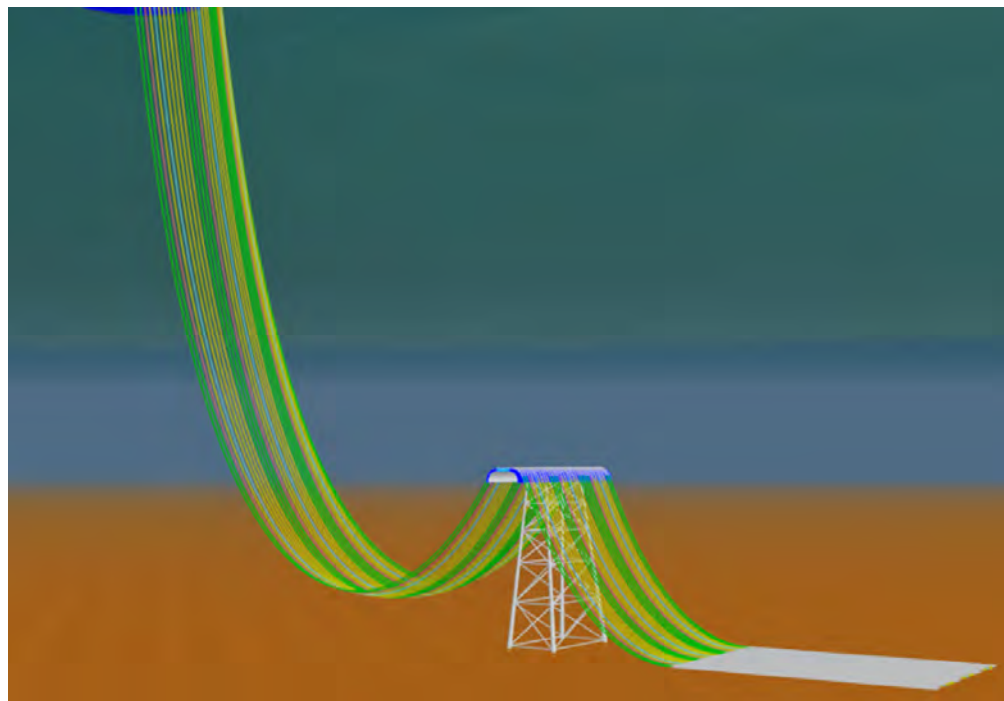


Figure A1.10: Lazy-S with RSS, courtesy of 4Subsea

Table A1.17: Lazy S design challenges

Water depth	Challenges	Comment
Shallow / Moderate	Interference between risers and structure Seabed contact Over-bending near hang-off Over-bending near buoy/MWA MWA clamp design Installation of a large RSS may be complex	
Deep	As for Shallow and moderate depths Hang-off tension	

#### A1.4.2.8 Hybrid systems Chinese lantern

A Chinese lantern configuration (see Figure A1.11) is a typical configuration of the offloading hoses on a CALM buoy. The hose has buoyancy modules attached and reinforced end connections to maintain reasonable tension in the system and avoid over bending near the ends.

Advantages include:

- Limited subsea space required
- Lower end moments than a lazy wave

For Chinese lantern design challenges, see Table A1.18.

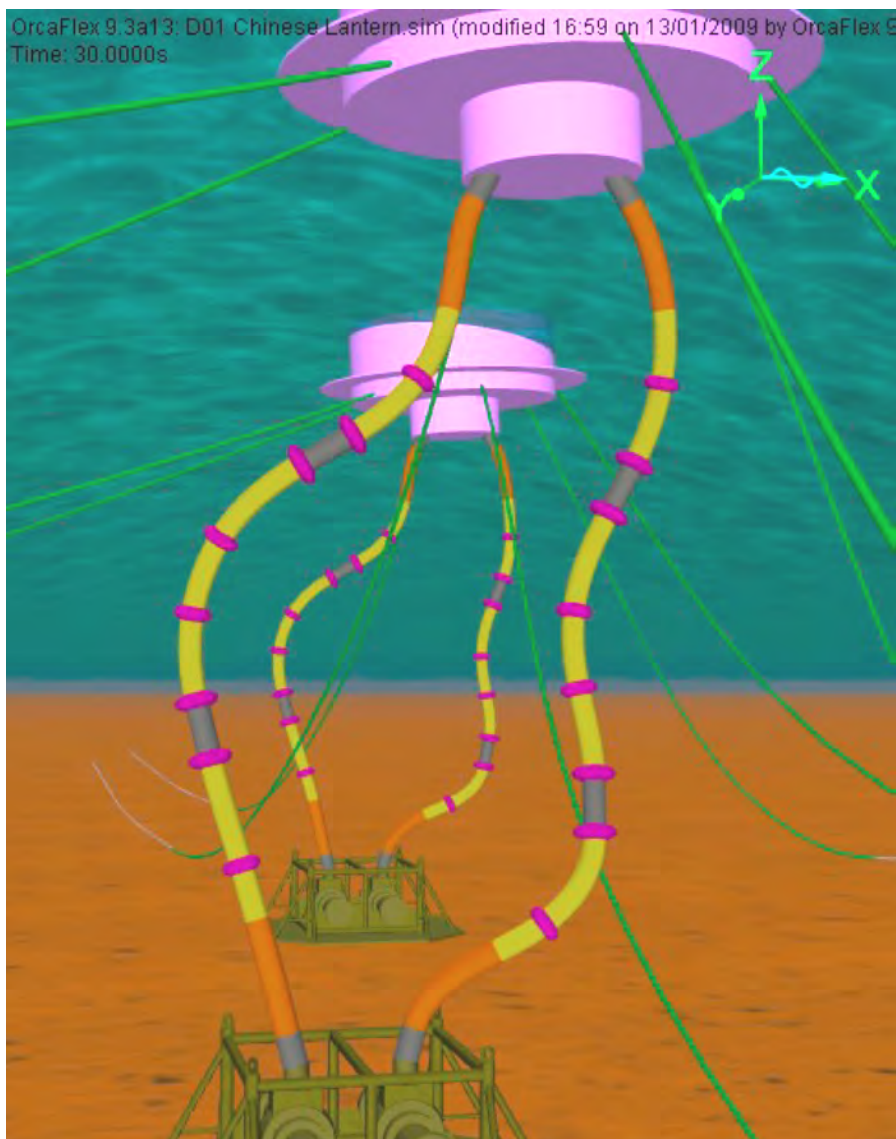


Figure A1.11: Chinese lantern from a CALM buoy to the seabed, courtesy of Orcina Ltd.

Table A1.18: Chinese lantern design challenges

Water depth	Challenges	Comment
Shallow / moderate	Interference between risers Over-bending	
Deep	As for Shallow and moderate depths Hang-off tension	

### A1.4.2.9 Vertical tower and jumper

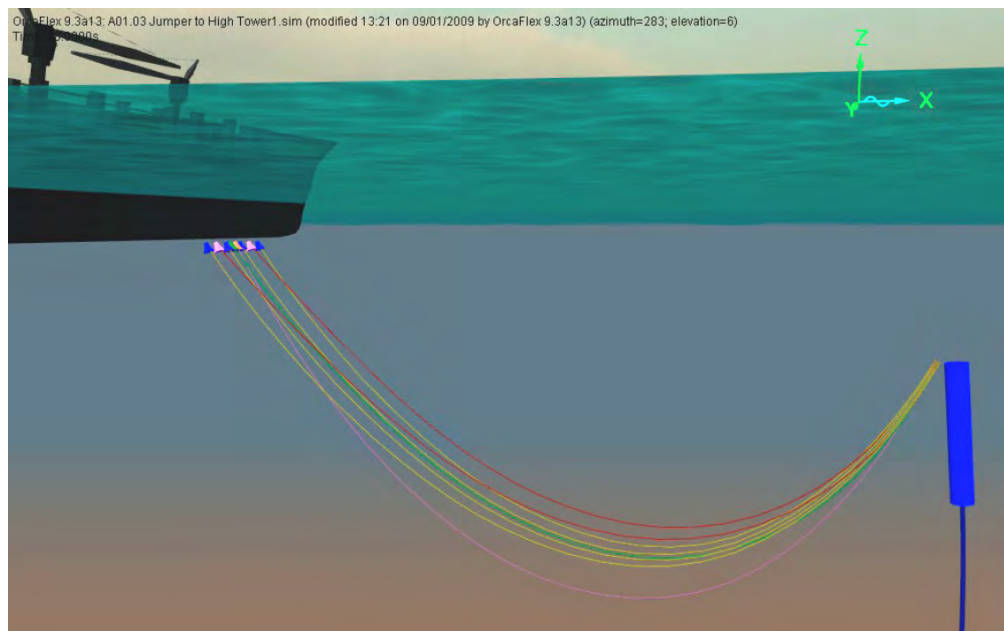


Figure A1.12: Riser Tower with jumpers, courtesy Orcina Ltd

Hybrid systems combine steel and flexible pipe systems. The hybrid systems currently known are used for deep water locations with moderate wave loading to achieve a cost-effective system. The fluid is transported in a steel riser connected subsea and to a large buoy located at a certain depth. The buoy has sufficient buoyancy to keep the steel riser in tension at all times. The platform is connected to the buoy via a catenary flexible jumper, with sufficient length to allow the vessel to offset from the buoy as needed. If necessary, the platform can disconnect from the buoy and retrieve the jumper to resume production. The system is complex to install.

Advantages include:

- Use of cost effective thermal insulation
- Low production cost
- Not sensitive to fluid content density
- No seabed contact issues
- Compact solution
- Low top tension for all depths

Table A1.19: Hybrid system design challenges

Water depth	Challenges	Comment
Shallow	Not presently used	
Moderate	Not presently used	
Deep	Buoy design Buoy dynamics Interference VIV on tower	

#### A1.4.2.10 Dynamic Jumper



Figure A1.13: Dynamic jumper. (Base picture is courtesy Øyvind Hagen - Statoil ASA).

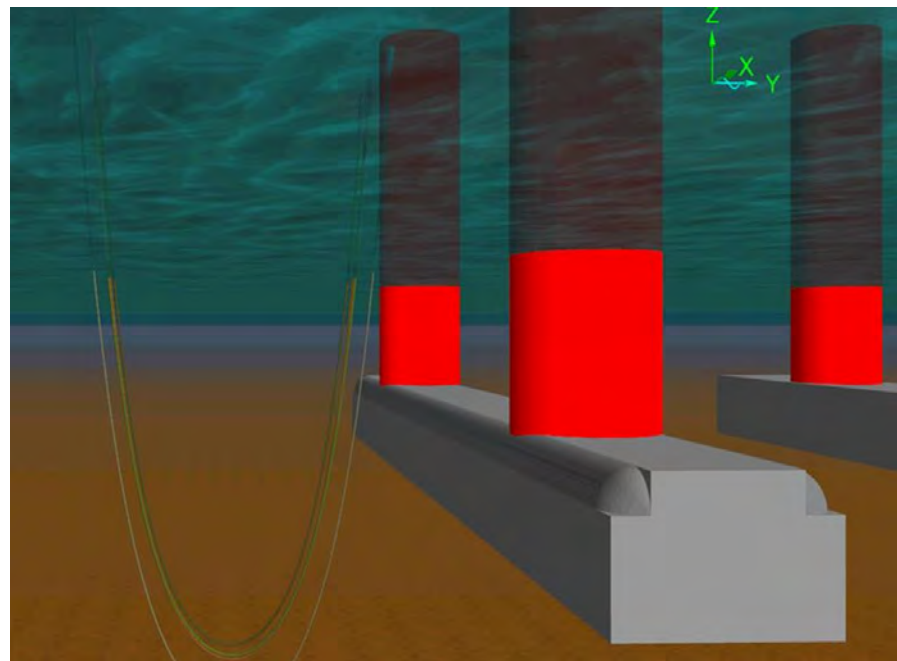


Figure A1.14: Dynamic jumper sagbend

Table A1.20: Jumper design challenges

Water depth	Challenges	Comment
Shallow Moderate Deep	Interference Overbending Handling Compression Dropped objects	Jumper vs. structure clashing

Jumpers are often used to connect two platforms or vessels that are very close. The jumper will hang between the riser and forming a single sag bend which will absorb the relative motions of the vessels as well as the environmental loads. Bonded jumpers are commonly used for offloading purposes.

Advantages include:

- Not sensitive to variation in fluid density
- High floater offset tolerance
- Simple

### A1.4.3 In-service experience overview

Figure A1.16 and Figure A1.17 sum up number of flexible risers per floater for FPSOs and FPU for 2011, based on data from [Offshore Magazine Mustang Engineering, 2011]. By investigating the data we may identify some trends and typical solutions by region. The list is obviously not complete on all details; however some general observations may be done:

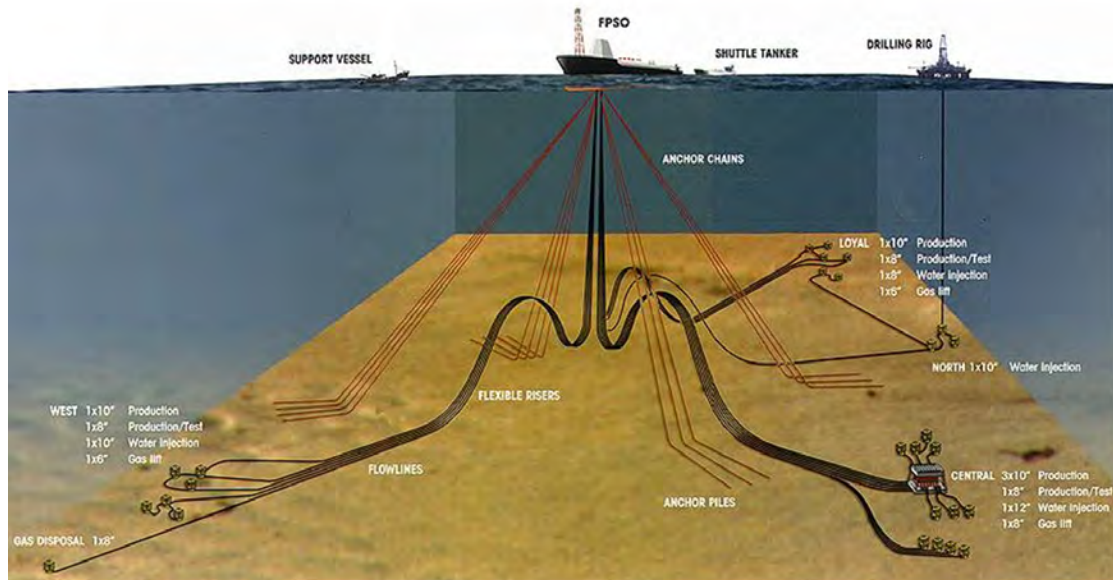
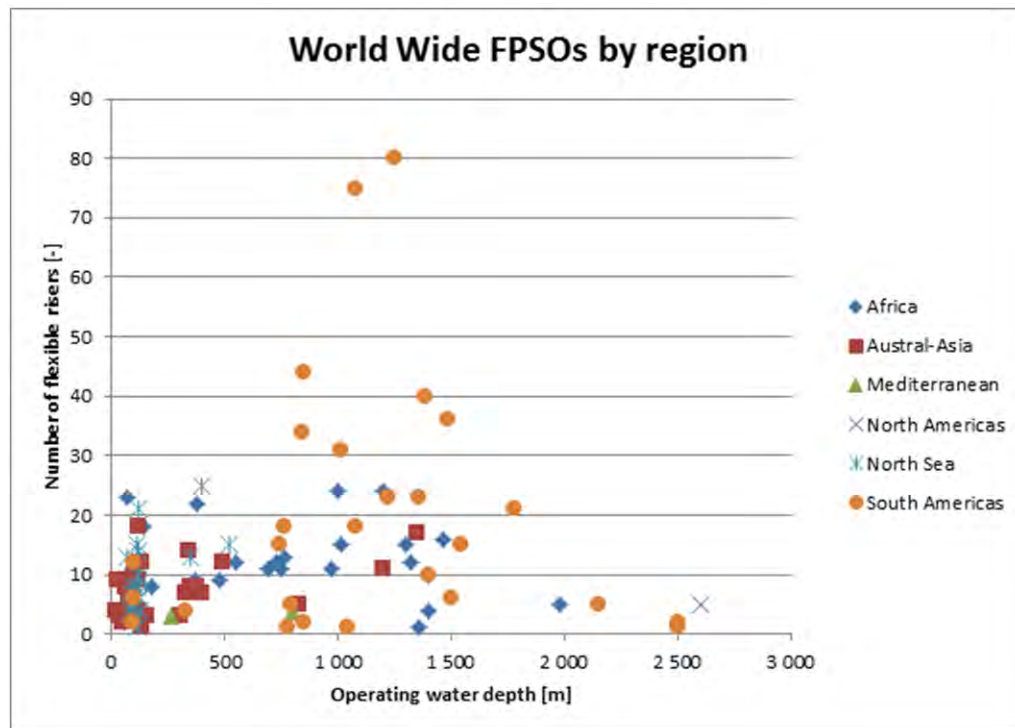


Figure A1.15: In-service Flexible riser system examples

Figure A1.16: Number of flexible risers connected to FPSOs per region in 2011 (based on data from [\[Offshore Magazine Mustang Engineering, 2011\]](#))

- The largest no. of risers is found offshore Brazil, most of these systems are free hanging configurations
- In the North Sea, flexible riser systems with additional flexibility, lazy, RSS or steep configurations are mainly used, and number of risers per unit is often limited to about 20, although 3 units with several more risers are seen

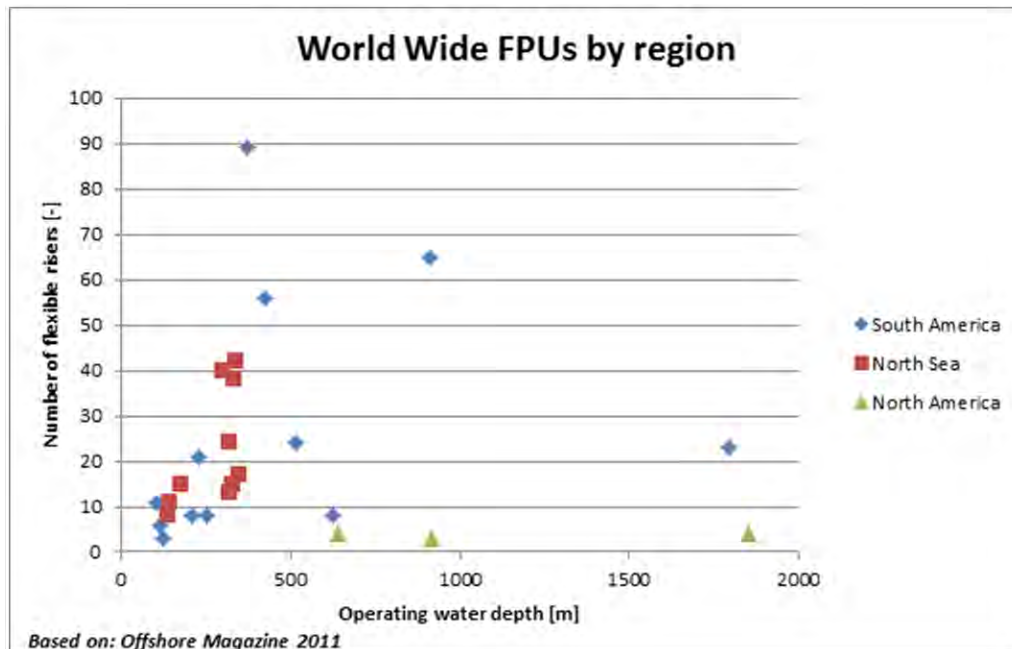


Figure A1.17: Number of flexible risers connected to FPUs per region in 2011 (based on data from [[Offshore Magazine Mustang Engineering, 2011](#)])

- In North America steel catenary risers connected to TLPs and spars has been frequently used as an alternative to flexible riser systems, hence the number of flexible are low
- In Africa FPSOs are widely used typically with 10 - 20 flexible risers each
- FPSOs are in all regions widely used in relatively shallow water (50-150m) with typically less than 12 risers, indicating that this solution now is attractive even at water depth previously developed by fixed units
- The deepest installed FPSOs are in Brazil and North Americas with about 2500m water depth with less than 10 flexible risers
- The deepest installed FPUs are also in Brazil and North Americas closing 2000m water depth, and seems to be able to carry more flexible risers than the corresponding FPSOs

## A1.5 Flowlines and tie-ins

### A1.5.1 General

This section is focusing on guidance for flexible flowlines and tie-ins. The analyses are closely linked with both flexible pipe design and system considerations for flowline and tie-ins. Recommendations related to use of analysis tools are hence included in this flowline section.

For both flexible risers and flexible flowlines the analysis tools section should be consulted when selecting software and defining load cases.

Flexible flowlines are in most areas of the world left unprotected on the seabed. In the North Sea, protection by trenching and rock dumping has been extensively used for trawl protection and thermal insulation.

Flowlines typically have lengths in the range 1-5 km. Instead of mobilizing an expensive pipe laying spread, it is often preferred to use flexible pipe installed from a dynamically positioned vessel.

The functional requirements to a flexible flowline are generally the same as for a steel pipe. However, for flowlines no dynamic loading or motions in the operational phase is expected. The flexibility requirements are mainly related to the transport and installation phases. This means that the bending flexibility requirement does not need to be associated with large internal pressures.

Furthermore, a flowline will be subjected to only a few cycles of bending, depending on the laying configuration.

Flexibility requirements are related to:

- Diameter of storage and transport reels
- Weight and tension control possibilities in the installation phase.

In general, the installation procedure can be designed to cope with the curvature limitations. It may be difficult to maintain a tension controlled curvature in deep water because the suspended pipe weight will be large compared to the required horizontal force. It may be advantageous to design the pipe to be 'self-supporting', so that the curvature is limited by the bending stiffness.

Examples where the use of flexible pipe results in simplified flowline design or installation include the following:

1. subsea flowline end connections where expensive or difficult operations, such as exact orientation measurements for spool pieces or the use of large alignment equipment to reposition the flowline, can be eliminated
2. situations involving gross movements and damage to flowlines because of mudslides can be reduced through the use of compliant sections of flexible pipe
3. applications in which field hardware and flowline location change with the field's production characteristics, which may necessitate the recovery and reuse of flowlines
4. applications with uneven seabed to avoid seabed preparation

5. in deep water or severe environment applications, where flexible pipe installation is economically attractive relative to rigid pipe installation

Flexible pipe flowlines generally range in internal diameter from 0.05m to 0.5m (2 inches to 20 inches) although some low pressure bonded flexible pipes, such as oil suction and discharge hoses, have internal diameters up to 0.91 m (36 inches). Section lengths are limited by transport capabilities, and diameter is limited only by current manufacturing capability. The functional requirements of a flexible pipe flowline are generally the same as for a steel pipe flowline. Significant dynamic loading or motions are generally not experienced, so the flexibility properties of flexible pipe simplify the project transport and installation phases.

### A1.5.2 Selection of Flexible pipe (alternatives)

A flowline may be configured with flexible pipe throughout, or as a combination of rigid pipe and flexible tails for tie-in sections (i.e. as an alternative to rigid tie-in spool). The following factors influence the selection process:

- Flow Assurance
- Selected subsea equipment (determines hub capacity and tie-in tooling)
- Chemical composition, design pressure and temperature

Flow Assurance (transport of the production fluids) leads to specifications for:

- Pipeline length and diameter
- Minimum and maximum design pressures and temperatures
- Start-up temperature transition (downstream and local to subsea choke)
- Maximum/design flow rate (hottest)
- Minimum flow conditions (minimum flow rate, insulation needed - multiphase)
- Hydrate control strategy
- Insulation required - product arrival temperature and no-touch time during shut-down
- Pipeline heating system required (e.g. DEH, Bundle only with rigid pipe)
- Risk of undetected hydrate plug (can lead to damage for flexible pipe)
- Target for pressure loss per meter (based on flow velocity and arrival pressure requirements) e.g. smooth bore flexible pipe is suitable for water injection but is not suitable where there may be pressure build up in the annulus. Flexible pipe internal carcass is 'rough' with significantly higher pressure loss than rigid/smooth bore pipe

Subsea interfaces (equipment):

- Tie-in limitations/cost e.g. existing hubs may be designed for Flexible tie-in
- Routing complexity (congested tie-in approach favours flexibles)

Chemical composition of the transported fluid will influence material and installation related issues:

- Material selection (Flexibles always include some CRA, if carbon steel pipe is suitable, rigid pipe cost can be very competitive)

- Availability/Competition for manufacturing, transport and installation (Procurement strategy)

Installation:

- Pipeline length; Installation vessel reel capacity determines number of transit days for transport and need for mid-line couplings

Flexible pipe can be routed directly to typical (standard) subsea manifolds/hubs. Flexible jumpers are often used in combination with rigid pipelines, thus exploiting advantages of flexible pipe for tie-in only. Making the complete flowline from flexible pipe avoids the cost of PLETs; however this may not meet the functional requirements for the system with respect to pressure loss, temperature upon arrival, or diameter. Selection between rigid pipelines and flexible is a multi-discipline process dominated by system considerations. This work is normally performed by the purchaser. In case of EPIC contracts it may be the EPIC contractor's scope to select.

### A1.5.3 Flowline restraint and tie-in flexibility

The flowline should be divided into two distinct zones during the design process, i.e. the 'tie-in' zone and the 'rest'. Intervention should be managed to avoid residual tension in 'tie-in' zones and to maximise residual tension in the 'rest'.

A flexible pipe should be left free to move on the seabed if it is found that none of the following justify the high cost and risks inherent in restraining the flowline using trench with backfill, or rock placement.

- Insulation enhancement by burial
- Protection against dropped object design loads
- Protection against trawling activity

GRP covers, with rock placement against both sides for trawl deflection, is used where it is necessary to allow the flexible pipe to move and provide trawl protection. More substantial structural covers are used over hub porches and are provided by the template/manifold supplier and usually referred to a 'near protection structure'. The 'near protection covers' interface with the template, extend out 10-15m from the hub face, and are installed after tie-in.

Mooring line and anchor footprints shall be avoided based on sensible routing. Probable anchor location shall be given a wide berth ( $\approx 200\text{m}$ ). If compromise is unavoidable due to routing restrictions, a pre-installed anchor (e.g. pile with some recoverable rigging for connection to anchor line), should be considered to mitigate risks associated with dropping anchors with allowance for drag during pretensioning/seabed penetration and miscellaneous tolerances.

### A1.5.4 Crossings

#### A1.5.4.1 The field layout should be arranged so as to avoid crossings.

Crossings should be as few as possible and follow internal guidelines as to separation. Transitions on both sides of a crossing shall be constructed with consideration to avoid a UHB challenge at the associated 'prop'. It seems that no background to the phenomena of Upheaval Buckling (and snaking for non-buried pipelines) is provided in the present document. Since the present text is much concerned with upheaval buckling it seems that some (possibly) brief introduction to the phenomenon should be given as it is not guaranteed that all readers are familiar with the associated physics.

Where crossing occurs, responsibilities and interfaces need special attention. In the event that two different operators are involved, a protocol should be established based on application/request for crossing being submitted by the crossing Party. The primary concern is to identify and manage risk. The crossing shall be designed so that the lines can be operated independently, neither line setting operating limitations on the other.

The first line (underneath) shall be stabilised laterally and axially (in so far as possible) at the crossing. This may involve finding a suitably stabilised location on an existing line. The second line shall be laid on a prepared (vertically profiled) path where sufficient separation is provided by e.g. rock dump or matresses. If the crossing line (second) is to be trenched, the up/down transitions to trench depth shall be completed with sufficient distance before and after the crossing to ensure that associated risks to the first line are as low as reasonably possible. The vertical profile of the crossing, including transitions in/out of trench, shall take into consideration upheaval buckling control. Pre-lay preparation of the crossing approaches is part of the overall upheaval buckling design.

The pre-laid rock (or carpet) profile determines the vertical imperfection of the crossing pipeline; it is an initiation point for upheaval buckling and will require rock cover to control UHB. Key parameters for the pre-lay profile are:

- Minimum width at top of support (consider lay corridor width, tolerances, and the probable footprint needed for post lay rock cover over the crossing line to control UHB)
- Side slopes (as gradual and smooth as possible/practical for a rock placement vessel)
- Vertical installation tolerances of support and transitions relative to the seabed
- Minimum height of the support measured from the seabed (UHB design is sensitive to height at crossing)

### A1.5.5 Installation

#### A1.5.5.1 Installation without intervention

The flowline should be laid with low back tension in order to minimise the risk of free spans on the flowline. Flexible flowlines are well suited to service on undisturbed seabed if unrestrained. The flexible flowline product is very robust with respect to vertical and horizontal curvature.

If it is required to restrain the flowline under rock cover protection or within a trench with backfill, then significant challenges arise in order to ensure that it remains under cover throughout its service life. This leads to a much more complex and interactive offshore campaign.

### A1.5.5.2 Offshore campaign planning

The following diagram highlights the interdependency of final analysis for a flowline, trenched, backfilled, and topped up with rock cover where needed to control upheaval buckling (this is a complex example for demonstration purposes, it is not a recommendation). The Out-Of Straightness (OOS) survey data and the residual tension represent key components of UHB control.

Implementation of residual tension into a flowline leads to an offshore campaign involving analysis based on as-installed information and survey data from a range of vessels; Installation vessel, Construction vessel, Survey vessel, Trenching vessel, Rock placement vessel and RFO vessel.

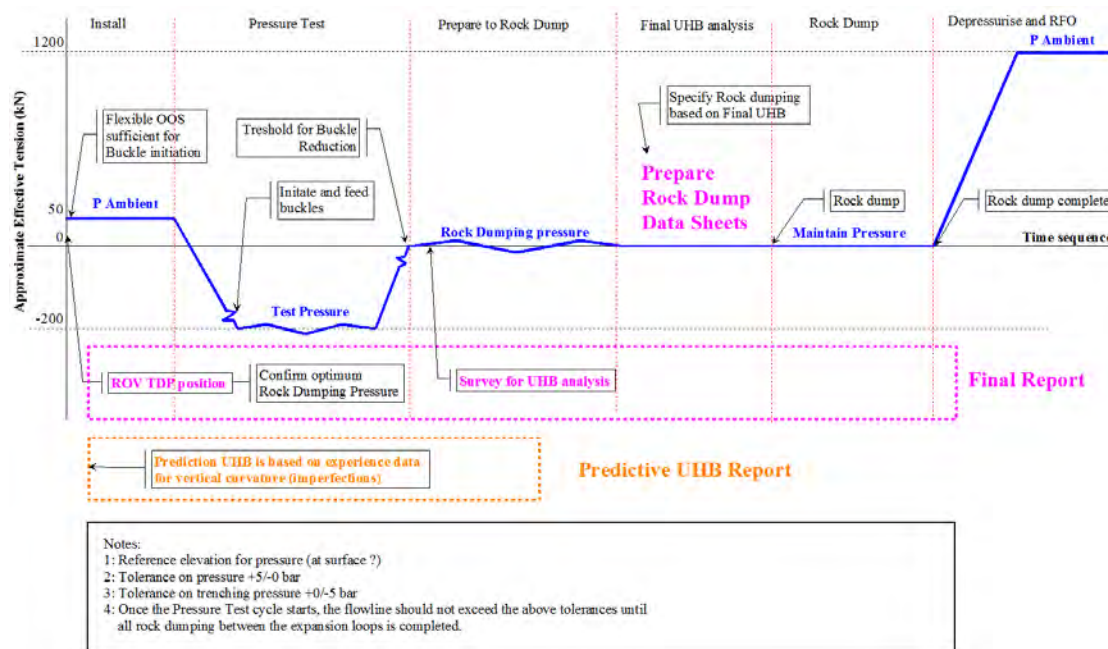


Figure A1.18: Example time-line for offshore activity and pressure in the line (RFO = ready for operation)

The goal in Figure A1.18 is to maximise residual tension in the flowline, thus reducing backfill and rock placement requirements. Residual tension in the tie-in free spans shall be avoided.

There are many variations on the above sequence, with and without trenching, which can also lead to a successful offshore campaign. The optimum sequence will be project specific and should be addressed during the planning phase in parallel with the predictive analysis.

In many cases, protection covers are required in the tie-in area to protect against trawling and dropped objects. The covers must be wide enough to allow for sufficient lateral movement in the expansion loop. By protecting with covers rather than rock, (i.e. in combination with

an expansion loop), the flowline can expand and retract when being subject to pressure and thermal expansion cycles. The lateral position of the covers over the flowline is dependent on the installation sequence. E.g. Positioning of covers prior to pressurisation should allow for lateral movement in the line due to expansion, while positioning of covers post pressurisation should have space between cover and line for lateral movement in the opposite direction (retraction) Once the flowline is pressurised, it should not be depressurised until it is completely/properly restrained. If it is trenched, sufficient time to let the soil backfill in the trench consolidate, must be included in the schedule. A survey of the pipe configuration after trenching is normally the input needed to decide how much (if any) rock is required, in addition to trenching/backfill, to lock in the residual tension and avoid UHB. A high performance trencher in combination with a flat and uniform seabed will often lead to a pipe configuration with sufficient burial to avoid rock placement after trenching. Planning of the sequence of the offshore campaigns for pressurisation, trenching followed by survey and/or rock dumping is important.

The predictive report includes a compendium of all analysis work leading up to receipt of the first hand (as-installed) surveys from the offshore campaign. The predictive report is superseded by the final report and associated surveys.

#### A1.5.3 Trenching

There is a range of trenching alternatives and relevant experience from adjacent developments is the best source of guidance for selection. Uniform conditions along the line are conducive to successful and uniform trenching. Areas with Ice Berg scars or irregular bathymetry (both often indicative of large local variations in seabed soil properties) lead to limited success, and in extreme cases can have a negative effect with respect to Rock volume needed to control UHB (i.e. deep trench in troughs (soft soil) and no trench at crests (stiff soil) along the route will amplify vertical curvature).

Avoid compression in the line during trenching. Liquidised suspension behind the trenching machine relieves compression and may allow it to accumulate to a degree that can disturb trencher performance (lift – jump out of trench). A small reduction from the maximum pressure is included in the above example schedule in order to relieve the compression level associated with the threshold load needed to drive (grow) buckles prior to trenching.

Backfill is also a matter of taking advantage of relevant experience. It is important that backfill which is liquefied during the trenching process (jetting) is given sufficient time to recover some of its bearing capacity before it is expected to provide restraint. At least seven days are used, however field specific evaluation is recommended.

#### A1.5.4 Rock Placement

The following is an example rock dumping data sheet – summarizing the flow of information from the UHB analysis to Rock Placement instructions offshore.

Check both lateral and in-line rock stability at all locations where the seabed slope exceeds 3°, taking into account local bathymetry (i.e. extent of area with slope both longitudinally and transverse to pipe). Rock placement sequencing from low towards high may be required in order to build up a s rock berm at some locations (i.e. support berm on low side first to

Project:													
Line:													
Document Number:													
Date:													
Revision:		0 Issue for Construction											
Prepared:													
Checked:													
Approved:													
Notes:													
1. Data sheet is based on LHD analysis to be presented in "Final in place LHD analysis report No. 4 subsea report no. 30242"													
2. Reference for Kp/Iz survey presented on sheet 2													
3. Ambient pressure in flowline during rock dumping													
4. Transverse seabed slope < 3 degrees - very flat seabed													
5. Minimum cover 0.6m, exception made for 0.5m for 1:15 to 1:19 analysis is sufficient for LHD prevention													
6. Transition in/out of trench means cross section varies from "on seabed" to "deep trench"													
Kp		Minimum		Comments		H rock							
Item		Start (km)		End (km)		W (m)							
		H (m)		W (m)		t (m)							
		Status				vol (m³)							
1						0.00							
2						0.00							
3				e.g. cross slope > 3 degrees		0.0							
4													
5													
Nominal Rock volume (m³)													
0													

Figure A1.19: Example Rock–Placement Data sheet

ensure stability before rock placed on pipe). Rock consuming locations should be identified as early as possible so that these may be avoided at the route selection phase.

## A1.5.6 Design and Analysis

### A1.5.6.1 Pipe soil interaction

For each of the construction stages identified in Figure A1.18, resistance between the flowline and the supporting seabed soil is mobilised in a different manner. The main modes are axial, lateral and uplift displacements for both the surface laid and buried cases.

Comprehensive guidance is provided by [DNV-RP-F110, 2007] for establishing the equivalent friction coefficients that may be used to approximate resistance per unit length of flowline. This resistance may then be used to construct force-displacement relationships to model the interaction of the flowline with the seabed, assuming particular values of relevant parameters, such as the strain required to mobilise peak resistance.

For the cases considered here, compatible axial, lateral and uplift force-displacement relationships were established for critical burial and cover depths. Uncertainties are introduced by this design approach that is not clearly considered by the guidance in [DNV-RP-F110, 2007].

The initial break-out resistance during lateral buckling under hydro-test conditions could be readily predicted using [DNV-RP-F110, 2007]; however, lateral resistance at large displacement is not explicitly covered. In this case, it is feasible that a berm may form adjacent to the pipe during the lateral 'sweep', and so require additional modelling to achieve an accurate prediction of resistance. Upper and lower bound pipe/soil interaction curves in combination with break-out and residual resistance phases for large displacements lead to a hysteretic behaviour, and thus loading duration and sequence can be important.

Some of the uncertainty is managed by being consistent, e.g. when considering that pipe/soil resistance is both leading to resistance (when locking in residual tension) and to load (allowing build-up compression loads and/or expansion feed into an imperfection).

Following jet trenching operations, backfill on top of the flowline is expected to be in a fluidised and super-loose state. An understanding of the time required for this backfill to densify, so that axial resistance and lateral restraint can be reliably mobilised, is critical for calculating the axial tension that may be 'locked in' to the system when the flowline is depressurised. This time requirement introduced dependencies in the construction schedule. For silty fine sand soils, the time period was taken to be seven days. Centrifuge testing is recommended to quantify this in specific projects.

Lateral resistance of a buried pipeline is often considered to be so large as to be a trivial consideration, e.g. virgin soil properties. When considering UHB to be a two dimensional phenomenon i.e. with a degree of freedom in the vertical and axial plane, this is a convenient assumption. However, in the case where horizontal curvature is significantly greater than vertical curvature, then an estimate of the force-displacement response in both vertical and lateral direction is required to accurately model the flowline system.

### A1.5.6.2 Flexible flowline bending stiffness and load history

The following section outlines challenges related to hysteretic pipe bending properties that vary with internal pressure and temperature. Flexible pipes have complex bending stiffness characteristics. For example the bending stiffness characteristics of a flowline may be presented as follows for bending relative to straight pipe. The curves represent a range of

pressures (e.g. 'P471' = 471 bar) and temperature ('T79' = temperature of internal fluid 79°C above ambient).

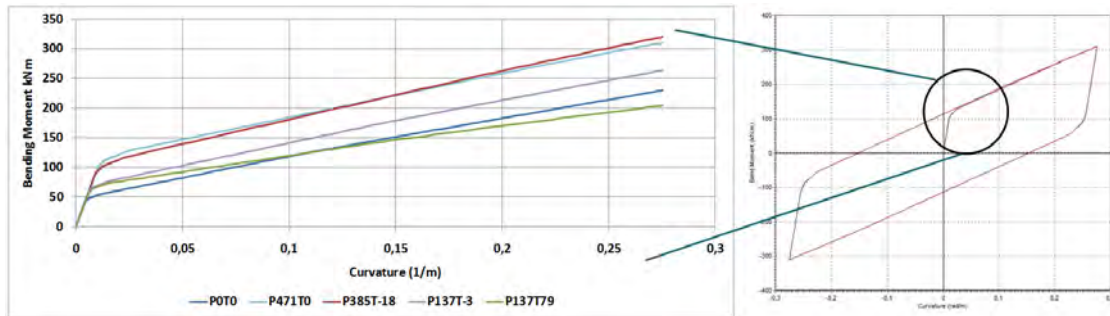


Figure A1.20: Example of flexible pipe bending stiffness curves. Hysteretic bending stiffness envelope.

The initial bending stiffness of the pipe may be in the order of 10 000 kNm<sup>2</sup>, i.e. approaching the stiffness of a rigid spool. The stiffness changes when the bending moment level overcomes the interlayer friction (stick/slip threshold) and the flexible pipe layers start to slide over each other. The interlayer contact forces are dependent on internal pressure and thus for a given friction coefficient the stick/slip threshold increases with internal pressure. The highest stick/slip threshold in the above figure occurs at a bending moment of approximately 115 kNm, under a pressure test scenario.

The post slip stiffness is much lower and variations with temperature become evident because the E modulus of the plastic layers varies with temperature. The steel layers are sliding over each other in the post slip phase. Only the first quadrant of the bending stiffness is shown in Figure A1.20. The pipe bending stiffness is thus hysteretic, so in the analysis, a complete stiffness curvature envelope for a given pressure and temperature would be modelled as shown in the figure.

It is important to consider the load history for a flexible pipe. The bending moments at a flexible tail tie-in hub are an example where load history is important due to hysteretic pipe bending during installation and tie-in.

During tie-in a flexible pipe is open ended and at ambient temperature; 'P0T0'. The resulting tie-in free span configuration is determined by back-tension, weight distribution, level and elevation tolerances, and a bending stiffness with a relatively low stick/slip threshold. The operating phase starts some months later and some shake-down of residual bending moment in the flexible can be expected in addition to the short term interlayer slippage occurring during the installation. The flexible will migrate towards a pre-bent shape in-situ where moments relying on interlayer friction are largely mitigated before start-up.

For an Operating scenario (expansion cycle), the hysteretic pipe bending stiffness corresponds to the maximum pressure during the cycle and the start/static configuration corresponds to a 'pre-bent' tie-in configuration. This assumes that the change in bending stiffness due to pressure and temperature variations precedes the corresponding elongation. Thus the high bending stiffness associated with interlayer stick/slip is included in the expansion cycle analysis and the advantage of a pre-bent flexible pipe is captured in the start configuration. The pipe stiffness used in UHB analysis of the flowline, where it is restrained, takes into consideration the fact that high stiffness will improve resistance to UHB (greater driving force required for given curvature). The bending stiffness in UHB analysis is reduced to

50 % of the nominal stiffness as presented above. For a UHB analysis, fulfilling the UHB acceptance criteria, the change in curvature is very small. UHB is dominated by the initial curvature.

#### A1.5.6.3 Survey data validation and interpretation

Survey quality is a key to good design and successful operation of covered pipelines, Rubbish in, rubbish out! There is a need for multiple surveys during such a project, starting with general routing and finishing with e.g. as-laid after rock-placement using pipe tracker to confirm successful completion of the installation in accordance with documented design.

Figure A1.18 demonstrates a sequence of surveys and how they are integrated into the offshore campaign in order to provide input to design/analysis. UHB analysis is on the critical path to completion of rock placement and RFO.

Curvature is a double derivative of the survey geometry, thus amplifying spurious variations inherent in raw survey data streams. Key stages in transforming a flowline survey into a FE model for UHB are:

1. Kp data is considered as a label
2. Easting, Northing and top-of-pipe-elevation coordinates describe the pipe profile in 3D
3. The raw survey is visualised and patched/pruned e.g. bridge gaps and crop obvious glitches
4. Each of the three patched/pruned coordinate streams are passed through a Blackman filter (weighted moving average)
5. The filtered data streams are used to generate a FE model with exactly 1m long elements (if survey at average 0.2m resolution, then intermediate data points are first ignored at this step)
6. Analysis and reporting is relative to the FE analysis model from step 5

Focusing on step 4, an adaptation of 'Time' domain filtering is used for the filtering process. The three separate data streams are assumed to be time histories with equal time steps (note gaps are patched in step 3). Important characteristics of the filter are that it should not generate ripples at steps in the data, and it should not generate any phase shift in the pseudo time domain as this would equate to moving the pipe in space in later steps.

Considering a moving average filter on a data stream, one uses a window function and a convolution algorithm. Alternative window functions are presented in Figure A1.21 and the basis for selection of a 'Blackman' filter is presented in Figure A1.22.

In the example presented in Figure A1.22, the window is progressively applied to 31 sequential data points to generate a 'filtered value' for the mid-point (30 increments 0.2m resolution is 6m window in this case). The Blackman window function is selected because it combines 'best' coherence to the survey with 'best' filtering of the curvature. The 'best' selection criterion is visual rather than numerical. This is demonstrated below where depth (top-of-pipe elevation) and absolute three-dimensional curvature are presented for a 150m section of survey data with a range of filter windows.

y comparison, the moving average (flat) filter leads to the largest change in the raw survey data (depth) and though it usually leads to the lowest curvature, it does not do so consistently,

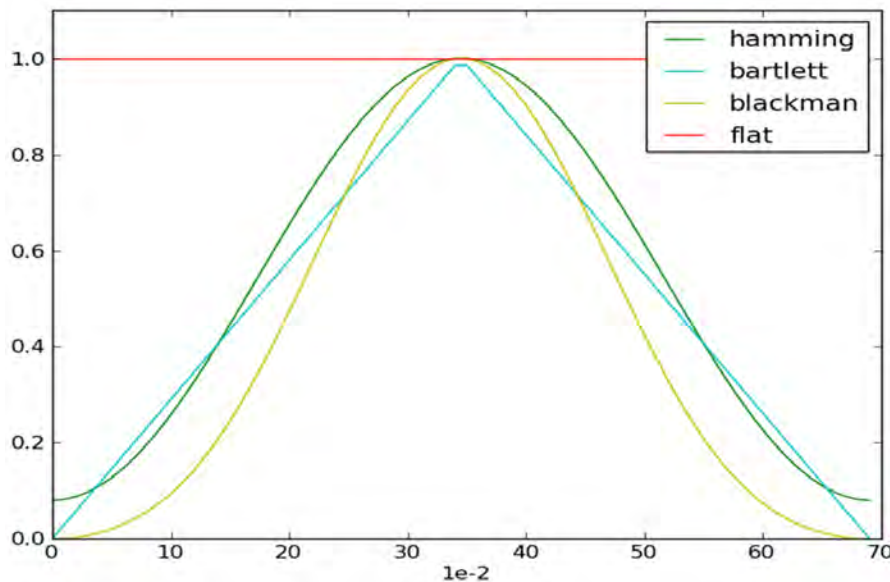


Figure A1.21: Filter windows overview

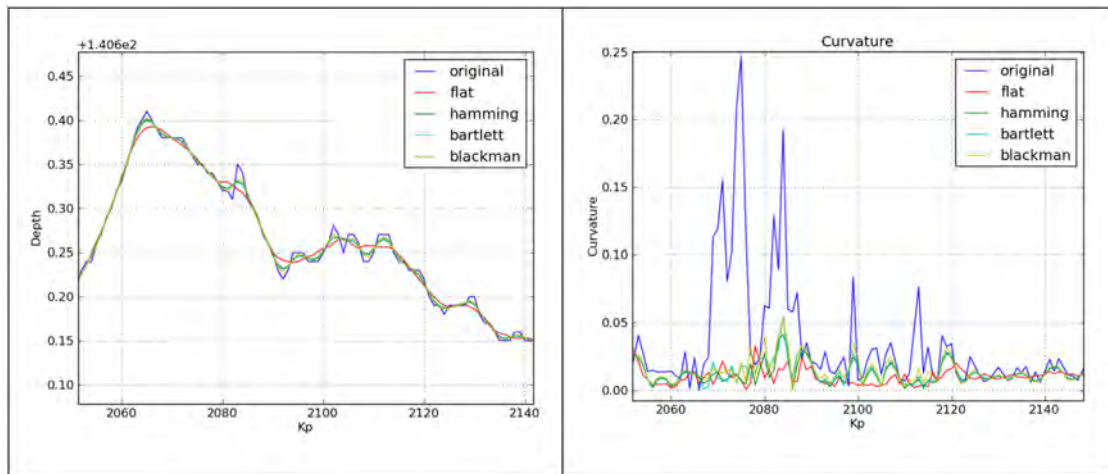


Figure A1.22: Examples filtering depth and curvature

some locations are higher than all other filters presented and the peak curvature locations are offset from the curvature peak location in the original data. The weighted filters have curvature peaks at the same K<sub>p</sub> as in the original data. It is important to compare original and filtered data, information herein may provide guidance but every survey can have its own specific interpretation challenges.

Step 5 transposes the three filtered data streams back into three-dimensional space. The filtered survey data streams are run through a script that generates a full 3D FE beam model with exactly 1m long elements. Attached to each node are three non-linear springs that point in the directions of the local coordinate system of the element. Horizontal and vertical springs are very long in order to follow the expected axial displacements while remaining nominally perpendicular.

The soil springs model the soil-pipe interaction. Each spring along the model is generated from a call-up library of springs pre-solved from pipe/soil interaction simulations or empirical

formulae. The call-up library for the springs covers the range of soil types along the line, the depth of lowering, depth of cover, and expected/design rock dump height and should have resolution appropriate for UHB analysis.

Logic is included so that the FE analysis iterates automatically to a design rock dump profile that meets the UHB acceptance criteria in [DNV-RP-F110, 2007] i.e. if the trenching and backfill provide insufficient restraint.

#### A1.5.6.4 Predictive UHB analysis and design for residual tension

Away from the end zones, one of the most important design considerations is UHB. Locking in of pre-tension and curvature control are the primary design tools. The flowline should be pressurised before being trenched to stretch it towards its maximum length in service and the pressure is not released until at least one week after being trenched and buried and rock-placement (as needed) is completed. One week after trench backfill is to allow the liquidised backfill to recover sufficient capacity to restrain the pipe and lock in pretension (residual tension).

During pressurisation for trenching, the elongation is resisted by pipe/seabed friction, and this leads to compression corresponding to the driving force for feed-in of elongation into expansion loops (buckles) along the line. Experience indicates that there are sufficient OOS along the flowline to initiate buckles at regular intervals (lay with low back tension), such that the driving force (compression) will not be high. However, it is a challenge to be sure during predictive engineering phase, so evaluation of the need to provide some deliberate OOS is a typical predictive engineering activity.

During trenching, the pipe is progressively suspended in frictionless slurry of liquidised seabed, and there are indications that accumulation and release of residual compression (elastic strain energy) during trenching can lead to significant local horizontal curvature within the trench. This can be an advantage for UHB, but also a risk if challenging OOS is observed as-trenched. It is recommended to consider reducing the pressure in the order of 15% from the peak pressure during preparation for trenching to avoid residual compression related risk. Predictive analysis should provide project specific guidance.

Trenching is not always a cost effective investment. For some soil conditions, trenching has been observed to result in similar rock dumping volumes as a 'no trenching' scenario. A route specific assessment of geological / geotechnical conditions should identify this risk. Successful trenching will lock in most of the pipe elongation, i.e. the elongation corresponding to the pressure during the trenching campaign. UHB driving force will not initiate in service until this locked in elongation is exceeded. The driving force corresponding to the locked in elongation is referred to as residual tension. A locked in elongation level corresponding to recurrent design conditions is a 'nice to have' target for a flowline (but not in tie-in zones as previously discussed).

In UHB analysis, rock is added incrementally at buckles that exceed the upward displacement criterion under the effective UHB load. The 'add rock' iteration process continues until the DNV UHB capacity check is fulfilled throughout the line. The cover height increments are commonly 0.2m of additional cover over a minimum length of 5m to each side of the node under consideration.

For final UHB analysis, the as-trenched or rock dumped pipe survey is used and supersedes all of the predictive analysis work.

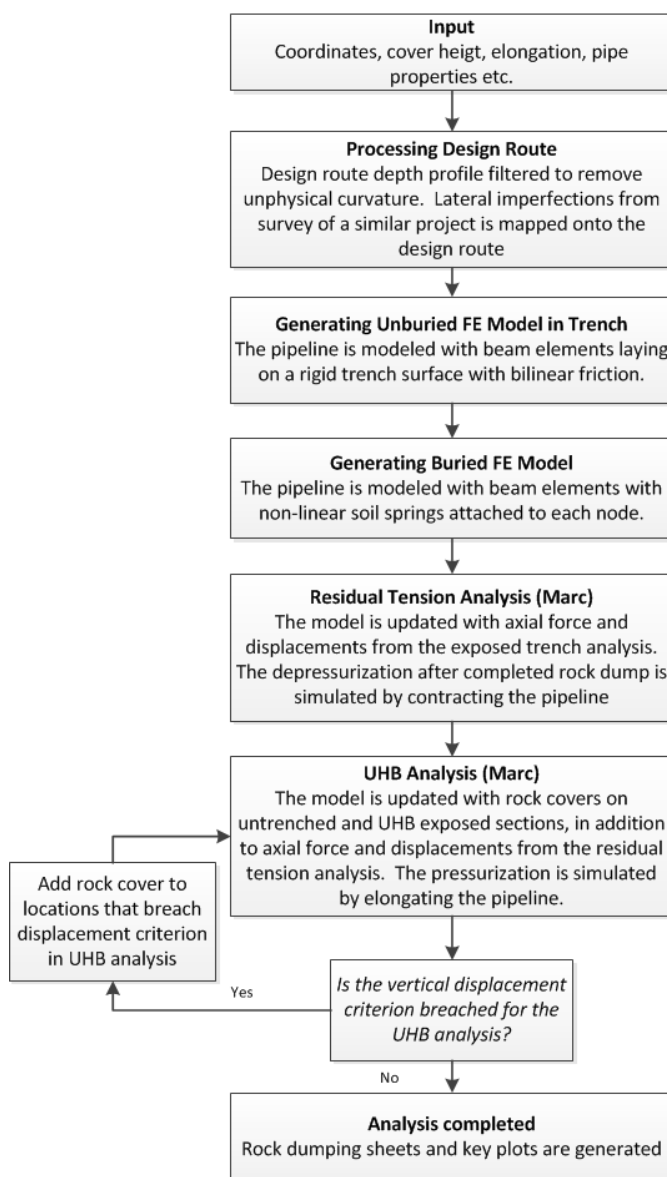


Figure A1.23: Example of Analysis methodology for predictive analysis of flowline laid in a pre-cut trench

#### A1.5.6.5 UHB Final analysis

The residual tension used for final analysis is solved based on the as-laid survey, the pressure cycle associated with the trenching campaign preparations, and the depth of burial and cover achieved prior to subsequent depressurisation. The design case elongation applied to the UHB model takes into account the residual tension in the line. The UHB model initial shape is derived from as-trenched survey data. The design case elongation is applied to the UHB model and an example of the deformed shape is presented on the following figure. The z displacement is in the vertical (upheaval) direction and a scaling factor of 300 is used to amplify the displacement.

The peak vertical displacement of the location with maximum vertical displacement is 3.6mm (yellow range). This occurs at the same location in both views, but seems different due to

view point/origin.

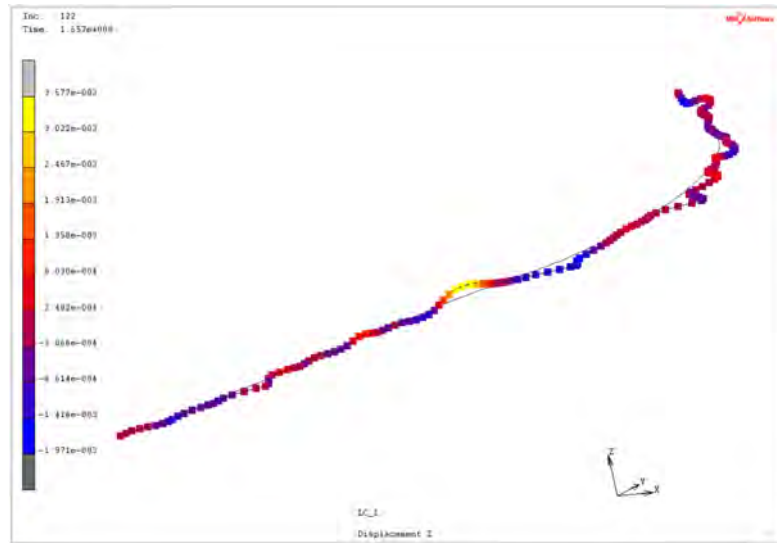


Figure A1.24: Side view (almost - see axes) - vertical displacement flowline elongation (yellow at Kp 0.342 in both views)

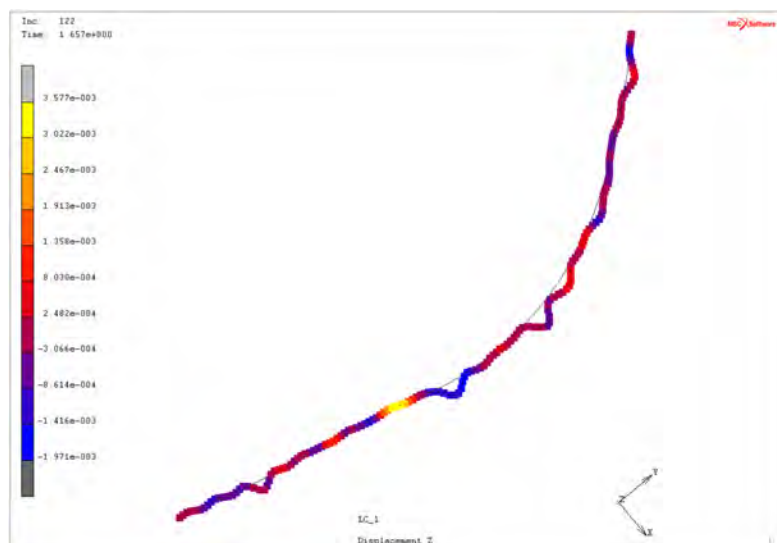


Figure A1.25: Top view - vertical displacement flowline elongation (yellow at Kp 0.342 in both views)

The maximum is at a location where the initial vertical curvature is high and the initial horizontal curvature is low as shown in Figure A1.26.

The horizontal soil resistance is approximately three times the vertical soil resistance for this example, so there is a structural bias preventing horizontal displacement in the FE model. However, the horizontal curvature is generally so much greater than the vertical curvature that the flowline elongation is mainly absorbed by horizontal displacement in this example. Thus at other locations along this section, some having marginally higher vertical curvature, the horizontal curvature is high enough to mobilise pipe buckling in the horizontal plane. These lateral buckles absorb most of the elongation and reduce the driving force at potential UHB locations such as Kp 0.342.

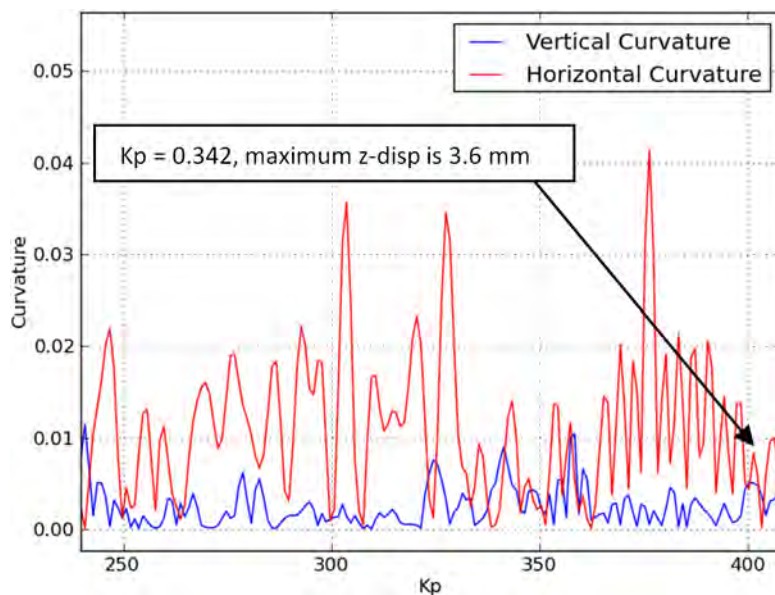


Figure A1.26: Vertical and horizontal curvature along example flowline

Figure A1.27 shows the vertical displacement and the corresponding vertical profile (initial) for the flowline plotted against Kp. Note the horizontal axes have different scales. At Kp 0.342 the vertical displacement is 3.6mm and this corresponds to a physical high point (hog bend) on the flowline. This again provides a visual quality check on results.

The UHB analysis acceptance criterion typically used is as follows:

- $\gamma_{UR} = 1.0$  [API 17B, 2008] formula (21)[DNV-RP-F110, 2007], standard deviation of survey accuracy is 0.05m.
- $\gamma_{UF} = 1.15$  [API 17C, 2010] formula (28)[DNV-RP-F110, 2007], i.e. safety class normal

The displacement in the upheaval buckle shall not exceed the displacement needed to mobilise peak upward resistance taking into account  $\gamma_{UR}$  for the cover/resistance and  $\gamma_{UF}$  on the load due to applied internal pressure and temperature. Residual tension is not factored.

#### A1.5.6.6 Follow-on and Final UHB report

Follow-on resources are needed throughout the offshore campaign in order to provide advice and support as needed during preparations for the offshore campaign. Rock dumping data sheets are provided where relevant, and issue of a 'Final UHB report' based on as-built data.

#### A1.5.6.7 Expansion loops (isolate tie-in span from flowline)

Care is necessary to provide expansion loops to avoid end expansion being fed into the tie-in free span. The tie-in free span has very limited capacity to absorb length changes between the hub and the touch down point, and this may lead to very high interface loads on the hubs. An adjacent expansion loop should be used to isolate the tie-in free span from flowline feed-in or out. It is particularly important to apply the flowline restraint (rock dump) adjacent to

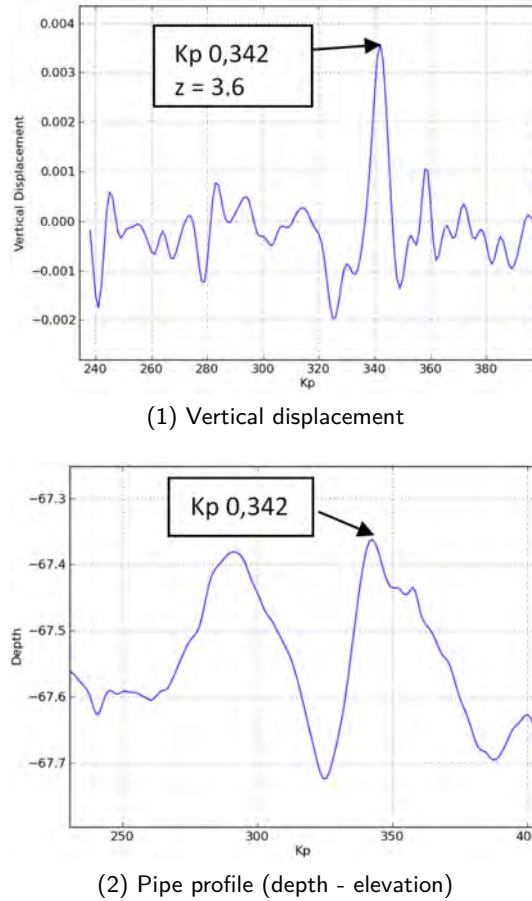


Figure A1.27: Flowline vertical displacement and vertical profile

the tie-in free span with ambient pressure and temperature in the flowline so that it will be biased towards compression due to elongation in operating phases. If restrained when pressurised, high tension due to shortening of the pipe will arise during each shut-down cycle. Avoid restraining of tie-in free spans with pressure in the line.

#### A1.5.6.8 Flexible tail tie-in and in-place analysis

A flexible tail is taken as an example of flexible pipe subsea tie-in. Considerations are similar for riser tail tie-in to a riser base, and for subsea Jumpers connecting subsea hub to hub. Use bending restrictors at the end fitting transition as default. These may be removed, pending risk/responsibility evaluation process with the Operator, the Installation Contractor and the flexible pipe supplier.

The laydown configuration will be defined by the Installation Contractor and provide a starting point for tie-in analysis. The tie-in analyses will provide a range of tie-in free span configurations to be considered in the in-place analysis (with associated back tension and touch down points). Account should be taken for tolerances and uncertainties. This is an important interface that is difficult to coordinate as, quite often, the tie-in analysis is carried out by the Installation Contractor and in-place analysis is in the flexible Pipe supplier scope of work.

Loads on the hub are predominantly static (weight/buoyancy). Guidance: maximum design moment is in the order of 1.3 times the static estimate. If more than 1.3, then heads-up, something is outside typical range, e.g. hub very high, soil friction unusually high, modelling error, and high tension due to restraint.

A flexible tail is typically arranged as shown in Figure A1.28 when tied in.

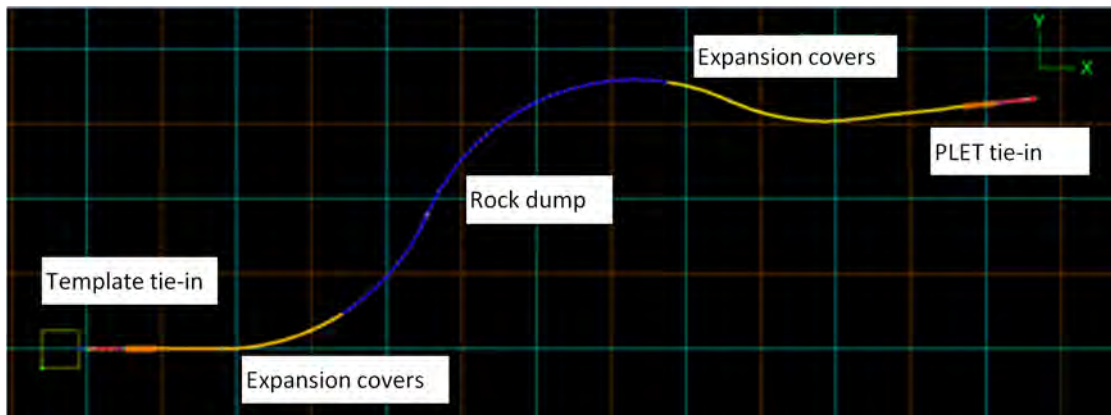


Figure A1.28: Covers and rock dumping overview

At both ends a free span is created when the flexible tail is pulled up to the interface hub and tied in. It can be challenging to maintain interface loads within hub capacity using flexibility in the tie-in free span alone, and it is therefore recommended to consider extension of the tie-in zone into a horizontal expansion loop under expansion covers, i.e. allow for horizontal displacement in a curve adjacent to the tie-in free spans. In the case of a short jumper, the intermediate section may be rock dumped or covered as best suited for specific projects. A flexible tail has thus five sections:

1. Template tie-in free span (e.g. arc length 0 to 20m)
2. Expansion covers over first expansion loop (e.g. arc length 20 to the 35m)
3. Rock berm (e.g. arc length 35 to 77m)
4. Expansion covers over second expansion loop (e.g. arc length 77 to the 122m)
5. PLEM tie-in free span (arc length 122 to 142m)

The load cases are applied as expansion cycles corresponding to the combined effect of the pressure and thermal variations. An example is presented based on an expansion cycle of 0.018% relative to as-installed (ambient) length. The magnitude of nodal displacements during this expansion cycle combined with 0.5m feed-in of the PLET, are presented in the Figure A1.29. Movement is primarily under the expansion covers. The pipe is restrained to within the resistance mobilisation displacement under the rock covered zone.

An example of loads cases for in-place analysis of a production jumper is presented in Figure A1.30.

The interface loads at tie-in hubs are governed by the radius in the adjacent expansion loop and pipe/soil friction. A range of expansion cycles corresponding to operating scenarios as above leads to interface loads as follows, see Figure A1.31. The effective tension range corresponds to mobilisation of the local expansion loop to absorb expansion (+/- 40 kN for feed-out or pull-in to the tie-in free span). The moment range varies relatively little as it is

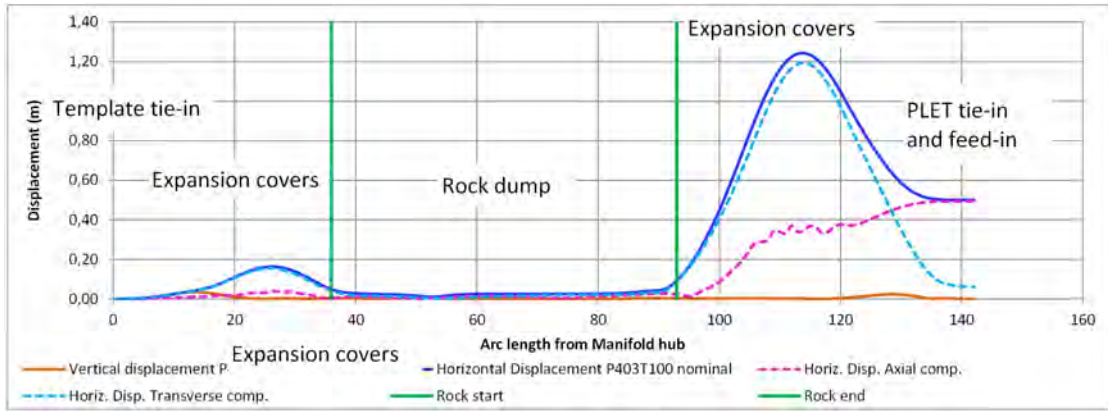


Figure A1.29: Nodal displacement magnitude along Jumper P403T100 and 0.5 m PLEM feed-in

Scenario	Scenario	As-built	Empty	Leak test	Design	Operation	Operation	Design
Parameter		LC1	LC2	LC3	LC4	LC5	LC6	LC7
Water Depth	m	253	253	253	253	253	253	253
ID incl carcass voids	m	0.238	0.238	0.238	0.238	0.238	0.238	0.238
End cap area	mm <sup>2</sup>	44488	44488	44488	44488	44488	44488	44488
Internal temperature	°C	8	8	11	95	90	5	-20
External temperature	°C	8	8	11	11	11	5	5
Pipe wall ΔT relative to 8°C	°C	0.0	0.0	3.0	87.0	82.0	-3.0	-28.0
α thermal expansion	1/°K	1.20E-05						
Internal Pressure	barg	26.5	0	404	351	131	0	0
External pressure	barg	26.5	26.5	26.5	26.5	26.5	26.5	26.5
Differential pressure	barg	0	-26.5	377.5	324.5	104.5	-26.5	-26.5
Pressure expansion only		-0.00025	-0.00041	0.00211	0.00177	0.00040	-0.00025	-0.00041
Thermal expansion only		0.00000	0.00000	0.00004	0.00104	0.00098	-0.00004	-0.00034
<b>Total elongation, original lgt. 1,0</b>		<b>0.99975</b>	<b>0.99959</b>	<b>1.00215</b>	<b>1.00281</b>	<b>1.00138</b>	<b>0.99971</b>	<b>0.99925</b>
Contents density	kg/m <sup>3</sup>	1 025	0.001	1 025	0.800	0.800	0.001	0.001
PLEM feed-in	m	0.000	0.000	0.250	0.250	0.250	0.000	0.000
End cap load	kN	0	-118	1 679	1 444	465	-118	-118

Figure A1.30: Example of load case matrix for tie-in in-place analysis

predominantly static (submerged weight of the hang-off assembly, end fitting etc.) and the tension range is well controlled.

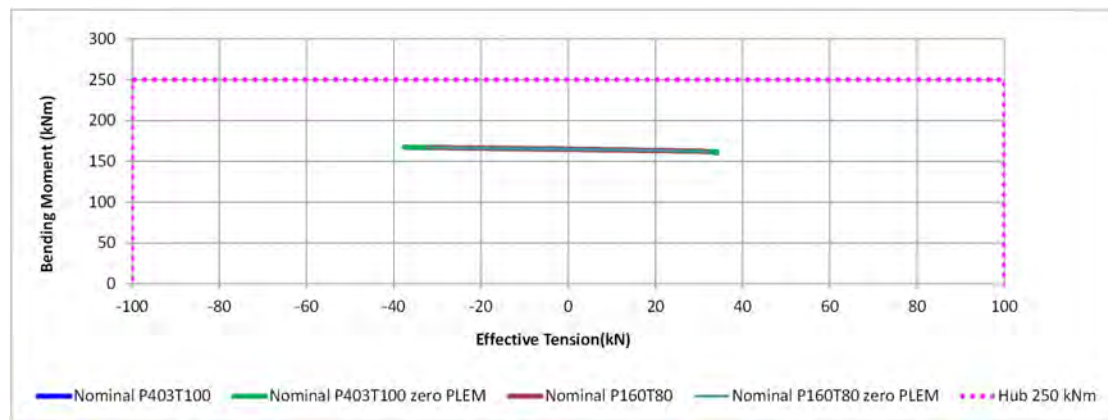


Figure A1.31: Hub loads, effective tension and moment combinations, at tie-in hub (P403T100 is an example in-place load cycle correspond to a change of internal pressure by 403 bar and contents temperature by 100°C. Note thermal expansion is based on average wall temperature which is approximately midway between ambient (external) and internal fluid temperature for un-insulated flexible pipe.

## A1.6 Other flexible pipe systems

### A1.6.1 Offloading

The following systems are used for offloading of hydrocarbons from FPSOs to tankers:

- Loading buoy moored a few kilometers away from the FPSO. Flexible risers and seabed flowline often used as a permanent connection between the FPSO and the loading buoy. Midwater e.g. camel shaped line with mid length buoyancy section has also been used. Tanker connect to buoy, several alternatives used e.g. APL, SBM.
- Floating hose from FPSO to tanker midship manifold, ref. Figure A1.32. Bonded hose from 10" to 24" internal diameter is normally used. The hose is normally stored on reel between offloadings. Floating hoses are not used in harsh environment.
- Catenary hose suspended from an FPSO reel to a bow loading system on the tanker. Submerged bonded hoses from 10" to 20" inside diameter are normally used. The hose is stored on reel or in separate areas onboard the FPSO between offloadings. This system is often used in harsh environment e.g. North Sea.

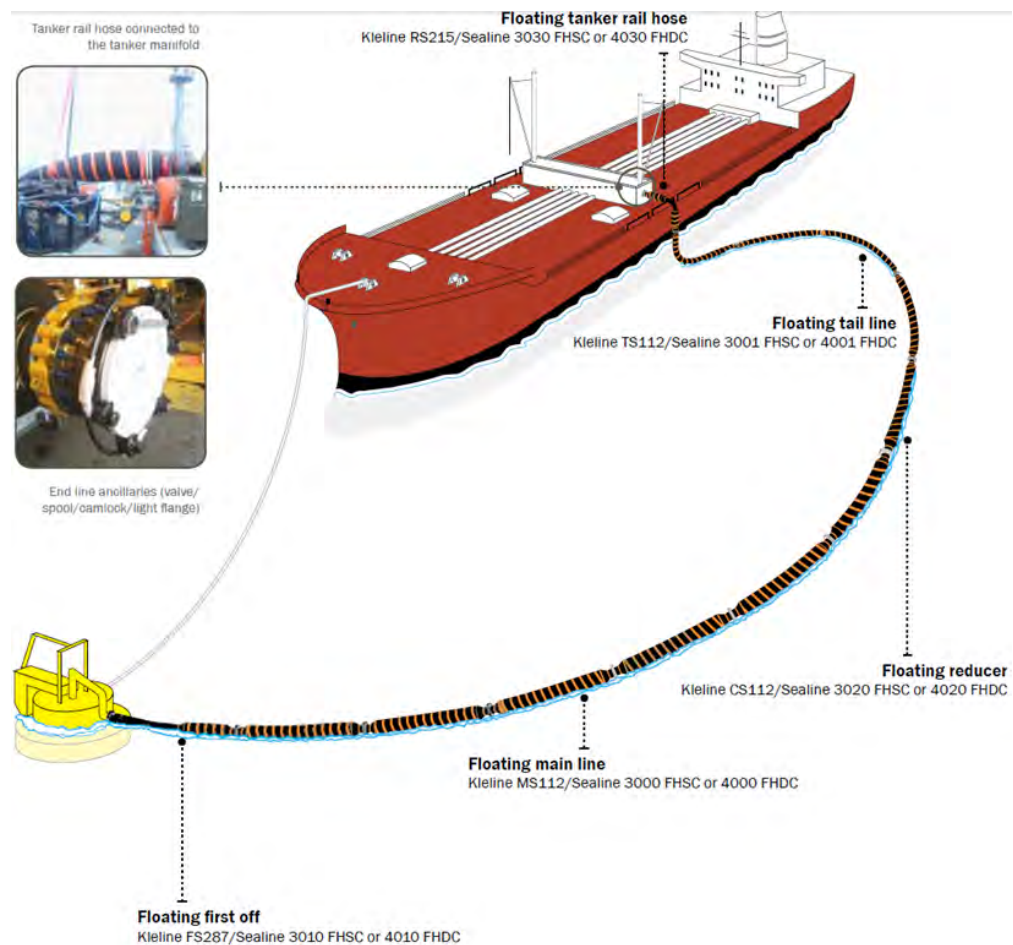


Figure A1.32: Floating hose offloading system, courtesy of Trelleborg Oil & Marine SA

## A1.7 Installation

### A1.7.1 Introduction

The installation phase cost for both rigid and flexible pipe systems are high compared to the procurement and operation phases. While the rigid pipe systems require either equipment to straighten oval pipe sections, weld stations at joints – or both, the installation phase for flexible systems is shorter and requires less equipment. Depending on the size of the vessel, a number of reels can be transported to the installation site in one mobilization phase, and installed. The equipment and actions required for installation of flexible pipes are listed in the following sections.

As an example, a pipe lay installation campaign for a flowline, jumper or riser to be wet-stored will commence along these lines:

1. The manufacturer spools the pipe onto reels or reels the pipe onto a carousel.
2. If necessary, either the reels are transported to the site where the installation vessel will mobilize or the installation vessel mobilizes at the manufacturer base
3. The installation vessel either lifts the reels onto the deck or reels the pipe onto a carousel in the ship

4. The vessel moves to the installation site
5. ROVs are deployed from the vessel to provide observation possibilities and low-level interaction
6. Installation aids are deployed subsea
7. The vessel moves to the initial position for pipe initiation
8. The reel with the pipe to be installed is engaged in a reel drive system
9. Winches and cranes are used to transport the first end of the riser over lay tower and through tensioners (caterpillars). The tensioners are closed around the pipe to take the weight it as it is discharged from the vessel
10. The pipe is fed through the tensioners - tension and lay speed can be adjusted according to the installation procedures
11. The pipe end is lowered down to the seabed and initiated towards a connecting structure or a temporary clump weight
12. Sufficient length is deployed to lay the head of the pipe down on the seabed
13. When the head has been landed, the vessel starts to move along the route according to procedure while feeding out pipe
14. Ancillary equipment is installed along the flexible pipe at a work table below tensioners
15. Either an A&R winch wire or the crane wire is connected to the second pipe end and is used to lower the pipe in place on the seabed
16. A separate tie-in operation will be performed, which can be performed by either the same vessel or a separate vessel at a later time

The installation phase includes large, high-cost equipment, which has a substantial mobilization-cost. The additional cost of performing work with an installation vessel that is in-field is low compared to the start-up costs, thus it is of great benefit to plan the offshore campaigns accordingly.

The installation vessels have weather limitations on most activities, thus the majority of activities are performed during late spring - summer – early fall, while the operations are planned and analyzed in the winter months. Few vessels are able to operate in seastates with  $H_s$  more than 4 m. This means that even during summer, installation vessels will spend time waiting for sufficient weather windows. If an operation requires 24 hours for completion, the weather must be below the weather window restrictions for the whole period. This complicates the detailed planning of the offshore campaign, and delays are not uncommon.

## A1.7.2 Vessels

### A1.7.2.1 Capabilities

Various types of installation vessels are used to install subsea assets, see Table A1.21. The day-rate of hiring a vessel is close to proportional to the size of the vessel. The larger vessels usually have better station keeping capabilities, making them more suited for riser installation/recovery operations which normally require close proximity to the production units, see Figure A1.33 for a typical example. DP III class requirement [[IMO MSC 645, 1994](#)] is becoming more and more common. Larger vessels are also able to store more equipment onboard and do not require as many mobilizations, and the larger vessels have motion characteristics that increases the possibility of crew change by helicopter. Hence, the total cost of each vessel must be assessed for each individual project.

Table A1.21: Vessel types

Vessel category	Description
Supply vessel	Used to transport equipment on deck, often used to base ROV operations and dive support. Very common and comparatively low cost. Does not have crane or winching possibilities.
Anchor handling vessel	Used to manipulate anchor systems. Comparatively low cost vessel with winch for anchor system interaction.
Light construction vessel (IMR vessel)	Used mainly for inspection and light subsea construction tasks. Are usually fitted with ROVs and medium sized crane(s). Varying station keeping capabilities
Offshore subsea construction vessel	Vessel with large cranes, pipe lay tower, large work ROVs and deck space for pipe reels. Larger vessels have carousels where the pipes are stored. Vessels usually have very good station keeping (DP III class [IMO MSC 645, 1994]) capabilities. The vessels have capability for performing most installations operations offshore. Given the size and complexity of the vessel, the pipe lay vessels are usually high-cost, with large variation in price.



Figure A1.33: Typical large Offshore Subsea Construction Vessel with a VLS mounted at the side of the vessel. Image courtesy of Emas AMC ([www.emas.com](http://www.emas.com))

### A1.7.2.2 Equipment

A list of equipment used for a typical offshore riser installation/recovery is included in Table A1.22

Table A1.22: Installation vessel equipment

Name	Description
Aft deck	Large deck space on the aft of the vessel where all the installation equipment is located. The aft deck is usually configured and outfitted for each specific job
Carousel	A rotating, cylindrical compartment used to store pipe or umbilicals either on or underneath deck
Installation aids	Sand bags, turning bollards, mattresses, clump weights, buoyancy modules, subsea winches, lifting clamps
Lay tower	Large tower structure that guides the pipe in a controlled manner into the water. May be located aft, on either of the sides or over a moonpool.
Moonpool	Opening in the vessel where either equipment/ROVs are launched through or pipe is installed through. Pressurised air can be used to lower the water level
Reel	Large cylindrical storage unit for pipes and umbilicals
Reeldrive system/Dolly base	Motorised equipment that holds and turns the reels.
ROV	Remote Operated Vehicle that is lowered into the water to perform interactions with equipment or serve as observation posts. The ROV pilot controls the ROV via an umbilical cord with hydraulic supply lines and video transfer.
Deck tugger winches	Used to handle pipe ends on deck and guide the pipe into the lay tower
A&R winch	Abandon Recover winch used to either lower or pick up pipe ends from the seabed. Usually fitted as part of the lay tower
Sand bags	Used to manipulate the routing of the pipes or build up pipe
Mats	Used for landing objects on the seabed to avoid them sinking into the soil.
Temporary anchors / clump weights	Used as attachment points / hold-back resistance on the seabed or as counterweights to buoyancy
Vessel Crane	Dictate how much weight can be manipulated on the seabed. Larger vessels can utilize larger cranes. Usually heave-compensated.

### A1.7.3 Installation Operations

#### A1.7.3.1 General

The initiation of a large number of failure modes for flexible pipes can be traced to mistakes that have been done during or events from fabrication, transportation or installation. Typical

non-conformances are related to handling issues, where the outer sheath is exposed to sharp objects, over-bent or compressed, and it is important that handling issues are addressed and mitigated by the installation contractors. Common non-conformances from installation are shown in Table A1.23, and operations related to the flexible pipe installation are listed in Table A1.24

Table A1.23: Common non-conformances from installation

Non-conformance	Description
Damaged and pierced outer sheath	Sea water filled annulus with subsequent potential corrosion of armor wires and reduced pipe service life.
Compression	The tensile armor wires may radially expand/birdcage, possibly affecting cross-section strength and deform outer sheath.
Open annulus vent port	Same as pierced outer sheath.
Buoyancy not clamped correctly	Loss/movement of buoyancy module.
Over-bending	Excessive straining and damage of pressure liner and potential unlocking of pressure armour
Dropped objects	Outer sheath damages, loss of equipment, damaging subsea equipment
Attaching the end fitting to reel	Incorrect attachment of the end fitting may lead to damage to the end-fitting itself or over-bending of the pipe
Bending stiffener over-bending	Wrinkling of the bending stiffener. This will alter the performance of the bending stiffener for a period, while the bulges may return to their original shape after a few years
Incorrect placement of tethers	The riser configuration will not be as designed, the consequence of this is project-specific.
Incorrect placement of buoyancy modules	The riser configuration will not be as designed, and the consequence of this is project-specific.
Touchdown area compression	See Compression.
Damage neighboring equipment	Project-specific. Damage to the external sheath of other risers, high tension and movement of other subsea equipment, tears in umbilicals.
Vessel drift-off and over pull / over bending	The flexible pipe, the structure it is connected to and the installation vessel equipment may be significantly damaged
Incorrect handling of clump weights	The clump weights may come loose, fall onto equipment or personnel. Large vessel motions while handling clump weights may be hazardous.

Table A1.24: Common operations related to flexible pipe installation

<b>Operation</b>	<b>Description</b>
Tie-in	The pipe ends are connected to subsea structure.
Pipe-lay	The pipe is laid along a predefined route.
Flowline retrieval	Retrieval of flowlines.
Trenching	Use of jet or other means to dig trenches for the flowlines to be lowered below sea-bed. Trenching machines will usually lower the pipe into the trench immediately before the trench walls collapse.
Rock dumping	The rock is dumped onto the pipe to provide trawl protection and prevent upheaval buckling
Riser installation	Installation of riser sections.
Riser replacement	Removal of risers.
Subsea equipment installation	Installation of PLEM/PLETs, T-joints, SSIV and more.

### A1.7.3.2 Flowline installation

During a typical flowline installation, the pipe is lowered to the seabed, usually using a VLS or a HLS and by deploying installation aids to maneuver to and land the first pipe end in the target box. Then the vessel moves along a predefined route and lays the pipe on the seabed. The second pipe end is lowered using the crane and installed in the second end target box.

Typical problems encountered during flowline installation operations include:

- Pipe sliding along the sea bed
- Difficulties maintaining the correct tension
- Vessel drift-off
- Flexible pipe handling issues on the vessel
- Repair of outer sheath damages

Remember to

- Avoid over-bending
- Avoid sharp edges against outer sheath
- Maintain tension according to procedure
- Monitor touchdown point

### A1.7.3.3 Trenching

Specialized vessels are lowered onto the seabed to control the trenching process. The remotely operated vessel will jet or dig a trench while lowering the pipe into the trench.

Typical problems encountered during trenching operations include:

- Unexpected high density soil sections in the trenching route

- Trench wall collapse
- Over-bending of the pipe during transitions

Remember to

- Avoid sharp transitions
- Avoid sharp edges
- Verify the trenching is successful

#### A1.7.3.4 Rock-dumping



Figure A1.34: Rock dumping illustration, courtesy of 4subsea

The rock dumping is performed by lowering a funnel on top of the flexible and dropping rocks onto the flexible, see Figure A1.34. This provides trawl protection and more details for the operation is found in Section A1.5.

Typical problems encountered during trenching operations include:

- Obtaining the required rock dump height
- Obtain the rock dump flow into the funnel

- Maintaining the correct vessel speed

Remember to:

- Maintain correct pressurization and content
- Avoid damage to outer sheath

#### A1.7.3.5 Tie-in

The tie-in operation is required to connect the wet-stored pipe ends to the subsea structures. Many proprietary tools have been developed for these operations, and issues regarded the tie in process is discussed in detail in Section [A1.5](#).

In general, the pipe end is fitted with a specific connector which corresponds to the subsea structure that it will be connected to and that interfaces with a tie-in tool. Tie-in tools are usually connected to and deployed with ROVs. A common procedure is for a ROV to connect a wire onto the pipe end which is connected to the tie-in tool docked onto the subsea structure. The wire is winched until the pipe end is located near the subsea structure connection. The tie-in tool then aligns and locks the head in the position and connects the subsea structure. The tie-in tool is then retrieved.

Typical problems encountered during tie-in operations include:

- Subsea head being outside tolerances of tool
- Manipulation of pipe with winch/buoyancy to assist operation

Remember to:

- Install subsea head within tolerances of the tie-in tool required.

#### A1.7.3.6 Flowline retrieval

In general, the operation is the tie-in, rock dump and flowline installation in reverse. The pipe ends are left in a target box, the rock removed, the crane or/and A&R winch is used to lift the pipe back onto the deck and the vessel starts reeling pipe onto the vessel.

Typical problems encountered during retrieval operations include:

- Damage to outer sheath due to process for removing rock dump
- Over-bending
- Burst of outer sheath due to annulus gas expansion

Remember to:

- Monitor Gas Relief Valves to verify gas is escaping the annulus

#### A1.7.3.7 Riser installation

A riser installation usually involves installing a flexible pipe that is hung-off from a platform and connected to a subsea structure or a connecting flowline on the seabed. Risers are

usually installed from reels. A riser can be installed with both the topside and the subsea end as first end of the vessel depending on the type of riser configuration, but the latter is the most common. An installation usually starts with initiating the subsea end towards a connecting structure or an initiation clump weight. The subsea head is then landed and the pipe is laid down on the seabed by moving the vessel in along a predefined route. Buoyancy modules are fitted onto the pipe to form the hog and sag bend. The topside end (the second end) is deployed from the vessel by lowering the head either with an A&R winch or by using the crane and cross-hauling it to a winch wire from the platform. The installation vessel will then disconnect from the riser, and the platform will pull the riser in and hang off.

When replacing existing risers, the new riser is normally installed between neighboring risers, implying strict requirements to vessel station keeping capabilities and adherence to weather criteria to avoid contact with existing risers.

Typical problems:

- Contact with neighboring risers and potential damage
- Damage to existing risers by ROV
- Installing risers in pliant waves require extensive movement of platform to install static route underneath platform.
- Overbending of pipe
- Damage to outer sheath from installation equipment

Remember to:

- Perform detailed analysis of the operation to understand installation limitations

#### A1.7.3.8 Riser Recovery

A riser recovery is in principle the reverse operation of a riser installation. Normally the riser being recovered will be scrapped, implying less weather limitations to the operation. Operations close to platforms are still as critical as for installation.

Typical problems:

- Contact with neighboring risers and potential damage
- Damage to existing risers by ROV
- Recovering risers in pliant waves require extensive movement of platform to install static route underneath platform
- Old riser being stuck in mud
- Gas leaks from outer sheath breaches

Remember to:

- Perform detailed analysis of the operation to understand installation limitations

### A1.7.3.9 Subsea Equipment installation

Installation of subsea equipment is varied, and only a few general comments will be included here. Large subsea structures like manifolds, X-mas trees and other equipment is not part of the scope, thus the focus will be on PLEMs, SSIVs, seabed suction anchors and other.

### A1.7.4 Post-Installation Procedure

After finishing the installation, the field will be cleaned for installation aids, the vessels will de-mobilize and the as-built documentation is gathered in a Design, Fabrication and Installation resume and delivered to the client.

### A1.7.5 Documentation

The design documentation may change over time as the design and analysis iterations progress. To obtain an overview of the installation package and as built configuration, the following documents are useful.

Table A1.25: Documentation

Operation	Description
Design, Fabrication and Installation resume (DFI)	The DFI includes as build data sheets, non-conformances, and configuration drawings.
Packing plan	The packing plan shows the reels that are being transported.
Daily reports	A journal that gives an overview of the activities on deck during installation for each day, planned and completed activities for the campaign.



## **Chapter A2**

# **Flexible Pipe Properties and Materials**

*Author: Stig Berge (NTNU), Morten Eriksen (4Subsea)*

## A2.1 General remarks

Non-bonded flexible pipe is a key to floating production of offshore oil and gas, and is used in many and diverse applications:

- Production risers for oil and gas
- Water or gas injection
- Gas lift
- Oil or gas export
- Test production
- Drilling
- Well maintenance
- In-field flowlines
- Jumpers

Depending on the specific application the demands in terms of dimensions, strength, flexibility, chemical compatibility, temperature tolerance and other properties may vary within wide margins.

The main global strength characteristics of a flexible pipe are:

- Small bending stiffness; can be repetitively bent to a small radius of curvature and laid from a reel
- Large volume stiffness and strength; containment of high pressure fluids, resistance against external pressure and forces
- Large axial tensile stiffness and strength; can be deployed at large water-depths

These favourable properties come at the expense of properties that are less favourable:

- Small torsional stiffness and strength
- Small axial compressive stiffness and strength

Table A2.1: Characteristic properties of flexible pipe.

Property	Comment
<i>Flow related</i> <ul style="list-style-type: none"> <li>▪ Internal diameter</li> <li>▪ Pressure capacity</li> <li>▪ Materials, composition</li> </ul>	<i>Relevant for transport function of the pipe</i> <ul style="list-style-type: none"> <li>▪ Transport capacity</li> <li>▪ Pressure ranges</li> <li>▪ Chemical compatibility with respect to internal flow. Prevention of diffusion and leakage</li> </ul>

<i>Support related</i>	<i>Relevant for structural integrity verification for installation and operation phases</i>
<ul style="list-style-type: none"> <li>▪ Bending flexibility</li> <li>▪ Weight</li> <li>▪ Radial compression strength</li> <li>▪ Axial force capacity, torque behaviour</li> </ul>	<ul style="list-style-type: none"> <li>▪ Entire motivation for using flexible pipe</li> <li>▪ Governs requirement to tension capacity</li> <li>▪ Water-depth limitation</li> <li>▪ Relevant with respect to static and dynamic loading</li> </ul>

Table A2.2: Overview of support related properties

Property	Symbol	Comment, relations
<b>Weight</b>	$m$ $w_a$ $w_w$ $\rho_\rho$	mass per unit length weight in air weight in water, water filled average material density of pipe wall $w_a = mg$ $w_w = mg(1 - \rho_w/\rho_\rho)$
<b>Bending</b> Curvature  Bending moment - curvature relationship Bending stiffness	$R_{MIN,s}$  $R_{MIN,d}$  $EI$	Minimum radius of curvature, static, storage. $R_{MIN,s} \approx 5.5 - 7 \cdot d_{ext}$ Do., dynamic. $R_{MIN,d} \approx 8 - 12 \cdot d_{ext}$ Complex relationship, also involving hysteresis and visco-elastic properties. Simplest model. Some data available
<b>Tension</b> Capacity  Axial stiffness	$T_{max}$ $T_c$ $EA$ $k$	Max allowable support force (effective tension) Collapse tension Elastic stiffness. Nonlinearities and hysteresis / visco-elastic properties may be significant but not as important as for bending
<b>Torque</b> Capacity  Torsional stiffness	$\theta_w$ $\theta_c$ $GI_t$	Max allowable torsion angle Collapse torsion angle Stiffness may be nonsymmetric

This combination of properties is obtained by a composite pipe wall, as shown in Figure A2.1, combining steel and polymer materials in a non-bonded structure, i.e. each layer may slide relative to adjacent layers. The basic concept of a flexible pipe is a fluid barrier made from a flexible polymer that can be bent to a small radius of curvature, layer 2 in Figure A2.1. The function of all the other layers is to provide strength, support and protection of the fluid barrier, while maintaining the low bending stiffness of the pipe. This is achieved by using helically wound steel armour in combination with flexible polymer materials, in a non-bonded structure. The number and construction of the layers depend essentially on the diameter and pressure rating of the pipe. Large diameter pipes for high pressure applications may have around 20 layers in the pipe wall.

Flow related properties are related to the transport function and are mainly determined by pressure capacity and internal diameter. These parameters may be measured and documented

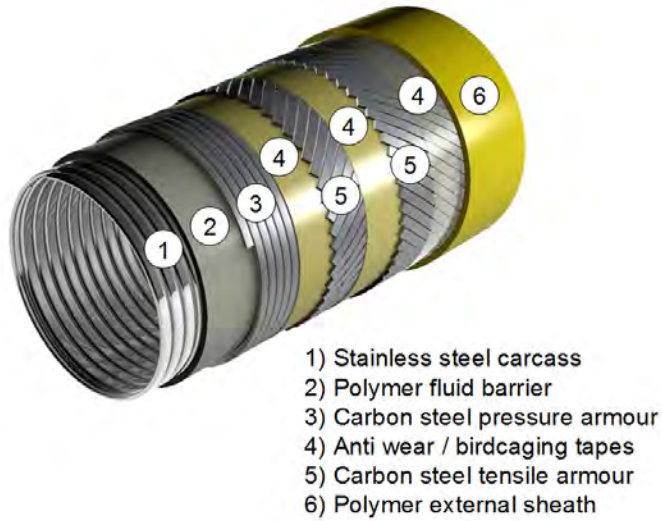


Figure A2.1: Typical cross section of a non-bonded flexible pipe. (*Courtesy of GE Oil & Gas*)

fairly easily. Chemical compatibility and temperature tolerance are also important flow related parameters that are not so easily documented.

## A2.2 Pipe wall structure and materials

The wall of a flexible pipe including ancillary components is a composite structure (Figure A2.1) where a wide spectrum of materials is used:

- Polymer materials
- Steel materials
- Synthetic fibres
- Foam materials

Each layer has a specific function and is interacting with the other layers. The complexity of the structure may be illustrated by the range of elastic moduli of materials that are used, Table A2.3. In addition to the range of elastic properties the materials also differ widely in terms of strength, ductility, wear, creep, thermal expansion and other characteristics.

Table A2.3: Elastic moduli for flexible pipe materials.

Material	Elastic modulus (MPa)
Polyurethanes	2-12
LDPE	55-410
Polyamide 11	300-1300
PVDF	500-1600
XLPE	600-1500
HDPE	690-1800
Polyamide 12	1200-1550

Silica glass	71 000
Aramid fibre	124 000
Carbon fibre	165 000
Steel	210 000

The combination of materials that are used for a given flexible pipe design depends on the specific application. [API 17B, 2008] gives a generic description of the grades of materials that are used for the different layers. [API 17J, 2008] gives detailed specifications for the qualification testing requirements. Herein a brief and descriptive review is given on each layer and function, and the materials that are used based on [Berge and Glomsaker, 2004].

### A2.2.1 Pipe wall structure

In Figure A2.2 is shown a pipe wall in more detail. As described above, the internal pressure sheath (liner) is the fluid barrier. The polymeric liner has very little strength relative to the forces that are acting, from the inside as well as the outside, and a number of additional layers are added to provide strength and protection.

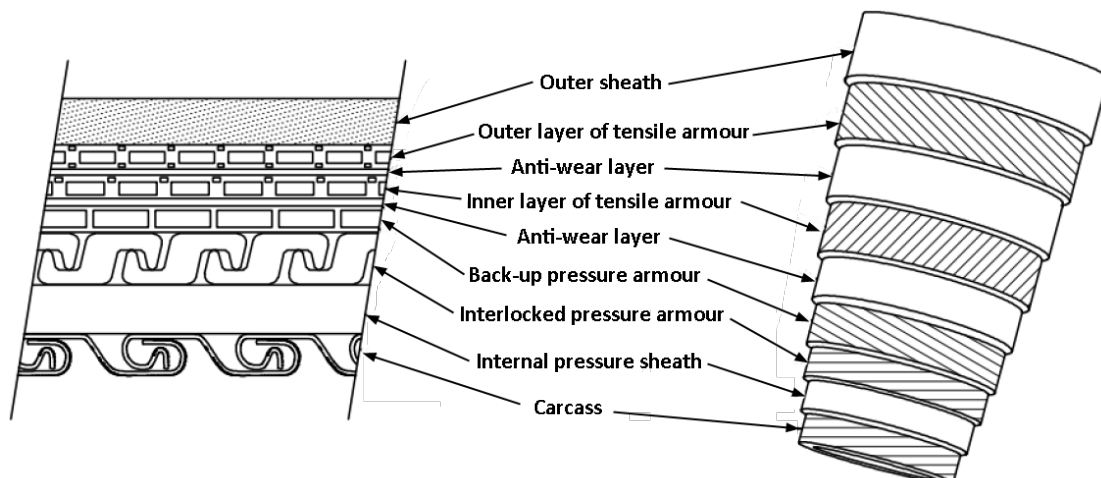


Figure A2.2: Pipe wall structure, in more detail.

### A2.2.2 Carcass

The carcass is the innermost layer of a pipe, and the only metallic component that is in direct contact with the fluid in the bore. The material must be compatible with the chemical constituents of the transported liquids and/or gases. A wide variety of austenitic and duplex stainless steels have been used as carcass materials for unbonded flexible pipes. The main drivers for selection of material for carcass are corrosion resistance to operating environment, mechanical strength and price.

For most applications austenitic stainless steel, typically AISI 304L, 316L or similar is used. For less corrosive bore fluids carbon steel or ferritic stainless steel may be used. More demanding applications may require high-alloy stainless steel (duplex), nickel-alloyed or molybdenum-alloyed steel. Table A2.4 A2.4 gives a list of typical grades used as carcass materials in flexible

pipes, [Gudme and Steen Nielsen, 2009]. A procedure for qualification of carcass materials is described by [Gudme and Steen Nielsen, 2009].

Table A2.4: Standard material grades considered as carcass grades.

Grade name	UNS number	Microstructure	Yield (MPa) Typical values	UTS (MPa) Typical values
304L/316L	S30403/S31603	Austenitic	270-350	520-670
Lean duplex	S32101	Duplex	580-700	700-900
Duplex	S32205	Duplex	600-800	750-1000
Super duplex	S32750	Duplex	750-900	900-1100
6Mo	S31254	Austenitic	340-430	680-900
6Mo-high Ni	N08367	Austenitic	310-400	690-900

Before going into the carcass machine the strips are welded into continuous lengths, usually by gas tungsten arc welding (GTAW). Weldability needs to be considered, [Tavares et al., 2010].

The function of the carcass is to provide strength against external hydrostatic pressure. The carcass also provides strength to resist crushing loads during installation operations and handling of the pipe. At large water depths the hydrostatic as well as the crushing loads will increase. A final function of the carcass is to provide mechanical protection of the liner against pigging tools and abrasive particles.

The carcass is produced from continuous strip of material onto a mandrel. In the carcass machine the strip is formed as a helix of folded S-shaped strip which is geometrically locked each turn into the next, to form an interlocked tube, Figure A2.3. The cylindrical structure provides stiffness and strength in the radial direction. Bending flexibility is obtained by the ability of each profile to slide with respect to the neighbouring profiles. The carcass is an open structure and does not provide any containment of internal pressure, i.e. oil and gas can flow across the carcass, albeit with severely restricted flow rate.

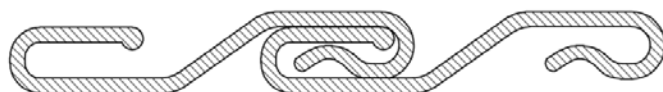


Figure A2.3: Typical carcass profile.

The armour structure outside of the liner is open Figure A2.2. In the case of a ruptured outer sheath, sea water will penetrate into the structure and the external pressure will be acting directly onto the liner. The carcass thus needs to carry the entire load from external water pressure. A basic design criterion is given by the external pressure at maximum water depth, assuming empty pipe. For the clamping or handling loads the steel armour outside of the liner contributes significantly to the strength.

Carcass collapse may also be caused by release of absorbed gas in the liner. During high pressure operations the liner will become saturated with gas, which will be released in the case of a low pressure shut-down. For multilayer liners, if proper venting is not provided for the slits between the layers of liner, pressure may build up to cause collapse of the carcass. The carcass is normally not designed for this condition, which must be avoided by design (venting of the liner) or by operational restrictions. Also for single layer liners depressurisation may be a problem. If the pressure drops rapidly, the restricted rate of flow through the carcass

may lead to build-up of pressure between the carcass and the liner that could cause collapse of the carcass.

The collapse capacity is strongly dependent on whether the carcass is fully supported by the surrounding structure (liner/pressure armour) or whether there is a gap. A gap may be caused by several mechanisms:

- Stretching and possibly deformation of the carcass due to force of gravity.
- Shrinking of liner due to deplastification, possibly counteracted by swelling due to absorption of hydrocarbons and/or gas.
- Pressure induced creep of liner into gaps in pressure armour profiles.

The forming of a carcass profile from metal strip is a cold-forming process. For a given material there are technological limitations with regard to the thickness of a strip that can be formed to a carcass profile like the one shown in Figure A2.3. The collapse strength of the carcass, which is essentially determined by the stiffness (moment of inertia) of the profile, has basic limitations for this reason. Collapse strength to resist hydrostatic pressure as well as crushing loads from installation equipment may be a limiting factor for deep water applications of large diameter pipe.

More compact and stiffer profiles are under development, [Rytter and Nielsen, 2002], that may extend the deep water range of flexible risers.

Flexible pipe with a carcass layer are termed rough bore pipe. For transport of fluids with no gas content, e. g. water injection, smooth bore pipe may be an option, with less flow resistance and reduced cost.

### A2.2.3 Liner

The liner is the sealing layer, made from a thermoplastic by extrusion over the carcass. In some applications a multi-layer liner is used, with sacrificial layers on the inside and/or the outside of the sealing layer. The purpose of the sacrificial layers is to provide protection against the metallic components on the inside and the outside. The liner is exposed to the fluid in the bore. The properties of the liner give the basic limits for the upper service temperature of the riser and the chemical composition of the fluids that may be transported through the line.

Different materials may be used, depending on the design conditions. Three generic classes of materials used as liner are:

- High density polyethylene (HDPE) and cross-linked polyethylene (XLPE)
- Polyamide (nylon) (PA11 or PA12)
- Poly vinylidene fluoride (PVDF)

Within each class of materials a number of grades with a large variability in properties are available. Some of the materials used are brand names, protected by patents or licenses as shown in Table A2.5. There is a continuous development of polymer materials for liner applications, and the table is not claimed to be complete.

A major criterion for selection of liner material is the design temperature. In general, HDPE has very good chemical resistance and maintains good mechanical properties up to 60 °C.

Table A2.5: Polymers used in the liner for flexible pipes.

Material	Description
Rilsan®	PA11 + plasticizer
Solef® 60512	PVDF/CTFE (Copolymer with Chlorotrifluoroethylene)
Solef® 1015/078	PVDF + plasticizer
Gammaflex®	PVDF/HFP (Copolymer with Hexafluoropropylene)
Coflon®	PVDF + plasticizer
HDPE/XLPE	

However, hydrocarbons like crude oil, methane, methanol etc., are absorbed and may work as plasticizer. Therefore, if the bore fluid contains hydrocarbons, HDPE may be used at low and moderate temperatures only, generally below 20 – 30 °C. Crosslinking may in general improve high-temperature properties and in addition reduce the absorption of hydrocarbons, and thus XLPE may be used at somewhat higher temperatures than HDPE.

Polyamide materials may be used at higher temperatures but are very sensitive to humidity. In the case of a high water cut, polyamide suffers from hydrolysis at elevated temperatures. The main mechanism of hydrolysis of PA11 and PA12 is chain scissoring (reduced molecular weight), causing brittleness. Prediction of service life in various environments has been a major complication with this material, [Ottøy et al., 2001]. The Rilsan User Group (RUG), which is a collaboration between a range of operators and suppliers, has developed a new procedure for prediction of the life time and degradation rate for Rilsan®, published by American Petroleum Institute (API) as a Technical Report [API 17TR2, 2003]. According to [API 17TR2, 2003], the extrapolated service time for Rilsan® at 60 °C in a typical well flow (humid, pH4) is 20 years. Nevertheless, Rilsan® is considered as the most used liner material within the North Sea, [MCS Kenny, 2001].

PVDF may be used at higher temperatures, possibly 130°C with present brands. However, typically 20% plasticizer is added to PVDF homopolymer, in order to improve processing (extrusion) properties and reducing the possibility for defects like blisters. In contact with hydrocarbons, the plasticizer tends to be extracted from the PVDF, leading to permanent shrinkage of the material which again has contributed to several failure modes: Pull-out or rupture of the liner at the end termination and collapse of the carcass due to pressurized gaps in multilayer liners. The former problem has been mitigated by use of accelerated deplastification of the end section of the liner before mounting of end termination.

Developments are ongoing for liner materials to improve processability and to increase the high temperature performance, [MCS Kenny, 2001]. This development is mainly run by the suppliers and the material industry.

### A2.2.3.1 Annulus

The section between the liner and the external sheath is the pipe annulus. This is an open structure with no pressure barriers. In a pipe that is transporting a fluid under high pressure, gas and liquid will permeate through the liner and cause pressure build-up in the annulus. To prevent rupture of the external sheath, the annulus is vented at the end terminations, typically at 1–2 bar overpressure.

In the as-fabricated state, void space in the pipe annulus is filled with atmospheric air. During operation the chemical composition may change, for several possible reasons:

The outer sheath may become damaged, during installation or operation. This will lead to sea water flooding of the annulus. Depending on the nature of the leak, sea water in the annulus could be depleted of oxygen, or possibly saturated with air. If the leakage is located above the sea level, ingress of air and salt moisture may take place. Efficiency of cathodic protection is uncertain. Sea water may be combined with H<sub>2</sub>S and/or CO<sub>2</sub> due to permeation from the well flow.

Over time diffusion of water vapour through the liner may lead to condensation of water (H<sub>2</sub>O) in the annulus. In combination with gaseous components like hydrogen sulphide (H<sub>2</sub>S), carbon dioxide (CO<sub>2</sub>) and methane (CH<sub>4</sub>) the condensation may lead to a corrosive environment. In this case the environment will be anaerobic.

Risers which have been subjected to sea water ingress may be repaired, flushed with inhibitor, and re-installed. Inhibitor fluid, possibly with some residual sea water and with CO<sub>2</sub> or H<sub>2</sub>S due to permeation from the well flow, could have an effect on residual fatigue life.

These environments may have a significant effect on fatigue life of steel components, and need to be considered in design and operation.

#### A2.2.4 Pressure armour

The primary function of the pressure armour is to back up the liner and to provide resistance against the hoop stress caused by internal pressure. The pressure armour is also a strength component with respect to external forces, e.g. crushing forces due to handling or accidental loading.

The pressure armour is an interlocking profile made from rolled carbon steel with tensile strength in the range 700 – 900 MPa. Three different profiles are currently in use, Zeta/Flexlok, C-clip and Theta, Figure A2.4, Figure A2.5 and Figure A2.6. Some of these profiles are protected by patents or licenses.

The interlocking of the pressure armour is a limiting factor for the minimum bending radius of the riser. If this limit is exceeded, irreversible damage to the flexible line may occur, leading to perforation of the liner when subjected to internal pressure.

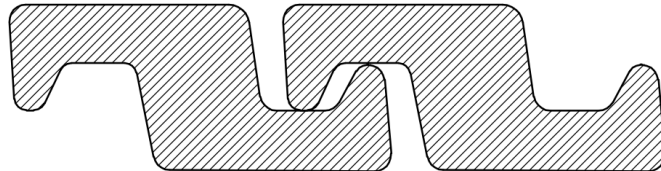


Figure A2.4: Zeta/Flexlok interlocking profile used as pressure armour.

For high pressure applications the interlocking layer may be strengthened by an additional layer of rectangular steel profiles that are not interlocked, cf. Figure A2.3.

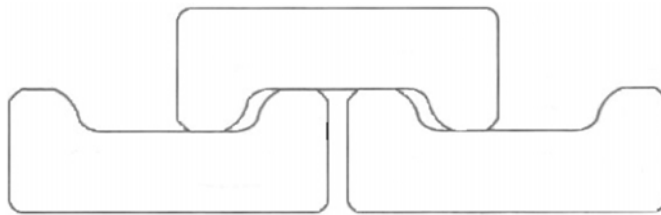


Figure A2.5: C-clip interlocking profile used as pressure armour.

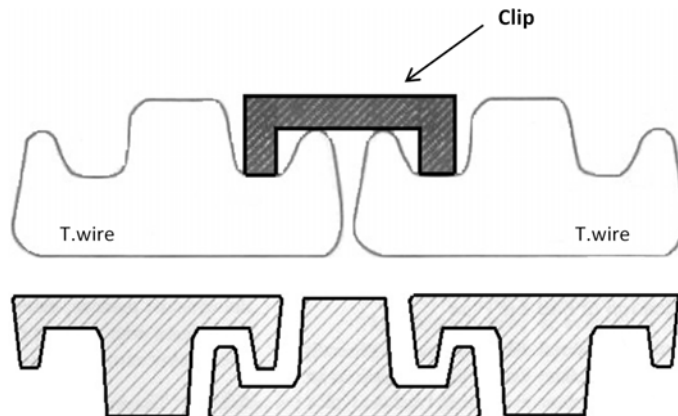


Figure A2.6: Theta-shaped interlocking profile (two variants) used as pressure armour.

### A2.2.5 Intermediate sheath

Smooth bore pipes with no carcass layer are vulnerable to external pressure from water ingress into the annulus. If the external pressure is exceeding the collapse pressure of the liner, an intermediate sheath must be provided, outside the pressure armour. The intermediate sheath is generally made from the same materials as the liner.

### A2.2.6 Tensile armour

The tensile armour is two or four layers of armour wire and provides strength against axial stress caused by internal pressure and by external loads. The layers are counter-wound to avoid torsion when axial loading is applied, Figure A2.1. The lay angle in most cases is 30 to 35 deg. The tensile armour also provides torsional strength to the pipe. However, for torsional loads in a direction leading to unwinding of the outer layer of armour (bird-caging) the strength and stiffness is poor.

The wire profile is rectangular, or close to rectangular, and is produced by cold rolling from drawn rods of carbon or low alloy steel. In general, armour wire is not made from standardized grades of materials, the grades are in most cases proprietary to each supplier of pipe. Heat treatment (quench and temper or annealing) is applied as needed to limit the yield strength. The strength is essentially governed by the carbon/alloy content and heat treatment. The governing factor for the use of high strength steel is whether hydrogen sulphide ( $H_2S$ ) is present.

Before going into the armour spinning machine the wires are welded into continuous lengths, usually by electrical resistance welding. Weldability needs to be considered. In dynamic

applications the tensile armour is subjected to fatigue loading, and fatigue strength of the welds may be an issue.

Tensile armour is generally classified on the basis of 'sweet' or 'sour' service, following the criteria given by NACE [[NACE TM 01-77, 1996](#)]. Sour service wire has tensile strength (UTS) generally below 900 MPa. Sweet service wire has a tensile strength in the range 1200-1500 MPa. In many cases the strength of the tensile armour needs to be optimised for specific designs, and other strength grades are also used.

The tensile armour alone carries the top tension of a riser, and is a critical component for deep water applications. The development of deep water risers is a driver for the use of higher strength steel, to reduce top tension. There is an ongoing activity to develop and to qualify higher strength steels with resistance to corrosive environments, in particular  $H_2S$ , cf., [[Rubin and Gudme, 2006](#)], [[Désamais et al., 2007](#)].

### A2.2.7 Composite armour

Beyond 2 000 metres of water depth the weight of conventional flexible pipe becomes critical not only for the pipelay equipment and vessel but also for the production floater. Substituting the tensile steel armour with composite armour made from fibre reinforced polymer has a potential of reducing the weight of pipe significantly.

[[API 17J, 2008](#)] specifies that it does not apply to flexible pipe that employs non-metallic materials for the pressure and tensile armour. However, in the next revision of [[API 17B, 2008](#)] a dedicated Annex H will be included on 'Composite Armour for Unbonded Flexible Pipe' with reference to [[DNV-OS-501, 2009](#)].

Carbon fibre composite armour has been qualified for flexible risers, [[Do and Lambert, 2012](#)], and concepts are under development for ultra-deep water risers utilizing this technology, [[Do et al., 2013](#)].

### A2.2.8 Anti-wear tape

In a flexible riser subjected to cyclic bending the tensile steel armour wires will slide cyclically relative to adjacent steel layers, with significant contact stress. If two layers of steel armour are in direct contact, wear or fretting fatigue may take place. For this reason anti-wear tape is applied between layers of steel armour. The tape is not leak-proof, and fluids in the annulus may flow through the tape.

The materials used for the tape are thermoplastic tape like Rilsan® with a thickness of around one millimetre. The tape is subjected to significant contact stress and large slip amplitudes. Cumulative slip for a 20 year design may be of the order of  $50 \cdot 10^3$  m. The tape must thus retain a minimum strength at the temperature of the armour, and to be resistant against wear, creep and other types of degradation mechanisms. If the tape fails during service, fatigue life may become significantly shortened, [[Berge and Sævik, 1993](#)].

ISO 13628 does not specify any criteria with regard to the wear properties of anti-wear tape, except general statements. Test procedures and qualification criteria are apparently not established.

### A2.2.9 Anti-buckling tape

Flexible pipe is vulnerable to torsion loading and to axial compression loading, which may occur during installation and in shut-down conditions. These loading modes may lead to radial buckling or 'bird-caging' of the tensile armour and to lateral buckling of tensile armour wires. For this reason anti-buckling tape may be provided outside the outer tensile armour layer. Aramid or glass fibre reinforced tape is used for this purpose.

### A2.2.10 Thermal insulation

In some cases thermal insulation of the pipe is required, made from foam materials or solid insulation. The insulation layers are located between the tensile armour and the outer sheath.

### A2.2.11 Outer sheath

The function of the outer sheath is to provide a seal against the sea water in order to prevent corrosion and to give mechanical protection to the steel armour. The loads that are typically applied on the outer sheath are impact, erosion and tearing as well as, in certain cases, external or internal pressure. The material is extruded thermoplastic x96 in most cases HDPE or Rilsan®. According to available information, MCS (2002), nearly 40% of the riser failures are due to external sheath damage and most of these took place during installation.

### A2.2.12 Bend stiffener

A flexible pipe is terminated with an end fitting where all layers are anchored and clamped in a rather complicated structure. At the interface the transition in bending stiffness is of the order 1:100. For bending loading of a pipe hanging from the end termination this will lead to a very large stress concentration. The same is the case for a pipe being deployed through an I-tube. A tapered bend stiffener is often used, to provide a gradual transition in stiffness from the pipe to the end termination or the I-tube and to limit the curvature.

Bend stiffeners are made from polyurethane, which may be cured to a range of elastic moduli. The mechanical connection to the end termination is provided by steel inserts. Bend stiffeners may have a large size, several metres in length and more than 1.5 m diameter at the base with a weight of more than 1.5 ton. The bend stiffeners need to be designed to the same fatigue life as the pipe.

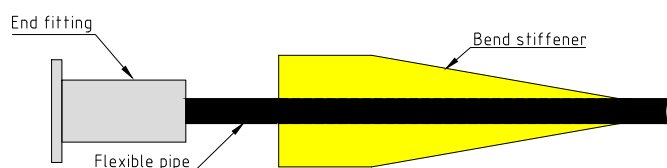


Figure A2.7: Polyurethane bend stiffener.

### A2.2.13 Smooth bore pipe

Flexible pipe with a carcass layer is termed 'rough bore' pipe. For transport of fluids with no gas content, e. g. water injection, 'smooth bore' pipe without a carcass may be an option, with less flow resistance and reduced cost. In the case of a damaged outer sheath the external hydrostatic pressure will act against the polymeric liner. A smooth bore pipe will thus have very little capacity against external hydrostatic pressure, and an anti-collapse sheath may be required, located between the pressure and the tensile armours, to utilize the collapse strength of the pressure armour.

### A2.2.14 Flowlines

Due to the low cost of installation relative to steel pipe, nonbonded flexible pipe is often used as in-field flowlines. In that case the tensile armour lay angle may be adjusted to the 'balanced' angle at which the pipe is neutral with respect to fluctuations in the internal pressure, i. e. there is no change in the length of the pipe due to pressure variations. In a pipe with no pressure armour and the internal pressure being resisted by the tensile armour alone the balanced lay angle is 54.7 deg. In pipes with pressure armour, which is generally the case, the balanced lay angle depends on the proportion of steel in the pressure armour and tensile armour respectively. The optimum lay angle is then typically 35 to 40 deg but may lie outside this range in some cases.

## A2.3 Polymers for liner applications

### A2.3.1 Introduction

#### A2.3.1.1 Purpose

The purpose of this section of the handbook is to provide

- an overview of polymers used in flexible pipes. Together with
- an update on status on field experience and knowledge built over recent years.

The main focus is on performance and service life issues of polymers used as pressure sheath.

#### Disclaimer

The review and discussion presented is not intended to be exhaustive on the subjects but address topics that to the knowledge of the author are relevant to the service life performance of polymer materials.

#### A2.3.1.2 Requirements and Guidance from ISO/API

The primary function of the pressure sheath is to provide adequate sealing for fluids and gas in the bore to ensure the required containment within the bore.

Industry requirements for design of the polymer layers and components in flexible pipes are defined in [API 17J, 2008]. The design criteria are defined in Table 6.3 in [API 17J, 2008]. The section relating to the pressure sheath is shown below:

Internal pressure sheath	Rupture	Thinning <sup>(4)</sup>	The maximum allowable reduction in wall thickness over the service life below the minimum design value, due to deformation into gaps in the supporting structural layer, shall be 30 % under all load combinations.
		Strain	For each polymer material for both static and dynamic applications, the allowable bending strain shall be as specified by the manufacturer, who shall document that the material meets the design requirements at that strain. The maximum allowable bending strain at nominal dimensions shall be 7,7 % for PE and PA, 7,0 % for PVDF in static applications and for storage in dynamic applications, and 3,5 % for PVDF for operation in dynamic applications <sup>(5)</sup> .

Figure A2.8: Section from Table 6.3 in [API 17J, 2008]

The background for the defined maximum strain limits is believed to be:

- When a flexible pipe is reeled on a reel with a diameter that is 12 times the diameter of the pipe the maximum strain in the outside cover is 7.7 % for the inner layer on the reel. This may originate from the cable industry where cables often have been reeled on drums with diameters that are 12 times the cable diameter. When the outside cover is strained to 7.7 % the pressure sheath is typically strained to 7 %. PVDF is never used as an outside cover which may be reason why the maximum strain has been specified as 7.0 %
- It has been suggested that the specific limitation on the maximum dynamic strain for PVDF is taken from a qualification test that Coflexip (at that time) carried out for a client where the maximum dynamic strain requirement was 3.5 %. The test was positive and this strain criterion adopted.

Even though the defined requirements not necessarily seem to be derived directly from functional requirements and material performance properties, field experience may be a good indication that they have been adequate for designs and materials that have been used extensively to now. A Relevant question may be whether these requirements are stricter than needed and therefore lead to more costly designs than needed. It should also be noted that the table imply that the ISO 13628-2 is only valid for Polyethylene, Polyamides and PVDF materials.

**In principle the following 3 requirements should be met throughout the service life:**

1. Adequate creep resistance under the operating conditions for the gaps between the pressure armours.
2. Suitable ductile behaviour to meet the static and dynamic strain requirements with adequate resistance against rupture and fatigue.
3. Adequate material performance to maintain sealing in the end fitting.

The meaning of 'adequate' must be defined from the margins required to meet the risk targets governing the integrity management for the pipes under consideration.

This section on Polymers in Flexible Pipes partly build on

- [API 17B, 2008], in particular Chapter 5 on materials and should be consulted for reference.

- [API 17TR2, 2003]

Guidance on use envelope in terms of temperature and pressure is available in these documents and these will be expanded on in later subsections.

## A2.3.2 Relevant Aspects of Polymer Performance

### A2.3.2.1 The role of polymers in flexible pipes

The primary function of the pressure sheath is to ensure containment of fluids and gases in the bore of the pipe throughout the service life for the pipe. This shall be achieved through interaction with neighbouring steel layers and sealing arrangements in the end fitting. The ideal pressure sheath would be a fully compliant layer performing its required function. Nevertheless fundamental properties of the polymer layer, such as stiffness, ductility, creep, thermal expansion, swelling, shrinking, permeation, thermal conductivity influence flexible pipe designs, properties and function. An example is that the polymer layers contribute to the overall bending stiffness of the pipes. Some polymers also have their own specific service life issues and operational limitations due to chemical ageing.

Since the function of the polymer layer is achieved in combination with steel layers it is also important to highlight some key differences in properties and performance of steel and polymers.

### A2.3.2.2 Typical properties

**A2.3.2.2.1 Polymer structure** A polymer molecule is a long chain of identical monomer units tied together. A polymer is normally identified through the monomer (for example ethylene) and a molecular chain can consist of several hundreds to several thousands monomer units. The long molecules can be organised in a crystalline structure or as a disorganised amorphous phase where the molecules are randomly entangled.

Thermoplastic materials used as pressure sheaths (and in other layers) in flexible pipes are semi-crystalline thermoplastics with a mixture of crystalline and amorphous regions on a microscopic level as illustrated in Figure A2.9.

The percentage volume of the material that is crystalline and the size of the crystalline region will vary between materials and will influence the material properties.

One of the characteristics of the crystalline regions is a melt temperature, which is often referred to as the melting temperature for the polymer. Above this temperature all the material is a visco-elastic amorphous phase. Below the melt temperature the amorphous regions remain visco-elastic. The viscosity and elastic properties will vary with temperature. A thermoplastic material is also characterised by glass transition temperature  $T_g$ , below which the amorphous phase becomes glassy (or frozen). The glass transition is not considered a phase transition. Below  $T_g$  the viscosity of the amorphous phase change and there will typically be an increase in stiffness. For relevant polymers there are no sharp step changes in properties associated with  $T_g$  but there will typically be transitions in their temperature dependence.

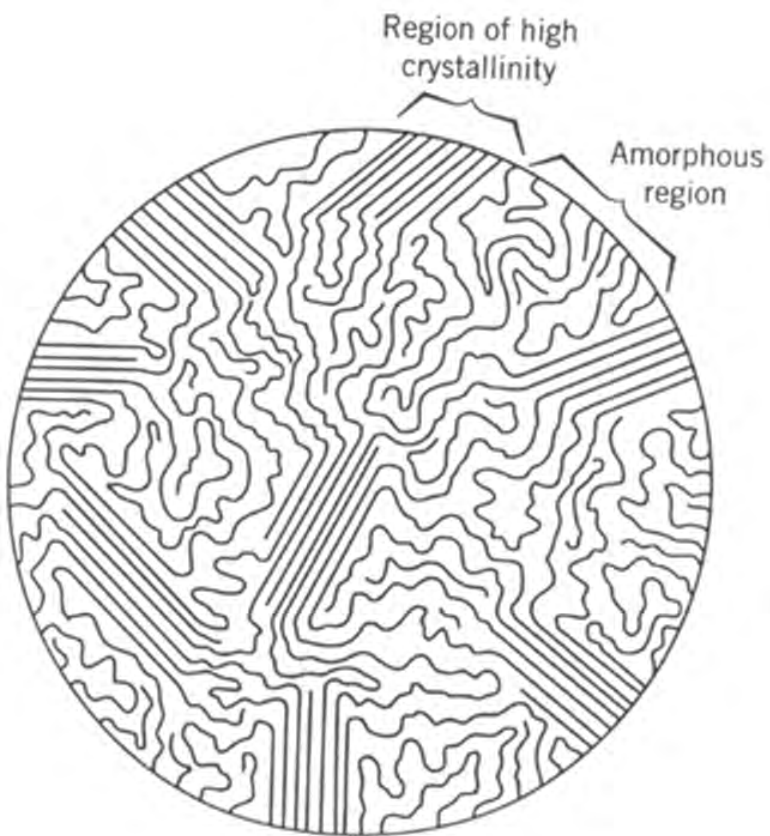


Figure A2.9: Illustration of a semi-crystalline polymer with a mixture of crystalline and amorphous regions

#### A2.3.2.2.2 Stress - strain

**A2.3.2.2.2.1 General response** The stress-strain behaviour of polymers is quite complex and it may be useful to be aware of some key features. The curve in Figure A2.10 below shows a typical stress strain relationship for a polymer (semi-crystalline thermoplastic) material.

The actual shape of the stress response curve will vary between materials and the strain at break can range from 50 to 1000% for relevant materials when tested according to ASTM D638 - 10 'Standard Test Method for Tensile Properties of Plastics' [[ASTM D 638, 1977](#)] at room temperature. Key parameters that characterise the materials are:

- The tensile modulus in the elastic region -> represent the material stiffness during use
- Strain at yield -> defines the strain where plastic deformation sets in
- Stress at yield
- Elongation at break -> gives a measure of the ductility of the material
- Ultimate strength

#### A2.3.2.2.2 Strain rate dependence

The stress strain curve and therefore the derived

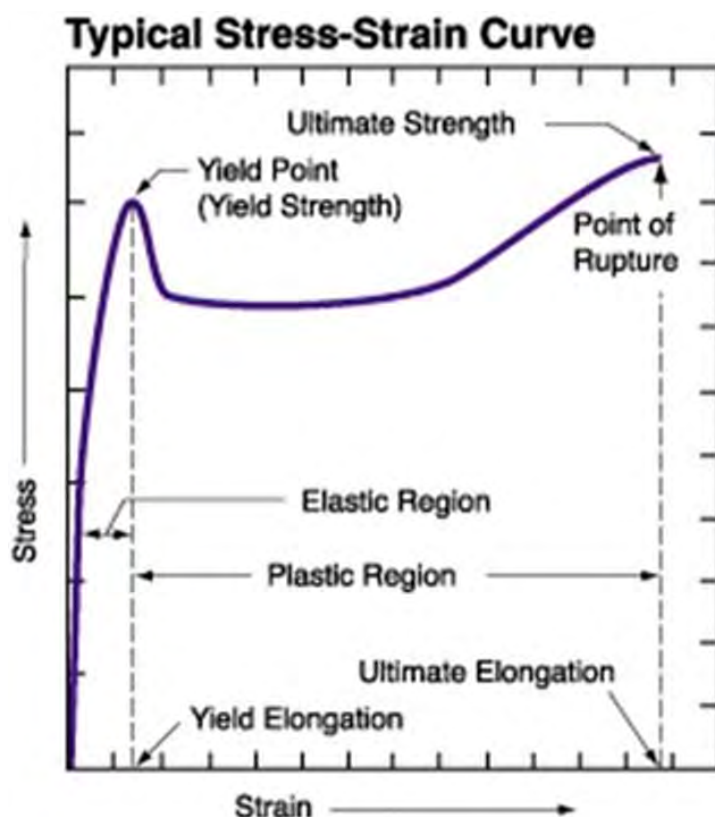


Figure A2.10: A typical stress-strain curve for a semi-crystalline polymer

parameters depend significantly on the rate of the applied strain. The higher the strain rate the stiffer the polymers and lower the ultimate elongation. When the strain rate becomes high enough the material will become brittle loosing its ability to ductile deformation. It is therefore important to ensure that mechanical properties used for design or response analyses have been derived from testing made at strain rates that are representative for the application.

**A2.3.2.2.2.3 Temperature dependence** The stress strain curve and all defined parameters will change significantly with temperature. For a given material the tensile modulus and the yield stress will go down and the ultimate elongation will increase when the testing temperature goes up. Thus the polymer sheaths in a flexible pipe used for oil and gas production will exhibit different mechanical response properties during shut down compared to the operational temperature.

In this context it is important to note that the axial, rupture and collapse strength of flexible pipes are provided by steel layers and are therefore not influenced by the stress/strain response of polymer layers.

**A2.3.2.2.3 Creep & stress relaxation** In the temperature ranges of interest the polymers used in flexible pipes exhibit viscoelastic properties. A constant load applied instantaneously (within the elastic response limits) will initially create an **elastic** strain response but over time the strain will increase due to slow **viscous** flow. The material will creep manifesting itself through a couple of phenomena for pressure sheaths:

- Creep of material into gaps between supporting pressure armours.
- Stress relaxation when the sheath is strained over long time.

Key features to observe are:

- Stress relaxation will never be 100% - there will always be some remaining stress (or elastic response).
- The viscoelastic behaviour is strongly temperature dependent in terms of
  - The rate of creep and relaxation
  - The degree of retained elastic deformation

Creep may induce orientation of polymer chains depending on the nature of the creep. This may impose some change in the tensile modulus but is not considered a significant issue for the function of polymers.

**A2.3.2.2.4 Ductile brittle transition** Polymers used in flexible pipes will exhibit ductile properties within the temperature ranges they are used. This means that when fractures are induced during testing they will be ductile. However, when the temperature is reduced the material will become more and more brittle and at some temperature the nature of induced fracture will become brittle. This will be the ductile/brittle transition temperature.

When the strain rate used to induce fracture is increased the brittle/fracture transition temperature will also increase. In a plot of strain rate versus temperature one can define a curve where the material on one side will have ductile behaviour and on the other side brittle.

When a material goes through ageing that make it more brittle the ductile brittle transition will go up in temperature for a given strain rate.

During shut down and in particular cooling from gas expansion, when the temperature in flexible pipes is low, the polymer materials will in general be closest to their ductile/brittle transition and thus be most prone to brittle rupture or crack initiation. Clearly cool down scenarios should be taken into consideration during design. For materials that loose ductility through ageing the margin with respect to the ductile/brittle transition may decrease and become a potential integrity issue.

**A2.3.2.2.5 Thermal expansion / contraction** In flexible pipes the polymer sheaths are functioning in close interaction with steel components. Differences in thermal response between polymers and steel may have impacts on design and the function of pipes. Relevant polymers have a thermal expansion coefficient that is in the order of a factor of 10 higher than steel. This means that a pressure sheath that has very low residual stress at high operating temperatures will experience increased stress during cool down as the steel components will limit the thermal contraction.

Typical thermal conductivity coefficients for a relevant thermoplastic is:  $150 \cdot 10^{-6} / K$

While a typical value for steel is:  $12 \cdot 10^{-6} / K$

**A2.3.2.2.6 Thermal conductivity** The much lower thermal conductivity exhibited by polymers compared to steel implies that the polymer layers govern the temperature profile through the pipe wall. Most of the temperature drops will take place through the polymers.

Typical thermal conductivity coefficients for a relevant thermoplastic is:	0.2 - 0.5 W / (m·K)
While a typical value for steel is:	43 W / (m·K)

**A2.3.2.2.7 Permeation** Contrary to steel, relevant polymers are permeable to several of the molecular species found in fluids and gases the pipes are exposed to when used for oil and gas production. Typically methane, ethane, CO<sub>2</sub>, H<sub>2</sub>S, water and other small molecules in gas or liquid form will permeate through polymer sheaths or membranes. The permeability properties depend on the solubility in the polymer of molecules in question and their diffusion properties in the polymer. There are significant differences in permeability between polymers and the rate of permeation vary with temperature.

The environment in the annulus will reflect the partial pressures of gases and vapours in the bore and their respective permeability constants. Thus the polymer pressure sheath will act as a filter allowing some species to get through more easily than others.

**A2.3.2.2.8 Blistering** The solubility of gases in a polymer is proportional to the pressures (partial pressures) of the respective gases. At high pressures the concentration of dissolved gas can be substantial. If the pressure is reduced the dissolved gases need to escape to match the concentrations of dissolved gases proportional to (in equilibrium with) their respective partial pressures. If the pressure drop is too fast for the gases to escape they may form micro-voids in locations such as impurities or at other imperfections where the bonding between molecule chains is weak. Pressure build-up in these micro-voids may become sufficient to create larger voids and lead to blistering with macroscopic voids.

Different polymer materials will exhibit different inherent resistance to blistering. The resistance to blistering will normally go down with increasing temperature partly due to weaker bonding between molecules in particular if the material swell. The acceptable maximum pressure and associated depressurisation rate for a given material will typically go down with increasing temperature. All relevant polymers could be brought to blister if the pressure is high enough. Among relevant polymers used for pressure sheath in flexible pipes Polyethylenes have the lowest resistance to blistering limiting their use envelopes in terms of temperature and pressure.

The blistering tendency will depend primarily on the gas composition but also to some extent on the fluid composition in particular if the fluid induces swelling. Thus resistance to blistering must be verified under simulated production conditions at adequately high pressures and depressurisation rates.

If blistering should become an issue for an existing pipe application one of the mitigations would be to avoid rapid decompression and if possible limit the maximum pressure.

**A2.3.2.2.9 Volume change** Some of the polymers used in flexible pipes are modified by the addition of plasticisers to improve extrusion properties and make the materials more ductile. This is the case for PA11 and PA12 and for some of the PVDF types used. The degree of plasticisation varies from a few % to 20%. Plasticisers will under many typical exposure conditions be extracted from the polymer to the surrounding environment causing reduction in the volume of the polymer (density changes are generally small). This will generate stresses in a sheath when it is not allowed to contract (as will be the case in the axial and circumferential directions in flexible pipes). Parts of these stresses may relax due to the viscoelastic properties of the polymers but not all. The thickness of the polymer sheaths will go down and may reduce the friction to neighbouring layers. This can be a problem for sealing in end fittings and must be taken into consideration for design and fabrication.

On the other hand some polymer will take up certain molecular species that it may be exposed to during service. This is quantified in terms of the solubility of a chemical substance in a polymer material. Polyamides will for instance take up water and Polyethylene type materials will take up hydrocarbons. This may for plasticised material compensate some of the volume change from loss of plasticiser and un-plasticised materials may swell.

Polyethylene materials will swell when exposed to crude oil. This swelling will increase with temperature and vary between types of Polyethylenes and will generate hydrostatic pressures in materials that are fully confined as is the case for many pressure sheaths. The pressures and forces generated from a confined material that is exposed to substances that cause swelling will eventually become substantial when the temperature is increased.

**A2.3.2.2.10 Cracking** Thermoplastic polymers will have varying susceptibility to crack initiation under cyclic loading. PVDF is considered to be notch sensitive and the possibilities of crack initiation must be taken into consideration in design and fabrication.

Within relevant temperature ranges the polyamides and polyethylenes used have low susceptibility to crack initiation. However, if materials degrade and become brittle crack initiation could eventually become an issue. Due to reduction in ductility with reduced temperature for the polymers the susceptibility to rupture, crack initiation and crack growth will be highest at low temperatures.

Another aspect of cracking is environmental stress cracking (ESC). This is a phenomenon where the material in locations of high persistent stress may induce increased solubility to certain chemicals that could be harmful for the polymer. This may lead to a local weakening of the material that in turn will promote stepwise initiation and growth of cracks.

One of the criteria for selecting polymers suitable for use in flexible pipes has been to ensure that they do have very low susceptibility to ESC for oil and gas environment. However, ESC could be of concern with some injection chemicals.

**A2.3.2.2.11 Structural changes** It is the amorphous regions that are the origin of the high ductility of thermoplastics. When a semi-crystalline material is exposed to elevated temperatures the crystalline structure may change. The percentage volume of the material that is crystalline and the average size of the crystalline regions may change. This may have impacts on bulk properties such as stiffness and ductility.

**A2.3.2.2.12 Crazing** Crazing is a phenomenon, also called whitening, where networks of micro-voids develop in highly stressed parts of the material. The consequence of crazing is not fully understood. There is a concern that crazing may affect the fatigue resistance. However, crazing developing in front of a crack tip, due to high stress levels, may represent energy absorption that slow down crack growth.

**A2.3.2.2.13 Chemical ageing** Polymer molecules may undergo chemical reactions caused by chemicals species entering the polymer or by radiation. This may modify properties of the bulk material. Such reactions may lead to chain cutting (reducing the length of the polymer molecules) or cross-linking between molecules affecting the ability if molecules to move relative to each other. Relevant reactions are:

- Oxidation leading to chain cutting in some material at high temperatures (in particular polyethylene and polyamides). Many polymers will include antioxidants providing a buffer against oxygen degradation.
- Hydrolysis where water takes part in a reaction causing chain splitting (in particular polyamides)
- Acids, bases or other chemicals causing or promoting chain cutting
- Ultra Violete radiation inducing chain cutting or cross-linking

The main impacts of chemical degradation for key use properties will first be increased stiffness and then embrittlement of the material.

**A2.3.2.2.13.1 Temperature dependence** The ageing rates for the described processes, apart from radiation-induced reactions, will increase with temperature. Typically reactions involved are characterized by their respective activation energy. The probability of overcoming the activation energy will increase with increasing temperature. Such processes obey the Arrhenius relationship  $r = Ae^{-E_a/kT}$  where  $r$  is the reaction rate,  $E_a$  is the activation energy,  $k$  is the Boltzmann constant and  $T$  is temperature on the Kelvin scale. The implication is that these ageing processes will become more severe when the temperature goes up and thus define upper temperature limits for use. Hydrolysis of Polyamides is a good example of an ageing process that leads to temperature limits for use.

**A2.3.2.2.14 Temperature use limitation** Temperature is the parameter that to a large extent governs the use range of polymers.

Increasing temperature will lead to:

- Softening and eventually excessive creep and blistering
- Increasing tendencies for structural changes (such as changes in crystallinity)
- Increasing swelling
- Enhanced ageing rates

On the other hand low temperatures will lead to:

- Brittleness that can lead to rupture and fatigue

- Generation of high stresses from cool down combined with differences in thermal expansion between polymers and steel

### A2.3.3 Polymers used in Flexible Pipes

#### A2.3.3.1 Overview

Table A2.8 identifies the different polymers in use as pressure sheath in flexible pipes.

Table A2.8: Different polymers in use as pressure sheath in flexible pipes

Type of Polymer	Grade name	Material supplier	Pipe Manufacturers	Plasticiser	Typical use envelope as pressure sheath
Polyamide	PA11 RILSAN BESNO P40 TL	Arkema	All	12% BBSA	Typical upper temp 60 - 80°C depending on pH and required service
	PA12 VESTAMID LX9020	Evonik	Wellstream (patented)	4-8% ?	Typical upper temp 60 - 80°C depending on pH and required service
	TP30 (Technip trademark)	Not known	Technip	Plasticised (but quantity and type not known)	Claimed by manufacturer to be 10-15°C higher than PA11
Polyethylene	MDPE	Several	All	0	
	HDPE	Several	All	0	Up to 60°C (Max pressure limited by blistering)
	Crosslinked PE - Crossflex (Silane cross linking)	?	Technip (patented)	0	Up to 90°C (Max pressure limited by blistering)
	Crosslinked PE - IR cured XLPE (Peroxide cross linking)	?	NKT (patented)	0	Up to 90°C (Max pressure limited by blistering)
PVDF	Coflon (Technip trademark)	Arkema (KYNAR 50HDC P900)	Technip	20% DBS (may have changed over time)	Up to 130°C
	Gammaflex (Technip trademark)	Arkema (KYNAR 400 HDC M800)	Technip	3% DBS elastomer particles	
	Coflon XD (Technip trademark)	?	Technip	2.5% ?	
	Solef 1015 / 0078	Solvay	Wellstream (phased out?)	19% DBS	
	Solef 60512 (PVDF with PVDF/CTFE copolymer)	Solvay	Wellstream	NKT 0%	

#### A2.3.3.2 Polyamides

**A2.3.3.2.1 PA11** PA11, supplied as Rilsan from Arkema, has been used for pressure sheath in flexible pipes for many years. It is based on amide bonding between monomer units consisting of a linear chain of 11 Carbon atoms. The degree of crystallinity is 20-30%.

It is promoted as a polymer, which is easy to process, with good resistance to chemicals, high

impact, and wear strength. The grade used for pressure sheath is Rilsan BESNO P40 TL contain 12% plasticizer by volume and an antioxidant package providing a certain capacity against oxygen degradation. The tensile modulus of fresh fully plasticized material is around 310 MPa at room temperature while loss of plasticizer will increase this significantly (fully de-plasticised and completely dry material has a tensile modulus around 1500 MPa). The elongation at break is in the order of 300 - 400%.

At 23 °C Rilsan will absorb around 2.5% water by weight. It should be noted that the water uptake in Rilsan is low compared to several other Polyamides such as PA6,6. The water uptake will contribute to plasticization and compensate for some of the impacts on mechanical properties from loss of plasticizer. It is the polarity (electrical dipoles) of the amide bonds that is responsible for the relatively high solubility of water, which is a highly polar molecule. Therefore other polar molecules such as alcohols (in particular methanol) and acids will have a relatively high solubility in PA11. Most hydrocarbons have a low solubility in PA11, which results in negligible swelling from exposure to crude oil. Aromatic hydrocarbons (containing benzene rings) have a non-negligible solubility in PA11. Arkema report blistering tests with no blistering after 20 cycles to 1000 bar at 90 °C with explosive decompression rate.

Guidelines for use of PA11 is available in [API 17TR2, 2003]. It is generally accepted that the main threat to PA11 is hydrolysis where water molecules react with the amide bonds cutting the polymer chains. Fluids and gas from oil wells are depleted from oxygen and oxidation is not considered an issue. Methanol is known to contribute to degradation, which is believed to be a separate reaction termed methanolysis, which is similar to hydrolysis.

The chain cutting (scission) caused by hydrolysis reduces the average length (and weight) of the polymer chains. When the molecular weight reaches a critical range the material starts to loose ductility and becomes brittle. Eventually this may lead to cracking and full rapture. The average Molecular weight has been adopted as the measure of degradation since it allows quantification of the degree of degradation. The most common way of measuring the molecular weight is through solution viscosity providing the Corrected Inherent Viscosity (CIV). Based on field experience and laboratory testing a recommended initial acceptance criterion of CIV= 1.2 dl/g has been defined. The basis for this is that PA11 pressure sheath failure has been observed in the field with CIV on the inside surface up to 1.05 dl/g which has been defined as the failure criterion.

The hydrolysis reaction rate increases with temperature. However, it is also known that there will be a reverse reaction where scissioned chains will recombine. In principle this would lead to a molecular weight plateau where the hydrolysis reaction rate and the reverse recombination rate are equal. This has been demonstrated in laboratory tests primarily in controlled water environments.

It is known that acids will enhance the hydrolysis reaction. The guidance in [API 17TR2, 2003] provide temperature and pH dependent service life curves for ageing of PA11 to reach the initial acceptance criterion of CIV=1.2 dl/g. There is also a curve to account for methanol exposure.

The service life curves in [API 17TR2, 2003] provide pH dependence but do not provide any discrimination between different types of acids. It is believed that the service life curves are based on ageing in buffered solutions using chemicals that may not necessarily be those generating acidity in oil and gas production environments. Thus there is no discrimination between acids. The pH is defined for water in contact with PA11 while hydrolysis reactions in

the material will be governed by the concentrations of chemical species inside the material. Different acids will have different solubilities in the PA11 thus it would be reasonable to assume that the type of acid can play an important role.

In the context of the impact of acids it is worth taking note of the types of acids that can be found in oil and gas production:

- CO<sub>2</sub> is always present in varying abundance. It forms Carbonic acid when dissolved in water.
- H<sub>2</sub>S is present in sour service environments and is an acid in itself. The concentrations can be negligible in some fields and relatively abundant in others.
- Water soluble organic acids such as methanoic (formic) acid, ethanoic (acetic) acid, propanoic acid etc. Ethanoic acid is always the most abundant of these and the concentration in produced water can be between negligible (less than 10 - 20 mg/l) to more than 500 mg/l.
- Larger organic acids such as Naphthenic acids are not soluble in water and stay in the oil phase. The acidity of oil is measured in terms of Total Acid Number (TAN), which is determined through titration. The TAN of crude oils varies significantly between fields ranging from negligible (less than 0.05 mgKOH/g) to more than 5 mgKOH/g. It is stated in [[API 17TR2, 2003](#)] that TAN below 3.5 mgKOH/g should not cause any concerns. It is also important to note that there are large numbers of organic acids that vary in structure and size. Thus the composition of acids in crude oil can be substantially different between 2 fields with the same TAN value.
- Injection fluids.

In the Joint Industry Project SESAM PA11 [[SESAM PA11, 2008](#)] tests were carried out to explore the impact of organic acids.

- Water soluble organic acids clearly enhanced the degradation. However, acetic acid enhanced the degradation but was not the worst at the test temperatures which were fairly high.
- A commercially available mixture of Naphthenic acids was mixed into a neutral oil. It was demonstrated that at around 100 oC, the degradation was enhanced even at concentrations as low as 0.5 mgKOH/g. It is not known how representative the tested Naphthenic mixture is for typical high TAN crude oils.

[[API 17TR2, 2003](#)] reports field experience based on analysis of flexible pipes with PA11 pressure sheaths that have been retrieved from service and analysed. 4 of the pipes were retrieved because of pressure sheath failures while others were retrieved due to suspicion of severe degradation.

- Two of the failed pipes were risers, one with an inside CIV=1.05 and the other with CIV= 0.95 next to the rupture. Both of these risers were exposed to crude oil with a total acid number (TAN) of around 1 mgKOH/g. The riser with CIV=1.05 showed signs of striations on the fracture surfaces indicating initiation and growth of a fatigue crack on the inside surface.
- Two flowlines that failed, one with CIV=0.89 and one with CIV=0.81 dl/g. Both of these lines have been exposed to relatively frequent batch treatment with methanol. It

is plausible to suspect that the methanol will have carried dissolved oxygen that may have contributed together with the methanol to create the substantial degradation.

The temperature histories for the exposure of the different pipes retrieved vary in quality but some histories are reasonably well known. There are indications of cases where the service lives predicted from [API 17TR2, 2003] are over-conservative but also cases where they are under-conservative. This suggests that the curves are not adequately discriminating between different environments.

Field experience over recent years show indications that fields with TAN below 1 mgKOH/g or with water soluble acid concentrations up in a few hundreds mg/l may cause more degradation than expected from available models.

There is clearly a need to develop more discriminating and precise models for degradation of PA11 in flexible pipes. A paramount issue, in relation to the development of service life models, is that PA11 ageing tests in neutral and nominally similar conditions produce very different results between laboratories. This is demonstrated in Figure A2.11 .

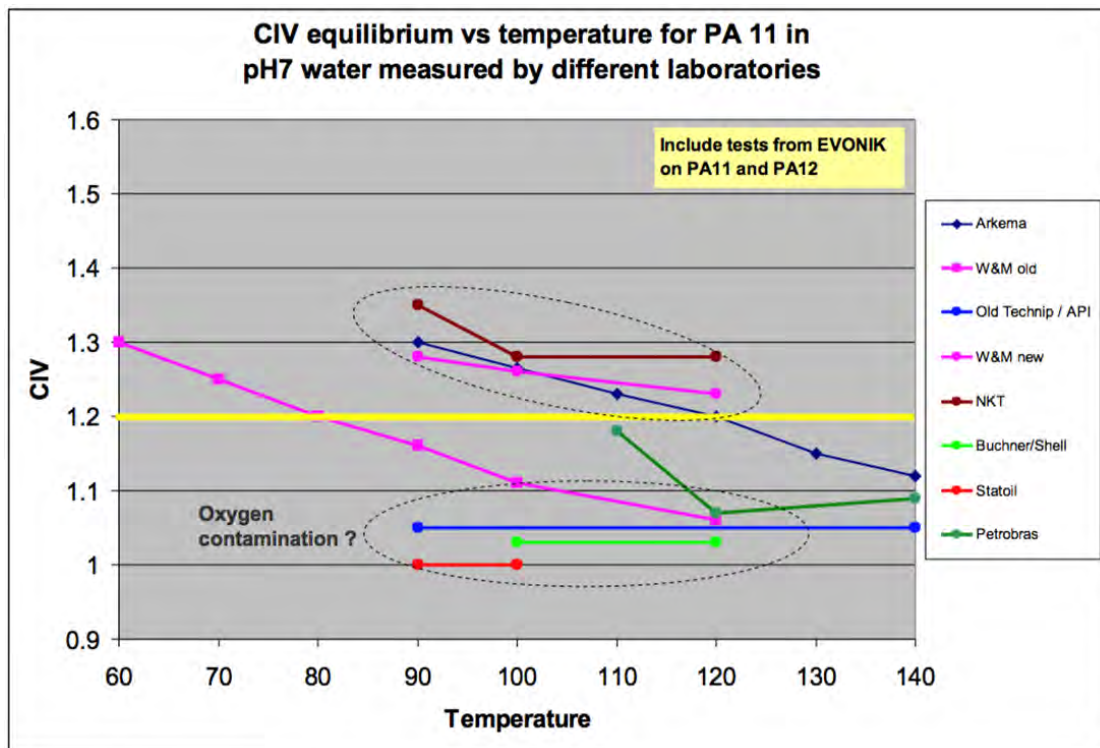


Figure A2.11: Comparison of the terminal CIV reported from different laboratories for ageing of PA11 in nominally neutral environments. (Courtesy of Einar Øren, Statoil)

This shows the substantial variation in reported CIV equilibrium or terminal CIV level at the end of tests. There is clearly a need to understand why different laboratories get such very large differences in CIV from similar tests. Questions that are asked are:

- Is the oxygen control inadequate in some laboratories?
- How important is the ratio between sample volume and water?
- What impacts are there from renewing the fluid every time sample is retrieved?

- How important is the starting water quality?

These questions may be a good starting point for development of harmonized test procedures to ensure reproducibility between laboratories. This would be a necessary starting point for testing to develop better service life models to discriminate better between different exposure conditions.

There are cases where the initial acceptance criterion, CIV=1.2dl/g, defined in [API 17TR2, 2003] may be too strict. In particular for exposure environments leading to a high CIV gradient through the thickness there may be good justifications for refining the acceptance criterion. Failures of PA11 pressure sheaths suffering from excessive hydrolysis will take place through either brittle fracture or through crack growth from the inside. Thus the margin against brittle fracture and the resistance against initiation of fatigue crack will define the actual margins with respect to failure. A better understanding of the mechanisms and drivers would enable development of more appropriate acceptance criteria.

Appropriate and adequately discriminating service life models and acceptance criteria should be of very high value to the industry. In some fields it may save substantial costs for replacement while other fields may operate PA11 pipes at a higher risk of failure than accepted.

#### **Summary of observations:**

- PA11 pressure sheaths exposed to oil production (including water) have remaining volatiles in the region of 4% - 7%. These volatiles will be plasticizer, water and some amount of hydrocarbons. A corresponding reduction in volume will develop compared to fresh material containing 12% plasticiser.
- PA11 pressure sheaths exposed to dry gas can loose more plasticizer and will not absorb much water since the gas is dry.
- The nature of the degradation process is that the ageing is cumulative. Short periods at high temperature only contribute to the ageing according to time and temperature.
- Be aware of batch treatment with chemicals such as methanol. They may carry sufficient oxygen to have an impact on PA11 after many repeated treatments.
- Even in aged condition the ductility of PA11 will depend on temperature and exhibit the lowest ductility at low temperatures. Thus aged PA11 pressure sheaths will be most prone to fracture during cool down or at start-up after shut down when high pressure may be re-applied.
- Operators that find that flexible pipes have expended more than 50% of their useful lives according to [API 17TR2, 2003] and have been exposed to environments with high concentrations of water soluble organic acids and/or crude oils with TAN above 0.25 mgKHO/g should consult with experts for advice.
- The anti-oxidant package in RILSAN was changed between 1995 and 2000. The different manufacturers took the new formulation into use at different times.

#### **A2.3.3.2.2 PA12** PA12 was used to a limited extent as pressure sheath back in late 80ies and early 90ies.

Wellstream has qualified the PA12 grade Vestamid LX9020 from Degussa Evonik in 2006 and since that have delivered significant lengths of flexible pipes with this grade. The grade is plasticized and was specially developed for application as pressure sheath in flexible pipes. Publications from the material supplier and the pipe manufacturer claim that this PA12 grade is better than PA11 Rilsan BESNO P40 TL in nearly all aspects from tests of the 2 materials in parallel [Buchner et al., 2007]. However, some of the results they have published for PA11 are significantly worse than those that have been reported by other laboratories that have tested Rilsan BESNO P40 TL. It would clearly be valuable to see testing of PA12 Vestamid LX9020 by independent laboratories using harmonized test procedures.

The polymer structure is similar: PA12 has one more Carbon atom with 2 associated Hydrogen atoms for each monomer unit. Apart from this PA11 and PA12 are identical in terms of the molecule structure but the average number of monomer units per polymer chain may differ. The PA12 from Evonik will probably be plasticized differently compared to PA11 and it may contain other stabilizer packages. The degree of crystallization and size of the crystalline regions may be different thus influencing some of the properties. It is very likely that PA12 is going to be affected by similar issues as those that have been experienced for PA11 but to different degrees.

The acceptance criteria and service life curves published in [API 17TR2, 2003] only apply to the PA11 grade used as pressure sheath in flexible pipes and should not be used for PA12 unless adequate documentation is provided.

**A2.3.3.2.3 TP30** Technip published a paper in 2013 [Chollet and Do, 2013] reporting that they had completed the qualification according to [API 17J, 2008] for a new Polyamide that they call TP30. The paper provides no information of the structure of the polymer. It is claimed that TP30 has improved hydrolysis resistance compared to PA11 and that it can be used at temperatures that are 10 to 15 °C above the upper limits for PA11 depending on pH and application. They report that permeation coefficients that are lower than for PA11 for both methane and hydrogen sulfide and the blistering resistance is reported to give no blistering after 20 cycles of 950 bar, 70 bar/min at 115 °C.

Many results are presented on graphs without dimension on one or both of the axes making it impossible to make quantitative comparisons to results for other polyamides.

Testing of HPPA by independent laboratories would be valuable to determine how much better than PA11 it is.

### A2.3.3.3 Polyethylene

Polyethylene is a low cost versatile polymer that comes in a variety of grades. It has good chemical resistance against most of the chemicals relevant in oil and gas production but it will degrade from exposure to oxygen at elevated temperature. However, one weakness is the high solubility of hydrocarbons, which leads to swelling and limited blistering resistance under rapid decompression in gas. These phenomena vary with grade type and increase with temperature.

Polyethylene can also be sensitive to Environmental Stress Cracking (ESC) where crazing and stepwise cracking is promoted by certain chemicals in high stress / high strain locations. Some relevant treatment chemicals could promote ESC.

Polyethylene is characterized by density, which reflects the degree of crystallinity. Primarily HDPE (High Density Polyethylene) and to some extent MDPE (Medium Density Polyethylene) are used in flexible pipes as pressures sheath or outside cover. In general the higher density improves properties such as swelling and blistering.

Pressure sheath applications for Polyethylene are limited to water injection and oil and gas production and transport at temperatures normally well below 60 °C at relatively low pressures.

**A2.3.3.3.1 Cross Linked Polyethylene (XLPE)** One of the reasons Polyethylene is sensitive to swelling and blistering is the relatively weak bonding (Van de Waals forces) between neighbouring polymer chains in the amorphous phase. To enhance the use-boundary, techniques have been developed to crosslink HDPE to establish links between molecule chains. There are several ways to introduce cross-linking but only two of these have proven to be suitable for flexible pipe pressure sheath:

- Crosslinking by Silane, where Silicon atoms take part in the crosslinking between chains. This method has been adopted for extruded flexible pipe liners by Technip and is protected by a patent. The cross linking must be activated by circulation of hot water after the flexible pipe has been completed with end fittings.
- Crosslinking with the help of peroxide that promote a direct Carbon-Carbon bond between neighbouring chains. NOV has developed and patented a technique for flexible pipes [Procida and Nielsen, 2007] where the cross linking is activated just after extrusion by heating with Infrared Radiation. This means that the cross linking takes place at temperatures above where crystal formation starts in the polymer thus ensuring crosslinking also in the crystalline phase.

Crosslinking will extend the use envelope both to higher temperatures and higher pressures. The manufacturers claim that the use temperature can be extended to 90 °C and operating pressure up to above 300 bar depending on temperature. The advantages from cross-linking HDPE are:

- Reduced swelling in the temperature region 60 - 90 °C
- Improved blistering resistance
- Better creep resistance

Cross-linking by peroxide and IR radiation is claimed to ensure a higher cross-linking density because the cross linking is done at temperatures above the formation of crystalline phase. This may influence the crystal structure and thus provide somewhat different mechanical properties than material cross-linked by Silane. But the differences may have limited impacts on the performance of the material in the flexible pipe. The technique used by NOV allows test samples to be taken of fully cross-linked liner before outer layers are put on and integration of end-fittings. NOV report blistering tests documenting no blistering after 20 cycles of 345 bar, 80 bar/min at 90°C

Swelling, reduced creep resistance and blistering are the properties that define the use limit for both PE and XLPE but with higher limits for XLPE. In Figure A2.12 the measured swelling of one type of XLPE is shown as function of temperature in 2 different types of crude oils.

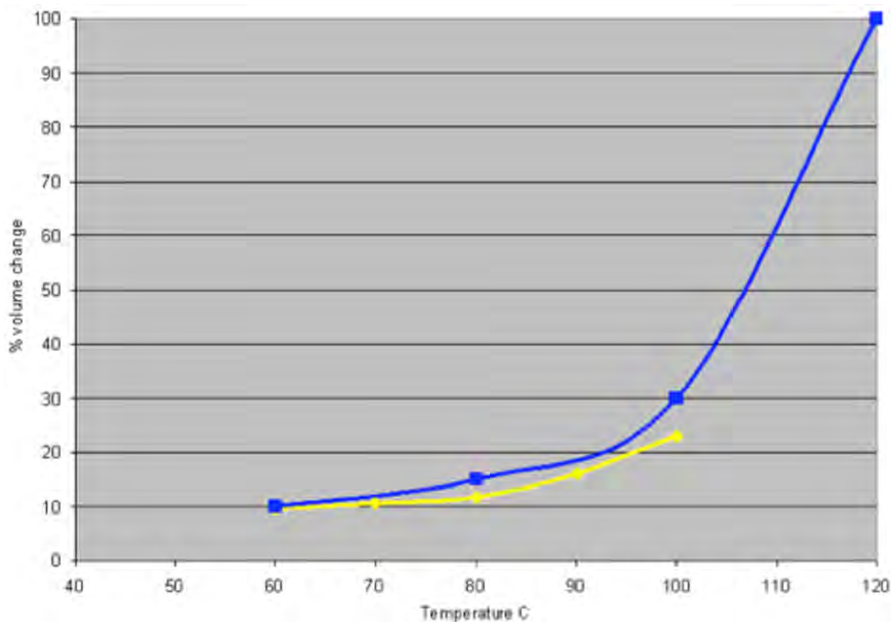


Figure A2.12: Swelling as a function of temperature of one type of XLPE in 2 different crude oils.

These swelling curves are generated on free samples directly exposed to the fluid. A pressure sheath in a flexible pipe is normally confined between the Carcass and the pressure armour. This means that the material is only allowed to expand to a limited degree and the tendency to swelling will generate a hydrostatic pressure. The confinement may well improve the blistering tendency and the softening from ingress of hydrocarbon species. However, the forces generated from the tendency to swelling will at sufficiently high temperature produce enhanced creep into available gaps and may eventually damage supporting structures. The implication of this is that exposure of XLPE and HDPE to very high temperature (relative to the design temperature) for a short period may cause permanent damage to supporting components in the end fitting or to the Carcass.

#### A2.3.3.4 Polyvinylidene Fluoride (PVDF)

PVDF is a chemically resistant polymer suitable for use at high temperatures. For flexible pipes it has been the only pressure material for high temperature applications - above 90 °C. It is also the most expensive of the pressure sheath materials and it is the material type that has created most pressure sheath related failures. The main chemical threat is alkaline fluids, which may have to be taken into consideration for some injection chemical (amines, sodium hydroxide)

PVDF is generally less ductile than the Polyamides and Polyethylene material and it is notch sensitive in relation to initiation of fatigue cracks. The first PVDF formulation taken into use by Technip was Coflon (Technip trade name), which contained 19% plasticizer (DBS). The plasticizer will in hydrocarbon environments be extracted to a significant degree resulting in corresponding shrinkage.

Axial (and circumferential) stresses are generated during cool down due to the differences in thermal expansion coefficients between the PVDF and steel. The stresses generated during

cool down of PVDF tend to become much higher than for other polymers because:

- PVDF is typically used at the highest temperatures giving larger temperature changes during cool down
- PVDF exhibit generally higher tensile modulus which in turn give higher stresses for a given level of strain

The shrinkage due to loss of plasticizer in combination with axial stresses and the weight of the Carcass resulted in pull-out of the Coflon pressure sheath from the sealing and anchoring arrangement in the end fitting used by Technip before 1995. This resulted in design changes for the sealing arrangement and better procedures including de-plasticization of the PVDF prior to termination in the end fitting.

After the problems with the end-fitting pull-outs other alternative PVDF formulations have also been taken into use with much lower or no plasticizer content. One of the new PVDF grades is a copolymer where the other chemical groups have been introduced together with VDF in the polymer chains to give the suitable properties for pressure sheaths. There has also been a drive to develop more fatigue resistant formulations.

Because of the notch sensitivity of PVDF sacrificial sheaths have been introduced to protect the main/middle sealing sheath in risers, in particular with Coflon barrier. There are now 2-layer and 1-layer solutions for PVDF barriers in risers depending on manufacturer and material used.

There have been a number of cases where the Carcass has collapsed in pipes with 3 layers. One of the explanations has been that under decompression and cool down hydrocarbon gas dissolved in the polymer may collect between the inner sacrificial layer and the sealing layer. When the drainage of the gas is not adequate in the axial direction the pressure build up can be sufficient to induce collapse of the Carcass. This failure mode is typically limited to high pressure/high temperature applications.

The different grades of PVDF will exhibit somewhat different properties and potential integrity issues will depend on the layer design. Thus the issues below will not necessarily apply to the same degree from grade to grade and from manufacturer to manufacturer:

- Fatigue and notch sensitivity is a concern for PVDF materials. Thermal cycling with large temperature variations is potentially a threat due to the differences in the thermal expansion coefficient between steel and PVDF [Melve, 2001]. Quality control during manufacturing and design solutions to avoid notches is recommended.
- There have recently been reports of tear out or fatigue of Carcass in the end fittings in 3 layer Coflon pipes. It has been demonstrated that one of the causes can be unrelaxed residual stresses from loss of plasticizer combined with stresses induced during cool down and reduced friction to outside layers inducing forces in the Carcass that can result in tear-out and fatigue [Farnes et al., 2013].
- Susceptibility to cracking at low temperatures and there have been cracking problems in connection with manufacturing for non-plasticised grades.
- Crazing has been observed in PVDF liner. The consequence of crazing is not fully understood. There is a concern that crazing may affect the fatigue properties.

Different manufacturers have different strategies for their PVDF pressure sheaths using 1 layer, 2 layers and 3 layer designs but the tendency is to go for 1-layer designs.

### A2.3.3.5 General aspects and comparison

**A2.3.3.5.1 Material properties** Some documented quantified performance properties of some of the polymers are shown in the Table A2.9:

Table A2.9: Properties of some pressure sheath materials

Grade / name	Dens- ity g/cm <sup>3</sup>	Pois- son ratio	Glass trans- ition T <sub>g</sub> C	Melt- ing temp T <sub>m</sub> C	Tensile Modulus at room temp Mpa	Tensile Modu- lus at elevated temp.	Thermal expansion coefficient 10 <sup>-6</sup> K	Ther- mal conduc- tivity W/(m·K)
PA11 / RILSAN BESNO P40 TL	1,03		42	182	310 (fresh) increase with loss of plasticiser	170 at 60°C 165 at 80°C	110 (-30 -> +50°C) 230 (+50 -> + 120 °C)	0.24 (at 60 °C)
PA12 / VESTAMID LX9020		0,47	36	171	450		160 (+23 -> +55 °C)	
TP30 (Technip)			?	?	661	198 at 100 °C	140 at 20 °C	0.26 at 25 °C
HDPE	0.94 -0.98	0,46	-80	120 - 130	500 - 1200		100 - 200	0.45 - 0.52
Coflon (Technip trademark)					1100 2000 (significant plasticiser loss)	600 at 60°C		
Solef 1015 / 0078	1.75 - 1.8		-40	170 - 175	1700 - 2500		140 (at ambient)	0,2
Solef 60512 (PVDF with PVDF/CTFE copolymer)	1.75 - 1.8	0,4	-40	170 - 174	1250 - 1400	800 (at 60 °C)	130 -> 180 (at ambient)	0,2

One important property that is missing in the table is permeability constants. These constants depend on test conditions and the variation between reported (nominally comparable) values is significant for several cases. A more in depth review is necessary to present useful data.

**A2.3.3.5.2 Guidance notes** In connection with material selection of polymers for new pipes it is important to identify all aspects of the exposure ranging from chemical composition of fluids and gases (including injection chemicals), physical conditions such as temperature & pressure, pH under production conditions, expected number of shut downs including pressure and temperature excursions and rates of changes. It is important to note that the pH measured in samples of formation water is not the pH under production conditions, which has to be calculated based the alkalinity of the produced water and the partial pressure of acid gases such as CO<sub>2</sub>.

If the material proposed for the application has limited field experience or will be operating close to or beyond earlier use limits, specific qualification tests should be carried out at harsher conditions (accelerated) than the service conditions. The test conditions and acceptance criteria should be determined with the involvement of experts on the performance of polymers in flexible pipes.

The manufacturer should specify the exposure limits for all relevant parameters and define what the consequence would be for operating outside these limits.

It is a good idea in many cases to install coupons taken from the extruded pressure sheath in the production stream in an arrangement where the coupons are directly exposed to all parameters of the flow. There should be enough coupons to allow periodic retrieval throughout the expected service life (including possibilities for life extension)

To assess the performance of polymer pressure sheaths it is essential collect and store temperature and pressure continuously for the full service life. It is also important to document on a regular basis the composition of fluids and gases and record all instances of injection of chemicals.



## **Chapter A3**

# **Failure Modes**

*Author: 4Subsea, Svein Sævik (NTNU)*

## A3.1 Purpose

### A3.1.1 Description of document objective

A comprehensive understanding of failure modes is essential for both the design phase and operational phases:

- Design phase: ensure that pipes are designed with adequate consideration and measures to avoid relevant failure.
- Operational phase: ensure that all relevant failure modes can be identified and assessed in terms of remaining service life, safety margins and quantification of risks as part of integrity management and lifetime assessment.

To meet the needs for insight into failure modes this chapter of the handbook has been developed with the following purposes:

- Define concepts and terminology relating to failure modes.
- Define a framework for assessment of failures in flexible pipes.
- Present state of the art for relevant failure causes and ultimate failure modes with description of failure and degradation mechanisms, consequences and mitigations.
- Present available and relevant failure statistics.

### A3.1.2 Scope of document

The primary scope of this document is to provide basis for systematic Integrity Management and Lifetime assessment of flexible pipes. Understanding of flexible pipe degradation mechanisms are essential in such work.

This chapter is concentrating on important failure causes relevant for flexible pipes in operation. The following should be noted:

1. It is assumed that the flexible pipe has been successfully designed, manufactured and installed according to [API 17J, 2008]. Failure mechanisms experienced during manufacturing and installation are hence not fully covered. Further, pipe designs are assumed to have the required design safety margins when installed. There are examples of installation damages and design weaknesses which have had significant impact on long term integrity and such long term effects are covered in the document, e.g. corrosion due to cover damage and collapse due to design with multilayer pressure sheath
2. Important failure mechanisms experienced in operation are covered
3. Failure mechanisms which ultimately may have large consequences and significant or unknown probability are covered
4. The probability of occurrence is briefly addressed by applicability, field experience and operational conditions
5. The chapter concentrate on failure mechanisms on the flexible pipe itself, failure mechanisms for ancillaries are partly addressed but such failure mechanisms will be design

dependent and the failure mechanisms addressed should be considered as examples only

The purpose of this document is to provide guidance on how to address important failure mechanisms when evaluating integrity of flexible pipes. The basis for the selection of failure mechanisms and associated assessment is best available knowledge in the JIP. It is recommended that these failure mechanisms must always be addressed. However, when designing a flexible pipe system or when using this document for IM or LTA purposes it is important that all requirements in [API 17J, 2008] as well as all failure mechanisms listed in [API 17B, 2008] are evaluated.

Further work on failure mechanisms is recommended. This would provide improved guidance related to all relevant failure mechanisms for flexible pipes and to quantify the probability of failure for the different failure mechanisms

## A3.2 Definitions of concepts and terminology

### A3.2.1 General concepts

#### A3.2.1.1 Ultimate pipe failure

The **ultimate failure** of flexible pipes will lead to loss of pipe functionality. This will either be loss of containment or blockage of the flow path. In more detail, it is possible to define 4 types of loss of functionality:

- Loss of containment - full pipe separation
- Loss of containment - leakage
- Blockage or restriction of the flow path caused by failure of a pipe layer (Carcass or liner collapse)
- Blockage or restriction of the flow path caused by the bore medium & bore conditions, or equipment used in pipe or well

It should be noted that blockage or restriction of the flow path caused by failure of a pipe layer might lead to subsequent processes and events leading to loss of containment. Blockage or restrictions of the flow path caused by the bore medium and bore conditions may in some cases be removed. In such cases it is important to be aware that the method to remove a blockage could introduce damages to pipe layers.

Examples of ultimate failure modes are:

- Progressive rupture of tensile armour leading to full opening of the bore of the pipe to the surrounding
- Rupture of the outer sheath when there is a leakage from the bore to the annulus
- Collapse of the carcass

### A3.2.1.2 Layer failure

Loss of functionality of a flexible pipe will often be the result of a sequence of damage events and/or time driven degradation mechanisms and layer (or component) failures.

Layer failure (or component failure) imply loss of layer (or component) functionality.

Loss of functionality of a layer will be the result of a time driven degradation process or a damage event. This can be described in terms of a degradation mechanism, events, root causes, failure mechanisms and consequences for the layer itself and for other parts of the pipe structure. The root cause of the degradation in one layer may be loss of functionality for another layer at an earlier stage.

In principle, layer failure where the degradation starts will be the result of operation outside design limits, unforeseen events or design incompatibilities. Layers in which known degradation mechanisms are taken into account during design should meet defined acceptance criteria at the end of the design life.

Integrity management should be directed at maintaining adequate margins against the failure modes (layer or component failures).

Detection of layer failure (through monitoring or inspection) is a valuable part of integrity management, in particular for failure sequences where the subsequent route to loss of pipe function gives adequate time for mitigation before ultimate pipe failure (for instance holes in outer sheath, small leakages from bore to annulus, flow restrictions).

### A3.2.1.3 Failure mechanism

Pipe failures should be described in terms of the failure mechanism:

1. Initiation of failure and deterioration of the layer (or component)
  - Time, event or condition based failure causes
2. Observed failure mode (layer or component failure)
  - Local failure effect (consequences for the layer or component itself)
3. Failure of subsequent layer(s) governed by associated failure cause
4. The ultimate loss of pipe functionality

### A3.2.2 Definitions

**Failure causes** includes the initiators, defects, processes and mechanisms generating damage or degradation and which are the basic reason for a failure. Failure causes may be divided into:

- **Degradation mechanisms** are time based physical or chemical mechanisms or processes by which the pipe layer degrades. Examples are: corrosion, fatigue, creep, embrittlement, erosion,
- **Damage event**. Examples are physical impact, unforeseen overloads loads, excessive bending etc.; by nature these are event driven. This can also be impacts from changing

properties of other layers or components such as forces generated on the carcass from changes in the pressure liner.

- **Service loads** are condition based threats to the pipe system such as changes in operational parameters

**Layer failure** is the loss of layer functionality.

**Failure mode** is the manifestation of loss of functionality for a layer in the pipe cross section, and it is the manner by which a failure is observed.

**Local effect** is the consequence of a failure on the layer itself, and is the actual damage to the pipe layer

**Subsequent effect** is the consequence of layer failure on other layers or components of the pipe, leading to the end-effect (ultimate pipe failure).

**End-effect** of a failure consists of two parts:

- The ultimate pipe failure mode is the manifestation of loss of pipe functionality, and it is the manner by which the ultimate pipe failure is observed.
- The ultimate pipe failure effect is the consequence of loss of pipe functionality: either loss of containment and/or blockage/restriction of the flow path.

#### **Failure mechanism**

Represents the chain of events, in terms of mechanisms and processes from the initial failure cause to the ultimate pipe failure

#### **Probability of Failure (PoF)**

The probability of the Ultimate Pipe Failure often annualized

### **A3.2.3 Probability of Failure (PoF)**

An important task in Integrity Management (IM) is to quantify the probability of failure as function of time in service. IM should focus attention on failure causes with the highest probabilities for leading to loss of pipe function.

IM rely on risk ranking where the risk is the product of Probability of failure PoF and Consequence of failure (CoF). Failure causes are assessed in terms of remaining time to loss of pipe function relative to required service life, relative utilization within Miner sum frameworks or safety margins relative loss of pipe function. In principle these parameters have to be converted to probability of loss of pipe function to enable consistent use in risk assessment.

Some ultimate failure modes can be initiated by damage events taking place during installation or operation.

- Damage events that have been detected and documented constitute a condition that has to be subjected to a separate assessment to determine the PoF based on calculated remaining service life or reduced capacity.
- PoF that relate to damaging events that have not been detected or events that may take place will typically be dominated by the probability of the event taking place.

The probability of failure for ultimate failure modes that are initiated through long-term degradation processes will be directly linked to the rate of degradation and the failure sequence following the initial layer failure.

It should be noted that the probability of failure in risk assessment is related to the ultimate loss of function and will thus represent the combined barriers against failure of the layer where the degradation process starts and for subsequent steps in the failure sequence.

#### A3.2.4 Format for Description of Failure Causes

One of the aims of this chapter is to identify relevant failure causes for all layers and components and described these to a level where it is possible to identify the level of susceptibility and estimate associated PoF. For each failure cause the following should be identified:

- Layer & layer function
- Material
- Applicability of failure cause for various pipe structures (design) and conditions
- Failure cause and promoting conditions
- Layer failure mechanism and the way it will manifest itself
- Acceptance criteria
- Procedure or models to predict remaining time to layer failure
- Identification of the operating or environmental conditions most likely to induce the layer failure
- Consequence of layer failure with identification of events and mechanisms leading to ultimate pipe failure
- Time scale for ultimate pipe failure after initial layer failure (imminent → long term)
- Parameters that will influence the time from layer failure to full pipe failure
- How will the ultimate pipe failure manifest itself
- Probability of failure considerations for pipe loss of functionality
- Possible mitigations against unacceptably high PoF
- Monitoring, inspection & prediction: methods and strategies
- Operational field experience

Failure trees should be specified identifying all degradation mechanisms that lead to one ultimate failure mode.

## A3.3 Flexible Pipe Failures

### A3.3.1 Overview of layer failures and failure causes

This section presents a list of known layer failures and failure causes for flexible pipes based on tables 30-31 in [API 17B, 2008] and a report from PSA Norway on flexible pipes [Muren, 2008] and JIP provided information. The list is revised to include only failures which imply loss of layer function. Defects in tables 30-31 in [API 17B, 2008] which are considered as causes rather than failures are categorized accordingly in Table A3.1. A selection of the failure causes are subject to a detailed evaluation in the next sections, also including ancillary devices as tether clamp, tethers and buoyancy modules. The selection is based on the dominant failures in historical data (details are given in Section A3.4 Failure Statistics) and failures which are considered important although considered carefully addressed in design.

Table A3.1: Layer failures and failure causes - ref: [API 17B, 2008], [Muren, 2008] and JIP provided information. Column 'Defect' refers to appropriate section in [API 17B, 2008]

Pipe Layer	Defect	Layer failure (loss of layer functionality)	Failure cause - Failure drivers and initiators - Degradation mechanisms and damage events
Carcass	1.2	Unlocking deformation or carcass tear-off	<ul style="list-style-type: none"> <li>- Overbending</li> <li>- Carcass axial overloading</li> <li>- Excess tension with bending</li> <li>- Pigging damage</li> </ul>
	1.3	Collapse	<ul style="list-style-type: none"> <li>Excessive pressure differential across carcass wall:</li> <li>- Pressure build-up between multilayer pressure sheaths</li> <li>- Rapid depressurization</li> <li>- Gas release of dissolved gases in the pressure sheath</li> <li>- Hydrate melting in the wall (hypothesis)</li> </ul> <p>Mechanical loads:</p> <ul style="list-style-type: none"> <li>- Overbending of the pipe</li> <li>- Mechanical crushing</li> </ul> <p>Erosion, corrosion or wear resulting in thinning of the carcass may lead to reduced collapse resistance</p>
	1.4	Circumferential crack or rupture (or fracture in carcass strip)	<ul style="list-style-type: none"> <li>- Carcass fatigue</li> <li>-&gt; Low cycle fatigue from loads imposed from the pressure sheath during shut down</li> <li>-&gt; High frequency vibrations due to vortex shedding at carcass cavities (in gas pipes)</li> <li>- Carcass-to-carcass (wire-to-wire) wear or friction</li> <li>- Rapid melting of hydrates formed inside the carcass structure</li> <li>- Stress corrosion resulting from high chloride content of the transported commodity</li> <li>- H<sub>2</sub>S corrosion (pitting) of the carcass material</li> </ul>

Pipe Layer	Defect	Layer failure (loss of layer functionality)	Failure cause - Failure drivers and initiators - Degradation mechanisms and damage events
Internal pressure sheath	2.1, 2.2 (2.4, 2.5, 2.6, 2.7, 2.8)	Crack, hole or rupture	- Ageing embrittlement -> (PA11 (hydrolysis, oxidation), -> PVDF (Deplasticization due to high temperature. Some types of PVDF are increasingly brittle at low temperatures), -> HDPE (oxidation)) - Excess creep (extrusion) of polymer into gaps between armours. - Blistering - Fatigue in polymer - Collapse inducing excessive deformation strains - Wear / nibbing due to abrasion between pressure sheath and carcass and/or pressure armour - Bonding between PVDF-sheaths (potential fabrication defect in multilayer pressure sheath structures)
	2.3	Collapse	Collapse a. Smooth bore: excessive pressure differential across pressure sheath b. Rough bore: associated with carcass collapse (see above: Carcass)
Pressure armour layer	3.1, 3.4, 3.5	Individual or multiple wire rupture	- Hydrogen induced cracking (HIC) or sulfide stress cracking (SSC) -> 'High' H <sub>2</sub> S levels in particular when material selection has not identified the need for sour service steel - Corrosion -> Acid species such as CO <sub>2</sub> diffusing from the bore to a water filled annulus. - Wire-to-wire wear and fatigue - Excess internal pressure - Failure of tensile or back-up pressure armour
	3.2	Development of excessive gaps between neighbouring wires through unlocking or separation of very long circumferential cracks.	- Overbending - Excess tension - Impact - Failure of tensile or back-up pressure armour - Radial compression (at installation) - Excess torsion (at installation)
	3.3	Collapse	- Impact or point contact - Excess tension - Radial compression (at installation)
	3.6	Longitudinal wire crack	Wire-to-wire contact and local stress concentration

Pipe Layer	Defect	Layer failure (loss of layer functionality)	Failure cause - Failure drivers and initiators - Degradation mechanisms and damage events
Back-up pressure armour layer	4.1, 4.4	Rupture (single wire or all wires)	- Hydrogen induced cracking (HIC) or sulfide stress cracking (SSC) -> 'High' H <sub>2</sub> S levels in particular when material selection has not identified the need for sour service steel - Corrosion - Acid species such as CO <sub>2</sub> diffusing from the bore to a water filled annulus. - Excess internal pressure - Failure of tensile or back-up pressure armour
	4.5	Individual or multiple wire crack	- Wear due to abrasion between back-up pressure armour layer and (inner) pressure armour layer - Fatigue
Tensile armour layer	5.1, 5.4, 5.5	Individual or multiple-wire rupture	- Corrosion leading to loss of cross section -> Acid species such as CO <sub>2</sub> diffusing from the bore to a water filled annulus -> Oxygen corrosion resulting in sea water ingress and renewal combined with inadequate cathodic protection - Hydrogen induced cracking (HIC) or sulfide stress cracking (SSC) -> 'High' H <sub>2</sub> S levels in particular when material selection has not identified the need for sour service steel - Excess tension or internal pressure - Fatigue - Rupture from Impact - Deformation from impacts leading to reduced fatigue life. - Wear between steel armor layers and other layers
	5.2	- Buckling of the pipe - Buckling of tensile wires: radial (bird-caging) or lateral buckling	- Excessive axial compression - Overtwist
	5.3	Kinking	- Impact or point contact - Error/defect from design, manufacturing or installation - Installation -> Handling on board vessel -> Stroke back before subsea tie-in
Anti-wear layer	6.1, 6.2	Excessive wear leading to radial contact between armour layers in dynamic pipes	- Ageing leading to embrittlement - Wear from excessive contact forces - Clustering (manufacturing)

Pipe Layer	Defect	Layer failure (loss of layer functionality)	Failure cause - Failure drivers and initiators - Degradation mechanisms and damage events
Insulation layer	7.1, 7.2, 7.3	Inadequate insulation (potentially causing pipe clogging)	- Crushed layer -> During installation -> External overpressure -> Inadequate pressure resistance - Flooded layer -> Ingress of seawater (e.g. hole in outer sheath) - Inappropriate design
Outer sheath	8.1, 8.3 (8.2)	Hole, tear, rupture or crack	- Impact - Wear or abrasion - Excessive annulus pressure build-up - Ageing embrittlement and degradation
End fitting	9.1	Internal pressure sheath pull-out	- Pressure sheath shrinkage - Pressure sheath creep - Loss of friction - Tear of pressure sheath with inadequate ductility
	9.2, 9.6	Tensile-armour pull-out (individual or all wires)	- See above: tensile armour wire rupture - Epoxy degradation (due to sour service or high temperature) - Loss of friction - Excess tension
	9.3	Outer sheath pull-out	- Outer sheath creep - Excess annulus pressure
	9.4	Vent-valve blockage	- Blockage due to annulus fluids, foreign fluids or objects from vent system, corrosion, fabrication error
	9.5	Vent-valve leakage	- Corrosion - Seal failure
	9.7	Failure of sealing system (sealing rings, etc.)	- Erroneous / inadequate design, fabrication or installation - Excess internal pressure, tension or torsion - Excessively low temperature
	9.8	Crack or rupture of pressure armour or back-up pressure armour	See above: pressure armour or back-up pressure armour wire rupture
	9.9	Crack or rupture of tensile armour	See above: tensile armour wire rupture
	9.10	Structural failure of end fitting body or flange	- Excess internal pressure, tension or torsion - Inadequate design - Hydrostatic collapse - Corrosion or chemical degradation -> Exposure to seawater (diminished anodes or coating break down) - Fatigue - Brittle fracture
	9.11	Cracking of pressure sheath	See above: internal pressure sheath (crack, hole or rupture)

### A3.3.2 Detailed evaluation of selected flexible pipe layer failure causes

#### A3.3.2.1 Carcass

**A3.3.2.1.1 Carcass collapse** Evaluation of failure causes for carcass collapse is presented in Table A3.2

Table A3.2: Carcass collapse

Layer & layer function	Carcass prevents collapse; protects pressure sheath from mechanical abrasion and to some extent also chemicals. However, the latter is mostly a drawback with the possibility of chemicals being trapped behind carcass prolonging the exposure
Materials	Mainly stainless steel, see [API 17B, 2008]
Applicability of failure cause for various pipe structures (design) and conditions. [Note limitations, ref Section A3.1.2]	Applicable for any multilayer pressure sheath pipe designs. Very rapid depressurization of any rough bore pipe (Depressurization rates within manufacturer's limits are considered safe for single layer pressure sheaths). Any rough bore pipe with reduced collapse resistance due to erosion, corrosion, ovalization, excessive bending or mechanical damage.
Degradation mechanisms.	Interlayer pressure build-up in the gap between carcass and pressure sheath, or for pipes with multilayer pressure sheaths: between the pressure sheaths, or pressure outside pressure sheath. Excessive pressure in annulus due to liquid filling at large water depth. At a sudden pressure drop in pipe bore, there is still an outside pressure which exerts a pressure force on the pressure sheath and/or the carcass; causing the ultimate collapse.
Layer failure mechanism and the way it will manifest itself	<p><b>I. Collapse due to high pressure in the annulus</b> Often due to hole in the outer sheath combined with reduced carcass collapse capacity.</p> <p><b>II. Rapid depressurization (the most probable cause)</b> The mechanism depends on the cross section and number of pressure sheaths. The failure and its three different modes are illustrated in Figure A3.1 and Figure A3.2 .</p> <p><u>Single layer pressure sheaths</u> Operation within operational limits and permissible depressurization rates is considered safe.</p> <p><u>Two layer pressure sheaths</u> The carcass and the second pressure sheath are both terminated in the pipe ends. The first pressure sheath lying between the carcass and the second pressure sheath is not terminated in the pipe ends. Hence, for a pipe in operation, fluids will over time migrate through the end-fitting and by diffusion through the inner pressure sheath and into the gap between the first and second pressure sheaths. The pressure in this gap is then approximately the same as the bore pressure. Slow depressurization is required to avoid large differential pressures across the inner pressure sheath. This is due to the small channel in the end-fitting. Thus, a rapid decompression of the bore may cause carcass collapse.</p>

	<p><u>Three layer pressure sheaths</u></p> <p>Here the pipe wall structure is similar to the two layer structure with an additional third pressure sheath on the outside of the second pressure sheath. This layer is terminated in the pipe ends.</p> <p>For a riser in operation, there will be diffusion through the pressure sheaths. Dependent on the operational and environmental conditions, the temperature gradient through the cross section may be so that the diffused gas accumulates and possibly condensates in the gap between the second and third pressure sheaths. This will in turn cause a pressure increase in this gap. For a pipe operating at 200 bars it is estimated that soon after pressure relief of the bore, a pressure of over 100 bars might be obtained in the gap between the second and third pressure sheath. Slow process of diffusion, slow depressurization is required to limit differential pressures across the pressure sheaths. On the contrary, a rapid decompression of the bore may cause carcass collapse.</p>
Conditions promoting degradation	<p><b>III. Gas release of dissolved gases in the pressure sheaths</b></p> <p>Reference is given to [Farnes et al., 2013]. This failure is applicable for pipes with multilayer pressure sheaths operating at high pressures (<math>\approx</math> 300-400 bars). Dissolved gases in the polymer are released and entrapped between the second and third polymer layers, causing pressure build up which ultimately results in collapse of the carcass and the two inner polymer sheaths after bore depressurization.</p> <p><b>IV. Bending of the pipe</b></p> <p>The carcass collapse capacity is reduced in bending; the reduction is significant close to MBR. Handling of the pipe may cause locally large curvature. For significant bending close to MBR, hydrostatic pressure may be sufficient to cause carcass collapse, all dependent upon the designed carcass collapse capacity.</p> <p><b>V. Hydrate melting in the wall (hypothesis)</b></p> <p>This failure mechanism is at present not fully understood. However, the components for hydrate formation may diffuse through the pressure sheaths and hydrates may form in the gap between the pressure sheaths under certain conditions (high pressures and low temperatures), during a shut-down. Then due to heating (e.g. start-up with circulation of oil during oil production) the hydrate melts and releases gas; resulting in a significant pressure increase sufficient to cause carcass collapse.</p> <p>The collapse manifests itself as carcass folding (typical heart shape) over a distance of the pipe, as illustrated in Figure A3.3, possibly with rupture of the carcass. The carcass collapse may progress in discrete steps: a starting collapse manifested as a dent, and subsequently a total collapse at a later depressurization event.</p> <p>Differences are seen with respect to the number of collapsed layers. In case of water and hydrostatic pressure in annulus, all layers (all pressure sheaths and the carcass) may collapse.</p> <ul style="list-style-type: none"> <li>- High operational bore pressure in combination with rapid depressurizations (frequent shut-downs)</li> <li>- Pressure sheath and carcass designs promoting interlayer pressure build-up: In particular <b>3-layer pressure sheaths</b>. Also promoted by end-fittings manufactured with limited passage for interlayer fluids to escape from the gap between pressure sheaths</li> </ul>

Acceptance criteria for degradation mechanism	No permanent deformations are allowed.
Procedure or models to predict service life or PoF for layer	- Full scale testing (performed by vendors) - Diffusion calculations - Analytical tools: Recommend 3D FEA
Identification of the operating or environmental conditions most likely to induce the ultimate layer loss of functionality	- Shut down with rapid depressurization - Pipe bending  - Heating after hydrate events in bore
Consequence of loss of layer functionality with identification of events and mechanisms leading to ultimate pipe failure	- Complete or partial bore obstruction - Loss of containment (leakage)  The pressure sheath(s) may be intact after the carcass collapse. However, it has lost its inner support and is vulnerable to pressure cycles: The pressure sheath will then unfold to somewhat near its original shape when the bore is pressurized and then collapse during bore depressurizations. Repeated cycling will ultimately lead to rupture of the pressure sheath with leakage to annulus and subsequently pipe leakage.
Time scale for loss of pipe functionality after initial loss of layer function (imminent → long term)	Imminent: Bore flow obstruction  Medium-long term: Damage to pressure sheath progressing to loss of containment (leakage)
Parameters that will influence the time from loss of initial layer functionality to full pipe failure	Bore flow obstruction: Carcass design and the pressure differential across the sheath at the time of collapse, the result may vary from a beginning collapse in form of a small dent to a near total pipe blockage. Loss of containment: Damage to pressure sheath in terms of crack initiation and/or pressure sheath deformation. The time to leakage is often governed by the progression into pressure sheath.
How will the ultimate pipe failure manifest itself	Loss of pipe function in terms of pipe blockage. Loss of containment: leakage.
Probability of failure considerations for pipe loss of functionality	3-layer pressure sheaths: Very high, provided high operational pressures and frequent/rapid depressurizations  1 or 2-layer pressure sheaths: Low
Possible mitigations against unacceptable high PoF	Operational procedures - Proper procedure for depressurizations. - For multilayer structures subject to possible hydrate formation: Maintain high pressure after restart and bore heat-up - Avoid breach in the outer sheath - Avoid excessive bending after periods with high pressure production
Monitoring, inspection & prediction: methods and strategies	- Annulus flow monitoring may provide early warning to avoid emerging loss of containment. - Pressure drop between subsea and topside pressure gauges may indicate bore obstructions - Internal inspection

Operational field experience	Many carcass collapses are experienced for 3-layer PVDF pressure sheath risers after decompression from high operational pressures. Carcass collapse is also experienced after seabed reconnection and local bending.
------------------------------	---

## Pipe wall pressures

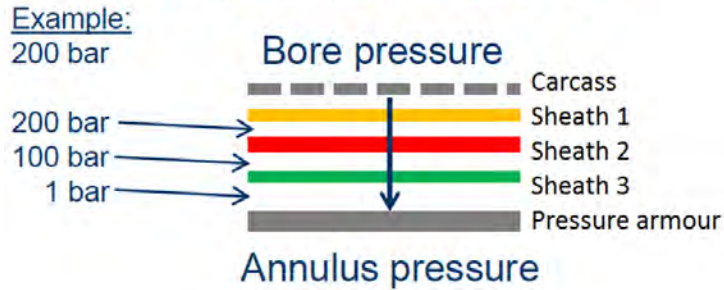


Figure A3.1: An example of possible pipe wall pressures

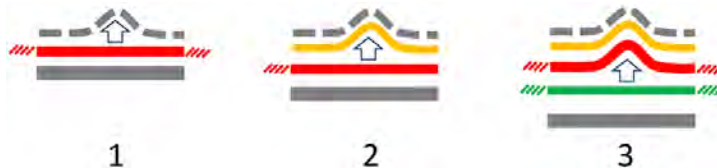


Figure A3.2: Carcass collapse mechanism for 1) Single layer 2) Two layer 3) Three layer pressure sheaths



Figure A3.3: Carcass collapse [Muren, 2008]

**A3.3.2.1.2 Carcass axial overloading** Evaluation of failure causes for carcass axial overloading is presented in Table A3.3

Table A3.3: Carcass axial overloading

Layer & layer function	Carcass prevents collapse; protects pressure sheath from mechanical abrasion and to some extent also chemicals. However, the latter is mostly a drawback with the possibility of chemicals being trapped behind carcass prolonging the exposure.
Materials	Mainly stainless steel, see [API 17B, 2008].
Applicability of failure cause for various pipe structures (design) and conditions. Note limitations, ref Section A3.1.2	Deepwater applications with high axial loading on carcass termination. Bore blockage (e.g. pigging, wax or hydrates). Multilayer pressure sheath riser with axial load contributions from both gravity and polymer crimp.
Degradation mechanisms.	<p><b>A) Pipe blockage and large differential pressure</b> Initiation by pipe blockage in terms of wax or hydrate formation, slug or erroneous pig. The degradation is then promoted by applying a high differential pressure across the blockage such as:</p> <ul style="list-style-type: none"> <li>- Large inlet pressure at start up</li> <li>- Injection at high pressure of chemicals/solvent to remove hydrates or wax</li> </ul>

	<p>The pressure force due to the differential pressure across the blockage is transferred by friction/mechanical coupling from the blockage to the carcass, resulting in potentially large axial loads. This also applies for gas producing pipes with liquid slugs where the differential pressure across the slug is transferred by friction to the carcass at high flow velocities.</p> <p>Subsequent progression is dependent on the radial contact between carcass and the other layers in the cross section. Sufficient radial contact/coupling may possibly save the carcass from axial overload.</p> <p><b>B) Loss of radial contact between the inner layers</b></p> <p>Reference is given to [Skeie et al., 2013]. In the absence of pipe obstructions, the main axial load contributions in the carcass and the pressure sheath(s) are due to gravity of the carcass and due to temperature stresses in the pressure sheath(s). These axial loads are intentionally transferred to the surrounding layers by friction and geometrical effects. The radial contact between the inner layers may decrease over time due to:</p> <ul style="list-style-type: none"> <li>- Changes in polymer properties (e.g. volume loss)</li> <li>- Temperature and pressure effects</li> <li>- Diffusion through the pressure sheaths or migration of fluids through the end-fittings; resulting in interlayer pressurized gas/liquid pockets.</li> </ul> <p>Dependent on the cross section, fabrication and operational conditions, the loss of sufficient radial contact may allow for axial movement within the pipe:</p> <p>Either</p> <ul style="list-style-type: none"> <li>- Axial movement of carcass relative to the remaining pipe</li> </ul> <p>Or</p> <ul style="list-style-type: none"> <li>- Axial movement of carcass and pressure sheath(s) relative to the remaining pipe</li> </ul> <p>Multilayer PVDF pressure sheaths are more vulnerable to the latter due to possible volume loss in the PVDF over time.</p> <p>The capacity against axial overloading is then dependent on the carcass axial capacity, in combination with the axial capacity of the polymeric pressure sheath in the latter case. Carcass axial overload is illustrated in Figure A3.4</p>
Layer failure mechanism and the way it will manifest itself	<p>The carcass geometry is important for the failure progression: the carcass is intentionally manufactured with a nominal pitch allowing for some extension or compression before taking significant load. Dependent on the carcass geometry relative to the axial load direction, the carcass will either reach the carcass profile limit for compression or the profile limit for elongation. When reaching one of these limits, the carcass will start to take significant axial load. The first of these limits to be exceeded will govern the further progression. The carcass axial load capacity is generally larger in compression than in elongation.</p> <p>When the carcass axial load exceeds the axial capacity, the failure will manifest itself in terms of carcass buckling, tear-off or spin out. In case of a failure near the topside end, provided loss of radial contact over a sufficient distance, the carcass - and possibly pressure sheath(s) - may fall down several meters through the pipe bore. The distance of the fall will then be limited by compression forces in carcass and radial contact with surrounding layers.</p>

Conditions promoting degradation	<ul style="list-style-type: none"> <li>- Fully extended carcass: the carcass does not allow for any additional extension before taking significant load.</li> <li>- Loss of radial contact in the cross section. This may be promoted by changes in polymers over time, geometry and by interlayer liquids</li> <li>- For blockage: Rapid pressure build-up without sufficient awareness on pressure measurement</li> <li>- Insufficient anchoring of the carcass in the end-fitting</li> </ul>
Acceptance criteria for degradation mechanism	<p>Primarily dependent on the cross-section and the allowable utilization of the axial capacity.</p> <p>For multilayer pressure sheaths: low temperature and high pressure limits may be established</p> <p>Also dependent on</p> <ul style="list-style-type: none"> <li>- Carcass condition (e.g. fully extended or nominal pitch)</li> <li>- Dynamic or static section. Vertical dynamic sections are more critical.</li> </ul>
Procedure or models to predict service life or PoF for layer	<p>Axial testing of carcass capacity, inspection of carcass condition and comparison of the two.</p> <p>See also description above for <i>Acceptance criteria for degradation mechanism</i>.</p>
Identification of the operating or environmental conditions most likely to induce the ultimate layer loss of function	<ul style="list-style-type: none"> <li>- Start-up sequences</li> <li>- Planned circulation at high pressure of chemicals for removal of pipe obstructions</li> <li>- Pressure testing of cold riser</li> </ul> <p>Important parameters:</p> <ul style="list-style-type: none"> <li>- The location of an obstruction</li> <li>- The amount and locations of liquids and gas in the pipe must be known in order to calculate differential pressures</li> <li>- Mechanical interaction between pressure sheath and layers inside/outside</li> </ul>
Consequence of loss of layer function with identification of events and mechanisms leading to ultimate pipe failure	<p><b>Worst case:</b> Carcass pull-out near end-fitting. Dependent on end-fitting design this may result in pull out of pressure sheath and pressure armour.</p> <p><b>Best case:</b> Reduced collapse capacity. Damage to pressure sheath and possibly further progressive damage:</p> <ul style="list-style-type: none"> <li>- If multilayer PVDF-pressure sheath: Axial loading in PVDF-sheath pulls the carcass sections apart, leaving the pressure sheath exposed to carcass - strip which may cause scratches in the pressure sheath. These scratches may promote PVDF-fatigue when subject to temperature (or pressure) cycles.</li> </ul> <p>The failure will eventually result in pipe leakage and loss of containment. The time scale is however significantly different for the best and worst case.</p>
Time scale for loss of pipe function after initial loss of layer function (imminent → long term)	<p><b>Worst case:</b> Carcass and pressure armour pull out in end-fitting, will cause leakage in very short time.</p> <p>Dependent on the location of the failure and the cross section, the time scale may be from imminent to long term.</p>
Parameters that will influence the time from loss of initial layer function to full pipe failure	<ul style="list-style-type: none"> <li>- Location of the failure relative to end-fitting and high/low pressure end</li> <li>- Cross section</li> <li>- Variations in pressure and temperature</li> <li>- Localized concentrated dynamics</li> </ul>
How will the ultimate pipe failure manifest itself	The ultimate failure will be pipe leakage preceded by pressure rise in annulus. Pipe leakage may be avoided by swift and proper response to an increased annulus pressure.

Probability of failure considerations for pipe loss of function	Lower operational and applied pressures promote safe operation. An example of risk evaluation for carcass capacity of selected risers is presented in [Farnes et al., 2013].
Possible mitigations against unacceptable high PoF	<ul style="list-style-type: none"> <li>- Operational procedures <ul style="list-style-type: none"> <li>-&gt; Avoid cold operation with high pressure</li> <li>-&gt; Operations should be planned with respect to carcass capacity.</li> <li>-&gt; Care should be exercised at start-up and procedures for start-up should reflect this failure mode.</li> <li>-&gt; During blockage (e.g. hydrate, wax or stuck pig) removal operation this failure mode should be considered</li> </ul> </li> </ul>
Monitoring, inspection & prediction: methods and strategies	<p>Monitoring of pressure and temperature both subsea and topside, particularly during start-up operation, to detect emerging pressure differences and recognize the larger differential pressures.</p> <p>Internal inspections of carcass for comparison with carcass capacity. Internal inspections should be performed after incidents where excessive carcass axial loads are expected, such as after hydrate removals. The carcass should be inspected both upstream and downstream of the hydrate plug location.</p>
Operational field experience	<p>The following degradation modes are observed in operation:</p> <ul style="list-style-type: none"> <li>- Pipe blockage and large differential pressure</li> <li>- Loss of radial contact between the inner layers</li> <li>- Axial overload due to gravity and polymer crimp in multilayer pressure sheaths.</li> </ul>

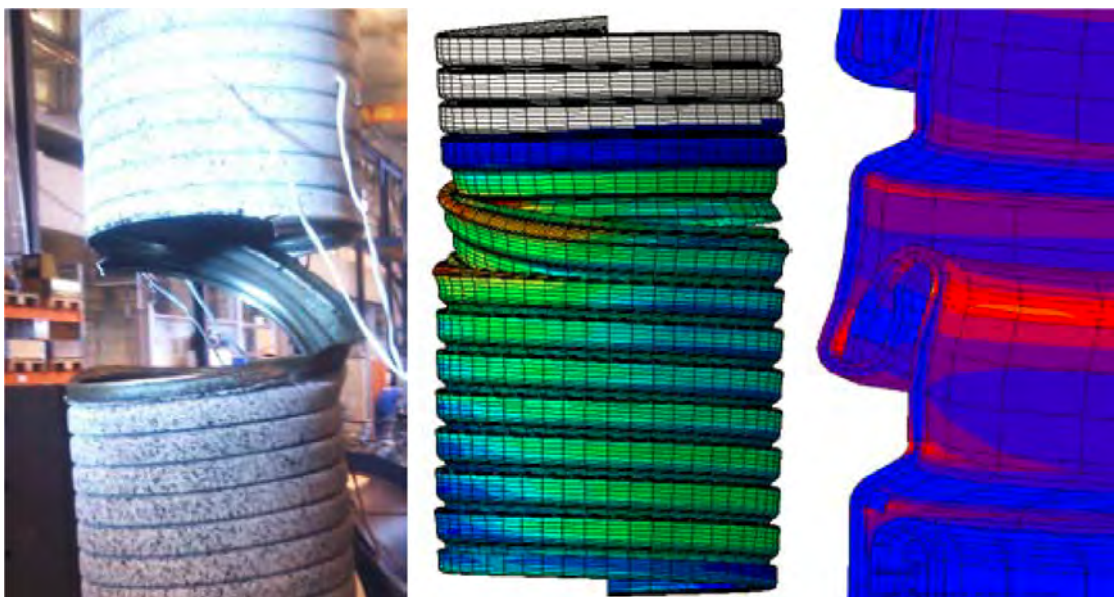


Figure A3.4: : Sample testing and FEM analysis [Farnes et al., 2013]

**A3.3.2.1.3 Carcass fatigue** Evaluation of failure causes for carcass fatigue is presented in Table [A3.4](#)

Table A3.4: Carcass fatigue

Layer & layer function	Carcass prevents collapse; protecting pressure sheath from mechanical abrasion and to some extent also chemicals. However, the latter is mostly a drawback with the possibility of chemicals being trapped behind carcass prolonging the exposure
Materials	Mainly stainless steel, for details reference is given to <a href="#">[API 17B, 2008]</a>
Applicability of failure cause for various pipe structures (design) and conditions Note limitations, ref Section <a href="#">A3.1.2</a>	Carcass fatigue is applicable to any dynamic rough bore pipes.  Consequence of carcass fatigue is most significant for pipes with PVDF pressure sheath due to risk for crack growth into pressure sheath.
Degradation mechanisms	Carcass should intentionally by design not have significant bending stiffness, and the carcass should have a nominal pitch allowing for some (small displacement) extension or compression before taking significant load. Typical carcass pitch lengths are heavily dependent on pipe dimensions and manufacturer (Recent measurements performed of carcass pitch length on a number of retrieved risers shows values in the range 13-22mm for 6"-9" ID risers (mainly pipes from one manufacturer)).

**Initiation**

- I. Fabrication: Carcass too 'tight', allowing for limited extension or compression before taking load, which causes high contact forces (increased bending stiffness) and high stresses in bending.
- II. Sand or deposits in carcass profile limiting the extension/compression, causing high contact forces (increased bending stiffness) and high stresses in bending.
- III. Dent or corrosion: limits (i.e. reduce) the extension and compression, causing stress concentration (i.e. partly locked) carcass
- IV. Fully stretched carcass
  - Due to fabrication
  - Developed over time in operation due to interaction with pressure sheath, e.g. due to stresses in the pressure sheath induced from temperature cycles and gravity of the carcass, see the *Degradation mechanism* in Section [A3.3.2.1.2](#) Carcass axial overloading.
- V. Clamp or interface load, over MWA. Cause of ovalization, changes the stress distribution, increased dynamic stresses in bending. MWA: All loading in bending (all cycles) concentrated in one location: promoting fatigue in the top section of the lower catenary
- VI. Pigging. Incompatible pig may cause local carcass deformations which in turn may provide weakened spots or points of stress concentration more susceptible to fatigue

Layer failure mechanism and the way it will manifest itself	Carcass fatigue: Circumferential fracture for failures experienced in operation. Fracture in carcass-strip (fracture parallel to pipe axis) considered to be unlikely compared to circumferential fracture.
Conditions promoting degradation	- Dynamic bending loading: large magnitude and frequently occurring. - Reduced carcass flexibility due to the issues listed above under <i>Initiation</i>
Acceptance criteria for degradation mechanism	Threshold value for stress level in carcass. Typically stress range above 100 MPa
Procedure or models to predict service life or PoF for layer	Concern for probability of failure: - Clamping: Clamps consisting of 2 half shells should be avoided, particularly if exposed to bending. Clamps are recommended to be made of 3 or 4 shells. In case of perfect fit of clamp, there are no differences between 2 half shells and 3 or 4 half shells. However, due to fabrication tolerances of the pipe, a poorer fit of the clamp may be the result. 3-4 shells provide a better distribution of contact force/stress - Fully extended carcass - Initial collapse, deformation or corrosion  Methodology: Structural model and evaluation
Identification of the operating or environmental conditions most likely to induce the ultimate layer loss of functionality	- High dynamic bending promoting fatigue loading - Pressure and temperature fluctuations promoting the progression into polymer layers  See description above of initiation (Degradation mechanisms) in combination with <i>conditions promoting degradation</i> .
Consequence of loss of layer functionality with identification of events and mechanisms leading to ultimate pipe failure	After carcass fracture: - Reduced collapse capacity. Damage to surrounding layers: - If multilayer PVDF-pressure sheath: Axial loading in PVDF-sheath pulling the carcass sections apart, leaving the pressure sheath exposed to carcass-strip which may cause scratches in the pressure sheath. These scratches may cause PVDF-fatigue when subject to temperature (or pressure) cycles.  Eventually resulting in leak from bore and subsequent pipe leakage.  If stiff carcass: after carcass circumferential fracture, concentration of pipe curvature at fracture location.
Time scale for loss of pipe functionality after initial loss of layer function (imminent → long term)	Long term
Parameters that will influence the time from loss of initial layer function to full pipe failure	- Polymer properties: PVDF is sensitive to notches, such that it is vulnerable when suffering from scratches and exposed to temperature cycles - Carcass loading: Worse conditions with liquid in annulus and low bore pressure

How will the ultimate pipe failure manifest itself	As for hole in pressure sheath: pipe leakage with loss of containment.
Probability of failure considerations for pipe loss of functionality	Probability reduced for new pipes as more QA on carcass is implemented.
Possible mitigations against unacceptable high PoF	<p>Generally, no mitigation actions in operation.</p> <p>Possible modifications:</p> <ul style="list-style-type: none"> <li>- Re-termination if hot-spot near pipe end, move the most loaded point.</li> <li>- Change average offset of installation, move the most loaded point.</li> <li>- MBR: Add a margin to dynamic MBR. For riser over MWA, change MBR for the pipe segment with fixed length (constant hot-spot for loading)</li> </ul> <p>These actions must be confirmed with calculations/analysis.</p> <p>Design: - Clamp: Use clamps made of 3 or 4 part shells, not 2 half shells.  - Fabrication follow up and QA in design. Carcass tolerances are now improved in fabrication</p>
Monitoring, inspection & prediction: methods and strategies	<p>Internal inspection to identify:</p> <ul style="list-style-type: none"> <li>- Deposits</li> <li>- Fully extended carcass</li> <li>- Initial defects</li> <li>- Fracture (at the correct time)</li> <li>- Concentrated bending e.g. at tether clamps or bend stiffeners</li> </ul> <p>There are several ways to perform carcass pitch measurements during an internal inspection. There exist specific tools for these measurements. However, some restrictions apply. In order to detect a fully extended carcass, specific information on carcass profile is required: detailed as-built data or a sample of the actual carcass.</p> <p>QA in design and fabrication is important to reduce the probability of occurrence for this failure mode.</p>
Operational field experience	Carcass fatigue resulting in ultimate pipe failure is experienced for one pipe, ref. Figure A3.5 and Figure A3.6.

Illustrations of a carcass fatigue fracture and initiating fatigue fractures in pressure sheet are shown inn Figure A3.5 and Figure A3.6.

H



Figure A3.5: Carcass fatigue fracture ref. [Talisman Energy Norge AS, 2005]

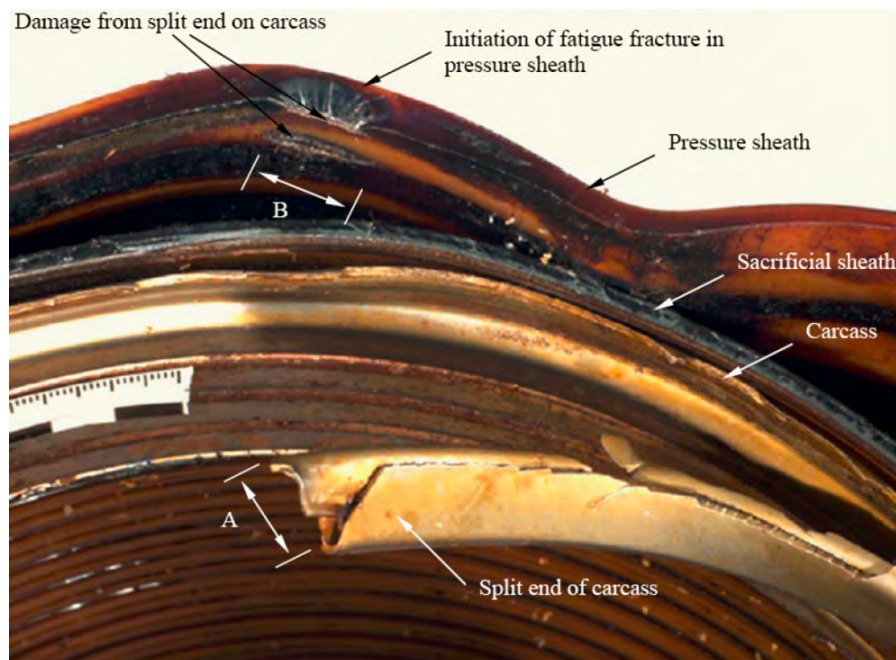


Figure A3.6: Carcass fatigue: carcass strip and initiating fatigue fractures in pressure sheath, ref. [Talisman Energy Norge AS, 2005]

### A3.3.2.2 Pressure sheath

**A3.3.2.2.1 Collapse of pressure sheath (Smooth Bore)** Evaluation of failure causes for Collapse of pressure sheath (Smooth Bore) is presented in Table A3.5.

Table A3.5: Collapse of pressure sheath (Smooth Bore)

Layer & layer function	Pressure sheath ensures containment of fluids and gas within the bore of the pipe
Materials	Polyamide Polyethylene
Applicability of failure cause for various pipe structures (design) and condition. Note limitations, ref Section A3.1.2	Only applicable to smooth bore flexible pipes, family I. Smooth bore risers are mainly used for water injection/transfer, however also used in gas export applications
Degradation mechanisms.	Pressure differential between pipe bore and annulus resulting in repetitive collapse of pressure sheath
Layer failure mechanism and the way it will manifest itself	<p>Failure mechanism:</p> <ul style="list-style-type: none"> <li>- Cyclic deformation of pressure sheath resulting in fatigue failure of pressure sheath or</li> <li>- Severe deformation directly resulting in failure of pressure sheath</li> </ul> <p>Failure mechanism will depend on actual polymer properties at the initiation- or repeated occurrence of the degradation mechanism</p> <p>The way the failure manifest itself:</p> <ul style="list-style-type: none"> <li>- Upon re-pressurization of pipeline, after pressure sheath has developed critical defect size, through thickness crack will occur allowing fluid flowing into annulus</li> </ul> <p>Temporarily blockage may occur due to pressure sheath collapsing. After repeated cycling however, loss of layer functionality is to be expected.</p>
Conditions promoting degradation	<ul style="list-style-type: none"> <li>- Rapid valve closure leading to vacuum in pipeline sections</li> <li>- Defects in intermediate sheath (if present)</li> <li>- Flooded annulus increasing static pressure differential</li> <li>- Failure of vent-system and trapped gas in annulus</li> <li>- Annulus testing where Ptest &gt; Pbore</li> <li>- Unintended removal of internal fluid or internal pressure, e.g. dewatering</li> </ul>
Acceptance criteria for degradation mechanism	Pressure sheath fluid containment, i.e. no through sheath defects
Procedure or models to predict service life or PoF for layer	<ul style="list-style-type: none"> <li>- Collapse capacity calculations</li> <li>- Verification of pressure differential between annulus and bore (pressure monitoring data, annulus testing if availability of vent-ports).</li> <li>- Reference testing of pipeline cross section</li> <li>- Leak testing of pipeline if critical defects are suspected.</li> <li>- Caliper pigging should not be used to validate condition of smooth bore pipe. All internal inspection should be performed with care due to risk of unintentional damages to pressure sheath.</li> </ul>

Identification of the operating or environmental conditions most likely to induce the ultimate layer loss of functionality	<ul style="list-style-type: none"> <li>- Start-up and re-pressurization after event where bore pressure may have been below allowable operational- and design limits.</li> <li>- Upon flooding annulus - if bore pressure is less than external hydrostatic pressure. Where an intermediate sheath is used, this failure mode is only relevant if loss of layer function in intermediate sheath is present.</li> <li>- During annulus testing with incorrect procedures</li> </ul>
Consequence of loss of layer functionality with identification of events and mechanisms leading to ultimate pipe failure	<ul style="list-style-type: none"> <li>- The ultimate failure occurs upon burst of outer sheath, i.e. loss of containment.</li> <li>- Rupture and/or unlocking of armour wires may occur due to inability to withstand bore pressure</li> </ul>
Time scale for loss of pipe functionality after initial loss of layer function (imminent → long term)	<ul style="list-style-type: none"> <li>- Burst of the pipe could take place within seconds to hours (maybe days) after the pressure sheath rupture or through thickness crack.</li> <li>- Short term, in high-pressure systems imminent failure may occur</li> </ul>
Parameters that will influence the time from loss of initial layer functionality to full pipe failure	<ul style="list-style-type: none"> <li>- Operating pressure</li> <li>- Pipeline cross section design, e.g. separate pressure armour layer or 55deg structure</li> </ul>
How will the ultimate pipe failure manifest itself	<ul style="list-style-type: none"> <li>- Pressure loss in bore.</li> <li>- Burst of the pipe or rupture of the outer sheath with release of bore fluid (gas, water).</li> </ul>
Probability of failure considerations for pipe loss of functionality	<ul style="list-style-type: none"> <li>- Collapse capacity of pressure sheath</li> <li>- Pressure sheath material type and condition</li> </ul>
Possible mitigations against unacceptable high PoF	<ul style="list-style-type: none"> <li>- Operational procedures, i.e. avoid rapid valve closure or depressurization rates through adjusted valve closing sequences</li> <li>- Operational procedures, i.e. maintain positive pressure differential between bore and annulus</li> <li>- Vacuum breaker in pipe system</li> <li>- Vacuum in annulus</li> <li>- Annulus test procedures limiting test pressure differential across pressure sheath</li> </ul>
Monitoring, inspection & prediction: methods and strategies	<p>Pressure monitoring data review</p> <p>Annulus testing</p> <ul style="list-style-type: none"> <li>- Verification of intermediate sheath functionality (if present)</li> <li>- Verification of annulus conditions</li> <li>- Vent-port capacity verification</li> </ul> <p>Leak testing of pipeline if defect is suspected</p>
Operational field experience	<ul style="list-style-type: none"> <li>- Several failure have occurred, resulting in loss of containment and structural failure of cross section</li> <li>- Failure have been due to rapid valve closure and depressurizations resulting in bore vacuum combined with high annulus pressure, failure of vent-system combined with previous incidents, incorrect annulus testing combined with low bore pressure.</li> <li>- Indirect failures due to internal inspections after suspected collapse, resulting in damages to pressure sheath and pressure sheath failures.</li> </ul>

**A3.3.2.2.2 Pressure sheath embrittlement (Ageing of Polyamides)** Evaluation of failure causes for pressure sheet embrittleness is presented in Table A3.6

Table A3.6: Pressure sheath embrittlement (Ageing of Polyamides)

Layer & layer function	Pressure sheath ensures containment of fluids and gas within the bore of the pipe
Materials	PA11 - Rilsan BESNO 40 TL. Considerations around threats to PA11 may also be applicable to other Polyamides such as PA12 but the acceptance criteria are not directly applicable to other grades of polyamides.
Applicability of failure cause for various pipe structures (design) and conditions Note limitations, ref Section A3.1.2	Applicable to all pipes with PA pressure sheath.
Degradation mechanism	Embrittlement through polymer chain scission caused by hydrolysis enhanced by elevated temperature and stimulated by acids and methanol
Layer failure mechanism and the way it will manifest itself	Brittle rupture or crack growth through thickness. The length of the rupture will depend on the degree of embrittlement of the material and how it varies with position and the event initiating the final rupture.  Fresh PA11 (and other relevant Polyamides) is generally very resistant to fatigue. However, embrittlement of Polyamides from ageing will enhance the susceptibility to crack initiation. In particular strong degradation on the inner surface of a PA11 pressure sheath may lead to sufficient brittleness for cracks to initiate. After initiation a crack may grow into more ductile material. There is also a possibility that chemicals in the bore fluid may promote the crack growth by 'ageing' of material in the crack tip. Cracks can develop both parallel to the axis and around the circumference.
Conditions promoting degradation	Combination of 'high' temperature and 'high' concentration of acidic species, in water ( $\text{CO}_2$ and small organic acids) and in oil (naphthenic acids characterized by TAN), and alkalinity of the produced water. For a given acid condition increased temperature enhances the degradation rate.  Oxygen can also degrade PA11. It may be introduced through use of batch treatment chemicals with dissolved oxygen (in particular methanol) or could be introduced through air leaking into transport or process equipment. Oxygen induced degradation rates increase with temperature for a given oxygen concentration like an Arrhenius process.
Acceptance criteria for degradation mechanism	Through [API 17TR2, 2003] an acceptance criterion relating to a lower bound on the average size of the molecular chains has been established. This is measured in terms of Corrected Inherent Viscosity (CIV). The initial acceptance criterion has been defined as $\text{CIV}=1.2 \text{ dL/g}$ with the following recommendation: <i>'Once the initial acceptance criterion is reached, the pressure sheath has aged significantly. In order to continue using the pipe, an analysis of potential failure modes should be performed. This will aim to evaluate the margin of safety and address risk and criticality.....'</i> It is suggested in the [API 17TR2, 2003] that operators may justify using $\text{CIV}=1.1 \text{ dL/g}$ as the acceptance criterion for static applications of flexible pipes.

Procedures or models to predict service life or PoF for layer	<p>[API 17TR2, 2003] is the established industry guideline for predicting service life and acceptance criteria. (There are ongoing industry activities to develop improved methods for prediction of service life and acceptance criteria)</p> <p>It is generally accepted that if it can be documented through coupons or credible modeling that the CIV will stay above 1.2 dl/g through the service life the PoF is acceptably low. Based on recent knowledge (several field experience cases - no information in public domain at the time of writing):</p> <ul style="list-style-type: none"> <li>- For conditions with acetic acid concentration below 40 ppm (by weight) in produced water, pH&gt;5.5, Crude oil TAN &lt; 0.05 mgKOH/g and limited batch treatment with methanol, compliance with the service life curves in [API 17TR2, 2003] should ensure PoF= low</li> <li>- When Acetic acid concentration &lt; 200 ppm and TAN &lt; 0.2 combined with coupons that degrade no faster than predicted by service life curves in[API 17TR2, 2003] then PoF = medium/low (depending on the degree of utilization in relation to [API 17TR2, 2003]).</li> <li>- With TAN&gt;0.25 mgKOH/g or acetic acid concentration &gt; 200 ppm (by weight) PoF should be considered medium/high depending on the degree of utilization in relation to the API model. Investigation of the impact of the fluid conditions on PA11 is recommended.</li> <li>- With frequent batch treatment (reaching the bore of the pipe) with chemicals that can contain high levels of dissolved oxygen or other sources of oxygen exposure the PoF = medium / high depending on frequency, concentration of dissolved oxygen and the operational temperature when production is restarted after the batch treatment.</li> </ul>
Identification of the operating or environmental conditions most likely to induce the ultimate loss of function for the layer	<p>The ductility of polymers like PA11 will decrease with falling temperatures thus the embrittlement will be strongest at the lowest exposure temperatures. The thermal expansion coefficient of PA11 is much higher than that of steel (typically <math>120 \cdot 10^{-6}/K</math> versus <math>12 \cdot 10^{-6}/K</math>) and this may lead to build-up of stresses in the PA11 sheath during cool down. With this background the events and conditions that are most likely to lead to the final through thickness rupture is:</p> <ul style="list-style-type: none"> <li>- Cool down due to reduced ductility and circumferential (and possibly axial) thermal stresses that induce strains exceeding the strain at break limits for the material at the cool down temperature</li> <li>- During a shut-down coinciding with strong changes in bending inducing axial strains exceeding strain at break limits.</li> <li>- Pressure testing</li> </ul>
Consequence of loss of layer function with identification of events and mechanisms leading to ultimate pipe failure	<p>Leakage of the fluid and gases in the bore of the pipe into the annulus. The leakage will be limited by the flow restrictions through the Carcass and the pressure armour layer.</p> <p>The leakage rate will depend on:</p> <ul style="list-style-type: none"> <li>- Length and separation of the through thickness rupture/crack</li> <li>- Sealing capacity of the Carcass and the pressure armours</li> <li>- Composition of the fluid - assume gas will leak through faster than fluids.</li> </ul>
Time scale for loss of pipe function after initial loss of layer function (imminent → long term)	<p>Burst of the pipe could take place within seconds to hours (maybe days) after the pressure sheath rupture or through thickness crack.</p>

Parameters that will influence the time from loss of initial layer function to full pipe failure	Internal pressure, gas content, how the pressure sheath will rupture, and sealing properties of the Carcass and the pressure armour.
How will the ultimate pipe failure manifest itself	Burst of the pipe or rupture of the outer sheath with release of hydrocarbons. This may be preceded with an increase in the rate of gas through the annulus vent.
Probability of failure considerations for pipe loss of function	See description above in <i>Procedures or models to predict service life or PoF for layer</i>
Possible mitigations against unacceptably high PoF	<p>Operational Procedures:</p> <ul style="list-style-type: none"> <li>- Reduce (if relevant) use of batch methanol treatment.</li> <li>- Keep the temperature during normal operation as low as possible</li> </ul> <p>Design:</p> <ul style="list-style-type: none"> <li>- If a high PoF is based on uncertainties related to high TAN or high acetic acid, coupons exposed to the flow environment will be valuable to determine the impact provided the exposure temperature (in particular temperature) can be documented.</li> </ul> <p>Testing / Calculation:</p> <ul style="list-style-type: none"> <li>- If coupons are not available, laboratory testing of PA11 in real crude samples combined with simulated produced water conditions should be performed. (Testing will provide data to make a more precise service life/criticality estimate which may document a possibly lower PoF)</li> </ul>
Monitoring, inspection & prediction: methods and strategies	<ul style="list-style-type: none"> <li>- Use of coupons exposed directly to the flow environment is a very good contribution to the integrity management. The coupons should preferably be exposed in a location where the temperature of the flow is high compared to the exposure of the flexible pipe. Coupons should be retrieved and analyzed periodically to determine the rate of degradation.</li> <li>- Monitoring and recording of production conditions, in particular temperature is essential. Recording of shut-down will also provide valuable information.</li> <li>- Take out samples from a liner. It may be possible to find ways of taking out samples of the pressure liner for analysis without damaging the pipe. (For instance take a sample from the end of the liner, which is outside the sealing ring in the end fitting.</li> <li>- Online annulus vent monitoring can provide a warning system where a leakage through the pressure sheath can be detected before the outer sheath burst to enable shut down and other risk containment measures.</li> </ul>
Operational field experience	<p>PA11 Rilsan has been used extensively by the offshore industry. There have been several reported failures for pipes in operation above 60 deg C. More rapid degradation rate seem to be connected with significant use of methanol batch treatment with possible oxygen problems or high TAN.</p> <p>There are many reported cases where the PA11 pressure sheaths (analyzed after retrieval) degrade significantly slower and less than predicted by the service life model in [API 17TR2, 2003]. There are also cases where coupons and material from retrieved pipes have shown a stronger degradation than predicted by the model.</p>

**A3.3.2.2.3 Fatigue and overload cracks in pressure barrier (PVDF)** Evaluation of failure causes for fatigue cracks in pressure barrier is presented in Table A3.7

Table A3.7: Fatigue and overload cracks in pressure barrier (PVDF)

Layer & layer function	Pressure sheath ensures containment of fluids and gas within the bore of the pipe
Materials	PVDF grades
Applicability of failure cause for various pipe structures (design) and conditions Note limitations, ref Section A3.1.2	All pipes with dynamic stresses in PVDF pressure sheath, e.g. thermal stresses or dynamic pipe bending.  PVDF exposed to excessive stresses, e.g. more than permissible bending (UHB), impact loads or incidents during manufacturing or installation.
- Degradation mechanisms.	- Fatigue crack initiation and growth promoted by cyclic loading. - Crack propagating from notch or overload location.
Layer failure mechanism and the way it will manifest itself	Crack penetrating the sheath thickness leading to leakage from the bore to the annulus. Such leakages will most likely initially be small and then increase with the fatigue crack expansion.
Conditions promoting degradation	PVDF is notch sensitive with respect to crack initiation. The large difference in thermal expansion between PVDF and steel (typically $140 \times 10^{-6}/K$ versus $12 \times 10^{-6}/K$ ) may lead to the development of high stresses during cool down from high temperatures. The higher and faster the temperature drop is the larger will the induced stress be. Other loads such as weight may enhance the sensitivity to crack development. Typically the most susceptible location is close to the termination in the end fitting where the development of circumferential cracks has been observed during testing.
Acceptance criteria for degradation mechanism	In section 6.3.2.1.5 in [API 17J, 2008] it is stated that the thickness of the pressure sheath shall ensure that cracks will not propagate through the thickness. No considerations are made with respect to safety margins  Crack initiation is normally longer than the time for an established crack to grow through the thickness. In this perspective the acceptance criterion should be to avoid that crack initiation takes place.  Some PVDF materials have exhibited some susceptibility to brittle cracking at low temperatures. Excessive cooling cycles or overload events when the pipe is cold could represent increase in PoF. This kind of cracking would be expected to be substantial when it occurs and would show up un annulus vent rate.
Procedure or models to predict service life or PoF for layer	For PVDF the probability of crack initiation will increase with the - The magnitude of the temperature change during shut down - The rate of temperature change (high rate will allow less stress relaxation during cool down) - The number of shut-down cycles One approach could be to make comparison to other risers in service with similar or harsher exposure with respect to crack initiation.

Identification of the operating or environmental conditions most likely to induce the ultimate layer loss of functionality	The loss of layer function in terms of through thickness crack will most likely take place in connection with the cool down sequence in connection with a shut down.
Consequence of loss of layer functionality with identification of events and mechanisms leading to ultimate pipe failure	Pipe burst or leakage
Time scale for loss of pipe function after initial loss of layer function (imminent → long term)	<ul style="list-style-type: none"> <li>- Worst case: Burst could occur in seconds.</li> <li>- Best case: Leakage due to rupture of the outer sheath could take place within hours to days after the pressure sheath rupture or through thickness cracks.</li> </ul>
Parameters that will influence the time from loss of initial layer functionality to full pipe failure	Internal pressure, gas content, how the crack continues to grow, and sealing properties of the Carcass and the pressure armour.
How will the ultimate pipe failure manifest itself	Burst of the pipe or rupture of the outer sheath with release of hydrocarbons. This may be preceded with an increase in the rate of gas through the annulus vent.
Probability of failure considerations for pipe loss of functionality	See above in Procedure or models to predict service life or PoF for layer
Possible mitigations against unacceptable high PoF	<p>Operational procedures:</p> <ul style="list-style-type: none"> <li>- Keep the number of shut downs as low as possible.</li> <li>- Keep the cooling rate as low as possible</li> <li>- Control the rate of depressurization</li> </ul>
Monitoring, inspection & prediction: methods and strategies	<ul style="list-style-type: none"> <li>- Online annulus vent monitoring can provide a warning system where a leakage through the pressure sheath can be detected before the outer sheath burst to enable shut down and other risk containment measures.</li> <li>- Record the shutdowns in terms of frequency, magnitude of temperature drop and cool down rate.</li> </ul>
- Operational field experience	<ul style="list-style-type: none"> <li>- Experienced after notch induced by carcass fracture</li> <li>- Leakage with unknown origin of flowlines with PVDF pressure sheath in demanding applications (high bending) has been observed.</li> <li>- Temperature cycling induced fatigue resulting in cracks in PVDF pressure sheath in location of high curvature</li> </ul>

### A3.3.2.3 Pressure armour

**A3.3.2.3.1 Pressure armour corrosion:** See corresponding description in Section [A3.3.2.4.1](#)

**A3.3.2.3.2 Pressure armour fatigue and unlocking** Evaluation of failure causes for pressure armour fatigue is presented in Table [A3.8](#)

Table A3.8: Pressure armour fatigue and unlocking

Layer & layer function	Inner pressure armour (not back-up spiral) provides the pipe resistance to internal pressure, support to resist external pressures and give strength for mechanical crushing loads. The layer provides structural support for the internal pressure sheath
Materials	Carbon steel, with carbon content dependent on the design requirements. Typical yield strength in the range 650-1000 MPa. For details, reference is given to <a href="#">[API 17B, 2008]</a> .
Applicability of failure cause for various pipe structures (design) and conditions Note limitations, ref Section <a href="#">A3.1.2</a>	Dynamic pipes with high operational pressure
Degradation mechanisms.	<p><b>Possible initiation mechanisms for fatigue:</b></p> <ol style="list-style-type: none"> <li>1. Ovalization in bending</li> <li>2. Manufacturing outside tolerances: <ul style="list-style-type: none"> <li>- Fully extended spiral with inadequate bending flexibility</li> <li>- High inter-wire contact pressure giving high stresses during bending</li> </ul> </li> <li>3. Fretting: wire-wire friction</li> <li>4. Transverse relative displacement and rotation in bending</li> </ol> <p><b>Possible initiation mechanisms for unlocking:</b></p> <ol style="list-style-type: none"> <li>1. Overbending</li> <li>2. Impact</li> <li>3. Excess tension</li> <li>4. Pipe design and manufacturing: <ul style="list-style-type: none"> <li>- Size of wire interlock insufficient to avoid un-locking during manufacturing, relevant for large bore pipes with thin hoop spiral layer and stiff pressure sheath</li> <li>- Wire welding or repair during manufacturing</li> <li>- Manufacturing halts, e.g. guide roller problems</li> </ul> </li> <li>5. Failure of tensile or back-up pressure armour</li> <li>6. Radial compression (at installation)</li> <li>7. Excess torsion (at installation)</li> </ol>
Layer failure mechanism and the way it will manifest itself	Gap in pressure armour with polymer sheath extending into the gap and subsequent breach of pressure sheath. Eventually resulting in pipe leakage or pipe rupture with loss of containment.

Conditions promoting degradation	<p><b>Fatigue:</b></p> <ul style="list-style-type: none"> <li>- Corrosive annulus environment</li> <li>- Annulus condition with access to oxygen (hole in the outer sheath)</li> <li>- Bore conditions; particularly H<sub>2</sub>S content if not designed for H<sub>2</sub>S service, and to a less extent CO<sub>2</sub> content.</li> <li>- Inaccurate pressure armour profile design or fabrication; affecting load transfer</li> <li>- High internal pressure and dynamic motion</li> </ul>
	<p><b>Unlocking:</b></p> <ul style="list-style-type: none"> <li>- Most flexible pipes have larger radial pressure on the hoop spiral during operation than during manufacturing and installation. Unlocking during normal operation is hence unlikely.</li> <li>- Buried flexible flowlines may be an exception where high axial compression due to thermal loads combined with upheaval buckling (UHB) may give unlocking.</li> <li>- Unlocking or partial un-locking (nub riding on nub) from manufacturing will normally propagate during FAT pressure testing, however, this is not always the case and detail evaluation is required before a pipe with a potential unlocking is accepted for operation</li> <li>- Unlocking or partial un-locking from installation will often not propagate during SIT as the external pressure (tension and pressure induced) on the hoop spiral is large and test pressure is lower</li> </ul>
Acceptance criteria for degradation mechanism	<p>The fatigue life calculation shall be performed using a valid and appropriate SN-curve and verified design tool.</p> <p>Unlocking is not permitted</p>
Procedure or models to predict service life or PoF for layer	<p><b>Fatigue:</b></p> <p>There are robust global and local analysis methodology and tools available for pressure wire fatigue calculations. Reference is given to [API 17B, 2008] for details. The probability of failure is taken into consideration through the methodology. The main points are:</p> <ul style="list-style-type: none"> <li>- The development and choice of SN-curves</li> <li>- The typical application of a safety factor (SF) of 10 between fatigue life and fatigue service life,</li> <li>- Reasonably conservative assumptions</li> </ul> <p>Sensitivity calculations should be performed to assess the influence of the main parameters on the resulting fatigue life.</p> <p><b>Unlocking:</b></p> <p>Detail FEM analysis of hoop spiral with neighbouring layers have successfully been used for evaluation of manufacturing and installation induced event with potential unlocking. The models need to take into account complex contact conditions as well as time and temperature dependent properties of the polymer layers.</p> <p>Potential un-locking during UHB must consider relevant bending stiffness distribution along the line, high bending stiffness far from the UHB due to interlayer friction locking and temperature effects along the line are important.</p>

	<p>For most hoop spiral designs the bending moment will have marked increase when bending radius goes below locking radius. For events with limited and known bending moment loads it may hence be possible to compare the actual load with the pipe capacity. Note that this method must never be used for load cases where pipe bending is controlled by geometry or the bending load is uncertain.</p> <p>Long term propagation of an unlock during normal operation will normally not occur. The consequence will either be manifested quickly or develop as a consequence of another event.</p>
Identification of the operating or environmental conditions most likely to induce the ultimate layer loss of functionality	<p>High operating pressure and frequent dynamic bending</p> <p>Continued operation after bending incident</p>
Consequence of loss of layer functionality with identification of events and mechanisms leading to ultimate pipe failure	<p>Unlocking of hoop spiral resulting in loss of integrity and possibly pipe rupture.</p> <p>Normally more than one hoop spiral wire is used such that a single wire rupture will only result in a local hole in the pressure sheath underneath.</p>
Time scale for loss of pipe functionality after initial loss of layer function (imminent → long term)	<ul style="list-style-type: none"> <li>- Short term, unlocking propagating until failure of pressure sheath</li> <li>- Long term;</li> <li>-&gt; Circumferential fatigue cracks of hoop spiral propagating until failure of pressure sheath is unlikely. However, such crack may get side branches giving wire rupture</li> <li>-&gt; Cross wire fatigue cracks due to repetitive ovalization, e.g. dynamic contact with support structure</li> </ul>
Parameters that will influence the time from loss of initial layer function to full pipe failure	<p>Parameters promoting shorter time to ultimate failure:</p> <ul style="list-style-type: none"> <li>- Higher internal pressure will affect the time. Increased pressure increases loading on both tensile and pressure armour</li> <li>- High temperature may contribute</li> <li>- Dynamics</li> </ul>
How will the ultimate pipe failure manifest itself	<p>Pipe leakage (loss of containment).</p> <p>Pipe burst is possible.</p>
Probability of failure considerations for pipe loss of functionality	<p>Pressure armour fatigue: seldom/rarely</p> <p>Pipe failure due to pressure armour fatigue: Very seldom</p> <p>Unlocking due to overbending during manufacturing and installation observed as latent defect ultimately resulting in pipe leak</p>
Possible mitigations against unacceptable high PoF	<p>Operational procedures:</p> <ul style="list-style-type: none"> <li>- Reduced bore pressure</li> </ul> <p>Design:</p> <ul style="list-style-type: none"> <li>- Robustness in global configuration designs (dynamic response, upheaval buckling)</li> <li>- Increased size of hoop spiral dimension</li> </ul> <p>Replacement:</p> <p>Unlocking: pipe replacement. Generally no mitigating actions available/possible</p>

Monitoring, inspection & prediction: methods and strategies	- Annulus environment - Pressure time series (see tensile armour fatigue) - Pressure test record (instruments and piping disconnected)
Operational field experience	Unlocking experienced on pipe in operation. For known cases the initiation of unlocking took place during fabrication, installation or accidental impact.

#### A3.3.2.4 Tensile armour

**A3.3.2.4.1 Tensile wire corrosion** Evaluation of failure causes for tensile wire wire corrosion is presented in Table A3.9

Table A3.9: Tensile wire corrosion

Layer & layer function	All steel armour layers in the annulus: <ul style="list-style-type: none"> <li>- Inner pressure armour and back-up spiral provides the pipe resistance to internal and external pressures and mechanical crushing loads and provides structurally support for the internal pressure sheath (the pressure armour layer is omitted in family II pipes)</li> <li>- Tensile wire provides axial structural capacity of the pipe (tensile wire provide both axial and hoop strength for family II pipes)</li> </ul>
Materials	Carbon steel and Low alloy steel
Applicability of failure cause for various pipe structures (design) and conditions Note limitations, ref Section A3.1.2	H <sub>2</sub> S driven SSCC and HIC is only applicable to high strength steel. All other corrosion mechanisms are applicable to all armour wire steels  All corrosion mechanisms require the presence of a liquid water phase. Most flexible pipes, including dry gas applications, will most likely have condensed water in annulus.
Degradation mechanisms.	Different corrosion mechanisms: <ul style="list-style-type: none"> <li>- CO<sub>2</sub> corrosion</li> <li>- Oxygen corrosion</li> <li>- COv corrosion enhanced by oxygen</li> <li>- H<sub>2</sub>S driven corrosion and cracking mechanisms</li> <li>-&gt; Sulfide Stress Corrosion Cracking (SSCC) requires high stress levels relative to UTS.</li> <li>-&gt; HIC can take place at low stress levels.</li> </ul>
Layer failure mechanism and the way it will manifest itself	Corrosion can lead to: <ul style="list-style-type: none"> <li>- Reduced cross section of wires reducing the load bearing capacity. When the capacity becomes lower than the applied load, wires will rupture.</li> <li>- Surface irregularities and pitting that will reduce the fatigue resistance. This may lead to premature crack growth and eventually rupture of wires.</li> <li>- For hoop strain armours corrosion can lead to reduced resistance against unlocking and longitudinal cracks. This may in the first instance lead to wider gaps between pressure armour wires and possibly excessive creep of the pressure sheath.</li> </ul> <p>High strength armour wires suffering Sulfide Stress Corrosion Cracking (SSCC) and HIC would fail through brittle rupture.</p>

Conditions promoting degradation	<p>Several corrosion mechanisms can take place depending on design application and scenario. The highest risk scenarios are:</p> <ul style="list-style-type: none"> <li>- Breach in the outside cover, in particular in the vicinity of the splash zone or above.</li> <li>- H<sub>2</sub>S in flexible pipelines with high strength steel armours, in particular family II structures. The total pressure in the annulus of flow lines is the sum of the hydrostatic pressure at the vent port and the differential release pressure of the vent valves for pipes with intact outer sheath or just the hydrostatic pressure if there are breaches in the outer sheath. When the total pressure is high there will be correspondingly high partial pressures for acid gases such as H<sub>2</sub>S and CO<sub>2</sub>. This will in particular for H<sub>2</sub>S increase the susceptibility for SSCC and HIC.</li> <li>- Cases with other leakages of oxygen into the annulus</li> <li>Cases with water condensing repeatedly (in vent tubes and other cold locations in regions where the annulus is gas filled)</li> </ul>
Acceptance criteria for degradation mechanism	Acceptance criteria will be defined by damage leading to unacceptable stress utilization or fatigue capacity.
Procedure or models to predict service life or PoF for layer	<ul style="list-style-type: none"> <li>- CO<sub>2</sub> corrosion in stagnant/confined water filled annulus is in the order of 0.01 mm/year.</li> <li>- A worst case estimate for corrosion in annulus with hole in the outside cover is typically 1mm/year</li> </ul>
Identification of the operating or environmental conditions most likely to induce the ultimate layer loss of functionality	<p>Situations with:</p> <ul style="list-style-type: none"> <li>- High amplitude stress cycles</li> <li>- High load</li> <li>- Pressure testing</li> </ul>
Consequence of loss of layer functionality with identification of events and mechanisms leading to ultimate pipe failure	<p>Excessive corrosion in risers may lead to full pipe rupture and significant release of gas and oil. When the load carrying capacity of axial armour layer goes below the applied load, the pipe rupture may be catastrophic with full opening to the bore of the pipe.</p> <p>SSCC or HIC failures of armours in flow lines lead to gaps in the support of the pressure sheath. The pressure sheath will eventually extrude through the gap and create hole in the pressure sheath. Bore content will flow into the annulus and relatively soon induce rupture of the outside cover.</p>
Time scale for loss of pipe functionality after initial loss of layer function (imminent → long term)	<ul style="list-style-type: none"> <li>- Loss of pipe function will for risers take place immediately after loss of layer function.</li> <li>- For SSCC or HIC cases it may take some time before the pressure sheath fails. (typically short to medium time)</li> </ul>
Parameters that will influence the time from loss of initial layer functionality to full pipe failure	For risers where the tensile layer fails due to applied load exceeding the remaining load capacity the loss of pipe functionality will be imminent.
How will the ultimate pipe failure manifest itself	<p>For risers: Full pipe rupture</p> <p>For flowlines: Full rupture or major leakage</p>

Probability of failure considerations for pipe loss of functionality	PoF for loss of functionality for the pipe should be the same as loss of layer functionality
Possible mitigations against unacceptable high PoF	<p>For risers:</p> <ul style="list-style-type: none"> <li>- Avoid damage to outer cover as far as possible</li> <li>- Ensure early detection and repair or exclude oxygen.</li> </ul> <p>For flow lines susceptible to SSCC and HIC:</p> <ul style="list-style-type: none"> <li>- Reduce H<sub>2</sub>S</li> <li>- Reduce pressure</li> </ul>
Monitoring, inspection & prediction: methods and strategies	<p>For risers: Vent gas monitoring and testing to detect outer cover breaches.</p> <p>For SSCC and HIC issues: Monitor for H<sub>2</sub>S increase in conveyed gas and fluid.</p>
Operational field experience	<p>Some of the most serious failures of flexible pipes have been caused by corrosion of armour wires. Based on available information failures or near misses for flexible pipes can be summarized in the following:</p> <ul style="list-style-type: none"> <li>- At least 4 risers - 1 in Africa and 3 in the North Sea region outside Norway</li> <li>- At least 2 near misses on risers - 1 in Norway and 1 in Africa.</li> <li>- At least 7 flexible flow lines with high strength steel wires have failed through mechanisms that are believed to be driven by H<sub>2</sub>S. None of these have been in Norway but have taken place in North Sea region, West Africa and Arabian Gulf.</li> </ul> <p>Many of these incidents represent cases with unacceptable high personnel risks and all have resulted in significant cost to operators. All the riser issues are related to outer cover damages and the best way to avoid this would be to prevent cover damages. However, it is unlikely that the industry will manage to eradicate outer cover damages completely. It is therefore important to develop better understanding of the corrosion mechanisms and influencing parameters to enable prediction capabilities.</p> <p>There are examples where risers have survived long periods with breaches in the outside cover and there are indicators such as breach location, type of damage, pipe configuration that would lead to higher probability of corrosion.</p> <p>All the corrosion failures of flexible flowlines have come as surprises to the operators. Retrospectively some of them seem to relate to H<sub>2</sub>S but it has not been possible for any of the cases to explain the full sequence of events and detailed mechanisms. Knowledge gaps clearly exist.</p> <p>It is premature to assume that issues will not appear related to corrosion inside intact annuli.</p>

**A3.3.2.4.2 Tensile wire axial compression failure** Evaluation of failure causes for tensile wire aware axial compression failure is presented in Table A3.10

Table A3.10: Tensile wire axial compression failure

Layer & layer function	Tensile wire providing axial structural capacity of the pipe
Materials	Carbon steel, with carbon content dependent on the design requirements. For details, reference is given to [API 17B, 2008].
Applicability of failure cause for various pipe structures (design) and conditions Note limitations, ref Section A3.1.2	Deepwater pipes.
Degradation mechanisms.	<ul style="list-style-type: none"> <li>- Compressive loads in riser due to 'reverse end cap' effect and additional bending.</li> <li>- Bird caging above (in front of) caterpillar during deep water installation</li> </ul> <p>The failure is most likely during installation and in the touch-down section where the pipe may be exposed to true wall compression from the external pressure end cap effect, and also bending promoting buckling.</p> <p>The failure is also possible for installed pipes with low or no bore pressure, and the failure is then expected at touch-down point or in another dynamic section with bending.</p>
Layer failure mechanism and the way it will manifest itself	<p>The compressive loads may cause buckling of the tensile wires. There are two buckling modes for the tensile wires:</p> <p><b>Radial buckling:</b></p> <ul style="list-style-type: none"> <li>- Lower energy mode: weak wire axis bending</li> <li>- Prevented by <ul style="list-style-type: none"> <li>-&gt; Anti-birdcage tape (commonly applied)</li> <li>-&gt; High external hydrostatic pressure (deep waters)</li> <li>(Intact outer sheath and atmospheric annulus vent)</li> </ul> </li> </ul> <p><b>Lateral buckling:</b></p> <ul style="list-style-type: none"> <li>- Higher energy mode: strong wire axis bending</li> <li>- The resulting buckling mode will be the buckling mode with lowest required energy. Hence, for lateral buckling to occur, radial buckling must be prevented until exceedance of the required energy for lateral buckling.</li> <li>- Buckling of wires will cause disorganization of the wires and shortening of the pipe. This will in turn introduce increased loading on pressure armouring and carcass, and may also result in outer sheath damage.</li> <li>Corrosion of the buckled wires may ultimately result in wire breakage.</li> </ul>
Conditions promoting degradation	<ul style="list-style-type: none"> <li>- Low internal pressure</li> <li>- Low pipe tension</li> <li>- Deep waters (i.e. larger external hydrostatic pressure)</li> <li>- Bending</li> <li>- Repeated dynamic cycling at touch down point</li> <li>- Vessel dynamics may contribute to overcoming internal friction for the tensile wires.</li> </ul>

Acceptance criteria for degradation mechanism	- Intact outer sheath (only for risers with atmospheric vent) - No plastic wire deformation - In case of plastic deformation, evaluate maximum strain in wires. - Reliable anti bird cage tape
Procedure or models to predict service life or PoF for layer	New analysis tools. Analytical methods and full scale testing.
Identification of the operating or environmental conditions most likely to induce the ultimate layer loss of functionality	See description above under <i>Degradation mechanisms</i> .
Consequence of loss of layer functionality with identification of events and mechanisms leading to ultimate pipe failure	Axial buckling is considered to be an ultimate loss functionality for the tensile armour. The pipe is no longer suited for operation. Loss of containment is likely. Full pipe rupture is not unlikely.
Time scale for loss of pipe functionality after initial loss of layer function (imminent → long term)	Imminent. See also description above under <i>Consequence of loss of layer function</i>
Parameters that will influence the time from loss of initial layer functionality to full pipe failure	Not applicable. See description above under <i>Consequence of loss of layer function</i>
How will the ultimate pipe failure manifest itself	Loss of containment is likely. Full pipe rupture is not unlikely.
Probability of failure considerations for pipe loss of functionality	Low.
Possible mitigations against unacceptable high PoF	Design: - Increased buckling resistance by application of anti-birdcage tape (mainly to prevent radial buckling) - Increased wire dimensions - Double outer sheath
Monitoring, inspection & prediction: methods and strategies	ROV inspection at touch down during and after installation. Visual inspection: - Radial buckling: detect bird caging. - Lateral buckling: Deformations of the outer sheath - Pipe elongation when pressurized
Operational field experience	Only experienced during installation and testing

**A3.3.2.4.3 Tensile armour wire fatigue** Evaluation of failure causes for tensile armour wire fatigue is presented in Table A3.11

Table A3.11: Tensile armour wire fatigue

Layer & layer function	Tensile wire provides axial structural capacity of the pipe
Materials	Carbon steel, with carbon content dependent on the design requirements. Typical yield strength in the range 650-1400 MPa. For details, reference is given to [API 17B, 2008].
Applicability of failure cause for various pipe structures (design) and conditions Note limitations, ref Section A3.1.2	Dynamic service, most critical for high operational pressure.
Degradation mechanisms.	<p>Initiation:</p> <ul style="list-style-type: none"> <li>- Corrosive environment in annulus: Corrosion fatigue</li> <li>- Intact pipe, dry annulus: Fatigue</li> </ul> <p>The mechanism is stress cycling leading to wire breakage</p>
Layer failure mechanism and the way it will manifest itself	<p>Typically, the inner tensile wires are the most critical with respect to fatigue for intact pipes, while for a pipe with outer sheath damage and corrosion, the local corrosion on the outer tensile wires may be governing (for instance in the splash zone in damage cases).</p> <p>The failure will manifest itself in terms of multiple wire breakage in the most loaded tensile wire layer. Wire breakage may cause loss of axial capacity and reduced radial support for the layers inside. Loss of axial capacity may cause local failure resulting in leakage and possibly full pipe rupture.</p> <p>Wire breakage may also cause twisting of the pipe as the loss of intact wires introduces an unbalance in the torsional force distribution</p>
Conditions promoting degradation	<p><b>Changes from design premise:</b></p> <ul style="list-style-type: none"> <li>- Increased internal pressure which increase the wire stress, pipe bending stiffness and contact pressure</li> <li>- Changed annulus environment</li> <li>- Dynamic bending</li> <li>- Excessive wear of the anti-wear tape between the metal layers, resulting in steel-steel friction</li> <li>- Unfavorable local design of bending stiffener, bellmouth or clamp on devices</li> <li>- Corrosion. Hence, degradation is promoted by: <ul style="list-style-type: none"> <li>-&gt; Annulus condition with access to oxygen (hole in the outer sheath)</li> <li>-&gt; Bore conditions; particularly H<sub>2</sub>S content, and to a less extent CO<sub>2</sub> content.</li> </ul> </li> </ul>
Acceptance criteria for degradation mechanism	The fatigue life calculation shall be performed using a valid and appropriate SN-curve and a verified analytical tool. Generally, only limited corrosive damage is allowed

Procedure or models to predict service life or PoF for layer	<p>There are robust global and local analysis methodology and tools available for tensile wire fatigue calculations. Reference is given to [API 17B, 2008] for details. The probability of failure is taken into consideration through the methodology.</p> <p>The main points are :</p> <ul style="list-style-type: none"> <li>- The development and choice of SN-curves</li> <li>- The typical application of a safety factor (SF) of 10 between fatigue life and fatigue service life.</li> <li>- Reasonably conservative assumptions</li> </ul> <p>Sensitivity calculations should be performed to assess the influence of the main parameters on the resulting fatigue life.</p>
Identification of the operating or environmental conditions most likely to induce the ultimate layer loss of functionality	Worse annulus environment (SN-curve is ruling) and higher pressure than design.
Consequence of loss of layer functionality with identification of events and mechanisms leading to ultimate pipe failure	Loss of integrity and possibly pipe rupture
Time scale for loss of pipe functionality after initial loss of layer function (imminent → long term)	Imminent after multiple wire rupture
Parameters that will influence the time from loss of initial layer functionality to full pipe failure	Internal pressure can affect the time to pipe rupture.
How will the ultimate pipe failure manifest itself	Leakage or pipe rupture
Probability of failure considerations for pipe loss of functionality	<p>The initial probability of pipe failure is low for an intact pipe where this failure mode is handled by design.</p> <p>Changes from design premise may affect the probability of failure.</p> <p>See description above for <i>Conditions promoting degradation and Procedure or models to predict service life or PoF for layer</i></p>
Possible mitigations against unacceptable high PoF	<p>Modifications</p> <ul style="list-style-type: none"> <li>- Repair outer sheath damages</li> </ul> <p>Design</p> <ul style="list-style-type: none"> <li>- Appropriate SN-curves (annulus environment)</li> </ul> <p>Operational procedures</p> <ul style="list-style-type: none"> <li>- Avoid ingress of seawater</li> </ul>

Monitoring, inspection & prediction: methods and strategies	<p>Inspection and monitoring</p> <ul style="list-style-type: none"><li>- Verify outer sheath integrity: annulus test</li><li>- Annulus monitoring (annulus gas and volume)</li></ul> <p>Calculations</p> <ul style="list-style-type: none"><li>- Improved analysis models/methods</li><li>- Improved input data for fatigue re-calculation:<ul style="list-style-type: none"><li>-&gt; Measured response</li><li>-&gt; Measured pressure time series</li><li>-&gt; Measured environmental (weather) data</li></ul></li></ul>
Operational field experience	<p>Experienced. Critical location could be in transition between pipe body and end-fitting.</p> <p>Corrosion will have significant negative effect on fatigue life and may have contributed to experienced failures believed to be caused by corrosion.</p>

### A3.3.2.5 Outer sheath

#### A3.3.2.5.1 Impact, wear and pressure induced rupture creating hole in the outer sheath

Evaluation of failure causes for impact, wear and pressure induced rupture creating hole in the outer sheath is presented in Table A3.12

Table A3.12: Impact, wear and pressure induced rupture creating hole in the outer sheath

Layer & layer function	Outer sheath prevents the ingress of external fluids
Materials	Hole, tear, rupture, wear - possibly ingress of seawater
Applicability of failure cause for various pipe structures (design) and conditions Note limitations, ref Section A3.1.2	PA-11, PA-12, PE: HDPE, MDPE (medium density polyethylene); PU; TPE (thermoplastic elastomer)
Degradation mechanisms	All pipes
Layer failure mechanism and the way it will manifest itself	- Accidental impacts - Blocked annulus - Abrasive contact with seabed / line / other surface - Handling/installation - Manufacturing defects
Conditions promoting degradation	I. Impact causing hole in the outer sheath. II. Blocked annulus vent causing pressure build up in annulus until burst of outer sheath. III. Abrasive contact with seabed / line / guide tube, midwater arch / other surface causing hole in the outer sheath IV. Cut in outer sheath during handling  Further development dependent on location along the pipe: above water, splash zone or subsea.
Acceptance criteria for degradation mechanism	I. Exposed to falling objects: crane activities or scaffolding above pipe / riser location. II. Impact due to trawl board or broken mooring lines III. Restricted annulus vent in combination with high diffusion rates IV. Sharp edged attachments to neighboring structures, rough surfaces, small spacing V. Incidents during installation
Procedure or models to predict service life or PoF for layer	Outer sheath integrity affects armour wire fatigue and corrosion Inspection and models to evaluate susceptibility to wear
Identification of the operating or environmental conditions most likely to induce the ultimate layer loss of functionality	Operator's actions to control the conditions promoting degradation. Assessment of the probability of the different causes, also taking into account external interfering activity and the actual integrity management program.

Consequence of loss of layer functionality with identification of events and mechanisms leading to ultimate pipe failure	Consequences of layer failure: corrosion (and wear) of armour wires, pipe failure Causes for outer sheath failure: Accidental/unintended contact with other objects/structures Relative movement and wear between pipe and support structure, e.g. guidetube, MWA or seabed Installation/field specific: Crane activity, ship traffic, fishing/trawling
Time scale for loss of pipe functionality after initial loss of layer function (imminent → long term)	The consequence of a hole in the outer sheath will depend on the location of the hole and on whether there is more than one hole. If the hole is in a location that is submerged in sea water either continuously or intermittently the annulus will be fully or partially flooded with seawater. The degree of flooding will depend on whether the pipe configuration will lead to trapping of gas pockets or whether oil leaking into the annulus from the bore may block the sea water from reaching some parts of the annulus.  The potential threat to the integrity will primarily be <b>corrosion</b> of steel armours and reduced <b>fatigue</b> resistance due to change of environment. Further details are given in Chapter B4 Annulus environment and corrosion.  Corrosion and fatigue may eventually lead to wire breakage with loss of axial and/or radial capacity and possibly full rupture of the pipe with loss of containment.
Parameters that will influence the time from loss of initial layer functionality to full pipe failure	Corrosion & fatigue are long-term processes. A worst case scenario is a hole in the splash zone which could lead to oxygen corrosion and rapid loss of cross section resulting in failure in less than a year.
How will the ultimate pipe failure manifest itself	- Changes in annulus environment compared to design - Location of damage: Above or below sea level / splash zone. - The corrosion impact on the fatigue life or load capacity - Repair of the outer sheath damage
Probability of failure considerations for pipe loss of functionality	Loss of axial capacity (loss of pressure capacity). Possibly full rupture of the pipe with loss of containment
Possible mitigations against unacceptable high PoF	High: Significant in the splash zone or if multiple holes (circulation) Medium: Above water Low, provided repair: Submerged damage. Slow degradation. New designs shall account for de-aerated water filled (flooded) annulus (ref. proposed change of [API 17J, 2008]).
Monitoring, inspection & prediction: methods and strategies	Modifications: Repair of outer sheath damage as soon as possible. Injection of inhibitor
Operational field experience	- Regular (annual) annulus volume test, vent capabilities & annulus vent rate (diffusion) - Annulus monitoring - External Visual inspection
	Most frequently experienced failure mode.  There are indications that outer sheath bursts due to excessive annulus pressure or other large breaches of outer sheath may be most critical.

**A3.3.2.5.2 Outer sheath embrittlement** Evaluation of failure causes for outer sheath embrittlement is presented in Table A3.13

Table A3.13: Outer sheath embrittlement

Layer & layer function	Outer sheath prevents the ingress of external fluids
Materials	PA-11, PA-12, HDPE, MDPE (medium density polyethylene); PU; TPE (thermoplastic elastomer)
Applicability of failure cause for various pipe structures (design) and conditions Note limitations, ref Section A3.1.2	Pipes with polyamide outer sheath at high operational temperatures and external insulation e.g. ancillaries as dry bend stiffeners or buried pipes
Degradation mechanisms	<p>Embrittlement that can be caused by:</p> <ul style="list-style-type: none"> <li>- Hydrolysis (by water) and/or oxygen degradation of Polyamides.</li> <li>- Oxygen degradation of Polyethylenes (HDPE, MDPE) and PU &amp; TPE</li> </ul> <p>Temperature (and to some extent chemistry) is a key parameter promoting the degradation</p> <p>Degradation by UV is also possible, but materials used for outer sheaths above sea level should include protection against UV.</p> <p>Details are given in Chapter B4 Annulus environment and corrosion.</p>
Layer failure mechanism and the way it will manifest itself	Sheath rupture or cracks growing through the full thickness. This will lead to ingress of air or water depending on the position of the defect.
Conditions promoting degradation	<p>Embrittlement of the outer sheath will be of concern when the combination of bore temperature and outside insulation (bend stiffeners (or restrictors), under buoyancy modules or in sections covered by mud or sediment) result in temperatures in the outer sheath that could lead to high degradation rates.</p> <p>Hydrolysis will also be affected by the chemistry in the annulus (in particular any acids). Oxygen in the air or dissolved in water is also a potential threat.</p>
Acceptance criteria for degradation mechanism	Maintain sufficient ductility to ensure adequate margin against rupture and against crack initiation.
Procedure or models to predict service life or PoF for layer	<p>Modelling of the temperature in the outer sheath as function of bore temperature would allow determination of the temperature history. This could be used in combination with degradation models to predict remaining service life.</p> <p>For outer sheaths using RILSAN BESNO P40 TL the [API 17TR2, 2003] can be used (see pressure sheath embrittlement). It should be noted that some manufacturers may use modified PA11 formulations for outer sheath for which the criteria and models in [API 17TR2, 2003] cannot be applied.</p> <p>For oxygen degradation criteria and models may have to be developed.</p>

Identification of the operating or environmental conditions most likely to induce the ultimate layer loss of function	The ultimate loss of function will probably be a brittle fracture of the outer sheath.
Consequence of loss of layer function with identification of events and mechanisms leading to ultimate pipe failure	See the equivalent section under: 'Section <a href="#">A3.3.2.5.1</a> Outer sheath hole/wear'
Time scale for loss of pipe function after initial loss of layer function (imminent —>long term)	See the equivalent section under: 'Section <a href="#">A3.3.2.5.1</a> Outer sheath hole/wear'
Parameters that will influence the time from loss of initial layer function to full pipe failure	See the equivalent section under: 'Section <a href="#">A3.3.2.5.1</a> Outer sheath hole/wear'
How will the ultimate pipe failure manifest itself	See the equivalent section under: 'Section <a href="#">A3.3.2.5.1</a> Outer sheath hole/wear'
Probability of failure considerations for pipe loss of function	See the equivalent section under: 'Section <a href="#">A3.3.2.5.1</a> Outer sheath hole/wear' and the above Applicability of failure cause for various pipe structures (design) and conditions
Possible mitigations against unacceptable high PoF	<p>Modifications</p> <ul style="list-style-type: none"> <li>- Reduce the temperature or the thermal insulation of the outside.</li> <li>- Repair of outer sheath if damage type and pattern allows.</li> <li>- Use of Inhibitor when rupture or cracks have been discovered and the damage has been repaired</li> </ul>
Monitoring, inspection & prediction: methods and strategies	<ul style="list-style-type: none"> <li>- Regular (annual) annulus volume test, vent capabilities &amp; annulus vent rate (diffusion)</li> <li>- Continuous annulus monitoring</li> <li>- Degradation models. Temperature sensors locally in bend stiffeners could provide more accurate input data</li> </ul>
Operational field experience	Several layer failures have been observed - some detected visually and others by annulus testing.

### A3.3.3 Examples of Ancillary devices failure causes

#### A3.3.3.1 General

Integrity of ancillary devices is important for safe operation of flexible pipes. This is reflected in the design specifications where a separate standard and recommended practice are issued to cover ancillary devices; [API 17L1, 2013] and [API 17L2, 2013]. As shown in the table below, failure of ancillary devices may be critical for the flexible pipe integrity. Ancillary devices and flexible pipe interfaces must hence be duly considered in design phase as well as in integrity management of a flexible pipe.

Three examples are included in subsections below to serve as examples for how to use the methodology. These examples are not intended to cover the most important failure modes for ancillary devices.

Table A3.14: General

Ancillary	In field experience	Consequence	Comment
Bending stiffener	Failure has occurred on dynamic risers	May result in riser loss of integrity due to local overbending, refer to Section A3.3.2.3.2  Fatigue performance will normally be unacceptable upon loss of bend-stiffener functionality, refer to Section A3.3.2.4.3	
Bend restrictor	Failure has occurred on static flexibles	May result in loss of integrity due to local overbending, refer to Section A3.3.2.3.2	- Installation loads are important - Polymeric bend restrictors should not be exposed to long term loads
Bellmouth -			Important interface as bellmouth size and shape may be critical for integrity of flexible pipe
Buoyancy and ballast module Subsea buoy clamp and tether clamp	- Loss of modules and sliding of module clamp have been experienced - Loss and sliding of tether clamp has been experienced	- Outer sheath damage of flexible pipe - Overbending - Tether clamp failure may result in loss of containment	Examples are given in Section A3.3.2 and Section A3.3.4
Tether Riser and tether bases	Damaged tethers Twisted tethers Tether hinge pin almost fallen off	Tether failure may result in loss of containment	Example is given in Section A3.3.3
Subsea buoy			Important riser interface. Criticality is design dependent
Piggy-back spacer			Design dependent

Ancillary	In field experience	Consequence	Comment
I/J-tube seals			Design dependent
Pull-in heads			Design dependent
Chinese fingers/cable grips			Design dependent
Connectors			Design dependent
Load-transferring devices			Design dependent
Mechanical protection			Design dependent
Fire protection	Fire protection not designed to environment and falling off	Reduced capacity against fire	

### A3.3.3.2 Sliding tether clamp

Evaluation of failure causes for sliding tether clamp is presented in Table A3.15

Table A3.15: Sliding tether clamp

Layer & layer function	Tether clamp contributes to maintaining the riser configuration
Materials	Tether clamp materials according to [API 17L2, 2013]: - High strength structural steel - GRP composites
Applicability of failure cause for various pipe structures (design) and conditions Note limitations, ref Section A3.1.2	
Degradation mechanisms	Loss of pretension and sliding clamp due to: - Creep in polymer (outer sheath material) - Erroneous pretension - Bolt failure
Layer failure mechanism and the way it will manifest itself	Failure mechanism: - Clamp pulling the outer sheath. Most probably, outer sheath torn, i.e. hole in outer sheath and ingress of seawater - Excessive bending of the pipe, dependent on riser configuration, possibly unlocking of pressure armour with subsequent loss of containment  The way the sliding manifest itself: - Small sliding movement: Detection by inspection - Large sliding movement: Small change in riser configuration as long as the clamp is sliding and have not lost contact with tether and gravity base
Conditions promoting degradation	N/A
Acceptance criteria for degradation mechanism	No sliding allowed
Procedure or models to predict service life or PoF for layer	- Global analysis model: clamp loadings - Calculation: clamp capacity - Testing of actual clamps. <i>Note on testing:</i> Should be performed on an appropriate flexible pipe, not on a steel pipe covered with polymeric layer

Identification of the operating or environmental conditions most likely to induce the ultimate layer loss of functionality	Max tension at the clamp location: Vessel in far offset and low pipe content density (gas filled).
Consequence of loss of layer functionality with identification of events and mechanisms leading to ultimate pipe failure	The ultimate failure is due to the outer sheath damage causing a corrosive environment in annulus
Time scale for loss of pipe functionality after initial loss of layer function (imminent → long term)	Long term.
Parameters that will influence the time from loss of initial layer functionality to full pipe failure	<ul style="list-style-type: none"> <li>- The annulus environment.</li> <li>- Dynamic loading at the exposed section</li> <li>- Inspection intervals (detection of progressing failure)</li> </ul>
How will the ultimate pipe failure manifest itself	<ul style="list-style-type: none"> <li>- Outer sheath damage progressing to ultimate failure: → Loss of axial capacity (loss of pressure capacity).</li> <li>→ Possibly full rupture of the pipe with loss of containment</li> <li>- Excessive bending of the pipe causing unlocking of pressure armour with subsequent loss of containment</li> </ul>
Probability of failure considerations for pipe loss of functionality	<p>Low.</p> <p>Most likely to occur during the first year after installation. The loading on the clamp is relatively static and only small variations are expected over the clamp's lifetime.</p>
Possible mitigations against unacceptable high PoF	<p>Design:</p> <ul style="list-style-type: none"> <li>- Accurate design taking creep into account, and with improved tolerances.</li> </ul>
Monitoring, inspection & prediction: methods and strategies	<ul style="list-style-type: none"> <li>- Visual inspection of clamp: → Verify no sliding. → Inspection to look for corrosion products, scratches and outer sheath anomalies near the clamp.</li> <li>- Visual inspection of the pipe configuration including depth measurements along the configuration. This is to be compared with the as-installed survey report.</li> </ul>
Operational field experience	Not experienced

### A3.3.3.3 Tether rupture

Evaluation of failure causes for tether rupture is presented in Table A3.16

Table A3.16: Tether rupture

Layer & layer function	Tether contributes to maintaining the riser configuration
Materials	Fiber ropes: synthetic tethers made from polyester, polyethylene and/or aramid fiber - often coated. Chain and wire ropes made from steel. For details, reference is given to [API 17L2, 2013].
Applicability of failure cause for various pipe structures (design) and conditions Note limitations, ref Section A3.1.2	
Degradation mechanisms.	Primarily wear. Material dependent: Corrosion and hydrogen induced stress concentration  Inappropriate design or excessive marine growth: Slack in wire, resulting in tether snatch loads and increased maximum tether loading.
Layer failure mechanism and the way it will manifest itself	Tether rupture may cause a significant change in the riser configuration. Dependent on the water depth and riser configuration, the riser may possibly float to the surface.
Conditions promoting degradation	- Erroneous installation - Slack in tether, e.g. resulting in undesirable bending in sockets - Excessive marine growth
Acceptance criteria for degradation mechanism	- No visible wear allowed - Intact outer hose on fiber ropes - Corrosion level (limited corrosion allowed) - No slack in tether
Procedure or models to predict service life or PoF for layer	Design. Tests and analytical methods.
Identification of the operating or environmental conditions most likely to induce the ultimate layer loss of functionality	Accidental event in extreme conditions: Maximum loading occurring with vessel in extreme offset (i.e. stretched/compressed riser configuration) and heavy dynamics. Minimum loading (possibly slack) occurring with extensive marine growth and heavy pipe content density, possibly additional loss of buoyancy.
Consequence of loss of layer function with identification of events and mechanisms leading to ultimate pipe failure	Dependent on riser configuration and field lay-out: - Interference, and possibly entanglement, with neighboring structures and lines with subsequent damages to those structures: e.g. outer sheath damages, damages to ancillaries and loss of buoyancy modules. Then, the neighboring structures are more vulnerable. - Excessive bending of the pipe
Time scale for loss of pipe function after initial loss of layer function (imminent —>long term)	Short term. During a heavy storm

Parameters that will influence the time from loss of initial layer functionality to full pipe failure	<ul style="list-style-type: none"> <li>- Weather</li> <li>- Small clearance to neighbouring structures</li> <li>- PLEM near anchor point: increased risk of excessive bending</li> </ul>
How will the ultimate pipe failure manifest itself	Leakage or tear-off at pipe end interface resulting in loss of containment.
Probability of failure considerations for pipe loss of functionality	<p>Damage to neighboring structures is more likely than damage to the pipe itself.</p> <p>For the pipe itself the probability of pipe failure is primarily dependent on the riser configuration with respect to distance between anchor and PLEM interface and the possibility for excessive bending near the PLEM. Additionally, the FPSO Hull may be close over the riser configuration with the possibility of interference between riser and hull.</p> <p>For an intact pipe system, the probability of failure is low. After a tether rupture, the probability for pipe failure is medium.</p>
Possible mitigations against unacceptable high PoF	<p>Design.</p> <ul style="list-style-type: none"> <li>- Design to allow for tether rupture</li> <li>- Verify by analysis (no loss of containment if loss of tether)</li> <li>- Redundancy</li> </ul> <p>-&gt; Double tethers</p> <p>-&gt; Both vertical and horizontal tethers and anchors</p> <p>Note: Although there may be redundancy in number of tethers, if similar bolts are used throughout, the system is dependent on the bolt quality.</p>
Monitoring, inspection & prediction: methods and strategies	<p>Visual inspection of the tether system.</p> <p>Extreme vessel offsets (caused by accidental event) should trigger inspections of the tether system.</p> <p>Elsewise: The riser must float to the surface in order to be detected within reasonable time</p>
Operational field experience	<p>Poor material quality of bolts is experienced causing lost anchoring of tether clamp and changed riser configuration; riser floating to surface.</p> <p>Wear on fiber ropes is experienced in both clamp and anchor ends (pad-eye)</p>

### A3.3.3.4 Altered buoyancy

Evaluation of failure causes for altered buoyancy is presented in Table A3.17

Altered buoyancy is here limited to lost or re-distributed buoyancy modules including excessive marine growth. Mid Water Arches (MWA) are not considered.

Table A3.17: Altered buoyancy

Layer & layer function	Buoyancy modules contributes to maintaining the riser configuration
Materials	Composite synthetic foam encapsulated by a polymeric external skin, reference is given to [API 17L2, 2013].
Applicability of failure cause for various pipe structures (design) and conditions Note limitations, ref Section A3.1.2	
Degradation mechanisms	<ul style="list-style-type: none"> <li>- Clamp failure</li> <li>- Splitting of or fallen off buoyancy modules</li> <li>- Water ingress</li> <li>- Hydrostatic collapse</li> </ul>
Layer failure mechanism and the way it will manifest itself	<p>One or more of the following:</p> <ul style="list-style-type: none"> <li>- Loss of buoyancy modules</li> <li>- Re-distribution of buoyancy modules</li> <li>- Excessive marine growth</li> </ul> <p>This may result in one or more of the following:</p> <ul style="list-style-type: none"> <li>- Change of riser configuration</li> <li>-&gt; Globally as a lower configuration</li> <li>-&gt; Locally as a 'camel hump'</li> <li>- Reduced tether tension</li> <li>- Increased top tension</li> <li>- Changed conditions for interference</li> </ul>
Conditions promoting degradation	<ul style="list-style-type: none"> <li>- Events of interference</li> <li>- Erroneous installation</li> </ul>
Acceptance criteria for degradation mechanism	<ul style="list-style-type: none"> <li>- The amount of allowable water ingress (lost buoyancy) is given in [API 17B, 2008].</li> <li>- Allowable number of lost buoyancy modules according to [API 17B, 2008] and [API 17L2, 2013].</li> <li>- Marine growth is accounted for in design.</li> </ul>
Procedure or models to predict service life or PoF for layer	Robust global analysis methodology also accounting for loss of buoyancy modules. This is considered to be proven technology
Identification of the operating or environmental conditions most likely to induce the ultimate layer loss of functionality	<p>Loss of buoyancy modules:</p> <ul style="list-style-type: none"> <li>- Insulated pipes may pose special challenges to clamping</li> <li>- Material selection</li> <li>- Installation</li> <li>- Interference</li> </ul>
Consequence of loss of layer functionality with identification of events and mechanisms leading to ultimate pipe failure	<ul style="list-style-type: none"> <li>- Excessive bending</li> <li>- Interference with possibility of entanglement</li> <li>- Slack in tether; increased loads in tether system. May subsequently promote tether failure</li> </ul>

Time scale for loss of pipe functionality after initial loss of layer function (imminent → long term)	Long term. Most critical just after installation and through the splash zone.
Parameters that will influence the time from loss of initial layer functionality to full pipe failure	- Dynamics - Riser configuration - Neighboring structures
How will the ultimate pipe failure manifest itself	Dependent on the failure: Excessive bending of the pipe may lead to unlocking of pressure armour with subsequent breach of pressure sheath and ultimately pipe leakage (loss of containment) Interference with entanglement may allow for several scenarios, including outer sheath damages.
Probability of failure considerations for pipe loss of functionality	Low
Possible mitigations against unacceptable high PoF	Design and installation: - Proper testing of clamp and buoyancy modules - Proper procedures for installation Modifications: - Inspection and replacement of buoyancy modules - Removal of marine growth
Monitoring, inspection & prediction: methods and strategies	Visual inspection is recommended after the first storm in addition to an annual inspection.  Visual inspection of the buoyancy modules should assess the relative spacing between each module, the absolute location of each module with reference to the pipe end and the number of buoyancy modules. Inspection to look for corrosion products, scratches and outer sheath anomalies near the clamp.  Inspection of the pipe configuration including depth measurements along the configuration. This is to be compared with the as-installed survey report.  Proper documentation from installation is required to verify that modules are in correct location.
Operational field experience	- Axial sliding of modules is observed such that a module rests on a neighboring module. - Excessive marine growth lowering the entire riser configuration

## A3.4 Failure Statistics

Historical data of failure and damage of flexible risers, jumpers and flow lines as presented in the SureFlex- JIP reports [[MCS Kenny State of the Art, 2010](#)] and [[MCS Kenny Guidance Note, 2010](#)] are considered representative. The incidents of flexible riser failure and damage are sorted by failure and presented graphically in Figure A3.7. These data are collected worldwide. However, a complete and comprehensive overview of all flexible pipe failures is not available. The data are in line with 4Subsea experience and data published by PSA Norway [[PSA Norway, 2013a](#)], [[Muren, 2008](#)]. The most frequent failures are external sheath damage (35%), ancillary device failure (10%) and carcass failure (10%). Among the elements included in ancillary devices are buoyancy elements, bend stiffener, bend restrictors, interface to turret or deck, riser base, tether base, mid-water arch and its riser interfaces [[MCS Kenny Guidance Note, 2010](#)].

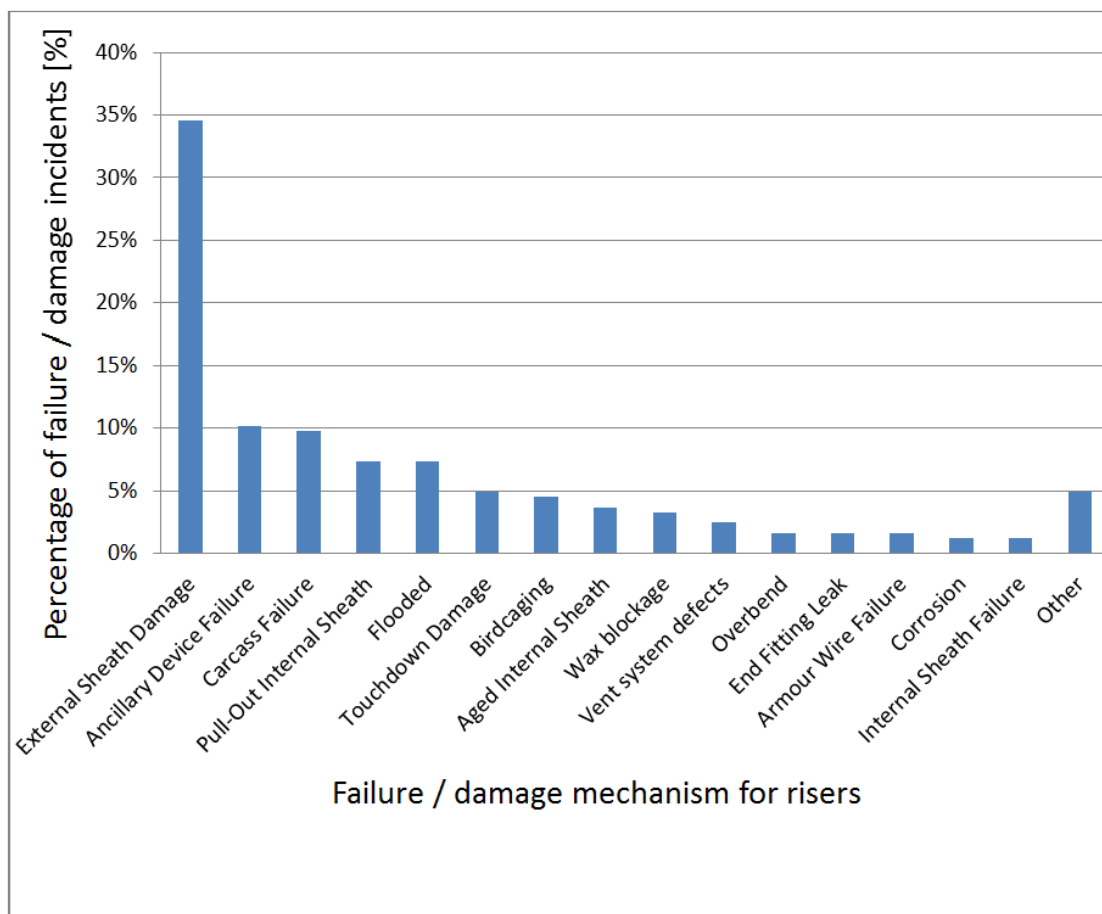


Figure A3.7: Flexible pipe failure / damage incidents [[MCS Kenny State of the Art, 2010](#)], [[MCS Kenny Guidance Note, 2010](#)]

Historical data of flexible pipe incidents in the PSA Norway CODAM database in the period 1995 - 2012 are presented in Figure A3.8. The categorization of the failure entries are performed with an interpretation of the individual failures as reported in the database. Each entry in the database is counted only once although some of the reported failures may apply to more than one category. Hence, there are some inaccuracies related to the exact numbers in the figure.

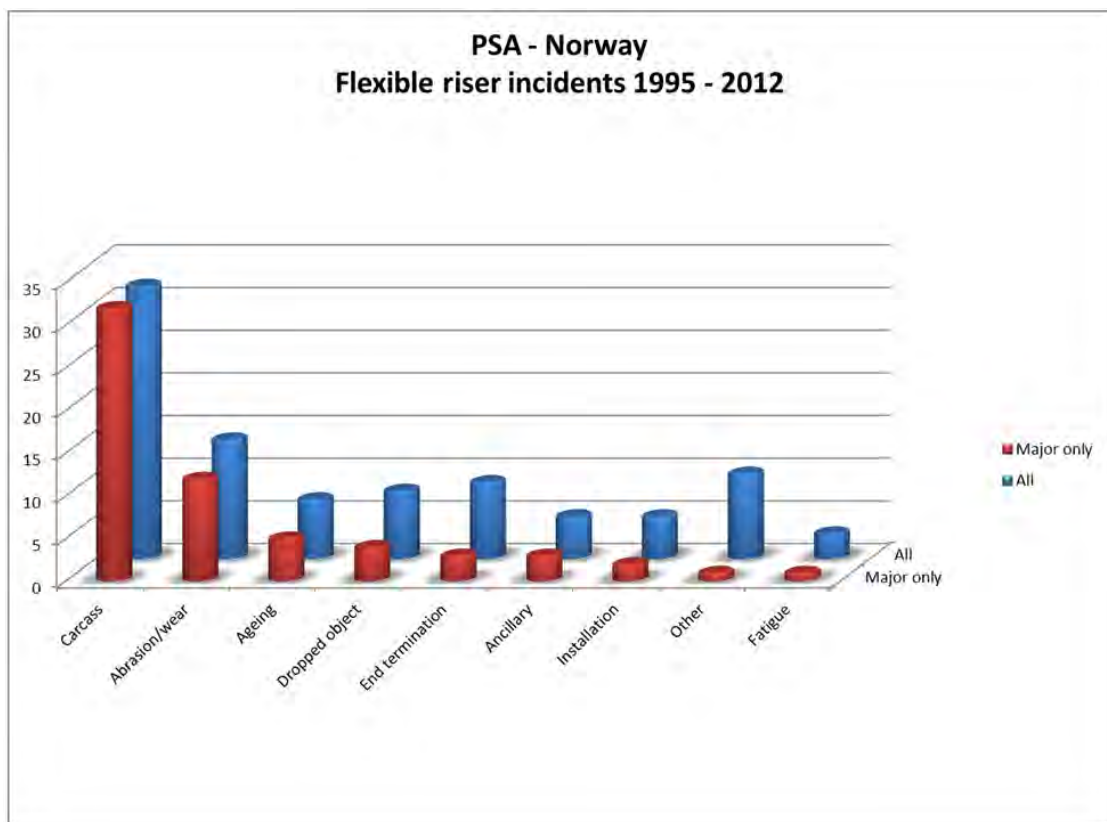


Figure A3.8: Failure incidents for flexible pipes [PSA Norway, 2013a]

## **Part B**

# **Design and Analysis Tools**



## **Chapter B1**

# **Design Analysis**

*Author: Carl Martin Larsen (NTNU), Svein Sævik (NTNU) and Jacob Qvist (4Subsea)*

## B1.1 Introduction

The main purpose of this Handbook is to provide background and guidance on methods for design and operation of flexible pipes. The intention is to give a better basic understanding of mechanisms and conditions governing a rational design and operation. The recommendations and guidelines in this text are not intended to serve as regulations, and there has been no attempt to write the Handbook in a style of a 'recommended practice'.

Since the earlier days of the previous version of the Handbook [Berge et al., 1992], the flexible pipe technology has developed by:

- Larger diameter pipes
- Higher internal and external pressure
- Higher temperature and flow rates
- New designs
- New materials
- New failure modes

The design analysis procedure may correspondingly be characterized by:

- Basic methods for global analysis have not changed; non-linear FEM time domain analyses are dominant
- Research in 1992 is engineering practice in 2010
- Improved computers makes 'non-linear stochastic analysis' available for design engineers
- The analysis of the complex flexible pipe cross sections has developed significantly
- Calculation of response and fatigue damage from vortex shedding (VIV) has made significant improvements. Uncertainties are still significant, but today's models have common understanding of the phenomenon and gives consistent results, which was not the case in 1992.
- Coupling between global and local analyses
- Significant improvements in the model visualization during design work

This chapter of the Handbook briefly mentions the Design Criteria in Section B1.2 before providing a more thorough description of Cross Section Analysis in Section B1.3. Based on a description of stress components and wire geometries, the behavior due to axisymmetric loads, bending and buckling is described, before commenting on computational methods.

In Section B1.4 aspects of the Global Analysis is covered, along with some fundamental concepts of flexible riser behavior.

## B1.2 Design Criteria

The main source for requirements and criteria on flexible pipes are API and ISO. However, very little background and guidance on methods is given in API / ISO, and the Handbook is complementary to the available API / ISO documents. For the majority of flexible pipes discussed in this Handbook the main specification is the [API 17J, 2008]. A descriptive summary is listed below.

### API Spec 17J:

- defines the technical requirements for flexible pipes that are designed and manufactured to uniform standards and criteria.
- minimum requirements are specified for the design, material selection, manufacture, testing, marking and packaging of flexible pipes, with reference to existing codes and standards where applicable.
- applies to unbonded flexible pipe assemblies, consisting of segments of flexible pipe body with end fittings attached to both ends.
- does not cover flexible pipes of bonded structure.
- does not apply to flexible pipe ancillary components.
- does not apply to flexible pipes that include non-metallic tensile and pressure armour wires.
- the applications addressed by [API 17J, 2008] are sweet and sour service production, including export and injection applications. Production products include oil, gas, water and injection chemicals.
- applies to both static and dynamic flexible pipes used as flowlines, risers and jumpers.
- does not apply to flexible pipes for use in choke-and-kill line applications.

For guidelines on the use of flexible pipes API has provided recommended practice [API 17B, 2008].

### Other relevant API specifications are:

- [API 17L1, 2013], Guidelines on Flexible pipe ancillary components
- [API 17L2, 2013], Recommended Practice for Flexible Pipe Ancillary Components
- [API 17K, 2005], Specification for Bonded Flexible Pipes
- [API 17E, 2010], Specification for Umbilicals
- [API 17C, 2010], Specification for Through Flowline (TFL) Systems
- [API 17TR2, 2003], The Ageing of PA-11 in Flexible Pipes
- [API 17TR1, 2003], Evaluation Standard for Internal Pressure Sheath Polymers for High Temperature Flexible Pipes

ASTM, ref<sup>1</sup>, and ISO, provides normative and informative references on material production (steel, alloys, plastics), and on fabrication and testing of components.

<sup>1</sup>American Society for Testing and Materials, 100 Barr Harbor Drive, West Conshohocken, PA 19428, USA

## B1.3 Cross Section Analysis

### B1.3.1 General remarks

The understanding of pipe performance characteristics and related failure modes is important for obtaining a reliable design of flexible pipe systems. The experience gained from flexible pipe applications over the last two decades has identified a significant number of failure modes. The performance with respect to these failure modes may be determined by the use of analytical and computational methods in combination with testing procedures. A detailed description of experienced failure modes and test methods are found in Section A3 and Section B5, respectively.

With reference to [API 17B, 2008], design of flexible pipes is carried out in stages:

- Material selection considering the temperature and chemical conditions in terms of pH (sweet or sour service).
- Cross-section configuration design based on what to be transported (gas, oil, water) and at which pressure rating.
- System configuration design based on the surrounding infrastructure and environment.
- Dynamic analysis design, identifying the curvature and tension extreme responses.
- Detail and service life design verifying that sufficient service life is obtained.
- Installation design, ensuring that the pipe can be safely installed.

The cross-section strength is governed by the steel helix layers and the design analyses used to define the amount of steel needed are normally carried out according to the requirements of [API 17J, 2008] which applies the *allowable stress format*. This means that a load condition specific utilization factor is applied to the yield stress defining a stress limit that is not to be exceeded. The cross-section design analysis is normally based on the pressure rating and use of analytical models considering axisymmetric effects alone (internal and external pressure, tension and torsion) and based on the mean stress approach. The latter means that only stresses due to the axial load in the wires are included when calculating the stresses. Secondary stresses in the wire due to bending and friction is not included. This relies on the assumption that the flexible pipe is a compliant structure where the secondary stresses can be taken care of by introducing a maximum curvature limit to ensure that no over bending takes place.

This section focus on methods for analysis and design of non-bonded flexible pipes with respect to known metallic layer failure modes that can be described by analytical or computational methods and are part of the design requirements reflected in [API 17J, 2008]. The failure modes addressed here are:

- Overload, i.e. excessive yielding in the metallic layers.
- Collapse of the cross-section due to external pressure.
- Buckling of the tensile armour.
- Metal fatigue.
- The effect of corrosion on metal fatigue and tensile armour buckling.

Analytical formulas are included for estimation of mechanical properties and structural capacities for specific cases. These formulas are primarily given for verification purposes, enabling capacity and performance parameters to be calculated in a simplified way and under specific conditions.

### B1.3.2 Governing stress components

The nonbonded flexible pipe consists of a layered structure where each layer is free to slide (under the restraint of friction) relative to each other. Each layer has its specific function as described in Chapter [A2](#), Flexible pipe properties and materials.

In order to understand the mechanical behaviour of flexible pipes it is important to clarify which layers and stress components that contribute. In the general case, the stress components include 3 normal stress components  $\sigma_{11}$ ,  $\sigma_{22}$ ,  $\sigma_{33}$  and 3 shear stress components  $\sigma_{13}$ ,  $\sigma_{23}$ ,  $\sigma_{32}$ , see Figure [B1.1](#)

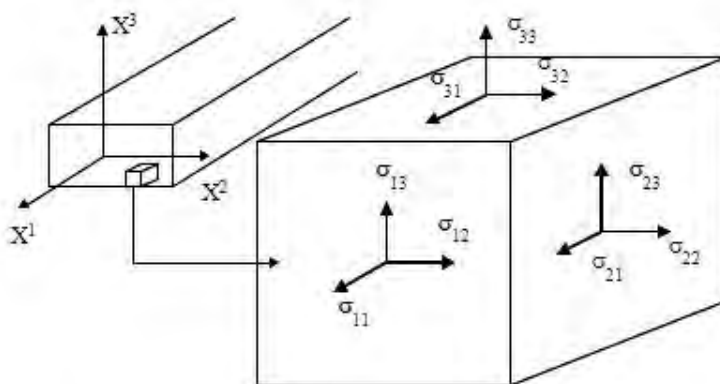


Figure B1.1: General components of stress

The load response is primarily governed by the steel layers, however, the plastic layers influence how the load is shared between the layers. This is exemplified in Figure [B1.2](#) showing how internal pressure is transferred throughout a typical flexible pipe cross-section. This pipe cross-section includes starting from the inside; the carcass, a pressure sheath, pressure spiral wires in two layers, 4 layers of cross-wound tensile armour separated by antiwear tapes and an external sheath.

It is seen that the carcass do not carry pressure (pressure on inside and outside of carcass is the same), due to its corrugated structure. The plastic layers are in this example assumed to have a Poisson's ratio of 0.5. Hence, these layers behave hydrostatic (same stress in all three directions) and the contact pressure (starting from internal pressure at the outside of carcass) is seen to be transformed directly to the next steel layer. The contact pressure from the tensile armour onto the pressure spiral wire results from the end-cap effect (tensioning the tensile armour) and act as a support of the two pressure spiral wire layers, reducing the associated pressure differential that need to be taken by the pressure spiral wires.

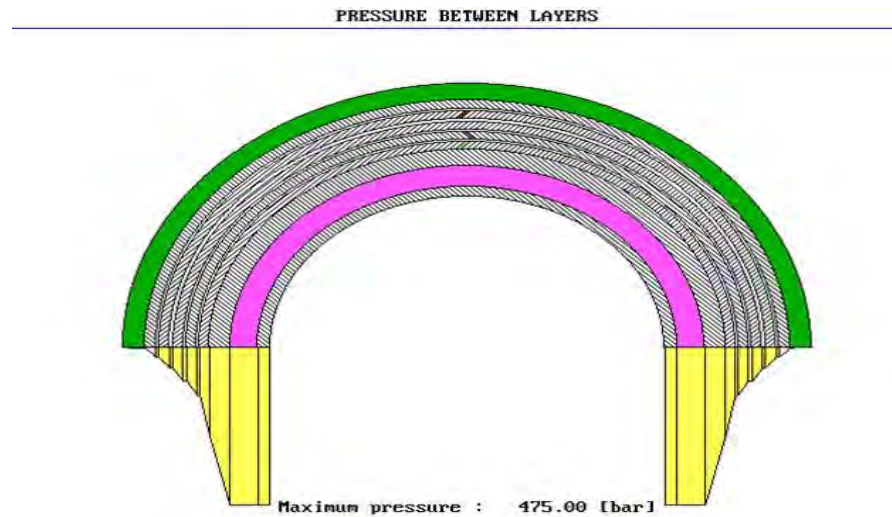


Figure B1.2: Pressure distribution in a typical flexible pipe exposed to internal pressure

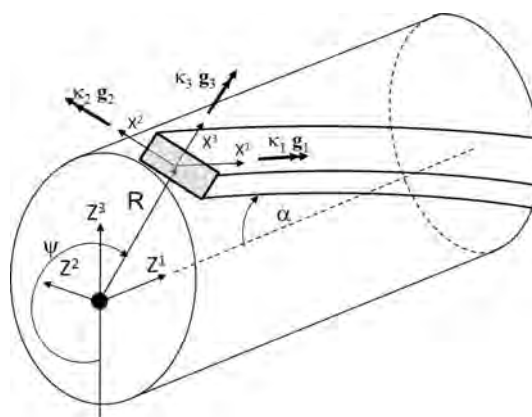
From the above it is clear that the stress state in each layer of a flexible pipe is in nature 3-dimensional. However, since the steel layers are governing with respect to structural strength and these basically consist of long slender curved beams, the primary load carrying effect will be by membrane action. Hence, the primary stress components to be included in strength calculations will be the axial stresses resulting from the axial load in each wire.

The wires are normally assumed to rest stress free in the helix configuration as the manufacturing procedure involves plastic straining. With reference to Figure B1.3 (a), this results in an initial torsion  $\kappa_1$  and an initial normal curvature  $\kappa_2$  whereas  $\kappa_3 = 0$  along the helix. Hence, curved beam theory that include the coupling between initial curvature, membrane and bending effects is needed to describe the structural behaviour. The stresses are related to the governing stress resultants defined in Figure B1.3 (b) and the load scenario, which can be divided into:

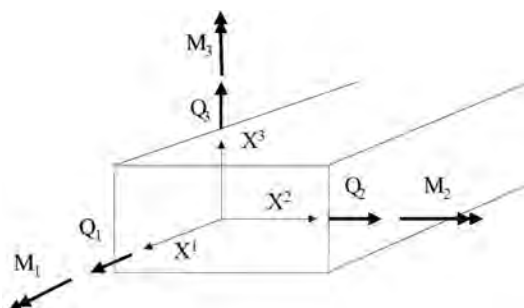
- Axisymmetric loads that only change the length and diameter of the straight pipe cylinder and with small relative deformations between wires. This includes tension, torsion, internal and external pressure loads, the latter assuming that no local buckling or collapse effects occur.
- Bending loads where the straight pipe cylinder is bent into a torus and where significant relative deformations will occur between the wires.

The significant stress components are shown in Figure B1.4 and include components from axial force (basis for strength calculation), torsion moment and bidirectional bending. The components of shear stresses  $\sigma_{12}$  and  $\sigma_{13}$  related to the local shear forces  $Q_2$  and  $Q_3$  are small and can be neglected.

For axisymmetric loads, the stresses related to torsion and bending are insignificant, hence the stresses resulting from the axial load in the wire will govern. It is noted that for non-symmetric pressure spiral wires, such as the Z-spiral, significant stresses may result from rotation as a result of the  $M_3$  moment about the strong radial axis resulting in a significant stress gradient along the cross-section, see Figure B1.5. However, since the spiral wire will be locked when the gaps are closed, these stresses are not essential for equilibrium and can be neglected in static strength calculations. This is one of the reasons why [API 17B, 2008] refers to



(1) Initial torsion and curvature quantities



(2) Wire stress resultants

Figure B1.3: Definition of wire coordinate axes and mechanical quantities

the concept of *mean stress* when dealing with strength calculations, i.e. neglecting the contribution from the bending moment resulting in each wire. It is noted that this approach rests on the assumption that the steel material used have sufficient fracture toughness to accommodate the involved strain level and where the minimum allowable curvature radius will represent the limiting criteria with respect to controlling the total strain involved in most cases.

For bending fatigue calculations, the axial, torsion and bending components need all to be included for both the tensile and pressure armours. In the latter case, the bending process also gives variation in  $\sigma_{22}$ ,  $\sigma_{23}$  and  $\sigma_{33}$  that need to be taken into account, see Section B1.3.5

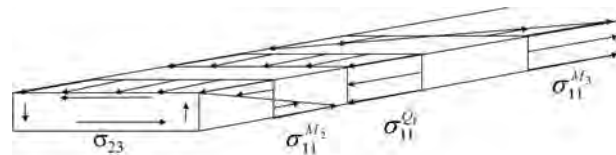


Figure B1.4: Stress components - tensile armour

### B1.3.3 Wire geometries

The tensile armour consists of flat rectangular profiles, with rounded corners to create a smooth profile thus avoiding notch effects. For each layer, all wires are simultaneously cold

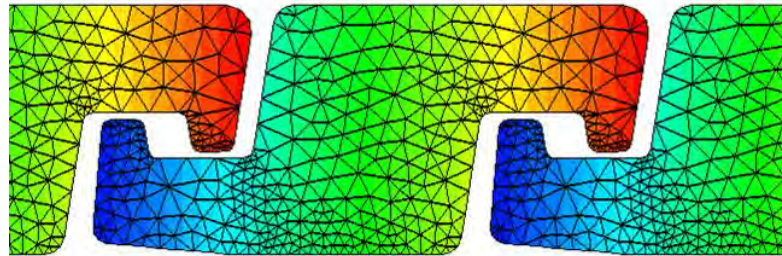


Figure B1.5: Longitudinal stress distribution in Z-profile

formed onto the pipe surface, 40–80 wires in each layer at lay angles  $29^\circ$ – $55^\circ$ . The fraction filled ratio  $F_f$  is usually around 0.9. For the tensile armour, the fill factor is defined by:

$$F_f = \frac{nb}{\cos \alpha 2\pi R} \quad (\text{B1.1})$$

where  $n$  is the number of tendons in the layer,  $b$  is the width of the tendon,  $R$  is the mean layer radius and  $\alpha$  is the lay angle. The applied wire dimension depends on the pipe diameter, some typical thickness/width mm values are 3/7.5, 5/17.5, 4/17.5, 6/12 and 6/15.

The pressure armour consists of interlocked spiral wires, normally 1-2 spiral wires per layer in 1-2 layers. The different manufacturers supply different geometries such as the Z-spiral, the C-clip and the Theta-clip. Different wire configurations are illustrated in Figure B1.6. For high pressure applications a rectangular back up spiral wire may be applied to increase the pressure capacity. The fraction filled ratio is normally in the range of 0.85 for these layers. For the pressure armour and carcass, the fill factor is normally defined by:

$$F_f = \frac{nA}{L_p t} \quad (\text{B1.2})$$

where  $L_p$  is the pitch length of the  $n$  spiral wires in the layer (normally 1 or 2) with cross-section area  $A$ . The pitch length is defined as:

$$L_p = \frac{2\pi R}{\tan \alpha} \quad (\text{B1.3})$$

The carcass is manufactured from a flat steel plate and formed into a corrugated profile as illustrated in Figure B1.7. A typical fill factor is 0.55.

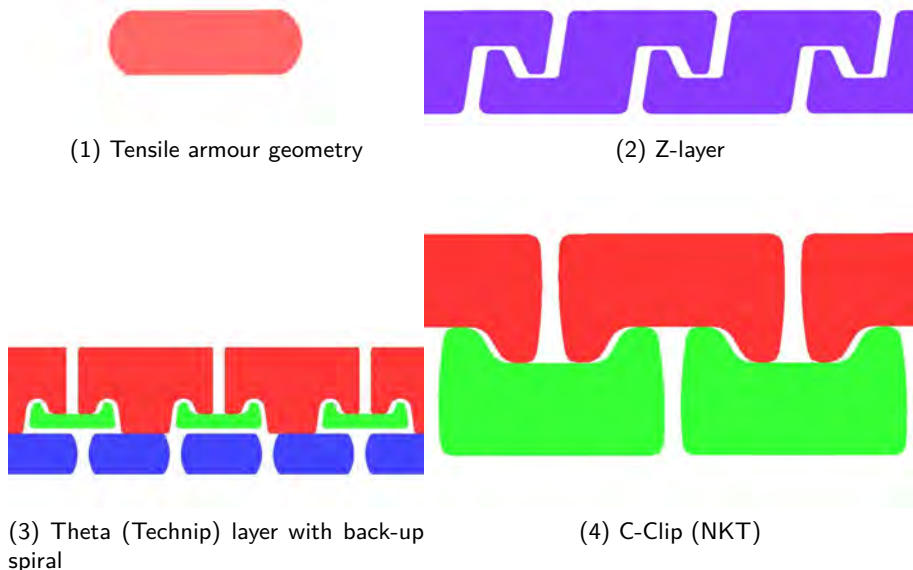


Figure B1.6: Tensile armour profile and alternative pressure spiral configurations

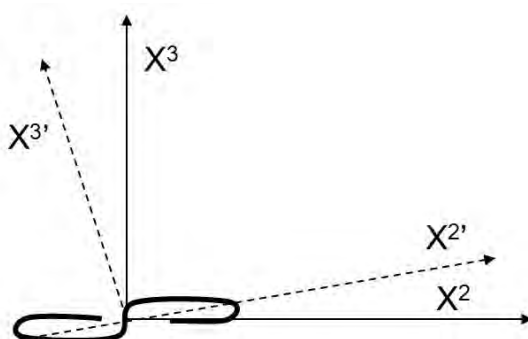


Figure B1.7: Carcass corrugated profile - principal outline

### B1.3.4 Behaviour due to axisymmetric loads

#### B1.3.4.1 General

In this section, the behaviour due to axisymmetric loads, i.e. tension, torsion, internal and external pressure loads will be explained in terms of an analytical approach assuming that the cylindrical straight pipe shape is kept during deformation. It is noted that with respect to external pressure loads this assumes that no local buckling or collapse effects will occur. Buckling effects are treated separately in Section B1.3.6.

As noted above, the response due to axisymmetric loads are primarily governed by the response of the metallic layers which all consist of helices. The wires are normally assumed to rest stress free in the helix configuration as the manufacturing procedure involves plastic strains. With reference to Figure B1.3, the initial torsion  $\kappa_1$  and curvatures components  $\kappa_2$  and  $\kappa_3$  along the helix can be expressed by the lay angle  $\alpha$  and the helix radius  $R$  as:

$$\kappa_1 = \frac{\sin \alpha \cos \alpha}{R} \quad (\text{B1.4})$$

$$\kappa_2 = \frac{\sin^2 \alpha}{R} \quad (\text{B1.5})$$

$$\kappa_3 = 0 \quad (\text{B1.6})$$

The long and thin wires can be described by curved beam theory and the wire equilibrium equation when only considering axisymmetric loads can be written as [Sævik, 2011]:

$$-\kappa_2 Q_1 + \kappa_1 Q_2 + q_3 = 0 \quad (\text{B1.7})$$

$$-\kappa_2 M_1 + \kappa_1 M_2 + Q_2 = 0 \quad (\text{B1.8})$$

where  $Q_i$  and  $M_i$  respectively represent the forces along and moments about the  $X^i$  axes defined in Figure B1.3 and  $q_3$  is the contact line load in the radial direction. For the slender armour wire, the contribution from  $M_i$  and  $Q_2$  is small and can be neglected. This means that wire equilibrium can be described by the axial load  $Q_1$  alone. The contact pressure line load  $q_3$  is then obtained from Eq. B1.7 and Eq. B1.5 as:

$$q_3 = \kappa_2 Q_1 = \frac{\sin^2 \alpha}{R} Q_1 \quad (\text{B1.9})$$

#### B1.3.4.2 Axial loading

**B1.3.4.2.1 Primary effects** By considering all steel layers and neglecting the contribution from the plastic layers, pure axial equilibrium yields:

$$\sum_{j=1}^{N_a} n_j \sigma_{11j} A_j \cos \alpha_j = T_w = T + \pi p_{int} R_{int}^2 - \pi p_{ext} R_{ext}^2 \quad (\text{B1.10})$$

where  $N_a$  is the number of contributing layers,  $T_w$  is the true wall tension,  $n_j$  is the number of wires in layer  $j$ ,  $\sigma_{11j}$  is the axial stress in the layer,  $A_j$  is the cross-section area,  $T$  is the effective tension (the total cross-section resultant),  $p_{int}$  is the internal pressure,  $p_{ext}$  is the external pressure,  $R_{int}$  is the internal pipe radius where the internal pressure is acting (normally outside the carcass) and  $R_{ext}$  is the external pipe radius where the external pressure is acting (depend on whether damaged outer sheath is to be assumed). It seen that since the lay angle of the pressure spiral wire is close to  $90^\circ$ , the axial load is primarily taken by the tensile armour layer.

For a two layered cross-wound structure where the lay angles are assumed to be equal in size but opposite in lay direction (torsion balanced), the below formulas can be used to estimate the stresses in the tensile armour.

$$\sigma_t = \frac{T_w}{nA_t \cos \alpha} = \frac{T_w}{2\pi R t_{tot} F_f \cos^2 \alpha} \quad (\text{B1.11})$$

where  $n$  is the total number of tensile armour wires,  $A_t$  is the area of the wire,  $t_{tot}$  is the thickness including both layers and  $F_f$  is the fill factor. By assuming same fill factor and number of tendons for the two layers, the nominal external pressure from the tensile armour layer onto the pressure spiral wire can further be approximated by:

$$p_t = 2 \frac{q_3}{b} F_f = 2 \frac{\sigma_t A_t \sin^2 \alpha}{R b} F_f = 2 \frac{T_w}{2n_j \cos \alpha} \frac{\sin^2 \alpha}{R b} \frac{n_j b}{\cos \alpha 2\pi R} = \frac{T_w \tan^2 \alpha}{2\pi R^2} \quad (\text{B1.12})$$

where  $R$  is taken to be the mean layer radius.

With reference to Figure B1.8 and Figure B1.9, the axial strain in the helix can be described by standard beam quantities at the cross-section centre and the radial motion  $u_3$  of each layer as:

$$\varepsilon_{11} = \cos^2 \alpha \epsilon_p + \frac{\sin^2 \alpha}{R} u_3 + R \sin \alpha \cos \alpha \tau_p \quad (\text{B1.13})$$

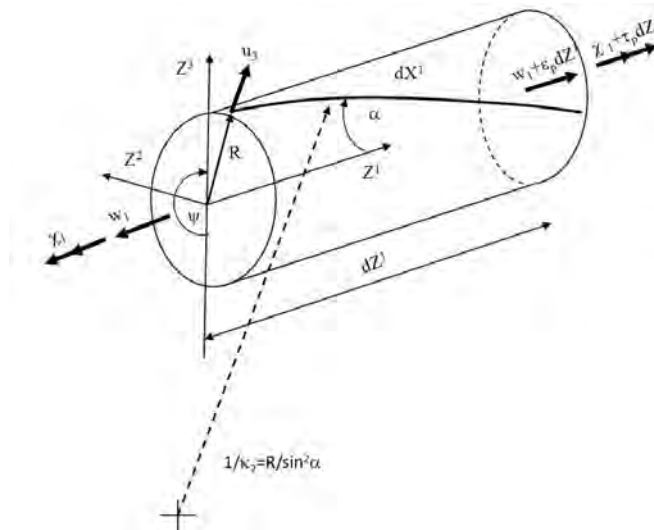


Figure B1.8: Kinematic quantities for axisymmetric deformation

where  $\epsilon_p$  and  $\tau_p$  are the overall pipe strain and torsion at the pipe centre, cfr. Figure B1.8 and Figure B1.9. The axial stiffness of the two layered pipe can then be obtained by assuming no torsion coupling, i.e. neglecting the last term in Eq. B1.13 and using energy principles as:

$$EA = nEA_t \cos \alpha (\cos^2 \alpha - \nu_a \sin^2 \alpha) = EF_f \cos^2 \alpha (\cos^2 \alpha - \nu_a \sin^2 \alpha) 2\pi R t_{tot} \quad (\text{B1.14})$$

where  $\nu_a$  is the apparent Poisson's ratio defined by the relation between axial straining and radial contraction:

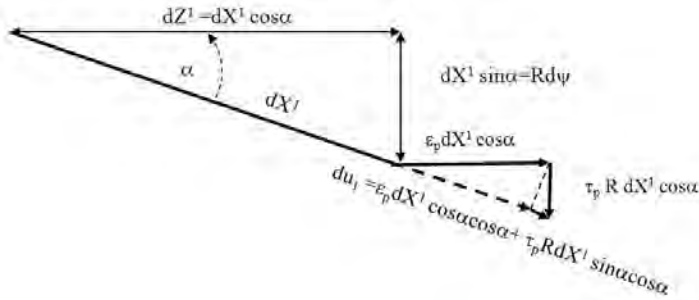


Figure B1.9: Infinitesimal segment strain

$$\nu_a = -\frac{u_3}{R\epsilon_p} \quad (B1.15)$$

The first term in Eq. B1.14 describes the stiffness contribution from the tensile armour, whereas the second term describes the softening effect of the radial contraction associated with the helix. For nonbonded pipes with a stiff pressure armour and carcass,  $\nu_a \sim 0.2$ . Consequently, the first term in the stiffness expression in Eq. B1.14 dominates. It should also be noted that the expression in Eq. B1.14 assumes small geometric deformations and that the layers remain in contact. The last assumption signifies that initial gaps introduced during fabrication or due to the load condition may influence the axial pipe stiffness significantly. This is particularly the case for compressive axial loads.

Figure B1.10 shows experimental results on the axial load -relative elongation behaviour of an 8m long 4" Technip smooth bore dynamic pipe, [Skallerud, 1991a], with zeta layer and pressure back-up layer. The results are presented for different levels of internal pressure and signify:

- Relatively little hysteresis
- Axial stiffness ranging from 11.05-21.05 MN, depending on internal pressure

Figure B1.11 indicates that increasing frequency increases the hysteresis, but the stiffness is not significantly affected. The discontinuity at the loop ends are due to resolution problems at the high frequency, and is not a physical effect of the pipe. It is likely that the hysteresis seen for high frequencies is caused by visco-elastic effects induced by the plastic layers.

The results showed that a linear relation can be assumed between axial force and strain with an associated equivalent damping ratio less than 3 % for the tested pipe.

For a given design,  $\nu_a$  can also be calculated based on information given in terms of the axial strain at a given internal pressure and the axial stiffness. The axial strain at a given pressure  $\epsilon_p$  can be approximated as:

$$\epsilon_p = \frac{(1 - 2\nu_a)p_{int}\pi R_{int}^2}{EA} \quad (B1.16)$$

which can be used to find  $\nu_a$ , in most cases giving the same value of  $\sim 0.2$  for the standard non-bonded pipe (not 55° designs with no pressure spiral wire).

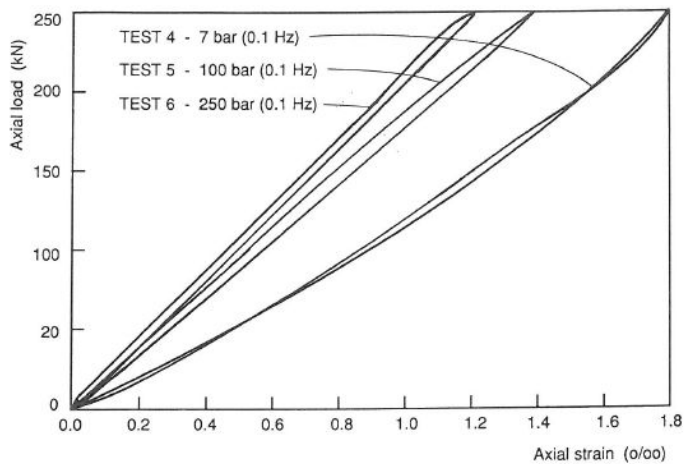


Figure B1.10: Axial elongation behaviour of a 4" Technip pipe. Loading frequency = 0.1 Hz, [Skallerud, 1991a]

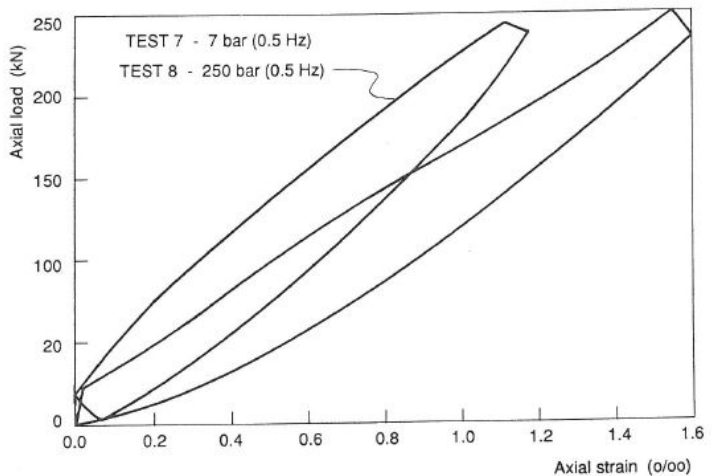


Figure B1.11: Axial elongation behaviour of a 4" Technip pipe. Loading frequency = 0.5 Hz, [Skallerud, 1991a]

Existing methods for the determination of pipe response to axial tension are fairly reliable. However, this is not the case for axial compression, which is a more complex area. During installation and shut-down conditions where the pipe bore may be exposed to external overpressure, the tensile armour will be in compression, even if the effective tension is positive. This may lead to radial gaps followed by radial or transverse buckling of the tensile wires, leading to overall torsion instability. For deep water pipe designs, anti-buckling tapes may be applied on the outside of the outer tensile armour to limit the radial motions and formation of gaps. The instability failure mode was reported by Bectarte and Coutarel [Bectarte and Coutarel, 2004] describing both bird caging (radial failure) and lateral buckling. Test procedures for lateral buckling were described that included the effect of cyclic bending. A computer model was also mentioned, but no details with respect to methods or results were given. The methods used to validate the pipe capacity with respect to this failure mode include laboratory testing, Deep water Immersion Performance (DIP) testing and mathematical models. Reference is given to Section B1.3.6.

**B1.3.4.2.2 Bending and torsion in the wire due to axial wire loads** The change in lay angle induced by the beam deformation quantities also leads to small changes in the curvature of the wire about the weak axis of the wire and torsion. These quantities can be approximated by [Sævik, 1992]:

$$\omega_1 = \frac{\sin^3 \alpha \cos \alpha}{R} \epsilon_p - \frac{\sin^3 \alpha \cos \alpha}{R^2} u_3 + \cos^4 \alpha \tau_p \quad (\text{B1.17})$$

$$\omega_2 = -\frac{\sin^2 \alpha \cos^2 \alpha}{R} \epsilon_p + \frac{\sin^2 \alpha \cos^2 \alpha}{R^2} u_3 + (2 \sin \alpha \cos^3 \alpha + \sin^3 \alpha \cos \alpha) \tau_p \quad (\text{B1.18})$$

where  $\omega_1$  represents the change in torsion and  $\omega_2$  is the change in normal curvature. As noted above, the contribution from the above quantities can normally be neglected due to the small tensile armour cross-section and the limited overall axial strain allowed for in flexible pipes. It should, however, be noted that for torsion unbalanced structures consisting of large helical elements, the contribution is significant and should be included. The above equations have been compared to FE analysis and are considered valid as long as the helix lay angle is not significantly altered [Sævik and Li, 2013].

**B1.3.4.2.3 Bending stresses induced by axial wire loads at end fittings** Axisymmetric loads is associated with small changes in the initial lay angle. In the end fitting where the wires are terminated, this change in lay angle may be restrained. In the case of restraint, this will give rise to local bending stresses, [Thorsen, 2011]. Longitudinal stresses due to bending will add to the total axial stress and this may possibly constitute a danger when it comes to fatigue of the pipe, specially if it is reasonable to believe that metal to metal contact occurs.

In the unloaded configuration the angle between the tensile armour wires and the longitudinal axis of the pipe (the lay angle) is  $\alpha_0$ , see Figure B1.12.

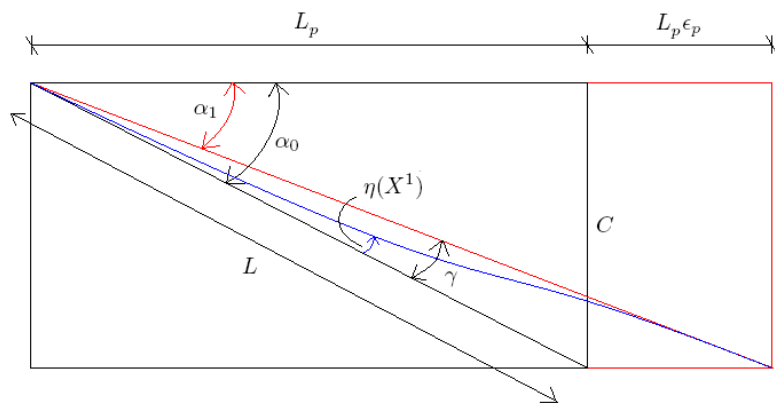


Figure B1.12: Definitions related to the wire behaviour at end fitting, [Thorsen, 2011]

As the pipe is axially strained, the curve which the wires follow must change. If no end restraints are present, the change in lay angle would be the same at all points along the wire, and the wire would assume a path like the red one in the figure. The new lay angle is denoted  $\alpha_1$ . The displacement pattern ( $\alpha_1$ ) and wire strain ( $\epsilon_{11}$ ) is only possible when no

end restraints are present. The wire is in fact fixed at the end fitting, meaning that the lay angle must remain at  $\alpha_0$  at the end fitting and gradually increase towards  $\alpha_1$  as one moves away from the end. This is illustrated in Figure B1.12 with a blue line. Therefore the *actual* change in lay angle is introduced as the variable  $\eta(X^1)$ , meaning that the new lay angle at any point along the wire is given as  $\alpha_0 - \eta(X^1)$  which in the limit reaches the change in lay angle  $\gamma$ . For the no friction case, the local bending stress about the wire strong axis can be approximated as [Thorsen, 2011]:

$$\sigma_{11}^{M_3} \simeq 1.73E\gamma \cos \alpha \epsilon_p^{\frac{1}{2}} \quad (\text{B1.19})$$

where  $\sigma_{11}^{M_3}$  is defined in Figure Figure B1.5(a) and  $\gamma$  is the change in lay angle. Eq. B1.19 has been used to calculate numerical values for a wide range of pipe strain. The calculations have been performed assuming standard steel properties and the results are shown in Figure B1.13, where the ratio between local bending stress and axial stress are shown for two different wire dimensions. The blue line shows results for a wire of width 9 mm and thickness 3 mm, while the red line shows a larger wire of width 15 mm and thickness 6 mm. The radius of the pipe is 0.1 meters and the lay angle is 35° in both cases.

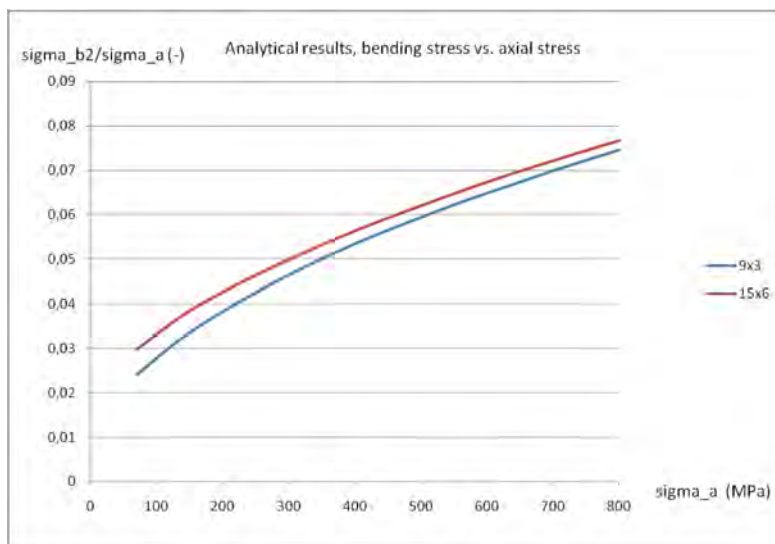


Figure B1.13: Analytical results for the ratio between bending and axial stress., [Thorsen, 2011]

As seen in the figure, the bending component grows larger relative to the axial stress as the stress increases, and the bending stress exceeds 6 % of the axial stress for an axial stress above 500 MPa. The rate of increase in bending stress is relatively large at low strain levels, but it does however decay as the axial stress increase. Even so, the relative magnitude of bending stress continues to increase. It is also observed that the two curves in the figure are located very close to each other despite the relatively large differences in wire dimensions.

A major limitation of the analytical model is the assumption of zero friction. Friction will restrain the wire motion and force the wire into the new lay angle over shorter length. FE analyses have been carried out to investigate the effect of friction in a single wire [Thorsen, 2011] for wire dimensions 9 x 3 mm wire and 15 x 6 mm. The results are presented in Figure B1.14 and Figure B1.15.

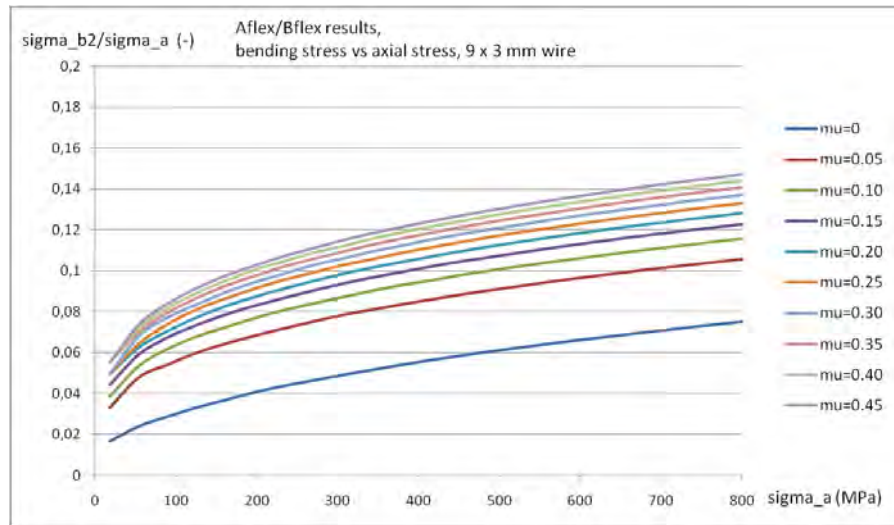


Figure B1.14: FE results for end fitting bending stress, 9 x 3 mm wire, [Thorsen, 2011]

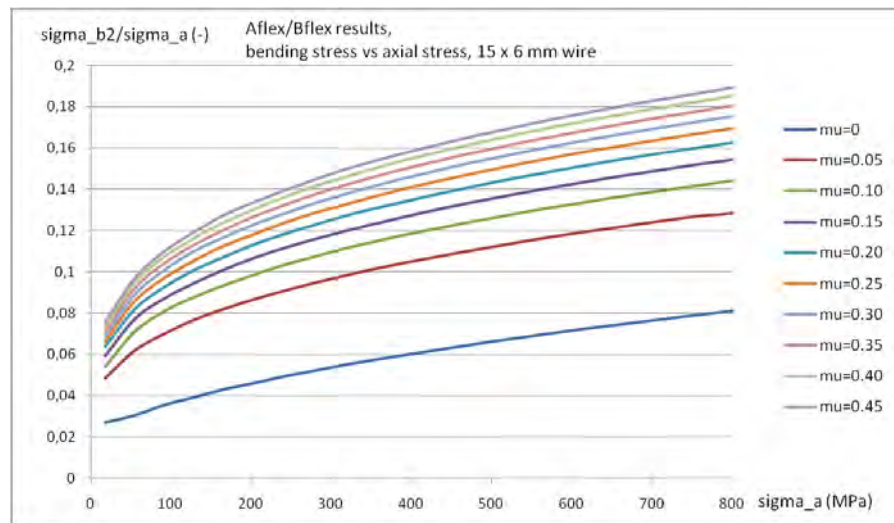


Figure B1.15: FE results for end fitting bending stress, 15 x 6 mm wire, [Thorsen, 2011]

As seen, the friction greatly increases the bending stress at the end fitting and for a two layered structure, one may experience a localized bending stress of approximately 16 % of the axial stress if the pure axial stress is 400 MPa. This is significant, and should be considered in fatigue evaluations of the armour wires if significant dynamic tension occurs. It is however noted that all the above calculations rests on the assumption that the armour wires are fully fixed at the end fitting. The accuracy of this assumption depends on the end fitting construction, and more detailed analyses taking the end fitting behaviour into the calculations should be performed in the general case.

#### B1.3.4.3 Torsion

Excessive torsion may give lock-up of the wires causing "birdcaging" or structural damage to the pipe. This is not a very likely failure mode under normal operational conditions where the torsional loads are small. However, there have been cases of excessive torsion

during pipe installation, which have caused failure in the pipe. An axial tensile force will prevent torsional damage. This positive effect is normally taken into account by verifying the torsional strength for a tensile force not greater than the minimum axial force predicted from the dynamic analysis of the riser system. The torsional resistance from all  $N_a$  resisting layers must equal to the torsional moment  $M_t$  given as:

$$\sum_{i=1}^{N_a} n_j \sigma_{11j} A_j R_j \sin \alpha_j = M_t \quad (\text{B1.20})$$

The major contribution to the torsional resistance comes from the helically wound tensile armours, which leads to the following formula for a quick evaluation of the stresses in the tensile layers:

$$\sigma_{11} = \frac{M_t}{R n A_t \sin \alpha} \quad (\text{B1.21})$$

where  $n$  is the total number of wires in the armouring layers,  $A_t$  is the cross section area of each wire and  $R$  is the mean radius of the armouring layers. Again, two tensile armour layers with equal but opposite lay angles have been assumed. By combining Eq. B1.21 and Eq. B1.13, disregarding the  $\epsilon_p$  and  $u_3$  components, the following expression may be used for an approximate evaluation of the torsional stiffness of the pipe

$$GI_t = n A_t E R^2 \sin^2 \alpha \cos \alpha = E F_f \sin^2 \alpha \cos^2 \alpha 2\pi R^3 t_{tot} \quad (\text{B1.22})$$

The above formulas assume that all layers remain in contact. It should be pointed out that there is an asymmetry in the torsional stiffness. When the pipe is twisted, gaps will tend to occur between the layers as one layer will tend to move outwards and the other inwards. The presence and location of these gaps therefore depends on the direction of the applied moment, the load condition and the pipe design (A  $55^\circ$  degree structure will behave different from a standard  $35^\circ$  structure). Considering a standard  $35^\circ$  structure and load cases dominated by tension and internal pressure, the tensile armour will be squeezed against the pressure armour and the torsion stiffness will be high. In cases where axial compression occurs, eg. during installation, the tensile armour will be supported by the soft outer sheath/anti-buckling tape and the torsion stiffness will be lower.

Experimental studies of the torsional behaviour of a 4" Technip pipe are reported [Skallerud, 1991a]. The pipes exhibit torsional behaviour which is similar to the axial behaviour shown in Figure B1.10, although the hysteresis is less dependent on the load frequency, the latter most likely being caused by friction induced in the pressure armour and due to the relative rotation between layers. Since friction effects are sensitive to the gap conditions, the torsion damping will vary with the load condition. However, the results showed that a linear stiffness relation can be assumed between torque and torsion as for the axial load case.

#### B1.3.4.4 Internal and external pressure

Bursting of a pipe by excessive internal pressure can occur if the pipe is not properly designed, or if the maximum internal pressure is considerably underestimated. However, if the internal pressure is known this failure mode is not likely to occur, see Section A3. The design pressure

includes operating pressure and allowances for surges or other factors affecting the internal pressure. This should be combined with atmospheric external pressure. For selection of design parameters, see [API 17J, 2008].

When a pipe is subjected to internal pressure the load will be carried by the tensile and pressure armour layers. The equilibrium between stresses and radial forces may be expressed by the following equation:

$$\sum_{j=1}^{N_a} \frac{n_j \sigma_{11j} A_j \sin^2 \alpha_j}{R_j} \frac{1}{\cos \alpha_j} = 2\pi(p_{int} R_{int} - p_{ext} R_{ext}) \quad (\text{B1.23})$$

where  $N_a$  is the number of pressure resisting layers. The first term on the left hand side is related to the axial force in the wires which when multiplied by the normal curvature gives the radial line load, as in Eq. B1.9, whereas the  $\frac{1}{\cos \alpha_j}$  term describes the relative amount having this line load per unit length of pipe. A good approximation is to assume that the plastic sheaths transmit pressure, i.e. there is no pressure differential through the plastic layers. The interlocked carcass does not carry any part of the internal pressure. Consequently, the pressure resisting layers are the pressure spiral wire layers and the cross-wound armour layers, with the pressure spiral wire layers taking the major role.

Eq. B1.23 and Eq. B1.1 may be combined to arrive at the following expression for the tensile armour contribution to burst pressure resistance:

$$p_h = \frac{t_{tot}}{R} F_f \sigma_u \sin^2 \alpha \quad (\text{B1.24})$$

where  $t_{tot}$  is the total thickness of the double tensile armour layers,  $R$  is the mean radius of the helical armour layers and  $\sigma_u$  is the ultimate tensile strength of the layer. Eq. B1.11 may be used to derive the following expression for the tensile armour contribution to end cap pressure resistance:

$$p_a = 2 \frac{R}{R_{int}^2} t_{tot} F_f \sigma_u \cos^2 \alpha \quad (\text{B1.25})$$

In the case of no zeta or back-up pressure layer, the stress in the helical armours alone must balance the hoop and end cap effects of the internal pressure, i.e.  $p_h = p_a$ . Assuming  $R_{int} \sim R$ , this gives  $\tan^2 \alpha = 2$ , or  $\alpha = 54.7^\circ$ . This is the "neutral" or "balanced" lay angle at which there is no tendency for the helical armour to change shape under load. Since a pipe is usually reinforced by several layers, the balanced angle will depend on the relative amount of steel in the helical armour layers and the pressure layers. The optimum lay angle is then typically  $35 - 40^\circ$ , cf. [Nielsen et al., 1990]. The contribution to burst pressure resistance from the pressure layers,  $p_p$  may be obtained from the following expression

$$p_p = \sum_{j=1}^{N_p} \frac{t_j}{R} F_{fj} \sigma_{uj} \quad (\text{B1.26})$$

where  $t_j$  denote the thickness of pressure spiral wire layer number  $j$  and  $R$  is the mean radius of the  $N_p$  pressure layers, respectively. The fill factor  $F_{fj}$  for pressure spiral wire layer  $j$ .

The total hoop pressure resistance is then obtained by summing the contribution from each layer as:

$$p_{hoop} = p_p + p_h \quad (\text{B1.27})$$

The burst pressure is then given by the smallest of  $p_{hoop}$  and  $p_a$  i.e. hoop and axial resistance:

$$p_b = \min(p_{hoop}, p_a) \quad (\text{B1.28})$$

In pipe design, the lay angle is usually chosen to give equal burst resistance in the axial and hoop directions. The procedure for burst pressure calculations, described above, is quite simple and straightforward. Experimental results, reported by [Chen et al., 1992], show that the above procedure gives quite reliable estimates of burst pressure. The average deviation from test results was reported to be within 3%, and with a maximum deviation of 7-8%.

### B1.3.5 Behaviour in bending

#### B1.3.5.1 General

The bending behaviour of flexible pipes is a more complex phenomenon to analyse than the axisymmetric load case. The flexural response shows a pronounced hysteresis behaviour. This is illustrated by the moment/curvature relation in Figure B1.16. The hysteresis behaviour of nonbonded pipes may be explained by the internal slip mechanism. Such pipes have a number of helical reinforcing layers, which tend to slip relative to each other when the pipe is bent. This is particularly the case for the two crosswound tensile layers. When the curvatures are small, slip is prevented by the internal friction between the layers, giving a high initial tangent stiffness,  $EI_s$ , corresponding to the sum of contributions from all layers when assuming plane surfaces remain plane as for standard beam theory. The moment needed to overcome the friction forces,  $M_f$ , is called the friction moment.  $M_f$  depends on the contact pressure between pipe layers, and consequently on the loads applied to the pipe. When the friction moment is exceeded, the curvature varies linearly with the moment variation. The slope of this line corresponds to the elastic bending stiffness  $EI_e$  represented by the sum of contributions from elastic bending of the plastic layers and each individual wire. This stiffness is rather low and the main part of it is due to the stiffness of the plastic sheaths. It should also be noted that when the direction of the curvature is changed, the change in moment has to exceed twice the friction moment before reversed slip behaviour occurs.

#### B1.3.5.2 Minimum bend radius

Excessive bending can lead to local buckling destruction of the pipe as the interlocking elements or helical armour elements interfere and touch each other as well as plastic layer overstraining. [API 17J, 2008] defines the minimum bend radius from the concepts of minimum storage radius,  $\rho_s$ , and the minimum locking radius,  $\rho_l$ , needed to cause unlocking of the interlocked layers where a primary requirement is that  $\rho_s$  is always greater than  $\rho_l$ . Different safety factors are then applied based on the load type and condition to prevent damage when the pipe is bent in dynamic, static, installation and storage configurations, see Section A3 for a more detailed description of related failure modes.

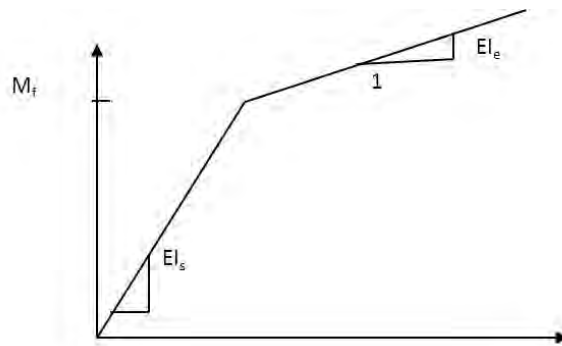


Figure B1.16: Typical moment curvature relation for non-bonded flexible pipe

The locking radius at which contact occurs between elements within the different helical layers, may be computed when the layer geometry is known. Figure B1.17 shows the relevant geometric quantities for both the tensile armour and the interlocked profiles used in the pressure armour. The locking radius is found considering the bending strain needed to close the gap at the tensile or compressive sides of the pipe. For the interlocked profiles, this can be formulated at the compressive side where shortening occurs as:

$$\frac{L_p R}{n \rho_l} = \frac{L_p}{n} - \frac{b_{min}}{\sin \alpha} \quad (\text{B1.29})$$

and at the tensile side where elongation occurs;

$$\frac{L_p R}{n \rho_l} = \frac{b_{max}}{\sin \alpha} - \frac{L_p}{n} \quad (\text{B1.30})$$

For the tensile armour, either of the above equations apply and can also be calculated on the basis of the fill factor as:

$$\rho_l = \frac{R}{1 - F_f} \quad (\text{B1.31})$$

The locking radius for the pipe is taken to be the largest \$\rho\_l\$ for all helical layers. In order to maintain integrity of the plastic layers, this is governed by the maximum allowable strain, see [API 17J, 2008]. This gives the following limit for the bending radius of the plastic layer:

$$\rho_\epsilon = \frac{R}{\epsilon_{lim}} \quad (\text{B1.32})$$

The minimum bend radius is established from considering both \$\rho\_\epsilon\$ and \$\rho\_l\$ and including relevant safety factors as specified in [API 17J, 2008].

### B1.3.5.3 Stresses and stress resultants related to the tensile armour

As stated above, the static reference stress level in the tensile armour is given by the mean static effective tension and associated internal and external pressures. This gives a mean axial stress and associated contact pressures that governs the friction moment. In a flexible

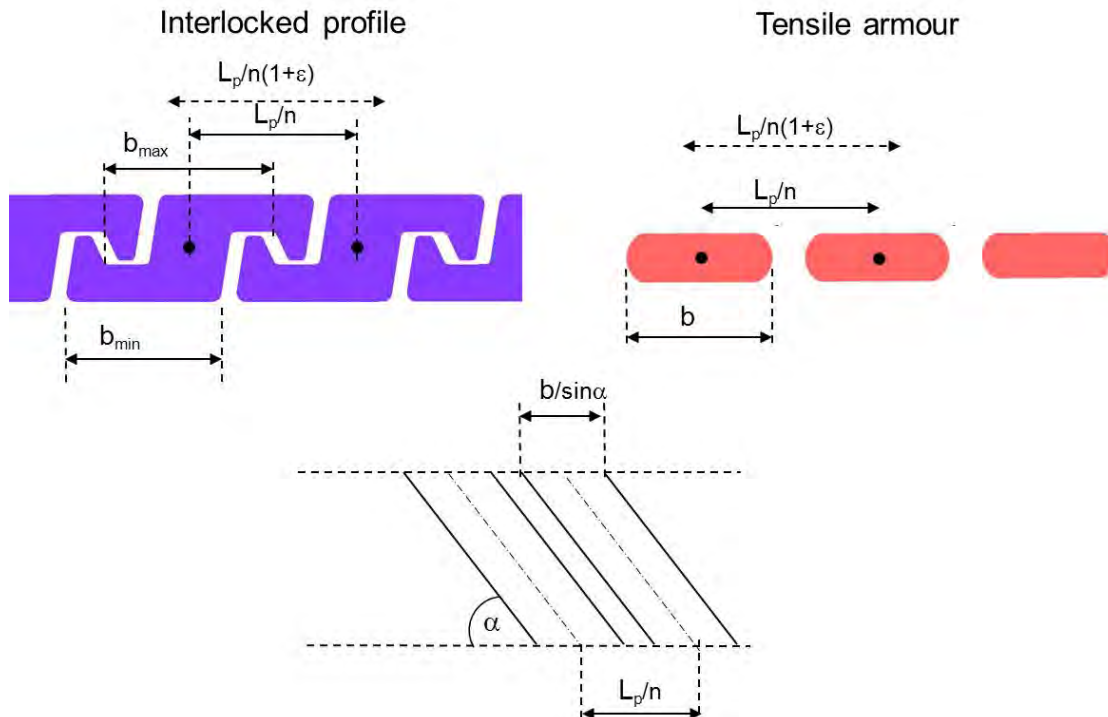


Figure B1.17: Geometrical properties of armour layers relevant for minimum radius prediction

riser the tension and external pressure will vary along its length, hence the friction moment will also change along the riser. Further, due to the differences in contact pressure between layers, the response in terms of dynamic stresses due to bending induced by floater motion and hydrodynamic loads will be different between layers. Hence, the nature of dynamic stresses will be characterized by both variation between layers and along the length of a flexible riser.

For the tensile armour layers, the dynamic stresses will consist of an axial friction stress associated to the slip between layers, axial stresses from dynamic tension and local torsion and bending stresses resulting from the components of global curvature along each wire.

**B1.3.5.3.1 Local wire bending stresses in tensile armour** In the stressed state, the local bending behaviour can be described by assuming that each wire follows an assumed path along the curved pipe surface and application of differential geometry. With regard to which path each wire will follow, there are two assumptions that have been commonly used, see [Feret et al., 1986b] and [Sævik, 1993] and Figure B1.18:

- The *Geodesic*
- The *Loxodromic*

The loxodromic curve represents the curve that would represent the initial path of each wire on the circular cylinder as if the path was fixed relative to the surface. The geodesic represents the shortest distance between two points, respectively on the tensile and compressive sides of the pipe along the same helix. It has no transverse curvature and both longitudinal and transverse slip relative to the loxodromic is needed to reach the geodesic path as illustrated in Figure B1.18.

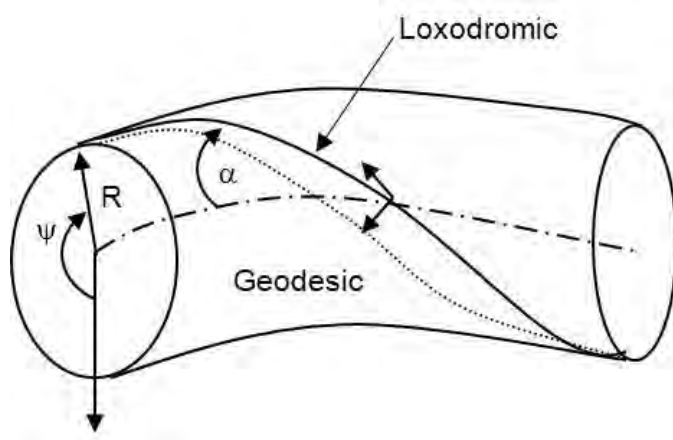


Figure B1.18: Definition of curve paths

As a result of bending, shear forces will build up between each wire and the pipe until slip starts. Due to the relative large axial stiffness of each wire, longitudinal slip is enforced to eliminate the length difference between the compressive and tensile sides of the pipe. However, based on the work by Sævik [Sævik, 1993], the transverse wire displacements towards the geodesic will be restrained by transverse friction forces. Hence, the dynamic bending torsion and curvature in each wire,  $\omega_{ip}$ , will be somewhere between the solution given by the above limit curves. If no slip is assumed, the loxodromic curve applies and the torsion and curvature quantities can be determined with reference to Figure B1.19 as:

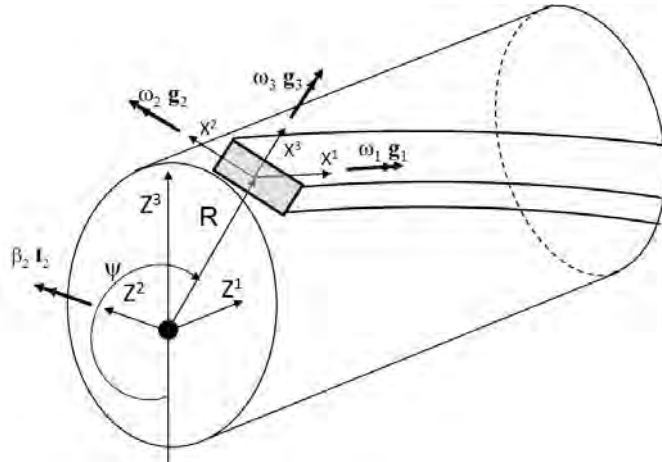


Figure B1.19: Definition of curvature quantities

$$\omega_{1p} = \sin \alpha \cos^3 \alpha \cos \psi \beta_2 \quad (B1.33)$$

$$\omega_{2p} = -\cos^4 \alpha \cos \psi \beta_2 \quad (B1.34)$$

$$\omega_{3p} = (1 + \sin^2 \alpha) \cos \alpha \sin \psi \beta_2 \quad (B1.35)$$

where  $\beta_2$  is the global curvature at the cross-section centre and  $\psi$  is the angular coordinate starting from the lower side of the pipe, see Figure B1.19.

However, since longitudinal slip is unavoidable, this will change the curvature quantities even if no transverse slip occurs. If no axial friction is assumed, the longitudinal relative

displacement is given by:

$$u_1 = R^2 \frac{\cos^2 \alpha}{\sin \alpha} \sin \psi \beta_2 \quad (\text{B1.36})$$

which then changes the above torsion and the weak axis curvature into:

$$\omega_{1p} = 2 \sin \alpha \cos^3 \alpha \cos \psi \beta_2 \quad (\text{B1.37})$$

$$\omega_{2p} = -\cos^2 \alpha \cos 2\alpha \cos \psi \beta_2 \quad (\text{B1.38})$$

where it is noted that the transverse curvature  $\omega_{3p}$  (bending about strong axis of the flat wire) is unaffected.

The corresponding quantities along the geodesic curve which assumes both longitudinal and transverse slips are , [Sævik, 1992]:

$$\omega_{1p} = -\sin \alpha \cos \alpha \left[ \frac{1}{\sin^2 \alpha} - 3 \right] \cos \psi \beta_2 \quad (\text{B1.39})$$

$$\omega_{2p} = -3 \cos^2 \alpha \cos \psi \beta_2 \quad (\text{B1.40})$$

$$\omega_{3p} = 0 \quad (\text{B1.41})$$

The slip towards the geodesic also involves a transverse slip component in addition to the longitudinal component in Eq. B1.36:

$$u_2 = \frac{R^2}{\tan \alpha} \left[ \frac{\cos^2 \alpha}{\sin \alpha} + 2 \sin \alpha \right] \sin \psi \beta_2 \quad (\text{B1.42})$$

**B1.3.5.3.2 Moment-curvature behaviour and associated friction stresses** As noted above, the pipe initially behaves as a rigid pipe according to Navier's hypothesis during increased bending. At a certain point, however, the shear stress at the neutral axis of bending will exceed the shear capacity governed by friction and slip will occur between layers. With reference to Figure B1.19, considering plane deformation only i.e.  $\beta_2 \neq 0$ , the axial force  $Q_1$  in the wire before slip is given by:

$$Q_1 = -EA_t \cos^2 \alpha R \cos \psi \beta_2 \quad (\text{B1.43})$$

The associated shear force  $q_1$  per unit length along the wire needed to fulfil the plane surfaces remain plane condition is obtained by differentiating the above equation with respect to the length coordinate  $X^1$  and applying the relation  $\psi = \frac{\sin \alpha}{R} X^1$ :

$$q_1 = EA_t \cos^2 \alpha \sin \alpha \sin \psi \beta_2 \quad (\text{B1.44})$$

where the maximum is found at the pipe neutral axis of bending as for standard beam theory. The shear stress increases until the maximum possible shear stress  $q_{1c}$  is obtained:

$$q_{1c} = \mu(q_3^I + q_3^{I+1}) \quad (\text{B1.45})$$

where  $\mu$  is the friction coefficient and the index  $I$  refers to the inner and outer surfaces of the wire. The critical curvature  $\beta_{2c}$  is then found by equating  $q_1$  and  $q_{1c}$  as:

$$\beta_{2c} = \frac{\mu(q_3^I + q_3^{I+1})}{EA_t \cos^2 \alpha \sin \alpha} \quad (\text{B1.46})$$

and the maximum stress at the outer fibre of the pipe at this stage is:

$$\frac{\mu(q_3^I + q_3^{I+1})R}{\sin \alpha A_t} \quad (\text{B1.47})$$

which is noted to be a factor  $\pi/2$  less than the value found by equilibrium assuming full slip along the quarter pitch helical path.

Assuming harmonic helix motion and no end effects, an arbitrary cross-section can be divided into two zones as illustrated in Figure B1.20 where one part of the cross-section will be in the slip domain (Region II), whereas the other will still be in the stick-domain (Region I). Considering one quarter of the cross-section and at the tensile side (the upper right part of Figure B1.20), the transition between these two regions can be defined by the angle  $\psi_0$ :

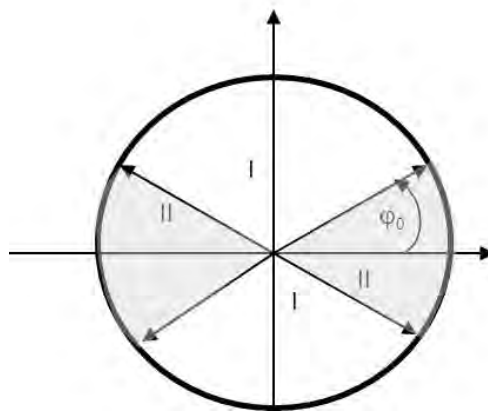


Figure B1.20: Cross-section slip zone

$$\psi_0 = \frac{\psi_0}{\sin \psi_0} = \frac{\beta_2}{\beta_{2c}} \quad (\text{B1.48})$$

where  $\beta_2$  represents the actual curvature of the cross-section at any stage beyond slip. At this stage, the stress distribution along Region II in the considered cross-section quarter can be expressed by:

$$\sigma_{11}(\psi) = \frac{\mu(q_3^I + q_3^{I+1})R}{\sin \alpha A_t} \psi \quad (\text{B1.49})$$

whereas the stress in Region I can be expressed by:

$$\sigma_{11}(\psi) = E \cos^2 \alpha R \beta_2 (\sin \psi - \sin \psi_0) + \frac{\mu(q_3^I + q_3^{I+1})R}{\sin \alpha A_t} \psi_0 \quad (\text{B1.50})$$

where it is noted that at full slip  $\psi = \psi_0 = \frac{\pi}{2}$ , the cross-section stress reaches its full value given by:

$$\sigma_{11} = \frac{\pi}{2} \frac{\mu(q_3^I + q_3^{I+1})R}{\sin \alpha A} \quad (\text{B1.51})$$

The associated bending moment can be found by integration, utilizing symmetry and considering the layer as a thin shell layer with thickness  $t$  as:

$$M = 4F_f \cos^2 \alpha R^3 t \left[ \int_0^{\psi_0} \frac{\mu(q_3^i + q_3^{i+1})}{\sin \alpha A_t} \psi d\psi \right. \\ \left. + \int_{\psi_0}^{\frac{\pi}{2}} E \cos^2 \alpha \beta_2 (\sin \psi - \sin \psi_0) + \frac{\mu(q_3^I + q_3^{I+1})}{\sin \alpha A_t} \psi_0 \sin \psi d\psi \right] \quad (\text{B1.52})$$

From the above, the start slip bending moment contribution from each layer is found to be:

$$M_c = \frac{R^2 \mu(q_3^I + q_3^{I+1}) n}{2 \tan \alpha} = F_f \frac{\pi R^3 \cos^2 \alpha \mu(q_3^I + q_3^{I+1})}{b \sin \alpha} \quad (\text{B1.53})$$

whereas the full slip bending moment from the same layer is determined to be:

$$M_f = \frac{2R^2 \mu(q_3^I + q_3^{I+1}) n}{\pi \tan \alpha} = F_f \frac{4R^3 \cos^2 \alpha \mu(q_3^I + q_3^{I+1})}{b \sin \alpha} \quad (\text{B1.54})$$

It is noted that the difference between this two moment values is a factor  $\frac{\pi}{4}$  which is in agreement with the value obtained when comparing the initial and full yield bending moments for a steel pipe having a perfect elastic-plastic material characteristic.

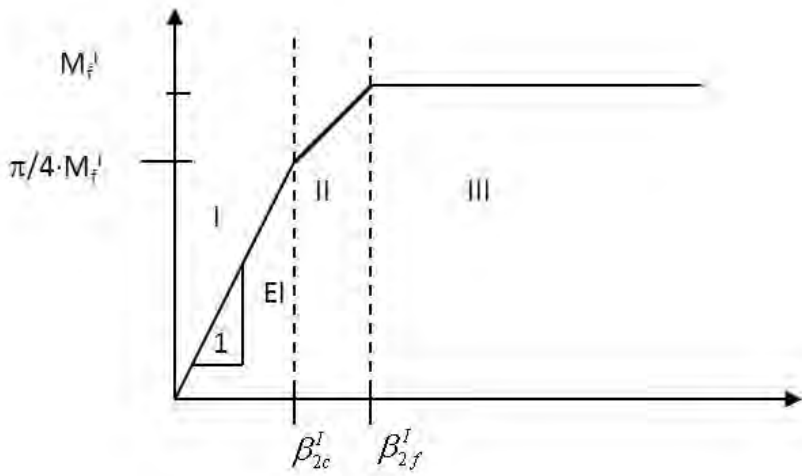


Figure B1.21: Moment curvature contribution from each layer

By application of Eq. B1.48 and Eq. B1.52 a moment curvature diagram can be constructed for each layer as illustrated in Figure B1.21. This diagram represent the friction contribution to the moment curvature relation from each tensile armour layer and can be represented as a three-linear function. The contact pressure will vary between layers and the total moment

curvature diagram will therefore include a sum of three-linear relations, one for each layer. However, since the transition to start slip to end slip is small in terms of curvature increase, the diagram can be approximated as sum of bi-linear relations and the contribution from one tensile armour layer to the bending stiffness before slip can be found by dividing the slip bending moment of Eq. B1.53 with the slip curvature in Eq. B1.46. The bending stiffness contribution from friction in each layer can then be written as:

$$\begin{aligned}\beta_2 &\leq \frac{4}{\pi} \beta_{2c} : EI_s = F_f \cos^4 \alpha \pi R^3 t \\ \beta_2 &> \frac{4}{\pi} \beta_{2c} : EI_s = 0\end{aligned}\quad (\text{B1.55})$$

This gives the following total bending stiffness relation for the flexible pipe:

$$EI = EI_e + \sum_{j=1}^{N_t} F_{fj} \cos^4 \alpha_j \pi R_j^3 t_j f(\beta_2, \beta_{2cj}) \quad (\text{B1.56})$$

where  $f$  is a function that is 1 for  $\beta_2 \leq \beta_{2cj}$  and 0 for  $\beta_2 > \beta_{2cj}$  for each layer  $i$ . It is noted that for dynamic loading the slip curvature range will be twice the amplitude limits described above.  $EI_e$  represents the sum of elastic contributions from the plastic layers and local wire bending. The local wire bending contribution is also influenced by the wire tension which increases the geometric stiffness against bending. By assuming the loxodromic curve representation for the tensile armour, the following expression may be applied to estimate  $EI_e$ :

$$\begin{aligned}EI_e &= \sum_{j=1}^{N_{pl}} \frac{\pi}{4} E_j [(R_j^o)^4 - (R_j^i)^4] \\ &+ \frac{1}{2} \sum_{j=1}^{N_t} n_j [G_j I_{1j} 4 \sin^2 \alpha_j \cos^5 \alpha_j + E_j I_{2j} \cos^3 \alpha_j \cos^2 2\alpha_j + E_j I_{3j} \cos \alpha_j (1 + 2 \sin^2 \alpha_j + \sin^4 \alpha_j)] \\ &+ \sum_{j=1}^{N_t} F_{fj} \sigma_{11j} \pi R_j^3 t_j [9 \cos^4 \alpha_j \sin^2 \alpha_j + 6 \cos^2 \alpha_j + 6 \cos^4 \alpha_j + \frac{\cos^8 \alpha_j}{\sin^2 \alpha_j} + \frac{\cos^4 \alpha_j}{\sin^2 \alpha_j} + 4]\end{aligned}\quad (\text{B1.57})$$

Since, the behaviour of the plastic layers is sensitive to temperature and the geometric stiffness and slip limit depend on pressure and tension, several moment-curvature relations may have to be used in strength calculations, depending on the condition to be evaluated.

It is also to be noted that the above model is based on the assumption that no significant end effects are present, i.e. the curvature takes place away from the end fitting where each wire is anchored. In cases where this is not the case, more advanced formulations based on individual wire modelling using general or specialized FE softwares, may be needed.

For most cases, however, the moment-curvature based model presented above have proven to give good stress and fatigue estimates for the tensile armour as compared to test data, see [Sævik, 2011].

**B1.3.5.3.3 Influence of shear deformations in the tape layers** If the tensile armour is supported by thick plastic layers, shear deformations might occur. If that is the case, plane surfaces no longer remain plane before the slip begins. The shear stress between the wire and the antiwear layer will then be governed by the inherent shear deformations and the tape material shear modulus. This is illustrated in Figure B1.22

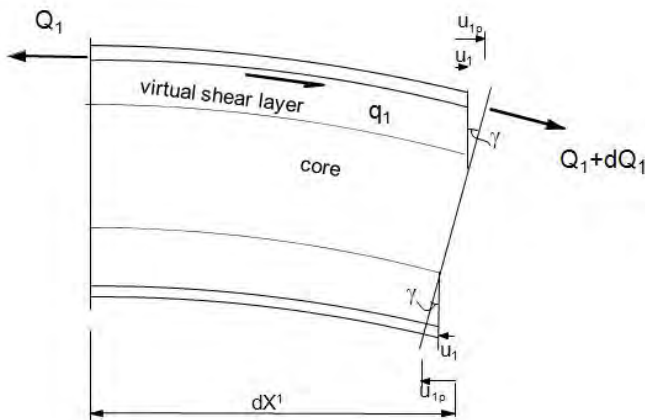


Figure B1.22: Shear deformation model

By equilibrium, the following differential equation can be formulated along the wire:

$$EAu_{1,11} - ku = -ku_{1p} \quad (\text{B1.58})$$

where  $u_{1p}$  is the displacement corresponding to plane surfaces remain plane from Eq. B1.36 and  $k$  is the shear stiffness parameter defined by:

$$k = G \frac{b}{t} = \frac{E_p b}{2(1+\nu)t} \quad (\text{B1.59})$$

where  $E_p$  is the Young's modulus of the plastic layer. By only considering the particular solution, the following solution is obtained for the slip curvature:

$$\beta_{2c} = [1 + \frac{\sin^2 \alpha EA}{kR^2}] \frac{\mu(q_3^I + q_3^{I+1})}{EA \cos^2 \alpha \sin \alpha} \quad (\text{B1.60})$$

It is seen that the  $k$  parameter will cause the slip curvature to increase, hence reducing the stress in the stick domain at a given curvature.

In [Skallerud, 1991a] and [Skallerud, 1991b] the results from testing two 4 inch pipes in bending at variable pressures were presented. The inner tensile armour in the two pipes were respectively supported by 1.5 mm and 2 mm antiwear layers and in the latter case the two armour layers were separated by another 2 mm antiwear layer. The results from these tests are presented together with the results obtained by the BFLEX software, [Sævik, 2015] in Figure B1.23 and Figure B1.24. The model includes using both the plane surfaces remain plane assumption in Eq. B1.46 and the shear slip model in Eq. B1.60 given above. The initial straight line illustrates the pre-slip bending stiffness calculated analytically from Eq. B1.56. It is seen that the shear model seems to describe the slip transition better than the

plane surfaces remain plane model. However, the plane surfaces remain plane model will be conservative in a fatigue calculation and since the resulting stress is sensitive to the k parameter selected, a large number of model tests are needed in order to provide sufficient confidence level in the above shear interaction model.

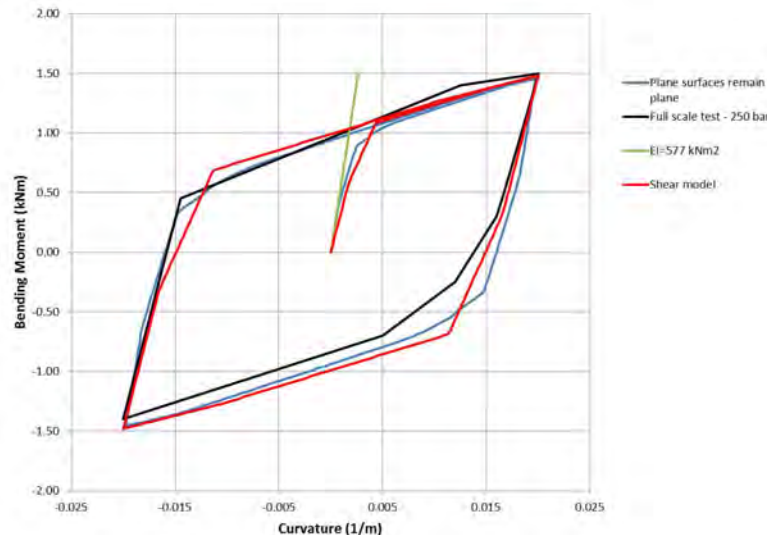


Figure B1.23: Correlation between model and bending tests, Pipe 1 [Skallerud, 1991a]

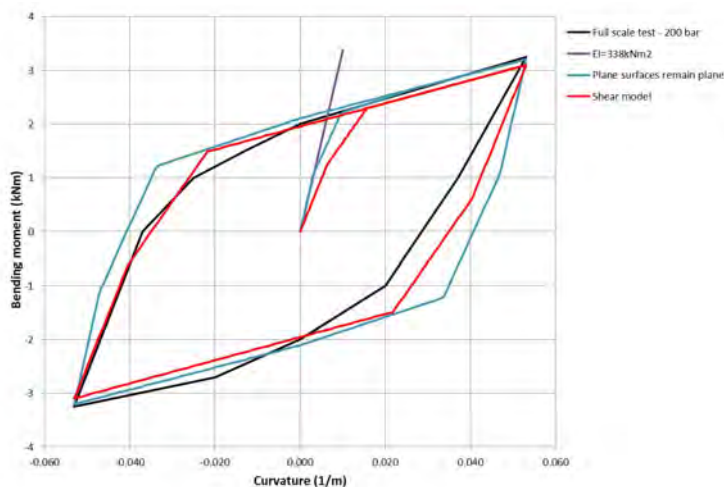


Figure B1.24: Correlation between model and bending tests, Pipe 2 [Skallerud, 1991b]

#### B1.3.5.4 Stresses related to the pressure armour

With respect to bending stresses in the pressure armour, there are two significant contributions to consider with reference to Figure B1.1:

1. Bending induced longitudinal  $\sigma_{11}$  stresses in the hoop direction.
2. Stresses introduced in the cross-section plane, primarily  $\sigma_{22}$ ,  $\sigma_{23}$  and  $\sigma_{33}$  stresses.

**B1.3.5.4.1 Longitudinal stresses** Due to the large lay angle and interlocked nature of the pressure armour, the relative displacements and associated longitudinal friction stresses introduced by bending will be insignificant and can be neglected. Further by studying Eq. B1.33-Eq. B1.35, the only first order term in  $\cos \alpha$  is found for the transverse curvature in Eq. B1.35. Hence, in terms of bending fatigue calculations it is common practice to only include this term with respect to local elastic bending of each wire.

The Carcass and the pressure spiral wire acts to keep the cross-section circular. During bending, however, ovalization and membrane stresses will be introduced due to the following effects with reference to Figure B1.25:

1. The reaction forces due to the support from bending restrictors, bend stiffeners or other external structures termed the *Tension and shear force differential effect*.
2. The bending moment itself termed the *Bending moment effect*.
3. The shear stresses resulting from the variation of contact pressure in the tensile armour, termed the *Shear stress membrane effect*.

With respect to the *Tension and shear force differential effect*, the reaction line load  $q$  resulting from plane pipe bending about the  $Z^2$  axis in Figure B1.3 can be described by standard beam theory as:

$$q = EI \frac{\delta Q}{\delta Z_1} + T\beta_2 \quad (\text{B1.61})$$

where  $Q$  is the shear force,  $T$  is the effective tension and  $\beta_2$  is the global curvature. The line load  $q$  results in an intensity  $w$  and the resulting ovalization bending stresses can be estimated by using the circular ring formula of Table 9.2 in [W.C.Young and Budynas, 2002].

The *Bending moment effect* comes primarily from the plastic layers and the tensile armour due to friction and elastic bending. The bending stresses in these layers in combination with global curvature gives an harmonic squeeze load intensity  $w$  given by:

$$w = \frac{M}{\pi R^2} \cos \psi \beta_2 \quad (\text{B1.62})$$

where  $M$  is the total bending moment. This effect will act to increase the ovalization.

The *Shear stress membrane effect* does not cause additional ovalization bending stresses. However, realising that the friction stress introduced by bending in the tensile armour will cause an increased tensile stress and contact pressure at the tensile side and a subsequent reduction at the compressive side, this must be balanced by simultaneous variation in the pressure armour hoop stresses to fulfil equilibrium at any section in the hoop direction. This requires that the variation in contact pressure is balanced by shear stress and normal stresses at the tensile/pressure armour interface.

This will not result in additional ovalization bending moments, however, at the tensile side there will be a reduction in the hoop stress (reduction in the axial force and the longitudinal stress) and at the compressive side there will be an increased hoop stress in the pressure spiral wire. An illustration of the longitudinal stress variation resulting from the above effects is seen in Figure B1.26

**B1.3.5.4.2 Stresses in the cross-section plane** As noted in Section B1.3.2 the interlocked nature of the pressure spiral wire causes stresses in the cross-section plane due to

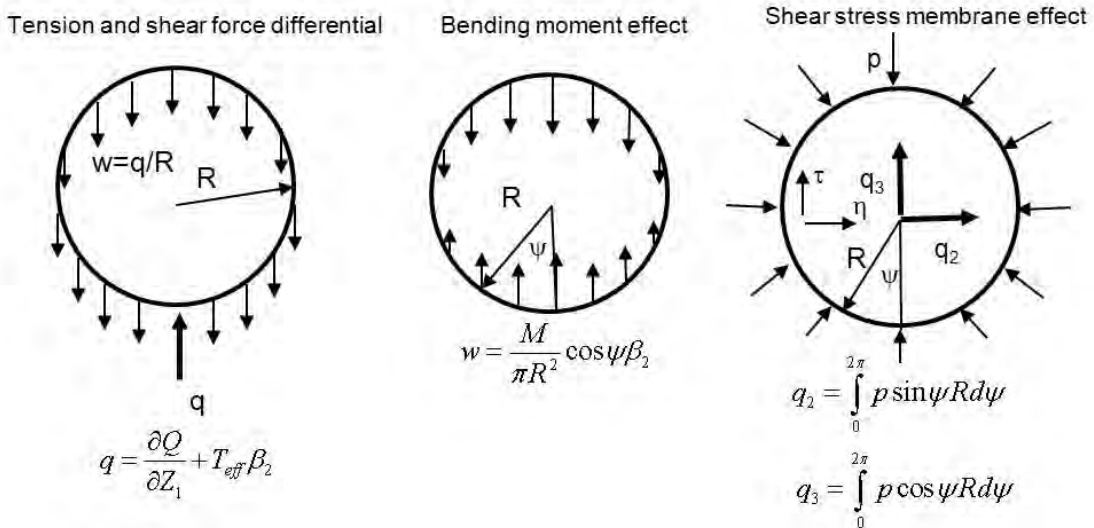


Figure B1.25: Physical effects related to ovalisation

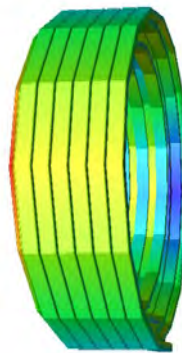
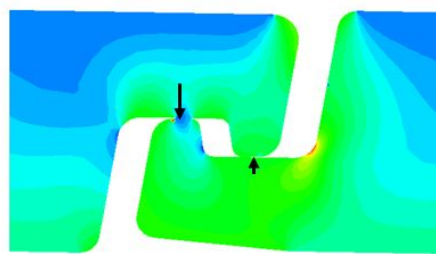
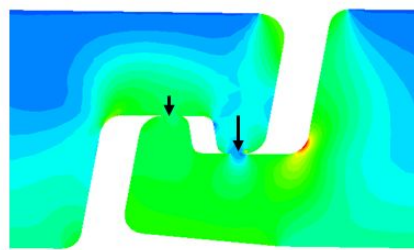


Figure B1.26: Longitudinal stress variation in pressure spiral wire

the axi-symmetric loads, primarily  $\sigma_{22}$ ,  $\sigma_{23}$  and  $\sigma_{33}$  stresses with reference to Figure B1.1. During bending, the pressure spiral wires are forced into the overall pipe curvature. This causes two effects relevant with respect to dynamic variation and fatigue:

1. At the tensile and compressive sides each winding will be forced to move relative to each other
2. At the same sides the nubs and valleys will be opened or closed in order to accomodate the overall pipe curvature

The first of the above effects will cause friction to be mobilised at the metal interfaces giving rise to variations in the  $\sigma_{22}$  and  $\sigma_{23}$  components. The second effect will primarily cause variations in the  $\sigma_{33}$  and  $\sigma_{23}$  components. As illustrated in Figure B1.27 for the Z-spiral this can be looked upon as a thick cantilever beam exposed to a pair of varying point loads. Since the length/height ratio of the beam is small, shear stresses are important and so also are the local geometries in terms of the profile curve radii with respect to stress concentrations. These stresses are therefore more difficult to describe by analytical methods. Using general FE softwares is an alternative, however, challenges with regard to selecting

(1)  $\sigma_{33}$  - State 1(2)  $\sigma_{33}$  - State 2Figure B1.27: Variation in  $\sigma_{33}$  during a bending load cycle

appropriate boundary conditions and computational effort have been noted. Special FE models have been developed to overcome these problems, see [Sævik et al., 2001]

### B1.3.6 Buckling

#### B1.3.6.1 Collapse

Excessive external pressure may lead to collapse of the pipe. Collapse usually involves flattening of the pipe which impedes the flow through it. However, this is not considered to be a critical failure mode since the design depth is usually well defined. This is also reflected in design recommendations for flexible pipes, where the safety factor is smaller than for bursting strength, see [API 17J, 2008]. The ultimate depth rating is to be verified for atmospheric internal pressure. When a pipe is subjected to external pressure, the loads are carried by the helical pressure layers and the interlocked carcass, all having a lay angle close to 90°. However, the collapse pressure given by the producers is often taken as the collapse strength of the interlocked carcass, disregarding the contribution from the other pressure spiral wire with regard to pressure load sharing. This is based on the pessimistic view that the outer sheaths may have been damaged in such a way that the external pressure acts directly on the inner plastic sheath. Therefore the interlocked carcass is normally designed to carry the full external pressure alone, however, the contribution in terms of bending stiffness support in the hoop direction from the other pressure layers is normally included.

The external pressure needed to initiate carcass collapse can be calculated based on the method by Timoshenko [Timoshenko and Gere, 1963]. The Timoshenko approach is based

on considering the bending moment in a steel ring having an initial imperfection characteristic described by the function  $R\delta_0 \cos 2\psi$ , see Figure B1.28, where  $\delta_0$  represents the initial ovality either caused by manufacturing tolerances or bending loads. This definition of  $\delta_0$  is consistent with the API definition  $(D_{max} - D_{min})/(D_{max} + D_{min})$ . According to API [API 17B, 2008], if specific information about the actual carcass is not available, the initial ovality to be used for collapse calculations should not be less than 0.002.

If no gaps are present between the pressure armour layer, the elastic buckling pressure of the carcass may be determined as the sum of contributions from the carcass and the pressure armour layers as:

$$p_{cr} = \sum_{i=1}^{N_p} \frac{3EI_{eq}^i}{R^3} \quad (\text{B1.63})$$

where  $R$  is the radius of the carcass and  $EI_{eq}^i$  is the equivalent ring bending stiffness of each layer per unit length of pipe. For a cylinder:

$$EI_{eq} = \frac{Et^3}{12(1 - \nu^2)} \quad (\text{B1.64})$$

where  $\nu$  is the Poisson's ratio. For the carcass and the pressure layers:

$$EI_{eq} = Kn \frac{EI_{2'}}{L_p} \quad (\text{B1.65})$$

where  $n$  is the number of tendons in the layer,  $L_p$  is the pitch and  $I_{2'}$  is the smallest inertia moment. For the non-symmetric carcass and Z-shaped profiles the weakest axis will be the  $X^{2'}$  in Figure B1.7 and being obtained as:

$$I_{2'} = \frac{I_3 + I_2}{2} - \frac{1}{2} \sqrt{(I_3 - I_2)^2 + 4I_{32}^2} \quad (\text{B1.66})$$

$K$  is a factor that depends on the lay angle and the moment of inertia in the section. For massive cross-sections  $K \simeq 1$ .

The equivalent stiffness may also be determined from a static ring test carried out on a piece of the carcass. Such a test consists of measuring the deformation  $\delta$  of an interlocked carcass subjected to a radial force  $F$  as shown in Figure B1.29. The equivalent ring bending stiffness may then be determined from the following relation:

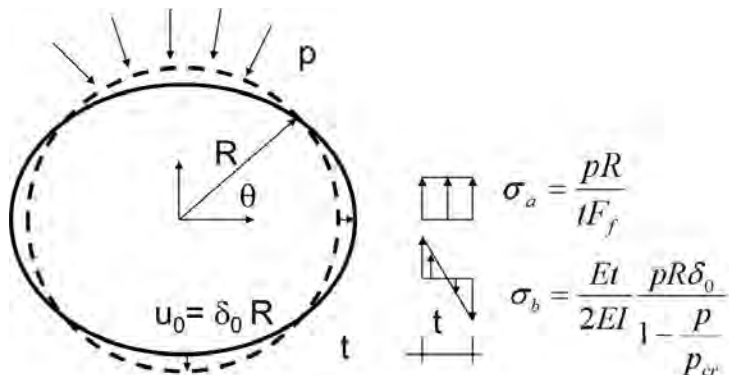


Figure B1.28: Timoschenko collapse model

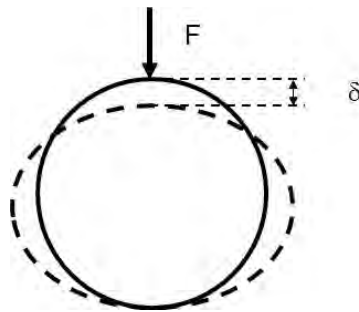


Figure B1.29: Ring stiffness test

$$\frac{EI_{eq}}{R^3} = \left(\frac{\pi}{4} - \frac{2}{\pi}\right) \frac{F}{\delta} \quad (\text{B1.67})$$

The maximum bending moment introduced by the combined action of external pressure and the eccentricity parameter  $u_0$  can then be found from:

$$M_{\max} = pR \frac{u_0}{1 - \frac{p}{p_{cr}}} \quad (\text{B1.68})$$

which has a direct analogy to Euler buckling analysis of imperfect beams. Collapse is assumed to occur when the outer fibre stress from bending and hoop stress in the carcass reaches the yield stress of the carcass material. Generally, if a residual stress  $\sigma_r$  occurs in the outer fibre, the yield stress  $\sigma_f$  will be reduced to an effective available yield stress  $\sigma_{fe}$  as:

$$\sigma_{fe} = \sigma_f - \sigma_r \quad (\text{B1.69})$$

The residual stress can be estimated based on assuming that the cross section is fully plastified at constant ultimate stress  $\sigma_u$  during manufacturing and that elastic unloading occurs to zero moment. In that case, the residual stress can be calculated as:

$$\sigma_r = \sigma_u \frac{W_p}{W_e} - \sigma_u \quad (\text{B1.70})$$

where  $W_p$  is the plastic area moment and  $W_e$  is the elastic area moment.

Collapse will then occur when:

$$\sigma_{fe} = \frac{tEpRu_0}{2EI_{eq}(1 - \frac{p}{p_{cr}})} + \frac{pR}{tF_f} \quad (\text{B1.71})$$

where  $t$  is the overall radial thickness of the carcass and the carcass fill factor  $F_f$  is determined from Eq. B1.2. The above leads to the following second order equation to determine the collapse pressure  $p$ :

$$p^2 - \left( \frac{F_f t \sigma_{fe}}{R} + p_{cr} \left( 1 + \frac{Et^2 F_f R \delta_0}{2EI_{eq}} \right) \right) p + \frac{p_{cr} \sigma_{fe} t F_f}{R} = 0 \quad (\text{B1.72})$$

where it is noted that if it can be assumed that there is full contact between the carcass and the other pressure spiral wires,  $EI_{eq}$  will be the sum of contributions from the carcass and the other pressure spiral wires. According to Chen et.al. [Chen et al., 1992] if the gap between the carcass and the other spiral wires in a 6" flexible pipe is greater than 2.5 mm, the support effect from the other spiral wires can be neglected and the  $EI_{eq}$  will be determined by the carcass contribution alone. This may result in a significantly reduced external pressure collapse capacity.

If the pipe is exposed to bending and external reaction forces, this will increase the ovality  $\delta_0$  and thus reduce the capacity.

### B1.3.6.2 Tensile armour buckling

**B1.3.6.2.1 General** During installation and shut-down conditions where the pipe bore is exposed to external overpressure, the tensile armour will be in compression, even if the effective tension is positive. This may lead to local radial and transverse buckling of the tensile wires, leading to overall torsion instabilities. This failure mode was reported by Bectarte and Coutarel [Bectarte and Coutarel, 2004] including both bird caging (radial failure) and lateral buckling. Test procedures for lateral buckling were described that included the effect of cyclic bending. A computer model was also mentioned, but no details with respect to methods or results were given. The methods used to validate the pipe capacity with respect to this failure mode included laboratory testing, Deep water Immersion Performance (DIP) testing and mathematical models.

With respect to mathematical models Tan et al. described the behaviour of tensile armour wires under compression [Tan et al., 2006]. A strain energy approach for modelling the buckling and post-buckling behaviour of the wires is outlined, but no expressions or results were presented. However, some test results were presented stating that lateral buckling of the wires was observed under cyclic bending and wet annulus conditions. Vaz and Rizzo [Vaz and Rizzo, 2011] presented a finite element (FE) model, studying the influence of friction, interlayer contact conditions and anti-buckling tape capacity on the collapse load behaviour under pure external pressure loading but no bending, identifying four different modes of failure, depending on the amount of friction and the properties of the anti-buckling tape. Based on FE analysis Brack et.al. [Brack et al., 2005] pointed out the importance of radial gaps, interlayer friction and the torsional resistance from the anti-buckling tape with respect to the axis of individual wire buckling. Østergaard et. al [Østergaard et al., 2011] presented a model that was capable of describing the coupling between the individual wire buckling and overall global behaviour for combined external pressure and bending loads, however, assuming zero friction to provide conservative estimates of the buckling load. Sousa et.al. [de Sousa et al., 2012] presented correlation studies between FE analysis and full scale testing describing the coupling between wire buckling and bird caging failure.

With reference to the above, the buckling process may be divided into two different categories:

- Radial buckling
- Transverse buckling

### B1.3.6.3 Radial buckling

The radial failure mode is also known as *bird-caging*, and was first observed in 1989 [Bectarte and Coutarel, 2004]. This failure mode can occur as an interaction process having contributions from the following physical effects:

1. Failure of supporting layer (anti buckling tape) as a result of the outward squeeze pressure from underlaying layers.
2. Elastic buckling without tape failure.
3. Yield failure of the wires

where the latter will be the most likely one to occur.

The first mode above is not really a buckling failure, it is simply triggered by the loss of support. When the ultimate strength of the anti buckling tape is exceeded, a sudden radial expansion of the tensile armour layers will take place. The second mode is a true buckling phenomenon which is quite similar to buckling of a straight beam on an elastic foundation.

When the annulus is flooded, there is nothing but the layers on the outside of the tensile armour to restrain radial expansion. Thereby, it is the anti buckling tape alone that must carry the radial pressure due to expansion of the tensile armour, and it is the ultimate strength of the anti buckling tape that will determine the critical external pressure.

The external pressure leads to a compressive load which further will give a contact pressure acting on the anti buckling tape, see Figure B1.31(a). By considering the hoop stress in the thin tape layer and assuming that the tensile armour and tape lay radii are approximately the same, the external axial force needed to trigger this failure mode  $P_{b1}$  of a two layered structure can be estimated as:

$$P_{b1} = \frac{R}{\tan^2 \alpha} \left[ \frac{n_t \sigma_{ut} A_t \sin^2 \alpha_t}{\cos \alpha_t R_t} + 2\pi E_s \epsilon_{ut} t_s \right] \quad (\text{B1.73})$$

where  $R$  is taken as the mean radius of the tensile armour layers,  $\epsilon_{ut}$  is the ultimate strain of the anti buckling tape,  $E_s$  is the sheath Young's modulus,  $\sigma_{ut}$  is the tape ultimate stress,  $n_t$  is the number of tape filaments,  $A_t$  is the cross-section area of the tape filament,  $\alpha_t$  is the tape lay angle,  $t_s$  is the sheath thickness and  $R_t$  is the tape radius.

The second radial failure mode is an elastic buckling mode, as also noted by [Vaz and Rizzo, 2011], where the armour wires deflect radially in a sinusoidal pattern. The solution to a similar problem, which is buckling of a straight beam on an uniform elastic support is described in [Søreide, 1985]. The critical load can also be found based on curved beam theory and will include contributions from bending of the wire and the straining of the elastic foundation. In this case, the foundation is the anti buckling tape/outer sheath, and their stiffness will be a governing factor. In the analyses performed here, it is assumed that each wire behaves equally, meaning that there is no interaction between wires. The total number of wires are taken into account by scaling the stiffness of the supporting tape. Hence, the buckling load may be determined by looking at a single wire.

The elastic foundation stiffness  $c$  will have contributions from both the anti-buckling tape and the outer sheath. The spring stiffness contribution from the outer sheath  $c_1$  is found

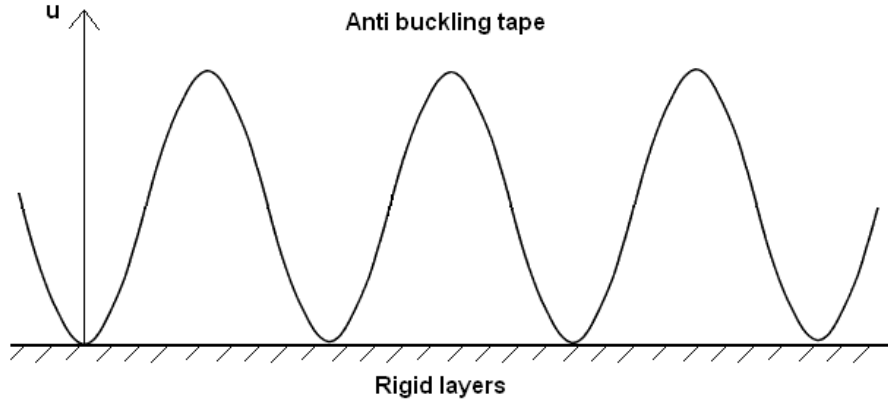


Figure B1.30: Assumed radial buckling shape

from considering one wire width's contribution to the hoop stiffness found as:

$$c_1 = \frac{q_2}{u_2} = \frac{2\pi}{n} \frac{E_s t_s}{R} \cos \alpha \quad (\text{B1.74})$$

where  $t_s$  is the sheath thickness,  $E_s$  is the sheath Young's modulus and  $n$  is the number of armour wires. For the antibuckling tape, the corresponding radial stiffness parameter  $c_2$  is determined to be:

$$c_2 = \frac{q_2}{u_2} = \frac{n_t}{n} \frac{EA_t \sin^4 \alpha_t}{R^2} \frac{\cos \alpha}{\cos \alpha_t} \quad (\text{B1.75})$$

where  $EA_t$  is the tape's axial stiffness,  $\alpha_t$  is the tape lay angle and  $n_t$  is the number of tape plies.

As the tensile armour wire is restrained from deflecting inwards due to the large stiffness of the underlying layers, it is assumed that it only deflects outwards. A possible buckling shape is shown in Figure B1.30.

By assuming a sinusoidal buckling shape:

$$u = u_0 \sin \frac{m\pi X^1}{l} \quad (\text{B1.76})$$

the critical buckling load  $Q_{1,cr}$  of one single wire can be expressed by using the Principle of Minimum Potential Energy and assuming straight beam theory as:

$$Q_{1,cr} = \pi^2 EI_2 \left( \frac{m}{l} \right)^2 + \frac{c}{\pi^2} \left( \frac{l}{m} \right)^2 \quad (\text{B1.77})$$

It is seen that the elastic buckling load depends strongly upon  $\frac{m}{l}$ , the number of half waves per unit length. The critical load will be the lowest possible, and may be found graphically by plotting the solution for different  $\frac{m}{l}$  or by differentiating Eq. B1.77 with respect to  $\frac{m}{l}$ , which in terms of the minimum axial force in each wire needed to cause buckling gives:

$$Q_{1,cr} = 2\sqrt{EI_2 c} \quad (\text{B1.78})$$

where  $n$  is the number of armour wires.

Table B1.1: ANALYTICAL BUCKLING FORCE VERSUS DE SOUSA ET.AL. RESULTS

Assumption	$\bar{P}_{b1}$	$\bar{P}_{b2}$	$\bar{P}_{b3}$	$\frac{D}{L}$	$\bar{P}_{rad}$
Tape+Sheath	1.24	4.33	5.36	2.14	0.82
Tape	1.04	3.98	5.36	2.13	0.72

Finally, the axial load capacity including the contribution from all wires can be obtained from Eq. B1.78 as:

$$P_{b2} = n \cos \alpha Q_{1,cr} \quad (\text{B1.79})$$

The axial force leading to wire yield failure is calculated as:

$$P_{b3} = n \cos \alpha \sigma_y A \quad (\text{B1.80})$$

where  $\sigma_y$  is the yield stress of the wire having a cross-section area  $A$ .

Intuitively, the critical radial buckling axial force may be taken to be the smallest of the quantities  $P_{b1}$ ,  $P_{b2}$ ,  $P_{b3}$  from Eq. B1.73, Eq. B1.79 or Eq. B1.80. However, since it is reasonable to believe that there will be interaction between these modes of failure, an interaction formula is proposed to determine the resulting axial load that governs radial failure  $P_{rad}$ :

$$\frac{1}{P_{rad}} = \frac{1}{P_{b1}} + \frac{1}{P_{b2}} + \frac{1}{P_3} \quad (\text{B1.81})$$

Three flexible pipe specimens were tested by Sousa et.al. [de Sousa et al., 2012] under axial compression until tape failure, where it is noted that the specimens were exposed to a constant compressive axial force until radial failure occurred.

The developed formulas describing radial failure are sensitive to which assumptions that are applied. With respect to the radial capacity failure as formulated in Eq. B1.73, the tape will dominate independent of whether or not the sheath is participating in the displacement process. Using Eq. B1.73, the corresponding axial force capacities are 1020 kN for the no outer sheath case and 1110 kN by including both layers. On the other hand, the sheath will influence the radial stiffness and the results obtained by either using straight beam (SB) theory according to Eq. B1.79. In Table B1.1 the sensitivities are demonstrated. In the table the capacities have been normalized with respect to the average capacity encountered during the tests of 256 kN. It is seen that Eq. B1.79 gives good correlation, however, somewhat on the conservative side. The number of half waves per diameter,  $\frac{D}{L}$ , is found to be around two, which appears to be in good agreement with the observations from the picture shown for the actual failure [de Sousa et al., 2012].

#### B1.3.6.4 Lateral buckling

As shown in Figure B1.31 there are two fundamental different conditions in terms of available friction acting to resist the buckling process: the intact outer sheath condition and the damaged outer sheath condition where the damaged outer sheath condition is consistent with the assumption made with respect to carcass design, see Subsection B1.3.6.1. As a

result of the end cap force, the two tensile armour layers will be squeezed against the anti-buckling tape creating a gap between the tensile armour layers and the pressure spiral wire. If the anti buckling tape is sufficiently strong to prevent radial buckling, the wire has only one way to go, and that is sideways. The friction forces available to resist buckling is smallest for the inner layer, hence the inner layer will loose its axial load capacity first. The buckling process will therefore be initiated in the inner layer. As the axial load capacity is reduced in the inner layer, this must be compensated by a loss in the axial compression forces in the outer layer as well to keep the cross-section in torsion balance. Hence the pipe must rotate in the same direction as the lay angle of the outer layer. Anti buckling tapes that are wound in the outer layer lay direction will therefore contribute to circumvent this behaviour by providing additional radial support acting to maintain some of the overall axial and torsion stiffness. When exposed to cyclic loading, a certain plastic rotation will, however, take place during each cycle until overall torsion failure of the cross-section occurs.

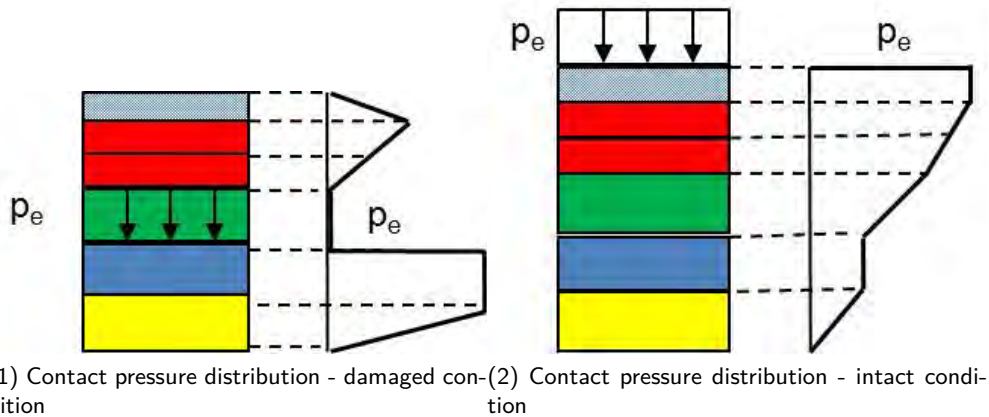


Figure B1.31: Contact pressure distributions for pipe exposed to external pressure during intact and damaged outer sheath conditions, red = tensile armour, green = pressure spiral wire, yellow= carcass, blue = plastic layer, rubber blue=antibuckling tape

Under the assumption of no friction, a conservative estimate of the buckling load can be obtained from the curved beam differential equation as:

$$P_{lat} = P_1 = n \frac{\cos \alpha}{R^2} [GJ \sin^4 \alpha + (4EI_2 + EI_3 - GJ) \sin^2 \alpha \cos^2 \alpha] \quad (B1.82)$$

The results from Eq. B1.82 has been compared to the test and analytical results obtained by [Østergaard, 2012a] for three different pipe dimensions, see Table B1.2. It is noted that these tests were based on cyclic bending and simulating the end-cap force only, i.e. assuming damaged outer sheath condition. The test value reported in the table is further taken as the largest axial force that did not cause a grow in overall torsion deformation of the test specimen during repeated cyclic bending. It is seen that the proposed model is well correlated with the Østergaard model. The effect of friction is to increase the buckling capacity. The cyclic tests done by Østergaard shows that the maximum compressive load that can be allowed without ultimately causing pipe damage when exposed to cyclic loading is a factor 1.7-1.9 higher than the value predicted by the above equation assuming no friction.

Table B1.2: COMPARISON BETWEEN LATERAL BUCKLING LOADS

Case	[Østergaard, 2012a] model (kN)	Proposed (kN)	model	Test result (kN)
6 inch pipe	100	93		160
8 inch pipe	256	226		400
14 inch pipe	157	139		269

### B1.3.6.5 Wire buckling capacity

An estimate of the buckling load is then obtained as the minimum of  $P_{lat}$  and  $P_{rad}$ .

## B1.3.7 Fatigue

### B1.3.7.1 General

The fatigue life of dynamic flexible risers is in most cases performed by a three step procedure:

1. A global analysis in order to obtain time series of tension, curvatures or end angles representing the annual fatigue load.
2. A local stress analysis transforming the global quantities into time series of stress.
3. The stress time series is transformed into classes of stress ranges and the fatigue damage calculated by application of the Miner sum.

The Miner sum is given by:

$$D = \sum_{i=1}^N \frac{n_i}{N_i(\Delta\sigma_i, \bar{\sigma}_i)} \quad (\text{B1.83})$$

where  $n_i$  is the number of occurrences of a certain stress range  $\Delta\sigma_i$  at mean stress  $\bar{\sigma}_i$  and the number of allowable cycles  $N_i$  given from an S-N diagram based on the following format:

$$\lg N_i = \lg a - m \lg(\Delta\sigma_i) \quad (\text{B1.84})$$

where  $\lg a$  and  $m$  are constants obtained by fatigue testing considering the expected annulus environment.

Normally, the tensile armour is taken as the governing layer with respect to metal fatigue. The tensile armour is made of cold formed carbon steel with high yield stress and a limited corrosion resistance. Until mid nineties common fatigue design practise was based on assuming dry air environment, relying on an intact outer sheath and no leakage of gas from the bore to the annulus. Assuming that no welds were present in the dynamic section of the flexible pipe, the fatigue limit approach was applied where no stress range was allowed to exceed the defined limit, which for non-welded cold formed steels under in-air condition is in the range 400-600 MPa. At the early stages, the pipe designs were further based on not having antiwear tapes between the tensile armours and using wear models to estimate the cross-section reduction of the tensile armour as a function of time. This was based on Archard's formula considering the distance of relative displacements, the contact pressure, the wear coefficient and the material penetration hardness, see [Feret et al., 1986b]. Fatigue

failure was assumed to occur when the mean stress due to the loss of tensile armour cross-section caused the stress range to exceed the fatigue limit, normally defined at  $10^6$  cycles of constant amplitude loading.

During the fatigue tests on two 4 inch flexible pipes [Sævik et al., 1992a] and [Sævik et al., 1992b], fretting effects due to metal to metal contact was identified as a possible failure mechanism. Fretting occurs if an alternating stress in one direction is combined with contact stresses in the transverse direction, which may cause crack growth initiated from the contact surface. Since then anti-wear tapes have been introduced to avoid this failure mode is now rarely seen. One critical section where fretting may still be an issue, is the top end fitting where the tape layers are removed to allow anchoring the wires in the end fitting.

It is noted that the performance of the anti-wear tapes is sensitive to parameters as operating temperature, manufacturing tension and thickness. If the temperature is too high, the layer may simply melt whereas too thin or too large manufacturing tension can cause tape breaking due to the shear loads introduced by the tensile armour sliding process. Extruded anti-wear layers further need sufficient venting to avoid damage from annulus pressure build-up. Normally this is obtained by making vent holes in the layer, however, if these are too few or too small, the armour sliding process my ultimately close these and the venting is lost.

During the nineties it was realised that the in-air annulus assumption cannot be assumed, both due to a number of failures found in the outer sheath causing sea water ingress and leakage of corrosive ingredients such as  $H_2S$  and  $CO_2$  from the bore into the armour annulus. The fatigue limit approach was therefore replaced by the Miner sum approach defined above.

### B1.3.7.2 Mean stress correction

Using the principles outlined in [Sines and Waisman, 1959] one way of formulating the criterion for a multi-axial fatigue failure can be stated in terms of the Von Mises equivalent stress range as:

$$\begin{aligned}\Delta\sigma &= (\Delta\sigma_{11}^2 + \Delta\sigma_{22}^2 + \Delta\sigma_{33}^2 - \Delta\sigma_{11}\Delta\sigma_{22} - \Delta\sigma_{11}\Delta\sigma_{33} - \Delta\sigma_{33}\Delta\sigma_{22} \\ &\quad + 3\Delta\sigma_{12}^2 + 3\Delta\sigma_{13}^2 + 3\Delta\sigma_{32}^2)^{\frac{1}{2}} \\ &= A - \alpha(\bar{\sigma})^\beta\end{aligned}\tag{B1.85}$$

The constants  $A$ ,  $\alpha$  and  $\beta$  can be determined from fatigue testing at three different mean stress levels, i.e. expressing how sensitive the number of cycles needed to cause fatigue failure is with respect to the variation in the mean stress  $\bar{\sigma}$  at a certain stress range.

Fatigue testing of tensile armour wires is normally carried out by uni-axial testing either by keeping the mean stress or the  $R - ratio$  constant, where:

$$R = \frac{\sigma_{\min}}{\sigma_{\max}}\tag{B1.86}$$

It is noted that a positive value is needed to avoid compression. Therefore armour wire testing in tension-tension mode is normally carried out for R-ratios in the range 0.1-0.5. The stress range applied in a fatigue test at a given R-ratio can be expressed in terms of the mean stress as:

$$\Delta\sigma = 2\bar{\sigma} \frac{1-R}{1+R}\tag{B1.87}$$

which means that each fatigue test at a given stress range for a fixed R-ratio represents a data point along a straight line in the Haig diagram as illustrated in Figure B1.32.

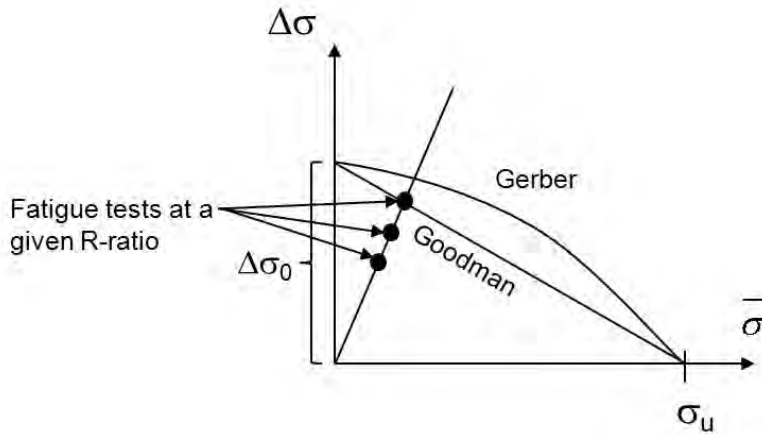


Figure B1.32: The Haig diagram

In many cases, only one R-ratio is available and it is therefore common practice to use either of the Goodman or Gerber assumptions to transform between different mean stress levels, see Figure B1.32. This is done by transforming the calculated stress range  $\Delta\sigma$  into the stress range  $\Delta\sigma_0$  this would correspond to at zero mean stress ( $R = -1$ ) using the Goodman or Gerber assumptions and the calculated mean stress. Using the Gerber assumption the transformation reads:

$$\Delta\sigma_0 = \frac{\Delta\sigma}{1 - (\frac{\bar{\sigma}}{\sigma_u})^2} \quad (\text{B1.88})$$

where  $\sigma_u$  is the ultimate stress of the material. In the Goodman case the transformation is:

$$\Delta\sigma_0 = \frac{\Delta\sigma}{1 - (\frac{\bar{\sigma}}{\sigma_u})} \quad (\text{B1.89})$$

For a given S-N diagram defined by a certain R-ratio the corresponding value at  $R = -1$  using the Gerber assumption is:

$$\Delta\sigma_0 = \frac{\Delta\sigma^*}{1 - (\frac{(1+R)\Delta\sigma^*}{2(1-R)\sigma_u})^2} \quad (\text{B1.90})$$

and by applying the Goodman assumption:

$$\Delta\sigma_0 = \frac{\Delta\sigma^*}{1 - (\frac{(1+R)\Delta\sigma^*}{2(1-R)\sigma_u})} \quad (\text{B1.91})$$

where  $\Delta\sigma^*$  represents the stress range to be used in the S-N diagram to find the number of cycles until failure for each load case. The stress range  $\Delta\sigma^*$  is found by equating Eq. B1.88 and Eq. B1.90 which for the Gerber case will give a second degree equation in  $\Delta\sigma^*$ . The same procedure is applied for the Goodman case, equating Eq. B1.89 and Eq. B1.91 resulting in a linear equation for  $\Delta\sigma^*$ .

For high pressure cases, the multi-axial alternating stress of the pressure armour in combination with high mean stresses may cause the pressure spiral wire to be the governing layer with

respect to fatigue. For the Z-spiral, high mean stresses may result both from the manufacturing procedure and longitudinal stresses introduced by transverse curvature when closing the gaps during onset of pressure, see Figure B1.5. Such stresses may be circumvented by applying an elevated fabrication test pressure (FAT).

#### B1.3.7.3 Mean and dynamic stresses in the tensile armour

A flexible riser hanging from a floater will be exposed to cyclic loads from top motions and hydrodynamic effects resulting in cyclic riser motions and global responses in terms of tension and curvature variations. This results in dynamic longitudinal and shear stresses in the tensile armour where the longitudinal stress represents the most important contribution with respect to fatigue. The longitudinal stress and associated mean stress being input to the fatigue calculation consists of different contributions. For the tensile armour cases these are:

$$\Delta\sigma_{11} = \Delta\sigma_{11}^{Q_1,T} + \Delta\sigma_{11}^{Q_1,F} + \Delta\sigma_{11}^{M_2} + \Delta\sigma_{11}^{M_3} \quad (\text{B1.92})$$

where  $\Delta\sigma_{11}^{Q_1,T}$  is the stress range from dynamic tension variation,  $\Delta\sigma_{11}^{Q_1,F}$  is the dynamic stress range from friction effects,  $\Delta\sigma_{11}^{M_2}$  is the dynamic stress from bending about the wire weak axis and  $\Delta\sigma_{11}^{M_3}$  is the stress range from bending about the wire strong axis.

Considering one load cycle, the stress response at one point in the wire cross-section exposed to a  $\beta_2$  curvature cycle at constant tension and pressure will typically look like the one in Figure B1.33. The steep part of the curve is primarily governed by the stick regime where the armour behaves as a stiff pipe until the layer friction is exceeded and the stress increase from that point will be governed by local bending of the wire. Since the rate of stress increase in the stick regime is much higher than for local elastic bending of the wire, small curvature ranges often governs the fatigue life. This is specially the case for corrosion fatigue calculations where no cut-off is applied in the fatigue curve (all stress ranges counts in the Miner sum).

The stick slip behaviour depends on the contact pressure conditions, whether the outer sheath is intact or not or whether the load condition is dominated by external as illustrated in Figure B1.31 or by internal pressure and tension as illustrated in Figure B1.34. It is difficult to accurately describe this behaviour for all load conditions by a simple analytical model and therefore computational models are needed to accurately capture these conditions in the general case, see [Feret et al., 1986a], [Often and Løtveit, 1990], [Custodio and Vaz, 2002] and [Sævik, 2011].

For a typical flexible riser, the most critical section will be the upper hang off where the contact pressure conditions are dominated by internal pressure and tension. In this case the inner tensile armour will be exposed to the largest contact pressures and associated friction stresses and will therefore govern the fatigue behaviour. By assuming:

- No end effects, i.e. the dynamic curvature acts away from the end fitting
- Plane loading
- Two-layered torsion balanced pipe with lay angle magnitude  $\alpha$ , mean helix radius  $R$ , wire area  $A_t$ , width  $b$  and summed layer thickness  $t_{tot} = 2t$
- The pipe is exposed to a constant mean true wall tension  $\bar{T}_w$  (from effective tension and internal pressure), dynamic effective tension  $\Delta T$ , mean curvature  $\bar{\beta}_2$  and dynamic

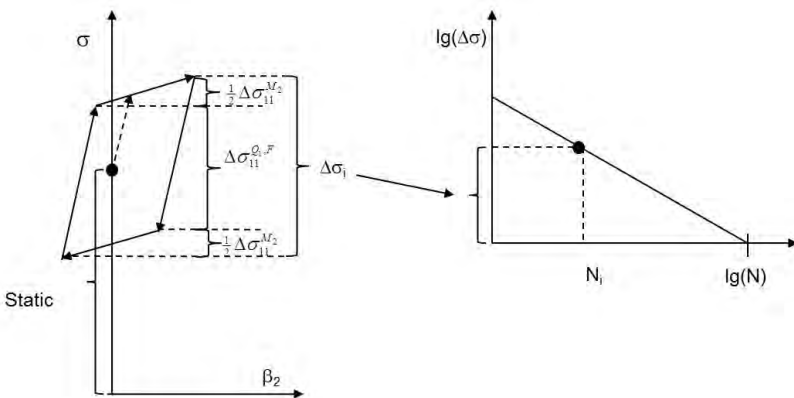


Figure B1.33: Typical stress history and fatigue calculation procedure

curvature  $\Delta\beta_2$

the mean stress and the stress range can be estimated from the geodesic and loxodromic assumptions respectively as:

$$\bar{\sigma}_{11} = \frac{\bar{T}_w}{2\pi R t_{tot} F_f \cos^2 \alpha} - 3EX_3 \cos^2 \alpha \cos \psi \bar{\beta}_2 \quad (\text{B1.93})$$

$$\begin{aligned} \Delta\sigma_{11} = & \frac{\Delta T}{2\pi R t_{tot} F_f \cos^2 \alpha} \\ & + \min\left(\frac{3\bar{T}_w b \mu \tan^2 \alpha}{4F_f A_t R \sin \alpha} \cos \psi, ER \cos^2 \alpha \cos \psi \Delta\beta_2\right) \quad (\text{B1.94}) \\ & + EX_3 \cos^2 \alpha \cos 2\alpha \cos \psi \Delta\beta_2 \\ & + EX_2(1 + \sin^2 \alpha) \cos \alpha \sin \psi \Delta\beta_2 \end{aligned}$$

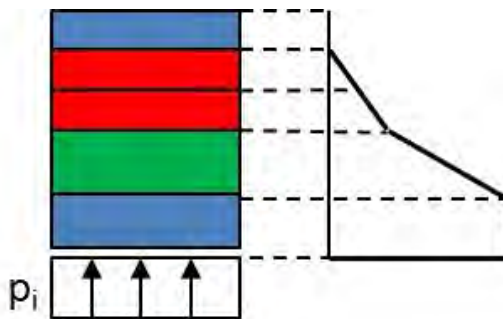
where it is noted that the wire coordinates  $X^2$  and  $X^3$  must be varied to include all four corners of the wire and the circumferential coordinate  $\psi$  varied to ensure sufficient cross-section resolution of the fatigue calculation.

#### B1.3.7.4 Mean and dynamic stresses in the pressure armour

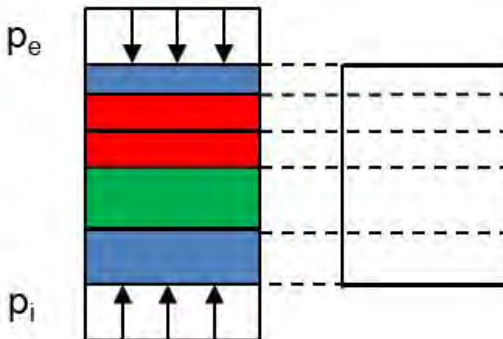
The mean and dynamic stresses in the pressure armour include the three-dimensional stress state where the  $\sigma_{11}$ ,  $\sigma_{22}$ ,  $\sigma_{33}$  and  $\sigma_{23}$  are the governing components as outlined in Section B1.3.4 and section B1.3.5.3. The stress levels and associated variations are sensitive to the

cross-section geometry and local contact conditions and cannot be described by a simple analytical model. One way of describing the stress range and associated mean stress used as input to the fatigue calculation procedure as described in Section B1.3.8.3 Bending and fatigue is to use the Von Mises approach by only neglecting the components of bending shear stresses as:

$$\Delta\sigma = \sqrt{\Delta\sigma_{11}^2 + \Delta\sigma_{22}^2 + \Delta\sigma_{33}^2 - \Delta\sigma_{11}\Delta\sigma_{22} - \Delta\sigma_{11}\Delta\sigma_{33} - \Delta\sigma_{33}\Delta\sigma_{22} + 3\Delta\sigma_{23}^2} \quad (\text{B1.95})$$



(1) Contact pressure distribution - damaged condition



(2) Contact pressure distribution - intact condition

Figure B1.34: Contact pressure distributions for pipe exposed to internal and external pressure for intact and damaged outer sheath conditions, red = tensile armour, green = pressure spiral wire, blue = plastic layer

$$\bar{\sigma} = \sqrt{\bar{\sigma}_{11}^2 + \bar{\sigma}_{22}^2 + \bar{\sigma}_{33}^2 - \bar{\sigma}_{11}\bar{\sigma}_{22} - \bar{\sigma}_{11}\bar{\sigma}_{33} - \bar{\sigma}_{33}\bar{\sigma}_{22} + 3\bar{\sigma}_{32}^2} \quad (\text{B1.96})$$

### B1.3.7.5 The effect of corrosion failures in terms of bursting and fatigue performance

Under the condition that some tensile armour wires fail in one layer due to corrosion or corrosion fatigue, this will have several consequences:

- The axial load capacity will be reduced. Hence, for a given true wall tension, axial elongation takes place.
- Further in order to keep the torsion balance, a torsion rotation of the cross-section in the helix direction of the failed layer will take place.
- The mean and dynamic stresses will increase both in the tensile armour and in the pressure spiral wire.

The number of tensile armour wire failures that can be accepted depends on the loading conditions and the material state, however, important questions are whether the failure happened in the inner tensile armour layer and whether multiple failures have occurred at the side of each other. If the latter is the case, the pressure spiral wire will start to lose support involving excessive local moments at the span shoulders which may lead to burst

failure, see Figure B1.35. Due to the large number of tensile wires, this will generally be more critical than the loss in axial load capacity. Having this in mind, one important issue is whether it is possible to detect torsion rotation before risking overload failure in the pressure spiral.

The effect in terms of torsion (rotation per length)  $\tau_p$  can be estimated by applying Eq. B1.13 and studying the resulting stiffness relation in tension and torsion. By assuming a two layered tensile armour with opposite layer angles of same magnitude consisting of in total  $n$  wires of which  $n_f$  wires have failed in one layer (no anti-buckling tape):

$$\tau_p = \frac{\frac{n_f}{n}}{(1 - 2\frac{n_f}{n})} \frac{T_w}{E2\pi R^2 t_{tot} F_f \cos^3 \alpha \sin \alpha} \quad (\text{B1.97})$$

By application of the above it is concluded that it will be very difficult to conclude with respect to how many wire failures that have actually occurred from such calculations. The main reason for this is that a significant number of failures are needed to obtain a rotation that can be measured, whereas the number of allowed failures in the inner tensile armour will typically be  $< 10$ . However, it may be possible to identify which of the outer or inner tensile armours that has failed. If the inner armour has failed, the pipe will tend to rotate in the inner armour lay direction to increase the strain in the inner armour and reduce it in the outer armour to keep the torsion balance.

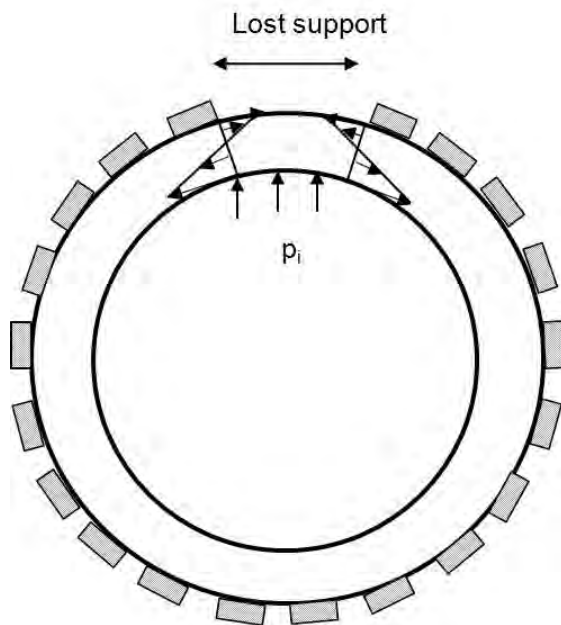


Figure B1.35: Stress in the pressure spiral wire due to lost tensile armour support

Generally the above effects need to be evaluated on a case to case basis by FE analysis.

If it is concluded that the risk for burst failure is small, the fatigue life needs to be re-evaluated taking the stress concentrations from the corrosion failure into account. Due to the nature of a corrosion failure in the tensile armour, the change in the conditions of stress will be both in terms of increasing the axial force in the wires and by introducing additional bending moments that were not present before failure. Having identified the increase in mean and dynamic stress from the failure, noting that the primary effect is related to changing the wire axial force distribution within the layer, see [Ji, 2012], its effect on the stress range and mean stress can be evaluated by:

$$\Delta\sigma_{11}^{Q_1,*} = \Delta SCF^{Q_1} \Delta\sigma_{11}^{Q_1} \quad (B1.98)$$

$$\bar{\sigma}_{11}^{Q_1,*} = SCF^{Q_1} \bar{\sigma}_{11}^{Q_1} \quad (B1.99)$$

where \* denotes the modified stress range and mean stress with reference to the nominal intact values.  $\Delta SCF^{Q_1}$  is the stress concentration factor describing the increase in the axial stress range during a cycle and  $SCF^{Q_1}$  is the associated mean stress concentration factor describing the increase in the mean axial stress from the failure.

### B1.3.7.6 The effect of corrosion in terms of lateral wire buckling

Corrosion will reduce the inertia moment of the cross-section and hence reduce the lateral buckling capacity Eq. B1.82. If an even corrosion factor  $c$  is assumed so that the corroded wire width  $b^* = b(1-2c)$  and the corroded wire thickness is  $t^* = t(1-2c)$  then the associated lateral buckling capacity reduction factor can be obtained from Eq. B1.82 as:

$$F_b = (1 - 2c)^4 \quad (B1.100)$$

## B1.3.8 Computational methods

### B1.3.8.1 General

The general FE softwares such as ANSYS®, MARC®, ABAQUS® have become increasingly popular with regard to analysing stresses in flexible pipes.

The major advantage of these tools is that arbitrary geometry, kinematic and material effects can be modelled. However, due to the large number of degrees of freedom (DOFS) needed to describe the inherent complexity of a flexible pipe, long computing times still limits application of these tools with respect to standard engineering analyses and they are therefore mostly used to investigate special effects where the required model length is limited. In the following, the relevance of alternative methods for stress and fatigue analysis are discussed.

### B1.3.8.2 Axisymmetric stress analysis

Axisymmetric stress analysis of flexible pipes can be carried out by several approaches:

1. By analytical methods.
2. By use of general FE softwares.
3. By specialised tools based on the concentric layer approach.

For the bursting and tension failure modes the gaps between layers will be closed before reaching the ultimate capacity. Hence, these can in most cases be adequately described by analytical methods similar to those outlined in Section B1.3.4.

However, when it comes to more advanced load cases or fatigue evaluations, these relies on correctly describing the initial conditions with regard to the gaps and contact pressures

between layers. In order to cover all relevant load combinations for a flexible riser, more advanced methods that consistently describe layer interaction is therefore needed. Due to the assumptions that can be made considering the layered structure of flexible pipes when exposed to axisymmetric loads, specialized procedures gives a significant computation benefit as compared to general FE softwares and these are therefore rarely used for standard design analyses.

Specialised procedures for calculating the axisymmetric layer response of flexible pipes have been dealt with by many authors. The main reference is the pioneering work by Ferét and Bournazel [Feret et al., 1986a] who formulated a model based on the following principles:

1. Divide the flexible pipe into a set of concentric layers.
2. Describe the strain resulting in each layer from the overall pipe axial strain quantities  $\epsilon_p$  and  $\tau_p$  in Figure B1.8 and Figure B1.9, i.e. all layers are forced to respond in the same 2D plane.
3. Each layer is allowed to move and deform radially.
4. For the plastic layer, the strain kinematics is based on thin shell theory ( $\epsilon_{11}$  and  $\epsilon_{22}$ ), however, also including the  $\epsilon_{33}$  term from the contact pressure and the  $\epsilon_{23}$  term introduced by pipe torsion  $\tau_p$ .
5. For the helix layers, the strain kinematics is based Eq. B1.13, however, also including the  $\epsilon_{33}$  term from the contact pressure and the  $\epsilon_{22}$  from hydrostatic pressure.
6. Assume linear elastic behaviour and apply Hooke's law for describing the stress-strain relation for each layer.
7. Establish algebraic equations for each layer based on the above, linking the response of each layer in terms of radial, torsion and axial motions to the external true wall force, torsion moment, external and internal pressures. The algebraic equations include the gap between layers as separate unknowns which is similar to treating the contact pressure as Lagrange multipliers in the algebraic equations.

The above procedure still represent the state of the art in terms of flexible pipe axisymmetric stress analysis and was implemented in the CAFLEX computer program which also is an integrated part of the BFLEX program system, see [Feret and Momplot, 1989] and [Sævik, 2014].

Later similar algorithms have been presented, see e.g. [McNamara and Harte, 1989], [Often and Løtveit, 1990]. Several modifications have been proposed to the above procedure serving different purposes. Custodio and Vaz [Custodio and Vaz, 2002] studied the axisymmetric response of umbilical cables, introduced improvements to previously published models with regard to allowing non-linear material models and [Sævik, 2011] presented an extension of the Ferét model to take circumferential gaps into account. Skeie [Skeie et al., 2012] proposed a similar model based on treating the contact conditions as an optimization problem, resulting in a similar set of equations.

### B1.3.8.3 Bending and fatigue stress analysis

Tensile and pressure armour bending stress analysis can be carried out by several approaches:

1. By analytical methods.

2. By use of general FE softwares.
3. By specialised FE tools.

**B1.3.8.3.1 Tensile armour** Analytical methods according to the principles outlined in Section B1.3.5 is widely used in the industry for tensile armour fatigue calculations. By additionally including the non-linear moment curvature relation as outlined in Section B1.3.5 in the global analysis, accurate results may be obtained taking the load carrying capacity of the flexible pipe into account. These methods, however, relies on the assumption of constant curvature and no end effects.

In cases where severe bending gradients are present, i.e. mostly cases of severe bending that is not controlled by external measures such as bending stiffeners or bending restrictors, the resulting stresses may be underestimated. That is also the case where the length from the end fitting where each wire is anchored to the curved section is short, typically less than half of a pitch length, depending on the loading condition.

The above may be of special concern for installation load cases and for full-scale test program designs. In the latter case, the specimen length is limited and the challenge is to design the test program in such a way that it simulates the operation load cases in a realistic way without introducing test specific failure modes. Such failures have been observed as specimen pig-tailing changing the mean stress and stress range levels giving reduced life during testing. In order to simulate such behaviour FE analysis is needed either by general or specialised software where of each wire is modelled. This can be done by either combinations of volume, membrane, shell and beam elements in combination with layer contact and friction models.

**B1.3.8.3.2 Pressure armour** The pressure armour requires representation of both longitudinal  $\sigma_{11}$  stresses and the  $\sigma_{22}$ ,  $\sigma_{33}$  and  $\sigma_{23}$  stress components in the cross-section plane. This can be obtained by analytical models that are calibrated with respect to testing such as the TECHNIP SLPM model, by application of general FE tools or by specialised software, see [Sævik, 1999] and [Sævik et al., 2001].

The models need to include the longitudinal stress variation resulting from ovalisation as outlined in Section B1.3.5, the friction introduced in the nubs and valleys resulting from relative motions between winding and the alternating lift and close effect as described in Section B1.3.5.

#### B1.3.8.4 Special cases

There are several cases which can only be modelled by general FE softwares. This includes:

- Localized loads from other mechanical devices such as tensioners, caterpillars, clamps etc.
- Bend stiffener and end fitting details
- Redistribution of stresses due to wire failures.
- Buckling effects including annulus pressure induced collapse.

- Manufacturing and installation effects.
- Carcass end fitting slip effects.

Example of such models are shown in Figure B1.36 - Figure B1.38

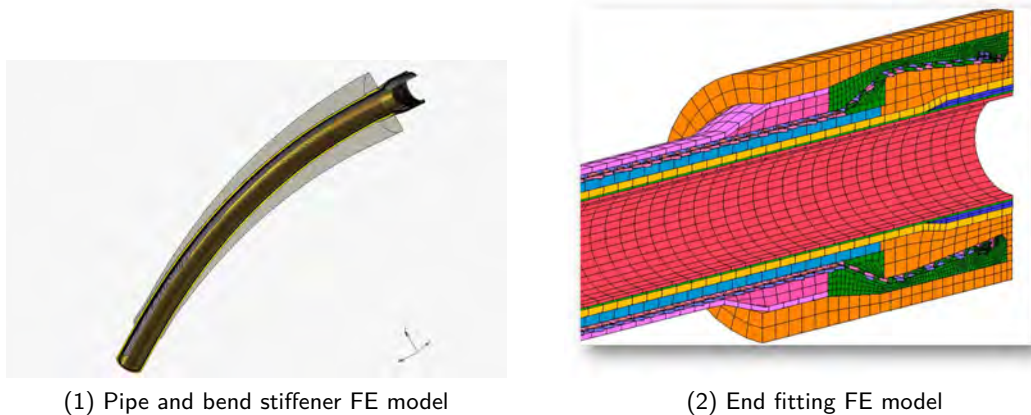


Figure B1.36: Example FE model including pipe, end fitting and bend stiffener in MARC® (4subsea)

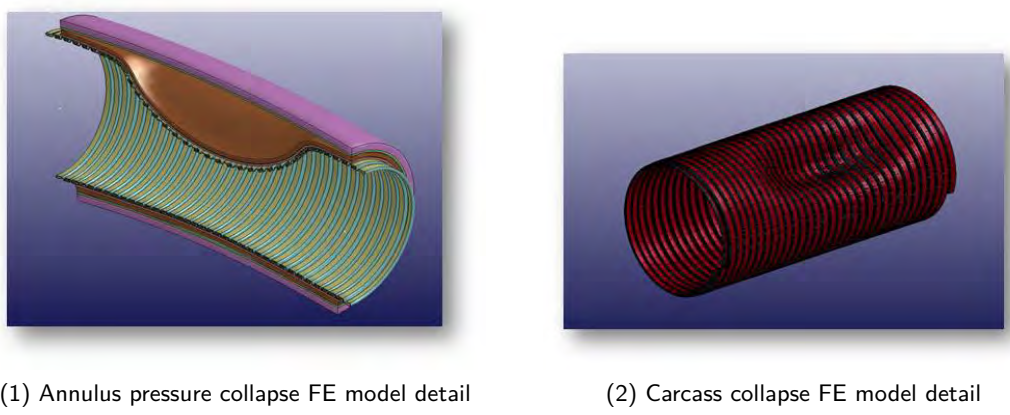


Figure B1.37: Example FE model to analyse Carcass collapse from annulus pressure build-up in MARC® (4subsea).

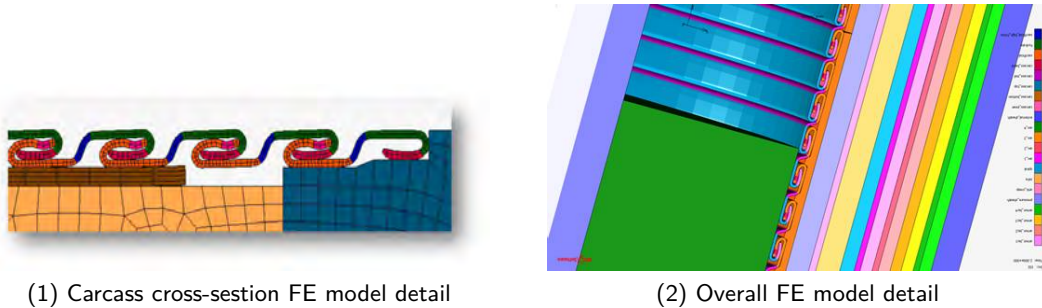


Figure B1.38: Example FE model to analyse Carcass and end fitting slip in MARC® (4subsea).

## B1.4 Global Analysis

### B1.4.1 Use of global analyses

#### B1.4.1.1 Initial design

Global analysis is usually performed as an integrated part of the riser system design and concept selection. The global analysis is typically performed at various stages of the project with various levels of detail, from an early concept study to the detail design phase.

In the very early concept study phase of a field development the level of detail required may be limited to only static analyses in order to provide sufficient confidence in feasibility. However, as the project phases approach riser delivery the required detail level of the global analysis increases significantly. A large set of load cases is typically required to demonstrate the fitness for purpose of the riser system.

In the detail design phase the global analysis is often performed as an iterative process with the following analysis steps:

1. Suggestion of a suitable riser system concept
2. Extreme analysis
3. Interference analysis
4. Fatigue analysis

Any or all of the 4 steps may be driving the design, but for many riser systems one may perform the analyses sequentially, i.e. start out with finding an appropriate starting point for a riser configuration. This may often be done with static analysis only and sometimes through analytical solutions, e.g. catenary equations etc. During any of the 4 steps one may have to reiterate to step one.

Once a riser system concept has been selected, the riser section lengths and various ancillary equipment properties have been determined (often through experience but occasionally through optimization routines), the extreme analysis can commence. The extreme analysis is a dynamic analysis applying either regular or irregular waves as a load input. The purpose of this analysis is to verify the integrity of the riser system during extreme events, i.e. often environmental loading with annual occurrence probability of  $10^{-2}$  or even down to  $10^{-4}$  is applied. In addition to extreme environmental conditions the riser system may experience extreme events like vessel mooring system damages, or alternatively the riser may see extreme temperature and pressure. Often the full set of extreme load cases may be combined to a significant number of different cases and it may take skill to determine which cases are governing. If the governing set of load cases can be kept to a minimum, the iteration on configuration design is greatly simplified. Tools for period/frequency screening are often handy to determine peak load drivers.

The initial extreme analyses are usually performed with a pinned riser at the top end to determine input to the bend stiffener design. Subsequent analyses are then performed with bend stiffener included with the purpose of verifying the riser/bend stiffener design and obtaining interface loads.

Following an understanding of the riser system extreme response, interference analyses may

be performed. This may be to determine any interference between riser-riser, riser-mooring, riser-platform/vessel or riser-subsea structure. Depending on the nature of the environmental conditions of the field the initial interference analysis may be a quasi-static analysis with extreme current loading only. This often provides a good indication of governing interference load cases, however for some systems the waves are the interference drivers. The interference analysis should include the full design range of operational criteria, e.g. variation in marine growth, variation in density contents etc.

Often the last step in a global analysis is to perform fatigue analysis, i.e. document the service life of the armour layers. The global fatigue analysis is performed by simulating the operating conditions, such as pressure-dependent hysteretic bending stiffness, applying wave scatter diagram (either full scatter diagram or lumped in to a selection of wave classes) and extraction of fatigue loads for local analysis. If sufficient fatigue life is not found a redesign of the riser cross section or some ancillary equipment may be necessary. Steps 1-4 above may then have to be performed again.

Validation of the global analysis for fatigue is often a good option at this stage. The selection of sea state included in the analysis should demonstrate a shared contribution by a reasonable number of sea states. Simulation time of fatigue sea states is often limited, say for instance 30 - 60 minutes. The analysis should demonstrate that a further increase in simulation time does not have significant impact on fatigue damage.

There are several commercial software packages available for performing global analysis. The most commonly used are:

- OrcaFlex (by Orcina)
- DeepLines (by Principia and IFP)
- Flexcom (by MCS Kenny)
- RIFLEX (by SINTEF and MARINTEK) [[Fylling et al., 1995](#)]

#### B1.4.1.2 Design verification

As a part of the delivery of a riser product the riser suppliers are usually required to document that their products are fit for purpose. This will often include the performance of a global analysis of the riser system. The purchaser of the risers may require that the global analyses performed by the riser supplier are verified by a third party.

As global analyses can be quite complex there are many sources for discrepancies between results from analyses performed by the riser supplier and a third party. For any discrepancies found it is important that a stepwise approach is used in finding the sources for deviation.

A typical start is to compare static loads in a Start-Of-Life (SOL, initial buoyancy, no marine growth) and then move on to End-Of-Life Condition (EOL, final buoyancy, full marine growth profile).

When a static agreement has been found, the next typical step is to compare the vessel response in a regular Airy wave. The Response Amplitude Operator (RAO) is a common source of mistakes as there are many different formats and conventions used, and these may not always be described in full detail. It is hence always wise to evaluate the RAO inputs and to perform a visual check of the vessel motion in waves with different periods and headings.

When an agreement has been found on the vessel motion, the next major hurdle is the comparison of environmental data input and riser/ancillary equipment properties, incl. bend stiffener stiffness.

One of the critical properties of the riser should be examined carefully, that is, how the stiffness of the riser is defined in the global modeling. In most cases, nominal elastic stiffness is used as a simplification. However, a hysteretic moment-curvature relation may be used as input as well.

Hydrodynamic properties of riser and ancillaries may vary significantly and a critical evaluation of these should be performed. When performing verification of fatigue analyses it may sometimes be difficult to initially directly compare fatigue damage or service life when S-N data is not available to the verifying party. So it is often a good idea to compare at response level.

#### B1.4.1.3 Installation of risers

Global analysis is used extensively in installation analysis of flexible risers. The global analysis is used at various stages through the project phase and onboard platforms and installation vessels.

The goal of the analysis is to evaluate the installability of the riser configuration by:

- Ensuring that the riser configuration is installable
- Identification of critical parts of the installation and splitting of the installation sequence into phases that may be performed separately
- Determining behavior, including loads on riser and ancillary equipment during installation, e.g. MBR at touch down , MBR over installation chute and top tension
- Determining installation loads (required winch capacities and/or tensioner hold-back and squeeze force)
- Determining requirements to installation vessel and/or platform positioning during the installation
- Determining installation limitations, e.g. w.r.t. weather criteria
- Creation of lay tables with required lay back and installation procedure input

Early evaluation of the installability of the configuration may be performed implicitly, i.e. by engineering judgment or experience. However, proper global analysis should always be performed during the detail design phase.

In general, visual checks of the model/riser behavior in the global analysis model are advised in order to obtain a proper understanding of the operation.

An important part of the installation analysis is to determine contingency plans for the various phases of the installation process, to ensure that the operations can be aborted safely at all times in the event of unexpected complications or onset of severe weather conditions.

Extra care should be taken when evaluating the process of lowering risers and other equipment through the splash zone, due to the possibility of slamming loads on the equipment and snatch loads on the lifting arrangement.

#### B1.4.1.4 Re-analysis during system lifetime

Global re-analysis of risers is often performed during system lifetime. Re-analysis is required if risers are to be replaced or additional risers to be installed. Also a lifetime assessment of a riser system will require re-analysis. In both cases it is important to account for new relevant input information to the analyses e.g.:

- Updated standards and operator technical requirements
- Updated metocean specifications
- Updated vessel/platform data (RAO and offsets)
- As-built, as-installed and as-surveyed data

In case of a riser system life extension it is suggested to initiate the work with a gap analysis to determine if input information to the analysis and current requirements have changed from the original design analysis.

#### B1.4.2 Weight and buoyancy; the effective weight concept

A key feature of slender marine structures is that the global geometry is strongly related to axial tension. The main contribution to stiffness versus lateral loads from waves and current, originates from axial tension. Equilibrium is obtained by change of geometry and hence also change of axial force direction. This type of stiffness is referred to as 'geometric stiffness', which gives a contribution to structural stiffness in addition to the traditional beam stiffness.

##### B1.4.2.1 Geometric stiffness

Figure B1.39 illustrates a simple example of geometric stiffness. The structure consists of a rope with constant tension  $T$  and is exposed to a concentrated load  $F$  at the midpoint of a free span with length  $L$

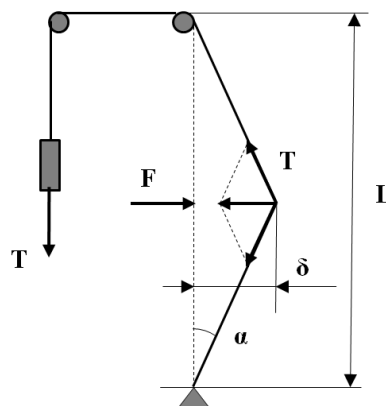


Figure B1.39: Rope structure with concentrated load

The deformation will lead to a change of direction of the rope, which means that the rope forces will have a horizontal component at the point load. Equilibrium is obtained when the

sum of the horizontal components is equal to the external load. From the figure we can see that the equilibrium condition can be written as:

$$F = 2T \cdot \sin \alpha \quad (\text{B1.101})$$

If we assume that the displacement is small, we can write

$$\sin \alpha = \tan \alpha = \alpha = \frac{2\delta}{L} \quad (\text{B1.102})$$

where  $\delta$  is the displacement at the load and  $L$  the length of the free spanning rope. The relation between force and displacement can hence be found as

$$F = \frac{4T}{L} \delta = K_G \delta \quad (\text{B1.103})$$

which means that the geometric stiffness for this case is

$$K_G = \frac{4T}{L} \quad (\text{B1.104})$$

The geometric stiffness terms are easily found for beam elements in a finite element formulation, and will always be directly added to the ordinary stiffness matrix for a beam element. The linear version of the geometric stiffness matrix from beam tension is described by [Larsen, 1976], while [A. Engseth, 1988] present a non-linear formulation that allows for unlimited rotations.

#### B1.4.2.2 Buoyancy effect

Figure B1.40 shows a vertical pipe in water. The pressure acts perpendicular to the pipe wall, which means that the pressure resultant on a pipe element is zero. The pressure resultant on the pipe from surface to bottom is hence also zero.

Figure B1.41 shows a part of an inclined pipe that is isolated form a continuous pipe between the seafloor and a floating vessel. In this case we will not have any end cap pressure, which means that the forces  $p_1 A_e$  and  $p_2 A_e$  are not present.  $A_e$  is the external area of the pipe, and the pressure  $p_e$  at water depth  $h$  is given by the well known relationship

$$p_e = \rho_e g h \quad (\text{B1.105})$$

where  $h$  is the water depth and  $\rho_e$  is the density of surrounding water. The vertical force from buoyancy  $B_V$  is given as the weight of displaced water (Archimedes), but since the end cap forces are not present the effect of buoyancy will become different from what Archimedes stated. The sum of the end cap forces is an axial force  $B_T$ . By subtracting this force from the vertical buoyancy force  $B_V$ , we can find the net buoyancy force on the inclined, continuous element,  $B_R$ , see Figure B1.41 c:

$$B_R = \rho g A L \cos \alpha \quad (\text{B1.106})$$

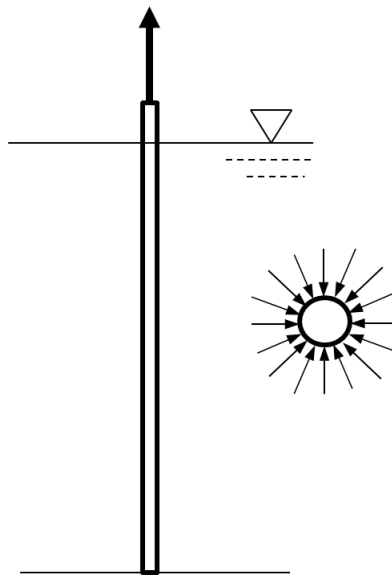


Figure B1.40: Illustration of buoyancy on a vertical pipe

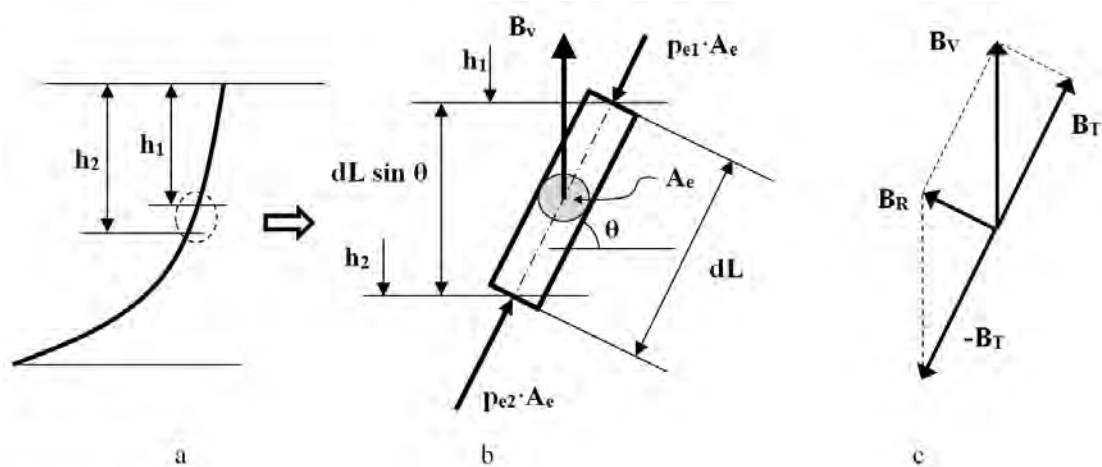


Figure B1.41: Pipe segment in a continuous pipe

The consequence of this is that the net buoyancy force will depend on the orientation of the element. A vertical pipe will not have buoyancy forces along its length, but a horizontal pipe will have buoyancy forces according to Archimedes' law. Hence, forces from buoyancy will become non-conservative, which causes formal problems for calculation of static and dynamic equilibrium. It is, however, possible to obtain a load description that leads to displacement independent forces, which will be shown in the following.

Figure B1.42 b shows all forces that act on the element. Bending moment and curvature are not considered, but the main observation and conclusion from this discussion are not influenced by this simplification. Figure B1.42 a shows the forces acting on the segment. They consist of axial stress resultant  $\sigma_x(A_e - A_i)$ , external and internal pressure  $p_e$  and  $p_i$ , and weight of the pipe itself  $w_p \cdot dl$ . This condition can be described as a sum of three contributions that are illustrated on Figure B1.42 b, c and d. External pressure on an equivalent closed pipe element is shown on Figure B1.42 b. External end cap pressures

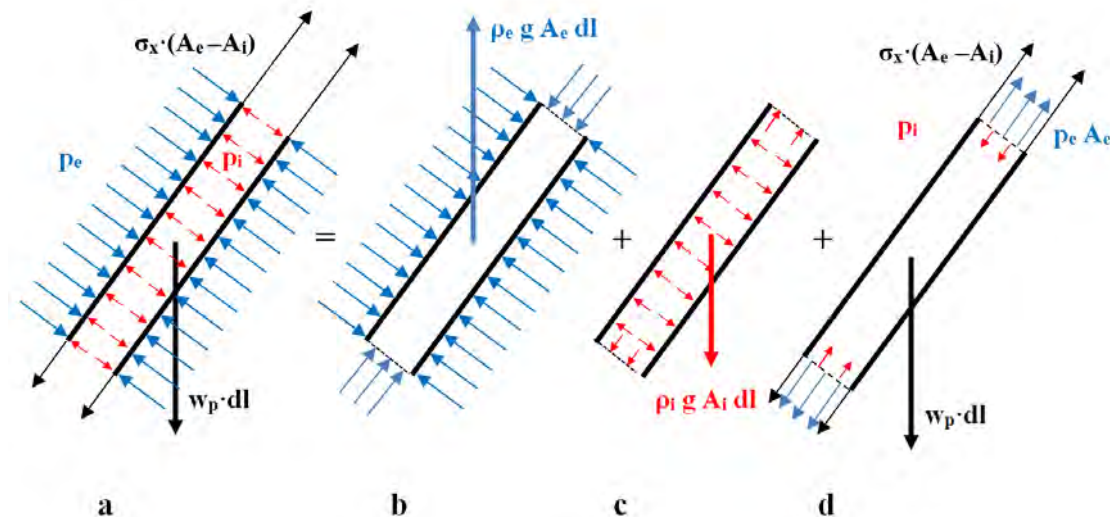


Figure B1.42: Forces on a section of a continuous pipe

are included, which means that the pressure resultant becomes vertical and found from Archimedes' law:

$$B_V = \rho_e g A_e dl \quad (\text{B1.107})$$

End cap pressure is also included from internal pressure on Figure B1.42 c, and the resultant must be equal to the weight of the content:

$$W_c = \rho_i g A_i dl \quad (\text{B1.108})$$

The third contribution is illustrated on Figure B1.42 d, and is simply found as the difference between a and (b+c). The weight of the pipe and axial stresses are included, but also end cap pressures in opposite direction that are needed to balance the non-existing pressures on b and c. By summing up vertical and axial forces on Figure B1.42 b, c and d, we will obtain the 'effective weight'  $w_e$  and 'effective axial force'  $T_e$ :

$$\begin{aligned} \text{Effective weight: } w_e &= w_p + \rho_i g A_i - \rho_e g A_e \\ \text{Effective axial force: } T_e &= T_\sigma + p_e A_e - p_i A_i \end{aligned} \quad (\text{B1.109})$$

where  $T_\sigma$  is the axial stress resultant given as  $\sigma_x(A_e - A_i)$ . Equilibrium can be found by consideration of effective weight and effective axial force (often referred to as effective tension), or by use of the real weight and pressure resultant, and axial stress resultant. Both methods are correct, but use of effective weight is far more convenient.

Note that the effective axial force is used to calculate the axial force for beam buckling, and also the geometric stiffness due to tension in a slender beam. The effective weight/effective tension concept is used in all computer programs for static and dynamic analysis of marine risers, and does not represent any loss of accuracy.

If the effective weight concept is used, we have to calculate stresses by use of the relationship between stress resultant and effective force. However, if the 'real' weight and pressure

resultant are used, axial stress will become a direct result from the analysis, but the effective force need to be calculated if geometric stiffness or buckling conditions are wanted.

Effective weight and axial force have been found without considering bending moments or pipe curvature. It is possible to include these effects, but the end results in terms of effective axial force and weight will no be influenced. The effective axial force may also be used to calculate equivalent stresses in the pipe cross section, see [Sparks, 1984].

### B1.4.3 Simplified analysis for preliminary design

#### B1.4.3.1 Initial analysis of lazy wave configuration

The purpose of this type of analysis is to have an easy way of generating an initial design of a lazy wave riser. Initial design means to define needed buoyancy and position of the buoyancy zone in order to obtain sufficient flexibility with respect to upper end motions without excessive bending or axial tension.

The starting point for this type of analysis is a riser without horizontal force. By neglecting the influence from bending stiffness, the riser will have three vertical sections as illustrated on Figure B1.43. Note that the figure shows a horizontal distance between the sections that ideally should not be there.

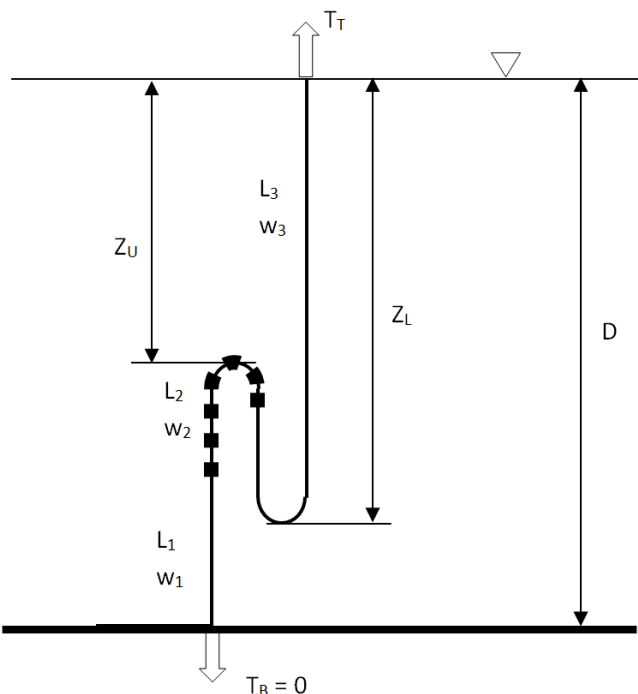


Figure B1.43: Initial condition of lazy wave riser. Upper end is assumed to be below or at sea surface level.

**Definitions**

- Segment 1 is the lowest segment that partially rests on the bottom. In the initial condition a length  $L_1$  is vertical and the effective tension  $T_B$  is zero at the touch-down point.
- Segment 2 is the segment with uniform buoyancy. Its total length is  $L_2$ . This segment will in the initial condition have a horizontal tangent at a distance  $z_U$  from the upper end (or surface on the figure). This point is referred to as the upper bend. Note that a horizontal tangent means that tension in the riser must be zero in the initial condition since the horizontal force is zero and the pipe has no shear force.
- Segment 3 is the segment that ends at the floater. Segment length is  $L_3$ . This segment will in the initial condition have a horizontal tangent at a distance  $z_L$  from upper end. This point is referred to as lower bend. The effective axial force at upper end will be  $T_T$ .
- $w_i$  Effective (or submerged) weight per unit length of segment  $i$  (N/m).
- $D$  Vertical distance from upper end to bottom.

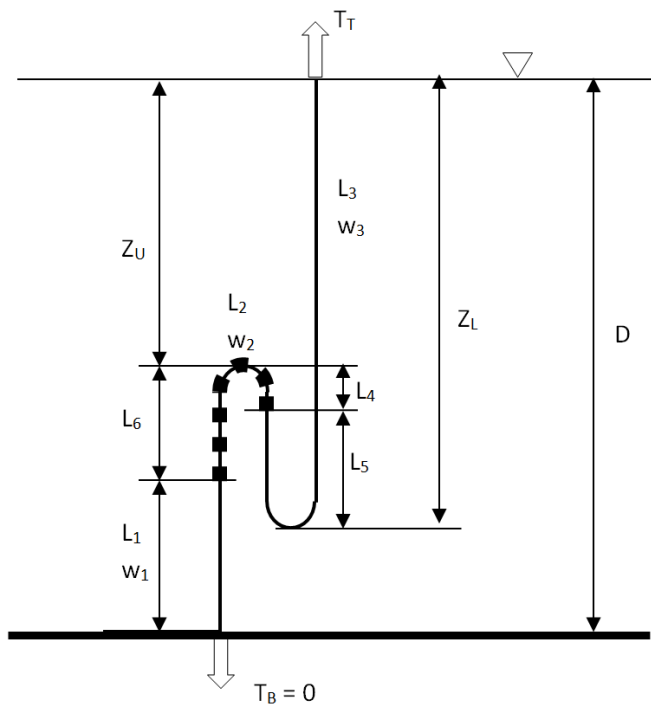


Figure B1.44: Initial condition and design parameters, Case 1.

An acceptable design will have allowable bending at the two bends in a 'near' position, and allowable tension at upper end in a 'far' position. Vertical equilibrium and compatibility equations can be established and allow for calculation of unknown design parameters. Solutions will be given for three different design situations.

**Option 1: Initial positions of upper and lower bend, and effective weight of segments given; segment lengths can be calculated**

When wanted positions of bends and effective weight of all segments are known, it is possible to calculate the needed lengths of the segments. According to Figure B1.44 we have 6

unknown length parameters, but we have also 6 equations; 4 are based on compatibility and 2 on vertical equilibrium:

$$\begin{aligned}
 \text{Length of segment 1:} & L_1 = D - z_u - L_6 \\
 \text{Length of segment 2:} & L_2 = L_4 - L_6 \\
 \text{Length of segment 3:} & L_3 = Z_1 + L_5 \\
 \text{Total length of riser:} & L_1 + L_2 + L_3 = D + 2(z_L - z_u) \\
 \text{Equilibrium bottom - upper bend:} & L_6 w_2 + L_1 w_1 = 0 \\
 \text{Equilibrium of reversed section:} & L_4 w_2 + L_5 w_3 = 0
 \end{aligned} \tag{B1.110}$$

$$\begin{aligned}
 L_1 &= \frac{w_2(z_u - D)}{w_1 - w_2} \\
 L_3 &= \frac{(D - z_u - L_1)w_2 + z_L w_3 - w_2[D + 2(z_L - z_u) - L_1]}{w_3 - w_2} \\
 L_2 &= D + 2(z_L - z_u) - L_1 - L_3 \\
 L_5 &= L_3 - z_L \\
 L_6 &= D - z_u - L_1 \\
 L_4 &= L_2 - L_6
 \end{aligned} \tag{B1.111}$$

**Option 2: Effective weight of segments given, and also the length of buoyancy zone and upper segment. Calculation of position of bends.**

The unknown parameters are

$$\begin{aligned}
 \text{Tension of upper end} & T_T \\
 \text{Length of suspended part of segment 1} & L_1 \\
 \text{Vertical position of upper bend} & z_U \\
 \text{Vertical position of lower bend} & z_L
 \end{aligned}$$

For this case we will have 3 equilibrium equations and one that defines compatibility:

$$\begin{aligned}
 \text{Equilibrium top - lower bend:} & T_T = w_3 Z_L \\
 \text{Equilibrium bottom - upper bend:} & (D - L_1 - Z_U)w_2 + L_1 w_1 = 0 \\
 \text{Global equilibrium:} & L_1 w_1 + L_2 w_2 + L_3 w_3 = T_T \\
 \text{Global compatibility:} & L_1 + L_2 + L_3 - 2(Z_L - Z_U) = D
 \end{aligned} \tag{B1.112}$$

Standard manipulation of these equations gives the following solutions:

$$\begin{aligned}
 z_L &= \frac{2A_1 w_1 + A_2 w_1 w_2 - 2A_3 w_1 + A_3 w_2}{2w_1 w_3 - w_2 w_3 - 2w_1 w_2} \\
 z_U &= \frac{A_2 w_1 - A_3 - w_3 z_L + 2z_L w_1}{2w_1} \\
 L_1 &= \frac{A_3 + w_3 z_L}{w_1}
 \end{aligned} \tag{B1.113}$$

The A parameters are found from Eq B1.112 and given by:

$$\begin{aligned} A_1 &= -Dw_2 \\ A_2 &= D - L_2 - L_3 \\ A_3 &= -L_2w_2 - L_3w_3 \end{aligned} \quad (\text{B1.114})$$

**Option 3: Initial positions of upper and lower bends, effective weight of upper and lower segments, and length of upper segment given. Length and effective weight of buoyancy segment must be calculated.**

Vertical equilibrium at the initial position can be applied to calculate the needed length and weight of the buoyancy segment if the wanted bend positions are given. The unknown parameters are  $L_1$ ,  $L_4$ ,  $L_5$ ,  $L_6$  and  $w_2$ . These can be found from the following relations:

$$\begin{aligned} L_5 &= L_3 - z_L \\ L_4 &= z_L - z_U - L_5 \\ w_2 &= -\frac{L_5w_3}{L_4} \\ L_1 &= \frac{(D - z_U)w_2}{w_2 - w_1} \\ L_6 &= D - z_U - L_1 \end{aligned} \quad (\text{B1.115})$$

#### B1.4.3.2 Catenary theory for analysis of lazy wave riser

Figure B1.45 shows the geometry of a lazy wave riser and defines all necessary geometry parameters. If the horizontal force  $H$  and all weights and segment lengths are known, and the bottom segment is assumed to be sufficiently long to maintain zero vertical force at the bottom end, the unknown parameters will be:

$$\begin{array}{ll} \text{Suspended length of lower segment} & L_1 \\ \text{Vertical position of upper bend} & z_2 \end{array}$$

If these parameters can be found, the riser geometry can easily be calculated from classical catenary theory.

It is not possible to find a direct solution for the two unknown parameters. An iterative procedure must therefore be established. Firstly, a relation between  $L_1$  and  $z_2$  must be found, and secondly we need to have equations that describe compatibility for all segments.

The vertical position of the connection between segment 1 and 2 (bottom and buoyancy segments) is  $z_2$ . For given horizontal force the following relation between  $z_1$  and  $L_1$  is known from catenary theory:

$$L_1 = \sqrt{z_1^2 + \frac{2z_1H}{w_1}} \quad (\text{B1.116})$$

At the connection between segment 1 and 2, tension in the riser can be found by considering segment 1 or the part of segment 2 between the connection point and upper bend. This is possible since we assume that there is no shear force in the riser. Hence we have:

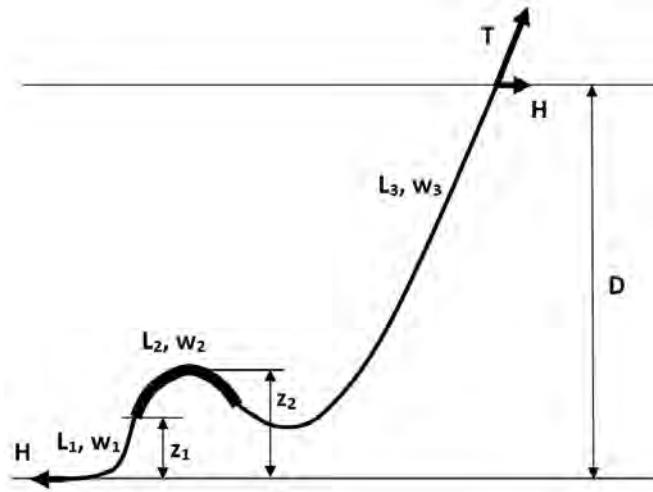


Figure B1.45: Geometry for lazy wave riser

$$T_1 = H + w_1 z_1 = -T_2 = -[H + w_2(z_2 - z_1)] \quad (\text{B1.117})$$

Note that  $w_2$  in Eq B1.117 is negative since the buoyancy for segment 2 obviously will be larger than its weight. If we assume  $z_2$  to be known, we can solve this equation with respect to  $z_1$ :

$$z_1 = \frac{w_2 z_2}{w_1 - w_2} \quad (\text{B1.118})$$

By introducing Eq B1.118 into Eq B1.116 we can find a relation between  $L_1$  and  $z_2$  without other unknowns:

$$L_1 = \left[ \left( \frac{w_2 z_2}{w_1 - w_2} \right)^2 - \frac{2H w_2 z_2}{w_1(w_1 - w_2)} \right]^{0.5} \quad (\text{B1.119})$$

Compatibility can be checked by adding the vertical projection of all segments and compare this sum to the known vertical distance between upper and lower end. Additional parameters are defined in Figure B1.46

The vertical distances  $z_3$  and  $z_4$  are given by:

$$\begin{aligned} z_3 &= \frac{H}{w_3} \sqrt{1 + \beta_3^2} - \frac{H}{w_3} \sqrt{1 + \beta_2^2} \\ z_4 &= \frac{H}{w_2} \sqrt{1 + \beta_2^2} - \frac{H}{w_2} \end{aligned} \quad (\text{B1.120})$$

The angles at segment boundaries and upper end can also be found when the segment lengths, the horizontal force and riser weights are known:

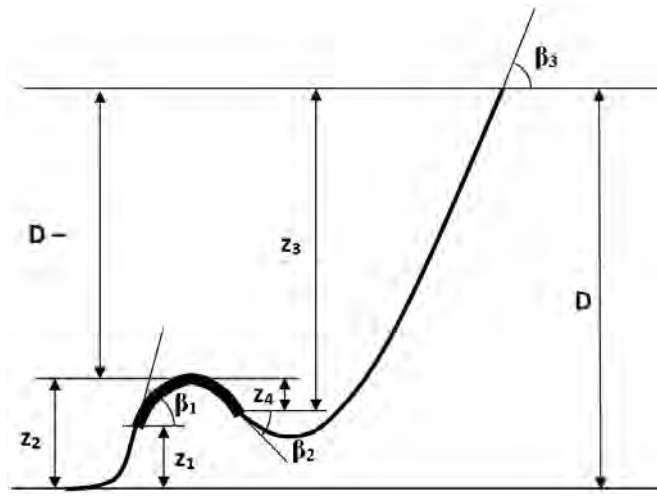


Figure B1.46: Definition of geometry parameters

$$\begin{aligned}\beta_1 &= \frac{w_1 L_1}{H} \\ \beta_2 &= \beta_1 \frac{w_2 L_2}{H} \\ \beta_3 &= \beta_2 \frac{w_3 L_3}{H}\end{aligned}\quad (\text{B1.121})$$

Finally we can find the vertical position of upper bend  $z_2$ :

$$z_2 = D - z_3 + z_4 \quad (\text{B1.122})$$

Equations B1.119 to B1.122 can be solved by iteration if weights,  $L_2$ ,  $L_3$  and  $H$  are known. The following scheme may be applied:

1. Assume an initial value for  $z_2$ ;  $z_2^0$ ;
2. Calculate  $L_1$  from Eq. B1.119
3. Calculate the angles at segment boundaries from Eq. B1.121
4. Calculate  $z_3$  and  $z_4$  from Eq. B1.120
5. Calculate  $z_2^*$  from Eq. B1.122
6. Compare the assumed value  $z_2^0$  to  $z_2^*$
7.
  - a) If the difference is smaller than a pre-set error tolerance, the calculated values are accepted as the final result
  - If the difference is too large, a new assumption for  $z_2$  is found from  

$$z_2^1 = z_2^{i-1} + (z_2^* - z_2^{i-1})f$$
where  $f$  is a factor that from experience should give a fast convergence. For most cases of practical interest 0.3 is recommended.

### B1.4.3.3 Stiffened catenary

The stiffened catenary method is probably the most successful attempt to find an approximate solution to the shape of a slender beam lifted at one end from a horizontal plane. The method was originally suggested by [Plunkett, 1967] and later applied by [Dixon and Rutledge, 1968] to find the configuration and stresses in a pipeline suspended between the sea floor and an inclined ramp that is free to rotate and hence give a moment free upper end of the pipeline. These boundary conditions are identical to the ideal conditions for a catenary riser, which means that the method should be well suited to analyse this type of structure. The method is limited to analyse a uniform beam loaded by its own weight only. Varying cross section, buoys or current forces can therefore not be considered. [Larsen, 1976] extended the method to account for a constantly curved stinger as frequently applied for pipelaying. A detailed discussion on the limitations of the method is also found in this reference. The theoretical foundation of the method will be briefly outlined in the following. The catenary riser in its simplest version may be described as a beam with small bending stiffness loaded by its own weight only. The idea of the stiffened catenary solution is that the bending stiffness causes secondary effects in boundary regions only, and that the deviation from the simple catenary solution can be found as a rapidly converging series expansion.

Figure B1.43 shows a beam element. The moment equilibrium of this element is seen to be given by:

$$\frac{dM}{ds} = H \cos \theta - V \sin \theta \quad (\text{B1.123})$$

where  $s$  is a length coordinate following the pipe axis and have its origo at the touch-down point. Notations are defined in Figure B1.44

By introducing the well-known moment - curvature relationship

$$M = -EI \frac{d\theta}{ds} \quad (\text{B1.124})$$

to Eq. B1.122, we have:

$$EI \frac{d^2\theta}{ds^2} + H \cos \theta - V \sin \theta \quad (\text{B1.125})$$

A non-dimensional curve coordinate  $z$  is introduced. At the point where  $z = 0$  we have zero vertical force in the beam. At upper end  $z = 1$ , and at the touch-down point  $z = z_0$  where  $z_0$  is unknown, but always negative. All global beam parameters are defined in Figure B1.48.

Eq. B1.125 is made non-dimensional by introducing the  $z$  coordinate and the following non-dimensional parameters:

$$m = \frac{ML}{EI} = -\frac{d\theta}{dz}; h = \frac{H}{wL}; \alpha^2 = \frac{EI}{wL^3} \quad (\text{B1.126})$$

$L$  is the (unknown) length between the point on the beam where  $V = 0$  and upper end, and  $w$  is the submerged weight per unit length of the beam. Hence,  $wL$  is equal to the vertical force at upper end of the beam. Eq. B1.125 can now be written as:

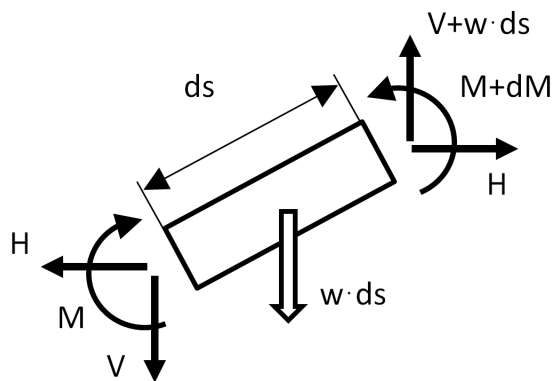


Figure B1.47: Element in suspended beam

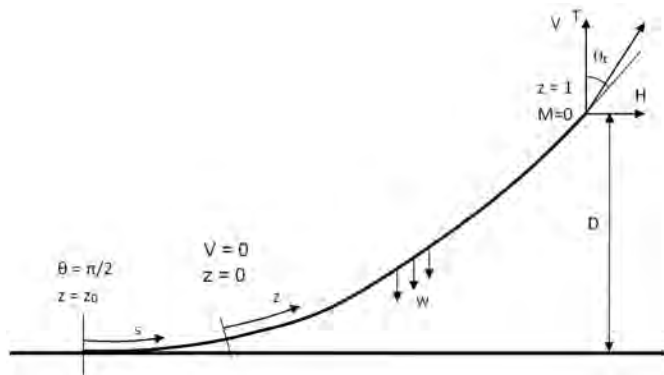


Figure B1.48: Global beam configuration and definition of boundary conditions

$$\alpha^2 \frac{d^2\theta}{dz^2} + h \cos \theta - z \sin \theta = 0 \quad (\text{B1.127})$$

An approximate solution to this equation that satisfies the actual boundary conditions was found by [Plunkett, 1967] and given as

$$\theta(z) = \tan^{-1} \left( \frac{h}{z} \right) - \frac{\alpha}{h^{\frac{3}{2}}} \left[ -\frac{1}{\alpha} q_1(z) \right] + \frac{\alpha h}{(h^2 + 1)^{\frac{5}{4}}} \exp \left[ -\frac{1}{\alpha} q_2(z) \right] \quad (\text{B1.128})$$

$q_1$  and  $q_2$  are functions found by integration from lower and upper end respectively. These integrals are given by

$$\begin{aligned} q_1(z) &= \int_{z_0}^z (x^2 + h^2)^{\frac{1}{4}} dx \\ q_2(z) &= \int_z^1 (x^2 + h^2)^{\frac{1}{4}} dx \end{aligned} \quad (\text{B1.129})$$

The first term of Eq. B1.128 is recognized as the classical catenary equation. The second term gives the correction to this solution from bending stiffness of the beam suspended between the actual point  $z$  and the seafloor, while the third term introduces the influence from bending in the upper part of the beam.

The accuracy of the method depends on how well the influence from bending is described by these two terms. [Plunkett, 1967] has shown that the series these terms are developed from are absolutely convergent if two conditions are satisfied:

$$\begin{aligned} 0 &\leq \alpha^2 \leq 1 \\ \alpha^2 &< h^3 \end{aligned} \quad (\text{B1.130})$$

Eq. B1.128 gives the angle at any position along the beam as function of a set of non-dimensional coefficients. Coordinates may then be found by a simple numerical integration procedure. For the case that the horizontal force at upper end is known, the coefficients are seen to depend on two unknowns,  $L$  and  $z_0$ . These are found from a nonlinear relation between the vertical distance from upper end to bottom,  $D$ , and the characteristic length  $L$ :

$$\frac{D}{L} = \sqrt{h^2 + 1} - \sqrt{h^2 + z_0} + \alpha^2 \left[ \frac{1}{\sqrt{h} \cdot (h^2 + z_0)^{0.75}} - \frac{h^2}{(h^2 + 1)^2} \right] \quad (\text{B1.131})$$

In addition the following relation for  $z_0$  is valid:

$$z_0 = -\frac{\alpha}{\sqrt{h}L} \quad (\text{B1.132})$$

Eq. B1.131 can be solved for the unknown length  $L$  by a standard iterative procedure. All non-dimensional parameters are then available and the angle  $\theta$  can be calculated from Eq. B1.128 and Eq. B1.129 at any position. It can also be shown that the angle at upper end of the riser is given by:

$$\theta_t = \tan^{-1}(h) + \frac{\alpha h}{(h+1)^{1.25}} \quad (\text{B1.133})$$

While the horizontal force is constant along the entire length of the riser, the vertical force can be found by:

$$V(z) = w \cdot L \cdot z \quad (\text{B1.134})$$

Total force, axial force and shear force can now be found from well known relationships:

$$\begin{aligned} T &= \sqrt{V^2 + H^2} \\ A &= H \cos \theta + V \sin \theta \\ Q &= V \cos \theta - H \sin \theta \end{aligned} \quad (\text{B1.135})$$

Note that the axial force found from this equation is the so-called effective axial force and not the axial stress resultant.

### B1.4.4 Loads from internal fluid flow

Non-stationary internal fluid flow will cause time varying forces in a flexible riser, and hence also lead to structural vibrations. It is also well known that riser dynamics may influence internal flow. This means that riser dynamics and internal flow should be analysed by use of an integrated simulation model. Such models have been published, but are normally not used for riser design. Three cases of influence from internal flow will be discussed in the following:

- Stationary flow in a pipe with constant internal diameter
- Slug flow; quasi static, dynamic, and coupled riser dynamics/flow models
- High frequency vibrations

#### B1.4.4.1 Stationary flow in a pipe with constant internal diameter

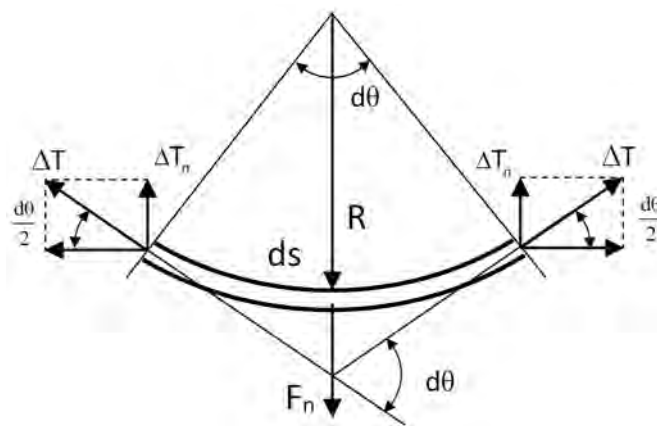


Figure B1.49: Geometry and forces in a pipe segment with stationary internal flow

Figure B1.49 shows a pipe segment with length  $ds$ . The segment has a radius of curvature of  $R$ , the density of the fluid is  $\rho_i$ , internal cross section is  $A_i$ , and the flow velocity is  $u$ . The acceleration related to the change of flow direction in the bend will lead to a force acting outwards and perpendicular to the tangent to the pipe. The magnitude of the force on this segment will be given by

$$F_n = \rho_i A_i u^2 \frac{ds}{R} \quad (\text{B1.136})$$

This force must be counteracted by a change of pipe forces. If we neglect the shear forces – which normally is a valid assumption for flexible risers – we realize that the vertical component of tension increase must be given by

$$\Delta T_n = \frac{F_n}{2} \quad (\text{B1.137})$$

Since we are dealing with small angles  $d\theta$ , we can write

$$\Delta T = \frac{2 \Delta T_n}{d\theta}, \quad d\theta = \frac{ds}{R} \quad (\text{B1.138})$$

By combining these equations we can see that tension increase from a stationary flow becomes independent of the curvature:

$$\Delta T = \rho_i A_i u^2 \quad (\text{B1.139})$$

The consequence of this equation is that stationary internal flow does not influence the shape of a riser. During an acceleration or deceleration period there will be a transient dynamic response, but the shape of the riser will be the same before and after these transient periods. The only exception is related to possible cross section effects from varying pressure.

We have two options for including the effect from a stationary fluid flow in a static analysis:

1. Neglect the lateral forces in the analysis, but calculate axial stress resultant from the relationship

$$T_\sigma = T_e - p_e A_e + p_i A_i + \rho_i A_i u^2 \quad (\text{B1.140})$$

where  $T_e$  is the effective axial force that is a result from the static analysis when effective weight is applied.

2. Include the lateral forces according to Eq. B1.136, but increase the effective axial force according to Eq. B1.139. Note that this method will give lateral forces that depend on the deformations, which may cause problems for an iterative search for static equilibrium. If this approach is applied the axial stress resultant must be calculated as

$$T_\sigma = T'_e - p_e A_e + p_i A_i = T_e + \rho_i A_i u^2 - p_e A_e + p_i A_i \quad (\text{B1.141})$$

The two methods will lead to identical results both with regard to shape and axial stress, but the first method should be preferred for ordinary riser analyses. For further details see [Back-Pedersen, 1991].

#### B1.4.4.2 Slug flow; quasi-static model

A slug with total mass  $M_s$  travels through a flexible pipe at constant velocity  $v_s$ . An approximate solution for this case can be found by use of a quasi static model, see [Fylling et al., 1988].

Figure B1.501 shows the static shape of the pipe without slug.

The radius of curvature at the position with horizontal tangent is given by

$$R_0 = \frac{H_0}{w_e} \quad (\text{B1.142})$$

where  $H_0$  is the horizontal force in the pipe and  $w_e$  is the effective pipe weight per unit length. At the instance of time when the slug with a length of  $l_s$  and total mass of  $q_{sl}s$  passes the point on the pipe with horizontal tangent, there will be a vertical force  $F_s$  from the slug given by

$$F_s = q_{sl}s = m_s \left( g + \frac{v_s^2}{R_0} \right) l_s \quad (\text{B1.143})$$

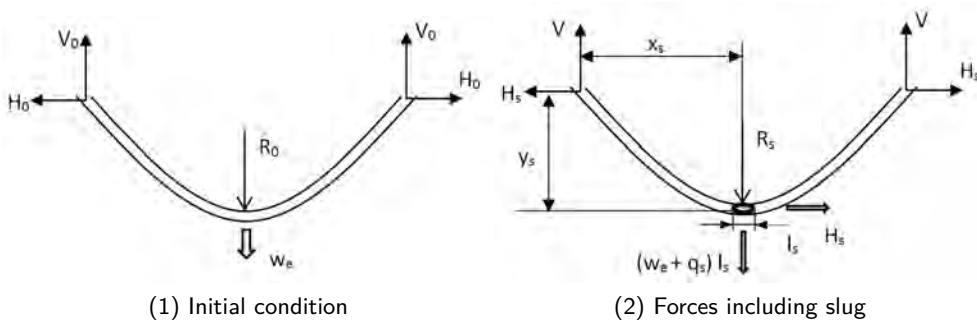


Figure B1.50: Quasi static slug model

The horizontal force  $H$  at this point must increase since the moment must be zero at the end support:

$$H_s = H_0 + q_s l_s \frac{x}{z} \quad (\text{B1.144})$$

The curvature in the sag bend during the slug passage can now be approximated by:

$$R_s = \frac{H_s}{w_s}; \quad w_s = w_e + q_s = w_e + m_s \left( g + \frac{v_s^2}{R_0} \right) \quad (\text{B1.145})$$

The bending moment relative to the static bending moment can be expressed by the ratio of the curvature radii:

$$\frac{M_{slug}}{M_{static}} = \frac{R_0}{R_s} \quad (B1.146)$$

#### B1.4.4.3 Slug flow; simple dynamic model

A simplified analysis of slug flow can be carried out as a non-linear time domain analysis with prescribed slug velocities through the pipe. The mass matrix must be updated according to the defined slug position at every time step in the simulation, and forces from gravity and centripetal acceleration must be added to other force contributions. This type of analysis is available in the RIFLEX computer program.

Formally the following equation is solved

$$\mathbf{M}(t) \ddot{\mathbf{r}} + \mathbf{C} \dot{\mathbf{r}} + \mathbf{K}(t) \mathbf{r} = \mathbf{F}(t) \quad (\text{B1.147})$$

The forces are illustrated on Figure B1.51.

Note that both curvature and inclination must be found at the slug position in order to calculate the centrifugal force component. The gravity force from the slug mass must also be added to the ordinary force vector. The travelling mass will not introduce these forces by the inertia term in Eq. B1.147, since the mass matrix takes care of inertia effects from structural acceleration only. A Coriolis' force term may also be relevant for cases with high velocities combined with large pipe response, see [Fylling et al., 1995].

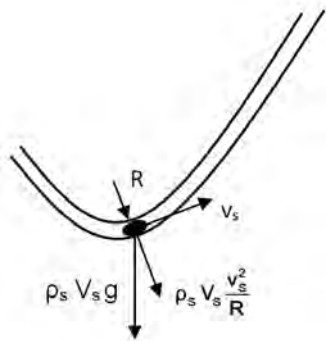


Figure B1.51: Travelling slug in a flexible pipe

#### B1.4.4.4 Advanced slug-flow model

It is well known that slug flow will give vibrations, but also that dynamic changes of the pipe geometry will have an influence on the slug flow development. Hence, in order to analyse this type of fluid-structure interaction, an integrated simulation of slug flow and mechanical vibrations should be carried out. A program system based on this principle is described by [Ortega et al., 2012]. The system consists of one program for calculation of two-phase slug flow dynamics, and another program for dynamic response of risers. Both programs apply a time integration method, but the two codes need to exchange information during the integration process. Information exchange is established by making a federation based on High Level Architecture (HLA). The flow code computes the flow development in a flexible pipe spanning between two fixed ends. The input flow at one end must be defined, and also the position at discrete points along the suspended riser. This program applies a Lagrangian tracking model for slugs that are considered as objects in the flow model. The liquid slugs are treated as incompressible units whereas the gas bubbles are treated as compressible units, see Figure B1.52.

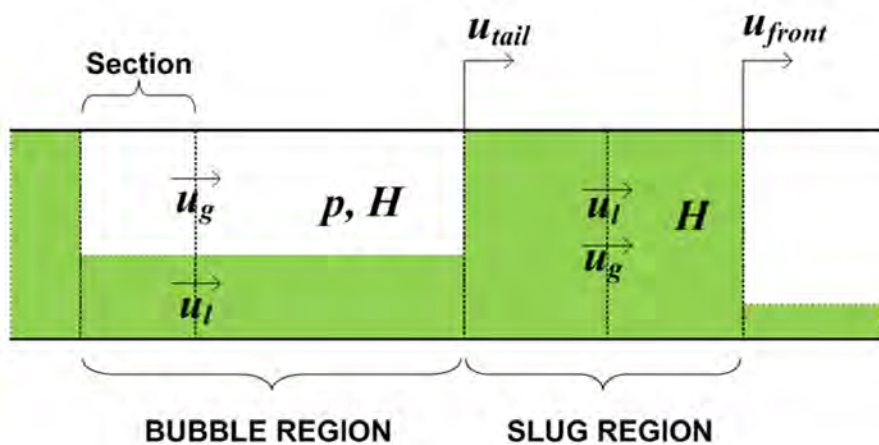


Figure B1.52: Definition of slug and bubble regions

Riser dynamics is computed by a computer program based on a finite element formulation. This program may also account for wave loads and end motions from a floating vessel. By use of the HLA standard, these two programs can carry out synchronized time integration

and exchange information for each time step.

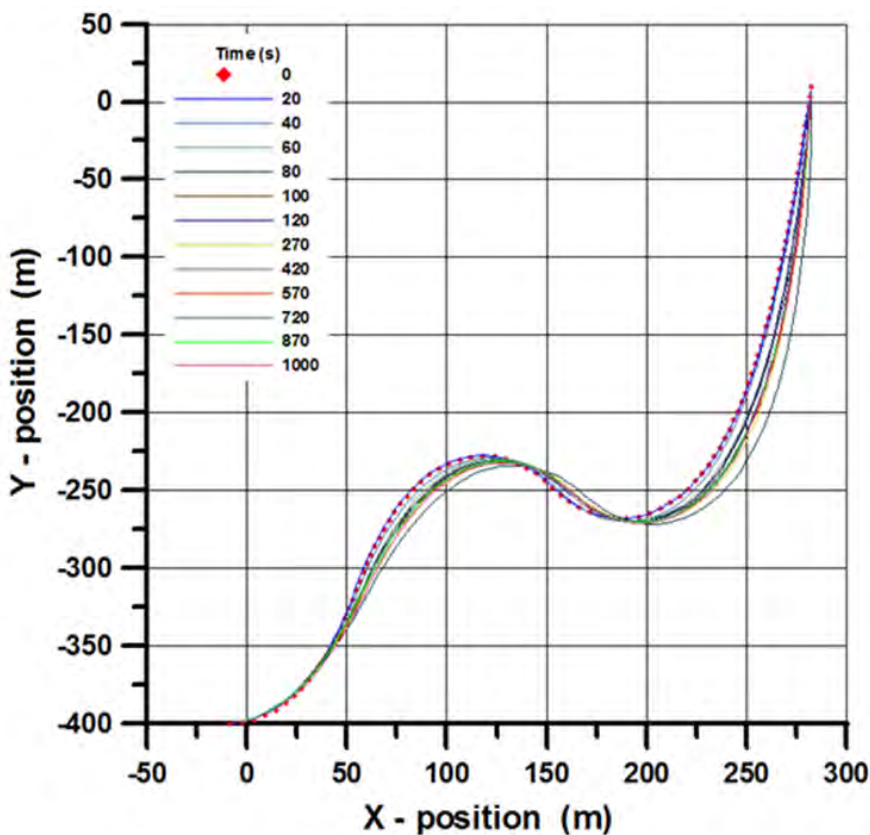


Figure B1.53: Snapshots if flexible riser subjected to slug flow. From [Ortega et al., 2012]

Figure B1.53 shows snapshots of the geometry for a lazy wave flexible riser. The oscillations are caused by slug flow only. The dynamic response is seen to be significant, and is caused by change of gravity forces from oil and gas inside the riser, and the time varying inertia forces from the internal flow. This type of analysis can be used to study the influence on riser stresses from slug flow, but also how the two-phase flow is influenced by riser dynamics in a situation with waves and vessel motions. Examples of results from coupled analyses are presented in Figure B1.54. Further details are given by [Ortega et al., 2013].

#### B1.4.4.5 Singing risers

Flexible risers will often have a corrugated inner liner. The offshore petroleum industry has experienced 'singing risers', which is a loud whistling sound followed by unexpected vibrations in the fixed pipe system coupled to the riser. This phenomenon is caused by a complex interaction between fluid dynamics (vortex shedding), acoustics (pressure propagation) and structural vibrations (response in rigid pipe system). Experiments and numerical models have been applied to increase the insight and establish guidelines from first principles, but there are still unanswered questions. The only safe way to avoid this type of unwanted response has in some cases been to limit the gas flow speed, which of course is an unwanted situation. Key results from a large research project at SINTEF are presented by [Reinen, 2008]. Figure B1.55 illustrates an experiment by [Kristiansen et al., 2011] that investigated vortex formation and pressure propagation in a corrugated pipe.

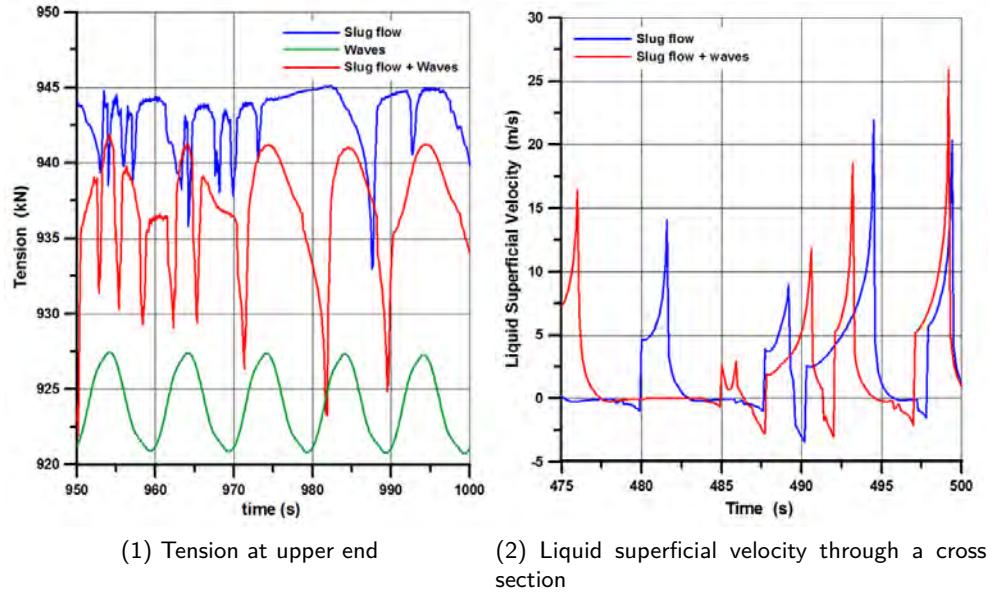


Figure B1.54: Results from integrated analysis of flexible riser subjected to slug flow and wave effects

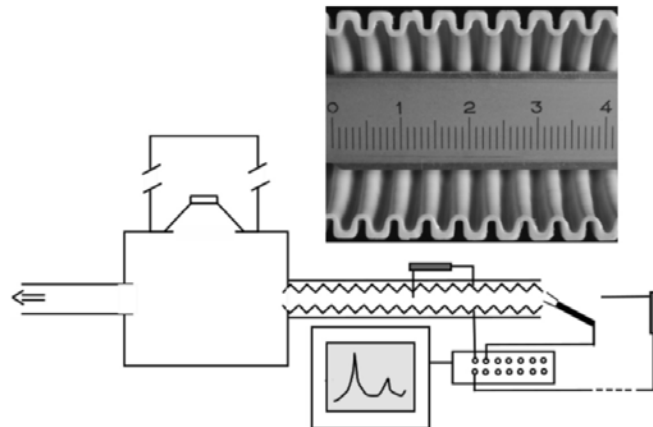


Figure B1.55: Experimental investigation of 'singing riser'

## B1.4.5 External loads

### B1.4.5.1 Introduction

External loads from waves and current on slender structures can be defined without accounting for the influence from the structure on the incoming flow (diffraction). This means that the loads can be found from Morison's equation. Key features of this load model are:

- The force has one drag term linked to the projected area of the cylinder, and one inertia term linked to the volume.
- Drag forces are non-linear and must be calculated from the relative velocity. In its simplest one-dimensional form this equation reads:

$$F_D = \frac{1}{2} \rho_w C_D D |v_w - v_s| (v_w - v_s) dL \quad (\text{B1.148})$$

where

$FD$  Drag force on a section with length  $dL$

$\rho_w$  Density of water

$D$  Diameter of cylinder

$v_w$  Velocity of water

$v_s$  Velocity of structure

- Inertia (volume) forces are linear and have contributions from the Froude–Krilloff term (undisturbed fluid flow, follows fluid acceleration) and one term from the presence of the structure (follows relative acceleration):

$$\text{Froude-Krilloff term : } F_{FK} = \rho_w \frac{\pi D^2}{4} a_{w,N} dL \quad (\text{B1.149})$$

$$\text{Presence of structure: } F_S = \rho_w C_M \frac{\pi D^2}{4} (a_{w,N} - \ddot{r}_{s,N}) dL \quad (\text{B1.150})$$

where

$F_{FK}$  Froude–Krilloff force

$a_{w,N}$  Acceleration of fluid perpendicular to pipe axis

$\ddot{r}_{s,N}$  Acceleration of structure perpendicular to pipe axis

$C_M$  Added mass coefficient; 1.0 for circular cross section

These force components are normally reformulated to an added mass term in the mass matrix in a finite element model, and an external force term in the load vector:

$$\begin{aligned} \text{Added mass: } & \rho_w C_M \frac{\pi D^2}{4} dL \\ \text{External force: } & \rho_w (C_M + 1) \frac{\pi D^2}{4} a_{w,N} dL \end{aligned} \quad (\text{B1.151})$$

In addition to these components that always will be present in waves, there might also be forces related to vortex induced vibrations (VIV) or slamming. VIV is normally assumed to be initiated by current while slamming forces may occur on partially submerged pipe sections in very steep waves.

### B1.4.5.2 Flow characteristics

Morison's equation contains the empirical coefficients  $CD$  and  $CM$ . These depend on the flow condition normally characterised by the non-dimensional parameters Reynolds number,

Keulegan-Carpenter number and the frequency parameter  $\beta$ , and also cross section shape and surface roughness. The non-dimensional parameters are defined by

$$\text{Re} = \frac{uD}{\nu}; \quad KC = \frac{u_a T}{D}; \quad \beta = \frac{\text{Re}}{KC} = \frac{D^2}{\nu T} \quad (\text{B1.152})$$

where  $\nu$  is the kinematic viscosity of the fluid,  $u_a$  is the amplitude of a periodic wave induced velocity and  $T$  is the wave period. For fresh water at 20°C the value of  $\nu$  is  $1.01 \cdot 10^{-6} \text{ m}^2 \text{s}^{-1}$ .  $\text{Re}$  originates from the ratio of inertia force and viscous force, while  $KC$  represent a memory effect from the ratio of a characteristic traveling amplitude for a fluid particle and the diameter of the cylinder. Large  $KC$  values define a flow situation similar to current, which means that a vortex shed from the cylinder will never return to the cylinder.

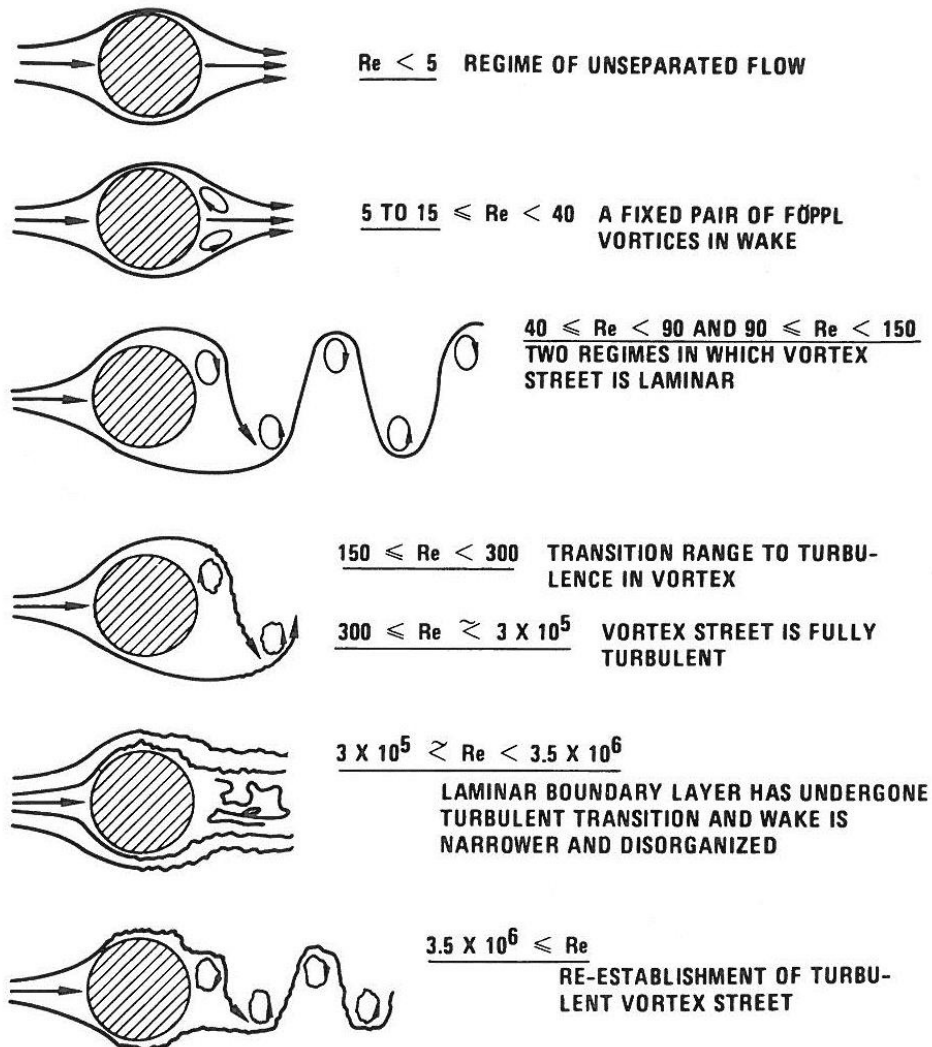


Figure B1.56: Vortex shedding patterns for varying  $\text{Re}$ , from [Lienhard, 1966] as reported by [Blevins, 1990]

Figure B1.56 illustrates the vortex shedding patterns for varying Reynolds number. The three regimes of interest for flexible risers are the stable subcritical regime ( $10^4 < \text{Re} < 3 \cdot 10^5$ ), the critical regime ( $3 \cdot 10^5 < \text{Re} < 3 \cdot 10^6$ ) and the super-critical regime ( $\text{Re} > 3 \cdot 10^6$ ). The transition between sub-critical and critical regimes is caused by the boundary layer, which changes from laminar to turbulent. Most model tests will be carried out in the subcritical

regime, while full scale structures often will experience super-critical conditions. This makes the use of model tests for investigating the behaviour of slender structures like flexible risers questionable. Figure B1.57 shows the variation of the drag coefficient for a smooth cylinder with Reynolds number. Note that both axes are logarithmic. The drag coefficient is seen to drop considerably in the critical flow regime. The critical regime is therefore often referred to as 'the drag crisis'.

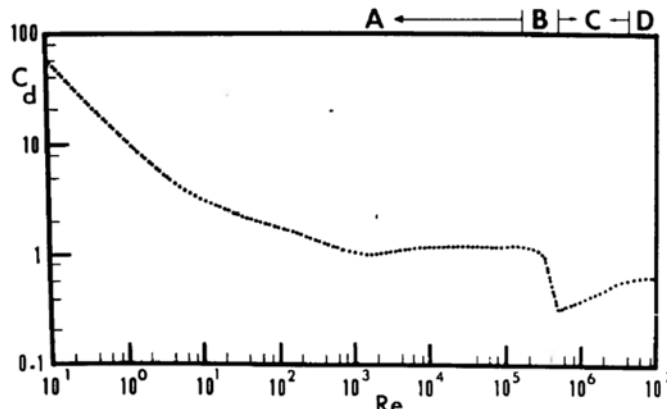


Figure B1.57: Drag coefficient for a circular cylinder as function of  $Re$ , [Sarpkaya and Isaacson, 1981]

The added mass coefficient will not show large variations with  $Re$  to the same extend as the drag coefficient. The reason is that added mass is less influenced by viscous effects than drag. However, when it comes to KC number and the  $\beta$  parameter, both CM and CD will be influenced. This is illustrated in Figure B1.58. These curves can be applied in a time domain simulation of structures subjected to current and waves.

#### B1.4.5.3 Cross-section shapes and surface roughness

Since the transition from sub-critical to critical flow is followed by transition from laminar to turbulent boundary layer, surface roughness will have an influence. Roughness will initiate turbulence for lower  $Re$  values than seen for a smooth surface. Figure B1.59 illustrates this effect, but also the trend to give less drag reduction within the 'drag crisis'. Large roughness will completely eliminate drag reduction, which is the reason for not apply reduced drag coefficients in design analyses. The drag coefficient will depend on the shape of the cross section, which is illustrated on Figure B1.60.

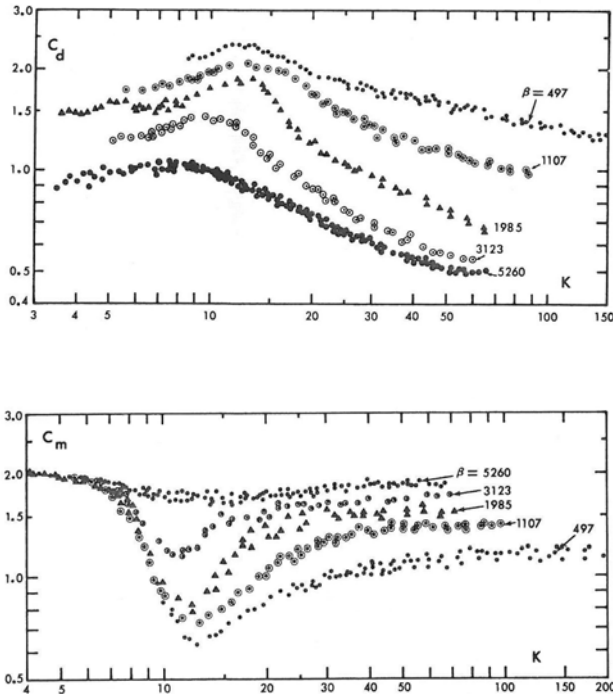


Figure B1.58: Variation of added mass and drag coefficients for varying KC and  $\beta$ , ref. [Sarpkaya and Isacson, 1981]

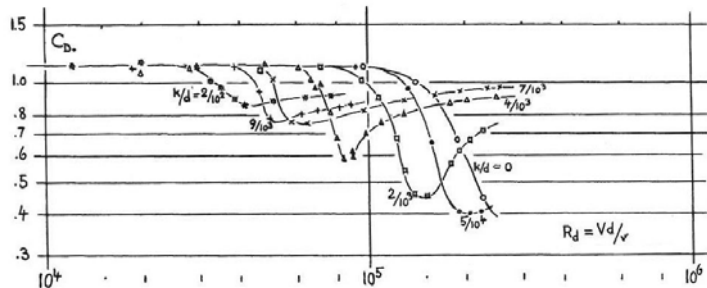


Figure B1.59: Influence of roughness on  $C_d$ , ref. [Hoerner, 1965]

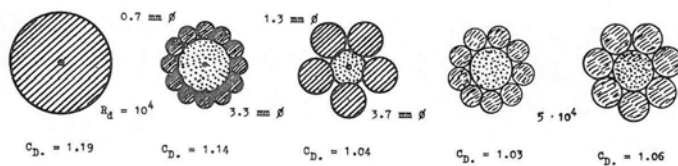


Figure B1.60: Drag coefficients for typical cross sections, ref. [Hoerner, 1965]

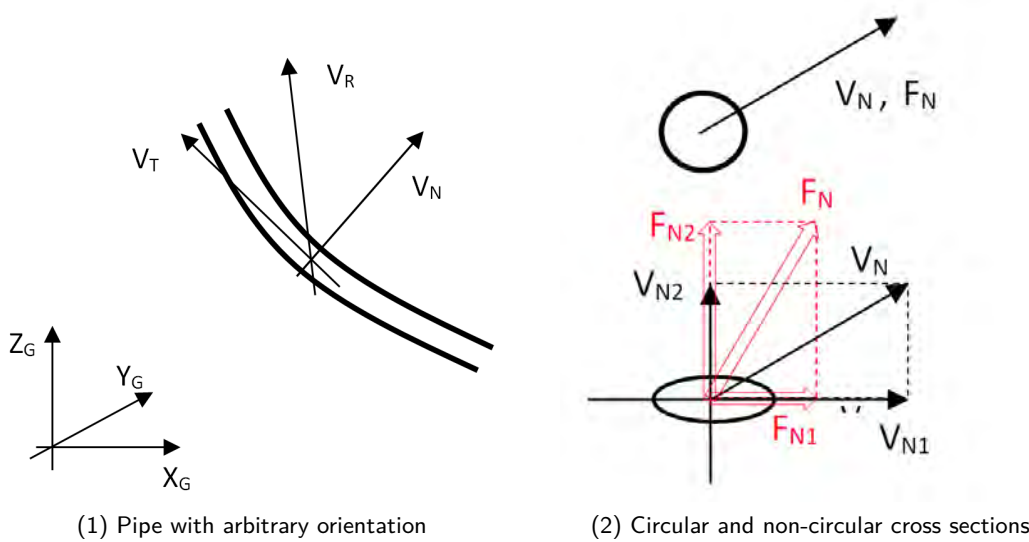


Figure B1.61: Force components from current

#### B1.4.5.4 Forces from current, static analysis

The direction of incoming flow can be arbitrary relative to the orientation of the structure, but it will always be possible to define a local coordinate system with a tangential and a normal flow component as illustrated in Figure B1.61. Calculation of drag from the normal flow component is referred to as the 'cross-flow principle' and is an established standard for slender structure. If the cross section is circular, the normal flow component will give a load component in the same direction as the flow. However, for non-circular cross sections one must normally know the drag coefficient for specific flow directions given by symmetry properties as illustrated in B1.61. This leads to different drag force equations for the two types of cross sections:

Circular cross section: Drag force will act in the direction of the normal flow component:

$$F_N = \frac{1}{2} \rho_w C_D D |v_N| v_N dL \quad (\text{B1.153})$$

Non-circular cross section with two symmetry axes

$$\begin{aligned} F_N &= \sqrt{F_{N1}^2 + F_{N2}^2} \\ F_{N1} &= \frac{1}{2} \rho_w C_{D1} D_1 |v_{N1}| v_{N1} dL \\ F_{N2} &= \frac{1}{2} \rho_w C_{D2} D_2 |v_{N2}| v_{N2} dL \end{aligned} \quad (\text{B1.154})$$

An alternative to the above equation for non-circular cross sections is to have direction dependent drag and lift coefficients, which normally is not the case.

It is easy to realize that if we apply (B1.154) to a circular cross section we will have a force resultant different from what (B1.153) gives. We must therefore apply different sets of equations for the two classes of cross sections. A non-symmetric cross section in constant

current will be exposed to the so-called Munk moment that will lead to torque in the riser. The moment can be calculated from the following equation:

$$M_{Munk} = \rho_w v_{N1} v_{N2} (\pi C_{M1} D_1^2 + \pi C_{M2} D_2^2) dL \quad (B1.155)$$

where CM1 and CM2 are the added mass coefficients for orthogonal symmetry axes. Other parameters are defined in Figure B1.62

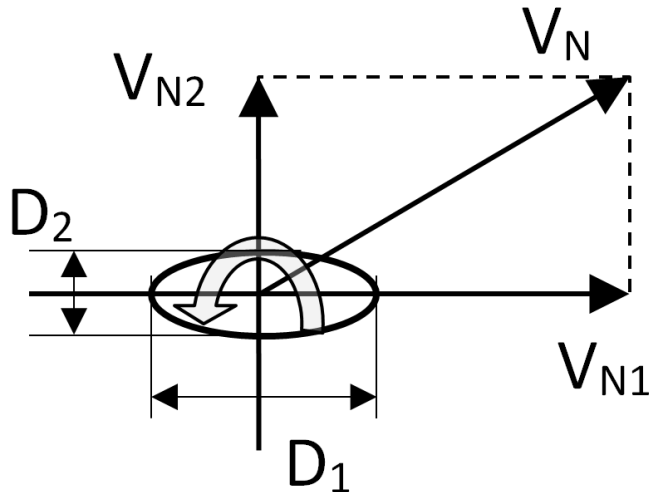


Figure B1.62: Munk moment

Tangential drag forces are in particular important for long risers with large dynamic axial displacements. Catenary riser linked to a floater with large heave motions is a typical example. The tangential force on a pipe section with length  $dL$  can be calculated from the following equation:

$$F_T = \frac{1}{2} C_{Dt} \rho_w D v_R^2 dL \quad (B1.156)$$

$$C_{Dt} = C_D (0.03 + 0.55 \sin \alpha) \cos \alpha$$

where  $\alpha$  is the angle between the pipe tangent and vector of relative velocity  $v_R$ . The force is seen to be zero if the flow is perpendicular to the pipe, and 3% of the ordinary drag force for zero angles. The tangential drag force will depend on surface and shape parameters that are not accounted for in this equation, but the equation should give reasonable values of tangential drag forces for ordinary flexible pipes. Buoyancy elements on a riser will have a strong influence on drag forces. The flow will become more three-dimensional, and the cross-flow principle becomes questionable. A commonly used simplification is still to apply the cross-flow principle and calculate the lateral drag force from the normal velocity component:

$$F_N = \frac{1}{2} C_D \rho_w D_H |v_N| v_N dL \quad (B1.157)$$

$v_N$  is the normal velocity component and DH is a hydrodynamic diameter that gives a correct projected area of the riser section with buoyancy modules, see Figure B1.63.

The drag coefficient should be taken as for ordinary circular cross sections unless data from tests of the actual design is available.

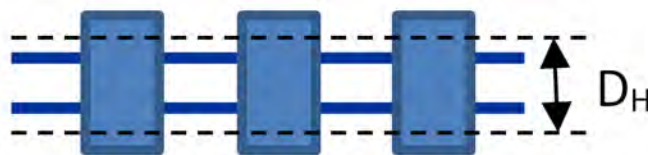


Figure B1.63: Definition of the hydrodynamic diameter  $D_H$

Tangential drag is more complicated since there will be a strong interaction between the individual buoyancy elements. [Huse and Reitan, 1990] carried out a set of experiments with buoyancy elements as shown on Figure B1.64.

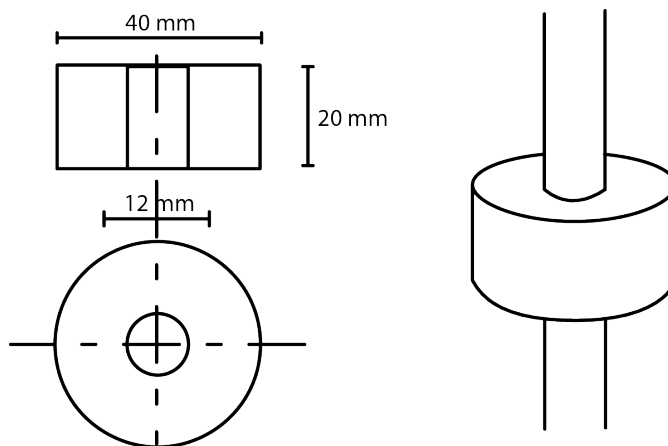


Figure B1.64: Buoyancy element used in MARINTEK tests [Berge et al., 1992]

A varying number of such elements were mounted on pipe segments with varying spacing. Tests with one element were used as a reference, and results were used to find the effective tangential drag coefficient for segments with  $N$  modules. Figure B1.65 shows the results for tests with one buoyancy module as function of the KC number. Large KC values can be considered to be valid for current.

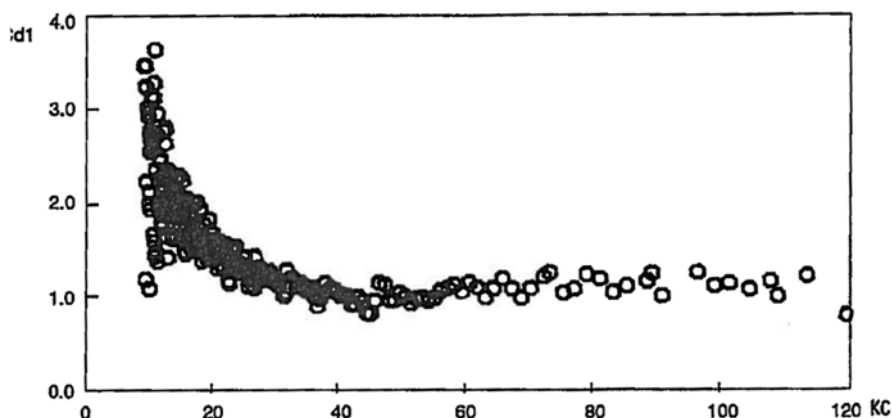


Figure B1.65: Tangential drag coefficient for pipe with one buoyancy module [Berge et al., 1992]

Figure B1.66 show the interaction coefficient  $I_B$  as function of KC, spacing between modules

SB relative to the diameter of the buoyancy module. Figure B1.67 illustrates how  $N_B$  can be defined from the geometry of the riser, and the parameters that defines the geometry parameters.

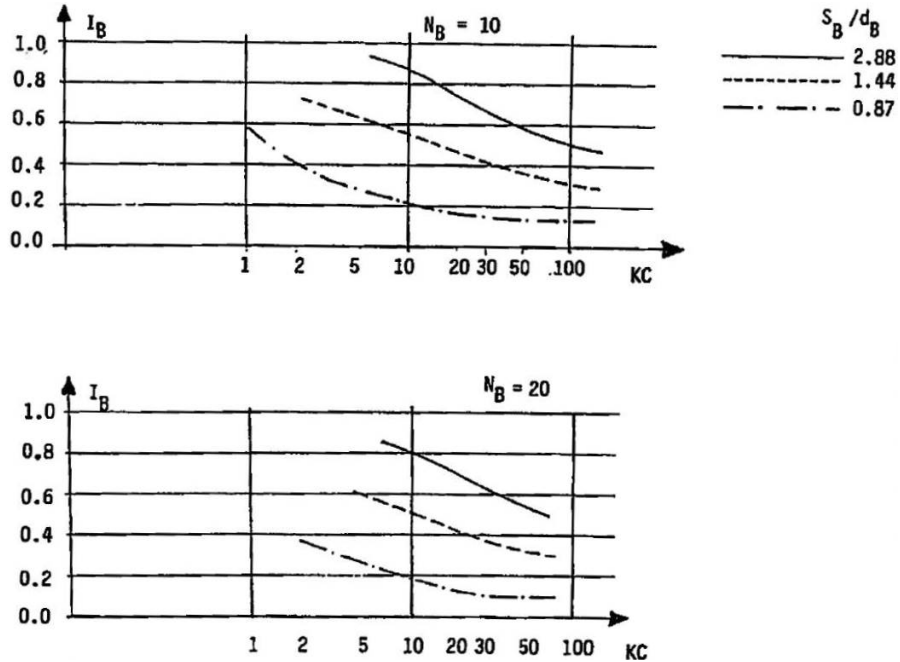


Figure B1.66: Interaction coefficient  $I_B$  as function of KC number, spacing and number of modules [Berge et al., 1992]

The use of these results in a practical analysis can be described in steps as follows:

1. Define segment length,  $L_B$  and number of modules in each segment, see Figure B1.67
2. Find the coefficient valid for one module,  $C_{D1}$ , from Figure B1.65 . Note that the values on this figure is strictly valid for the actual design of the tested buoyancy module
3. Find the interaction coefficient  $I_B$  for each segment based on number of modules, spacing and actual KC number. Large KC values are valid for static cases with current

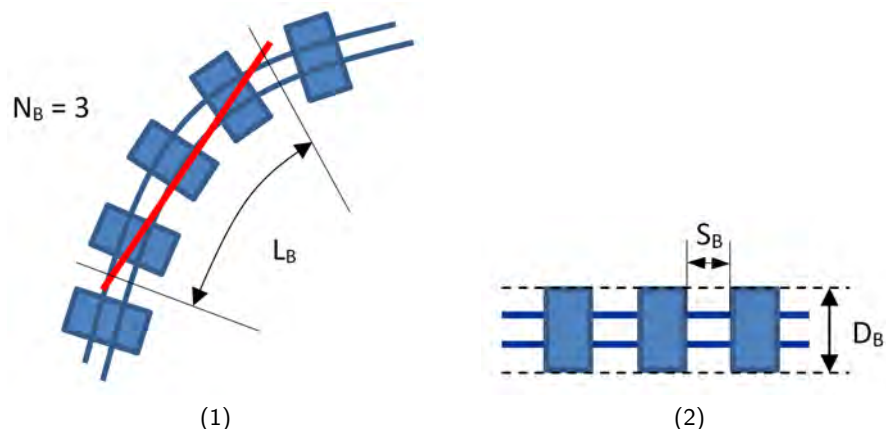


Figure B1.67: Definition of parameters for riser with buoyancy modules

4. Calculate the coefficient that defines the tangential force on the segment from

$$C_{DT,N} = C_{D1} N_B I_B \quad (\text{B1.158})$$

5. Calculate the tangential drag coefficient to be used for calculation of force on an element in the actual segment from

$$C_{DT} = C_{DT,N} \frac{\pi D_B^2}{4 D_H L_B} \quad (\text{B1.159})$$

where  $D_H$  is the hydrodynamic diameter to be used in the final force calculation

6. Calculate the force on an element with length  $dL$  from

$$F_T = \frac{1}{2} C_{DT} \rho_w D_H |v_T| v_T dL \quad (\text{B1.160})$$

#### B1.4.5.5 Wave Models

Most riser analyses will deal with stochastic waves, but regular waves may still be applied in some cases. Aspects of stochastic analysis will be discussed in Section B1.4.8, but some comments regarding modelling of waves will be given here.

Regular waves are often represented by the linear Airy wave theory [Airy, 1845]. This theory is valid for an infinitesimal wave height. The solution is therefore inconsistent in the sense that it describes the motion of a water particle without accounting for its change of position in the fluid. The theory can therefore not give values for flow velocity or acceleration in a wave crest, and the absence of fluid between mean water level and a wave trough is not formally described. Extrapolation of the wave potential in a wave crest - either by use of the exponential function, linear extrapolation or by using the surface values to give a constant profile in the crest - is in general not recommended since wave forces will become overestimated. A better way to improve the theory is to apply Wheeler stretching [Wheeler, 1970] or to move the profile for pressure, velocity and acceleration to the instantaneous sea surface, see Figure B1.68.

Irregular waves are normally described by a summation of linear wave components. Extrapolation of the individual wave components to instantaneous free surface will give meaningless results. Wheeler stretching or move of profiles similar to what is suggested for regular waves is a reasonable way to improve load calculation.

There exist a large number of wave theories that represent improvements of the simple Airy theory. Stokes non-linear theory [Stokes, 1847] has later been solved to 5<sup>th</sup> order [Skjelbreia and Henderson, 1961]. The wave potential is solved to the actual free surface to fifth order, and the result is a wave profile that is asymmetric: the wave crest is far steeper than the wave trough, and the theory can predict accelerations and velocities to the actual free surface. This wave model should always be preferred for regular wave cases. Irregular waves are normally described by summation of linear wave components. A theory for describing irregular waves to second order exist and might be applied in riser analysis [Mei, 1983].

A better description of near breaking waves is the Stream function theory [Dean, 1965]. The Solitary wave theory [Munk, 1949] gives a good representation of waves in the surf zone, and predicts a wave that do not have a trough but travles above mean water level only. A periodic shallow water wave is described by the Cnoidal theory [Korteweg and Vries, 1895].

An important feature of linear wave theory is that there will not be any mass transport of water. This is in contrast to theories of higher order, and also to observations of ocean waves. Wheeler stretching will give a mass transport, while moving the velocity profile to actual free surface will not - at least not for deep water waves. The difference between these two methods will in most cases be minor.

A good description of wave theories for engineering applications is given by [Dean and Dalrymple, 1984].

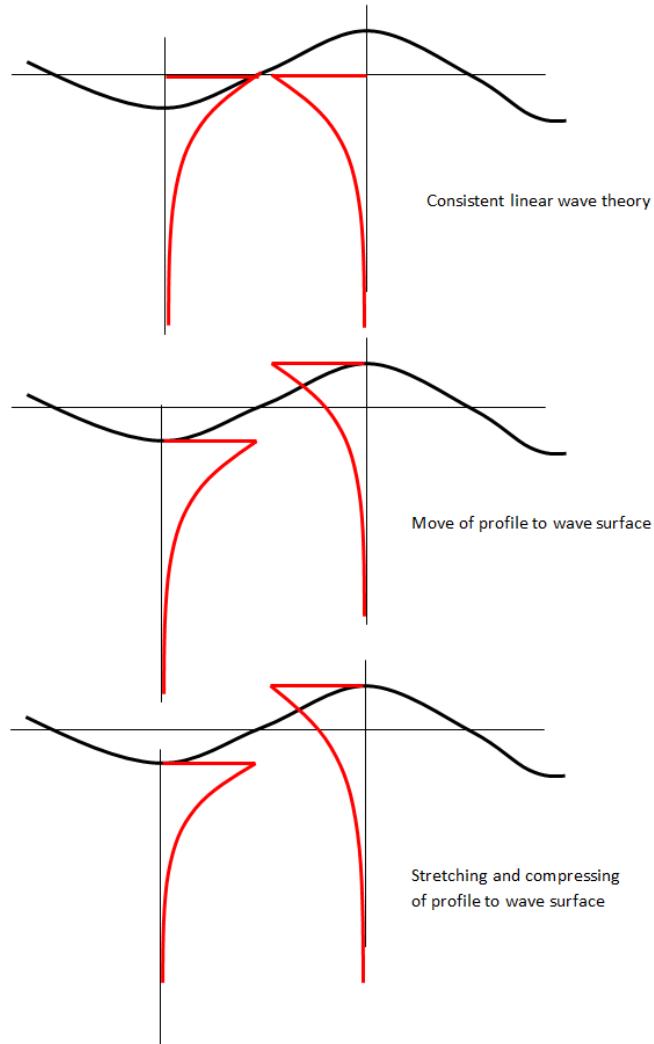


Figure B1.68: Use of linear wave theory to describe profiles to true surface

#### B1.4.5.6 Forces from waves; dynamic analysis

Due to direct wave actions and top end excitation from wave induced floater motions, marine risers will be subjected to oscillatory fluid flow. A considerable effort has been made over the last decades to develop practical load models for slender structures. Models based on

numerical methods for fluid forces - often referred to as computational fluid dynamics (CFD) - are available, but not as a tool for engineers due to extreme computing time. Morison equation with constant coefficients is the only model in common use, and uncertainties with regard to coefficients are accounted for by sensitivity analyses and safety factors, confer [Lienhard, 2010].

The general equation for the lateral hydrodynamic force on a slender member can be written as

$$F_{N,H}(\ddot{r}_N, a_{N,w}, v_{N,rel}) = [-C_M \frac{\pi D_V^2}{4} \ddot{r}_N + (C_M + 1) \frac{\pi D_V^2}{4} a_{N,w} + \frac{1}{2} C_D D_D |v_{N,rel}| v_{N,rel}] \quad (B1.161)$$

The first term represent added mass and will normally be included in the mass matrix. The second term gives forces from fluid acceleration. The diameter  $D_V$  must give the correct average volume of the pipe over the length  $dL$ . The third term gives the drag force according to the cross-flow principle. The diameter  $D_D$  must give the correct projected area of the pipe. A 'hydrodynamic diameter' is often applied for non-circular cross section. Note that if the same diameter is used for the drag and inertia terms for arbitrary cross section shapes, the coefficients must be scaled in order to obtain the correct forces.

A pipe with constant diameter will not have tangential added mass since the tangential resultant of the dynamic pressure will be zero. The hydrodynamic mass will therefore be anisotropic. Figure B1.69 shows an inclined element in a local and global coordinate system. If added mass is zero in the local  $X_L$  direction, we can find the inertia forces in the global coordinate system from

$$\begin{bmatrix} F_{XG} \\ F_{YG} \end{bmatrix} = m_{a,YL} \begin{bmatrix} \sin^2 \alpha & -\cos \alpha \cdot \sin \alpha \\ -\cos \alpha \cdot \sin \alpha & \cos^2 \alpha \end{bmatrix} \begin{bmatrix} a_{XG} \\ a_{YG} \end{bmatrix} \quad (B1.162)$$

These terms must be included in the global mass matrix, which means that use of a concentrated (diagonal) mass matrix is inadequate for modelling of hydrodynamic mass of slender structures.

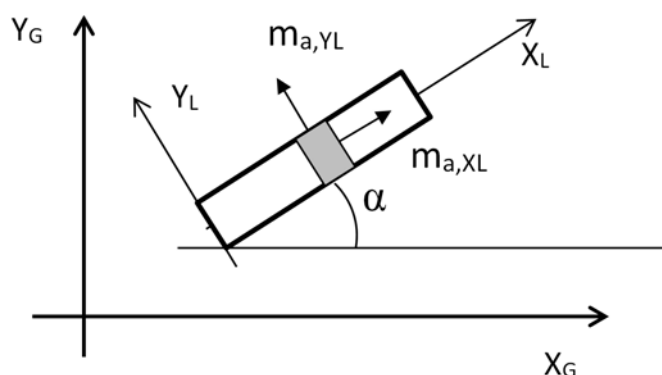


Figure B1.69: Added mass on an inclined element

Added mass in tangential direction for a riser with buoyancy elements will, however, not be zero, but will still be different from lateral added mass. The terms to be included in the global mass matrix from tangential added mass can be found as

$$\begin{bmatrix} F_{XG} \\ F_{YG} \end{bmatrix} = m_{a,XL} \begin{bmatrix} \cos^2\alpha & \cos\alpha \cdot \sin\alpha \\ \cos\alpha \cdot \sin\alpha & \sin^2\alpha \end{bmatrix} \begin{bmatrix} a_{XG} \\ a_{YG} \end{bmatrix} \quad (\text{B1.163})$$

These matrices must of course be extended for a 3D analysis. When it comes to selection of actual values of hydrodynamic coefficients, one have to follow recommendations from guidelines and design specifications. Some general comments may, however, be given:

- Added mass for circular cylinders should be taken as 1.0. Figure B1.58 indicates significantly lower values, in particular for low values of  $\beta$  - or Re. For ordinary pipes in waves of practical interest, however, added mass seems to be quite stable.
- In a sensitivity study to find variation of the response from varying  $C_D$  it is important to keep in mind both the excitation and damping effects of drag forces. The most unfavorable situation in a dynamic analysis will be a large  $C_D$  in the wave zone, and a low value at large water depth where drag will add damping.
- Many riser types will consist of a number of pipes like drilling risers with their 'kill and choke' lines. Coefficients will be direction dependent, but often not known in detail for the actual Reynolds number. The need for parameter variations for such cases is obvious.

#### B1.4.6 Finite Element Models

The finite element method is a general numerical technique for solving differential equations applied on field problems. Important applications in addition to structural analysis are hydrodynamics, temperature distribution, magnetism and rock mechanics. The continuum is divided into a number of elements, and the elements are linked at nodes. Interpolation functions and state variables at nodes are applied to describe the field parameters within each element. A set of algebraic equations for the unknown node parameters can be established and solved. The quality of the solution depends on the ability of interpolation functions to describe the state variables within the element, and the characteristic size of the element.

Compatibility for deformations and equilibrium between external and internal forces are the two basic requirements that have to be satisfied in structural analysis. This is ensured by introducing a material law that relates stresses to strains and leads to a stiffness matrix. In static analysis, a set of global equilibrium equations relates internal and external forces at each node for unknown displacements. Node displacements are found by solving these equations, and the deformations, strains and stresses within the elements can either be found from the interpolation functions or directly from the element stress resultants. A dynamic analysis additionally includes velocity and acceleration at each node in order to include inertia and damping forces in the equilibrium equations.

By using a linear finite element method, deformations and stresses are found without accounting for the fact that deformations will change the geometry or material properties of the structure. Deformations will hence always become proportional to the load. A non-linear solution will update geometry and material properties on the basis of deformations and strains by introducing load increments in combination with equilibrium iteration. Hence, linear analysis cannot be applied in cases where deformations become large relative to the global geometry, or if stresses exceed the proportionality limits for the actual material.

A finite element analysis must start from a stress free condition or from a condition with known initial stresses. Non-linear effects will always be present for static analyses of flexible risers due to large deformations relative to a stress free condition. Dynamic response might however, be adequately analysed by linear methods, but non-linear analyses are normally preferred. The simplest way of analysing flexible risers is to find a static shape from catenary theory (see Sect. B 1.4.3) and apply a linear method for calculating the dynamic response as a perturbation of the static shape. Note that a linear dynamic analysis will calculate the dynamic response with reference to a static condition, and hence include dynamic forces only, while a non-linear dynamic analysis must apply the sum of static and dynamic loads in the calculations.

The reasons for applying non-linear analysis for flexible risers are not only large displacements and non-linear material behaviour. The geometric stiffness (see B 1.4.2.1) is linked to the tension in the riser, which often will have large variations in a dynamic condition. Contact between the riser and the sea bottom, and stick/slip between layers in the cross section are examples of other non-linear effects that often need to be accounted for.

#### B1.4.6.1 Beam and bar elements

Beam elements are normally used for all flexible riser analyses. However, one may still apply bar elements during initial design in order to find global geometry and optimum distribution of buoyancy elements for steep and lazy wave configurations. It might be convenient to apply a simple catenary model for static analysis (see Sect. B 1.4.3) combined with a linear 2D dynamic analysis with bar elements to investigate dynamic effects.

The stiffness matrix for a 2-D bar element (see Figure B1.70 and Eq. B1.164 ) will have contribution from the elastic stiffness defined by modulus of elasticity E, cross section area A and element length L, and geometric stiffness defined by axial tension P:

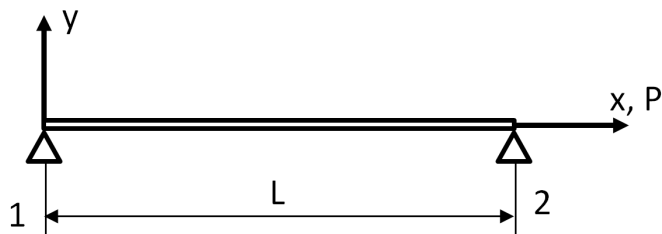


Figure B1.70: 2D bar element

$$\mathbf{K}_{\text{Bar},E} = \frac{EA}{L} \begin{bmatrix} 1 & 0 & -1 & 0 \\ 0 & 0 & 0 & 0 \\ -1 & 0 & 1 & 0 \\ 0 & 0 & 0 & 0 \end{bmatrix}, \quad \mathbf{K}_{\text{Bar},G} = \frac{P}{L} \begin{bmatrix} 0 & 0 & 0 & 0 \\ 0 & 1 & 0 & -1 \\ 0 & 0 & 0 & 0 \\ 0 & -1 & 0 & 1 \end{bmatrix}, \quad \mathbf{v} = \begin{bmatrix} x_1 \\ y_1 \\ x_2 \\ y_2 \end{bmatrix} \quad (\text{B1.164})$$

The physical interpretation of the geometric stiffness matrix is that it accounts for the contribution to restoring forces from the change of direction of the axial force, see Section B1.4.2.1

The 2-D beam element will have end rotations as additional degrees of freedom, see Figure B1.71. The elastic stiffness terms related to rotations are found from elementary beam

theory. The geometric stiffness matrix will now be modified since end rotations will influence the direction of the axial force, see Eq. B1.165.

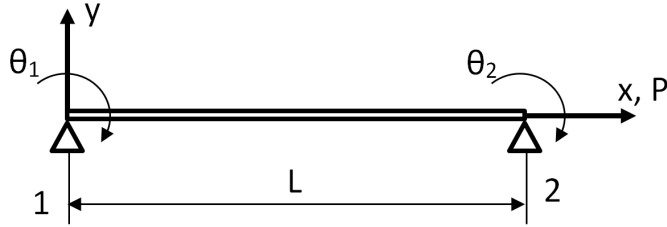


Figure B1.71: 2-D beam element

$$\mathbf{K}_{\text{Beam},G} = \frac{P}{L} \begin{bmatrix} 0 & 0 & 0 & 0 & 0 \\ 0 & \frac{6}{5} & -\frac{L}{10} & \frac{2L^2}{15} & 0 \\ 0 & -\frac{L}{10} & 0 & 0 & \frac{6}{5} \\ 0 & \frac{2L^2}{15} & 0 & 0 & -\frac{L}{10} \\ 0 & 0 & \frac{6}{5} & -\frac{L}{10} & \frac{2L^2}{15} \end{bmatrix}, \quad \mathbf{v} = \begin{bmatrix} x_1 \\ y_1 \\ \theta_1 \\ x_2 \\ y_2 \\ \theta_2 \end{bmatrix}, \quad (\text{B1.165})$$

$$\mathbf{K}_{\text{Beam},E} = \begin{bmatrix} \frac{EA}{L} & 0 & 0 & 0 & 0 \\ 0 & \frac{12EI}{L^3} & -\frac{6EI}{L^2} & \frac{4EI}{L} & 0 \\ 0 & -\frac{6EI}{L^2} & \frac{4EI}{L} & 0 & -\frac{12EI}{L^3} \\ 0 & \frac{4EI}{L} & 0 & \frac{EA}{L} & -\frac{6EI}{L^2} \\ 0 & 0 & 0 & \frac{EA}{L} & \frac{12EI}{L^3} \\ 0 & -\frac{12EI}{L^3} & -\frac{6EI}{L^2} & 0 & \frac{6EI}{L^2} \\ 0 & \frac{6EI}{L^2} & \frac{2EI}{L} & 0 & \frac{4EI}{L} \end{bmatrix}$$

Note that the above matrices are local in that sense that the x axes are horizontal. These matrices have to be transformed and assembled in a global stiffness matrix to represent the entire structure for an arbitrary geometry of a riser. The mass matrix for a 2-D beam element is shown in Eq. B1.166. This matrix is found by use of the same interpolation functions as the stiffness matrix, which means that the mass matrix is consistent.

$$M = \frac{\rho AL}{420} \begin{bmatrix} 140 & 0 & 0 & 70 & 0 & 0 \\ 0 & 156 & -22L & 0 & 54 & 13L \\ 0 & -22L & 4L^2 & 0 & -13L & -3L^2 \\ 0 & 0 & 0 & 140 & 0 & 0 \\ 70 & 0 & 0 & 0 & 156 & 22L \\ 0 & 0 & 0 & 0 & 0 & 4L^2 \end{bmatrix} \quad (\text{B1.166})$$

So-called concentrated mass matrices were often used in the early days of finite element history in order to reduce computing time and needed memory in computers. A concentrated mass matrix is diagonal, but has no relevance for today's element models. One important argument against the concentrated mass matrix for application on flexible risers is that added mass cannot be correctly described. Acceleration in one direction will give inertia forces in the perpendicular direction for an arbitrary oriented beam in water, which is impossible to describe by a diagonal mass matrix.

A beam element without any limitations for translations and rotations is needed in order to describe the global deformations of a flexible riser. This can only be achieved by applying

nonlinear analysis based on a so-called co-rotated ghost reference system, which will be described in the following.

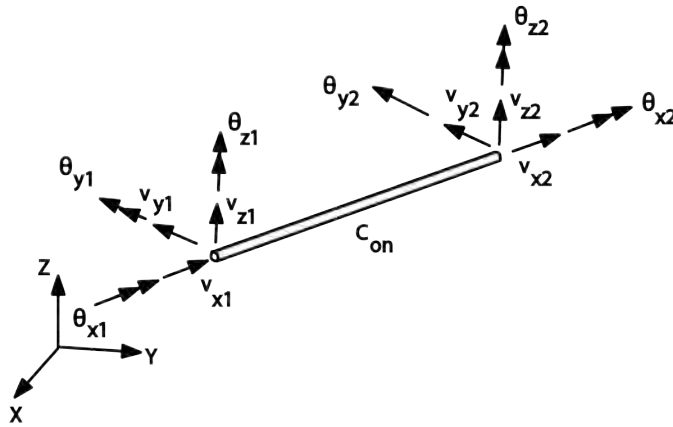


Figure B1.72: Degrees of freedom for a 3-D beam element

Figure B1.72 shows the 12 degrees of freedom that are needed to describe the deformation state for a 3D beam. An initial stiffness matrix for this beam can be found in the same way as for the 2D case. The only new type of deformation from Eq. B1.165 is rotation. What is important for the 3D case with large displacements is the description of rotations and the stress analysis.

3D rotations are not true vectors that can be described by components in a base coordinate system in the same way as translations. What is needed is to define a local coordinate system to each end, and fix this to the cross section. In a general deformation state with bending and torsion we need to know the directions of the local axes by their direction cosines. Instead of three rotations at each nodes, we need a  $3 \times 3$  matrix to define the actual position of the local coordinate system, see Figure B1.73.

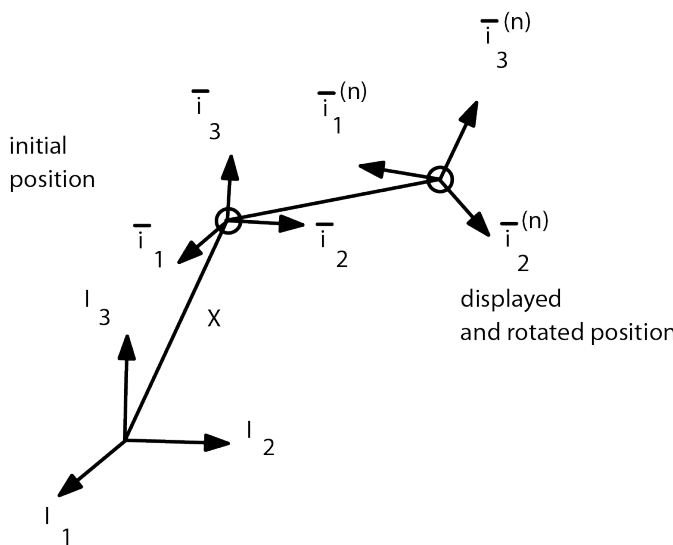


Figure B1.73: Local coordinate system to describe cross section rotations

Figure B1.74 illustrates how the global displacements and rotation vectors are used to define

the deformations of an element. Once the element deformations are found, internal forces (bending and torsion moments, shear and axial forces) can be found from elementary beam theory. Non-linear material behaviour may also be accounted for. Note that the stress analysis for each element is based on the assumption that local deformations are small. This is not an important limitation of the method since the large global displacements is dominated by rigid body motions.

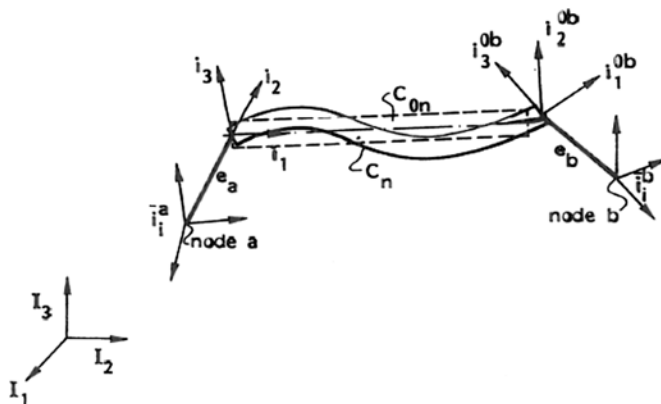


Figure B1.74: Global displacements and local deformations for stress analysis

A large number of textbooks and publications present the finite element method for static and dynamic analysis. [Livesley, 1964], [Zienkiewicz, 1971] and [Clough and Penzien, 1975] should be mentioned among the classical FEM literature, while [Cook et al., 1975] provides a more modern book on finite element theory. The 3D non-linear beam element and its application is described by [Mathisen, 1990] and [A. Engseth, 1988].

#### B1.4.6.2 Riser/ seafloor interaction

Several flexible riser configurations will have a contact zone on the sea bottom that varies with time. This represents a non-linear effect that may have a small influence on the global behaviour of the riser, but the local effect might still be significant. Modelling of this interaction should therefore be given some attention.

Figure B1.75 illustrates 3 different models that might be applied in a linear dynamic analysis. Model 1 is truncated at the touch-down point, and is assumed to have fixed positions but moment free rotation at the end. A dynamic response of the riser will transport energy to this end, and all energy will be reflected. Model 2 includes a riser segment on the seafloor, and linear springs are introduced to model the interaction between the riser and the seafloor. These springs will give a distributed reflection of energy, but the local bending moment will be strongly influenced by the stiffness of the springs. The third model includes dampers in parallel to the springs, and will therefore absorb some of the energy and reflect a smaller amount than for the other models.

Figure B1.76 presents results from a fatigue analysis where the first and second models have been used. The truncated model will eliminate the bending moment at the touch-down point, while the model with bottom springs will have maximum fatigue damage at the first node with bottom contact. The height of this peak depends strongly on the stiffness of the spring, and will almost always give a conservative estimate of fatigue at this point. One may also observe that the first peak for the truncated model is higher than for the model

with bottom springs at the same location. The reason for this is the concentrated energy reflection from the end support of the truncated model.

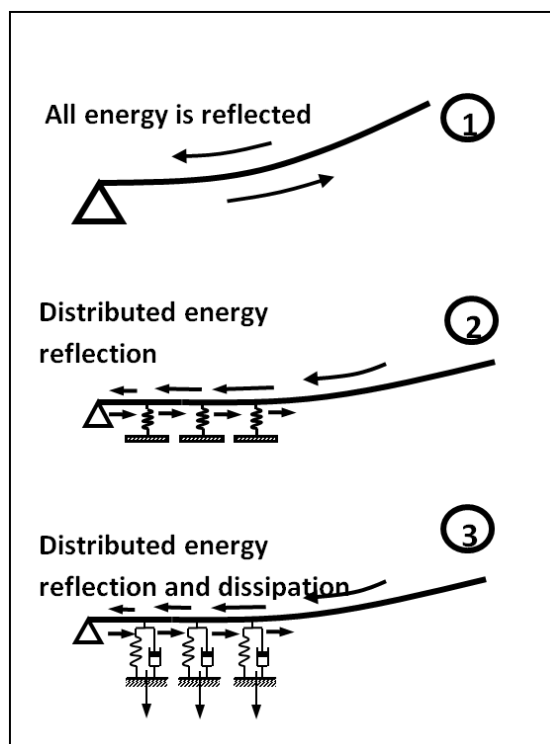


Figure B1.75: Alternative models for riser - seafloor interaction.

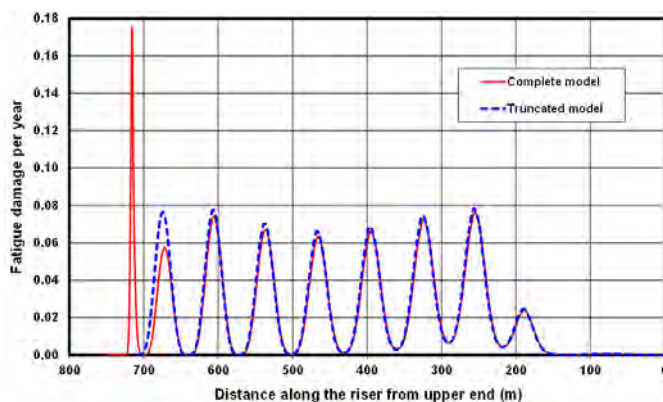


Figure B1.76: Fatigue damage along a riser with truncated model and model with bottom springs

The results on Figure B1.76 are obtained from linear analyses, which means that the springs may have experienced tensile forces. A more realistic model is therefore to apply a non-linear dynamic analysis, and account for varying contact length during a simulation. Figure B1.77 illustrates the difference between interaction forces in a linear and non-linear time domain simulation. Since a linear analysis will have constant stiffness, tensile forces in the springs may occur, and a node without initial bottom contact will not experience any interaction force during a simulation even if the node penetrates into the sea floor. Both effect will lead to increased bending moment close to the first contact node in the static condition.

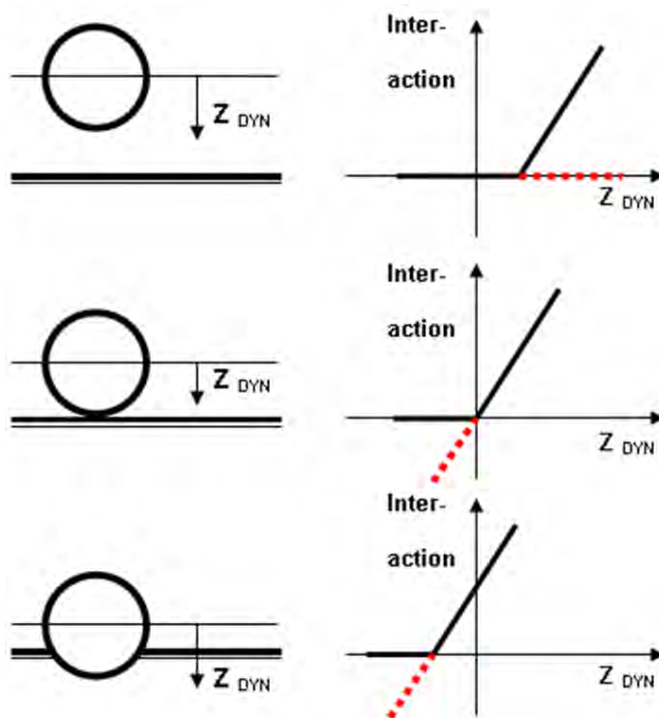


Figure B1.77: Spring forces in a linear and non-linear analysis

Figure B1.78 shows snapshots of the deformations close to the touch-down point from linear and non-linear time domain analyses. The linear model will give symmetric snapshots, while a non-linear model will prevent penetration and allow nodes to leave the bottom by adjusting the contact springs.

Another effect that will influence stresses in the touch-down zone is friction between the riser and the sea floor. This will in particular be important for distribution of axial force along the length of the pipe with seafloor contact, and bending stresses caused by response perpendicular to the catenary plane. Figure B1.79 shows the hysteresis curve for friction forces on the pipe by using a simple dry friction (Coulomb) model. The friction force will increase for increasing displacement, but the pipe will start to slide at a force level determined by the local friction coefficient. Sliding will take place at constant force, but unloading will follow a linear curve as soon as the external force reverses. This process can easily be included in a non-linear time domain simulation. Figure B1.80 shows local stresses from a variety of models for interaction between riser and seafloor. Note that the high and low friction models in frequency domain will give identical results.

Details from analyses of catenary risers with varying models for sea floor interaction are presented by Larsen and Passano (2006).

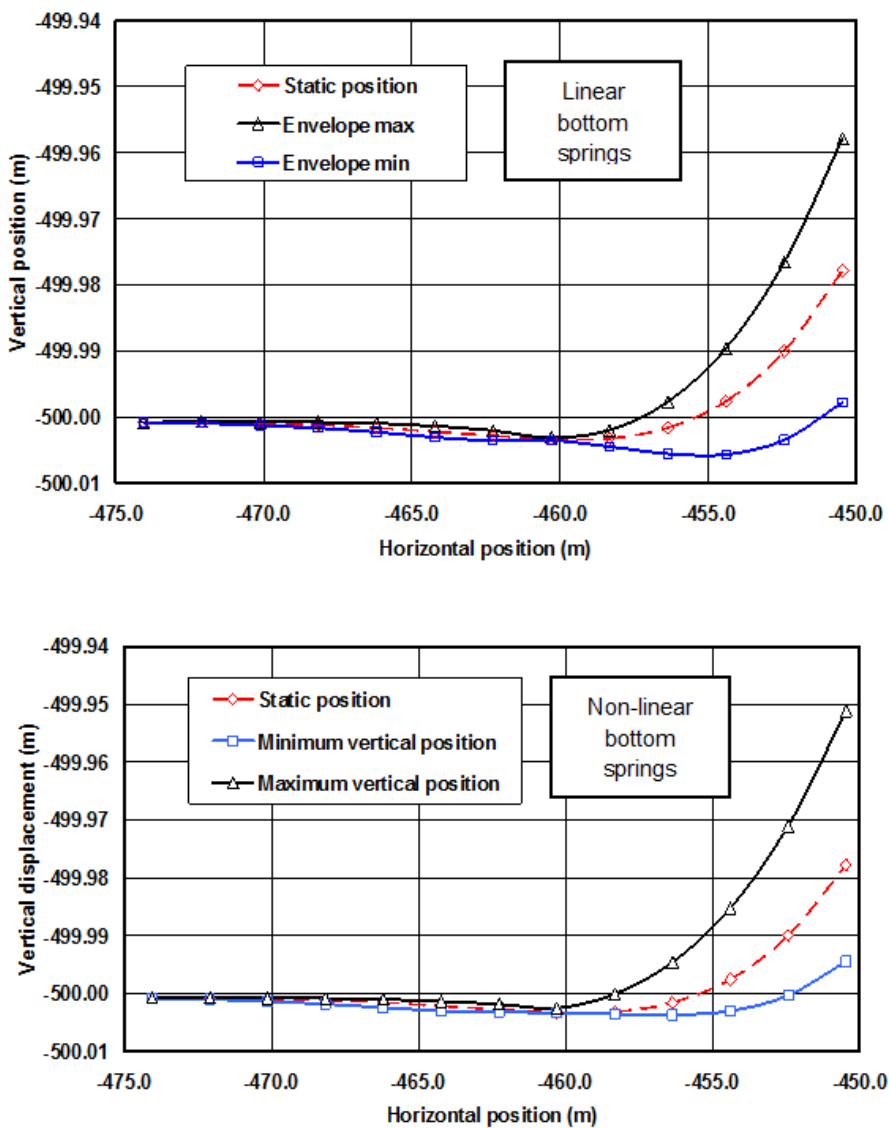


Figure B1.78: Comparison of vertical deformations for linear and non-linear bottom springs

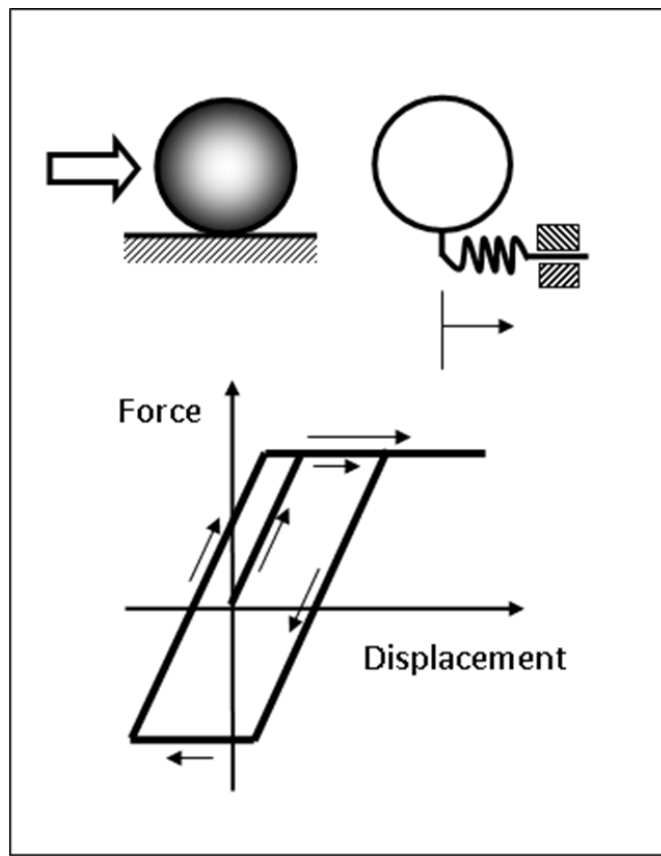


Figure B1.79: Dry friction model for horizontal displacements

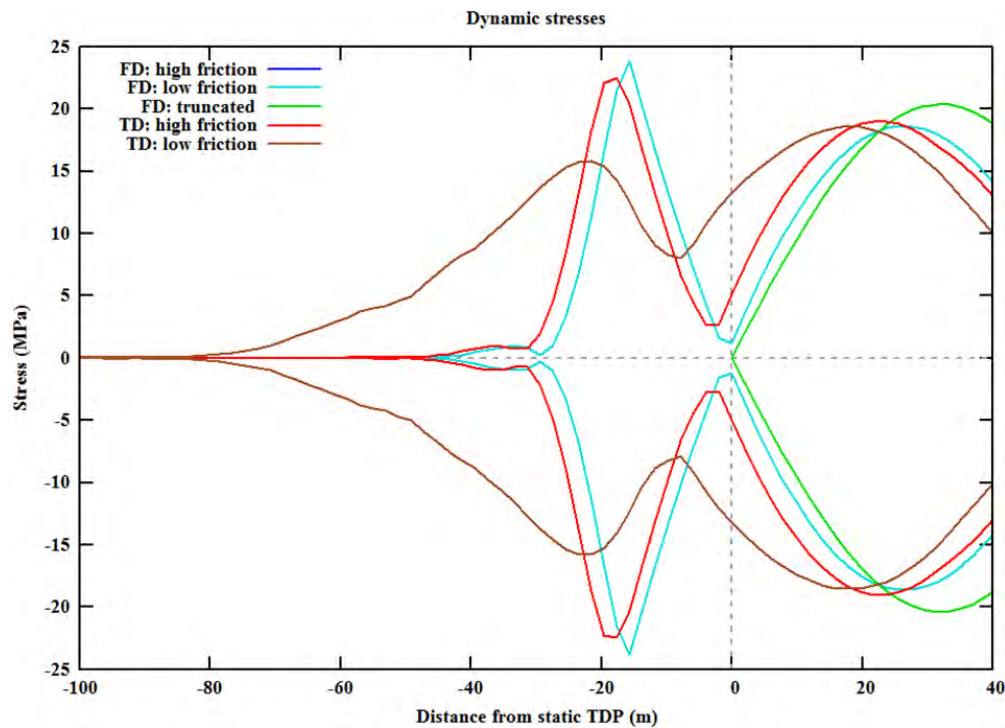


Figure B1.80: Local bending stresses close to the touch-down point from various models

### B1.4.6.3 Static analysis

The most general way to find the static condition for a flexible riser system is to define a stress free condition and introduce load contributions in a specific sequence until all static effects are included. Load types will normally consist of

- Volume forces (weight and buoyancy)
- Prescribed displacements at nodes with given boundary conditions
- Friction forces between riser and sea bottom
- Temperature and pressure
- Current forces

This list can also represent a recommended sequence for how the load groups are introduced. The initial (stress free) condition cannot have any curvature, and will hence be significantly different from the static shape. Figure B1.81 illustrates how one end of the riser must be moved down to the sea bottom, while the other must be moved to the termination point on a floater. The initial position may be defined at an arbitrary level, but should preferably be submerged in order to have buoyancy. The two ends need not to be at the same level, but the distance between the ends must be identical to the true length of the unstressed riser.

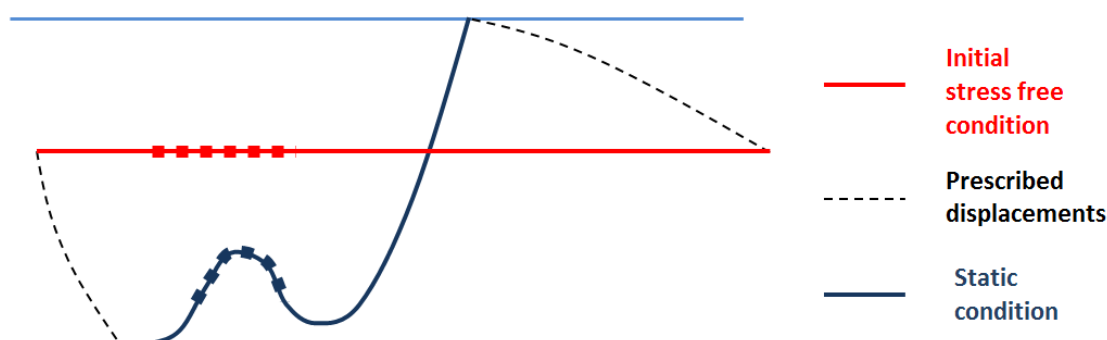


Figure B1.81: Initial and static condition of a lazy wave flexible riser

Number of load increments within a load group might be high - often of the order of 100. This is in particular the case for the prescribed displacements as shown on the figure. Note that equilibrium must be obtained for each load increment, which might be difficult at some intermediate end positions between the initial and final positions.

Equilibrium iteration will preferably follow the Newton-Raphson scheme. This is illustrated on Figure B1.82. Equilibrium requires internal forces to be equal to external forces at all degrees of freedom. Since the orientation of than element will influence current forces, both external and internal loads may vary with displacements, and the stiffness matrix will not be identical at the start and end position for an increment. Hence, the iteration will become a combination of load and equilibrium iteration. Both external and internal forces must therefore be calculated a number of times for each increment.

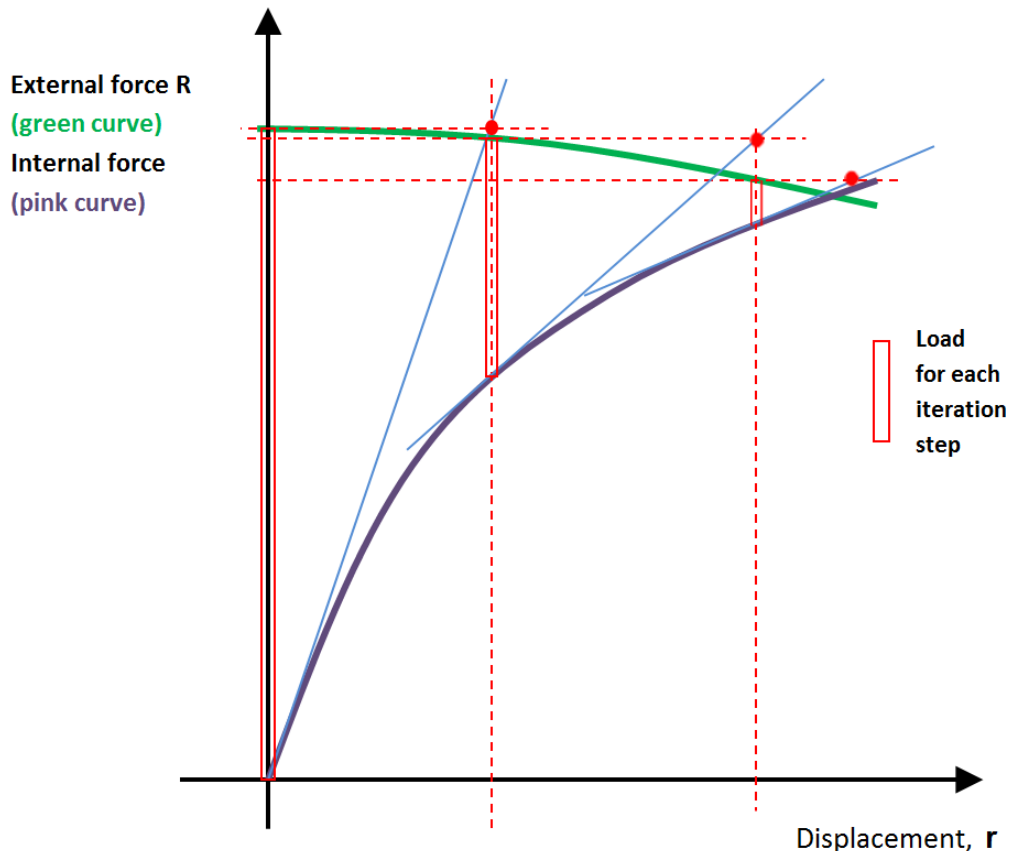


Figure B1.82: Illustration of combined load and equilibrium iteration

#### B1.4.6.4 Damping models

The main contributor to damping of most flexible riser system is the hydrodynamic damping on parts of the riser without significant wave induced water particle velocities. However, structural damping may also be important and should therefore be accounted for.

The mechanism for structural damping is complex, and requires a detailed analysis of cross section deformations including strains in non-metal layers, contact forces, 'stick and slip' and friction between layers. It is feasible to include this type of analysis in a global dynamic simulation, however, the computational time will increase. An alternative strategy is to use local cross section analyses to tune parameters for more simple damping models.

It is formally possible to define a non-linear model for structural damping by hysteresis curves for bending deformation of a cross section. Such models will require storage of recent time histories of bending at each node, and hence increase computing time and data storage. This type of model will vary not only from one cross section design to another, but also with temperature and pressure. Simplified global damping models are therefore in many cases preferred.

The Rayleigh damping model is often applied for structural damping. The model defines a damping matrix  $C$  as a weighted sum of the stiffness and mass matrix  $K$  and  $M$ :

$$C = \alpha_1 M + \alpha_2 K \quad (B1.167)$$

where  $\alpha_1$  and  $\alpha_2$  are coefficients that define the damping ratio  $\xi$  from the equation

$$\xi(\omega) = \frac{1}{2} \left( \frac{\alpha_1}{\omega} + \alpha_2 \omega \right) \quad (\text{B1.168})$$

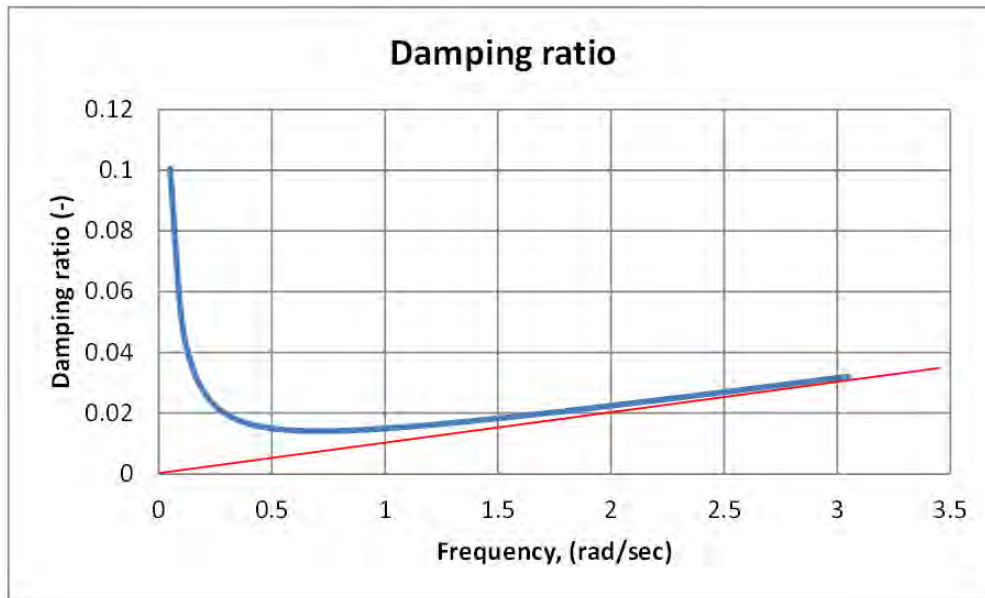


Figure B1.83: Damping ratio for  $\alpha_1 = 0.01$  and  $\alpha_2 = 0.02$

From Eq B1.168 it is seen that the  $\alpha_1$  will give high damping at low frequencies, while  $\alpha_2$  will give increasing damping for increasing frequencies. Figure B1.83 shows the damping ratio as function of frequency. The blue line presents the values from Eq. B1.167, while the red line gives the stiffness proportional contribution only. There are good reasons for using  $\alpha_1 = 0$  for flexible risers. One reason is that damping may easily become too high for low frequencies, but it is also important to note that a mass proportional damping will give damping from rigid body motions in the same way as inertia forces will do. This damping contribution is not desired since rigid body motions are damped by drag forces. A damping matrix with the same structure as the stiffness matrix will give damping from bending deformations, which is a reasonable assumption. The red line defines damping from the  $\alpha_2$  term only. The damping ratio is seen to increase from 0.5 to 2 % between period values of 12.56 to 3.14 seconds. One may argue that the stiffness proportional damping should follow the elastic stiffness matrix and not be influenced by the geometric stiffness matrix. The argument is reasonable, but it might be difficult to estimate the damping ratio for this case since the contributions from the two stiffness matrices are difficult to define.

Some time integration procedures like the Newmark beta family can introduce numerical damping by adjusting integration parameters and length of the time step. When using this type of damping it might be difficult to identify the actual damping level, in particular how damping varies with time step and load frequency. A general rule is therefore to avoid numerical damping and instead have a stiffness proportional Rayleigh damping.

The Rayleigh damping model can be applied for both time and frequency domain analyses. The model may also be used for non-linear simulations, but the simple relationship for damping ratio given in Eq. B1.168 is formally not valid. Rayleigh damping is still recommended

for ordinary design analyses, but should be avoided for cases with boundary condition changes like riser installation and accidental loss of integrity.

Damping is important for cases where load frequencies are close to one or several eigenfrequencies for the riser. Hydrodynamic damping from drag forces will normally be a domination damping effect, but structural damping might dominate for axial vibrations and systems in air. Such cases need special considerations, and should be checked for unphysical damping effects when approximate damping models are used.

Some more info on structural damping may be found in [API 17B, 2008] [MCS Kenny, 2006] and [Berge et al., 1992]

#### B1.4.6.5 Frequency domain analysis

Time domain simulation is the standard method for dynamic analysis of flexible risers. However, fatigue analyses can with acceptable accuracy be carried out in frequency domain, confer [Larsen, 1992]. In addition, most commercial programs for calculation of vortex induced vibrations apply frequency domain methods. The frequency response method combined with a three-dimensional finite element model is well suited for this application since the loads from vortex shedding are normally considered to act at one frequency or at a limited number of discrete frequencies.

Using standard finite element notation the dynamic equilibrium equation may be written as

$$\mathbf{M} \ddot{\mathbf{r}}(t) + \mathbf{C} \dot{\mathbf{r}}(t) + \mathbf{K} \mathbf{r}(t) = \mathbf{R}(t) \quad (\text{B1.169})$$

If the external loads  $\mathbf{R}(t)$  are harmonic, but not necessarily in phase at all degrees of freedom, a complex load vector  $\mathbf{X}$  can be applied to define amplitudes and phase angles. The time varying load will then be given as

$$\mathbf{R}(t) = \mathbf{X} e^{i\omega t} \quad (\text{B1.170})$$

The response will appear at the same frequency as the load, and will also be given by a complex vector and a harmonic time variation. Hence we have

$$\mathbf{r}(t) = \mathbf{x} e^{i\omega t} \quad (\text{B1.171})$$

By introducing the hydrodynamic mass and damping matrices dynamic equilibrium can now be expressed as:

$$-\omega^2(\mathbf{M}_S + \mathbf{M}_H)\mathbf{x} + i\omega(\mathbf{C}_S + \mathbf{C}_H)\mathbf{x} + \mathbf{K}\mathbf{x} = \mathbf{X} \quad (\text{B1.172})$$

The damping matrix  $\mathbf{C}_S$  represents structural damping and will normally be assumed to be a linear combination of the mass and the stiffness matrix (see Section B1.4.6.4), known as the Rayleigh damping matrix.  $\mathbf{C}_H$  contains terms from hydrodynamic damping. The solution can now be found from

$$\mathbf{x} = \mathbf{H}(\omega) \mathbf{X}$$

$$\mathbf{H}(\omega) = (-\omega^2(\mathbf{M}_S + \mathbf{M}_H) + i\omega(\mathbf{C}_S + \mathbf{C}_H) + \mathbf{K})^{-1} \quad (B1.173)$$

The hydrodynamic damping matrix CH represents damping from drag forces. Since these forces depend on the response velocity, Eq. B1.173 must be solved by iteration, confer Krokowski and Gay (1980). See also Section B1.4.7.2 for stochastic analysis in frequency domain.

#### B1.4.6.6 Mode superposition

Mode superposition is a method for calculating the response in a continuous system where the response is expressed as a linear combination (weighted sum) of selected mode shapes. The method represents an extension of generalized coordinates, but it is based on the same basic principles. The method has some similarities with the Rayleigh-Ritz (R-R) technique for calculation of eigenfrequencies for continuous systems. However, the arbitrary basic shapes in R-R are now replaced by known eigenmodes. The starting point for modal superposition is hence:

$$\mathbf{r}(t) = \sum s_i \phi_i q_i(t) = \Phi \mathbf{q} \quad (B1.174)$$

Here is a known modeshape,  $q_i(t)$  are time-dependant weight functions that must be calculated from a dynamic analysis. The weight functions determine the contribution from each mode shape to the total deformation state. It is important to know that the weights can change their relative quantity with time, hence the deformation is not necessarily a time scaling of a particular shape.

By introducing Eq. B1.174 to the dynamic equilibrium equation and neglect damping, we will obtain a set of uncoupled equations. The reason why the equations are uncoupled is that modeshapes are orthogonal - one mode cannot be defined as a linear combination of other modes. Another way of understanding orthogonality is to realize that each mode provides unique information - other modes are not able to give the same information. The uncoupled set of equations can be written as:

$$\begin{bmatrix} \bar{m}_1 & & 0 \\ & \bar{m}_2 & \\ & & \ddots \\ 0 & & \bar{m}_N \end{bmatrix} \begin{bmatrix} \ddot{q}_1 \\ \ddot{q}_2 \\ \vdots \\ \ddot{q}_N \end{bmatrix} + \begin{bmatrix} \bar{k}_1 & & 0 \\ & \bar{k}_2 & \\ & & \ddots \\ 0 & & \bar{k}_N \end{bmatrix} \begin{bmatrix} q_1 \\ q_2 \\ \vdots \\ q_N \end{bmatrix} = \begin{bmatrix} \bar{p}_1 \\ \bar{p}_2 \\ \vdots \\ \bar{p}_N \end{bmatrix} \quad (B1.175)$$

Line i will now give a second order differential equation for weight factor i:

$$\bar{m}_i \ddot{q}_i + \bar{k}_i q_i = \bar{p}_i(t) \quad (B1.176)$$

where the modal parameters are given by

$$\bar{m}_i = \phi_i^T \mathbf{M} \phi_i \bar{m}_i = \phi_i^T \mathbf{M} \phi_i \bar{p}_i(t) = \phi_i^T(x) \mathbf{p}(t) \quad (B1.177)$$

Damping must be introduced for each modal equation, normally in terms of a damping ratio  $\xi$ :

$$\xi_i = \frac{\bar{c}_i}{\bar{c}_{crit,i}} = \frac{\bar{c}_i}{2\bar{m}_i\omega_{0,i}} = \frac{\bar{c}_i}{2\sqrt{\bar{m}_i\bar{k}_i}}\bar{c}_i = 2\xi_i\sqrt{\bar{m}_i\bar{k}_i} \quad (\text{B1.178})$$

The differential equation for each modal weight factor will now be given as:

$$\bar{m}_i\ddot{q} + \bar{c}_i\dot{q} + \bar{k}_i q = \bar{P}_i(t) \quad (\text{B1.179})$$

This equation can now be solved by conventional methods; in frequency domain if the load can be described by harmonic components or by time integration for arbitrary load histories.

Drag forces gives coupling between the modal equations since they are nonlinearly related to the relative velocity. The only advantage by the use of mode superposition will then be to apply a significantly lower number of modes than degrees of freedom in the finite element model.

#### B1.4.6.7 Time domain analysis

Time domain calculation of the coupled set of equations for all degrees of freedom in the finite element model is the most frequently used approach for dynamic analysis of flexible risers. Two classes of methods might be used:

- linear analysis where the system matrices remain constant, and the dynamic response is calculated as a perturbation of the static condition
- non-linear analysis where the geometry is updated for each time step during the simulation

The two approaches are illustrated in Figure B1.84

Formally we can describe the linear dynamic analysis as

$$\mathbf{M}\ddot{\mathbf{r}} + \mathbf{C}\dot{\mathbf{r}} + \mathbf{K}\mathbf{r}_{DYN} = \mathbf{R}_{DYN}(t) = \mathbf{R}_{TOT}(t) - \mathbf{R}_{STATIC} \quad (\text{B1.180})$$

Dynamic stresses can be calculated directly from the dynamic displacements added to the static values. External forces in a linear analysis must be the difference between total and static forces. This is in particular important to have in mind if current forces are present in the static analysis, and the static condition includes waves. Because of the non-linear term in Morison's equation we have to add current velocity to the wave induced velocity, calculate the drag force and subtract the current force.

It is also important to realize that the hydrodynamic forces must be calculated with reference to the static shape of the riser. If an updated geometry is applied, one will calculate an incorrect dynamic response since forces will get local directions relative to the riser that are inconsistent to the geometry that is represented by the stiffness matrix. Forces that should act perpendicular to the riser will get an unwanted tangential component.

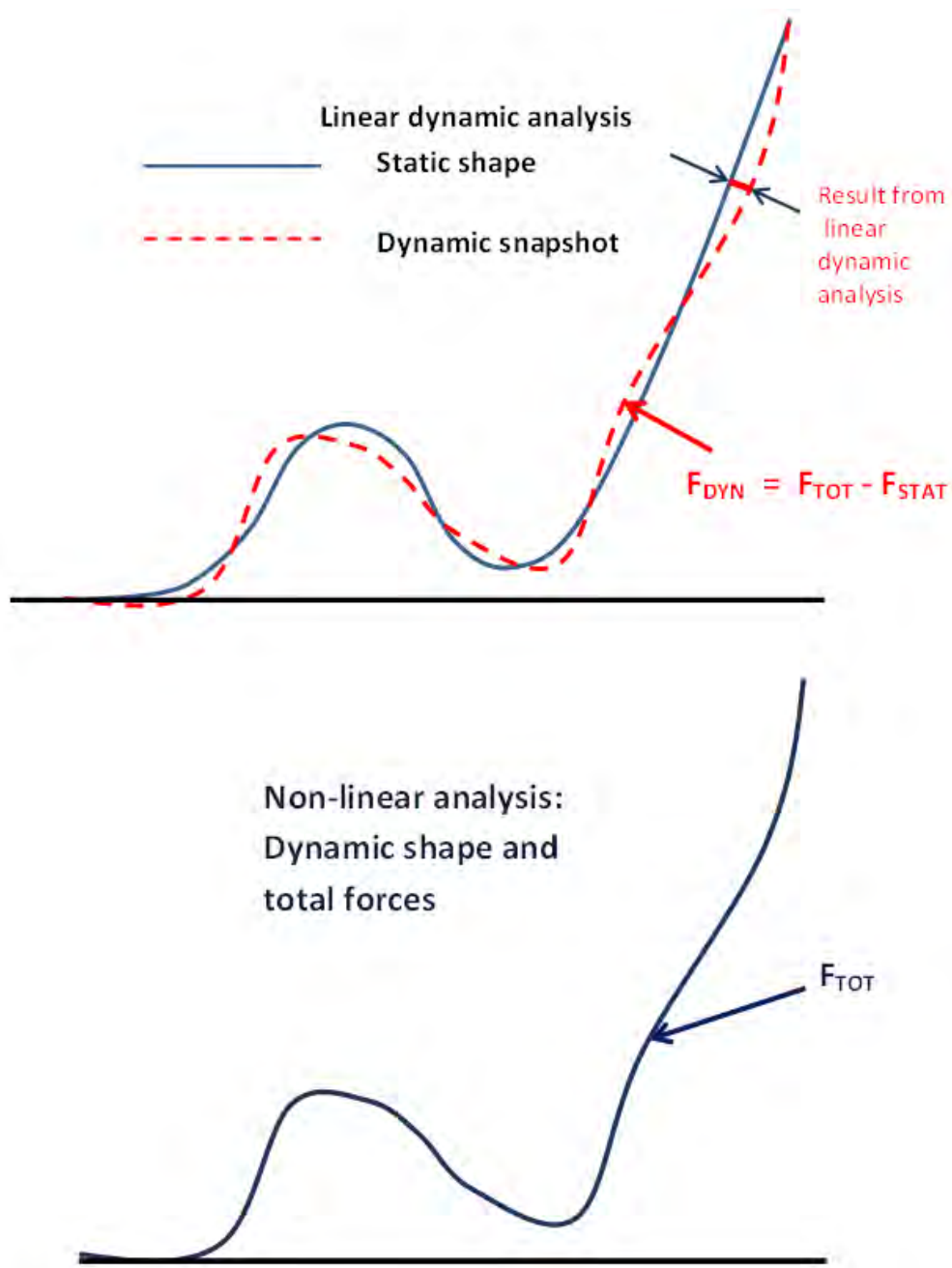


Figure B1.84: Linear and non-linear dynamic analysis

A linear time domain simulation should include load iterations at each time increment since drag forces must be calculated from the initially unknown relative velocity. This load iteration will in most cases - and for short time increments - have a fast convergence.

The Newmark  $\beta$  family is a convenient procedure for time integration. One may, however, experience unphysical variations of accelerations when using parameters that gives zero artificial (or numerical) damping. An alternative is to use Wilson's method or introduce some numerical damping by adjusting parameters in Newmark's method. It is recommended to test the numerical procedures for new applications.

A non-linear analysis should preferably carry out equilibrium iteration for every time increment during a simulation. Total loads including weight and buoyancy must be present, and the present geometry must always be considered when calculating the external loads. The dynamic equilibrium equation is normally reformulated to consider incremental parameters:

$$\begin{aligned}
 & (F_{k+1}^I - F_k^I) + (F_{k+1}^D - F_k^D) + (F_{k+1}^S + F_k^S) = R_{k+1} - R_k \\
 & R_k = F_k^I + F_k^D + F_k^S \\
 & \Delta r_k = r_{k+1} - r_k \\
 & \Delta \dot{r}_k = \dot{r}_{k+1} - \dot{r}_k \\
 & \Delta \ddot{r}_k = \ddot{r}_{k+1} - \ddot{r}_k \\
 & M_k \Delta \ddot{r}_k + C_{Ik} \Delta \dot{r}_k + K_{Ik} \Delta r_k = R_{k+1} - [F_k^I + F_k^D + F_k^S]
 \end{aligned} \tag{B1.181}$$

The index  $k$  defines the time increment, superscript  $I$  is inertia forces,  $D$  is damping forces and  $S$  is stiffness or restoring forces.  $K_{Ik}$  and  $C_{Ik}$  refer to incremental stiffness and damping matrices and together with displacement and velocity increments they will give incremental restoring and damping forces. Inertia forces are different since an inertia force always will appear as the instantaneous acceleration and mass matrix.

The last equation must be solved for each time increment, and normally one have to carry out a combined equilibrium and load iteration in order to ensure correct hydrodynamic forces and internal stress resultants. Note that the final equation in (B1.181) is strictly valid only if  $M$  is constant. Since  $M$  will vary with the displacements both due to transformations and added mass, a correction of inertia forces is also needed as a part of the iteration. This procedure is time consuming but has still become a standard method for dynamic simulation of flexible risers.

Wilson's method for time integration is difficult to apply on non-linear systems since the solution is found by an interpolation between an artificial time increment with dynamic equilibrium, and the real time increment. This is done in order to maintain a stable solution for linear systems, but a non-linear system must calculate all forces at the same time instant without any approximations. The Newmark procedure has shown to give excellent results for non-linear analysis of marine structures.

Integration methods are often split into explicit and implicit methods. Explicit methods give a set of linear equations for each time increments that can be solved directly, while some implicit methods will need iteration for each time increment. Some implicit methods like 'Newmark beta family' and 'constant average acceleration' can become explicit by simple reformulation of the set of equations.

More important than explicit versus implicit methods is how procedures behave with respect to stability. Some integration schemes are conditionally stable, which means that the length of the time increment is limited to a fraction of the shortest eigenperiod in the finite element model. This will lead to extremely short time increments and hence too long computing time in particular for non-linear stochastic simulations. Use of unconditionally stable methods is therefore recommended.

### B1.4.7 Coupled Analysis Models

The traditional model for global dynamic analysis of flexible risers applies pre-calculated forced displacements as boundary conditions for upper end, Morison's equation for calculation

of hydrodynamic loads from current and waves, and a 3D beam element model to represent the riser structure. The low frequency and wave frequency motions should be calculated from the same wave record as applied in the dynamic analysis for calculation of forces.

This type of model should give a fairly good result for riser displacements, axial forces and bending moments in the pipe, but may still not provide all needed information for design verification. The need to link the global riser model to other computer programs is therefore present - either by direct communication between programs during the simulation or by post processing of key results. Examples of such analysis models are

- Coupled analysis of floater motions and riser dynamics
- Coupled analysis of riser dynamics and internal non-stationary flow
- Coupled analysis of riser dynamics and hydrodynamic loads based on computational fluid dynamics (CFD)
- Post-processing of results from global riser analysis for calculation of local stresses in individual components in the cross section
- Post-processing of results for the design of bending restrictors

Comments related to these options will be given in the following.

#### B1.4.7.1 Riser dynamics and floater motions

The traditional way for calculation of floater motions and stresses in risers and anchor lines is to apply two sets of uncoupled analyses:

1. Floater motions are initially found as the sum of wave-frequency and low frequency components. The wave frequency component is calculated by use of transfer functions that has to be found from potential theory. Frequency dependent added mass will be accounted for, but anchor lines must be modelled as linear springs. Time histories of motions in a given sea state may then be generated by Fast Fourier Transform. Random phase angles for wave components must be known. The slowly varying component is normally found in time domain by use of stochastic wind forces and wave forces from the same wave record as applied for the wave frequency calculation. Anchor lines and risers without heave compensation may in this calculation be introduced as non-linear massless springs.
2. Dynamic response in anchor lines and risers are found by introducing known motions as boundary conditions at the connection points. Such analyses are normally carried out in time domain in order to represent drag forces correctly. If low frequency motions are neglected, the forced motions are found directly from the transfer functions, and consistent time histories for motions and wave generated fluid velocities and accelerations can easily be found prior to the stochastic dynamic simulation.

The uncoupled approach gives acceptable results for shallow water depth since non-linear restoring forces, damping and inertia effects from anchor lines and risers have minor influence on wave frequency motions. However, increasing water depth will lead to increased mass of anchor lines and riser, and also increased damping from these members. Low frequency motions will in particular be strongly influenced by line dynamics, and the need for coupled analysis becomes obvious. Coupled analysis must be carried out as a non-linear time domain simulation in order to give the best possible result. A particular problem will be to represent

frequency dependent added mass for the floater, but this effect is taken care of by use of retardation functions.

In the late 90-ties [Ormberg et al., 1997] and [Ormberg and Larsen, 1998] published models for coupled analysis. Comparison between uncoupled and coupled analysis for an FPSO with turret mooring was illustrated by [Ormberg et al., 1998]. There is a large number of publications about coupled and uncoupled analyses of floaters with anchor lines and risers. ITTC had a specialist committee on deep water mooring that discussed analysis options, confer [Aage et al., 1999]. Other important contributions are [Heutier et al., 2001] and [Garret, 2005].

#### B1.4.7.2 Riser dynamics and internal fluid flow

It is well known that a steady state flow through a flexible pipe with uniform cross section will not influence the global shape of the pipe. Axial stresses will, however, be influenced, but the effect of the flow can be calculated subsequent to a static or dynamic analysis. If the flow is non-stationary, dynamic effects may lead to vibrations. Slug flow is one example, and acceleration or deceleration of the flow will also give dynamic effects. A particular effect will be important for slug flow since the vibrations of the pipe will influence slug formation and propagation. An integrated riser response and slug flow analysis will hence be needed to give a correct result in such cases.

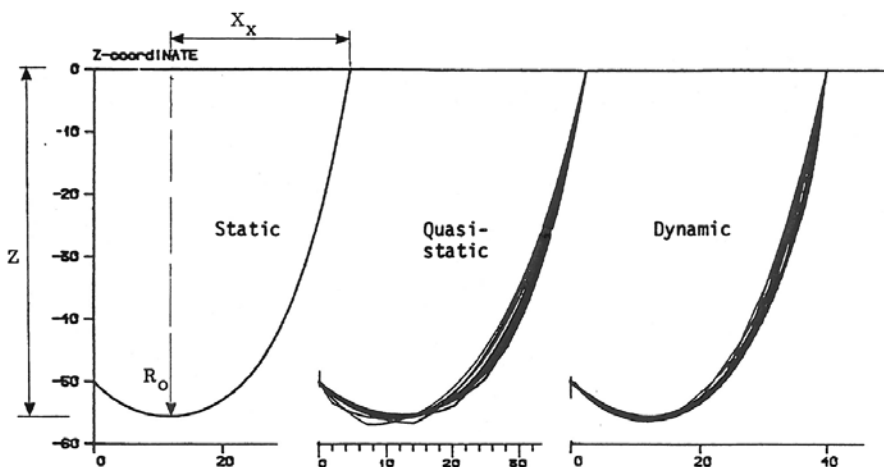


Figure B1.85: Global response from slug flow, quasi-static and dynamic simulations [Berge et al., 1992]

A simplified slug flow model was used by [Fylling et al., 1988] to investigate the response from a point mass travelling through a flexible pipe at constant speed. The global geometry is shown on Figure B1.85, and results from quasi-static and dynamic simulations are presented by snapshots. The difference between the two methods is significant, and caused by transient dynamic effects and the centrifugal forces that are neglected in the quasi-static model, [Fylling et al., 1988]. Other slug flow models published at that time followed similar principles, [Patel and Seyed, 1989].

The Reflex model had no feedback from the dynamic oscillations of the riser to the slug flow. The purpose of the work by [Ortega et al., 2012], [Ortega et al., 2013] was to combine a slug flow model and a dynamic riser response model. The slug flow model has been developed by

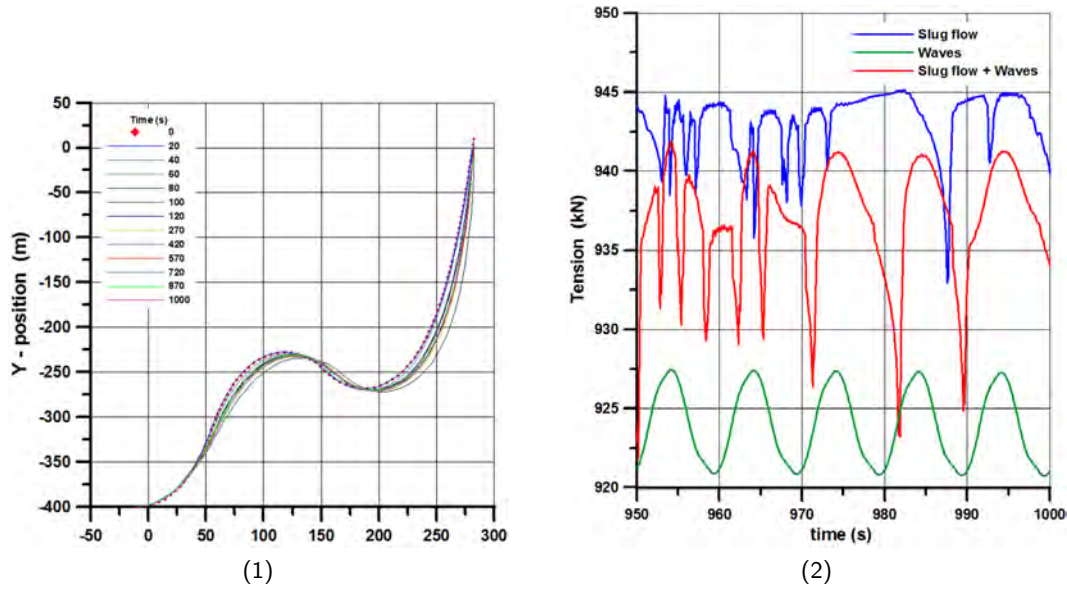


Figure B1.86: Snapshots of global shape (a) and end tension variation from slug flow in still water, waves and slug flow combined with waves ([Ortega et al., 2013])

[Nydal, 2010] and can describe the development of two-phase flow in a pipe with prescribed flow input and dynamic change of the riser shape. The riser and flow programs were coupled by use of HLA technology [IEEE Standard, 2010], which provides data flow between the programs and a synchronization of the two time integrations. The results from this type of model is not only the dynamic shape and tension in the riser (see Figure B1.86a), but also data to describe the internal flow process (see Figure B1.87).

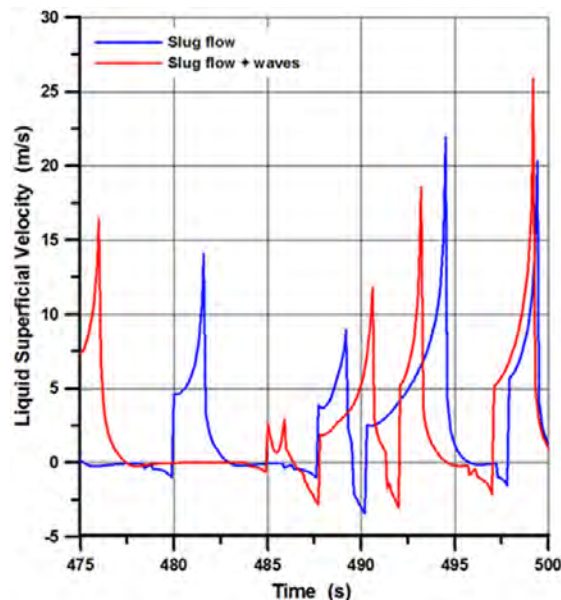


Figure B1.87: Liquid superficial velocity for slug flow in still water an waves [Ortega et al., 2013]

### B1.4.7.3 Numerical models for hydrodynamic forces

Morison equation is normally used to calculate hydrodynamic forces on slender structures. This load model is far from perfect, but is easy to use and gives results of acceptable accuracy in most cases. There are, however, situations when more sophisticated models are wanted. Slamming loads in steep waves, loads on curved pipes and buoyancy segments, and loads causing vortex induced vibrations (VIV) are examples. [Nestegård et al., 2004] applied a slamming model to calculate forces of short duration on guide tubes for protection of flexible risers in the splash zone. These loads could be pre calculated and added to ordinary Morison type loads in the simulation. A similar approach for calculating loads on curved pipes by a numerical method was investigated by de [de Vecchi et al., 2009]. Strictly speaking these cases are not examples of coupled analyses, but illustrates how additional load components can be introduced in a riser analysis.

VIV is a classical example of strong interaction between structural response and the local hydrodynamic loads. Today's approach for engineering purposes is to apply empirical load models, but these are not able to give reliable results in all cases. The approach may be described as an iterative process where the load on a specific cross section is calculated by an empirical model and parameters defined from the response at the same cross section. Convergence is obtained when all local loads are in agreement with the corresponding response. For a given frequency this means that the response amplitude defines the load amplitude, and that the phase angle of the response velocity corresponds to the phase of the load that transfers energy between the fluid and the structure. This means that the fluid is not a real part of the analysis model, but is substituted by empirical parameters.

The only way to include the fluid in this type of analysis is to apply a numerical method for calculation of flow patterns, velocities and thereby also dynamic pressure variations on the structure. An early attempt to this type of analysis was published by [Hansen et al., 1988]. The fluid model applied a 2D 'vortex-in-cell' method that is an approximate way to solve the Navier-Stokes equation (NSE) for high Reynolds numbers. This method is computationally efficient compared to the use of finite elements, and could be applied with reasonable speed on the computers that were available at that time.

Further development of combined computational fluid dynamics (CFD) and structural dynamics gave models based on 2D finite elements to solve NSE combined with turbulence models, [Halse, 1997] Figure B1.88, direct numerical simulations (DNS) that eliminated the use of turbulence models, [Evangelinos et al., 2000], and 3D DNS models combined with a flexible beam, [Bourguet et al., 2011] Figure B1.89. This figure illustrates the type of information that becomes available from a 3D DNS simulation. The aim is to calculate hydrodynamic forces, but it is also possible to see the complex vortex shedding formation and hence be able to understand the process that leads to the forces. This approach will hopefully replace the use of empirical methods for VIV calculations in the future, but computers must become cheaper and far more powerful than today.

### B1.4.8 Stochastic analysis

When dealing with dynamic analysis and stochastic processes, the terms 'time domain' and 'frequency domain' are often used. The two 'domains' represent alternative ways of describing processes and performing calculations, which will be described in the following.

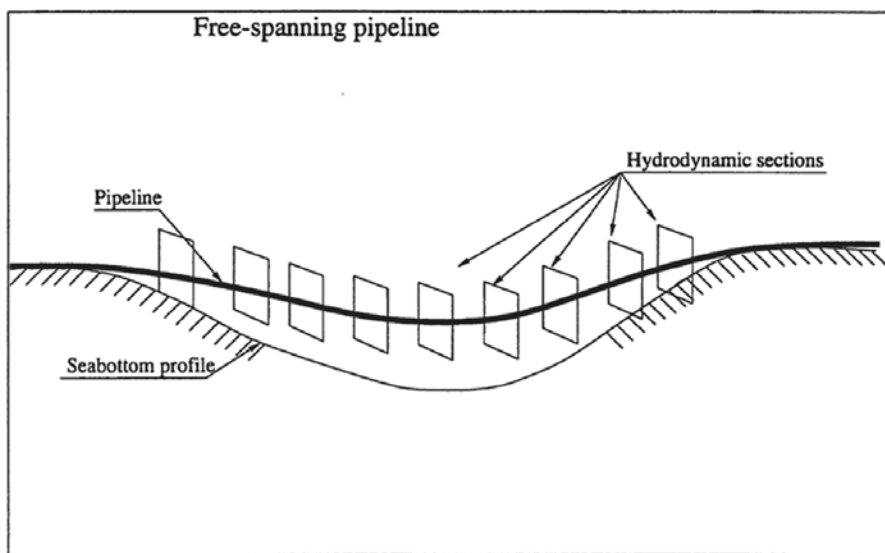


Figure B1.88: Use of 2D CFD combined with a flexible beam for VIV calculation of free spanning pipeline, [Halse, 1997]

A frequency spectrum is a way of presenting a Gaussian process that shows the intensity (or energy) of the process as a function of the frequency. Mathematically this type of spectrum is the Fourier transform of the auto correlation function for the process, and is referred to as the 'auto spectrum'. This is in contrast to the 'cross spectra' applied for description of correlated stochastic processes. A cross spectrum is defined as the Fourier transform of the cross correlation function for two processes, and is needed to describe phase relations in multi degrees of freedom systems.

An auto spectrum represents a Gaussian process, and if all spectrum moments can be calculated, the spectrum gives a complete description of the statistical properties of the process. Hence, standard deviation, zero up-crossing frequency, bandwidth and the distribution of individual maxima and extremes can be found without any statistical uncertainty. The frequency domain representation of a process (auto spectrum) is therefore a complete description and contains all necessary statistical information about the process.

If we measure the sea surface elevation in a limited time interval, we have a 'realisation' of the stochastic process. If the statistical properties of the wave process remains unchanged and we measure for a new time interval, we will have a new realisation from the same process. The two time records will be different, and if we estimate the standard deviation and other statistical parameters from the records, the two sets of estimates will be different, and none of them can be taken as the true values for the background process.

This means that estimates of statistical parameters from a record will have a statistical uncertainty, and the only way to reduce the uncertainty is to increase the length of the record. Dealing with time domain analyses will therefore require estimation of statistical parameters, and we should also be able to quantify the level of uncertainty for our estimates. A broad presentation of methods for stochastic analysis of marine structures is given by [Næss and Moan, 2013].

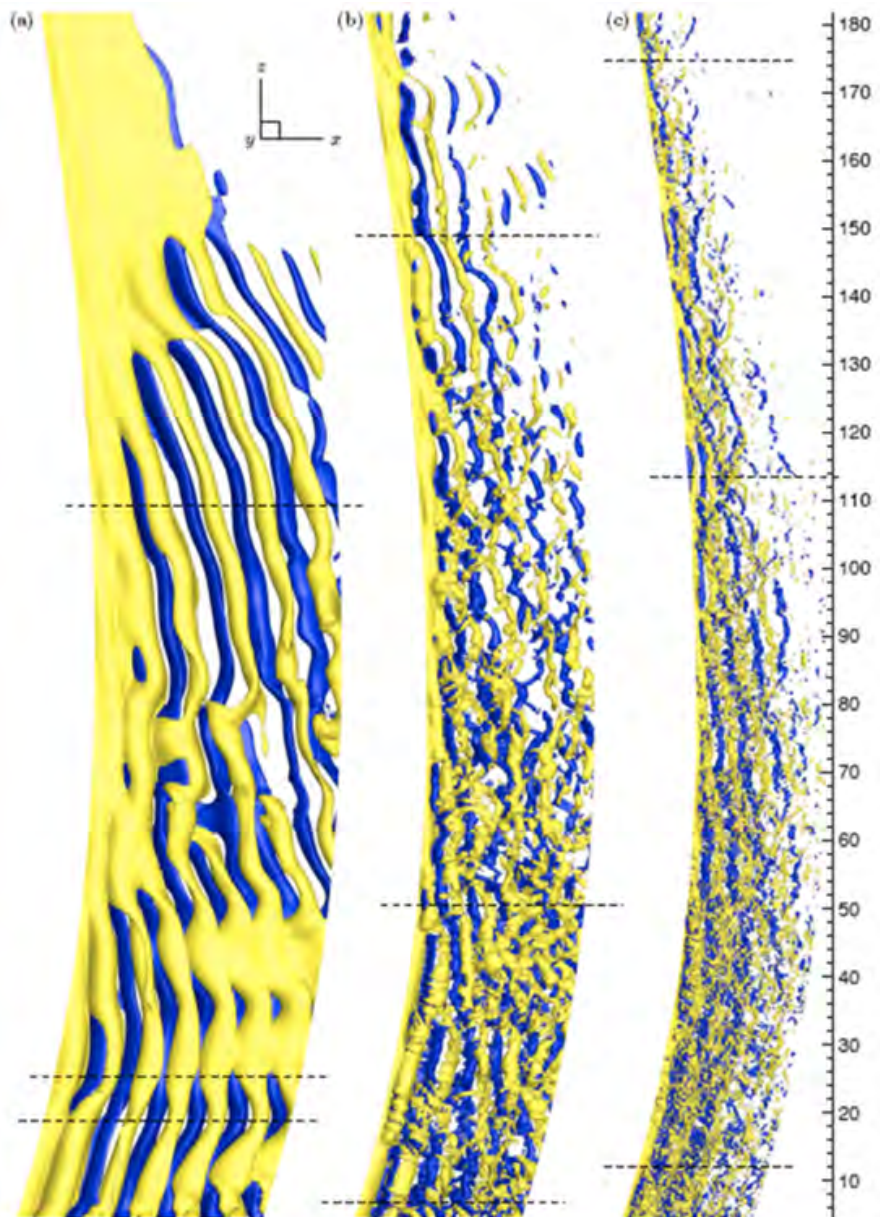


Figure B1.89: Wake visualization in a linearly sheared current. Maximum velocity at bottom equal to 1.1, minimum at top equal to 0.3. (a)  $Re=110$ ; (b)  $Re=330$ ; (c)  $Re=1,100$ . Reynolds number based on maximum velocity. Length to diameter ratio = 180. From [Bourguet et al., 2011], provided separately by Michael Triantafyllou

#### B1.4.8.1 Wave spectra

A large number of wave spectrum equations exist. These have been proposed for use in design of marine structures by individuals or organizations, and they help designers to apply stochastic theory for sea loads in a rational way. The most frequently used spectra are

- Pierson-Moskowitz, based on wave data from the North Atlantic Sea
- JONSWAP (JOint North Sea WAve Project, proposed after a large multi-national wave measurement project in 1968-69

- ITTC, proposed by International Towing Tank Conference
- ISSC, proposed by International Ship (and Offshore) Structures Congress
- Torsethaugen two-peak spectrum, proposed by Torsethaugen to combine wind generated waves with swell.

The general equation for the Pierson-Moskovitz wave spectrum is as follows:

$$[S(\omega)] = \frac{A}{\omega^5} \exp\left[-\frac{B}{\omega^4}\right] \quad (\text{B1.182})$$

A, B: Constants that define the wave spectrum  $A = 0.0081 g^2$ , where  $g$  is the acceleration of gravity  $= 9.81 \text{ m s}^{-2}$   $B = 0.74 (g/v)^4$ , where  $v$  is the wind speed at 19.5 meters above sea surface  $\omega$  Wave frequency (radians per seconds)  $= 2\pi/T$ , where  $T$  is the wave period in seconds  $= 2\pi f$ , where  $f$  is the wave frequency in Hz.

The general equation for spectrum moments is defined by:

$$m_n = \int_0^\infty S(\omega) \cdot \omega^n d\omega, \quad n = 1, 2, \dots \quad (\text{B1.183})$$

Significant wave height,  $H_S$ , defined as the average value of the 1/3 highest waves is found from  $m_0$ , which is the area of the wave spectrum:

$$H_S = 0.21 \frac{v^2}{g} = 4\sqrt{m_0} \quad (\text{B1.184})$$

Mean frequency, rad/sec, corresponding to the centre of gravity of the wave spectrum:

$$\omega_1 = 1.14 \frac{g}{v} = \frac{m_1}{m_0} \quad (\text{B1.185})$$

Average zero up-crossing period in seconds can be found from:

$$T_Z = 2\pi^{\frac{3}{4}} B^{-\frac{1}{4}} = 2\pi \sqrt{\frac{m_0}{m_2}} \quad (\text{B1.186})$$

Relations between spectrum moments and the parameters A and B are given by:

$$\begin{aligned} m_0 &= \frac{A}{4B} \\ m_1 &= 0.306 \frac{A}{B^{3/4}} \\ m_2 &= \frac{\sqrt{\pi}}{4} \frac{A}{\sqrt{B}} \end{aligned} \quad (\text{B1.187})$$

By combining Eq. (3.29) and (3.31) with the definition of B, we have

$$B = \frac{4A}{H_S^2} = \frac{0.0324 g^2}{H_S} \quad (\text{B1.188})$$

By use of this relationship we can define the wave spectrum by the significant wave height instead of the wind speed. An example of a P-M wave spectrum is given on Figure B1.90.

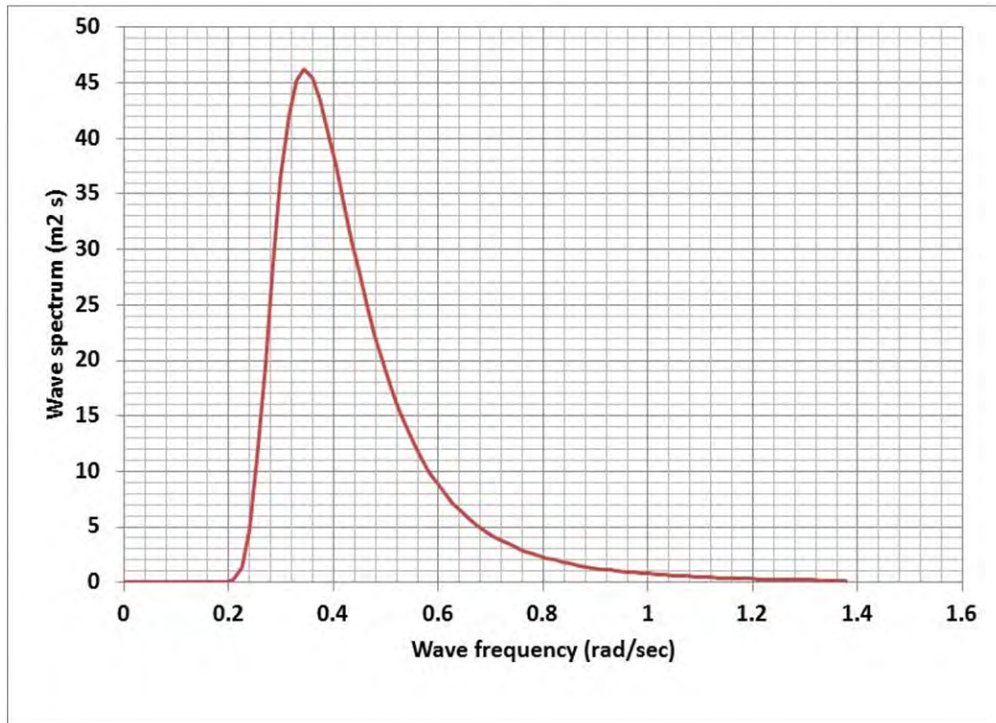


Figure B1.90: Pierson-Moskowitz wave spectrum for  $v = 25 \text{ m/s}$ , corresponding to  $\text{HS} = 13.4 \text{ m}$

#### B1.4.8.2 Generation of wave records

If we know the auto spectrum of a process, a realisation of limited duration can be established by an inverse Fourier transform formally given as:

$$x(t) = \sum_{n=1}^{N} [a_n \cos \omega_n t + b_n \sin \omega_n t] \quad (\text{B1.189})$$

Here  $a_n$  and  $b_n$  are independent Fourier coefficients found from the auto spectrum and  $\omega_n$  is the frequency for the  $n^{\text{th}}$  component. Instead of using sine and cosine components, one component  $c_n$  and a random phase angle  $\varepsilon_n$  are often seen:

$$x(t) = \sum_{n=1}^{N} c_n \sin(\omega_n t - \varepsilon_n) \quad (\text{B1.190})$$

The Fourier transformation means that we use the complete frequency domain representation of the process to go to the time domain where we have a sample of the process with limited duration. Two samples will be different if the sets of random parameters in the above equations are different.

Figure B1.91 shows 10 harmonic components taken from the spectrum shown on Figure B1.90, while Figure B1.92 presents a short part of a time series of the sum of the harmonic components.

#### Method 1. Use of stochastic amplitudes

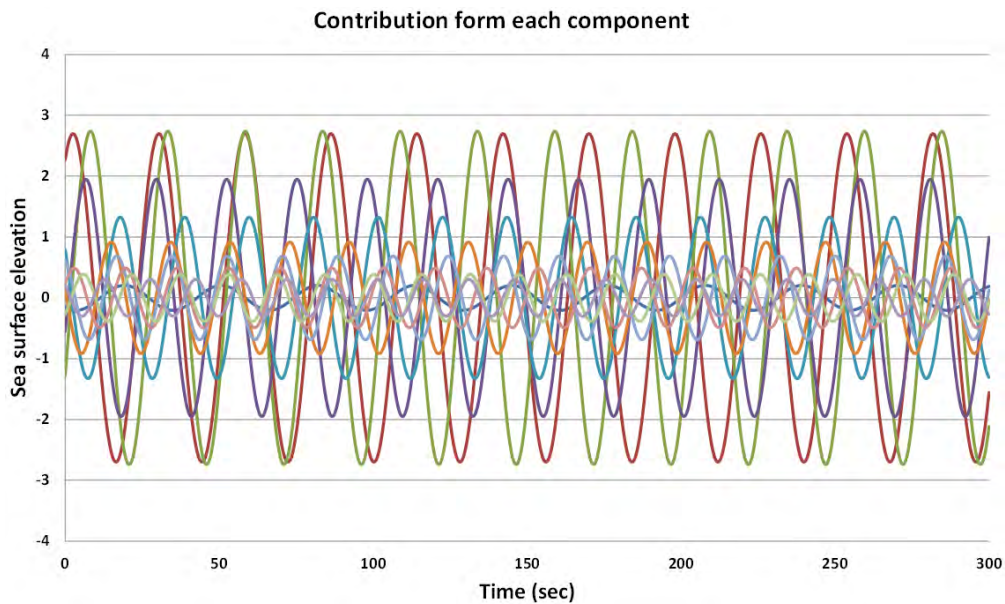


Figure B1.91: Harmonic components from the wave spectrum in Figure B1.90.

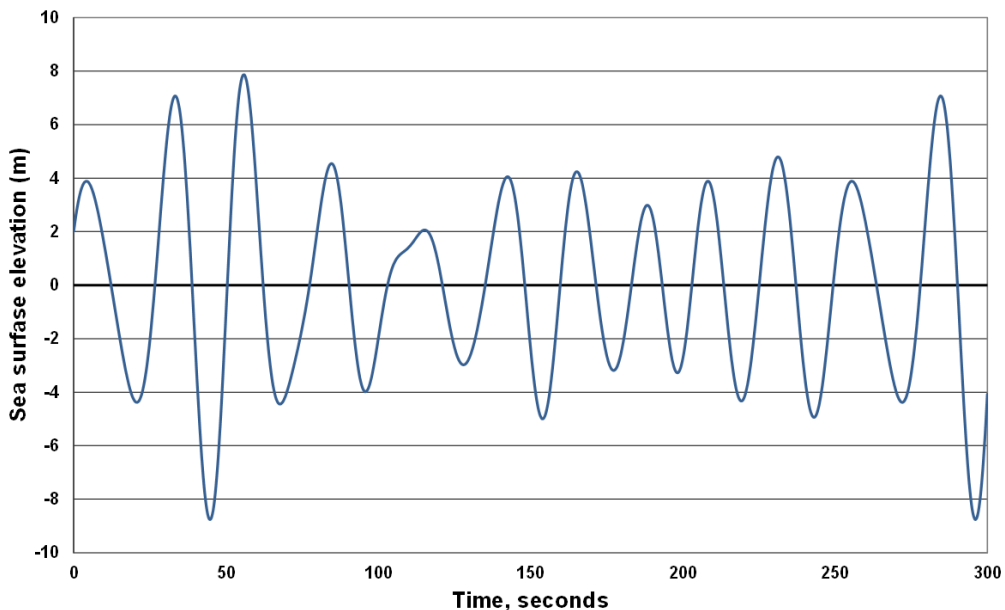


Figure B1.92: Short sample of a stochastic wave process

Using sine and cosine functions, both  $a_n$  and  $b_n$  should be independent stochastic variables:

$$x(t) = \sum_{n=1}^N [a_n \cos \omega_n t + b_n \sin \omega_n t] \quad (\text{B1.191})$$

Both should be taken from a Gauss distribution with zero mean and variance given by

$$\sigma_{a_n}^2 = \sigma_{b_n}^2 = \sigma_n^2 = S_x(\omega_n) \Delta \omega_n \quad (\text{B1.192})$$

Note that this method will require  $2N$  independent variables in order to define a sample with  $N$  frequencies. The result of this method will become a sample from a true Gaussian

process. The variance that may be estimated from each sample will vary from one sample to another, as is the case for true stochastic process. Such samples will also give correct estimates for statistical parameters for individual maxima and largest amplitude in a limited period of time. Note also that the relative value of  $a_n$  and  $b_n$  will define the phase angle for this component.

### Method 2. Use of one stochastic amplitude and stochastic phase

It is also possible to generate samples with correct statistical properties by using the cosine series with a random phase:

$$x(t) = \sum_{n=1}^N c_n \sin(\omega_n t - \varepsilon_n) \quad (\text{B1.193})$$

A stochastic amplitude  $c_n$  must be considered:

$$c_n = \sqrt{a_n^2 + b_n^2} \quad (\text{B1.194})$$

As  $a_n$  and  $b_n$  are Gaussian distributed with identical parameters,  $c_n$  will be Rayleigh distributed with a variance equal to the sum of the variances for the two components. Hence, the standard deviation of the stochastic amplitude  $c_n$  will be given by:

$$\sigma_{c_n} = \sqrt{\sigma_{a_n}^2 + \sigma_{b_n}^2} = \sqrt{2 S_x(\omega_n) \Delta \omega_n} = \sqrt{2} \sigma_n \quad (\text{B1.195})$$

The Rayleigh distribution is given by

$$F_Y(y) = 1 - \exp\left[-\frac{1}{2}\left(\frac{y}{\sigma}\right)^2\right] \quad (\text{B1.196})$$

where  $\sigma$  is the only free parameter. The variance of this distribution is given by

$$\sigma_Y^2 = 2\sigma^2 \quad (\text{B1.197})$$

By combining the three equations above we may write the Rayleigh distribution for the cosine amplitude  $c_n$  as

$$F_{C_n}(c_n) = 1 - \exp\left[-\frac{1}{2}\left(\frac{c_n}{\sigma_n}\right)^2\right] \quad (\text{B1.198})$$

The stochastic amplitude can now be found by the following procedure

1. Draw a random number  $p$  from an even distribution in the interval  $[0, 1]$
2. Calculate the random amplitude  $c_n$  by solving the equation for the Rayleigh distribution with respect to  $c_n$  :

$$p = 1 - \exp\left[-\frac{1}{2}\left(\frac{c_n}{\sigma_n}\right)^2\right] \quad (\text{B1.199})$$

or

$$c_n = \sqrt{\ln(1-p)} \sqrt{2} \sigma_n \quad (\text{B1.200})$$

By introducing the known relation for  $\sigma_n$  we have

$$c_n = \sqrt{\ln(1-p)} \sqrt{2 S_x(\omega_n) \Delta \omega_n} = \sqrt{\ln(1-p)} \cdot c_n^* \quad (\text{B1.201})$$

where  $c_n^*$  is the deterministic amplitude of a harmonic component, found from the auto spectrum by

$$c_n^* = \sqrt{2 S_x(\omega_n) \Delta \omega_n} \quad (\text{B1.202})$$

The phase angle  $\varepsilon_n$  is related to the stochastic amplitudes by

$$\varepsilon_n = \tan^{-1} \frac{b_n}{a_n} \quad (\text{B1.203})$$

$\varepsilon_n$  must be evenly distributed in the interval  $[0, 2\pi]$ .

Note that this method will have the same number of random variables as the first method, and will give time records with the same statistical properties. This method is simpler to implement as it uses random numbers from even distributions and one trigonometric function only, in contrast to the first method that must handle Gauss distributions and two trigonometric functions. This method is therefore more often applied than the first.

**Method 3. Use of deterministic amplitudes and stochastic phase** In this case the Fourier transformation will follow the equation

$$x(t) = \sum_{n=1}^N c_n^* \sin(\omega_n t - \varepsilon_n) \quad (\text{B1.204})$$

where the component amplitude  $c_n^*$  is deterministic and given from the auto spectrum according to Eq. B1.202). The phase angles  $\varepsilon_n$  are independent stochastic variables taken from an even distribution in the interval  $[0, 2\pi]$ . A random number generator may be used to generate these parameters.

When using this method, the generated time records will always have a variance exactly equal to the variance found by integrating the auto spectrum. This is, as previously mentioned, not the case for a sample of limited length from a real Gaussian process.

The samples produced by this method are therefore not samples from a true Gaussian process, and will not have the correct statistical distributions for extremes. They will also show differences in grouping effects for individual maxima as compared to samples from true Gaussian processes. These shortcomings might become important when samples are used to generate second order wave forces and when dynamic simulations are used to estimate the variability of extreme responses as is the case in a reliability analysis.

This method is frequently applied as it is the simplest method. In spite of its theoretical weaknesses the method will give a correct distribution for individual maxima, which in most cases is the result of primary interest.

**General comments on time series generation** The methods that have been described here have a common limitation with respect to length. If the frequency interval is  $\Delta\omega$ , the time record will start to repeat itself after a period  $c_n$  given by

$$T_P = \frac{2\pi}{\Delta\omega} \quad (\text{B1.205})$$

Periodicity is illustrated on Figure B1.93, where the record is seen to repeat itself after 50 seconds. This feature can be useful for stochastic time domain simulation of dynamic systems. In a time domain analysis there will be a transient phase in the simulation until damping has eliminated the influence from the initial condition. This period cannot be

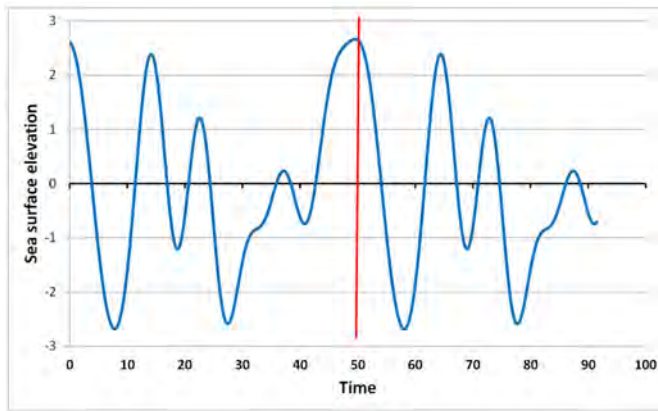


Figure B1.93: Illustration of periodic time series

included in a statistical analysis of the time record. Since the record is periodic with period  $T_P$ , the condition at  $T_P$  is a perfect match to the initial condition at  $T=0$ . By continuing the time integration beyond  $T_P$  we can obtain a record with length  $T_P$  without any influence from the initial condition, and the full length can be used to estimate statistical parameters. This is in particular useful for simulation of systems that have some eigenfrequencies lower than the wave frequencies since the associated modes will have a long transient period. Simulation of articulated towers subjected to first order wave forces is an example. The pendulum mode will have an eigenfrequency below the wave frequency range and hence contribute to the response during a large number of wave periods.

**Calculation of the spectrum function from a measured record** If we have a time record of limited length  $T$ , the spectrum for the process that we assume to be the source for the sample,  $S_x(\omega)$ , may be estimated by taking the Fourier transform of the time history. Formally the Fourier transform of a function  $x(t)$  may be expressed as

$$a_i = \frac{2\pi}{T} \int_0^T x(t) \sin(\omega_i t) dt \quad b_i = \frac{2\pi}{T} \int_0^T x(t) \cos(\omega_i t) dt$$

$$\omega_i = i \cdot \frac{2\pi}{T}, \quad i = 1, 2, \dots, N \quad \Delta\omega = \frac{2\pi}{T} \quad (B1.206)$$

$$x_i = \sqrt{a_i^2 + b_i^2} \quad S_x(\omega_i) = \frac{1}{2\Delta\omega} x_i^2$$

Number of frequency components  $N$  must be sufficiently large to represent the frequency content in the signal  $x(t)$  with wanted accuracy. The spectrum found when applying these equations on a measured signal will often show large variations from one discrete frequency to the next. Smoothing techniques are therefore often applied.

Using these equations will involve numerical integration to find the Fourier coefficients  $a_i$  and  $b_i$ . This type of computation is time consuming if long time series are handled. In many cases more than 10.000 time increments and frequency components might be involved. In order to speed up the computation, special numerical techniques have been developed, known as Fast Fourier Transforms (FFT). Use of FFT will give a considerable reduction as compared to straightforward use of the given equations, but some restrictions will apply. The time increment  $\Delta T$  and the frequency discretization  $\Delta\omega$  must be constant, and there will be a fixed relationship between number of time increments  $N\Delta T$ , number of frequency

components  $N\Delta\omega$ , time length of the generated record  $T$ , and cut-off frequencies  $\omega_{\max}$  and  $\omega_{\min}$ . These relations will become as follows

$$\begin{aligned}\Delta T &= T/N_{\Delta T} & N_{\Delta T} &= 2N_{\Delta\omega} & \Delta\omega &= 2\pi/T \\ \omega_{\min} &= \Delta\omega & \omega_{\max} &= \Delta\omega N_{\Delta\omega}\end{aligned}\quad (\text{B1.207})$$

The use of this method is discussed more in detail by [Tucker et al., 1984]. Verification of generated time series. Random numbers are needed to produce a record of stochastic waves. It is not easy to produce a large number of genuine random numbers. However, several algorithms have been made to generate 'pseudo random numbers'. By specifying a seed number, the algorithm will be able to generate a long sequence of 'random' numbers. The second number is a function of the seed, the third number is a function of the second number etc. A good algorithm can generate a long sequence without hitting the original seed number and hence avoid giving a periodic series of numbers.

Sophisticated tests of randomness exist, but it is also possible to have a simple control of the quality of the wave record that is produced by use of the pseudo random phase angles. Mean value and variance of the record will be correct unless there are errors in the computer code, but parameters linked to higher order moments of the probability density function might be used as indicators for accepting records.

Skewness is an indicator for symmetry of the probability density function and is found from

$$\gamma = \frac{m_{PD,3}}{m_{PD,2}^{\frac{3}{2}}} \approx \frac{\frac{1}{N} \sum_{i=1}^N x_i^3}{\left( \frac{1}{N} \sum_{i=1}^N x_i^2 \right)^{\frac{3}{2}}} \quad (\text{B1.208})$$

where  $m_{PD,N}$  is the nth order moment of the probability density function,  $N$  is number of time increments, and  $x_i$  is the discrete value of the process (sea surface elevation in our case). Skewness for a true Gaussian process is zero, and if the calculated value from a generated record is significantly different from zero one should not apply the record in a simulation. Kurtosis represents the property of the tails for the probability density function and is found from fourth and second moments:

$$k_x = \frac{m_{PD,4}}{m_{PD,2}^2} \approx \frac{\frac{1}{N} \sum_{i=1}^N x_i^4}{\left( \frac{1}{N} \sum_{i=1}^N x_i^2 \right)^2} \quad (\text{B1.209})$$

Kurtosis for the Gauss distribution is 3. Higher values indicate that the tail is higher than for a Gaussian distributed variable, which means that the sample contains more large values (positive and negative) than predicted by the Gauss distribution. Lower values tell that the sample contains less large values than wanted. The statistical variation of kurtosis between short samples might be large since  $x^4$  is a strong function, but long samples should have kurtosis close to 3.

### B1.4.8.3 Short term statistics

The fundamental assumption for short term statistics of waves is that the sea surface elevation is a stationary, ergodic Gaussian process with zero mean value. The three terms may be defined as follows:

- Stationary means that the statistical properties of the process are constant in time during an observation period
- Ergodic implies that all statistical information about the process is contained in each and every realization [Næss and Moan, 2013])
- A process is Gaussian if a set of measurements (process values) taken at time  $t + n \cdot \delta, n = 1, 2, 3, \dots$ , fits a Gaussian distribution, see Figure B1.94.

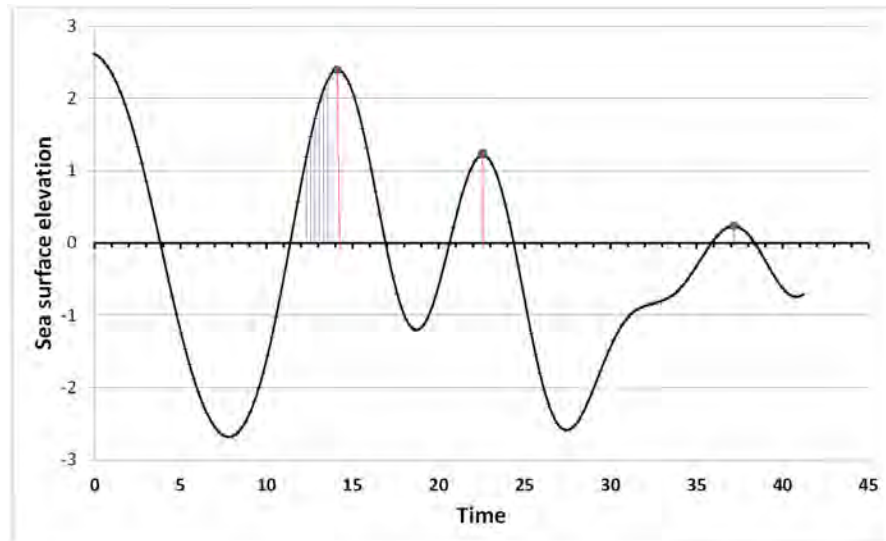


Figure B1.94: Illustration of process values (blue lines) and individual maxima (red lines)

The variance  $\sigma_x^2$  of the process  $x(t)$  can be found from the spectrum:

$$\sigma_x^2 = m_0 = \int_0^\infty S(\omega) d\omega \quad (\text{B1.210})$$

The bandwidth  $\varepsilon$  of a process indicates the range of frequency that contains significant energy. The mathematical definition of the bandwidth parameter for a Gaussian process is given by

$$\varepsilon = 1 - \frac{m_2^2}{m_0 m_4} \quad (\text{B1.211})$$

$m_n$  in Eq. B1.210 and B1.211 is the  $n^{th}$  order moment of the spectrum, see Eq B1.183.

A narrow banded process ( $\varepsilon = 0$ ) will have one individual maximum between each zero up-crossing, and all maxima will be positive, while broad banded processes may have multiple maxima between zero up-crossings, and also negative maxima, see Figure B1.95.

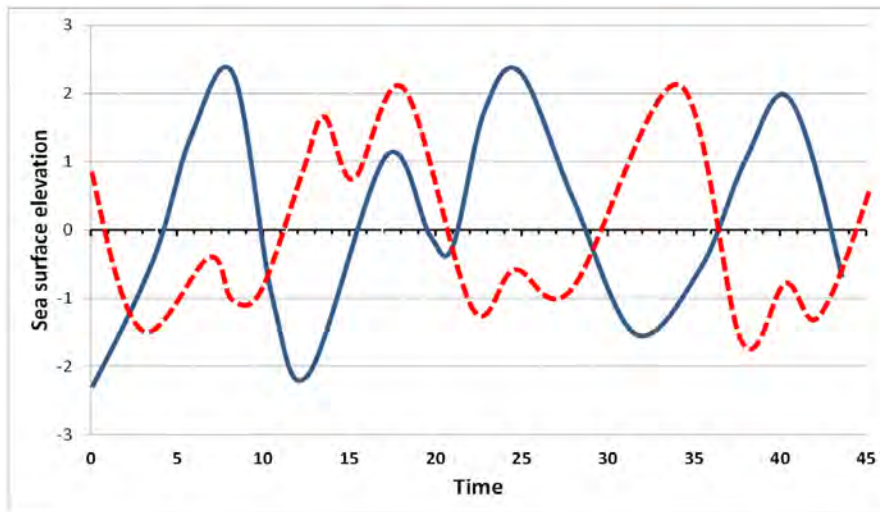


Figure B1.95: Illustration of broad banded (red dotted line) and narrow banded (blue line) processes

The distribution of individual maxima (see Figure B1.94) will depend on the bandwidth parameter, and is in general known as the Rice distribution (see Figure B1.96) given as

$$f_{X_a}(x_a) = \frac{\varepsilon}{\sigma_x \sqrt{2\pi}} \exp\left[-\frac{x_a^2}{2\sigma_x^2 \varepsilon^2}\right] + \frac{\sqrt{1-\varepsilon^2}}{2\sigma_x^2} x_a \exp\left[-\frac{x_a^2}{2\sigma_x^2}\right] \cdot \left[1 + \operatorname{erf}\left(\frac{x_a}{\varepsilon} \sqrt{\frac{1-\varepsilon^2}{2\sigma_x^2}}\right)\right]$$

where

$$\operatorname{erf}(x) = \frac{2}{\sqrt{\pi}} \int_0^x e^{-t^2} dt$$
(B1.212)

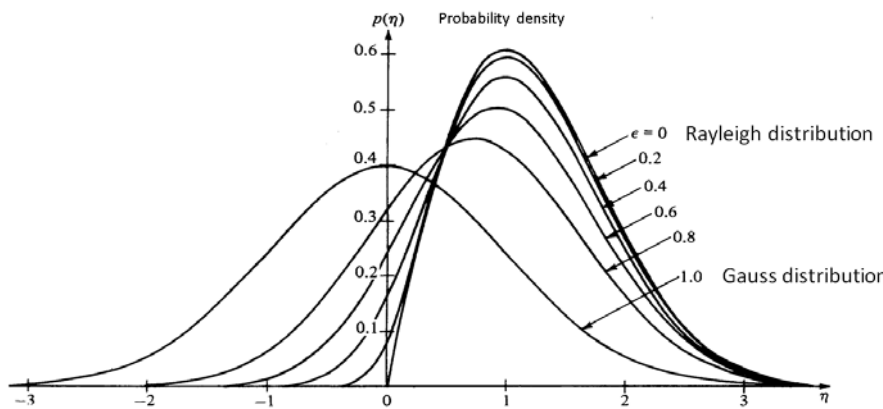


Figure B1.96: Transition from Gauss to Rayleigh distribution by the Rice distribution, [Berge et al., 1992]

The Rice distribution will be reduced to the Rayleigh distribution for a narrow-banded process ( $\varepsilon = 0$ ). Hence, the probability density function for individual maxima will become

$$f_{X_a}(x_a) = \frac{x_a}{\sigma_x^2} \exp\left(-\frac{x_a^2}{2\sigma_x^2}\right), \quad x_a \in [0, \infty] \quad (B1.213)$$

Note that the variance for the Gaussian process is the only parameter for the Rayleigh distribution. Hence, if we know the wave spectrum, we also know the distribution of individual

maxima in a wave record. The other extreme value for the bandwidth parameter is  $\varepsilon = 1$ . This means that the frequency bandwidth is unlimited, which tells that all frequencies have equal intensity in the process. The distribution for individual maxima will then become the Gaussian distribution defined by

$$f_{X_a}(x_a) = \frac{1}{\sqrt{2\pi} \cdot \sigma_x} \exp\left(-\frac{x_a^2}{2\sigma_x^2}\right), \quad x_a \in [0, \infty] \quad (\text{B1.214})$$

Figure B1.96 illustrates how the Rice distribution defines a transition between the Gauss and Rayleigh distributions. In design we often want to know how large the largest wave or response,  $x_{\max}$ , might be during a given duration of a sea state. Figure B1.97 illustrates how this type of distribution can be established. The process must be observed for several periods of time with duration  $T$ , and the largest individual maximum in each sample is recorded. The new sample consists of a number of largest maxima among  $N$  maxima,  $x_{\max}$ , where  $N$  is given by

$$N = \frac{T}{\bar{T}}, \quad \bar{T} \text{ is the average time between each zero up-crossing} \quad (\text{B1.215})$$

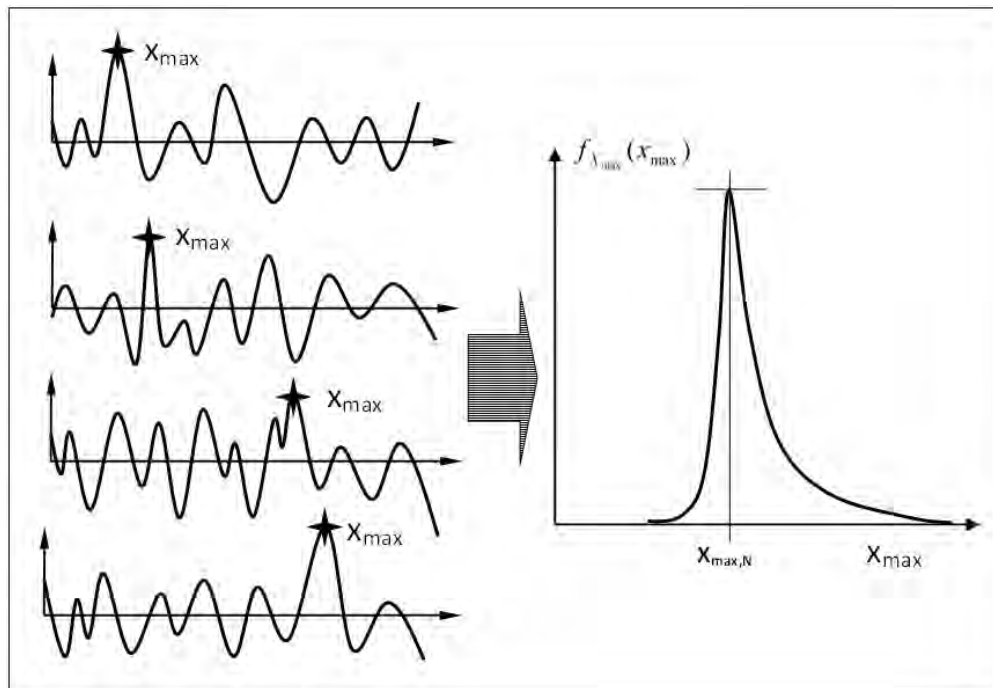


Figure B1.97: Definition of the extreme value distribution

Note that the distribution of individual maxima in a sea state is independent on the observation period, while the extreme value distribution depends on  $T$ . Figure B1.98 shows all distributions that have been discussed in this section; Gauss, Rice and Rayleigh, together with extreme value distributions for varying duration.

Two characteristic values from the extreme value distribution are often applied as reference values in structural design:

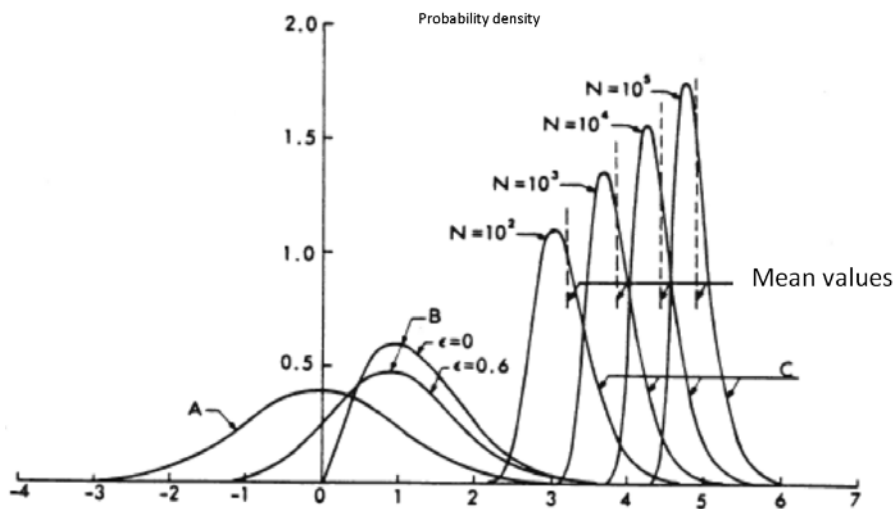


Figure B1.98: Distributions for individual maxima (Gauss, Rice and Rayleigh distributions) together with extreme value distributions for varying sea state durations, [Berge et al., 1992].

- The expected largest, or mean value:

$$\bar{X}_{\max,N} = \sigma_x \left[ \sqrt{2 \ln N} + \frac{0.5772}{\sqrt{2 \ln N}} \right] \quad (\text{B1.216})$$

- The most probable largest :

$$X_{\max,N} = \sigma_x \sqrt{2 \ln N} \quad (\text{B1.217})$$

The most probable largest corresponds to the maximum for the extreme value distribution since the value has the largest probability density.

#### B1.4.8.4 Long term statistics

The short term distribution for individual maxima (Rice or Rayleigh distributions) is valid for a specific sea state defined by its wave spectrum. The sea state is normally uniquely defined by the significant wave height  $H_s$  and a characteristic wave period  $T_p$  or  $T_z$ . In design we want to have a similar relationship for waves and response that is valid during the entire lifetime of a structure. Two types of statistical information are then required:

- Long term statistics of sea state parameters
- Statistics for individual maxima in each sea state

Long term statistics of sea states will often be presented by frequency tables for observed sea states with given combinations  $H_s$  and  $T_p$ . Figure B1.99 shows an example of this type of table with data from the Ekofisk field in the North Sea. Frequency tables might be defined for summer and winter season, and also split up in classes of dominating wave direction  $\alpha$ .

This type of data may be applied to define empirical distributions for sea state parameters. Haver and Nyhus (1986) proposed to use a marginal distribution for  $H_s$ ,  $F_{H_s}(h_s)$ , and a conditional distribution for  $T_z$  for given  $H_s$ ,  $F_{T_z|H_s}(T_z|h_s)$ . Data for the marginal distribution is found in the left column in the frequency table in Figure B1.99.

Hm0\Tp	< 4	4 - 5	5 - 6	6 - 7	7 - 8	8 - 9	9 - 10	10 - 11	11 - 12	12 - 13	13 - 14	14 - 15	15 - 16	16 - 17	17 - 18	18 - 19	19 - 20	20 - 21	21 <	
0 - 0.5	219	247	98	56	108	139	85	53	38	28	16	9	3	1	1	1	1	1	1102	
0.5 - 1.0	462	1444	1332	551	394	409	362	255	153	126	66	73	28	20	9	4	1	2	5691	
1.0 - 1.5	54	763	1991	1654	703	436	327	258	176	86	49	49	23	21	22	3	3	5	6626	
1.5 - 2.0	1	114	994	2015	1329	583	260	246	193	91	37	20	10	16	14	3	1	1	5927	
2.0 - 2.5		7	189	1122	1532	734	261	182	165	124	48	20	8	1	1	2	1	2	4399	
2.5 - 3.0			14	329	1082	958	309	137	139	96	39	13	6		1	1	1	1	3125	
3.0 - 3.5				59	533	983	382	140	87	72	33	15	4	2		1			2311	
3.5 - 4.0					10	133	660	418	144	65	36	23	14	3	4				1510	
4.0 - 4.5						28	313	417	149	41	25	7	10	4	1				995	
4.5 - 5.0							2	113	271	190	40	19	8	6	2	1			652	
5.0 - 5.5								23	154	136	49	23	7	12	4				408	
5.5 - 6.0									4	61	109	52	26	4	6	4				266
6.0 - 6.5										20	58	35	14	6	4	5				142
6.5 - 7.0											6	23	35	14	5	2	1			86
7.0 - 7.5											2	21	16	13	4	3	2	1	1	63
7.5 - 8.0												4	8	9	3	1				25
8.0 - 8.5												2	8	3	2	3	2			20
8.5 - 9.0													2	5	2					9
9.0 - 9.5													1	5	1	3	2			12
9.5 - 10.0																1				1
10.0 - 10.5														2	1	1				5
10.5 - 11.0															1					1
11.0 - 11.5															1					3
11.5 - 12.0																1				1
12.0 <																				
	736	2575	4618	5796	5844	5355	3335	2107	1303	818	362	267	111	70	48	15	6	5	9	

Figure B1.99: Example of frequency table for observed sea states defined by  $H_S$  and  $T_P$ , all seasons and directions, [Myrhaug and Lian, 2009].

If the long term distribution for sea state parameters is known, the long term distribution for individual maxima can be found as a weighted sum of short term distributions

$$Q_{X_a}(x_a) = \sum_{H_S} \sum_{T_Z} \sum_{\alpha} Q_{X_a|H_S, T_Z, \alpha}(x_a | H_S, T_Z, \alpha) \cdot w(H_S, T_Z, \alpha) \quad (\text{B1.218})$$

The weight function for a specific sea state  $w(H_S, T_Z, \alpha)$  must represent the probability for an arbitrary maximum to appear in this sea state. This probability must be the product of the probability for the sea state to occur (from the frequency table) and the ratio between the average and actual zero up-crossing period  $g(T_Z)$ :

$$\begin{aligned} w(H_S, T_Z, \alpha) &= P(H_S, T_Z, \alpha) \cdot g(T_Z) \\ g(T_Z) &= \frac{\text{mean } T_Z \text{ all sea states}}{\text{mean } T_Z \text{ actual sea state}} \end{aligned} \quad (\text{B1.219})$$

The long term distribution is normally presented as the cumulative probability of being larger than,  $Q_{X_a}(x_a)$ , and a logarithmic scale is used for the probability on the horizontal axis, see Figure B1.100.

If the average zero up-crossing period is 6.3 seconds, there will be 108 individual maxima during 20 years. A second horizontal axis can now be made to present number of waves that exceeds a given level during 20 years. Since the vertical axis in this example is positioned at a probability level of 10-8, the N axis indicate that only one maximum will in average exceed the  $x_a$  value at the intersection between the probability function and the vertical axis. This means that  $X_{\max, 20}$  on Figure B1.100 is the amplitude level that in average will be exceeded every 20th year, which means that this amplitude has a return period of 20 years. The third axis on Figure B1.100 presents the return period in years, which in general can be calculated

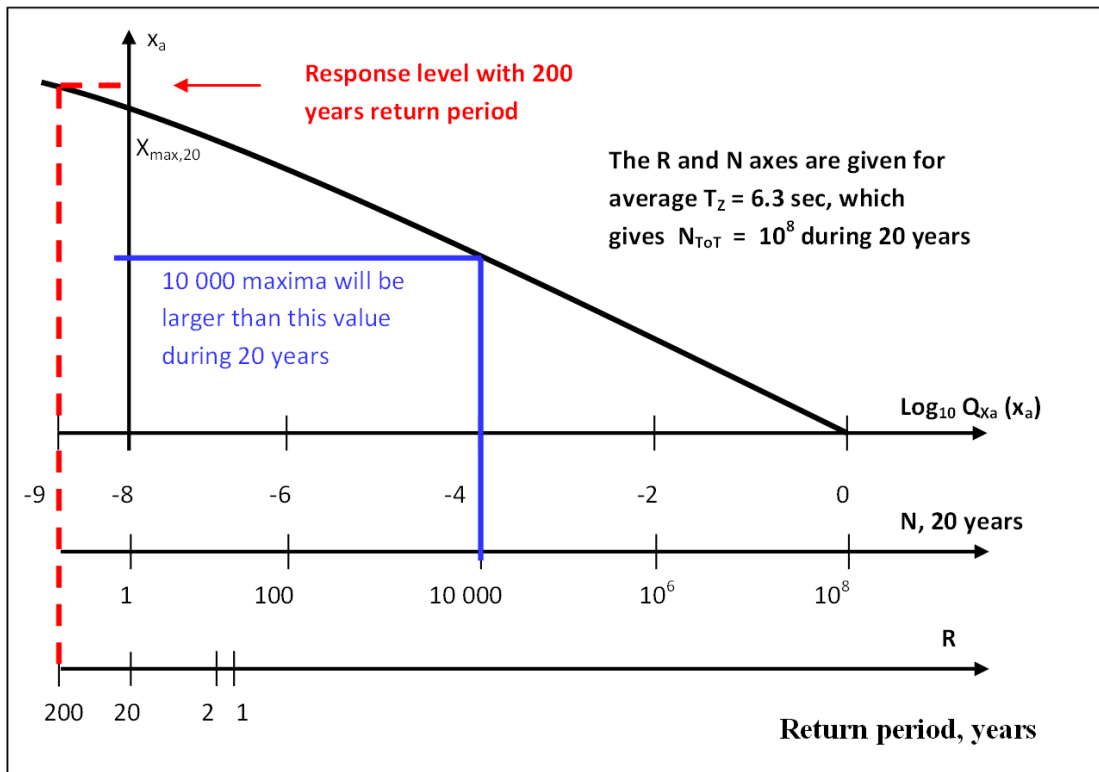


Figure B1.100: The long term distribution for individual maxima

by solving the equation

$$Q_{Xa}(x_{a,N}) = \frac{\bar{T}_Z}{N \cdot 365 \cdot 24 \cdot 60 \cdot 60} \quad (\text{B1.220})$$

where  $x_{a,N}$  is the individual maximum that has a return period of  $N$  years. Eq. B1.220 must be solved by iteration for a given value of  $N$ .

#### B1.4.8.5 Stochastic analysis in frequency domain

If a linear structure is subjected to a regular wave with amplitude  $\zeta_a$  and frequency  $\omega$ , the response amplitude  $x_a$  can in general be written as

$$x_a(\omega) = H_x(\omega) \zeta_a(\omega) \quad (\text{B1.221})$$

(49)  $H_x(\omega)$  is the transfer function for the actual response type, and gives a relationship between the wave amplitude and the response amplitude for the actual frequency. The transfer function will normally consist of a hydrodynamic and a mechanical component. The hydrodynamic part gives a relationship between the wave and the external load on the structure, while the mechanical part defines the relationship between the load and dynamic response. The relation between a bar in the wave spectrum  $S(\omega_i) \Delta\omega$  and the amplitude of a regular wave component that is represented by this bar is given by (see Eq (B1.202)).

$$\frac{1}{2} \zeta_{ai}^2 = S(\omega_i) \Delta\omega_i \quad (\text{B1.222})$$

By combining Eq (B1.221) and (B1.231) we understand that the response spectrum can easily be found if we know the wave spectrum and the transfer function:

$$S_x(\omega) = H_x^2(\omega) \cdot S_\zeta(\omega) \quad (\text{B1.223})$$

This type of calculation is frequently applied for calculation of vessel motions since we can assume that the motion components are uncoupled. Figure B1.101 illustrates that the response spectrum may have two peaks; one quasi-static peak at the wave spectrum peak, and one at the eigenfrequency of the structure. Note that this is not necessarily the case, but an illustration of what may happen. Another observation is that the phase information between the wave and response is not taken care of in Eq B1.223.

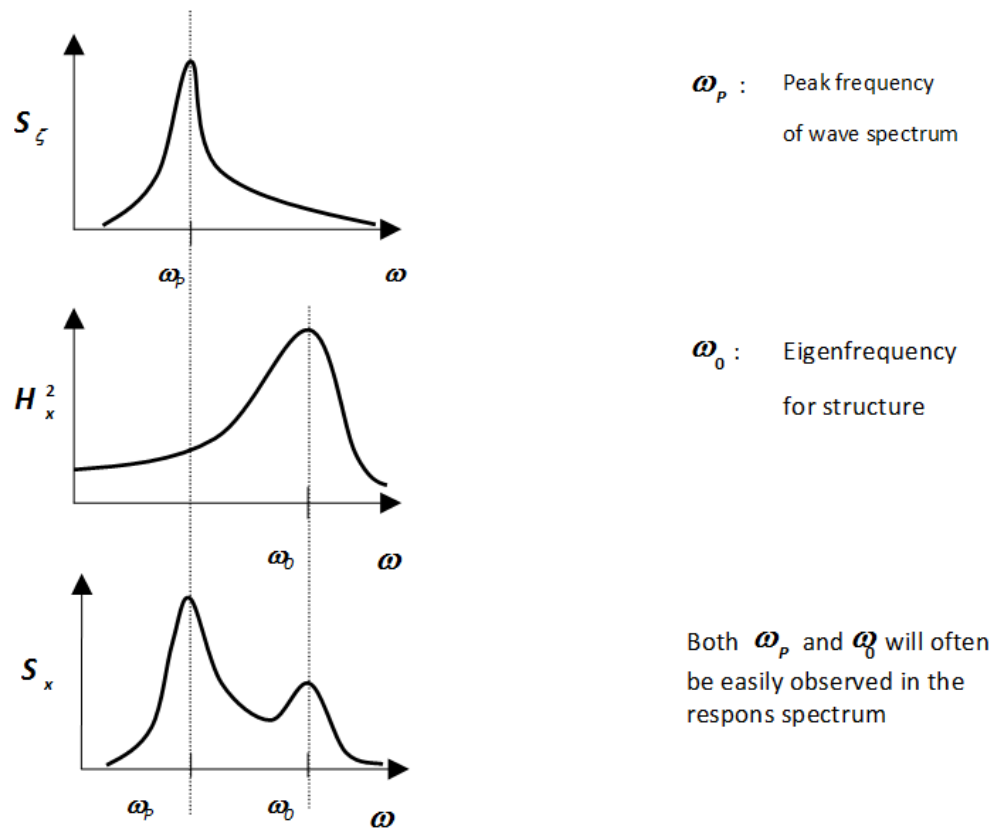


Figure B1.101: From wave spectrum to response spectrum, linear system

Dynamic analysis of flexible risers will almost always be carried out by use of finite elements. In this case we are faced to a multi-degree-of-freedom system, which cannot be solved by use of Eq B1.223 . One obvious reason is that the degrees of freedom are structurally coupled, and that the phase angle between response components must be known in order to calculate stresses.

Dynamic equilibrium for a finite element model can be formulated by relating the sum of inertia, damping and restoring (stiffness) forces to external forces:

$$\mathbf{M} \ddot{\mathbf{r}} + \mathbf{C} \dot{\mathbf{r}} + \mathbf{K} \mathbf{r} = \mathbf{R}(t) \quad (\text{B1.224})$$

This equation can be solved in frequency domain by restricting the load vector to be harmonic and limiting the application to linear systems. The load and response vectors  $\mathbf{R}$  and  $\mathbf{r}$  can now be written as:

$$\mathbf{R} = \mathbf{X} e^{i\omega t} ; \quad \mathbf{r} = \mathbf{x} e^{i\omega t} \quad (\text{B1.225})$$

The dynamic equilibrium equation can now be written as

$$\begin{aligned} & (\mathbf{K} + i\omega \mathbf{C} - \omega^2 \mathbf{M}) \mathbf{x} = \mathbf{X} \\ & \text{or : } \mathbf{x}(\omega) = \mathbf{H}(\omega) \mathbf{X}(\omega) \\ & \text{where : } \mathbf{H}(\omega) = (\mathbf{K} + i\omega \mathbf{C} - \omega^2 \mathbf{M})^{-1} \end{aligned} \quad (\text{B1.226})$$

The  $\mathbf{H}$  matrix is the complex frequency response function. Each element in the  $\mathbf{H}$  matrix,  $h_{ij}$ , represents the transfer function between a load in degree of freedom  $j$  and the response in degree of freedom  $i$ . By the use of a complex load vector, the phase information between load components is included. The complex frequency response matrix will define the phase between load and response. Hence, the complex response vector will describe both the magnitude of the response at all degrees of freedom and their phase angles. A stochastic analysis in frequency domain means that we have to reformulate Eq. B1.223 by introducing Eq B1.226. In order to represent the phase information correctly both for the loads and also for the response, we have to include the cross spectra in addition to the auto spectra in the calculation. The solution for one frequency can hence be found from the following equation:

$$\mathbf{S}_{rr}(\omega) = \mathbf{H}(\omega) \mathbf{S}_{LL}(\omega) \mathbf{H}^{*T}(\omega) \quad (\text{B1.227})$$

where the  $\mathbf{S}_{LL}$  matrix contains the complex load spectrum terms and  $\mathbf{S}_{rr}$  the complex response spectrum terms for the actual frequency. The main diagonal carries the auto spectrum terms (real values), while the terms  $S_{xx,ij} = S_{xx,ij}^*$  give the complex cross spectra terms where phase information is contained. The \* symbol defines the complex conjugate operator.

Eq. B1.227 gives us the solution for one single frequency. We need to find the solution for a large set of frequencies (100 is a typical number) in order to find the spectrum for the response and hence define its statistical distribution. Formally we can illustrate the computation process by Figure B1.102.

If we have calculated the load spectra for  $N$  frequencies, we will have the auto spectra terms on the main diagonal. Hence, the set of  $S_{L_i L_i}(\omega_n)$ ,  $n = 1, 2, \dots, 100$  contains all auto spectra terms that we need to define the auto spectrum  $S_i(\omega)$ . By replacing  $S_{L_i L_i}$  with  $S_{r_i r_i}$  we have the response spectrum for degree of freedom  $i$ . Once the spectra for deformations are found, spectra for stresses can be calculated by introducing standard equations for cross section analyses. Note that since phase information is carried through the computation, we can have correct stresses from combined action of axial forces and bending moments.

To apply this method to flexible risers we have to include an iteration since the drag forces are non-linear. The procedure for this type of iteration is described by [Krolkowski and Gay, 1980].

One may argue that this type of computation is far more complex than straightforward time integration, even for non-linear systems. The reason why frequency domain analyses still are in use, is that the statistical analysis following the response calculation becomes simple. The spectrum of stresses becomes available, and fatigue damage can be found

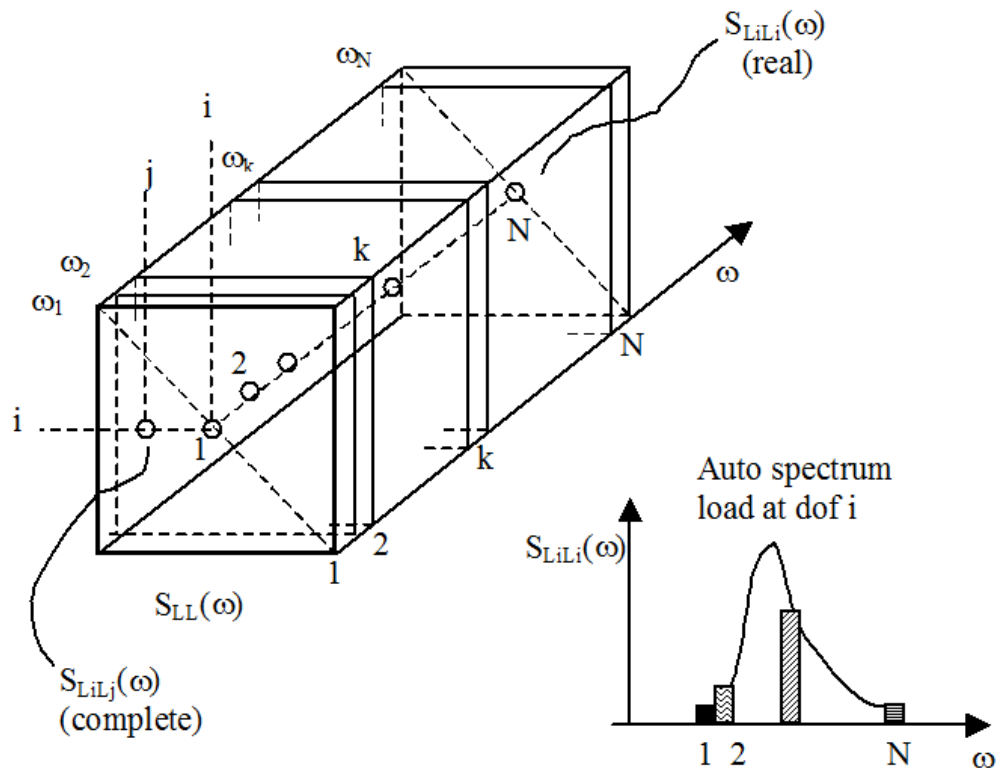


Figure B1.102: Illustration of the stochastic analysis process

from closed form equations. Non-linear analysis is mandatory for extreme response estimation, but fatigue may be calculated with acceptable accuracy in frequency domain, see also [Leira and Remseth, 1985].

#### B1.4.8.6 Stochastic response analysis, time domain

Time domain analysis is today the standard method for calculation of dynamic response of slender marine structures. The main reason is that most limitations we have in frequency domain methods are easy to overcome in time domain. This is in particular true for non-linear drag forces and forces in the wave zone since such effects can be accounted for even if the system matrices are kept constant.

The main difference between time and frequency domain from a statistical point of view is that the frequency domain analysis will calculate the response spectrum, while time domain will produce a sample of the stochastic response process. All needed statistical information is available from the spectrum, but from the time record we have to estimate statistical parameters. One may state that frequency domain will give a result with a large model uncertainty but without any statistical uncertainty, while time domain will reduce the model uncertainty but at the expense of an inherent statistical uncertainty. The only way we have to reduce the statistical uncertainty is to extend the duration of simulations.

Statistical uncertainty will play a different role for fatigue calculation than for extreme response estimation. Fatigue will be strongly linked to the variance of the stress process, while extremes are described by the tail of the distribution. It is also important to note that extreme sea state will not be important for fatigue since the average duration per year is low, see

Figure B1.103. Hence, linear (frequency domain) analyses will therefore often give sufficient accuracy for fatigue analysis, but will be inadequate for extreme response estimation.

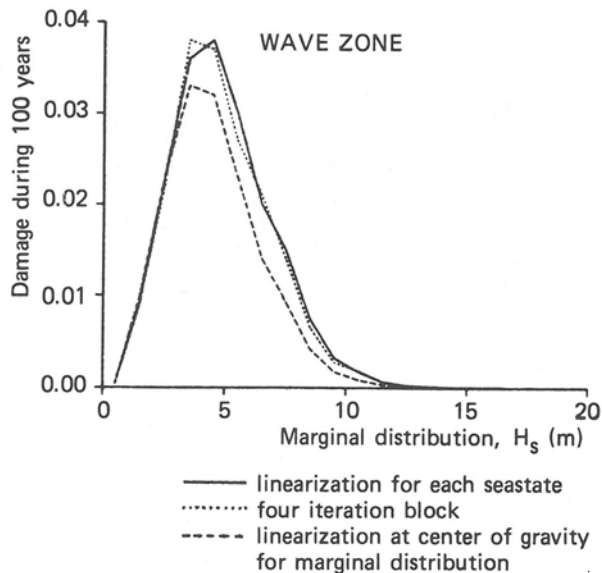


Figure B1.103: Illustration of contribution to fatigue damage versus significant wave height, tensioned steel riser in North Sea environment, from [Larsen and Passano, 1987]

A key issue for stochastic time domain analysis is to establish probability distributions for individual maxima from the calculated response history. Rayleigh and Rice distributions (see section Section B1.4.8.3) are valid for Gaussian processes only, and should not be used to describe the statistics of individual maxima from a time domain simulation.

The Weibull distribution is formally an asymptotic distribution for the lowest value of a variable with a lower limit. This distribution is, however, flexible with its 2 or 3 parameters, and is therefore often applied as a simple empirical distribution. The two parameter distribution is defined by a scale parameter  $\sigma$  and a shape parameter  $\eta$ , see Figure B1.104:

$$f_X(x) = \frac{\eta}{\sigma} \left(\frac{x}{\sigma}\right)^{\eta-1} \exp\left[-\left(\frac{x}{\sigma}\right)^\eta\right] \quad ; \quad x \geq 0, \quad \eta \geq 0, \quad \sigma > 0 \quad (\text{B1.228})$$

The moments for this distribution is given by

$$m_n = \int_0^\infty x^n f_X(x) dx = \sigma^n \Gamma\left(1 + \frac{n}{\eta}\right) \quad (\text{B1.229})$$

where  $\Gamma$  is the ordinary gamma function. The expectation value  $E[X]$  and variance  $\text{Var}[X]$  are given by

$$\begin{aligned} E[X] &= \sigma \Gamma\left(1 + \frac{1}{\eta}\right) \\ \text{Var}[X] &= \sigma^2 \left[ \Gamma\left(1 + \frac{1}{\eta}\right) - \Gamma^2\left(1 + \frac{1}{\eta}\right) \right] \end{aligned} \quad (\text{B1.230})$$

The three parameter Weibull distribution is a transformation of the two parameter model by introducing the location parameter  $\mu$ :

$$X = Y - \mu \quad (\text{B1.231})$$

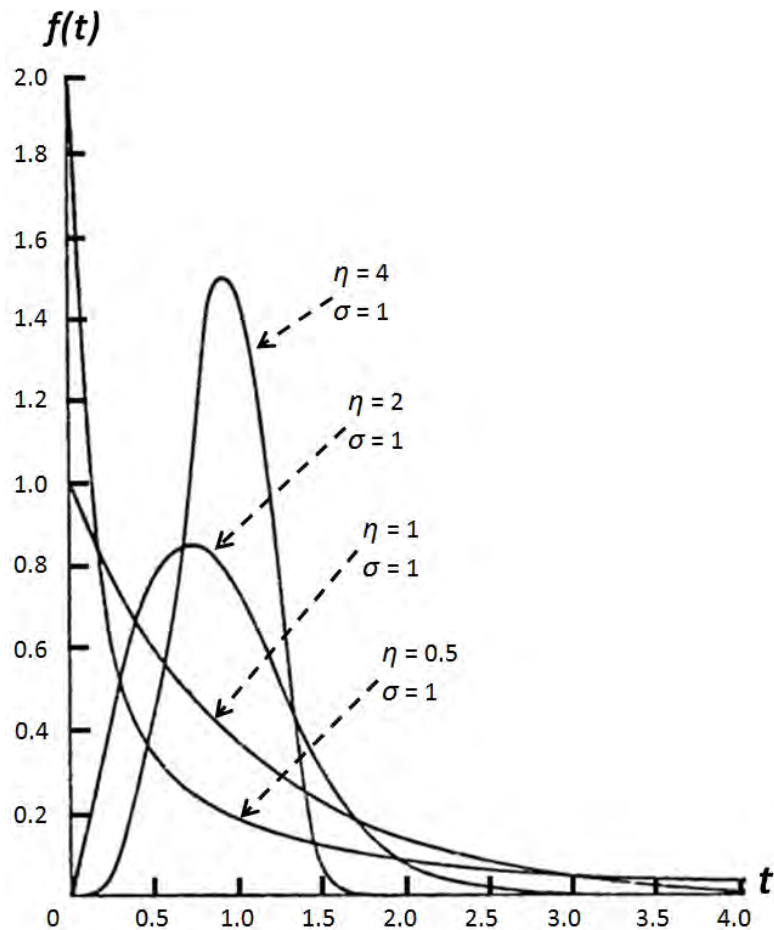


Figure B1.104: The two parameter Weibull distribution (from [Moan et al., 1980])

which gives

$$f_Y(y) = \frac{\eta}{\sigma} \left( \frac{y - \mu}{\sigma} \right)^{\eta-1} \exp \left[ - \left( \frac{y - \mu}{\sigma} \right)^\eta \right] \quad (\text{B1.232})$$

Expectation value and variance will now be given by

$$\begin{aligned} E[Y] &= \mu + E[X] = \mu + \sigma \Gamma \left( 1 + \frac{1}{\eta} \right) \\ Var[Y] &= Var[X] = \sigma^2 \left[ \Gamma \left( 1 + \frac{2}{\eta} \right) - \Gamma^2 \left( 1 + \frac{1}{\eta} \right) \right] \end{aligned} \quad (\text{B1.233})$$

The Weibull distribution will become identical to the Rayleigh distribution for  $\mu=0$  and  $\eta=2$ , and the exponential distribution for  $\mu=0$  and  $\eta=1$ .

#### B1.4.8.7 Extreme response estimation

It is easy to estimate extreme response at any probability level or return period from a known distribution of individual maxima  $x_a$ . If the probability of being smaller than a given value  $x_{max}$  is given by  $F_{X_a}(x_{max})$ , than the probability for all maxima among N to be smaller than  $x_{max}$  will be given by

$$F_{X_{max}}(x_{max}) = P(X_{max} < x_{max}) = [F_{X_a}(x_{max})]^N \quad (\text{B1.234})$$

This probability is the same as the probability for  $x_{max}$  to be the largest among N individual maxima. Formally we can use Eq. B1.234 to estimate extremes in a sea state or from a long term distribution of individual maxima if we accept that individual maxima are Rayleigh distributed. However, the response in flexible riser systems are strongly influenced by non-linear effects like drag forces and time varying stiffness due to tension variations. We will therefore not be able to have an analytical definition of the distribution of individual maxima. We have to estimate this distribution from our sample of response histories, and our estimates will always have a statistical uncertainty.

**Extreme response in a given sea state** If individual maxima  $X_a$  are Rayleigh distributed, the distribution for the largest among N maxima will be given by

$$F_{X_{\max}}(x_{\max}) = \left[ 1 - \exp \left( \frac{-x_{\max}^2}{2\sigma_x^2} \right) \right]^N \quad (\text{B1.235})$$

Two response levels are often referred to in design; the most probable largest and the mean value of the largest maximum during a specific storm duration. The most probable largest corresponds to the peak in the extreme value distribution, see Figure B1.97 and Eq. B1.216 and Eq. B1.217. If the distribution of individual maxima is unknown, we have to estimate the distribution  $F_{X_a}$  in Eq B1.234. It is normally difficult to identify the inherent statistical uncertainty, but we easily understand that the only way of reduce the uncertainty is to carry out very long simulations.

COMPARISON OF LARGEST SAMPLES FROM 10 SIMULATIONS  
SEA SURFACE ELEVATION. USE OF STOCHASTIC PHASE ANGLES,  
BUT DETERMINISTIC COMPONENT AMPLITUDES.

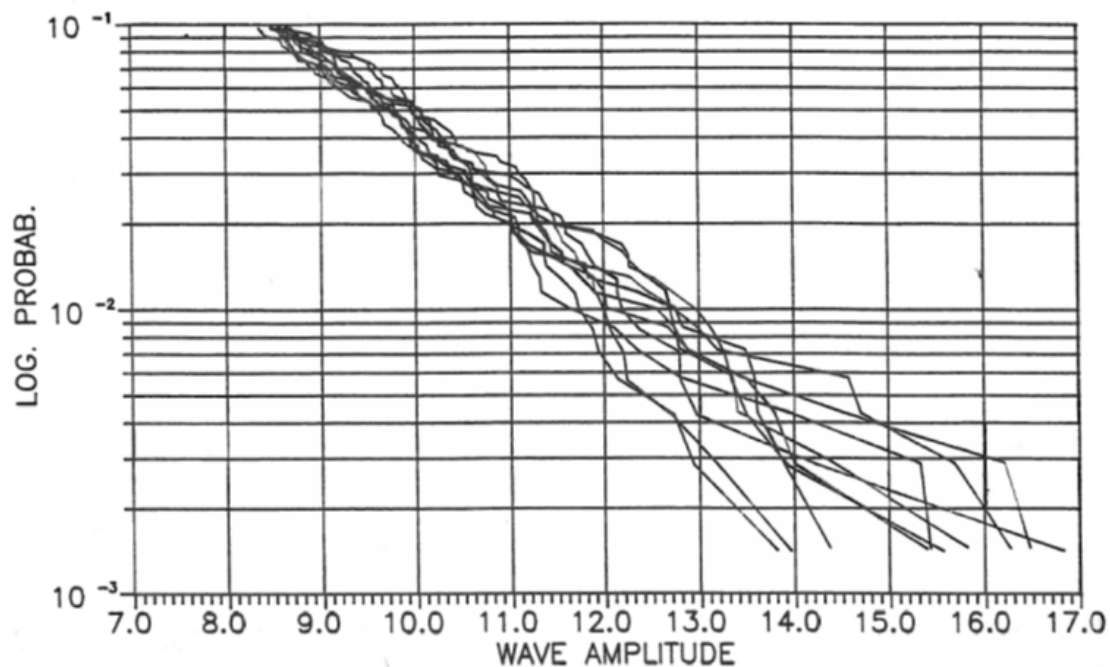


Figure B1.105: Illustration of statistical uncertainty, wave amplitudes from spectrum

Figure B1.105 illustrates the statistical uncertainty related to extreme values from a record. Ten wave records with 2 hours duration are generated from the same wave spectrum by using

different seed numbers for generation of pseudo-random phase angles. Each line represents the result from one simulation. The largest, second largest, third largest etc values from each sample have identical probabilities to be exceeded, but varying magnitude. By plotting probability and magnitude from each sample, we can have a good visual impression of the uncertainty. The largest wave amplitude is seen to vary between 13.8 and 16.8 meters. The 10 % largest maxima are included on the figure.

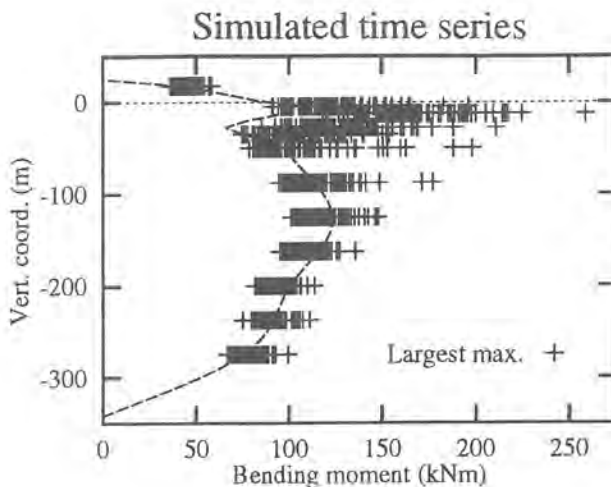


Figure B1.106: Illustration of statistical uncertainty; maximum bending stresses in tensioned riser during one hour, 100 samples from same wave spectrum, but varying set of phase angles, [Passano, 1994]

The variation of extremes for response will often become larger than for wave amplitudes because of non-linear effects, usually dominated by the drag forces. Figure B1.106 illustrates this point. The largest stress during one hour simulation from 100 records with identical wave spectrum but varying phase angles are shown. The variability is seen to be largest in the wave zone, but is significant along the total length of the riser.

Estimation of distribution parameters from sampled data (i.e. individual maxima from simulation) is offered by commercial software like Matlab, and will not be described here. Statistical uncertainty related to extreme response estimation for flexible risers is discussed by [Sødahl, 1991].

A practical approach may be to make several 3 hours realizations of the response in the design sea state. 30 cases is often used, but number of realizations should be based on the wanted statistical confidence for the final estimate, which again depends on the consequence of failure and applied safety factors. The largest response maxima in each sea state can be applied in a variety of methods to estimate an extreme value. The Gumbel distribution is frequently applied. This problem is discussed in detail in [Næss and Moan, 2013].

### **Estimation of lifetime extreme response**

The most consistent way to estimate lifetime extreme response is to establish a long term distribution for the actual response parameter. When dealing with non-linear systems like flexible risers in waves, a large number of long non-linear simulations are needed. Short term distributions must be estimated for each response parameter and sea state, which makes this approach time consuming. Statistical uncertainty will be present in each short term distribution, and should be found for the final estimate for the extreme response.

Use of design waves is inadequate for obvious reasons, but an alternative to long term statistics is to identify a design storm and a probability level for the lifetime extreme in this sea state. Two approaches for use of design storms have been applied for flexible risers - the contour line method (CLM) and the approximate long term distribution (ALTD). The contour line method was proposed by [Winterstein et al., 1993] and has been used for several types of structures, see [Haver and Kleiven, 2004]. The idea is to apply the long term distribution for sea states (frequency table for  $H_s$  and  $T_p$ ) to identify extreme sea states with equal return period, see Figure B1.107.

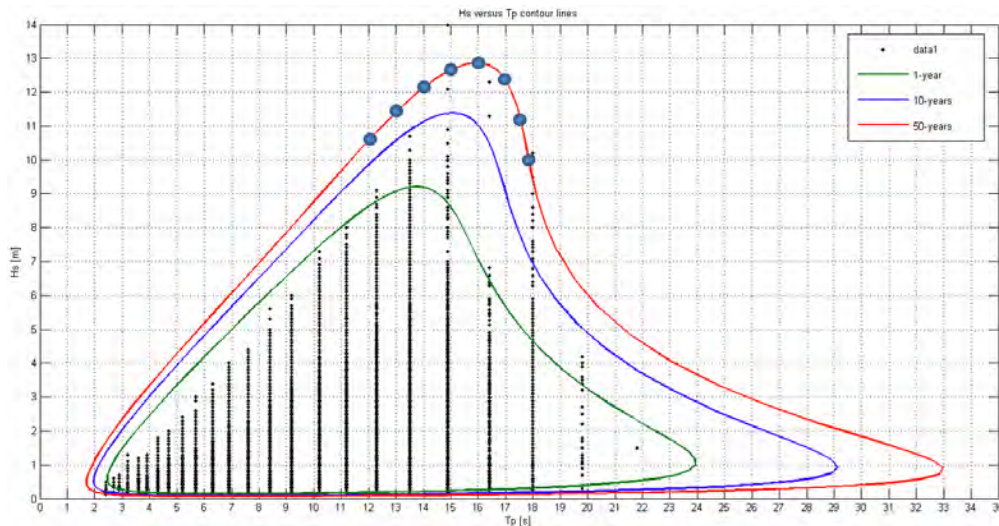


Figure B1.107: Contour lines for sea state parameters. The red line represents combinations of  $H_s$  and  $T_p$  with return period of 50 years, modified figure from [Nygaard and Mathiesen, 2008] (Courtesy of Statoil)

The variance for the actual response parameter (i.e. tension or curvature in the riser) can be estimated from non-linear time domain simulations in these sea states, and the sea state that gives the largest variance is defined as a design sea state. The short term distribution for the response in this sea state must be estimated from a longer simulation in order to have an acceptable statistical uncertainty for tail of this distribution (large response levels). The most difficult parameter to estimate is, however, the probability level (or return period) for the lifetime extreme response in the actual sea state. Formally this probability must be found from a long term distribution based on a large set of time domain simulations. One may however, define the probability level from experience or apply obviously conservative approximations. Hence, the response amplitude with hundred years return period may be found as the response amplitude with 3 hours return period in the selected design sea state.

An alternative to the contour line method was proposed by [Larsen and Passano, 1990] and applied to flexible risers by [Larsen and Olufsen, 1992]. The method applies frequency domain analyses to estimate a long term distribution, and a time domain simulation in a design sea state found from the long term distribution. The analysis can be described in steps as follows:

**Step 1: Establish an approximate long term distribution** This distribution should be based on a set of dynamic analyses in frequency domain, preferably including stochastic linearization of drag forces, see [Leira and Olufsen, 1992]. These analyses gives the response spectrum and hence also the variance and Rayleigh distributions of the response for the

selected sea states. Number of sea states in this selection will normally be below 20 since contributions to the tail of the long term distribution from moderate and calm sea states can be neglected. A typical selection of sea states is shown on Figure B1.108.

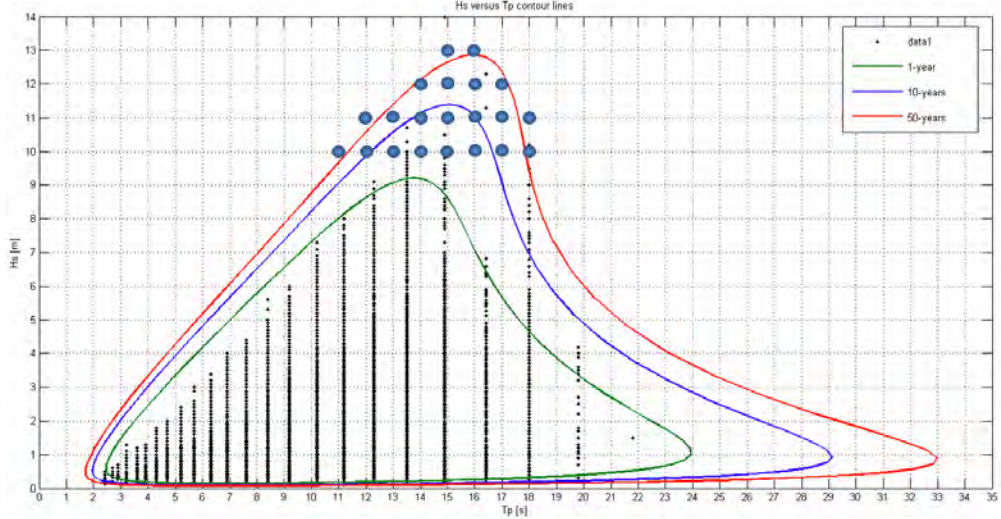


Figure B1.108: Selected sea states to define an approximation for the long term distribution for extreme response estimation, modified figure from [Nygaard and Mathiesen, 2008] (Courtesy of Statoil)

The long term distribution  $P^L$  can be found from a weighted sum of short term distributions  $P^S$ , confer also Eq. B1.218

$$P_{X_a}^L(X_a > x_a) = \sum_{i=1}^{N_R} P_{X_a}^S(X_a > x_a | H_S, T_P)_i \cdot P_{H_S T_P}(H_S, T_P)_i \cdot w(\bar{T}, T_P) \quad (\text{B1.236})$$

$N_R$  is number of sea states,  $P_{H_S T_P}$  is the short term distributions and  $w$  is the same weight factor as shown in Eq. B1.218. All short term distributions are Rayleigh distributions found from the variance of the response in the actual sea state.

**Step 2: Approximate extreme value** An approximation to the extreme response with return period D years,  $x_D^*$ , can be found by solving the equation

$$P_{X_a}^L(X_a > x_D^*) = \frac{1}{N_D} \quad (\text{B1.237})$$

where  $N_D$  is the total number of response zero up-crossings during D years, counted for the  $N_R$  selected sea states only.

**Step 3: Identification of the design storm** The contribution from each sea state to the total probability  $1/N_D$  can be found from the individual elements in the summation in Eq B1.236:

$$P_{X_a}^S(X_a > x_D^* | H_S, T_P)_i \cdot P_{H_S T_P}(H_S, T_P)_i \cdot w(\bar{T}, T_P)_i \quad (\text{B1.238})$$

These contributions can be ranked, and the sea state with the largest contribution must be the most important sea state for the extremes of the actual response parameter. Another

type of information is also achieved, namely the probability of the extreme value in the actual sea state, which is given by

$$P_S = P_{X_a}^S(X_a > x_D^* | H_S^*, T_P^*) \quad (\text{B1.239})$$

where  $H_S^*, T_P^*$  means the sea state that gives the largest contribution to the long term distribution at the actual response level, and  $x_D^*$  is the estimate for the lifetime extreme response.  $P_S$  is now the probability of the lifetime extreme to appear in this sea state.

**Step 4: Estimation of extreme response for the actual sea state** The final estimation of the lifetime extreme response  $x_D$  can now be found from a non-linear time domain simulation in the design sea state defined by  $H_S^*, T_P^*$ . The result from the simulation can be used to estimate the probability distribution for the response in the actual sea state. The lifetime extreme response  $x_D$  can then be found from the equation

$$F_{X_a}(x_D) = P_{X_a}^D(X_a > x_D) = P_S \quad (\text{B1.240})$$

where  $P_S$  is given in Eq. B1.239 and  $F_{X_a}$  is the short term distribution for the response in the design sea state.

It should be noted that the design sea state that is found in this way may vary from one response type to another, and the probability level for the lifetime extreme in the design sea state will also vary. The fundamental assumption for this method is that the non-linear effects are equally important for all sea states used to find the approximate long term distribution. Note that the probability level 1/ND in Eq. B1.237 is the same in the approximate long term distribution as for a correct distribution. Hence, the sum of probabilities in Eq. B1.236 is correct. If non-linearities have equal influence, we also realise that each contribution to this sum can be correct even if the estimated response level  $x_D^*$  is different from the final estimation  $x_D$ .

### B1.4.9 Vortex induced vibrations

The topic of vortex induced vibrations (VIV) is not covered by this editionn of the text. This complex and important part of the hydrodynamic load models, and the corresponding effects upon the hydrodynamic coefficents to be used, is beyond the scope of the present Handbook edition.

### B1.4.10 Use of results from global analyses

#### B1.4.10.1 Bending stiffener design

Design of bend stiffeners is usually designed in 3 steps.

1. Determination of input loads
2. Determination of bend stiffener geometry and material
3. Verification of the design

The determination of input loads is most often carried out with a pinned model, i.e. a model that is free to rotate at the end. Tension-angle relationships are extracted from extreme analysis using the pinned model, and the envelope is plotted from all governing load cases. In some cases this approach may be too conservative with regard to angle and it may then be beneficial to include a dummy bend stiffener in the global model in order to reduce the computed angle response. In this case the angle should be extracted at the bend stiffener tip or even further away from the end, ensuringn that the correct bending moment at the root of the bend stiffener is captured.

The main purposes of the bend stiffener design step is to find a geometry that keeps the curvature of the riser below the critical limit and at the same time

1. minimize the amount of bend stiffener material (to reduce cost)
2. ensure that it can be produced, e.g. with appropriate cone dimensions (to reduce cost)

The optimum bend stiffener geometry may either be found trough analytical approximations, through finite element software or through 'trial-and-error' methods in the global analysis model, see e.g. [Sødahl, 1991].

The design should finally be verified by global analysis for both soft and stiff conditions, i.e. in hot and cold operational conditions. The verification analysis should check that the riser bending is within its limits and that the bending stiffener strain is within the allowable.

When a feasible or optimum bend stiffener design has been found with regard to extreme loads, the design procedure may be re-performed to better distribute the curvatures in lower seastates, i.e. improving the fatigue performance.

#### B1.4.10.2 Detailed stress analysis of cross-section

Reference is given to Section [B1.3](#)

### B1.4.10.3 Fatigue damage calculation

For dynamic risers the governing load contribution is normally assumed to be 1st and 2nd order wave and current loads in combination with associated floater motions. In addition VIV may also be a concern, however, according to the state of art of today wave and VIV loadings require different response models. Whereas, the nature of wave responses includes large response amplitudes that requires a non-linear response model, most VIV models of today assumes a linear frequency domain model and small response amplitudes. In order to describe the extreme responses the effect of VIV is included in the time domain model in terms of selecting the drag coefficient such that drag amplification from VIV is included. For fatigue calculations the fatigue damage is obtained from separate models where the total damage is calculated as the sum of the wave and the VIV contributions.

The damping from bending hysteresis will influence the dynamic response and this is particularly the case for VIV calculations. In a time domain procedure this can be handled directly by applying an elastic-plastic material model for the pipe in bending, however, small time steps are needed to pass the stick-slip transition zone. Therefore, most irregular wave response analysis is still based on linear beam elements and application of equivalent viscous damping models. Since the bending hysteresis damping is amplitude dependent (frequency independent) different equivalent damping coefficients may have to be used from load case to load case. For VIV frequency response models, the equivalent damping coefficient related to each mode can be handled by iteration according to the procedure proposed by [Sødahl et al., 2011]. The moment curvature diagram needed for such procedures can be obtained from full-scale measurements or from mathematical models as outlined in Section B1.3.5. For the time domain equivalent damping case one alternative is to establish two linear material models, one based on the stick bending stiffness and one based on the slip bending stiffness, see Figure B1.16. For the load cases where the slip curvature is not exceeded standard material damping (no hysteresis) is used whereas for the remaining load cases an equivalent damping coefficient including both material and hysteresis damping is used, or alternatively by a moment curvature hysteresis model.

The wave fatigue calculation is in most cases performed by a two step procedure: A global analysis in order to obtain the tension, curvatures or end angles followed by a local stress analysis to transform the global quantities into time series of stress used as basis for calculating the final damage as a Miner sum. There are different strategies for local stress analysis in use. Among these are:

1. in combination with analytical stress models allowing direct transformation of the global time series into time series of stress.
2. Global irregular wave analysis in combination with a filter based on the outputs from non-linear FE analysis of the cross-section, transforming the time series of global responses into time series of stress.
3. Global irregular wave analysis calculating harmonic responses in terms of tension and curvature variations and use this as input to analytical models or non-linear FE stress analysis.
4. Global irregular wave analysis in combination with direct non-linear FE analysis. As the non-linear FE stress model is too time consuming to allow direct transformation of the global time series, the global responses need to be transformed, by e.g. rainflow counting, into classes of regular harmonic tension, curvature or end angle variations

prior to calculating the stresses. This means that choices need to be made with regard to which global response quantity to be used as basis for the rainflow counting procedure. By e.g. selecting the major curvature component as the master quantity, the time instants at which each curvature range is calculated need also to be used when calculating the other response ranges such as the tension ranges.

5. Global regular wave analysis resulting in harmonic timeseries of tension and angle/curvature. Care needs to be taken in this approach with respect to eigenfrequency vibration. Once the time series of stress have been established on an annual basis, the fatigue in each layer can be calculated by the Miner sum approach as outlined in Section [B1.3.7](#)

#### **B1.4.10.4 Interference analysis**

Interference analysis is often performed as a part of the original design analysis. Interference should, if applicable, be checked between:

- Riser and riser/umbilical
- Riser and mooring
- Risers and platform/vessel
- Riser and seabed structures
- Riser and seabed

The interference analysis may be performed with various levels of detail. Often the initial interference evaluation is performed as a quasi-static screening with current load and vessel/platform offset applied. The quasi-static approach is used to find governing load cases to which subsequent dynamic analysis is applied. Alternative approaches are to extract clearance results from the entire (or part of) extreme load case matrix or to base the interference load case selection on visual inspection of the extreme load case simulations.

Various levels of detail may be included in the determination of hydrodynamic coefficients, e.g. Reynolds number dependent drag coefficients or wake models.

If Reynolds dependent drag coefficients are used in the analysis the quasi-static approach should be used with care, as the riser drag loads can change significantly between the quasi-static and dynamic analyses, and results can hence be misinterpreted.

Wake models are generally computationally heavy and hence problematic to use in the riser system design phase where design iterations are often required.

The design requirements w.r.t. interference is usually determined by the operators' technical requirements and standards and may be evaluated in the following forms:

- Minimum distance of clearance in an extreme event
  - In case of interference/clashing it is good practice to:
    - \* Determine impact velocities (or clashing energy)
    - \* Evaluate limiting sea states (environment) and frequency of occurrence
- Possible crossing of risers under or over objects such as mooring lines, risers and umbilicals as well as over seabottom structures as flowlines, spools, etc.

Loads from the latest wave are often sufficient in a regular wave analysis approach. However, when extracting interference results care should be taken if only results from the latest wave are used. If contact is not modeled, the riser may in some scenarios move through and past the interfering object for which the software wrongfully may report positive clearances. If contact is modeled in the global analysis, interference results from the latest wave may suffice.

Interference analysis between risers should take into account various combinations of internal density and possible installation of new (marine growth free) risers between old marine growth covered risers.

### B1.4.11 Quality assurance and quality control

#### B1.4.11.1 General remarks

Flexible marine risers are quite complicated systems with regard to mechanical behaviour. Significant nonlinearities related to loads, global geometry and cross-section characteristics are present. In addition, stochastic methods are needed to handle the design principles in a rational way. The types of analyses involved in design are therefore complex, from mathematical, numerical and statistical points of view.

The complexity of the problem increases the probability of errors. It also makes the detection of errors more difficult. The reason for this is that unexpected results might easily be explained as effects from nonlinearities or other types of complex behaviour, and are therefore accepted instead of being subjected to a more critical review.

In general, the best method of quality assurance will obviously be to apply a well reputed computer program, and have a qualified staff to do the job. However, even the best program can have hidden bugs or be misused, and humans are never perfect. Quality control of design analyses must therefore never be limited to the verification of the applied computer program, but be an integrated part of the design process.

#### B1.4.11.2 Verification of computer programs

In recent years, several computer programs for the analysis of flexible risers have been developed. These programs apply various methods for static and dynamic analysis, and models for loads, damping etc. are also different. This is why the International Ship and Offshore Structure Congress (ISSC) initiated a study to compare the results from different computer programs. Riser data and environmental conditions were defined in addition to standards for result presentation. The purpose of the study was to investigate the modelling uncertainty in connection with design analysis of flexible risers. Furthermore, to define a 'benchmark' test case and make results available to designers and users of such programs. A complete description of this work is presented by [Larsen, 1991].

The test cases involve the following types of analyses:

- static analysis, buoyancy and gravity,
- static analysis, in-plane and out of plane current,
- eigenvalue analysis,

- dynamic analysis, forced upper end motions,
- dynamic analysis, forced motions and waves

The intention was to allow for a stepwise verification, involving new parts of the computer program and new model parameters in each step. A computer program is always tested as a part of the QA/QC process during its development, and commercial programs normally work as intended. However, all experience indicates that every large computer program has hidden bugs that normally do not influence the results. Such bugs may suddenly give rise to errors if the program is used in a new way, like rare combination of options or on problems on the border of the program's intended application. Therefore a computer program should never be trusted and users should never accept results without a critical review from an experienced person.

When installed on a new computer and introduced to a new group of engineers, it is important to check that the program works as intended. In addition, the new users should be qualified to use the program. Generally, a standard set of input files are delivered with the program, and results can be compared to a fact. A more comprehensive test that also involves the personnel is to define a problem and have at least two engineers working independently. The job must include establishing all needed input parameters from the physical description of the system, preparing the input files and evaluating the results. The previously mentioned standard cases can serve as test problems in this kind of work.

#### B1.4.11.3 Verification of models

The term 'model' means in this context the mathematical and numerical procedure established by a computer program on the basis of a specific set of input parameters provided by the user. Such a model may have errors since it does not represent the physical reality in an adequate way. Known limitations or inaccuracies are of course present due to simplifications in the applied methods, e.g. Morison's equation. Such limitations should be specified by the programmers and are hopefully known to the user. Even if a program works perfectly according to its intentions, unexpected errors may occur due to:

- **Use of a program outside its limitations**  
Example: Some programs neglect lateral friction between the riser and the sea floor. Such a program should not be used on problems where a long section of the pipe rests on the sea floor and lateral deformations are present.
- **Lack of understanding of the mathematical model related to the actual problems.**  
Example: Application of a Rayleigh damping model to represent structural damping of non-bonded pipes.
- **Inadequate discretization**  
Example: Too long elements, too long time increments or too large frequency intervals.
- **Lack of consistency between data sources**  
Example: Many riser analysis programs are linked to other computer programs by data files, or results are transferred manually. Data for static offset and motion transfer functions of anchored vessels are typical examples. A special attention must be given to transfer functions. There is no international standard for definition of phase angles between motion components, and transfer functions for rotations may be related to

wave amplitudes or wave surface angles at mean water level. Some definitions will normally be obvious for asymptotic values (long wave periods). However, the general rule for use of transfer functions is to check the definitions for the actual provider.

- **Errors and misunderstandings**

Example: Input parameters must be calculated from an engineering description of a riser system. This process gives unlimited possibilities for errors.

#### B1.4.11.4 Control of results

Quality control costs and these costs must always be seen in relation to consequences of errors and the probability of avoiding errors by quality control. It is therefore not possible to give general rules about how quality control should be carried out, but some advice and hints can be stated.

- **Use of independent computer programs**

Many institutions have more than one computer program for flexible riser analysis. A typical situation is that one simple 2-dimensional cable program is available in addition to a more sophisticated tool. In this situation it is possible to establish two independent models and perform some initial calculations for verification of the established model. Such calculations could be:

- Initial configuration
- Static analysis for a set of current profiles
- Eigenvalue analysis

- **Two independent models.**

Two engineers may prepare input files for the same problem independently. The two models can then be used for some initial analyses, and the results can be compared.

- **Discretization check**

If a large number of analyses are to be carried out, an initial check of the discretization (time increments and element lengths) should be performed by running some adequate examples. If the results from a refined discretization are close to the results from the ordinary model, the model can be accepted. Note that this control must cover all required response parameters. It is well known that bending moments will need shorter element lengths than axial forces to obtain the same level of accuracy.

- **Decay of transient effects**

A time domain solution is always influenced by the initial values of displacements, velocities and accelerations. This part of the solution is called the homogeneous or transient solution, in contrast to the particular or steady state solution. Transients influence the initial part of a stochastic simulation. Consequently, this part should never be considered when calculating statistical parameters from a simulated time series. When using FFT to generate time records of motions and wave induced velocities and accelerations, one may apply the initial part of the record as a continuation of the record. This is possible since the result at the end of the simulation is the perfect initial condition for the analysis since the time record is periodic. By continuing the analysis in this way, a longer record will be available for the succeeding statistical analysis of the response.

For regular wave cases, the problem is avoided simply by analysing several successive wave periods and using the results from the last period only. Systems with very long eigenperiods compared to the actual wave period may have transients that continue for a long time, say 10 periods or more. A typical example here is a disconnected riser. A good control of the influence from transients is obtained by producing a time plot of a displacement taken at a position along the riser where a long period eigenmode has a maximum value. An equivalent regular wave analysis can be performed to determine the length of a transient period present in a stochastic analysis.

- Control of stochastic simulations

Another type of error that may influence the results of a stochastic analysis is failures in the numerical processing. Normally, such failures are immediately discovered as they lead to a lack of convergence or instabilities and, hence, give meaningless results. However, some kinds of failures are more sophisticated and need special attention. An example here is the process of random number generation (see also Section 4.3.2.2) that may fail and thereby produce a series of numbers with hidden correlations. This results in a non-Gaussian wave process and, consequently, also in errors in the statistical description of the response, e.g. estimated extreme values. The best precaution here is always to check the quality of the wave process by computing the variance, skewness and kurtosis, and compare these values to the known facit:

$$\text{Variance} \approx H_s^2 / 16$$

$$\text{Skewness} \approx 0.0$$

$$\text{Kurtosis} \approx 3.0$$

In connection with stochastic analyses one should always plot the spectra of calculated time records in addition to the estimated probability distribution. The response spectra together with the (linear) transfer functions and a wave spectrum can easily indicate if some significant errors have been introduced.

In conclusion, one can state that the best quality assurance system one can have is well qualified engineers to do the job. In addition, time should be allowed for a careful detailed evaluation and control analyses on the basis of the actual project.

## **Chapter B2**

# **Risk Analysis Methodology**

*Author: Bernt Leira, NTNU*

## B2.1 Introduction

The main steps associated with quantitative risk assessment (QRA) can be summarized as follows:

1. Definition of system boundaries and identification of hazards
2. Development of fault trees and event trees
3. Evaluation of failure probabilities and consequences (risk matrix)
4. Development of decision networks (decision trees)
5. Definition of acceptance criteria
6. Risk reduction and/or risk mitigation

These topics are highlighted in the following in relation to flexible pipe systems. Furthermore, evaluation of probability for mechanical failure modes and the topic of risk-based riser integrity management are elaborated.

In order to perform a risk assessment for a given flexible riser or flowline system, the potential types of failure modes and the associated initiating events need to be identified. For some of the failure modes a certain amount of relevant historical/empirical data may be available such that failure rates can be estimated directly. However, in many cases such data are missing or they can be rather irrelevant due to technological developments and improved manufacturing methods. All the same, it may be possible to identify the mechanical failure modes which lead to different types of failure events and hence estimate the associated probabilities of failure by consideration of relevant mechanical models.

This requires that the specific models which represent a given failure criterion are identified, and these are generally referred to as mechanical limit states. For flexible pipes, a layer-by-layer and component-by-component approach is typically applied for identification of the failure modes which correspond to such mechanical limit states.

The mechanical limit states are frequently defined in terms of loads (or load effects) versus capacity terms. For some cases (such as in connection with assessment of fatigue and wear) the accumulated load effect is applied rather than its instantaneous value. Both the load effects and capacity associated with a particular limit state will frequently depend on a number of parameters for which inherent variability is present. This implies that they are more adequately represented as random variables than deterministic quantities.

In the present chapter, the risk concept is first briefly discussed. The main steps of quantitative risk assessment are next described in some more detail. Subsequently, methods and sources for evaluation of the probability of failure for relevant critical events are reviewed. Consequence analysis, acceptance criteria and decision making are also addressed.

Risk-based Riser Integrity Management (RIM) of flexible risers is also briefly considered. This topic involves e.g. the task of assessing the effect of inspection and monitoring of flexible pipes and evaluating the implications of the findings which arise from these activities with respect to decision-making and required actions. This includes decisions related to the need for repair, protective measures, remaining time in operation and future replacement or decommissioning of the flexible pipe.

The objective of the present chapter is to give an overview of the methods which are required for risk analysis of flexible pipes. Further details related to the various failure modes, also including new types of such modes, are given in Chapter [A3](#) of the present Handbook. The same applies to available failure statistics. Regarding risk assessment based on a more elaborate layer and component oriented approach, reference is made to Chapter [C1](#) (Section [C1.4](#)) Practical Integrity Management.

## **B2.2 Risk-based approach: risk definition, classification and quantification**

### **B2.2.1 General**

The risk concept is first reviewed. However, it should be kept in mind that in addition to the risk as such, the 'benefit' (e.g. in terms of income/utility) which is associated with a given operation/activity will also enter the picture when assessing the viability of a specific system. Hence, an optimization of the total benefit will be a relevant criterion as well as risk minimization.

### **B2.2.2 Definition of risk**

The risk concept is here defined as the expected consequences associated with a given activity. For an activity with  $n$  events where each event is characterized by a corresponding probability of occurring (i.e.  $P_i$ ) and a consequence (i.e.  $C_i$ ) the risk (i.e.  $R$ ) is similarly defined by :

$$R = \sum_{i=0}^n P_i \cdot C_i \quad (\text{B2.1})$$

For the case of a single event, the risk becomes simply the product of the corresponding probability of that event times the consequence. For the case of an 'infinite number of possible outcomes', e.g. where each event corresponds to a specific value of an operation parameter for a flexible pipe system, the summation becomes an integral expression.

### **B2.2.3 Risk categories**

There are three main risk categories:

1. Risk of human injuries and fatalities
2. Risk of environmental damage
3. Risk of financial losses

Generally, all three aspects need to be considered separately for each risk assessment. The relative importance of the three categories represents a multi-criterion decision-making issue. The relative weighting of the different categories will in some cases depend on the stakeholder which is involved.

## B2.2.4 Derived risk measures

Based on the outcome event frequencies (probabilities) for a particular Event Tree (see Section B2.3.5), derived risk measures can be obtained. These vary according to the category of persons that are affected by the outcomes, with the main distinction being between the workforce and the public in general. Some of these risk measures are briefly summarized here:

### B2.2.4.1 Risk to Workforce

**B2.2.4.1.1 Annual risk** The annual risk may be expressed as Potential Loss of Life which corresponds to the probability of fatalities per year for all the personnel involved in a particular operation. It is a risk measure which is valid for the whole installation rather than for a single individual.

**B2.2.4.1.2 Individual risk** The Individual Risk expresses the probability per year of fatality for one individual. For the operating personnel of an installation an *Average Individual risk* can also be computed.

**B2.2.4.1.3 Fatal accident risk** The *Fatal Accident Rate* is defined as the potential number of fatalities in a group of people exposed for a specific time interval to the activity in question. Generally, this rate is expressed as a probability of fatality per 100 million exposure hours for a given activity.

### B2.2.4.2 Risk to Public

**B2.2.4.2.1 FN curve** FN curves or F/N plots (also referred to as 'Cumulative Frequency Graphs') are probability versus consequence diagrams where 'F' designates the frequency of a potential event and 'N' denotes the number of associated fatalities for that event. Such graphs tend to be highly relevant for selection of the risk acceptance criterion to be applied. Frequently, they are also imposed by the Regulator. Hence, these curves will be considered in more detail in connection with acceptance criteria discussed below.

Regarding risk to the public, contour maps of physical effects (e.g. pressure levels due to explosion, concentration of oil pollution due to an accidental release) and individual risk can also be applied.

## B2.3 Building blocks of quantitative risk assessment (QRA)

### B2.3.1 General

The building blocks which are summarized in the Introduction to this chapter are elaborated in the following.

### B2.3.2 Definition of system boundaries and identification of hazards

For flexible pipe systems, a main distinction is made between on-bottom pipes (e.g. intra-field flowlines) and risers. A particular system can comprise one or both of these sub-systems. Furthermore, a clear specification of the other components to be included in the system under consideration is required. This applies e.g. to which parts of the pressure regulation system, safety valves and process equipment that are to be included in the risk analysis. The surrounding area which is influenced by a failure of the system also needs to be identified. For an oil or gas leakage with the possible sequence of events that are initiated by such a leakage, the extent of this area can be very large.

A hazard is typically referred to as a failure event for the flexible pipe system. Occurrence of a hazard is therefore also referred to as a system failure event. Identification of hazards comprises all events which might have an adverse consequence to people, environment or economy. There are a number of procedures that can be applied in order to support this process of hazard identification. These have been developed out of various engineering application areas such as the chemical, nuclear power and aeronautical industries. Examples of such are:

- Qualitative Failure Mode and Effect Analysis (FMEA)
- Quantitative Failure Mode Effect and Criticality Analysis (FMECA)
- Hazard and Operability Studies (HAZOP)
- Risk Screening (HAZID)
- Preliminary Hazard Analysis (PHA)

Further details of these procedures are given e.g. in [Stewart and Melchers, 1997], [Vinnem, 1999], [Aven, 1992] and [Rausand and Høyland, 2004].

In the following sections, a brief review and summary of the procedures associated with FMEA/FMECA and HAZOP is first given. Subsequently, application of so-called event trees and fault trees are discussed

### B2.3.3 FMEA/FMECA

Failure mode and effects analysis (FMEA) often represents the first step of a systems reliability study, see e.g. [Rausand and Høyland, 2004], [BS 5760-5, 1991], [IEC 60812, 1985], [MIL-ST-1629A, 1980] and [SAE-ARP 5580, 2001]. For each component of the system, the potential failure modes and their corresponding effects on the other parts of the system are summarized in specific FMEA worksheets.

If criticalities and priorities are assigned to the failure mode effects, the FMEA is referred to as a failure mode, effects and criticality analysis (FMECA). In the literature, sometimes no distinction is made between FMEA and FMECA such that the latter is applied in order to describe both types of analysis.

An FMEA is mainly a qualitative analysis while FMECA may comprise some gross quantitative features. Such analyses are best suited at the design stage for a system. Design areas where improvements are required in order to meet specified reliability requirements can then be identified. An updated FMECA may serve as an important tool in relation to design reviews and inspections.

In some cases, an FMECA can involve a coarse-grained categorization of the failure rate and the severity corresponding to the specific failure modes which are being considered. FMECA is best suited for systems where the system failure most likely will be caused by failure of single components. However, for systems with a fair degree of redundancy this approach may lead to examination of a large number of component failures that do not have any significant consequences for the system as a whole. For such systems a fault tree analysis is much more relevant.

### B2.3.4 HAZOP

'Hazard and Operability Analysis' (HAZOP) is usually applied in connection with planning and design of process plants, see e.g. [AIChE, 1985] Guidelines for Hazard Evaluation Procedures and [the Hazop Study Guide, 1977] Guide to Hazard and Operability Studies (the Hazop Study Guide). This can be performed as a complete risk assessment for the whole plant or as a pre-study for certain critical parts of the plant. The analysis is usually based on the drawings of the process plant and the instrument system (P& I diagrams), and the objective is to identify possible safety-related or operational problems that may arise during in-service operation or maintenance of the process plant. The main focus of a HAZOP is to identify possible problems rather than to find relevant solutions to the problems.

The analysis itself is carried out by a HAZOP group which typically consists of a leader, a secretary and 4–6 process specialists. A significant part of the analysis is performed in the form of 'brainstorming' meetings. This analysis process poses strong demands on the abilities of the leader who should have extensive experience and background from similar analyses.

The starting point for each brainstorming session is usually a major component of the plant such as e.g. a storage tank or a compressor. Each pipe flow into the unit, or out from it, is then analyzed one by one. The individual pipe flows are referred to as 'Study Nodes'. For each 'Study Node' it is aimed at identifying the normal condition as well as deviations from this normal condition. The reasons for the deviations and the potential consequences which are associated with them are then addressed by means of 'Guide Words' which are applied for the purpose of stimulating the brainstorming process.

### B2.3.5 Event tree analysis

An Event Tree is used to develop the consequences of an event. It gives a pictorial representation of the logical order in which the different events in a system can occur. An Event Tree is constructed by defining an initial event and works forward in time considering all possible subsequent events until the consequences are known. The initial event is usually placed on the left and the corresponding branches are drawn to the right. Each branch represents a particular scenario which corresponds to a particular sequence of events and terminates in an outcome.

The initial event is usually expressed as a frequency (events/year) and the subsequent splits are expressed as probabilities (events/demand). This implies that the final outcomes are also represented in terms of frequencies (events/year). Figure B2.1 illustrates a very simple example of an event tree related to the initiating event of a continuous gas release.

In Figure B2.1,  $f_1$  designates the frequency (in events/year) of the initiating event and the probabilities at the different branching points are denoted by  $p_1, p_2 \dots p_6$ . The uppermost

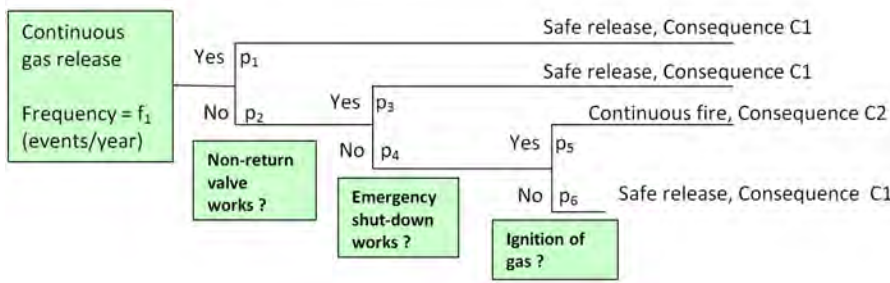


Figure B2.1: Simple example of an Event Tree

branch in this event tree corresponds to the scenario that there is a continuous gas release as the initiating event and that the non-return valve (NRV) is working such that the final outcome is a safe release (SF). The associated frequency (number of events per year) for this final outcome is accordingly expressed as  $f_{Upper\ branch} = f_1 \cdot p_1$ , which is based on the assumption that the two events are statistically independent from each other.

In this example it is assumed that no manual isolation of the release is possible. If this could be possible, the event tree would contain one additional intermediate branching point and additional final outcomes. Furthermore, in many cases there are more than two options at each branching point (which in the present example are of the yes/no type). This implies that the number of outputs at each branching point corresponds to the number of possible alternative events.

### B2.3.6 Fault tree analysis

Compared to an Event Tree the 'Fault Tree' analysis works in the opposite direction. A Fault Tree starts at a possible system failure mode (top event or undesirable event) and then works backwards. The strategy is to identify events (fault events) which may contribute to a failure event. These events are enumerated in logical sequences through logical connections (logic gates). The Fault Tree is both a qualitative and a quantitative technique. Qualitatively it is used to identify the individual scenarios (so called cut sets) that lead to the top (fault) event, while quantitatively it is used to estimate the probability (frequency) of the top event.

A component of a Fault Tree has one of two binary states, either in the correct state or in a fault state. An example of a very simple Fault Tree related to the failure of a valve is given in Figure B2.2 .

It is observed that each of the basic sub-events in this figure in turn can be expressed in terms of even more basic events, which implies introduction of more branches in the tree structure. The logic gate in the present example is of the OR type. There are also logic gates of the AND type which requires that all of the 'in-going' events take place for the output from the gate to be activated.

As a Fault Tree represents a logical formula it is possible to calculate the probability of the top event by ascribing probabilities to each basic event (denoted by  $p_1$  and  $p_2$  in Figure B2.2), and by applying the probability calculation rules. When the events are independent, and when the probabilities are low it is possible to roughly estimate the probability of the output event for an OR gate as the sum of the probabilities of the input events. Hence, for

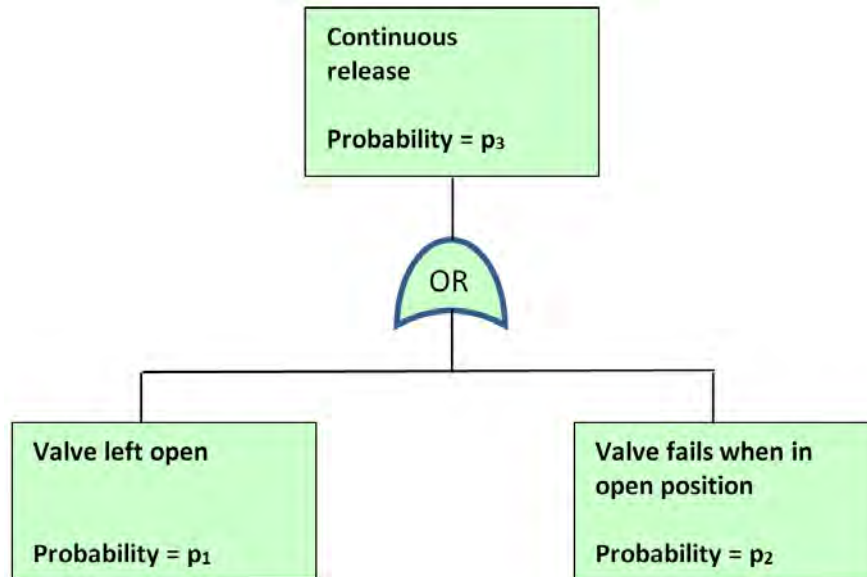


Figure B2.2: Simple example of a Fault Tree

in the present example it is obtained that  $p_3 \approx (p_1 + p_2)$ . (If the logic gate were an AND gate and the input events were independent, the probability of the output event would be the product of the two probabilities of the input events.)

### B2.3.7 Risk Matrix: Evaluation of failure probabilities and consequences

#### B2.3.7.1 Evaluation of failure probabilities

The different events for which evaluation of associated probabilities are required can be quite diversified. The main difference is between events which are directly related to human activities and those that do not explicitly involve human actions. The first category requires that the probabilities of human errors, slips and mistakes are dealt with. The second category is concerned with evaluation of failure probabilities for the individual components and sub-systems as such. For this category, two different approaches can be applied: direct application of observed failure rates for electrical and mechanical components is one option, and use of structural reliability methods for mechanical components represents another option.

Observed failure rates are available in various types of empirical data bases, and supplementary information can also be obtained from laboratory testing. Limitations associated with empirical data obtained from past experience is that frequently there have been significant technical developments associated with industrial products throughout the years. Hence, application of historical data can lead to significant errors in estimation of failure rates for products which are being applied at present. This needs to be kept in mind when such empirical data are to be utilized. One possibility will be to apply only the part of the data which is found to be relevant for the particular case to be analyzed.

Quantification of failure probabilities for mechanical components is discussed in more detail in Section B2.4 below (and in Chapter B3). The focus is on flexible pipe sections since these constitute the main topics of the present handbook.

For some of the relevant failure mechanisms of flexible pipes it may not always be possible to quantify the failure probability in numerical terms. This implies that in some cases more qualitative measures are applied (e.g. low, medium and high probability)

### B2.3.7.2 Consequence analysis

In accordance with the three different types of risk, there are three main types of consequences:

1. Human injury and fatality
2. Environmental damage
3. Financial losses.

The estimation of consequences given failure of the system requires a good understanding of the system and its interrelation with the surroundings. Accordingly, very specialized types of analysis skills and computer software may be required. For consequence assessment related to explosion and fire, application of calibrated computational fluid dynamics (CFD) software is frequently made. The same applies to oil dispersion in the ocean once a release has taken place.

### B2.3.7.3 The risk matrix concept

The arrangement of accident probability and corresponding consequence in a Risk Matrix can be a suitable visualization of risk in cases where many accidental events are involved and/or where calculation of a single risk value is difficult. A schematic structure of such a matrix is shown in Figure B2.3 . It is observed that the matrix is separated into three regions which correspond to low, medium and high risk, respectively. Clearly, the high risk region will generally correspond to unacceptable conditions. For the medium risk region, reduction of risk needs to be considered. This is discussed in further detail in connection with acceptance criteria below.

### B2.3.8 Decision trees

Decision trees are applied in order to compare the expected costs associated with different alternative system concepts. A decision tree can be considered as a special case of an event tree. For each branch of the tree, the consequences of the corresponding events are listed in addition to the probabilities. The expected consequences (i.e. quantified in terms of cost if this is possible) which are associated with each outcome of the tree can then be computed as a basis for decision-making.

### B2.3.9 Acceptance criteria

#### B2.3.9.1 General

In some cases, the accepted risk level can be formulated directly in terms of a given fixed value. More generally, acceptable regions are specified in relation to the risk matrix as

## Probability / Consequence matrix

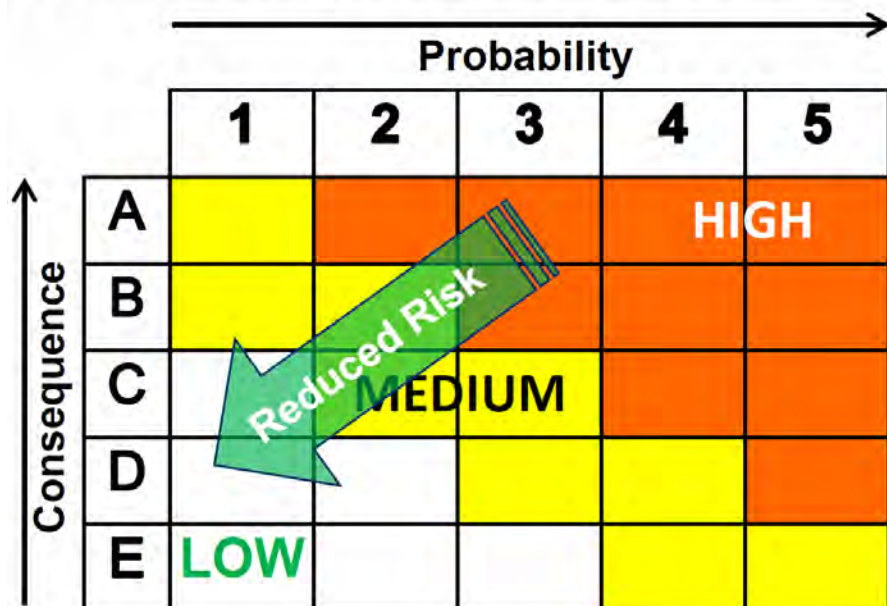


Figure B2.3: General layout of risk matrix

shown in Figure B2.3 above. Furthermore, the risk level can be specified in terms of derived measures such as values of Fatal Accidental Rates (FAR) or alternatively FN-curves. In some cases, risk reduction needs to be considered if events with non-acceptable risks are identified. The question regarding which reduced risk level should be aimed at is frequently based on the so-called ALARP principle as discussed in the next section.

### B2.3.9.2 The ALARP principle

The ALARP principle refers to the risk level and designates '**As Low As Reasonably Possible**', see e.g. [Sharp et al., 1993]. Sometimes this is replaced by the concept '**As Low as Reasonably Attainable**' (ALARA). The background for this notation is the transition zone between the non-acceptable region of the risk-matrix and the low-risk region where both the consequences and the probabilities are small. In the transition zone it is frequently possible to move as far as wanted towards the low-risk region. However, this is usually a matter of cost, time and effort. Hence, the situation can easily arise that the additional resources which are required to reduce the risk even by a small amount become disproportionate with these resources. It is natural to consider such a point (or risk interval) to be the minimum risk that reasonably be achieved. Such a criterion may seem to be quite subjective, but for a given type of system it may also be possible to translate this requirement into quantified specifications.

### B2.3.9.3 Target failure probabilities and safety classes

Excluding the 'external damage sources' of pipe failure and considering the probability of mechanical failure due to the load effect exceeding the mechanical strength, it is possible to identify probability levels which are considered to be adequate. For metallic pipes, such

probabilities are given e.g. in [DNV-OS-F201, 2010] and in [DNV-OS-F101, 2007]. These probability levels are also highly relevant for flexible pipes. The target values for dynamic risers are reproduced in Table B2.1

Table B2.1: Target failure probabilities as function of safety class for metallic risers according to [DNV-OS-F201, 2010]

Target failure probabilities (annual per riser) versus  
safety class for metallic risers

<b>Safety class</b>		
<b>Low</b>	<b>Normal</b>	<b>High</b>
$10^{-3}$	$10^{-4}$	$10^{-5}$

[DNV-OS-F201, 2010]: Dynamic Risers

It is generally possible to compute the inherently implied failure probabilities for pipes which are designed according to past and present design standards. This will reflect the reliability level which is found to be acceptable within the industry. In some sense, this will correspond to the ALARP criterion for engineering design as such. If new design formats, design guidelines or design standard are to be developed, these inherently implied probability levels can be applied as target (average) values for the updated codified rules.

The convenience of a permissible value of the probability of failure versus time is illustrated in Figure B2.4. In this figure, the failure probability for a flexible pipe system increases with time e.g. due to corrosion and fatigue. At certain points in time a transition from one safety class to a lower one takes place. If the new safety class is found to be unacceptable, some measures need to be introduced. This could e.g. correspond to upgrading of the pipe system, replacement, shut-down, modification of operation parameters etc.

In this figure the annual probability of failure is applied. In some cases the annual probability is quite low while the cumulative failure probability becomes unacceptable after a sufficient time in operation. Accordingly, limits should also be specified for the cumulative value of the probability of failure.

In Figure B2.4, it is also illustrated how the amount of test data may influence the permissible time in operation. An increasing number of tests will reduce the scatter as measured by the variance of the data. If the mean values of the strength parameters are constant for increasing sample sizes this reduction of scatter will hence imply smaller probabilities of failure.

For an increasing number of tests it is increasingly likely that 'weak samples' will be encountered if such exist. This may sometimes tend to a reduction of the mean value of the strength. In rare cases this may lead to a decrease of the characteristic strength properties rather than an increase. However, the confidence in the results will increase which results in a more proven design basis. This is also discussed in connection with qualification of new technology in Section B2.6.

### B2.3.10 Risk reduction

If the estimated risk is too high as compared to the maximum acceptable level (or above the ALARP range), risk reduction and risk mitigation must be considered.

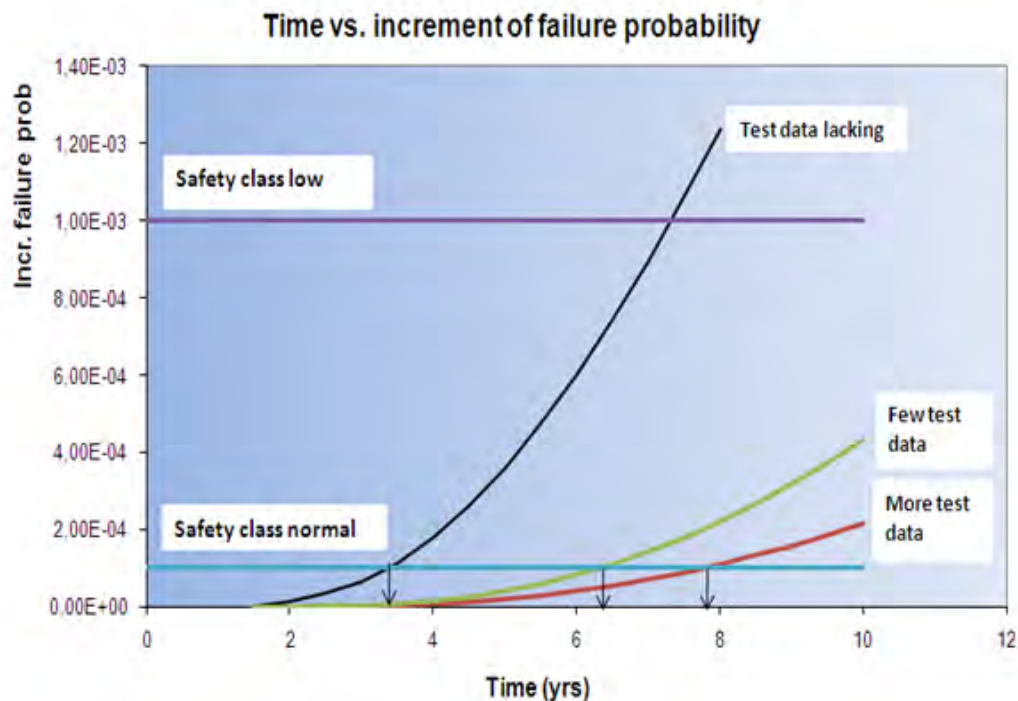


Figure B2.4: Example of computed failure probability versus time in operation

*Risk reduction* can be achieved by reduction of the probability of occurrence. In practice risk reduction is normally performed by a physical modification of the considered system (e.g. by introduction of sensors and warning systems). This also includes the possibility of modifying the operation parameters (e.g. maximum internal pressure or normal operating pressure).

*Risk mitigation* is implemented by modification of the system such that the consequences of an accidental event are lowered. This can be achieved e.g. by application of control systems of different types.

## B2.4 Quantification of mechanical failure probability

### B2.4.1 General

As seen above, quantification of failure probability is a very important part of the risk analysis. Such a quantification is required for all the different steps of each branch of the fault tree or event tree. This may be a challenging task, especially in relation to quantification of probabilities for events which involve human interaction. This is outside the main scope of the present handbook, and in the present section we focus solely on quantification of the probabilities associated with mechanical failures.

### B2.4.2 Flexible pipe failure data based on test results

Based on mechanical testing, probabilistic models of the associated physical properties can be established. This applies both to the ultimate limit state (e.g. yield stress) and the fatigue

limit state. For both cases flexible pipes represent materials for which extensive test data are not available, such that dedicated testing for the particular metallic alloys and plastic materials is required. Furthermore, the internal and annulus fluids in flexible pipes represent corrosive environments with time-varying composition for which extensive additional testing is typically required. This applies for example to fatigue testing and establishment of relevant SN-curves to be applied for design. The scatter in the SN test data forms the basis for identification of probabilistic models for the fatigue capacity. Further details of such testing are given in Chapter B5 of the present handbook.

In some cases, results from full-scale measurements are also available. Similarly, probabilistic models of the environmental processes and the corresponding external loads frequently require result from full-scale measurements and simulation in hydrodynamic laboratories.

Samples from decommissioned riser pipes that have been in operation for a number of years are sometimes available. By extracting samples from such pipes and subject these to testing under controlled laboratory conditions, the effect of relevant aggressive environments and corrosion defects on the fatigue properties can be assessed. Damaged pipes have also been instrumented and tested in strength laboratories.

#### B2.4.3 Probabilistic evaluation of mechanical limit states, including time-variation of loads and resistance

As the loads on floating structures are mainly due to the effects of wave-, wind and current, their statistical properties will fluctuate as functions of time. The same will accordingly apply to the load effects in risers and mooring lines which are attached to these structures. The resistance will also in general be a function of time e.g due to deterioration processes such as corrosion (unless this is counteracted by repair or other types of strength upgrading). Furthermore, a typical situation is that the extreme load effects will increase with the length of the time interval which is considered (i.e. the 20 year extreme value is higher than the 10 year extreme value, and the 3-hour extreme load-effect during a storm is higher than the 1-hour extreme load-effect).

This situation is illustrated by Figure B2.5 for a relatively long time horizon. Here,  $t$  denotes time, and  $t_0 = 0$  is the start time. The second 'time slice' is at 10 years, and the third slice is at 20 years. The corresponding probability density functions of the mechanical resistance and the load effect are also shown for each of the three slices.

The structural component will fail if (at any time during the considered time interval)

$$Z = R(t) - S(t) < 0 \quad (\text{B2.2})$$

where  $Z$  is referred to as the safety margin. The probability that the event described by B2.2 will take place can be evaluated from the overlap of the two probability density functions  $f_R(r)$  and  $f_S(S)$  at each time step, as shown in Figure B2.5. At  $t = 0$  and  $t = 10$  years, these two functions barely touch each other, while at  $t = 20$  years, they have a significant amount of overlap. The latter case represents a resulting significant increase of the failure probability.

If it is chosen to use time-independent values of either  $R$  or  $S$  (or both), the minimum value of the function in Equation B2.2 during the interval  $[0, T]$  should be applied, where  $T$  denotes the design life time or the duration of a specific operation under consideration. In relation

to the maximum load effect, an extreme value distribution is relevant, such as the Gumbel distribution (also referred to as the type I asymptotic form). Similarly, the probability density and distribution functions of the minimum value of the resistance is relevant. For durations of the order of a few days or less, simplifications can typically be introduced, since decrease of the strength properties on such limited time scales usually can be neglected.

The variation of the density functions will be different for the different types of limit states. For the fatigue limit state (FLS), the physical load effect corresponds to the cyclic stress time history. The resistance is characterized by the parameters of the SN-curve. However, for the purpose of reliability calculations, it is more convenient to apply the permissible Miner sum as 'derived resistance parameter'. This is a time-independent quantity which can be represented by a (time-invariant) random variable. The 'derived load effect' will now correspond to the (random) cumulative damage which is obtained from the probability distribution of the cycle range of the stresses (also comprising the SN-parameters). If other deterioration processes are also present (such as corrosion), the 'derived load effect' will clearly increase with time also for this type of limit state.

Based on the probability density functions of the load effect and resistance, the failure probability can be computed. The more overlap of the upper tail of the load effect density function with the lower tail of the resistance density function, the higher the failure probability becomes. With reference to Figure B2.5, it is seen that the width of the probability density function for the resistance typically increases with time (while the height of the peak decreases as the total area under the density function is equal to 1.0). The location of the peak is also shifted to lower values. For the probability density function of the load effect, the location of the peak is shifted upwards with time (while both the dispersion and the peak height are constant). The combined effects of these features imply that the overlap interval of the density functions increases with time which means that the probability of mechanical failure will be significantly higher at  $t = 20$  years than at  $t = 0$ . Hence, for mechanical components in general and flexible pipes in particular the development of the probability density functions with time must be predicted with sufficient accuracy in order to compute the resulting variation of the corresponding failure probability..

Expressions for evaluation of this probability are elaborated in Chapter B3 of the present handbook.

## B2.5 Risk-based Riser Integrity Management

Risk-based Riser Integrity Management (RIM) can be considered as a systematic framework for keeping the risks associated with riser operation within acceptable limits that also takes into account the results from inspection, monitoring and repair. Here, only an overview of the topic is given while further details are given in Chapters C1, C2 and C3.

A layout of the risk-based integrity management process is given in Figure B2.6. The first two steps correspond to the risk analysis process which was outlined in the previous sections, also including risk reduction and risk mitigation. The continuous risk reduction in the lower part of the figure is based on measurements and observations which are made during operation, inspection and possible repair of the system. Based on such additional information, decisions related to future operation and time of decommissioning are facilitated.

Figure B2.7 illustrates some more particular details of the feedback process in relation to

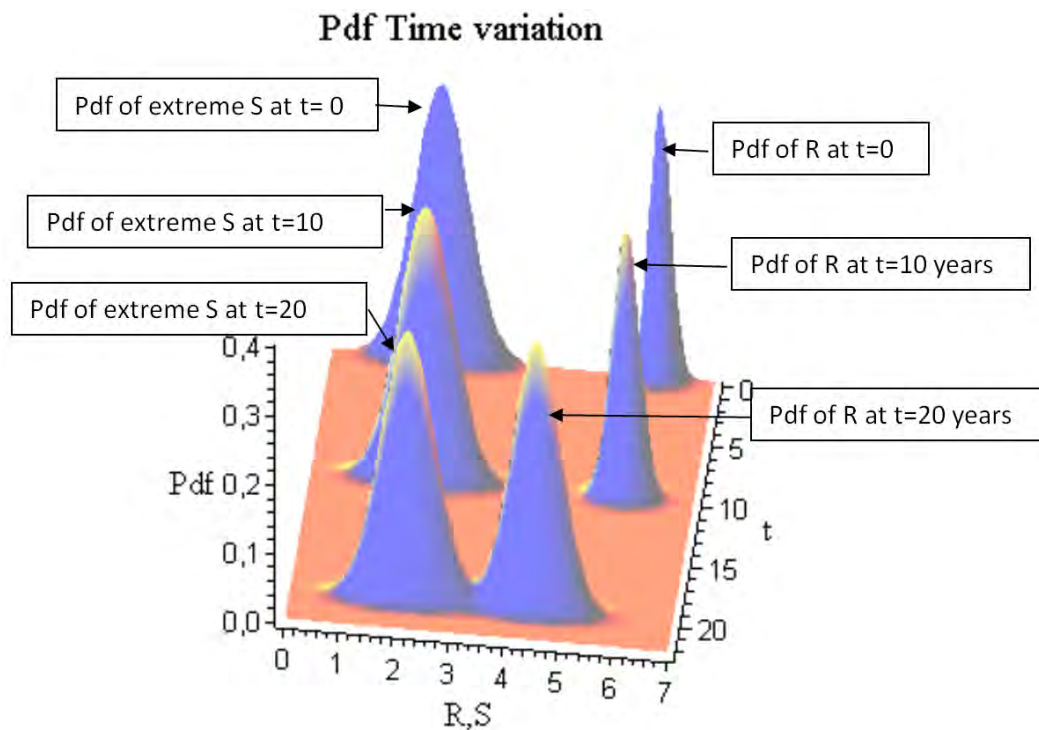


Figure B2.5: Illustration of the time-varying marginal probability density functions (Pdfs) of resistance,  $R(t)$ , and extreme load effect  $S(t)$ . (Note: Density functions are artificially scaled to the same maximum value)



Figure B2.6: General layout of risk-based management process

assessment of future corrosion, fatigue and ageing of polymers for the case of an aggressive annulus environment. Experience from past operation and all relevant information about present conditions are applied in order to assess the present level of corrosion and fatigue damage. This is combined with intrinsic knowledge about the material properties and planned future operation characteristics which allows prediction of the remaining time in operation at an adequate safety level.

## Risk management, particular

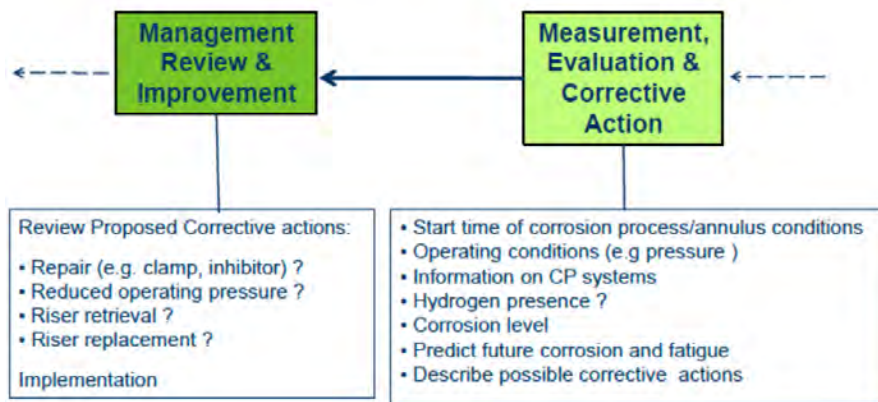


Figure B2.7: Particular considerations related to risk management in connection with corrosion and fatigue

## B2.6 Historical failure mechanisms and qualification of new technology

### B2.6.1 Historical failure mechanisms

A summary of historical failure mechanisms as reported by one particular operator based on 15 years of riser experience is given in [Olsen and Rongved, 2002]. This summary can be considered to be quite representative for the accumulated experience at that time.

Degeneration of the Rilsan *pressure sheath* was observed. Studies concluded that use of Rilsan as the inner thermoplastic sheet at temperatures above 65° C makes hydrolysis of the polymer a prevailing degradation mechanism.

Regarding the *outer sheath* it was found that vent ports had been blocked and that the pressure increase in the annulus resulted in burst of the outer sheath. Another failure mode of the outer sheath was mechanical damage during installation and replacement operations. In one case the sheath was damaged when it was hit by a dropped object from the platform. Furthermore, riser annuli were found to be flooded by seawater after installation due to missing vent plugs.

Vacuum testing of the risers indicated that there was water in the annuli in several risers. The indication of water-filled annuli resulted in a change of the design philosophy. The resulting corrosive environment had to be taken in account. Reanalyses of the risers were found to be required by applying new input regarding S-N curves for the relevant materials with the modified curves being established for a corrosive environment.

Risers with *PVDF pressure sheath* experienced some problems with leakage in the end termination. The plasticizer in the polymer layer was washed out by the hydrocarbons in the riser flow. Several temperature cycles could in some cases result in loss of anchoring of the pressure sheath in the end termination. A fracture mechanics approach to assessment of PVDF pressure sheaths was outlined by [Melve, 2001].

Hence, it was found that 'internal causes' associated with the pipe materials and pipe design as well as 'external causes' due to damage triggered by external events contributed to the failure statistics.

Further details of flexible pipe failure mechanisms are given in Chapter [A3](#) of the present handbook. where also references to more recent databases are given such as those of PSA and HSE, see also the SUREFLEX JIP reports, [[MCS Kenny State of the Art, 2010](#)] and [[MCS Kenny Guidance Note, 2010](#)].

### B2.6.2 Qualification of new technology

New designs of flexible pipes are continuously being considered. Modifications with respect to the geometrical layout of individual layers, the number of layers and/or new material properties are frequently proposed. Qualification of such new designs may as a first step involve extensive numerical analysis and small-scale sample testing. However, in the case of such modified design of flexible pipes, there could also be new types of failure mechanisms for the flexible pipe which are caused e.g. by interaction between the different materials and the different layers. Accordingly, systematic test programs for integrated pipe sections and full-scale pipe systems will generally be required in addition to testing of samples for the individual layers. In addition, expert opinions related to identification of potentially new failure mechanisms should be sought.

Identified failure modes can be submitted to a ranking based on the risk analysis procedures which are outlined above. Clearly, modifications of the new design will be required if the risk associated with any of the failure mechanisms is within the unacceptable region.

The long-term behavior of new pipe designs is also an important issue. Extended monitoring and inspection during installation and operation of the pipe system will typically be required in order to ensure adequate safety and performance.

Qualification of novel pipe design will in general be an iterative process. Based on feedback from the numerical analysis and the various experiments, modifications to the proposed design will often be necessary. This modification process is repeated until the specified design criteria are satisfied.

General procedures for qualification of new technology are found e.g. in [[DNV-DSS-401, 2012](#)] and [[DNV-RP-A203, 2012](#)].

## B2.7 Concluding remarks

In the present chapter the risk concept is first introduced, and subsequently the main steps related to a risk assessment of flexible pipe systems are summarized. Key items related to risk assessment of flexible pipes are then focused upon. In particular, methods for quantification of the probability of mechanical failure are considered in more detail as well as relevant acceptance criteria.

Further details related to some of the key topics which are highlighted in the present chapter can also be found in other parts of the present Handbook. Examples are:

- Flexible pipe failure modes (Chapter [A3](#))

- Reliability methods (Chapter [B3](#))
- Assessment of damaged pipes (Chapter [B4](#))
- Mechanical testing (Chapter [B5](#))
- Riser Integrity Management (Chapter [C1](#))
- Lifetime Assessment (Chapter [C2](#))
- Repair Methods (Chapter [C3](#))

Hence, it is emphasized that main factors related to prevention of failure of flexible pipe systems is a good understanding of the mechanical failure modes and their interrelation with relevant modes of operation for the pipe system throughout its lifetime.

## **Chapter B3**

# **Reliability Methods**

*Author: Bernt Leira, NTNU*

## B3.1 Introduction

In order to perform a risk assessment for a given flexible riser or flowline system, the potential failure modes need to be identified. For some of the failure modes a certain amount of relevant historical/empirical data may be available such that failure rates can be estimated. However, in many cases such data are missing or they can be rather irrelevant due to technological developments and improved production methods.

Still, it is frequently possible to establish a clearly defined mechanical model which corresponds to a given failure criterion. This model is generally referred to as a limit state, which is typically defined in terms of loads (or load effects) versus capacity terms. For some cases (such as for assessment of fatigue and wear) the accumulated load effect is relevant rather than its instantaneous value.

Both the load effects and capacity associated with a particular limit state will frequently depend on a number of parameters for which inherent variability is present. This implies that they are more adequately represented as random variables than deterministic quantities, which is accommodated within the framework of structural reliability analysis.

Another strong source of demand for application of such analysis methods is represented by cases which are not directly covered by existing design documents. Examples are life extension of flexible pipes beyond the intended service life as well as requalification and reuse of such pipes. Integrity management is another example.

Other examples of application are situations where additional information is to be taken into account in a systematic and consistent manner. Such updated information can e.g. be related to monitoring of operation parameters, metocean characteristics, pipe damage, accident scenarios as well as pipe annulus conditions

## B3.2 Mechanical Limit States

### B3.2.1 Limit states and levels of reliability analysis

In engineering design, distinction is typically made between different categories of limit states and associated design criteria. The three most common categories are the Serviceability Limit State (SLS), the Ultimate Limit State (ULS) and the Fatigue Limit State (FLS). Many riser design guidelines also introduce the so-called Accidental Limit State (ALS) in order to take into account the possibility of unlikely but serious event sequences.

The accidental events to be designed against are typically obtained by application of quantitative risk assessment (See Chapter B2). The requirement related to which accidental events that are to be considered also takes into account the probability for the events to occur. For static applications the accidental events typically include impact from trawl boards and dropped objects. For dynamic applications, accidental events which are typically considered include one or more mooring lines broken and partial loss of buoyancy.

Engineering design rules are generally classified as Level I reliability methods. These design procedures apply point values for the various design parameters and also introduce specific codified safety factors (also referred to as partial coefficients) which are intended to reflect the inherent statistical scatter associated with the parameters.

At the next level, second-order statistical information (i.e. information on variances and correlation properties in addition to mean values) can be applied if such is available. The resulting reliability measure and analysis methods are then referred to as a Level II reliability methods. At Level III, it is assumed that a complete set of probabilistic information (i.e. in the form of joint density and distribution functions) has been established.

In the following, procedures at Level III are focused upon as they allow the most accurate types of models to be applied.

### B3.2.2 A basic limit state formulation: Failure function and probability of failure

The common basis for the different levels of reliability methods is the introduction of a so-called failure function (or g-function) which represents a particular mechanical limit state as discussed above. The failure function gives a mathematical definition of the failure event in mechanical terms. In order to be able to estimate the failure probability, it is necessary to know the difference between the maximum load a flexible pipe is able to withstand, R (often referred to as resistance), in addition to the loads it will be exposed to, Q, and the associated load effects S. The latter are typically obtained by means of (more or less) conventional structural analysis methods. For this 'generic' case, the 'g-function' is then expressed as:

$$g(R, S) = R - S \quad (\text{B3.1})$$

As an example, R may correspond to the permissible fatigue damage for the flexible pipe and S will then correspond to the estimated fatigue damage after a specific period of time at the most critical cross-section. Failure of the pipe is then assumed to occur if the latter (accumulated response) quantity exceeds the permissible fatigue damage.

Hence, for positive values of this function (i.e. for  $R > S$ ), the structure is in a safe state. Hence, the associated parameter region is referred to as the *safe domain*. For negative values (i.e.  $R < S$ ), the structure is in a failed condition. The associated parameter region is accordingly referred to as the *failure domain*. The boundary between these two regions is the failure surface (i.e. presently corresponding to the line  $R=S$ ). The reason for application of these generalized terms is that the scalar quantities R and S in most cases are functions of a number of more basic design parameters. This implies that the simplistic two-dimensional formulation in reality involves a much larger number of such parameters corresponding to a reliability formulation of (typically) high dimension.

Here, a brief introduction is given to the basis for the Level III structural reliability methods which are required in the subsequent sections. Further details of these methods are found e.g. in [Melchers, 1987], [Thoft-Christensen and Baker, 1982] and [Madsen et al., 1986]. When concerned with waves, wind and dynamic structural response, it is common to assume that the statistical excitation and response parameters are constant over a time period with a duration of (at least) 1 hour. This is frequently referred to as a *short term statistical analysis*. A further assumption is typically that the stochastic dynamic excitation processes (i.e. the surface elevation or the turbulent wind velocity) are of the Gaussian type.

If the joint probability density function (or distribution function) of the strength and the extreme load effect, i.e.  $f_{R,S}(r,s)$  is known, the probability of failure can generally be

expressed as

$$p_f = P(Z = R - S \leq 0) = \iint_{R \leq S} f_{R,S}(r,s) dr ds \quad (\text{B3.2})$$

where the integration is to be performed over the failure domain, i.e. the region where the strength is smaller than or equal to the load effect. It is also noted that the computed failure probability refers to the same time period that the joint density refers to (e.g. 1 hour, 1 season, 1-year).

This is illustrated in Figure B3.11, where both the joint density function and the two marginal density functions  $f_R(r)$  and  $f_S(s)$  are shown (the marginal functions are obtained by a one-dimensional integration of the joint density function with respect to each of the variables from minus to plus infinity). The joint density function can then be split into two separate pieces as shown in part B3.12 and B3.13 of the same figure. The failure probability can then be interpreted in a geometric sense as the volume of the joint density function which is located in the failure domain, i.e. the part of the plane to the right of the line  $R=S$  (i.e. the region for which  $S>R$ ). This corresponds to the slice of the volume of the joint probability density function (pdf) which is shown in Figure B3.13.

For the case of independent variables, the joint density function is just expressed as the product of the two marginal density functions. The resulting expression for the failure probability then becomes:

$$p_f = P(Z = R - S \leq 0) = \iint_{R \leq S} f_R(r) \cdot f_S(s) dr ds \quad (\text{B3.3})$$

where it is assumed that  $R$  and  $S$  are independent. By performing the integration with respect to the resistance variable, this can also be expressed as

$$p_f = P(Z = R - S \leq 0) = \int_{-\infty}^{+\infty} F_R(x) \cdot f_S(x) dx \quad (\text{B3.4})$$

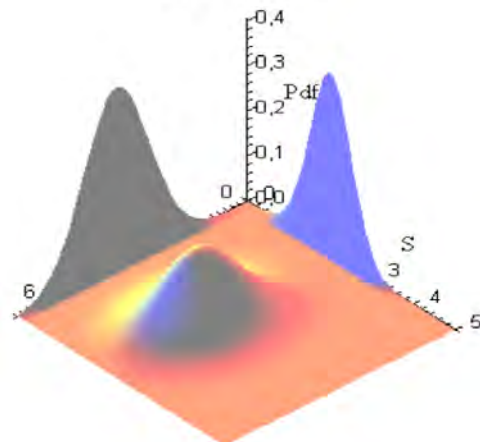
where

$$F_R(x) = P(R \leq x) = \int_{-\infty}^x f_R(r) dr \quad (\text{B3.5})$$

This situation is illustrated in Figure B3.2 where the two marginal density functions now are shown in the same plane. The interval which contributes most to the failure probability is where both of the density functions simultaneously have non-vanishing values (i.e. in the range between 1 and 3.5 for this particular example).

The integral in Equation B3.4 is known as a convolution integral, where  $f_R(r)$  denotes the cumulative distribution function of the mechanical resistance variable  $R$ . Closed-form expressions for this integral can be obtained for certain distributions, such as Gaussian distributed  $R$  and  $S$  variables.

The resistance probability density function in Equation B3.3,  $f_R(r)$ , is frequently represented as a Gaussian or Lognormal variable. The density function of the load-effect,  $f_S(s)$ , typically corresponds to extreme environmental conditions (such as wind and waves) and is frequently assumed to be described by a Gumbel distribution, see e.g. [Gumbel, 1958]. For this case, a closed- form expression for the failure probability can not be obtained in general.

**Pdf of R and S**

(1) Joint probability density function (pdf) of R and S

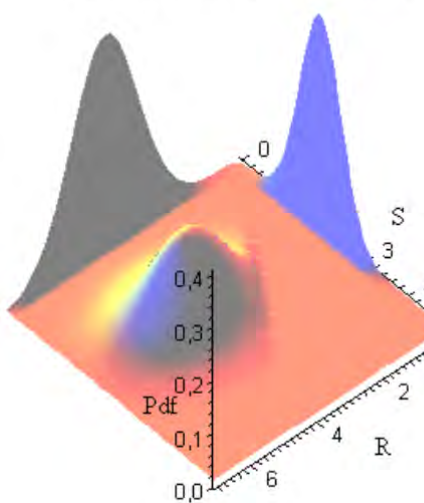
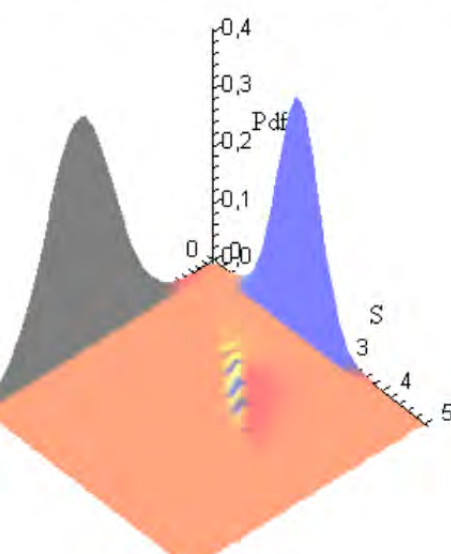
**Pdf of R and S: Failure domain****Pdf of R and S: Safe domain**(2) Safe domain volume ( $R > S$ )(3) Failure domain volume ( $R < S$ )

Figure B3.1: Illustration of failure probability when it is interpreted as a volume

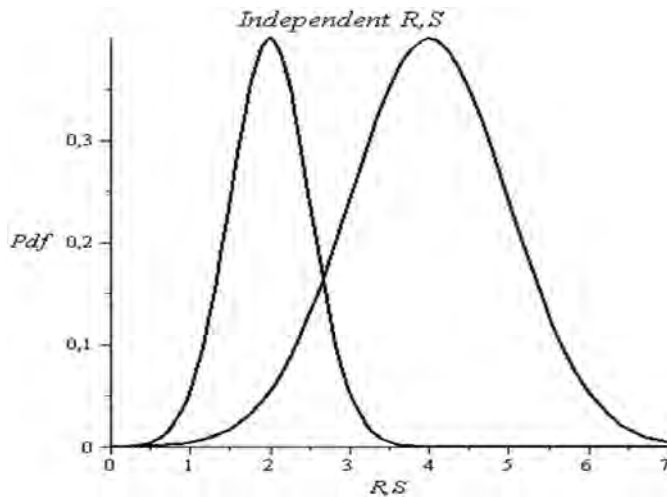


Figure B3.2: Marginal densities projected into same plane for the case of independent variables.

The present 'load effect versus capacity' formulation can be applied to all different kinds of limit states. In the present application the fatigue (FLS) and ultimate (ULS) criteria are mainly focused upon. In the former case, the derived load effect corresponds to the accumulated fatigue damage which is obtained from the long-term stress-cycle distribution. The derived capacity will then correspond to the permissible value of the Miner–Palmgren sum. For the ultimate limit state the load effect will correspond to the extreme response during a specified reference period (e.g. 1-year, 10-years or 100-years). The capacity will be the ultimate capacity which is intrinsic to the particular failure mode that is being considered (e.g. cross-section force resultants, stress, curvature).

### B3.2.3 Time-varying characteristics of load-effects and capacity

The time-varying nature of load-effects and capacity were already discussed in Chapter B2.5. Here, only a brief summary is given in connection with the illustration shown in Figure B3.3. Here,  $t$  denotes time, and  $t_0=0$  is the start time. The second 'time slice' is at  $t=10$  years, and the third slice is at  $t=20$  years. The corresponding probability density functions of the mechanical resistance and the load effect are shown for each of the three slices.

The figure illustrates that the structure will fail if (at any time during the considered time interval)

$$Z = R(t) - S(t) < 0 \quad (\text{B3.6})$$

where  $Z$  is referred to as the safety margin. The probability that the event described by Equation B3.6 will take place can be evaluated from the amount of overlap by the two probability density functions and at each time step, as shown in Figure B3.2 by application of Equation B3.3 or Equation B3.4. At  $t = 0$  and 10 years, the two density functions barely interact, while at  $t = 20$  years, they have a significant amount of overlap. The latter case accordingly represents a significant increase of the failure probability.

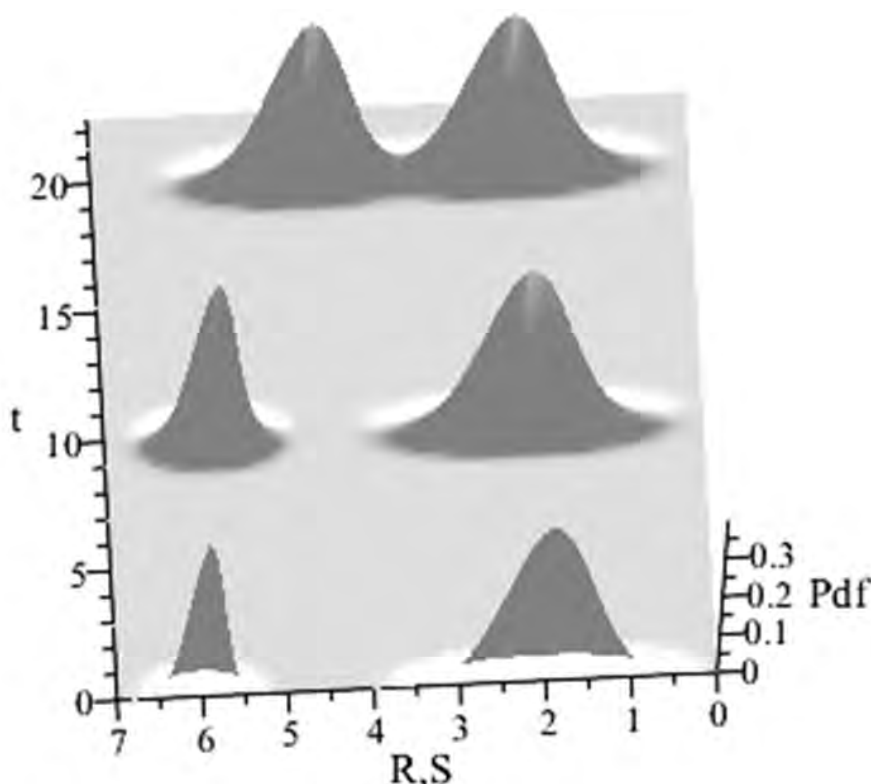


Figure B3.3: Illustration of the time-varying marginal Pdfs of resistance,  $R(t)$ , and extreme load-effect  $S(t)$

If it is chosen to use time-independent values of either  $R$  or  $S$  (or both), the minimum value of Equation B3.6 during the interval  $[0, T]$  must be used, where  $T$  denotes the design life time or the duration of a specific operation under consideration. In relation to the maximum load effect, an extreme value distribution, such as the Gumbel distribution, (also referred to as the type I asymptotic form) is typically applied. Similarly, the probability density and distribution function of the minimum resistance value is relevant.

The variation of the density functions will be different for the different types of limit states. For the fatigue limit state, the 'derived resistance' can e.g. correspond to the permissible cumulative damage. This is a time-independent quantity (which may still be represented by a (time-invariant) random variable). The 'derived load effect' will now correspond to the (random) cumulative damage which is obtained from the probability distribution of the stress cycles (also involving the SN-curve parameters). If other deterioration processes are also present (such as corrosion), the 'derived load effect' will clearly increase with time also for this type of limit state.

### B3.3 Data Basis and Input Modeling Relevant for Mechanical Limit States

The data basis is clearly essential for an adequate reliability assessment. This applies to the basis for estimation of probabilistic models in relation to flexible pipe capacity as well as probabilistic models for load effects. Some of the relevant parameters are of a general type

while others are intrinsic to the particular case that is being analyzed.

Examples of the general ('state of the art') category are probabilistic models related to environmental modeling, global and local response analysis and material properties (e.g. yield stress and fatigue capacity). These models are based on accumulated knowledge related to design, testing and operation of flexible pipes as well as other types of slender marine structures (e.g. mooring lines, tendons, metallic risers and pipelines)

Comparisons between measured and calculated stresses in flexible pipes based on application of optical fibers are reported in [Andersen et al., 2001], [Sævik and Ekeberg, 2002] and [Sævik, 2011]. For damaged pipes, comparisons between measured and computed stresses are made e.g. in

[De Sousa et al., 2011]. At the level of global response of flexible risers, results obtained by application of different computer programs were compared by [Larsen, 1991]. Comparisons between computation and full-scale measurements are reported e.g. in [Otteren and Hanson, 1990], [Hanson et al., 1994].

In relation to material properties of flexible pipes, multiple studies have been performed. Just to mention a few publications, plastic materials have been investigated by [Dawans et al., 1998], [Berger et al., 2011], [Shen et al., 2011].

A summary of relevant metallic materials and their properties is given by [Colquhoun et al., 1990]. Relevant requirements to such materials are given in [API 17J, 2008]. Results from fatigue testing of metallic specimens in various corrosive environments are reported e.g. in [Berge et al., 2008] and [Charlesworth et al., 2011].

Examples of the probabilistic models for the case-specific category are those based e.g. on available pressure and temperature records, measured floater motions and time series of environmental parameters at the particular site that is being considered. Examples of recorded pressure and temperature time histories are given e.g. by [Binet et al., 2003], see the time-traces which are reproduced in Figure B3.4.

When sufficient data are available, the best statistical model among relevant analytical expressions can be found. Various statistical test methods exist in order to quantify the 'suitability' of a specific model in relation to a particular data set. Such methods are most established for univariate ('one-dimensional') probability models. More efforts are generally required for multivariate models, in particular related to the modeling of correlation properties, see e.g [Kiureghian and Liu, 1986]. This implies that there will typically also be stronger requirements to the amount of available data for such cases.

As a main observation, it is very important that the probability distributions of the load effects as well as the resistance/capacity variables are validated by measurements or test data. If such data is lacking then the sensitivity of the computed results to distribution variations should be studied and new tests carried out.

## B3.4 Acceptance criteria

Procedures for Quantitative Risk Assessment are described in Section B3.5. As discussed, the ALARP principle is typically applied in order to decide whether risk mitigation is required. Having introduced adequate mitigation measures at the flexible pipe system level, adequate mechanical design of the individual components is subsequently required.

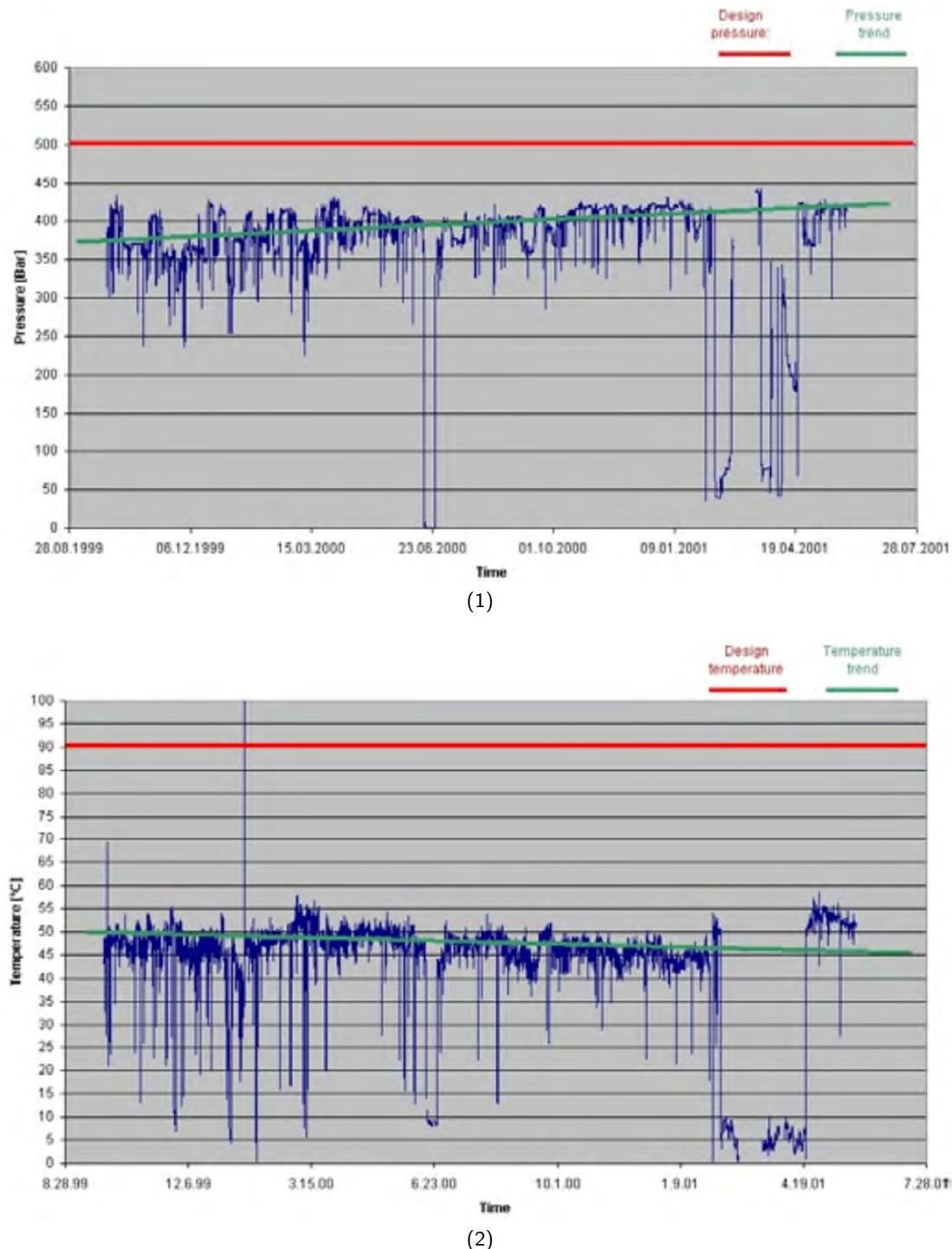


Figure B3.4: Examples of (a) pressure record and (b) temperature record, from [Binet et al., 2003]

Relevant target structural reliability levels (specified in terms of probability of failure) are also discussed in Section B3.5. The target value depends on the safety class which is relevant, and the safety class in turn depends on the consequences of failure. Three different safety classes are defined in [DNV-OS-F201, 2010] in relation to metallic risers. For safety class low, a target failure probability of  $10^{-3}$  is applied, for safety class normal the probability  $10^{-4}$  and for safety class high the value is  $10^{-5}$ . These values refer to annual failure probability per riser.

## B3.5 Analysis procedures

In most applications of reliability analysis, the load effect and resistance terms which enter the failure function are in turn functions of a number of more basic design parameters.

The random static load effects and the random capacity in the failure functions can frequently be expressed directly in terms of the basic variables. Such relationships can be obtained based on performing deterministic load effect analyses for different values of the relevant input parameters. For example, multidimensional polynomial expressions can be established that fit the functional relations as closely as required. This approach is referred to as response surface techniques. An example of application in relation to fatigue reliability analysis of flexible risers is given e.g. in [Leira et al., 2005].

On the other hand, the dynamic response is generally represented in terms of random processes. This implies that the statistical parameters (e.g. standard deviation, skewness and kurtosis) which characterize the dynamic response distributions can be determined as functions of the basic variables. Hence, the fitted response surfaces are related to the statistical parameters instead of a characteristic value (i.e. point value) of the response. This is due to the fundamental statistical variability associated with the sea-elevation and consequently the response processes.

The main steps of the reliability assessment comprise the following:

1. Step (i): Specification of the failure criterion (Limit State function) and corresponding random variables.
2. Step (ii): Variation of basic parameters and identification of corresponding response surface polynomials.
3. Step (iii): Calculation of failure probabilities and importance factors for the random variables.

In relation to the third step, a number of different techniques are available for calculation of the failure probabilities. These techniques can broadly be classified into two main categories, i.e. those based on Monte Carlo simulation methods and those based on local approximation of the failure surface by first- or second-order mathematical expressions (i.e. in the vicinity of the so-called *design point*). Further details related to both categories of methods are given in [Thoft-Christensen and Baker, 1982], [Madsen et al., 1986] and [Melchers, 1987] Melchers.

The basic principle behind Monte Carlo simulation techniques is to generate a statistical sample based on pseudo-random number algorithms. Such algorithms are readily available in many standard software packages such as Excel, Matlab, Maple, Mathcad etc. For a given sample, the number of outcomes which result in failure is simple divided by the total

number of outcomes to provide an estimate of the failure probability. By generating samples of adequate size, probabilities of any magnitude can in principle be estimated. The main drawback associated with this technique is typically the significant computational effort which is required for small failure probabilities since this demands large sample sizes.

In relation to the second category of methods, the simplest approximation to the failure surface is based on first-order (i.e. linear) expressions, which is the basis for the so-called FORM (First Order Reliability Method) technique. An example of such a linear 3D approximation at the design point in normalized space is shown in Figure B3.5. The search for the design point is performed in a normalised space by means of the so-called Rackwitz-Fiessler algorithm. Transition from basic variable space to the normalised space is based on the Rosenblatt transformation. Further details of this category of methods are found in [Pickands, 1952], [Cornell, 1969], [Hasofer and Lind, 1974], [Colquhoun et al., 1981], [Hohenbichler and Rackwitz, 1981], [Hohenbichler and Rackwitz, 1983]. Associated Second-order methods (SORM) are described e.g. in [Breitung, 1984] and [Tvedt, 1987].

### ***Failure function FORM approximation***

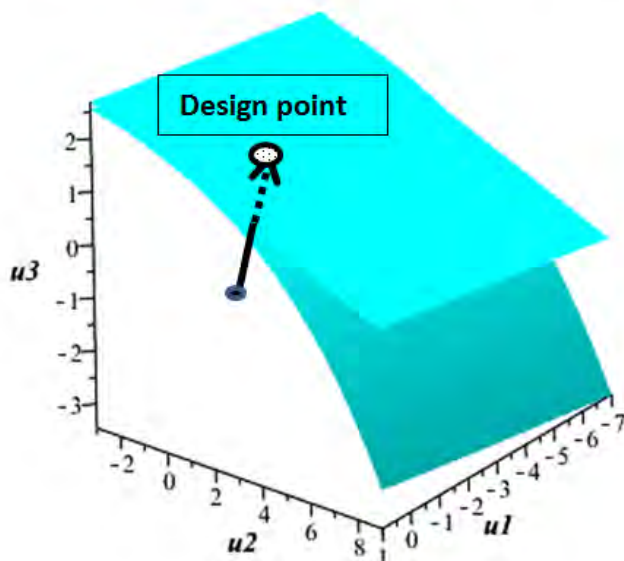


Figure B3.5: Example of FORM approximation of failure surface in normalized 3D space and associated design point.

In relation to FORM/SORM techniques, the parameter region where the highest accuracy is requested will hence be in the neighborhood of the *design point*. This is the neighbourhood where the highest contribution to the failure probability is located. A priori it may be anticipated that for load variables this neighbourhood will correspond to values well above the mean value. For resistance variables, lower fractiles (i.e. below the mean value) of the probability distributions are relevant.

Hence, an initial estimation of the location of the design point can frequently be made. Initial reliability analyses are then performed by first making a rough fit of the response surface expressions over a relatively wide parameter range around this region. Based on the resulting design point, more refined fitting is subsequently made for a restricted range. Information on

the more precise location of the design point also allows the relative importance of the various random variables to be computed. This is quantified in terms of the directional cosines of the radius vector at the design point, see e.g. [Madsen et al., 1986] and [Melchers, 1987].

Designating the distance from the origin to the design point in the normalized space by  $\beta$ , the failure probability is computed as

$$p_f = \phi^{-1}(\beta) \quad (\text{B3.7})$$

where  $\phi$  is the standard normal cumulative distribution function

## B3.6 Reliability Analysis for the Fatigue Limit State

### B3.6.1 General

For reliability analysis related to the fatigue failure mode, the load effect term in Equation B3.6 corresponds to the accumulated fatigue damage as a function of time. Due to the parameters which are input to the fatigue damage calculation being random variables, the left-hand side of the expression is also a random variable. The permissible threshold value is 1.0 for the fatigue damage (i.e. corresponding to  $R(t) = 1.0$  in Equation B3.6) which is based on the Miner-Palmgren hypothesis for summation of partial damage contributions. However, as there is a significant model uncertainty related to this summation method the threshold value is also generally represented as a random variable (with a mean value of 1.0).

Generic models are frequently based on lognormal probability models for both the 'derived resistance' and the 'derived load' terms. Based on such a model the resulting failure function can be expressed as:

$$g(R, S) = R - S(t) = R - D(t) \quad (\text{B3.8})$$

where  $R$  represents the lognormal distributed capacity (i.e. Miner Sum) with a mean value of 1.0, and the lognormal variable  $D(t)$  corresponds to the accumulated fatigue damage (also containing the SN-curve parameters). The statistical parameters of the latter are generally functions of time. A simple illustration of the resulting density functions and their relative location as a function of time is given in Figure B3.6. The mean value of the damage increases linearly with time for the present example (i.e.  $\mu_D(t) = 0.004 \cdot t$ ), and the variance is presently taken to increase in proportion to  $t^{1.5}$  (i.e.  $\sigma_D^2(t) = 0.00002 \cdot t^{1.5}$ ). It is seen that the probability density function of the accumulated damage has an increasing overlap region with the density function of the permissible damage. At time unit  $t=100$  the probability of failure calculated according to Equation B3.2 is computed (by FORM) as  $p_f = 0.02$  which reflects the proximity of the density functions at that time.

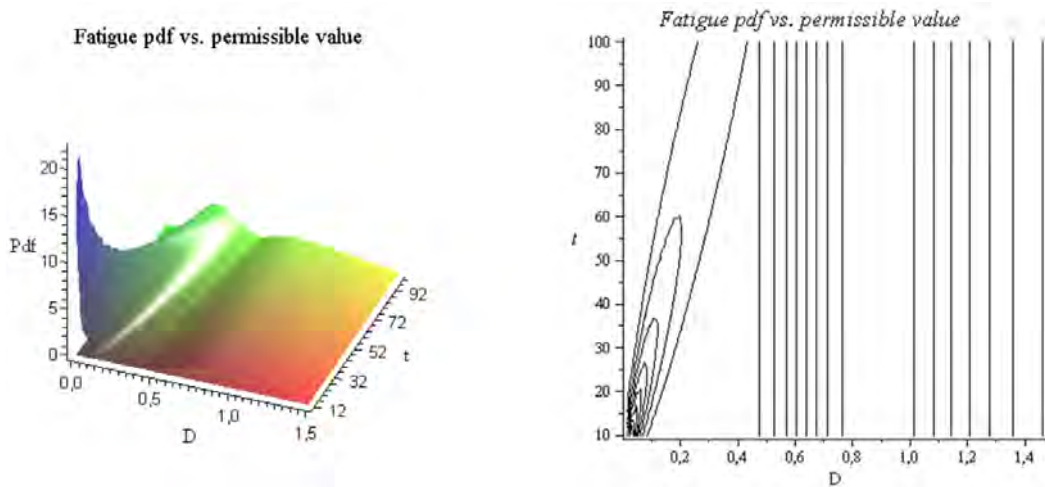


Figure B3.6: Example of time variation of probability density functions related to fatigue reliability.

Table B3.1: Base case lifetimes in years corresponding to different internal conditions

Case	Condition	Pressure Armour	Tensile armour
1	No $H_2S$ , Inhibited Fluid	400 yrs	2000 yrs.
2	$H_2S$ , Inhibited Fluid	60 yrs	120 yrs.

## B3.6.2 Example of application to fatigue assessment of a flexible riser

### B3.6.2.1 Introduction

As an example of a reliability analysis related to the fatigue limit state for a particular flexible riser system, a configuration of the lazy-wave type is considered. The riser is terminated at the upper end by a bending stiffener which is attached to an FPSO at a water depth of around 450m. The wave environment corresponds to rough North Sea conditions. For the initial period of operation, i.e. the first 15 years, the internal fluid is non-aggressive. Subsequently, a rather fast increase of the content of  $H_2S$  takes place, and after an additional period of 1 year (i.e. after 16 years in operation) the fluid in the annulus reaches the maximum  $H_2S$  concentration. For the subsequent period this concentration remains constant.

The fatigue damage is first calculated with all analysis parameters being equal to their base case (i.e. design values). The results are shown in Table B3.1 for both the pressure and tensile armors for the two different annulus conditions (i.e. with and without  $H_2S$ ). It is seen that the pressure armor is more critical than the tensile armor with respect to fatigue lifetime for both of the internal fluid conditions. Furthermore, it is observed that the annulus condition has a very strong influence on the lifetime (through the SN-curve parameters).

### B3.6.2.2 Parameter variations and response polynomials

Each of the input variables are subsequently varied at a number of different levels and the fatigue damage is recalculated for each case. The relevant parameters to be varied for the present configuration are the following:

- Riser drag coefficient used in global analysis models
- Floater dynamic surge amplitude
- Floater dynamic heave amplitude
- Floater dynamic pitch amplitude
- Floater static offset from reference position
- Armour wire friction coefficient used in local pipe analysis models
- Internal pressure

These parameters correspond to the random variables in the upper half of Table [B3.2](#).

By dividing the damage for each analysed case with the 'design damage' (i.e. corresponding to the base case), response surface polynomials for the resulting normalized damage are fitted for each of the design parameters.

The response surface polynomial for this normalized damage of the pressure armor which corresponds to parametric variation with respect to the drag coefficient is shown in Figure [B3.7](#) (corresponding to the SN-curve which applies to the  $H_2S$  condition). For this particular parameter fatigue calculations were repeated with the normalized drag coefficient at 95 % and 105 % of the base case value (i.e. 100 %). As observed, the variation of the fatigue damage is almost linear for the interval of the drag coefficient which is considered. A positive increment of 15 % leads to an increase of the fatigue damage of around 6 %.

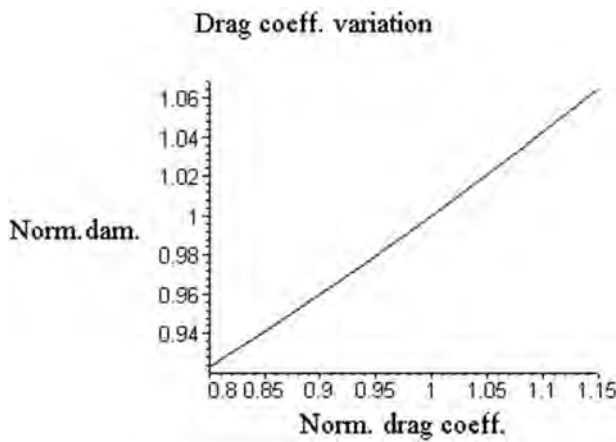


Figure B3.7: Response surface polynomial for (normalized) fatigue damage versus the (normalized) drag coefficient for pressure armor (longitudinal direction). (SN-curve corresponds to  $H_2S$  being present)

The response surface polynomial for the floater surge amplitude is shown in Figure [B3.8](#), and it has a shape which is quite similar to that for the drag coefficient. The increase of the fatigue damage is around 4% for a scaling factor of 1.1 for the surge amplitude.

The relationship between the fatigue damage and the heave amplitude is shown in Figure [B3.9](#). The curve is slightly non-linear for the present case. An increase of the scaling factor of 15% leads to an increase of the fatigue damage of around 1%, which is quite negligible. This variation is hence neglected in the following analysis.

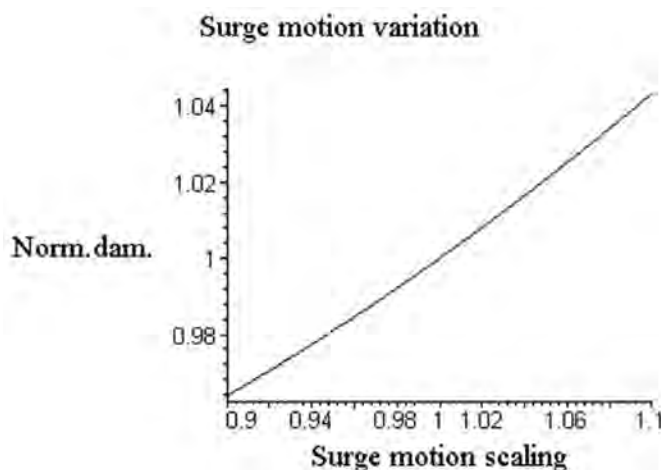


Figure B3.8: Response surface polynomial for the (normalized) fatigue damage versus the scaling factor for the surge motion ( $H_2S$  conditions)

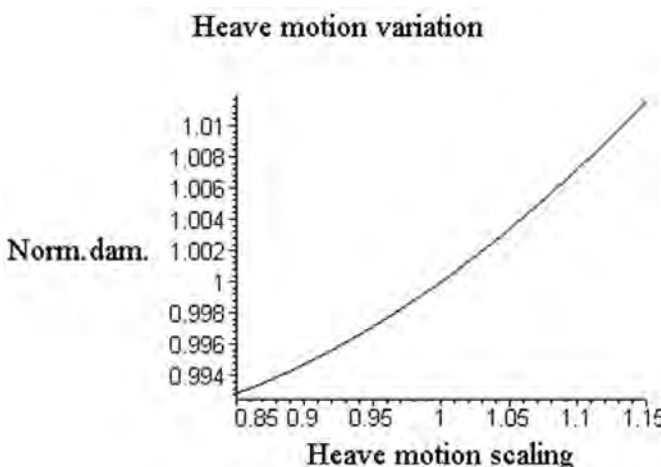


Figure B3.9: Response surface polynomial for the (normalized) fatigue damage versus the scaling factor for heave motion ( $H_2S$  conditions)

The relationship between the fatigue damage and the pitch amplitude is shown in Figure B3.10. Again, the shape is almost linear. A positive increment of 15% leads to an increase of the fatigue damage of the order of 20%.

The fatigue damage versus the static vessel offset is shown in Figure B3.11. As mentioned above, the mean value estimated from the measurements is around 0.5 when normalized with the value that was applied at the design stage (i.e. 45m relative to a given reference position). The fatigue calculations are performed for a number of offset scaling factors which are quite symmetric around this value. It is seen that if a static offset for the floater equal zero is relevant, the fatigue damage would be slightly less than 40 % of the base case value. If the offset is increased to 60m, the fatigue damage would be around 140 % of the base case damage (which corresponds to an offset of 45m)

The response surface polynomial for the friction coefficient is shown in Figure B3.12. This curve is quite linear for the range which is considered. The percentage variation in fatigue damage is roughly of the same order as the percentage variation of the friction coefficient.

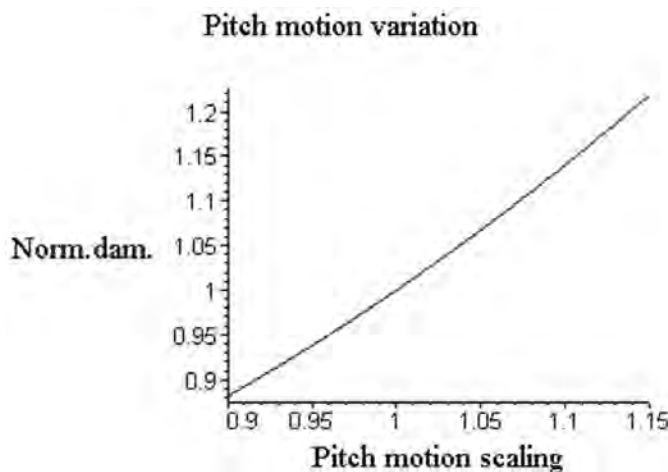


Figure B3.10: Response surface polynomial for the (normalized) fatigue damage versus the scaling factor for pitch motion ( $H_2S$  conditions)

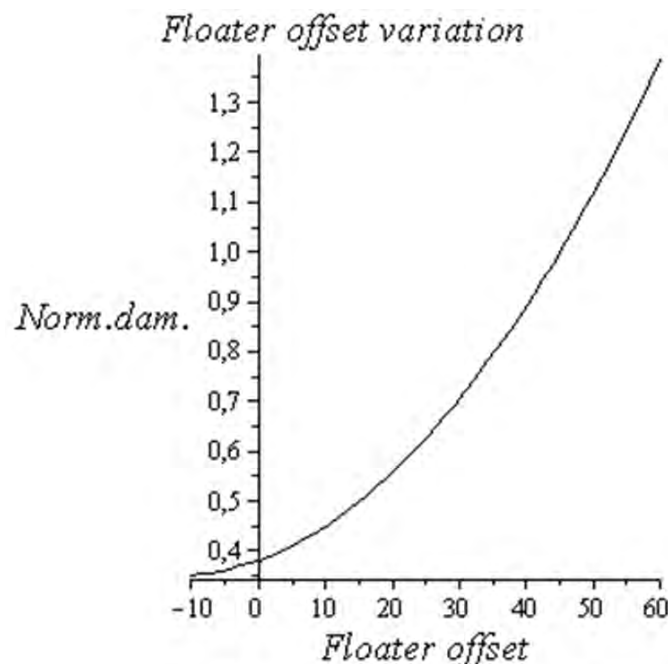


Figure B3.11: Response surface polynomial for the (normalized) fatigue damage versus the static floater offset in meters ( $H_2S$  conditions)

The resulting curve for the internal pressure within the range of interest is given in Figure B3.13. The base case value corresponds to the operation pressure that was assumed at the design stage. The polynomial is represented by a straight line. However, it must be noted that for large upward deviations from the operation pressure a quite nonlinear and rapid increase of the fatigue damage will be observed.

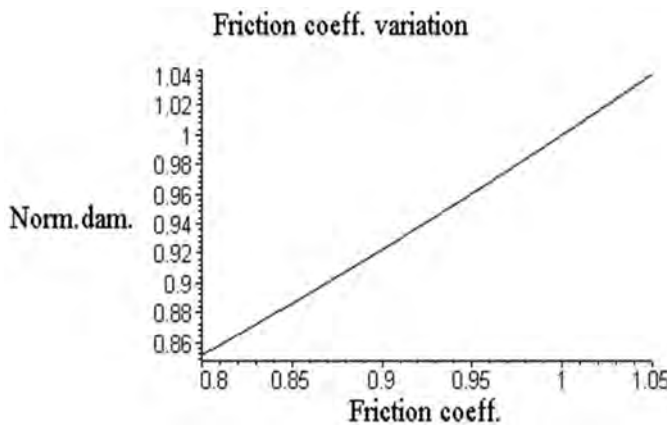


Figure B3.12: Response surface polynomial for the (normalized) fatigue damage versus the (normalized) friction coefficient ( $H_2S$  conditions)

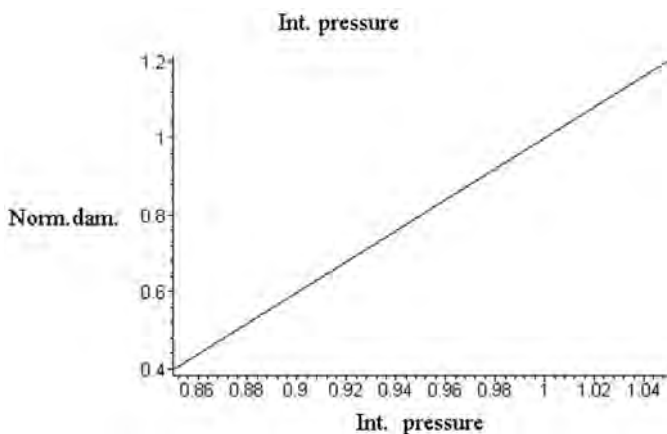


Figure B3.13: Response surface polynomial for the (normalized) fatigue damage versus the (normalized) internal pressure ( $H_2S$  conditions)

### B3.6.2.3 Reliability analysis

As a next step, the response surface polynomials are incorporated as part of the failure function (i.e. limit state function). In this way, the accumulated fatigue damage (i.e. the 'derived load effect') is expressed as a function of the base case damage (referring to either of the two annulus conditions) in addition to the design parameters which are considered as variables. Hence, the failure function can now be formulated on the following form:

$$\begin{aligned} g(\mathbf{X}) &= X_{Fail} - D(T_{op}, X_2, X_3 \dots X_N) \\ &= X_{Fail} - D_{Tref}(X_2, X_3 \dots X_N) \cdot (T_{op}/T_{ref}) \end{aligned} \quad (\text{B3.9})$$

where  $X_1 = X_{Fail}$  is a random variable which represents the Miner-Palmgren sum at failure,  $X_2, X_3, \dots, X_N$  are random variables related to the riser system which correspond to the parameter variations just described. Top is the time in operation for the riser system (i.e. time during which fatigue damage accumulation takes place). Tref is a given reference duration (which here is taken to be 1 year), and  $D_{Tref}(\dots)$  is the estimated fatigue damage for the same reference duration (i.e. 1 year). The last factor in Eq.B3.9 is due to the proportionality of the accumulated fatigue damage with respect to elapsed time in operation.

Subsequently, the variation in fatigue damage as a function of the random variables (i.e. X<sub>2</sub>, X<sub>3</sub>, ..., X<sub>N</sub>) is factored out and represented by a separate function. This is a smooth analytical function which is obtained as the product of the fitted response surfaces for the individual parameters. Each of the 'control points' which define the polynomials of the response surface is obtained by performing a dynamic response analysis by means of the Finite Element Method also including calculation of the fatigue damage. The resulting explicit form of the first factor in the second term in Eq. B3.9 then becomes:

$$D_{Tref}(X_2, \dots, X_N) = D_{Tref,Basecase}(N_{ref} \cdot f(X_2, \dots, X_N)) \quad (\text{B3.10})$$

The subscript 'Basecase' here refers to the value of the damage which is obtained as a result of the base case fatigue design analysis for the given pipe layer and for the given internal fluid condition.

The last factor on the right-hand side in Eq. B3.10 is further normalized such that when all the random variables are equal to their base case values (i.e. design values), the response polynomials all have a value equal to 1.0. Furthermore, normalized random variables are introduced. This is achieved by dividing each variable with its corresponding base case value. The base case values are here taken to be equal to the values applied for design of the riser system. Accordingly, the following set of new variables are introduced:

$$\begin{aligned} Y_1 &= X_1/X_{1,Basecase} \\ Y_2 &= X_2/X_{2,Basecase} \\ &\dots \\ Y_N &= X_N/X_{N,Basecase} \end{aligned} \quad (\text{B3.11})$$

The normalized version of the failure function is then obtained as:

$$g(\mathbf{X}) = Y_1 - D_{Tref,Bscs}(N_{ref}) \cdot f(Y_2, Y_3, \dots, Y_N) \cdot (T_{op}/T_{ref}) \quad (\text{B3.12})$$

where  $N_{ref}$  is the number of stress cycles during the reference time period for the base case analysis.

The cumulative failure probability as a function of time can subsequently be expressed in terms of the failure function (by introducing the time as a variable instead of the fixed duration  $T_{op}$ ):

$$P_f(T) = P(g(\mathbf{X}, T) < 0) = P([Y_1 - D_{Tref,Bscs}(N_{ref}) \cdot f(Y_2, Y_3, \dots, Y_N) \cdot (T/T_{ref})] < 0) \quad (\text{B3.13})$$

This probability can now be computed for a sequence of durations (corresponding to increasing values of the time in operation). Having calculated the cumulative failure probability, the incremental failure probability for an arbitrary 'sub-period' (i.e. mainly one-year increments) can then also be evaluated by taking the difference between the cumulative probability at the end and at the start of this specific 'sub-period'.

The failure function in Equation B3.13 is combined with the probabilistic models in order to compute the reliability measure (i.e. the reliability index, or equivalently: the failure

probability). The applied probabilistic models are summarized in Table B3.2. Note that four of the random variables represent model uncertainties, i.e. global and local analysis; environmental description and Miner sum at failure.

Table B3.2: Probabilistic models relevant for fatigue reliability of flexible risers (N= Gaussian, L = Lognormal)

Variable	Distr	Base Case	Mean value	St.dev.
Drag coefficient	L	1.0	1.0	0.20
Surge ampl., $X_s^*$	L	1.0	1.0	0.05
Pitch ampl., $X_p^*$	L	1.0	1.0	0.05
Static offset	L		see information in text	
Friction coefficient	L	1.0	1.0	0.10
Int. pressure	L	1.0	1.0	0.05
3D load and resp.effects, $X_{3s}^{**}$	N	1.0	1.0	0.05
Global analysis	N	1.0	1.0	0.05
Local analysis	N	1.0	0.9	0.15
Env. Descr.**	L	1.0	1.0	0.05
Miner-Palmgren sum at failure	L	1.0	1.0	0.30
Intercept of SN-curve	L		Mean value of $\log_{10} K$ varies	St.dev. of $\log_{10} K$ varies

\* The surge and pitch transfer function amplitudes are multiplied by the same respective scaling factor for all frequencies.

\*\* The variables representing uncertainty related to analysis method, environmental description and 3D load and response effects are assumed to apply for the *stress range* rather than the fatigue damage. These variables are hence exponentiated to a power equal to the m-exponent of the SN-curve in the reliability calculations.

The floater position is found to have a (non-dimensional) mean value of 0.5 and a standard deviation of 0.125, with a Lognormal model found to be a proper choice. Both of these values are normalized by the mean static offset which was assumed at the design stage, i.e. 45m. The statistical model is based on measurement for a period in operation of 15 years.

The internal pressure is found to have a mean value of 1.0 and a standard deviation of 0.03 based on the same measurement period. Both of these values are normalized by the normal operation pressure which was applied during the design phase. As observed, the standard deviation which is estimated from measurements is smaller than the value which was assumed a priori (i.e. referring to Table B3.2).

The procedure which is applied for calculation of the failure probability is presently based on the so-called FORM approach as explained above. As mentioned, Monte Carlo simulation methods would offer a good alternative (and supplement) to such calculations.

All the random variables are presently assumed to be statistically independent. Pairwise correlation can be included e.g. by application of the so-called Nataf model in a straightforward manner

Transition between different annulus conditions (i.e. a rapid increase of H<sub>2</sub>S concentration in the annulus for the present riser configuration) requires that the calculation scheme is

supplemented by an additional step. This step amounts to representation of the fatigue damage at the time of transition as a random variable. The permissible remaining value of the accumulated fatigue damage (with H<sub>2</sub>S being present) will hence also be a random variable. A further description of this procedure is given in [Leira, 2009].

The failure probability is computed by application of Eq. B3.7

The variation of the failure probability for the time span starting from 15 years and upwards is shown in Figure B3.14. It is found that a failure probability level of 10<sup>-4</sup> is reached after a time in operation of around 32 years. A failure probability level of 10<sup>-3</sup> per year is reached slightly after 41 years in operation.

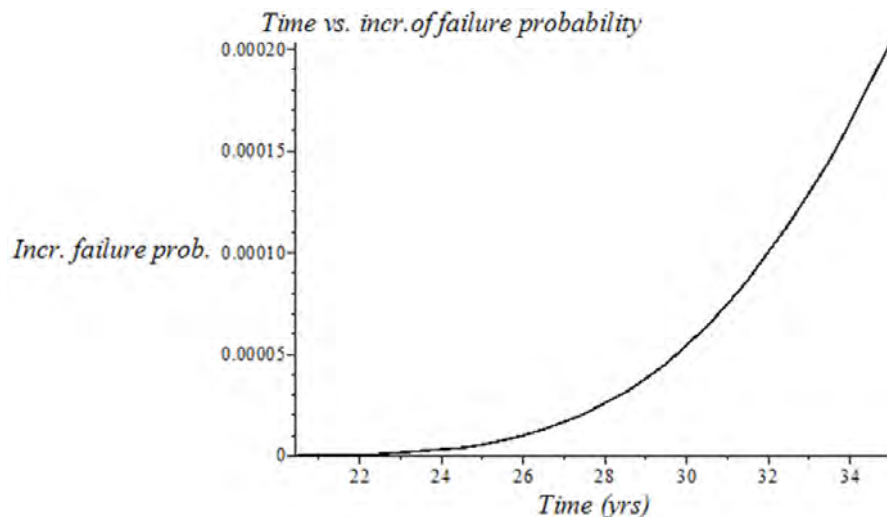


Figure B3.14: Failure probability per year versus time in operation

A summary of the time in operation until the three different probability levels of 10<sup>-5</sup>, 10<sup>-4</sup> and 10<sup>-3</sup> are reached is provided by Table B3.3.

Table B3.3: Summary of time in operation versus failure probability per year.

Time of failure prob. level [yrs]		
10 <sup>-3</sup>	10 <sup>-4</sup>	10 <sup>-5</sup>
41.0	32.5	26.5

The variable with the highest importance factor in the reliability analysis is the Miner sum uncertainty contributes with 32%, and the intercept of the SN-curve contributes with 24%. The variable which represents 3D load and response effects contributes with around 10% and the same applies to the global analysis uncertainty.

Note that interaction between corrosion and fatigue is not considered in the present analysis. If a linear (proportional) model of the corrosion process is applied (i.e. corresponding to a constant annual corrosion rate), a linear variation of the associated 'stress increase factor' is also relevant. In addition, possible stress concentration factors would need to be considered, somewhat depending on the shape of the corrosion defects. Further details related to this topic are given in Chapters B4 and B5 of the present Handbook.

## B3.7 Reliability Analysis for the Ultimate Limit State

### B3.7.1 General

Reliability analysis in relation to the extreme response level exceeding a specific capacity threshold can be based on the failure function from Equation B3.6 above, i.e.:

$$g(R, S) = R - S(t) \quad (\text{B3.14})$$

where the capacity threshold presently is represented by a time-invariant random variable. The time-varying load term  $S(t)$  can also be replaced by its extreme value (i.e.  $S_{E,T}$ ) during a specific time interval,  $T$ . For a short-term condition this gives:

$$g(R, S) = R - S_{E,T} \quad (\text{B3.15})$$

where the load effect distribution function is considered in more detail in the present section.

For reliability formulations involving a deteriorating threshold, a sequence of stationary conditions need to be analyzed. A conservative approximation which leads to simplified calculations can be based on application of the statistical resistance parameters which correspond to the end of the time interval under consideration. This implies that the extreme loading is assumed to occur at the time when the capacity reaches its lowest value.

Based on the distribution function for local maxima, the corresponding extreme value distribution for a given duration  $T$  can be obtained. The number of local maxima for a narrow-band process during this period can be estimated based on the zero-crossing frequency as:

$$N = \nu_x^+(0) \cdot T = \frac{\dot{\sigma} \cdot T}{2\pi\sigma_x} \quad (\text{B3.16})$$

Here,  $\sigma_x$  is the standard deviation of the response process,  $\dot{\sigma}_x$  is the standard deviation of the response process;  $\nu_x^+(0)$  is the zero-crossing frequency

A plot of the resulting density function of the Gumbel type (see [Gumbel, 1958]) is shown in Figure B3.15 below for increasing values of the exponent  $N$  (in the range from 50 to 5000). The ordinate axis in the figure corresponds to the normalized extreme value, i.e.  $z = \frac{x_{E,T}}{\sigma_x}$ . The figure clearly shows the increase of the mean value for increasing values of the exponent  $N$ .

The extreme value density function in general needs to be evaluated by consideration of all the sea-states corresponding to a specific scatter diagram. Basically, two different approaches can be applied. The most correct approach will be to express the parameters of the extreme-value distribution in terms of the sea-states characteristics (typically in terms of significant wave height,  $H_s$ , and peak period,  $T_p$ ). Alternatively, a long-term distribution of the relevant response quantity can be established by well-established procedures. The corresponding extreme-value distribution is subsequently obtained by exponentiation of the long-term distribution. The latter approach implies that the sea-state variables are taken care of outside the reliability analysis itself.

Extreme pdf vs. z and N

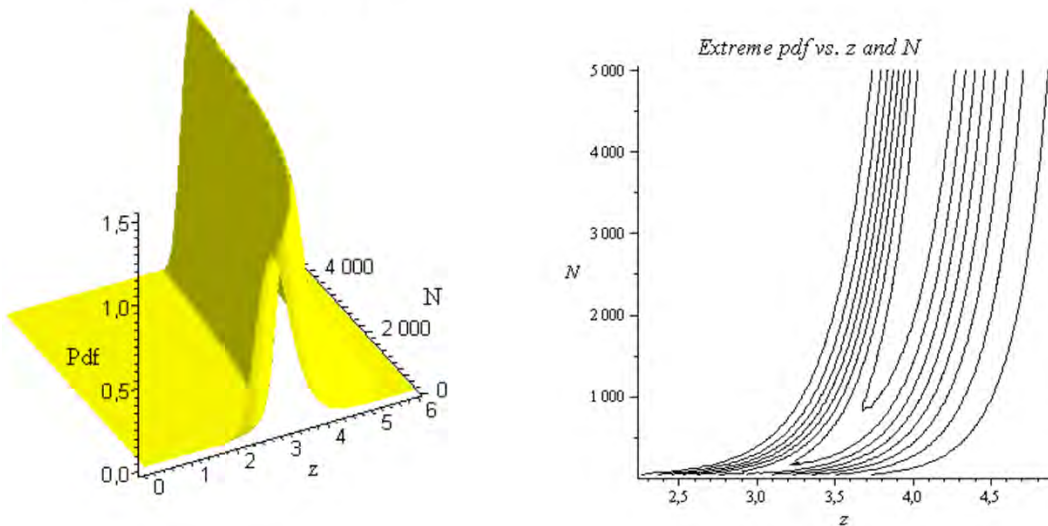


Figure B3.15: Extreme value density function for increasing  $N$  (i.e. number of local maxima for the parent Gaussian process)

### B3.7.2 A Simplified Example of Application to a Flexible Riser Configuration

To exemplify calculation of failure probability in relation to the ultimate limit state, we consider potential failure due excessive curvature of a riser cross-section. The following characteristics are given:

- The permissible minimum curvature is assumed to be reduced due to degradation of the pipe materials with time. The permissible bending radius is taken to be 75% of the minimum bending radius capacity (MBR) of the pipe, i.e.  $0.75 \cdot \text{MBR}$ .
- The static bending radius is represented as a deterministic value which is 50% of the minimum bending radius, i.e.  $0.5 \cdot \text{MBR}$ .
- The annual extreme dynamic curvature is assumed to be represented by a Gumbel distribution. The 90% fractile of this distribution is applied as a deterministic value in a preliminary analysis (the fractile is evaluated when all the design parameters are at their base case value). This value is equal to 14.5% of the MBR, i.e.  $0.145 \cdot \text{MBR}$  and corresponds to one particular sea-state which is found to be the most critical one for bending of the relevant cross-section.

The statistical variability of the drag coefficient is taken into account for the dynamic response component. The expression relating the normalized value of the 90% fractile of the extreme curvature distribution (i.e. normalized by the base case value), to the normalized drag coefficient is given by the following second-order polynomial expression:  $y = (1.35 \cdot x^2 - 2.04 \cdot x + 1.70)$ , where  $y$  is the normalized extreme curvature and  $x$  is the normalized drag coefficient. The statistical model for the drag coefficient is the same as that applied in the previous example, i.e. a Lognormal variable with a mean value of 1.0 and a coefficient of variation equal to 0.20. In addition, a variable which takes into account the analysis model uncertainty is included. This variable corresponds to the ratio between the computed critical load effect divided by the true one. It is represented by a Gaussian distribution with a mean value of 1.0 and a coefficient of variation equal to 0.15.

At a very early stage of the analysis, the following simplistic version of the failure function is accordingly applied:

$$g(X_1, X_2) = MBR \cdot [0.75 - 0.15 \cdot X_2 \cdot \{1/(1.35 \cdot (X_1)^2 - 2.04 \cdot X_1 + 1.70)\} - 0.50] \quad (\text{B3.17})$$

where  $X_1$  corresponds to the normalized drag coefficient and  $X_2$  represent the model uncertainty factor. It is noted that values of  $X_2$  which are smaller than 1.0 is more critical than values larger than 1.0.

The incremental probability of failure per year in operation is mainly constant (as long as this failure probability is low). The probability computed based on the failure function in Equation B3.17 is found to be  $4.8 \cdot 10^{-5}$ , which is acceptable if safety class normal is set as the target. For safety class high, this value is not quite satisfactory.

Regarding the relative ranking of the random variables, the variability of the drag coefficient contributes by around 84% to the failure probability, while the model uncertainty related to the load effect analysis contributes by the remaining 16%.

In the present simplified example, a single extreme sea state was applied as a basis for the reliability assessment. In order to identify such a critical sea state, a more comprehensive analysis involving a number of different sea states generally needs to be performed. The three main steps of the reliability analysis can then be summarized as:

1. Identify potentially important  $(H_s, T_p)$  combinations for the response quantities entering the specific failure function. This can be based on previous experience and/or simplified response analysis methods.
2. Fit initial relations of response quantities and their statistical parameters as functions of the basic parameters. Most emphasis is put on relatively accurate fitting for the identified  $(H_s, T_p)$  ranges.
3. Perform a reliability analysis with corresponding localization of design points for the various g-functions. If the design values of  $(H_s, T_p)$  deviate too much from the assumptions in step (1), a second iteration involving steps (2) and (3) must be performed. If it is considered necessary, refined fitting of the functional relations can also be performed in a more restricted neighborhood around the design point.

The attractiveness of this procedure lies in the possibility of monitoring the various steps of the calculation process. A fully automated reliability analysis with response analyses performed blindly, might miss important physical aspects. Furthermore, convergence to local instead of global design points could easily occur. An important aspect of the present scheme is that the response analyses should not miss nonlinear phenomena that may tend to increase the extremes significantly.

## B3.8 Effect of Monitoring/inspection/repair on reliability level

During operation of a specific flexible pipe system, measurements and observations collected as part of monitoring and inspections are typically obtained. In some cases repair (e.g. by application of riser clamps) is also performed. This implies that additional information (as compared to that available at the design stage) becomes available. Monitoring methods and integrity assessment of flexible risers are e.g. summarized in the reports from the Sureflex

JIP [MCS Kenny Guidance Note, 2010] and [MCS Kenny State of the Art, 2010], see also relevant Chapter C1 of the present handbook for further information.

When considering such additional information, it is important to make an assessment of the associated accuracy. This applies e.g. to the noise level inherent in measurement records, as well as probability of detection for various types of defects. In relation to repair actions, the updated capacity of the pipe after the repair needs to be estimated.

Some of the additional information is of the negative type. An example is increasingly corrosive environment which was not foreseen during design. Other types of information are of the positive type. Examples are smaller observed floater offset than assumed during initial design or lower internal pressure levels than applied during the design phase. A screening of the most critical riser configurations based on a gross assessment of operation parameters and experience is performed e.g. by [Lemos et al., 2008].

Based on measurements obtained during a certain period in operation, updated statistical models can be established. As examples, we may designate the initial probability density of the floater offset by and the initial probability density for the internal pressure by  $f_{\theta_{FO}}(\theta_{FO})$ . The corresponding updated probability densities can then be obtained by application of Bayes formula. These updated density functions are expressed by:

$$f_{\theta_{FO}|X_{FO}}(\theta_{FO}|x_{FO}) = C_{FO} \cdot f_{x_{FO,obs}|\theta_{FO}}(x_{FO,obs}|\theta_{FO}) \cdot f_{\theta_{FO}}(\theta_{FO}) \quad (\text{B3.18})$$

and similarly for the internal pressure:

$$f_{\theta_{IP}|X_{IP}}(\theta_{IP}|x_{IP}) = C_{IP} \cdot f_{x_{IP,obs}|\theta_{IP}}(x_{IP,obs}|\theta_{IP}) \cdot f_{\theta_{IP}}(\theta_{IP}) \quad (\text{B3.19})$$

where  $f_{x_{FO,obs}|\theta_{FO}}(x_{FO,obs}|\theta_{FO})$  is the likelihood function for the measured offset (or some derived characteristics), conditional on the statistical parameters which are contained in the vector  $\theta_{FO}$ . Similarly,  $f_{x_{IP,obs}|\theta_{IP}}(x_{IP,obs}|\theta_{IP})$  is the likelihood function for the measured pressure record. The constants CFO and CIP are the respective normalization coefficients for the resulting density functions.

As an example of application of the Bayesian updating procedure, the probability distribution of the mean value of the riser operation pressure is considered. The initial (i.e. prior) probability density function for the mean pressure is assumed to be Gaussian with a mean value of 100 bar and a standard deviation of 20 bar (i.e. a variance of 400 bar<sup>2</sup>). After a certain time in operation, a number of 1000 observations (i.e. 1000 pressure measurements) have been accumulated. These observations are found to be well fitted by a Gaussian distribution with a mean value of 70 bar and a standard deviation of 5 bar (i.e. variance of 25 bar<sup>2</sup>).

By applying the relevant expressions for updating the mean value and standard deviation of the probability density function for the mean value of the (mean) operation pressure, the new mean value becomes 72.7 bar and the new standard deviation is 2.6 bar. This implies that the scatter associated with updated distribution is significantly less than for the initial one. Here it has been assumed that the initial distribution was based on 100 observations, which implies that the relative weighting of the initial information and the measurements is 100 to 1000. From Figure B3.16, it seen that the updated density function accordingly has a very peaked shape.

### *Updating of mean value Pdf*

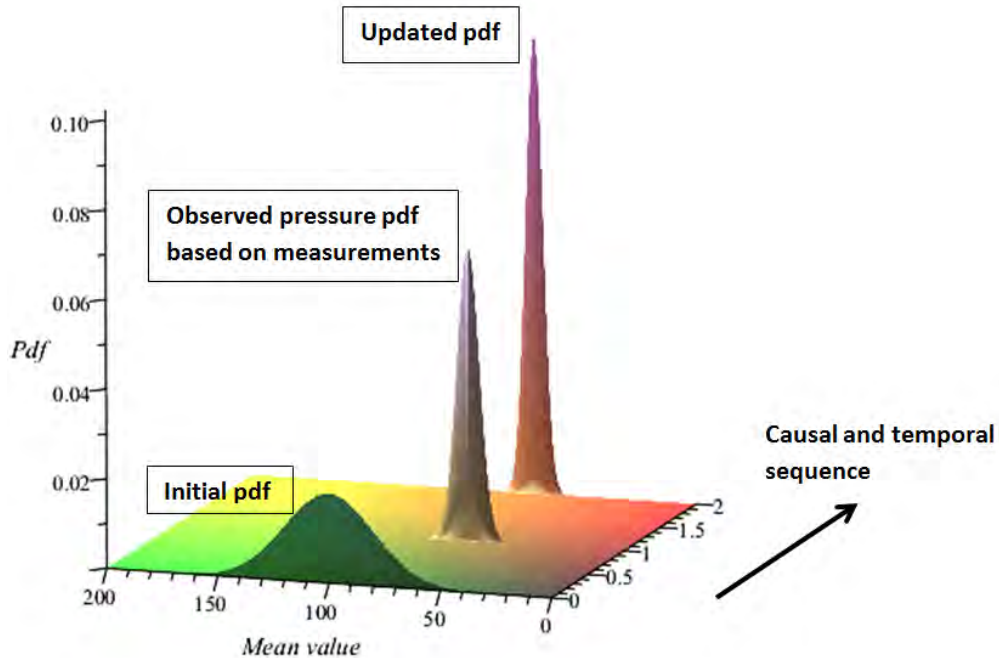


Figure B3.16: Example of Bayes updating related to the probability density function which characterizes the mean value of the internal riser pressure.

It is also possible to update the probabilistic models in a continuous way based on processing of the measured data at regular time intervals (e.g. one-year intervals). This will imply that significant weight is put on the measurements if the density functions are updated at each interval. Based on the updated probabilistic models, the estimated reliability (or equivalently: failure probability per year) can then also be updated by application of the new probabilistic models.

## B3.9 Concluding remarks

In the present chapter, reliability calculations corresponding to well-defined mechanical limit states for flexible pipes were outlined. Example calculations were performed for the fatigue limit state (FLS) and the ultimate limit state (ULS).

For the fatigue limit state, the time-dependent fatigue reliability of the tensile and pressure armours for a specific riser configuration was focused upon. A procedure for incorporation of relevant full-scale measurements related e.g. to surface floater motion, internal pressure and other internal flow parameters is also described. Furthermore, the method which is applied for calculation of failure probabilities is also described in some detail.

The reliability analysis procedure is applied for assessment of a specific riser configuration for the purpose of illustration. As a basis for the assessment, measurements of internal riser pressure and surface floater offset are utilized and three different target safety levels are

considered.

The obtained results are based on some key features (which are reflected by the measurements) which imply that application of standard fatigue design methods will give conservative results. These features are mainly:

- Results from dedicated fatigue testing are available
- The measurement of operation pressure implies that the initially assumed scatter associated with the pressure basically is removed. Furthermore, the recorded pressure is slightly lower than the value applied at the design stage.
- The (mean) static offset position obtained from the measurements is around half the value which was applied at the design stage.

For riser configurations where these features are not present, the results will change accordingly. Clearly, it is also assumed that there are no defects (e.g. due to manufacturing, transportation or accidental damage) in the relevant pipe layers.

The second example was a simplified reliability analysis of extreme curvature, which represents the ultimate limit state. The probability of exceeding a reduced bending capacity was estimated for the future time in operation of the riser system.

Multiple applications of the present reliability analysis procedure can be envisaged. One example is calibration of more refined design formats than those presently being applied. This can e.g. be achieved by introduction of partial safety factors instead of a single usage factor. Initial work in this direction can be found in [[Løtveit and Often, 1990](#)], [[Leira and Mathiesen, 1995](#)].

Other applications can be the ability to specify the required quality of the data basis in order to apply the presently codified safety factors. Situations where non-standard values of these factors are demanded in order to achieve a sufficient reliability level can hence also be identified.

## **Chapter B4**

# **Annulus environment and corrosion**

*Author: 4Subsea*

## B4.1 Introduction

The annular space in flexible pipes contains the steel armours that provide the structural support for containment of fluid and gas in the bore and the structural capacity required to carry axial, bending and torsion loads. The integrity of these armours is essential. They are arranged within a confined annular space in a way, which makes it challenging to model corrosion. The annulus conditions vary significantly between pipes in service and also along a given pipe.

Corrosion damage and cracks on armour wires are difficult to detect and characterise in detail by inspection through the outside cover or from inside the bore of the pipe. Locations with the highest stresses and consequences of failure will typically be under bend stiffeners where access for inspection is even more difficult.

Damage to the outer cover with subsequent ingress of seawater or exposure to air is a likely scenario based on field experience. There is no surprise that seawater ingress and exposure to moist air may cause problems in particular in locations where cathodic protection is non-existent or inadequate. However, corrosion concerns related to condensed water in the annulus or seawater ingress from cover damages well below the sea level, in combination with acid gases from the bore, must also be addressed. In-service field experience for flexible pipes is still limited and there may well be corrosion issued that have not yet been experienced.

The industry needs

- Models and procedures to assess the susceptibility and probability for corrosion of armours in flexible pipe annuli for relevant scenarios
- Solutions for monitoring, detection and predictions
- Guidance for how to deal with damage or other incidents.

Testing and monitoring of the conditions in the annulus through the vent ports provide information that may be useful for assessing the probability for corrosion. In principle leakage in the outer cover in topside jumpers and in the upper part of risers can be detected and the flow rates and composition of the vent gas can be determined with suitable equipment and verified procedures. Increased insight and understanding of the annulus environment is continuously developed, and there are still challenges to derive accurate information on the integrity of the armours with respect to corrosion.

The purposes of this chapter of the Handbook are to

- Define the span of possible conditions in flexible pipe annuli.
- Identify to what extent relevant conditions in flexible pipe annuli can cause corrosion
- Review literature to identify knowledge and models that can be used to predict corrosion under identified annulus conditions.
- Develop guidance relating to corrosion caused by damage to the outside cover in terms of:
  - Detection of outside damage
  - Susceptibility for corrosion as function of the location of cover damage
  - Risk assessment and possible mitigation

## B4.2 Annulus environment and conditions

### B4.2.1 Definition of the annulus

The annulus in flexible pipes is defined as the annular space between the pressure sheath and the outside cover as illustrated in Figure B4.1 and Figure B4.2.



Figure B4.1: Picture of flexible pipe to define the annular space. (Base picture, ref. [Muren and Gjendal, 2011])

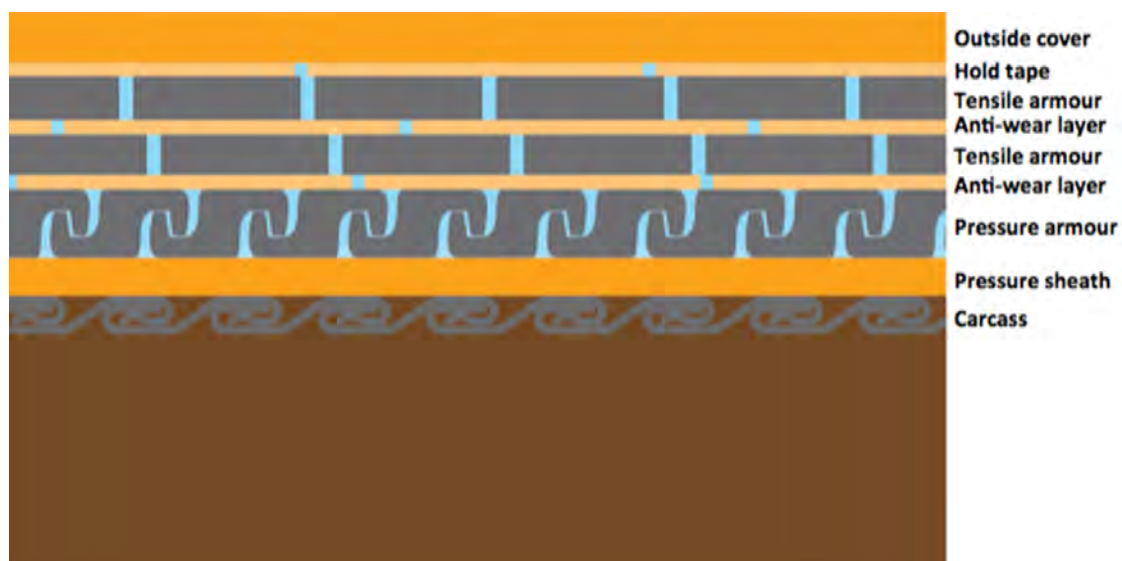


Figure B4.2: Schematic illustration of the layers through the annulus cross section

The pressure and tensile steel armour layers are in many pipe structures separated by anti-wear layers that will influence how fluids and gases distribute and flow in the annulus. The steel armours and the anti-wear layers will normally occupy 85-95% of available space in the annulus. The gaps between armours and gaps between tape layers will be filled with air or preferably an inert gas (FAT) and some lubrication oil after manufacturing.

The cross section profile of tensile armours is rectangular with slightly rounded corners.

Dimensions of the armour wires vary with pipe dimension and design. On average the gap between neighbouring armours in a layer will be between 0.5mm to 1.5mm but the gaps within one layer may vary more than this around the circumference. The total available free space is between 5 and 15% of the layer volume.

The anti-wear layers can be either polymer tape or extruded thermoplastics sheaths.

- The tapes used are typically 50 - 100mm wide helically wound with a separation of around 10mm. The thickness is typically from 0.25mm to 2 mm. The gaps between the tape layers represent narrow channels for fluid and gas flow and ensure that there is flow communication between the free volumes in consecutive armour layers.
- If the anti-wear layer is an extruded polymer sheath the flow connection between armour layers depend on punched holes through the layer and this has on occasions been observed to be insufficient. The consequence of poor flow communication between layers may lead to different environments in the radial direction in the annulus.
- Many pipes for static applications have no tape between armour layers creating a more open pattern for fluid flow between layers.

The armours will from manufacturing normally be covered by a lubrication oil. Depending on the amount and type, excess oil may collect in available free space in low points during storage and possibly redistribute during operation. Oil films on steel surfaces will provide protection against corrosion until the film is broken down or washed or worn away.

Dynamic flexible risers will experience dynamic loads and bending. This will result in armour wires moving relative to anti-wear tape. This relative movement with high contact forces may damage surface films or surface layers in locations with sliding contact. The oil layer may be partly removed and protective oxides or corrosion salt layers on steel surfaces may be destroyed. Bending of flexible pipes may also lead to contact wear between neighbouring hoop armour layers possibly damaging surface salts that may protect against corrosion.

The steel armours are made from carbon steel or low alloy steels with ultimate strength ranging from 700 to 1400 MPa depending on design and application. In cases of sour service ( $H_2S$ ) the material must comply with the NACE standard MR0175 Materials for use in  $H_2S$ -containing environments.

Axial armours are electrically connected in the end fittings typically by welding or loaded metal to metal contact to a steel ring that again is connected to the steel body of the end fitting. This should ensure that the axial armours are in electrical contact with each other and with the steel end fitting bodies of the pipe.

### B4.2.2 Permeation into the annulus

The annulus is sealed from the bore of the pipe by the pressure sheath and from the external environment by the outside cover. When the pipes are new the gas in the free volume is air at close to atmospheric pressure (probably somewhat depleted in oxygen due to oxidation processes).

The pressure sheaths are permeable to small molecules in the bore such as  $H_2O$ ,  $CO_2$ , methane and ethane. The permeation rates depend on different parameters ranging from their fugacity (partial pressure), temperature, type of polymer, sheath thickness etc. Other small molecular species such as  $H_2S$ , formic acid and acetic acid, that are present in bore to

varying degrees, will also permeate through pressure sheaths into the annulus. (also larger hydrocarbon molecules than those mentioned here will permeate but the rates will generally be lower).

Permeation rates are governed by permeability constants that depend on solubility and diffusion properties for a gas in the polymer. The permeability constants vary with temperature and will also depend on the pressures. When polymer lose plasticisers, swell or age in other ways the permeability constant will also change to some degree. The overall permeation rates for a gas will be proportional to its partial pressure (or fugacity) in the bore of the pipe relative to its partial pressure in the annulus. The 'pressurized' contact between the outside of the pressure sheath and the inside of the axial armours will provide partial shielding for the permeating gases to escape and thus reduce the total permeation rates. Many parameters influence the permeation and some of them will change through the field life. It is also important to note that it may take long time to establish steady state for permeation from the bore to the annulus.

There will also be permeation from the annulus through the outside cover and vice versa from the outside into the annulus. This is normally considered to be very low due to low partial pressure differences and lower temperature. However, this may be important for Hydrogen (from CO<sub>2</sub> corrosion processes) and for subsea flow lines vent directly to the sea and may build up annulus pressures exceeding the hydrostatic pressure. This may lead to significant differences between the partial pressures of gases in the annulus and the outside sea environments where the concentrations of these gasses are low. Permeation through the outside covers may thus become non-negligible.

### B4.2.3 Annuli environment evolvement

#### B4.2.3.1 Initial conditions

When a new pipe is taken into use permeation from the bore will start and the gas environment will soon be dominated by permeating gases. The total pressure in the annulus will depend on the vent arrangement.

Risers will normally vent at the top to atmospheric pressure either directly or via valves that may introduce a slight pressure drop. Direct ventilation to atmosphere should be avoided to avoid ingress of air. When there are no fluids blocking the annulus the annulus pressure is expected to be the same along whole pipe. If the vent rates are very high there may be a slight pressure gradient along the pipe annulus. A steady state condition in terms of pressure and gas composition will typically be reached fairly soon.

Subsea flow lines will vent directly to the sea through vent valves. Gas will be released when the annulus pressure exceeds the outside hydrostatic pressure plus the necessary differential release pressure for the vent valve. Thus the total annulus pressure will typically be higher in subsea flexible flow lines than in risers. It will therefore typically take longer for the pressure and gas composition in the annulus of the flow line to reach steady state conditions. High total pressure in the annulus will normally result in higher partial pressures of gases contributing to corrosion, such as CO<sub>2</sub> and H<sub>2</sub>S.

The composition would initially reflect the permeation rates of the different gases from the bore of the pipe. In some cases the partial pressures of the permeating gases build up in the annulus to levels that are non-negligible compared to their partial pressures in the bore. The

permeation rate will go down to reflect the reducing difference between the partial pressure in the bore and in the annulus. This may affect the gas composition in the annulus.

If corrosion reactions take place in the annulus the gas composition may be substantially modified in particular through production of Hydrogen from CO<sub>2</sub> corrosion.

#### **B4.2.3.2 Impacts of changing temperatures on gas in the annulus**

When a confined amount of gas undergoes changes in temperature there will be a corresponding change in pressure and/or volume that can be described in terms of the ideal gas law:

$$P_1 \cdot V_1 / T_1 = P_2 \cdot V_2 / T_2 = nR$$

Where n is the amount of gas and R is the ideal gas constant. This means that if the temperature in the annulus drops the pressure of the gas in the annulus will go down correspondingly under the assumption that the amount of gas remains the same. A drop in temperature of around 30 °C will result in a pressure drop of around 10% if the annulus is sealed off. Gases permeating into the annulus will compensate some of the pressure drop but in many cases the temperature drop during shut down will be faster than the rate of compensation from permeation.

When there is no valves blocking the reverse flow or there are holes in the outside cover, the pressure reduction will be compensated by sucking gas or liquids into the annulus. Thus if the pressure in the annulus is defined by the outside pressure, the gas in the annulus will contract by about 10% for the 30 °C drop in temperature. To compensate for the reduction in volume of gas (or liquid) will be sucked into the annulus. This could be air or water if there is a subsea hole in the outside cover.

The reverse effect will take place when the temperature goes up as for instance at start up of production. The gas will expand and lead to enhanced vent flow.

When assessing the effects of temperature changes on the gas in the annulus it is necessary to take into consideration the rate of permeation into the annulus during cool-down periods.

#### **B4.2.3.3 Condensation of water**

If the temperature on layers / components in the annulus is below the dew point for the water vapour building up in the annulus, water will condense and a liquid water phase may build up. Condensation would typically take place on 'cold' outer layers during normal operation or on any layers during shut down when the temperature goes down. When the temperature goes up again some or all of the condensed water may evaporate depending on conditions. Available permeation models can in principle be used to calculate whether water condensation will take place and how fast a liquid water phase may build up.

Initially the condensed water will most likely exist as dew on the coldest surfaces. If sufficient condensation takes place for water to run down from inclined surfaces it will tend to collect in low points such as sag bends, bottom ends of risers or low points in flexible flow lines.

- When the volumes are limited water accumulating in low points will initially only occupy the lower parts of the circumference. Gas permeating from lower parts of the riser will flow above the water in low points.

- When water builds up to a level where it occupies the full circumference of the pipe-annulus in low sections the flow of gas becomes more complex. In steady state situations the gas pressure will build up to a level where gas can escape (possibly intermittently) through water columns in the direction of the top end fitting where the gas is vented. A possible situation with condensed water building up in the annulus is shown in Figure B4.3 where the pressure in a gas pocket in the hog has built up to compensate for the water column above the sag bend. The release of gas up through the annulus may be intermittent as a burping phenomenon that has been observed for risers in service.

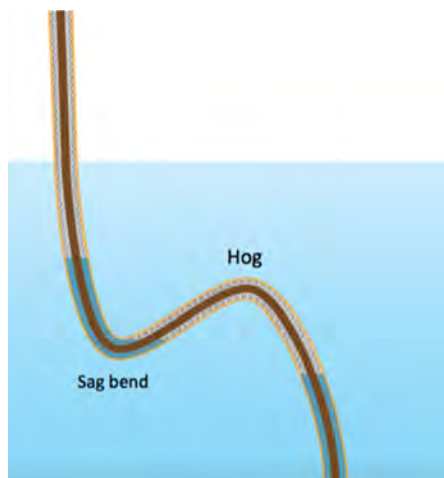


Figure B4.3: Possible case with gas pocket in hog in a annulus with build up of condensed water

Gas pockets will contract when the temperature is reduced as discussed in sub-section B4.2.3.2. The interface between condensed water and the gas will move: water columns in the annulus will shift taking armours out of water in some locations and into water submergence in others.

Condensed water will get into equilibrium with the gas and the different gases will dissolve to concentrations that reflect their partial pressures and their solubility in water at the prevailing temperatures. Water vapour will exist at a concentration in the gas phase that corresponds to the dew point for the temperature at the water/ gas interphase. If corrosion processes take place the respective gases, ions and salts from the corrosion reactions build up in the water. CO<sub>2</sub> corrosion will produce Hydrogen and result in build up of bicarbonates and Iron-carbonate that will precipitate as a solid film on steel surfaces when the concentration gets high enough.

Situations have been experienced where the pressure in the annulus in the hog has exceeded the burst pressure of the outside cover (annulus pressure minus the outside hydrostatic pressure) and resulted in outer cover rupture.

**B4.2.3.1 Water condensing in vent tubes** Water condensation in vent tubes is a potential source of water running back into the annulus. For many riser configurations the top end will see the highest static and dynamic loads on the tensile armours. Thus the consequences from corrosion may be high

#### B4.2.3.4 Seawater ingress

Water may enter the annulus through holes in the outside cover. Holes may result from impacts, contact with sharp objects, wear, rupture caused by excessive pressure in the annulus or cracking of aged outer covers. How water entering from a hole in the outer cover distributes in the annulus will depend on the location of the hole, the configuration of the pipe and how water will flow along the armour layers. Gas pockets will establish in high points (hog in risers or high points on the sea floor sections). The hydrostatic pressure from water columns building up in the annulus will compress gas trapped in pockets. Just after an ingress event a temporary steady distribution of water will be reached followed by a period where permeating gases may increase the pressure in gas pockets and push some water out again. A possible scenario where a gas pocket in the hog is still expanding before a steady state has been reached is shown in Figure B4.4.

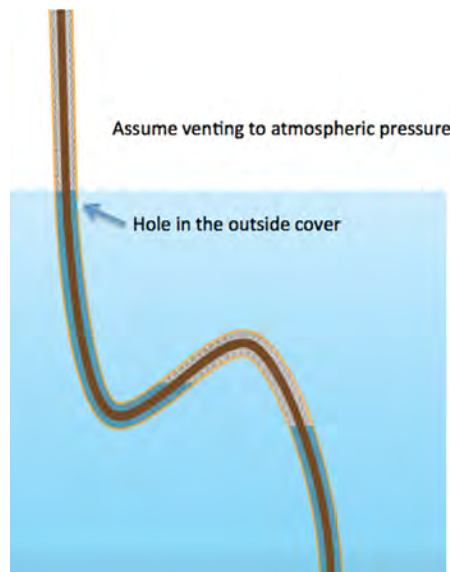


Figure B4.4: Example of distribution of water in annulus with hole in the outside cover, before steady state has been reached.

A steady state will eventually be reached where the total rate of gas permeation into the annulus is equal to the rate of gas escaping through holes and vent ports.

However, temperature changes will disturb the steady state situation due to the effects described in Section B4.2.3.2. A rapid temperature drop may lead to 'fresh' seawater being sucked in through holes in the outer cover to compensate for the volume reduction of gas pockets.

**B4.2.3.4.1 Renewal of seawater** Consider a case with a 50 m long gas pocket in the hog, a hole in the outside cover below the sea level and no gas pockets below the water column on the well side of the hog, as indicated in Figure B4.4. Assume that the temperature in the annulus is  $T_1=40\text{ }^{\circ}\text{C}$  (313 K) and that the amount of gas in the gas pocket stays constant. If the temperature in the annulus drops to  $T_2=10\text{ }^{\circ}\text{C}$  (283 K) there will be a reduction by around 10% in the product  $P*V$ . The pressure will go down as the water level in the section between the sag and the hog will creep up towards the hog. However, the

change in V will be higher than the change in P. The length of the gas pocket would in realistic cases go down by 3-4m. Thus an amount of fresh (aerated) seawater corresponding to the free annulus volume of 3-4 m of pipe will be sucked into the annulus through the hole in the outside cover.

Thus temperature changes in a riser with holes in the outside cover will result in a pumping effect for seawater. It is also possible to foresee pumping effects from ballasting changes and slow drift on FPSOs as well as waves. For fixed installations tidal variations may also be relevant.

A very concerning scenario would be two or more holes in the outside cover. This may lead to fresh seawater entering one hole while annulus water escaping through another. The possibility of circulating water will among several things depend on the relative locations of the holes and temperature distributions. Continuous renewal of fresh seawater may lead to armour wires away from holes being exposed regularly to oxygenated water.

#### B4.2.3.5 Ingress of air

**B4.2.3.5.1 In the splash zone** If a hole in the outside cover is located in the splash zone the armour wires inside the hole will regularly be exposed to moist air and seawater with a high oxygen level. It is assumed that anodes or impressed current systems will protect the directly exposed armours when the location of the hole in the outside cover is submerged. When a hole is located in the splash zone the protection will only be effective when the hole is fully submerged in the sea. When the hole is above the sea level steel armours near the hole will not be protected while being exposed to fresh seawater and air.

**B4.2.3.5.2 Above the sea level** Holes in the outside cover above the sea level will lead to ingress of air that often will be saturated with water. Depending on arrangements rain water and water spray from the sea may also enter the hole. The degree of exposure to air inside the annulus will depend on hole size and geometry and conditions in the annulus. It could range from a small hole where vent gas would be escaping most of the time to cases where air could circulate through the armour wire structure. A concerning scenario is cracking of the outer cover under a bend stiffener due to ageing. This may produce long and complex crack patterns and even partial separation of the outside cover and give constant oxygen exposure.

A key question when air enters the annulus is whether a water phase is present for significant times in combination with CO<sub>2</sub> potentially creating conditions for enhanced corrosion.

In a pipe with one or several holes in the outside cover of a riser located only above the sea level there have been examples where the water level in the annulus is at the same level as the lowest edge of the lowest hole. This requires either sufficient water in the annulus from condensation or ingress of rainwater or sea spray.

**B4.2.3.5.3 From the vent system** One should also be aware that unfortunate designs of vent systems could lead to air being sucked into the annulus when gas in the annulus contract during cool down associated with shut down. This could be a problem when venting goes

directly to air via short tubes. This would possibly combine with water condensing in the vent tubes and running back into the pipe annulus.

It is also worth noting that situations have been observed where water from the annulus of one riser has been pushed into the annuli of other risers through a common vent system.

#### B4.2.4 Conditions affecting corrosion of armour wires

##### B4.2.4.1 Surface protection of armour wires

The tensile armours will from manufacturing be covered with a layer of oil.. From pipes taken out of service it is observed that this coverage vary between individual wires and along wires, and areas without oil are observed, e.g. in contact areas between wires.

An interesting question is how well and how long the oil film on the exposed surfaces may protect against corrosion.

- Is it possible that localised break down of protective oil films may result in small steel areas being directly exposed to the environment?

##### B4.2.4.2 Exposure of armour wires

Gas permeating through the pressure sheath will enter the annulus in the gaps between the pressure armours. During operation the pressure sheath is supported by the inside surface of the pressure armours resulting in high pressure 'sealing' contact so that permeating gases must enter in the gaps between the wires as indicated in Figure B4.5 below (detail from Figure B4.2).

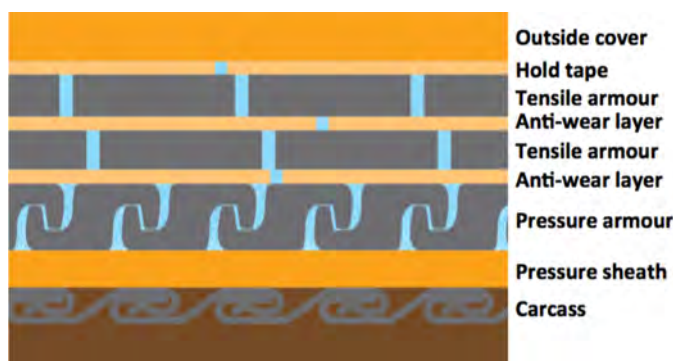


Figure B4.5: Illustration of permeating gases entering the annulus in the gap between the pressure armours.

The pressure armour is thus the first layer exposed to gases permeating from the bore. The gaps between the armours may be filled with water, there may be condensed water films on the armour surfaces or they may be filled with dry gas with water vapour below the dew point.

When the gaps between armours are water filled chemical constituents may go directly into solution in the water or exist within gas bubbles. This may lead to a concentration of some chemical species that is higher in the water between the pressure armours than in the water surrounding the axial armours. Diffusion and convection will tend to even out concentration

gradients but the paths may be narrow and partly obstructed by anti-wear layers. This may lead to significant time constants (or delays) associated with this transport process. If chemical constituents react with steel at rates that are higher than the 'transport' delay it is possible that the pressure armour would be more strongly affected than other armour layers.

The scenario with water films on the armour surfaces may also lead to higher reaction rates on the pressure armour layer. Higher concentrations of harmful chemical species in the gas will lead to correspondingly higher concentrations of these species dissolving in the water films.

**B4.2.4.2.1 Corrosive constituents and their abundance** Corrosion of steel armours in annulus environments depends on the presence of a liquid water phase and is driven by acids, acid formers or oxygen. O<sub>2</sub> may promote corrosion either as pure O<sub>2</sub> corrosion, or by influencing CO<sub>2</sub> corrosion processes preventing formation of effective protective films. It is also observed that O<sub>2</sub> corrosion of armour wires prior to CO<sub>2</sub> corrosion (without O<sub>2</sub>) may result in significantly increased CO<sub>2</sub> corrosion rates.

Typical acids or acid formers that may permeate through the pressure sheath are

- CO<sub>2</sub> from produced gas or dissolved in crude oil. CO<sub>2</sub> dissolves in water according to Henry's law and a small fraction of the dissolved CO<sub>2</sub> reacts with water to form Carbonic acid H<sub>2</sub>CO<sub>3</sub>
- Organic acids such as Formic (CHOOH), Acetic (CH<sub>3</sub>COOH) and Propanoic (CH<sub>3</sub>CH<sub>2</sub>COOH) acids). (Acetic acid is always the most abundant of the organic acids in oil and gas production environments)
- H<sub>2</sub>S is an acid present in some oil reservoirs and develop in some ageing reservoirs due to stimulation by water injection.

The permeation rates for acid gases will, when a steady state has been reached, depend on its permeation coefficients in the polymer used as pressure sheath, the thickness of the polymer layer and it will be proportional to its partial pressure in the bore of the pipe (or difference between the partial pressures in the bore and the annulus)

Possible sources of oxygen can be

- Ingress of seawater with naturally dissolved oxygen into the annulus.
  - Full flooding is a one time event and carry correspondingly limited oxygen
  - Pumping effects in the annulus due to temperature changes or sea level variations relative to the riser. This may lead to repeated ingress of oxygenated seawater with a limited reach into the annulus from the location of a hole.
- Air sucked into the annulus through faulty annulus vent systems or leaky seals between the end-fitting and the outside cover.
- Air ingress when the outside cover is damaged above the sea level.

### B4.2.4.3 Solution of annulus gases in water

The concentration of dissolved acid gases in the water in the annulus will be proportional to their partial pressures and their solubility (Henry's law). It is important to know the partial

pressures of potentially harmful gases in the annulus. In a dry annulus the concentrations of the permeating gases will reflect their partial pressures in the bore and the permeation coefficients. If CO<sub>2</sub> corrosion takes place hydrogen gas will be generated and become a part of the gas composition. If the hydrogen content becomes significant the partial pressures of the other constituents will go correspondingly down in a steady state situation (when the annulus is venting to a fixed pressure). It is also worth noting that if the temperature in an annulus with a fluid water phase is relatively high the water vapour may be a significant fraction of the gas phase if it is venting at a pressure just above one atmosphere.

In partially water filled annuli there may be gas pockets that are pressurized by water 'column'. The pressure in a gas pocket trapped in the hog of a riser with a hole in the outside cover higher up on the riser may end up at a pressure corresponding to the hydrostatic pressure in the sea at the level of the riser sag. This could be well above 10 bar and would lead to higher partial pressures for all constituents. If the pressure builds up 'rapidly' after damage to the outside cover the composition of the gas will stay constant and the partial pressure for each constituent will increase by the same factor. (the fugacity - describing real gases - will not necessarily increase by the exactly the same factors, but close enough). The consequence of the increase in partial pressures will be a corresponding increase in the concentration of the dissolved gas in the water in contact with the gas pocket. This will modify the composition of the water and will have impact on acidity alkalinity. After a gas pocket has formed by flooding of the annulus, a new steady state will form over time. The gas composition in the annulus will adapt to the modified permeation rates reflecting the new conditions. It is also important to be aware that the steady state conditions in the water phase will not only adapt to the changes in the gas phase but also to changes in corrosion related reactions. This will lead to changes in the concentrations of ionic species in the water.

The annuli of flexible **flow lines** vent directly to the sea at the water depth of the vent ports. The steady state pressure in the annulus will reflect the hydrostatic pressure plus the differential relief pressure of the vent valve. The steady state annulus pressure can be very high in some flow lines with correspondingly high partial pressures of the constituents such as acid gases. The total permeation rates in combination with dimensions of the annulus will determine the time for the pressure to reach steady state. This can take long time - months to years - depending on design and conditions.

#### B4.2.4.4 Possible impacts from the polymers

It is known from literature that some polymers may acidify water they are exposed to, especially when the material is fresh. This could be caused by stabilizers (eg plasticisers, antioxidants) leaching out of the polymer and it could also be small polymer molecules (oligomers) with acid end groups found in Polyamides. The amounts will be limited and will probably be most pronounced in early parts of the pipe life. An effect of inhibition is observed in laboratory corrosion experiments for polymers taken from intact pipe cross sections. However, there are variations between pipe designs and vendors where some designs do not exhibit any or negligible inhibiting effect. Experiments suggest this inhibition affects CO<sub>2</sub> corrosion, but not in the presence of O<sub>2</sub>.

### B4.2.5 Some relevant quantities

The large area of exposed armour wire surface compared to the available volume of water has been identified as an important parameter for long-term corrosion in flexible pipe annuli. As an example the ratio of water volume to steel surface area has been calculated for one of the axial armour layers in a typical 10" flexible pipe. The results are as follows:

- Taking all surfaces of all armours in the layer into consideration gives:  $0.016 \text{ ml/cm}^2$
- Taking only the edges of the wires (assume shielding of surfaces in contact with anti-wear tape):  $0.056 \text{ ml/cm}^2$

For the same case estimates have been made of the amount of oxygen that would enter with ingress of fresh sea water compared to the steel surface. Assuming that only the edges of the armour wires are exposed there will be  $0.4 \mu\text{g}/\text{cm}^2$  (oxygen / surface area of armour wire edges).

In connection with transport of permeating gases from the pressure sheath to the axial armour layers in a pipe with hoop strain armour the following example may be useful to understand the rates. We consider a 7.5" ID pipe and calculate a permeation rate of 0.15 l/day/m at STP for an internal pressure of 150 bar. Assume that gas escape from the polymer sheath only in the gaps between the pressure armours. The length of the gap can be calculated for 1m of pipe. Based on gap-to-gap separation of 10mm the length of the spiraling gap is 68m in a 1m length of pipe. For every 1 cm length of gap there will be  $6 \cdot 10^{-10} \text{ mol/min/cm}$  of methane escaping from the pressure sheath. If all the gas over one cm length of the gap went into forming a bubble in water in the gap it would take around 9 minutes to generate a 1 mm diameter spherical bubble if the pressure is close to atmospheric and correspondingly longer at higher pressures. Typically the concentration of acid gases will only be a fraction of the gas in a bubble forming on the annulus side of the pressure sheath.

### B4.2.6 Summary of Scenarios

The scenarios for how armour wires in flexible pipes can be exposed inside the annuli are found in Table B4.1 :

Table B4.1: Summary of exposure scenarios for armours wires in the annulus of flexible pipes

<b>Exposure scenarios for armour wires in the annulus</b>	<b>Comments / issues to be considered</b>
Dry gas no condensation	Low water contents in permeating gases
Intermittent wetting of surfaces	Typically condensation will take place during shut down. Condensed water forming on a dry surface will be non-buffered unless salts on the surfaces dissolve immediately
Submerged in water phase (Condensed water or sea water)	Water phase will be stagnant and most probably reach a steady state condition defined by constituents and chemical reactions.
Taken in and out of the water phase due to contracting and expanding gas pockets	Surfaces may dry out in periods between re-submergence in 'stagnant' water phase.
Periodically exposed to fresh seawater in the vicinity of a hole in the outside cover	The concern is that pumping effects from expanding / contracting gas pockets or from changes in sea level relative to the riser may expose armours shielded from cathodic protection to sufficient oxygen to contribute to harmful corrosion

In the vicinity of a hole exposed to splash zone conditions	This scenario is of significant concerns because of fresh seawater and air and periods without any cathodic protection.
In the vicinity of a hole located above the sea level - exposed to air	Ingress and renewal of air in locations where the armours are in contact with water will affect the corrosion conditions
In the annulus just below the entry to the vent tubes condensing water may run back to the annulus	Newly condensed water will not be buffered by salts and may become more corrosive than stagnant water in other locations in the annulus
Hoop strain wires in contact with the pressure sheath	Hoop strain wires will in several pipe designs create and represent a complex path for gases permeating out of the pressure sheath to reach other armour layers. For chemicals species with a relatively high reaction rate may lead to preferential reaction on the surfaces of the hoop strain layer

The concentration of harmful gases dissolving in condensed water or from water ingress will be proportional to their partial pressures in the gas phase in the annulus and the higher the total pressure the higher the partial pressures will be.

Thus the total pressure in the annulus gas phase is important and we must consider the following scenarios:

- Annulus vent in flexible risers normally vent to atmospheric pressure and will operate a little above 1 bar
- In risers with partially water filled annuli there may be gas pockets compressed by water columns in the annulus. Variations will be large but one can foresee situations with several tens of bars in gas pockets
- The annuli in flow lines vent to the sea at the depth of the vent ports. The hydrostatic pressure in the sea plus the differential release pressure of the release valves will define the release pressure. Thus the annulus pressure depends on the depth of the flow lines.

The typical availability of corrosive constituents can be present in flexible pipe annuli in the following ranges:

CO<sub>2</sub>: from a fraction of 1 bar up to few bar in the annulus

H<sub>2</sub>S: from negligible to several 10s of mBar (and even higher in extreme cases)

Acetic acid: traces have been found in annuli but permeation models do not cover acetic acid

O<sub>2</sub>: well aerated sea water contains around 8 ppm by weight of dissolved oxygen. This goes somewhat down with water depth.

For acid gases it will be their partial pressures in the bore, properties of the pressure sheath and the conditions in the annulus that will define their partial pressures in the annulus.

Assessment of corrosion must take into consideration that the armour wires will be covered by a oil film from manufacturing. As long as the film is intact it will provide significant protection against corrosion. Processes and mechanisms to break down or remove the oil film may be important for understanding and modeling corrosion on armour wires.

Dynamic flexible risers will experience dynamic loads and bending. This will result in armour wires moving relative to anti-wear tape. This relative movement with high contact forces

may damage surface films or surface layers in locations with sliding contact. The oil layer may be partly removed and protective oxides or corrosion salt layers may be destroyed. Bending of flexible pipes may also lead to contact wear between neighbouring hoop armour layers possibly destroying surface layers that may protect against corrosion.

## B4.3 Corrosion issues in flexible pipe annuli

### B4.3.1 Potential Consequences of Corrosion

There are in principle three concerns with corrosion of armour wires in the annulus:

- Loss of metallic cross section leading to reduced load capacity that eventually could lead to rupture and loss of containment.
- Reduced fatigue resistance caused by a combination of increased stress levels due to reduced metallic cross section and corrosion generated surface irregularities or notches that generate local stress concentrations which will be sites for crack initiation
  - General corrosion will in itself lead to increased surface irregularity
  - Surface conditions and local variations in chemistry may lead to the generation of pitting corrosion. These will represent sites with stress concentration and corresponding reduction in service lives
  - Corrosion mechanisms that generate crack like defects such as sulfide stress corrosion cracking and hydrogen induced cracking that can result from H<sub>2</sub>S in materials that are not suitable for such service.
- Impacts from the corrosion process on the fatigue resistance - modification of the SN curve for long-term fatigue.

An essential question is the threshold of shapes and sizes of defects that will lead to reduced fatigue resistance and the sensitivity to increasing defect sizes.

Failure of load carrying armour wires can lead to full pipe ruptures with the potential of significant release of hydrocarbons.

In a corrosive environment the fatigue resistance of relevant steels will go down since the corrosion processes influence both the crack initiation and the growth process. These effects are addressed in Chapter Section D1 (Sections D3 - D4).

### B4.3.2 The role of the steel

The steels used for axial armours and pressure armours in flexible pipes are either carbon steels or low alloy steels. Typical compositions are shown in Table B4.2.

Table B4.2: Typical compositions of steels used for axial armours and pressure armours in flexible pipes, [Dupoiron and Taravel-Condat, 2003], [Rubin and Gudme, 2006]

	<b>C</b>	<b>Mn</b>	<b>Si</b>	<b>S</b>	<b>P</b>	<b>Cr</b>	<b>Mo</b>	<b>Al</b>
Low Alloy 4130 (Technip)	0.33	0.73	0.28	0.003	0.009	1.03	0.18	–
C35 grade 2 (Technip)	0.36	0.75	0.2	0.008	0.007	0.05	–	–
Sour-800 (NKT)	0.6	0.70	0.25	0.003	0.01	–	–	0.04

The microstructure of the steel is the key to the required properties. This is achieved through controlled heat treatment processes. The manufacturers may have developed these processes for the steels they use. A key challenge for the manufacturers is to select or develop and qualify steels that have adequately high strength for sour service applications.

In terms of corrosion it is worth asking whether there will be any inherent differences in the corrosion resistance between types of armour wires due to differences in the steels. It is known that the formation of protective films on steel surfaces as part of the corrosion process is one of the most important contributors to limit the corrosion rate for relevant corrosion processes. This is discussed in detail for CO<sub>2</sub> in [Dugstad, 2006]. It is reported in the literature [Schmitt and Horstemeier, 2006] that the strength and quality of iron-carbonate films forming during CO<sub>2</sub> corrosion will be influenced by the microstructure of the steel. Thus the 'inherent' corrosion rate may vary between steels with similar mechanical properties. There is no open information available from the manufacturers to determine whether differences in corrosion resistance exist between the steels used in armour wires. The way to find out would be to run comparative corrosion tests on relevant samples.

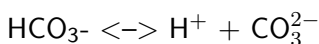
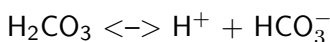
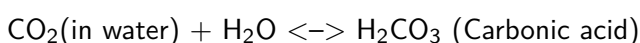
It is also to be expected that the condition of steel surfaces in terms of oxides and other deposits after manufacturing also affect the susceptibility to corrosion. Again this can only be determined through comparative testing.

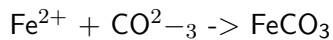
### B4.3.3 Corrosion mechanisms

#### B4.3.3.1 Pure CO<sub>2</sub> corrosion

**B4.3.3.1.1 The CO<sub>2</sub> corrosion reactions** A key focus for corrosion of armour wires in flexible pipes has been CO<sub>2</sub> whether the water phase is from condensation or seawater ingress. The oxygen contained in a single flushing with oxygenated seawater will produce negligible corrosion unless the oxygen is replenished. When the oxygen has been consumed it will primarily be impacts from the acid gases permeating from the bore of the pipe that will be of concern.

The reactions for CO<sub>2</sub> corrosion can be written as:





The corrosion rate is strongly dependent of the pH of the electrolyte (here referring to condensed water or seawater with dissolved CO<sub>2</sub>). It is important to note that the corrosion reaction leads to formation of hydrogen gas. Hydrogen may permeate out through the outer sheath, and the remaining hydrogen in the vent gas could represent a signature within the vent gas composition.

The CO<sub>2</sub> corrosion process will lead to formation of FeCO<sub>3</sub> which will precipitate when the concentration of the involved ions reach a limiting concentration. Protective films of FeCO<sub>3</sub> will develop on steel surfaces. These films will contribute to keeping the corrosion rate low.

**B4.3.3.1.2 Advantage of the annulus confinement** There are concerns that CO<sub>2</sub> should lead to longer term corrosion issues for steel armours in the annulus of flexible pipes even in pipes with intact outer covers. The condition in the annulus of a flexible pipe is, however, characterized by the following features that we have discussed in previous sections:

- There is a lot of steel surface compared to the space available for water. The water volume to steel surface ratio V/S is in the order of 0.03 ml/cm<sup>2</sup>
- The annulus space is confined leading to non or limited change out of water
- The gas phase is continuously renewed by permeating gases

This has been noticed by several research groups looking at potential corrosion issues in the annulus of flexible pipes [Clements, 2003] [Clements, 2008], [Désamais and Taravel-Condat, 2006], [Désamais et al., 2007], [Désamais and Taravel-Condat, 2009], [Duporion and Taravel-Condat, 2003], [Ethridge and Cayard, 1997], [Félix-Henry, 2007], [Joel, 2009], [Klust et al., 2011], [Remita et al., 2007], [Remita et al., 2008a], [Remita et al., 2008b], [Ropital et al., 2000], [Rubin and Gudme, 2006], [Santos et al., 2011], [Taravel-Condat and Désamais, 2006b], [Taravel-Condat and Désamais, 2006a], [Underwood, 2002].

A paper by [Ropital et al., 2000] was one of the first papers published on this matter and was based on work by Technip. They reported corrosion tests with S/V ranging from 100 to 0.25 ml/cm<sup>2</sup> in well controlled cells.

Tests were carried out for periods of 500 to 3000 hours at 20°C under one atmosphere of 100% CO<sub>2</sub>. Under these conditions the NORSOX CO<sub>2</sub> prediction model gives a yearly corrosion rate of 3.7 mm/year. The NORSOX model does not take account of confinement and the high steel surface to water volume ratio. The results obtained by [Ropital et al., 2000] are shown in Figure B4.6.

The average corrosion rate with VS = 0.25 was 0.005 mm/year after 813 hours. Monitoring during the testing showed that the pH and the dissolved iron content increase to much higher levels than predicted by corrosion models (pH 5.2 -> 6.2, iron content 100 ppm -> 600ppm). The high iron content is referred to as super-saturation. Thin protective layers of iron carbonate FeCO<sub>3</sub> (Siderite) was found on the steel surfaces in tests with low S/V ratio.

The authors also reported results from a similar test at 80°C with V/S=0.17. Similar results were obtained with much lower corrosion rates than predicted by NORSOX and higher pH and iron content. The corrosion rate was about twice what was observed at 20°C (since the tests were carried out at atmospheric pressure the partial pressure of CO<sub>2</sub> was 0.53 bar due to the higher water vapour pressure at 80°C)

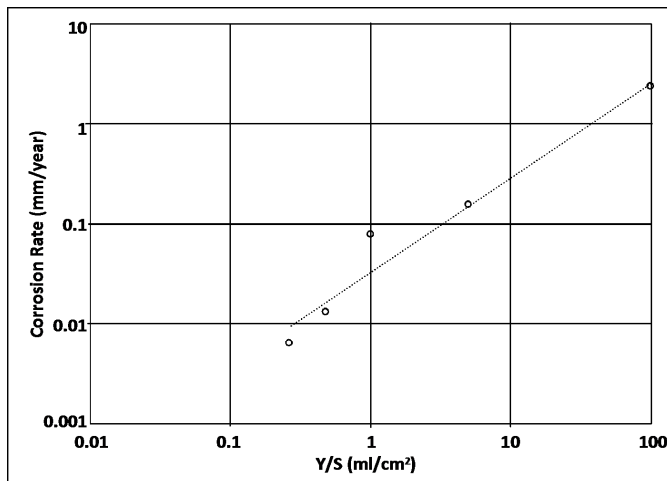


Figure B4.6: Corrosion rate as function of the ratio of water volume to steel surface area.  
Plot produced from paper by [Ropital et al., 2000]

Technip has continued the work reported in [Ropital et al., 2000] including tests with small amounts of H<sub>2</sub>S. Results have been published in a number of partly overlapping papers. Both Wellstream (GE Oil and Gas) and NKT (now NOV) have performed similar testing and assessment and reported results that to a large extent support the results and assessment from Technip. [Clements, 2008] in the paper from 2008 presented a summary of published results together with the latest (at the time) testing results from Wellstream. On a log-log plot of yearly corrosion rate versus V/S he fitted a non-linear curve to these points and extrapolated this beyond V/S=0.03 ml/cm<sup>2</sup> which is a typical value for flexible pipe annuli. The measured data point with the lowest V/S was at a value of around 0.2 ml/cm<sup>2</sup>. At V/S=0.03 ml/cm<sup>2</sup> the fitted curve would predict a corrosion rate of 0.00015 mm/year. The number of data points used in the plot is limited and the extrapolation carries significant uncertainty but it suggests that the in water filled, anaerobic and confined annuli the corrosion rates will be low.

These conditions are not taken account of in corrosion models like the NORSOX CO<sub>2</sub> corrosion model.

**B4.3.3.1.3 Potential CO<sub>2</sub> corrosion issues** Other acids permeating into the annulus or leaching from polymeric layers will disturb (reduce) the high pH conditions and may create a somewhat higher corrosion rate than with CO<sub>2</sub> only. The availability of other acids from permeation will govern this additional corrosion effect. Reported investigations on CO<sub>2</sub> corrosion in flexible pipe annulus have to limited degrees addressed this issue.

In steel pipelines one of the concerns with CO<sub>2</sub> corrosion is top of line above a gas phase where condensing water will run down along the pipe wall. The running water will take with it the ions providing the buffering capacity that will be generated by the corrosion process. Freshly condensed water will be un-buffered and start with a high corrosion rate. When this process keeps going the corrosion rate can be much higher than in a stagnant water environment with small V/S ratio. It is difficult to predict if similar processes can take place on steel armours in flexible pipe annuli. It could in principle go on in gas pockets such as in the hog if the water vapour pressure is high enough. Further investigation through modeling and possibly testing would be necessary to identify whether such situations may exist.

CO<sub>2</sub> corrosion as discussed above will not generally lead to pitting on a homogeneous steel surface. Published test results do not report any significant pitting effects. However, on surfaces, which are partially protected by oil or grease or where the surface layer may be damaged due to relative movement of contacting surfaces, the corrosion processes may take place on limited areas where the surface protection is destroyed. This can lead to higher localized corrosion rates that may lead to pit like corrosion defects. The susceptibility for such corrosion patterns should be investigated by testing and by dissection of flexible pipes that have been taken out of service.

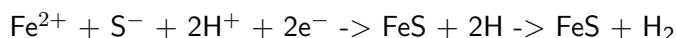
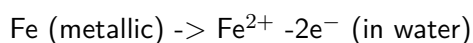
Summary of potential corrosion issues related to CO<sub>2</sub>

- Can high partial CO<sub>2</sub> pressure in gas pockets pressurized by water column or in subsea flow lines lead to higher corrosion rates than reported in the literature?
- Could good protection by oil films invalidate the assumed high ratio between steel surface and water volume?
- Can situation exist where water continuously or intermittently condense and run down on surfaces taking with it the ions creating the buffering capacity and thus cause high corrosion rates when water continues to condense?
- Can corrosion patterns develop leading to pitting like patterns?

#### B4.3.3.2 The effects of H<sub>2</sub>S

In many oil field production environment the level of H<sub>2</sub>S is very low and can be ignored as a potential corrosion mechanism. But there are fields, which naturally contain a lot of H<sub>2</sub>S. Some fields that start up with negligible H<sub>2</sub>S levels experience growing concentrations due to SRB (Sulfide Reducing Bacteria) activity as a result of water injection. Thus there are more and more cases where H<sub>2</sub>S is becoming a concern.

Typically the reaction of H<sub>2</sub>S with steel can be written in the following way:



Iron Sulfide FeS has a low solubility and would precipitate on the steel surfaces. It has also been reported [Sun and Nesic, 2007] that there can be a direct reaction between sulfide ions and Iron on the steel surface forming a very thin layer of FeS in the form of Mackinawite. Iron sulfide films tends to provide very good protection against corrosion but local damage to such films may create sites for localised corrosion to develop.

However, in flexible pipe applications H<sub>2</sub>S will mainly be accompanying CO<sub>2</sub>, which in most cases will be in much higher abundance than H<sub>2</sub>S. The main concerns with H<sub>2</sub>S are expected to be:

- Influences from H<sub>2</sub>S on the CO<sub>2</sub> corrosion process
- Potential of Sulfide Stress Corrosion Cracking (SSCC) and Hydrogen induced Cracking (HIC) in high strength steels

**B4.3.3.2.1 Possible Effects from H<sub>2</sub>S on CO<sub>2</sub> Corrosion** [Taravel-Condat and Désamais, 2006b]

report corrosion tests with different amounts of H<sub>2</sub>S (up to 1% compared to CO<sub>2</sub>) and showed that the confinement and low V/S ratio produce similar increases in pH compared to model predictions as for CO<sub>2</sub> on its own. They report corrosion rates of 0.025 and 0.030 mm/year (at 20 °C and 80°C respectively) for tests with 0.1 bar H<sub>2</sub>S together with around 0.9 bar CO<sub>2</sub> in a confinement of V/S=0.2 ml/cm<sup>2</sup>.

Desamais and Taravel-Condat [Désamais and Taravel-Condat, 2006] report from a long-term full scale test with exposure to both CO<sub>2</sub> and H<sub>2</sub>S that the corrosion rates have been measured to be in the range 0.005 - 0.015 mm/year.

In a review by [Schmitt and Horstemeier, 2006] of fundamental aspects of CO<sub>2</sub> corrosion it is pointed out that mixing in H<sub>2</sub>S can significantly change the corrosion rates depending on the conditions. H<sub>2</sub>S will react with the Iron Carbonate film formed by CO<sub>2</sub> corrosion. In steady state gas compositions the protective film on the steel surfaces may be dominated by carbonates or sulfides or mixtures depending on absolute and relative partial pressures of CO<sub>2</sub> and H<sub>2</sub>S. In some situations H<sub>2</sub>S can be beneficial but there are cases where the corrosion rates increase because of H<sub>2</sub>S compared to a pure CO<sub>2</sub> system. Based on available information it is not possible to say whether situations with enhanced corrosion rates on steel armours in the annulus can develop as a result of increasing H<sub>2</sub>S concentrations.

A. Dugstad of IFE (ref [Dugstad, 2013]) has pointed out that H<sub>2</sub>S may react quickly with FeCO<sub>3</sub> resulting from the CO<sub>2</sub> corrosion. This may lead to gradients in the H<sub>2</sub>S concentration in particular in the radial direction due to high consumption rates. There may be a concern that in the transition between H<sub>2</sub>S influenced and pure CO<sub>2</sub> dominated conditions that variations with time can lead to higher corrosion rates. This is an issue that may have to be investigated in further details. It may be that there are signatures in the generation of hydrogen gas that might be detected through annulus vent monitoring.

**B4.3.3.2.2 Potential for SSCC and HIC** The main concern with H<sub>2</sub>S is Sulfide Stress Corrosion Cracking (SSCC) and Hydrogen Induced Cracking (HIC) in high strength steel. This concerns steels with hardness exceeding a threshold and since hardness tend to be proportional to the ultimate yield strength the SSCC issue relates to steels with a UTS exceeding a threshold. Steels that exceed these thresholds can still be resistant to SSCC and HIC depending on composition and heat treatment. The [NACE TM 01-77, 1996] standard defines the requirements and test procedures to qualify specific materials.

Both SSCC and HIC are caused by atomic hydrogen diffusing into the steel structure where they may collect in micro-voids/inclusions and combine to form hydrogen molecules and build internal pressures that cause cracking or blistering. H<sub>2</sub>S corrosion lead to the formation of atomic hydrogen and sulfides tend to prevent hydrogen atoms H to combine to molecular hydrogen H<sub>2</sub> that would end up as gas. This leaves higher concentrations of atomic hydrogen close to the steel surfaces than for instance with CO<sub>2</sub> corrosion. The concentrations of atomic hydrogen will depend on the partial pressure of H<sub>2</sub>S and the pH of the electrolyte

SSCC takes place in susceptible materials that are under high stress (relative to their yield strength). Cracking typically starts in locations with the highest stresses, which could be in surface irregularities creating stress concentrations. Rather than a single crack a network of fine feathery-branched cracks will form.

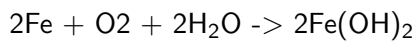
HIC is a mechanism that does not require high stress levels to be present but may take place

in materials with hardness above a threshold level. It is thought to be linked to long drawn out inclusions and will often appear as internal blister-like defects.

There are examples where flexible pipes, in particular flow lines with high annulus pressures, designed for sweet service have failed due to H<sub>2</sub>S related cracking because the reservoir turns sour with time. The observed damage patterns and locations do not necessarily fit what would be expected from SSCC and HIC. Thus the industry may benefit from developing further knowledge and insight into the potential corrosion mechanisms when H<sub>2</sub>S builds up in the annuli of flexible pipes.

#### B4.3.3.3 Effects from oxygen

**B4.3.3.3.1 Pure Oxygen Corrosion** Corrosion of steel in seawater with dissolved oxygen can be described by the following full reaction:



Further reactions with oxygen and water will also lead to other end products such as Fe(OH)<sub>3</sub>.

The reaction is clearly dependent on the availability of oxygen. The corrosion rate will directly depend on the concentration of dissolved oxygen and be influenced by parameters such as temperature and to a limited extent on pH. With constant concentration of oxygen the corrosion rate increases with temperature.

In seawater the corrosion rate will be limited by Calcium Carbonate, CaCO<sub>3</sub>, deposits forming on the steel surface. In seawater saturated with air and with continuous removal of surface deposits the corrosion rate will be around 0.6mm/year at 20 °C, [Bardal, 1994]. In reality, due to calcareous deposits, it turns out to be around 0.1 - 0.2 mm/year for uncoated steel in moving seawater without protection by anodes or impressed current systems. Since oxygen corrosion is also limited by the supply of oxygen the corrosion rates become fairly low when the movement of the water is limited. Other corrosion products building on steel surfaces will contribute to slowing down the corrosion rate.

In the splash zone exposed steel surfaces are intermittently submerged in seawater and exposed to air a significant fraction of the time. In such situations the steel surfaces may be covered by water films most of the time and protective deposits may be washed away. This may lead to a good availability of oxygen and corrosion rates up to 0.4 mm/year have been reported on other steel components [Bardal, 1994] in such conditions.

**B4.3.3.3.2 Possible impacts from Oxygen on other corrosion processes** The main concern from repeated ingress of oxygen, through aerated water or air, may be the impacts oxygen could have on other corrosion processes. The paper by [Schmitt and Horstemeier, 2006] state that Oxygen in CO<sub>2</sub> systems exhibits a strong effect on the corrosion rate and facilitates the formation of localized attack. Oxygen may damage the protective iron carbonate film (and the high pH) created from CO<sub>2</sub> corrosion in a confined annulus. With poorer protection by carbonate films and lower pH the CO<sub>2</sub> corrosion rate may increase significantly. Examples referenced in [Schmitt and Horstemeier, 2006] are not directly relevant for the conditions in annulus but magnitude of the effects (0.5 mm/y per ppm of oxygen) should create concerns also for annulus corrosion in locations with ingress of air. The effects of O<sub>2</sub> on CO<sub>2</sub> corrosion are also studied in recent experiments performed by IFE.

Relevant scenarios are situations where oxygen can enter and disturb low CO<sub>2</sub> corrosion rates. One scenario is air entering through the vent system or leakages in the sealing between the end fitting and the outer cover. Combined with the possibility of water condensing in the vent tubes and CO<sub>2</sub> in the vent gas it is possible to see cases of concern. The most frequent source of oxygen ingress would be holes in the outside cover which is discussed in Chapter B4.

Possible impacts from oxygen on H<sub>2</sub>S dominated corrosion processes should also be of concern. For instance ingress of aerated seawater into the annulus of subsea pipes with high partial pressures of H<sub>2</sub>S could change the corrosion mechanisms and corrosion rates. It is known that oxygen will react with hydrogen sulfide to form elemental sulphur that is a strong corrosion agent for steel. Other mechanisms could also be relevant.

#### B4.3.3.4 Other potential influences on corrosion

There may also be other chemical constituents that influence the susceptibility to corrosion. One possibility is chloride in the seawater that might have an impact on pitting corrosion by creating local damage to protective films.

### B4.3.4 Hole in the outside cover

#### B4.3.4.1 Holes in locations submerged in seawater

**B4.3.4.1.1 Corrosion from a single flooding** Possible scenarios for ingress of water and air as a result of holes through the outer cover have been described in Chapter B4.2.

A hole in the outer cover of a riser below the sea level will lead to partial flooding of the annulus of the riser with gas pockets trapped in high points such as in the hog for many riser configurations. A typical concentration of oxygen in seawater in equilibrium with air is a round 8 ppm by weight. In the water filled part of the annulus the water volume and therefore the amount of available oxygen in ratio to steel surface area is low. If the oxygen is evenly distributed over the steel areas of the edges of the tensile armour wires for a typical pipe design there will be 0.4 µg/cm<sup>2</sup> (oxygen / surface area of armour wire edges). If all the oxygen is consumed through the oxygen reduction cathodic reaction the amount of Iron going into solution would correspond to 1.4 µg/cm<sup>2</sup>. Distributed evenly over the edges of the tensile armours this corresponds to 1.8 nm (10<sup>-9</sup>m). Thus the oxygen from 1 flooding will represent a negligible potential material loss from oxygen corrosion.

**B4.3.4.1.2 Direct exposure to seawater and cathodic protection** Armour wires that are directly exposed to flowing/moving seawater will primarily be exposed to oxygen driven corrosion. Unprotected corrosion rates under these conditions would typically be up to the range 0.1 to 0.2 mm/year as described in Chapter B4. The highest corrosion rates will be found where the flow speed of water is highest and will decrease with reduced flow speed (for seawater in direct contact with steel surfaces).

If the configuration of the damage to the outside cover provides some shielding from the flowing water but still allow direct exposure to the seawater the pure oxygen driven corrosion

rate is expected to be lower than a damage case that gives direct exposure to the flowing water.

Most risers and flow lines are equipped with cathodic protection systems such as anodes or impressed current systems. These systems are expected to provide adequate protection potentials for directly exposed armour surfaces. This requires that the anode system has been designed with adequate reach to cover the full length of pipe to be protected and with sufficient capacity to provide protection over the service life.

[Festy et al., 2004] have reported investigations of cathodic protection efficiency. A simulation cell was made to investigate the protection efficiency under the cover in a hole with good exposure to oxygenated seawater. CO<sub>2</sub> bubbling was also included in the test to simulate annulus environment. The results showed that steel under a simulated cover was adequately protected well beyond the reach of the oxygen. The simulation of gaps or channels for water in the annulus deviated from the structure in a real annulus so the results may not be fully representative. The test did not include any simulation of 'pumping' actions that can drive oxygenated water into the annulus away from the hole. The test was not set up to investigate the protection of internal armour layers.

**B4.3.4.1.3 Effects of renewal of seawater - mixture scenarios** In locations where seawater is continuously renewed the environment will be dominated by oxygen in the seawater. An important question is how far into the armour wire structure will pure seawater corrosion dominate? This will most probably depend on the actual outer cover damage, its location and whether there are conditions that will have pumping actions that regularly 'pump' seawater in and out of the hole. Permeating gases will partly be venting through a hole in the outer cover. This may ensure relatively good supply of CO<sub>2</sub> to saturate seawater-reaching regions of the annulus fairly close to a hole.

One can foresee, in a region in the vicinity of a hole, a scenario where CO<sub>2</sub> dominated anaerobic conditions have developed before a pumping event, such as a cool down, drives fresh seawater to this region. Oxygen will dominate over CO<sub>2</sub> for a period until CO<sub>2</sub> regains domination either because of water being driven in the opposite direction or CO<sub>2</sub> building up from the transport of permeating gases. What impacts such oxygen exposure have on the CO<sub>2</sub> corrosion and how frequent must such event be to create long-term corrosion issues is not understood.

Another relevant question is how much oxygen is necessary to disturb the iron carbonate films sufficiently to push the CO<sub>2</sub> corrosion rate to a level where it will represent a concern?

It is worth noting that seawater has a pH around 8, which could contribute to limit the corrosion threat?

Summary of questions and issues:

- To what extent and how often is the seawater renewed in the annulus in the vicinity of a hole in the outer cover as function of
  - type and location of cover damage?
  - pipe configuration?
  - operation and other exposure conditions?

- Will possible patterns of seawater renewal create conditions in the annulus water that will lead to enhanced corrosion rates to levels that would be of concern?
- To what extent will cathodic protection help to limit potential corrosion pattern?
- What is the reach of effective cathodic protection into the annulus relative to the reach of renewed oxygenated seawater?
- The uncertainties relating to these issues should encourage
  - Investigations to understand the threat and quantify issues
  - Ensure that damage to outside covers are repaired as soon as possible

#### B4.3.4.2 Holes above the sea level and in the splash zone

Holes in the splash zone will regularly or in periods repeatedly be exposed to seawater. Steel surfaces that are directly impacted by seawater will:

- In periods be covered by water films rich in oxygen
- If the water impacts are vigorous they may damage protective corrosion deposits
- When the hole is above the water there is no effects from cathodic protection

The corrosion rates from oxygen could be up to 0.4 mm/y.

Waves that take a hole in and out of submergence will induce some pumping actions - possibly compressing gas pockets in the downwards direction and forcing water upwards in the annulus. The upward reach will be bounded by the wave height but flow impedance along the annulus combined with the submergence period will probably contribute to limit the reach. The consequence is that oxygenated water will be flowing in and out of parts of the annulus above a hole that is going in and out of submergence. Anti-wear layers will also impede the flow of water both in and out during a wave period and may contribute to partial trapping of water. Periods with high waves may lead to wetting of sections of the annulus that in following periods will not get in contact with fresh sea water. This may lead to CO<sub>2</sub> domination in water that may be partially trapped.

There is a multitude of possible exposure combinations that can exist for armour wires under and in the vicinity of holes in the splash zone. It is difficult to predict possible corrosion patterns but there are possibilities for high corrosion rate scenarios including oxygen, CO<sub>2</sub> and combinations.

For holes that are located above the splash zone the main threat will be ingress of air possibly in combination with ingress of rain water and/or seawater spray. It is possible that the annulus will have filled up with water to the level of the hole. In such cases there will be water in the annulus below the hole and water vapour may condense in the annulus above the hole. Any pumping effects will result in air being sucked in rather than oxygenated water if the holes had been submerged in seawater. On the other hand holes in outside covers in locations that are shielded from exposure to running water, as for instance inside I-tubes, may not lead to water filling of the annulus. The armours may stay dry depending of temperature conditions in relation to the dew point of water in the gas transported in the annulus. Thus a variety of conditions may exist with varying mixtures of water, oxygen and the corrosion threat must be assessed on a case-by-case basis.

There have also been reports in the industry of outside covers cracking due to ageing under bend stiffeners in applications with relatively high temperatures. This will lead to possible combinations of oxygen and CO<sub>2</sub> and a key question is whether condensed water may exist in this part of the annulus. The temperature in the annulus would be high, which should not lead to condensation of water but then there may be the possibility of water condensing in vent tube running back to the annulus. Again potential issues have to be assessed based on configurations and operating conditions.

### B4.3.5 Effects on fatigue resistance from corrosion processes

#### B4.3.5.1 Introduction

Fatigue of armour wires is in many cases a limiting factor for the design life of flexible risers. Until a few years ago, fatigue design was based on SN data obtained by component testing in air, with the implicit assumption that the environment in a pipe annulus is benign with regard to fatigue of armour wires. Service experience has shown that a pipe annulus may contain species that are aggressive with respect to steel, and could affect fatigue strength significantly. In a consistent design methodology these effects should be taken into account.

The essential components of dynamic loading of a flexible riser are global bending and tension. For shallow water risers bending loading will in general be dominating, and concentrated to the top end and (depending on the configuration) sag and hog bends and the touch-down zone. Deep-water risers in a catenary configuration will to a larger extent be subjected also to fluctuating tension in the top end, due to inertia and drag forces.

Fatigue design of armour wire is based on empirical SN-curves from component testing. A number of programs have been and are being carried out to determine SN-curves for simulated annulus environments. Most of the data is confidential. Some general results will be discussed here, based on [Berge et al., 2008].

#### B4.3.5.2 Environmental effects on fatigue strength

In the as-fabricated state, void space in the pipe annulus is filled with atmospheric air. However, for several possible reasons the chemical composition of the annulus may change during operation, as discussed throughout this chapter.

A corrosive environment may have an effect on fatigue strength through two different processes:

1. The long term cumulative effect of exposure to a corrosive environment may lead to deterioration of the surface of the armour, in particular by pitting corrosion. A number of studies have shown that pitting corrosion to a depth in the range 50-100 m may have a significant effect on fatigue strength of steel plate, due to an enhanced fatigue notch factor. Service experience has shown that armour wire in a flooded annulus may become subjected to pitting. However, no studies have been reported to give quantitative data on the effect on fatigue strength of armour wire.
2. A corrosive environment may interact with the cycle-by-cycle fatigue damage process (slip band formation, fatigue crack initiation and growth). A number of environmental effects may lead to accelerated fatigue damage (anodic dissolution of iron leading to

accelerated slip band formation or fatigue crack initiation and growth, local hydrogen effects causing embrittlement and stress corrosion, and so on). On the other hand, corrosion products (iron carbonate  $\text{FeCO}_3$ , iron sulphide  $\text{FeS}$ ) may form a protective layer, and reduce the detrimental effect of the environment. The relatively large scatter that is often observed in corrosion fatigue testing may be attributed to the competition between corrosive and protective processes.

It is important to note that a corrosion fatigue test to obtain an SN-curve normally is carried out over a time span of weeks or possibly some few months. The long-term cumulative effect of corrosion damage is thus not considered.

#### B4.3.5.3 Annulus environments

The factors of annulus environments that are most important for fatigue strength and need to be considered in design and in testing are discussed below.

**Sea Water Ingress** It is known from service experience that sea water flooding of flexible pipe due to leakage through holes in the external sheath or faulty vent valves is a scenario with a relatively high probability. The following issues need to be addressed:

- Effect of cathodic protection - possible shielding at some distance from the point of leakage.
- Chemistry of seawater, in particular oxygen level inside the annulus and also the possibility of microbial induced corrosion as sulphide reducing bacteria may develop in stagnant sea water.
- Diffusion of gases from the bore, in particular  $\text{CO}_2$  and  $\text{H}_2\text{S}$ , partial pressures.

**Diffusion from bore** Similar issues arise with respect to diffusion from the bore:

- Rate of diffusion of water vapour, condensation in the annulus.
- Ionic content in condensed water.
- Diffusion of gases from the bore, in particular  $\text{CO}_2$  and  $\text{H}_2\text{S}$ , partial pressures.

**Repaired pipe** Pipes that are subjected to seawater ingress may be flushed and repaired, and then re-installed. The following issues arise:

- Time frame for inspection and repair before corrosion fatigue damage may take place.
- Effect of inhibitor, possibly with residual seawater,  $\text{CO}_2$  and  $\text{H}_2\text{S}$ , on residual life.

**Diffusion from bore - prediction models** Prediction models have been developed for diffusion of species from the bore, based on Fick's laws, e.g. [Last et al., 2002]. The models may be used for prediction of annulus environment, in particular condensation of water and concentration of gases. A generic problem is that due to the number of parameters a test matrix to cover all possible design cases becomes very large. Test parameters are discussed more in detail in Chapter B5.

**Environmental parameters for design and test simulation** In corrosion fatigue testing to obtain design criteria (SN-curves) it is important to simulate operational conditions as truly as possible. For annulus environments this is a very difficult task, due to the large variability of possible scenarios. Another complication is that the conditions in an annulus are dynamic - gases ( $\text{H}_2\text{S}$  and/or  $\text{CO}_2$ ) that diffuse through the liner will be consumed

by chemical reactions with the steel. The conditions in a water-filled annulus in terms of partial pressures are thus very different from the nominal composition of the gas that diffuses through the liner. The current approach in design is to characterise the annulus environment by the nominal parameters, i.e the partial pressures of gases calculated from the diffusion models and disregarding consumption by chemical reactions. In testing the electrolyte is bubbled with a gas of the same composition. Simulation of the environment in testing is thus based on nominal parameters. Testing is discussed more in detail in Chapter B5 Test Methods.

#### B4.3.5.4 Current status

Service experience shows that armour wire in flexible risers may be exposed to aggressive environments. The detrimental effect on fatigue strength may be significant, in particular for long lives, [Berge et al., 2008]. There is a need for fatigue design criteria for a large number of design cases, specified by:

- Material grade, strength class
- Environmental factors
- Load parameters

Several programs have been carried out or are on-going with the aim of establishing such fatigue design criteria. However, very little information is public domain, and no standard industrial practice has been established. A further problem is that test data tends to be considered 'in-house' to the respective suppliers of flexible pipe, valid for proprietary brands of wire only. It would be beneficial for the industry if SN-data instead were presented and analysed on the basis of generic strength classes, for the following reasons:

1. The variability that in some test series is observed between different brands of armour wire (within the same strength class) is in most cases hardly significant. The scatter-bands are in many cases overlapping, and no systematic trend is seen to indicate that one brand is superior relative to other brands. It is likely that the variability is of type batch-to-batch rather than brand specific.
2. If SN-data were analysed on the basis of brand, each SN curve would represent one batch of material only. This would lead to much narrower scatter-bands than what is obtained if data representing many batches are pooled together. The design criteria that would be derived from this procedure could become unconservative.
3. In many cases fatigue design is carried out with no knowledge of which supplier will provide the riser. Using brand specific SN-curves would be complicated for such cases.

The analysis of SN-data that is underlying the current design codes for welded steel structures, [Gurney and Maddox, 1973], is based on data that deliberately were pooled from as many sources as possible, taken to represent materials and welding technology at large. In this way generic and robust design criteria were obtained that could be applied world-wide, provided basic quality requirements were met. In the same way, generic fatigue design criteria for flexible risers should be developed, to be sufficiently robust to be applied independent of brand.

For products that may be claimed to have better properties than what is given by the generic SN-curves there is still an option to use optimised design criteria for that specific product,

provided the improved properties can be documented.

## B4.4 Field experience

### B4.4.1 Cases with severe corrosion

#### B4.4.1.1 Subsea pipelines

An early paper reporting corrosion in the annulus was from a trial use a flexible pipe for gas lift with high H<sub>2</sub>S (2.5%) and CO<sub>2</sub> (6%) contents, [[j. Al-Maslamani, 1996](#)]. It culminated in failure after 3 years. Gas leakages were observed from several locations on both the riser and flow line sections. The leakage rates to the sea went up and down with the pressure in the bore suggesting holes in the pressure sheath.

A one meter section of the flow line was retrieved for dissection and assessment. Pictures in ref. [[j. Al-Maslamani, 1996](#)] give clear impression of severely corroded and ruptured armours.

Cracks and ruptures in the armours had clear signs of SSC, Hydrogen Induced Cracking and Hydrogen embrittlement confirmed by metallographic investigation. It was suggested that the hardness was higher than specified by NACE MR0175 for sour service steels. They also reported unacceptable steel structure in the surface of the pressure armour.

There was no discussion of the possible sequence of event - whether the pressure sheath had ruptured first or whether water in the annulus had led to ruptures and loss of support for the pressure sheath. The clear message is that selection and qualification of steel for sour service is essential.

Today we know about several cases where subsea flexible pipeline have failed due to corrosion/cracking of armour wires in the annulus: at least 3 cases in the North Sea, 1 in the Arabic Gulf and 2 cases I Africa. The main suspicion is increasing levels of H<sub>2</sub>S that have led to SSCC or related issues for high UTS armours. There is a growing need to understand the causes to limit future impacts.

#### B4.4.1.2 Severe corrosion of armours in risers

Very limited Information about cases where operators have experienced corrosion leading to pipe failures or near misses is available in the public domain. Some information has been provided through presentations in open forums and some information has spread through the industry. To our knowledge about corrosion issues with risers are:

- At least 4 riser failures caused by corrosion resulting from hole in outside cover:
  - 1 in UK sector
  - 1 in West Africa
  - 2 in South North Sea

A couple of these have led to catastrophic failures.

- At least 3 occurrences where severe corrosion was detected in time for corrective action

- 2 in North Sea
- 1 in Africa

We do, however, not know the specific corrosion mechanisms that have led to the failures whether it has been oxygen driven corrosion, oxygen + CO<sub>2</sub> or CO<sub>2</sub> + H<sub>2</sub>S with oxygen. We believe that all the failures originated from holes in the outer cover located in the sea level region or below. One of the near misses was due to damage well above the sea level.

In the years after the 2014 revision of this handbook corrosion issues are experienced related to outer sheath wear and wear of armour wires. Additionally, in two separate cases suspected corrosion processes are due to the combined effects of O<sub>2</sub> and CO<sub>2</sub>, and due to CO<sub>2</sub> and acids in the annulus.

Figure B4.7 and Figure B4.8 have been included to illustrate issues without reference to specific cases.



Figure B4.7: Corroded armour wire after breach of external sheath, [Out, 2010] (Courtesy of Hans Out, Shell)

#### B4.4.2 Other field experience

There are several cases where potentially concerning corrosion attacks have been found on armour wires from flexible pipes retrieved for other reasons. In some cases the damage has been equivalent to or more severe than the corrosion pits found on samples from the North Sea Riser and the Balmoral Riser that gave significantly reduced fatigue life compared to predictions from SN curves for new wires.

Information available points to the need for better understanding of corrosion mechanisms in the annulus and what level of surface damage they can create. If relatively modest corrosion takes place in locations that represent hot spot for fatigue loads the fatigue life for a riser can be significantly reduced, ref. Figure B4.9.

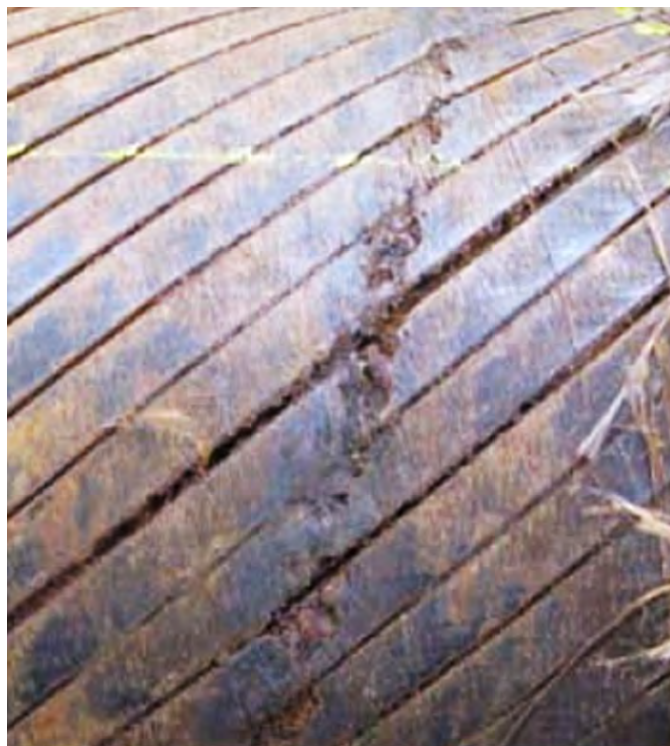


Figure B4.8: Armour wire corrosion (Courtesy of Statoil)



Figure B4.9: Example of pitting in axial armour wires [Nordsve, 2007]

There are numerous cases where damages to outside covers have been detected and repaired in time to avoid significant reduction in integrity [Anderson et al., 2007].

## B4.5 Summary and recommendations

### B4.5.1 Summary of field experience:

Pipe failures - loss of containment where corrosion was the main mechanism:

- At least 4 riser failures caused by corrosion resulting from hole in outside cover:
  - UK Sector
  - West Africa,
  - 2 in South North Sea
- At least 6 pipeline failures have been caused by sulfide stress cracking or HIC of high strength steel armour wires stimulated by H<sub>2</sub>S or cathodic protection of deformed armour wires inside damaged outside cover.
  - Arabic gulf
  - Africa
  - South North Sea
  - UK Sector
- At least 3 near misses on risers where severe corrosion was detected in time for corrective action
  - North Sea
  - Africa

4Subsea knows of at least 5 cases where 'significant' corrosion attack has been found on armour wires from flexible pipes retrieved for other reasons. On these wires the corrosion damage has been equivalent to or more severe than the surface damage found on samples from the North Sea Riser and the Balmoral Riser that came out with strong indications of significantly reduced service life.

There are numerous cases where damages to outside covers have been detected and repaired in time to avoid significant reduction in integrity.

### B4.5.2 Key findings relating to CO<sub>2</sub> corrosion

There is strong evidence that CO<sub>2</sub> corrosion rates on steel armours in anaerobic water phases in flexible pipe annuli are low - typically below 0.01 mm/year. The reason for this is the low ratio between available water volume and the steel surface area in a confined annulus. This will be the case for both condensed water and ingress of seawater.

Presence of acids or ingress of oxygen into CO<sub>2</sub> corrosion systems may lead to significantly enhanced corrosion rates.

### B4.5.3 Issues for concern

#### B4.5.3.1 Hole in the outside cover.

- Below sea level the main concern will be the reach and frequency of renewal of oxygenated seawater (pumping effects). There may be potential corrosion threats where oxygen may mix in with CO<sub>2</sub> or if conditions vary between CO<sub>2</sub> dominated and oxygen dominated. There are also uncertainties regarding the effectiveness of cathodic protection, due to shielding effects, for armour wires in the vicinity of a hole in the outside cover.
- Holes in the splash zone can lead to conditions with high corrosion rates. To mitigate severe loss of integrity, damage to outside covers should be detected very early - preferably within weeks or a few months.
- Holes above water can lead to serious corrosion depending on location. Issues are:
  - Damage patterns and vent system lay-out that lead to renewal of oxygen.
  - Possible enhanced corrosion in situations with mixtures of Oxygen and CO<sub>2</sub> (& Oxygen and H<sub>2</sub>S)
  - Condensation and formation of thin water films on armour wires
- A situation with multiple holes in outside covers with possible circulation of seawater or air from one hole to another is a high risk scenario.

#### B4.5.3.2 Other issues

- Growing H<sub>2</sub>S concentration in pipes with high strength steel - can lead to major corrosion / cracking damage
- Mixtures of H<sub>2</sub>S and CO<sub>2</sub> - can this lead to unforeseen corrosion damage
- Possible top of line CO<sub>2</sub> corrosion - should be investigated
- Possible enhanced CO<sub>2</sub> corrosion in connection with local damage of protective Iron-carbonate films (relative movement of contacting surfaces)
- Possible unforeseen effects of annuli with high total pressure with correspondingly high partial pressures of acid gases.

### B4.5.4 Mitigation:

#### B4.5.4.1 Motivation

Many of the serious corrosion issues experienced by the industry cannot be removed by design of the flexible pipes. It is essential for the industry to implement procedures, work practices, monitoring solutions and inspection programs to

- in the first instance, avoid damages or incidents that can lead to corrosion and
- secondly make sure that incidents or damages leading to corrosion in the annulus are detected as soon as possible.

#### B4.5.4.2 During Installation

Many incidents of outer cover damage take place during installation. The consequences can be serious. It is therefore essential to implement procedures and work practices during installation that limit the chance of damage to the outside cover. If damage should occur it is essential that these are detected and repaired appropriately as soon as possible.

#### B4.5.4.3 During Operation

In the operational phase the following mitigations are recommended

- Annulus vent should not be ventilated directly to the atmosphere, but either be directed to a closed vent system or ventilated through a pressure valve to avoid ingress of oxygen through the vent port and into the annulus
- By all means avoid blockage of the annulus vent system:
  - Blocked venting systems will lead to rupture of the outside cover.
  - Establish continuous monitoring or periodic inspection to verify adequate venting
  - Ensure periodic annulus testing to measure the flow rate (flow impedance) through the vent system.
- Limit the chance of falling objects and impacts that can damage the outer cover.
  - Ensure a strict system for reporting incidents that could have caused cover damage.
- Identify whether cracking of the outside cover under the bend stiffener is a potential issue based on the operating temperature and the thermal gradient through the pipe wall and bend stiffener.
  - If at risk, carry out modeling and implement possible mitigation (lower temperature / limit access of oxygen etc)
- Implement monitoring or inspection system to detect outside cover damage early enough to repair in time:
  - A hole in or just above the splash zone should be detected within weeks or months.
  - Annulus vent testing is a cheap and effective way to detect outside cover breaches in the upper part of risers
  - Regular visual inspection
  - Be aware of possible rupture of outside cover in the hog because of high pressure in gas pockets with a high water column in the annulus. (The risk can be assessed from configuration and measurement of free volume in the annulus in the top of the riser)
  - Regular ROV inspection to search for cover breaches
- Verify functional cathodic protection over the entire service life of the flexible pipe
- Assess the chances of Sulfide Stress Cracking or Hydrogen Induced Cracking based on possible increase in H<sub>2</sub>S and material used for armour wires.

#### B4.5.4.4 Limit impacts of outer cover damages

- Implement inspection and monitoring procedures to ensure early detection of cover damage
- Carry out assessment of corrosion scenarios and risk when a cover damage has been detected
- Ensure that damages are repaired as soon as possible to avoid/limit possible corrosion damage
- Immediate attention must be given to situation where there are multiple damages to the outside cover that can lead to circulation of seawater or air.

#### B4.5.5 Future challenges

To deal appropriately with integrity issues related to potential corrosion of steel armours in the annuli of flexible pipes there is a need to develop more knowledge and insight about annulus conditions and realistic corrosion scenarios such as:

- Conditions and corrosion in the annulus in the vicinity of holes in the outside cover
- The potential impacts of H<sub>2</sub>S, in particular for sweet service armours in field that turn sour

New knowledge about the processes must be combined with better solutions for monitoring and detection of corrosion threats such as characterization of signatures from relevant corrosion processes:

- Equipment and procedures to enhance the quality of annulus vent monitoring and testing
- Develop new methods for annulus monitoring and inspection to detect damage processes
- Address potential corrosion issues to enable prediction capabilities

In the long term the cost of developing sufficient knowledge and insight will be small compared to consequences of not being able to deal with the integrity threats in a diligent way.

## **Chapter B5**

# **Test Methods**

*Author: Stig Berge (NTNU)*

## B5.1 Introduction

Testing is an integral part of flexible pipe technology. [API 17B, 2008] and [API 17J, 2008] specify a large number of tests to be carried out during the phases of the life of a flexible pipe concept; design, qualification, characterisation, fabrication, acceptance, installation, commissioning and operation. The objective of this chapter is to give an overview of the different types of tests that are specified. Details are found in [API 17B, 2008], [API 17J, 2008] and referenced testing standards.

In addition, procedures for corrosion fatigue testing that is not detailed in the API documents are described in some detail.

## B5.2

### B5.2.1 Prototype testing

There are two objectives of prototype (qualification) testing [API 17B, 2008]:

- Evaluate the performance (i.e. structural, functional, fabrication) of a new or established pipe design (verification test).
- Qualification of an established pipe design for use outside its previously qualified envelope.

Prototype tests are generally carried out with full scale sections of pipe with end terminations, or medium scaled sections comprising only the layers required for the test, with or without end terminations. Many of the tests are destructive.

The number and range of prototype tests that can be performed on a flexible pipe is extensive, and requires for many tests special and expensive test rigs. The requirements for prototype testing are thus subject to agreement between the manufacturer and the purchaser. As an alternative to prototype testing the manufacturer may provide objective evidence that the product satisfies the design requirements. Objective evidence is defined as documented field experience, test data, technical publications, finite element analysis or calculations that verify the performance requirements.

Prototype tests are furthermore classified into three classes:

- Class I: Standard prototype tests, as most commonly used
- Class II: Special prototype tests, used regularly to verify specific aspects of performance, such as installation or operating conditions
- Class III: Tests used only for characterisation of the pipe properties.

In [API 17B, 2008] detailed guidance is given on the type of tests for each Class, with specifications for the test procedures and acceptance criteria. A brief summary is given here.

**Class I tests** The objective of Class I tests is to document the basic strength properties of a pipe; burst pressure, axial tension, hydrostatic collapse and cyclic temperature test of PVDF.

**Class II tests** The objective of Class II tests is to document properties that are important for specific applications, in installation or operation; full scale fatigue test, crush strength

test, combined bending and tensile test, sour service test, etc. The number of tests is large, for unbonded pipe 13 tests are listed in [API 17B, 2008].

**Class III tests** Class III tests, also termed characterisation tests are normally carried out as part of a prototype test program. The objective is to measure properties of a pipe that cannot readily be determined on the basis of design calculations. Properties that are assessed on the basis of testing are bending stiffness, torsional stiffness, axial compression strength, abrasion resistance, etc., cf. [API 17B, 2008].

**Validation tests** Prototype testing is not only a test of pipe performance, but also a test of the design methods used. The tests may thus be used to validate the design methods and tools, in particular software.

### B5.2.2 End termination tests

End terminations are complicated structures where all load-carrying components in a pipe wall are anchored, in principle with at least the same capacity and service life as in the pipe wall. The sealing layers (liner and outer sheath) must be sealed with a sufficient pressure capacity and endurance. Proof of capacity is to a large extent based on testing and - for established designs - service experience.

Testing of end terminations is integral to many of the prototype tests. But tests have been developed for specific testing of end terminations. The problem that is addressed is the anchoring and sealing of the liner. Under thermal cycling, e.g. during a shut-down of the riser, the liner will shrink and expand thermally, and large axial stresses will be developed. This applies in particular to polyvinylidene fluoride (PVDF), which is the preferred material for high temperature applications. The anchoring and sealing is provided by mechanical clamping of the liner. The axial thermal stress may cause slippage in the anchoring, and over time (many cycles) pull-out of the liner. Some PVDFs require an addition of a plasticiser to improve on the extrusion process. The plasticizer is volatile, and over time the loss of plasticizer leads to volumetric shrinkage of the liner, and loss of anchoring force.

Two special tests are specified in [API 17B, 2008] for testing of end terminations and liner material under cyclic thermal loading, one for liners with plasticizer and one for liners without. The tests require full scale or medium scale models with end terminations.

### B5.2.3 Vacuum tests

In a vacuum test the annulus of a pipe is partially vacuumed. The test may be applied with two objectives:

1. To demonstrate that the sealing layers (liner and outer sheath) are leak-proof.
2. To investigate (for a pipe in operation) whether the annulus is dry or water-filled.

### B5.2.4 Factory acceptance tests

Factory acceptance testing (FAT) is a procedure for verification that a pipe is manufactured to the requirements of [API 17J, 2008]. The following tests are specified:

- Hydrostatic pressure test, in general to 1.5 times the design pressure for risers and 1.3 times the design pressure for flowlines and jumpers
- Gauge test to detect blockages and gross deformations
- Electrical continuity and isolation test to ensure that the cathodic protection system will be efficient and the carcass is electrically isolated from the end terminations
- Gas venting test to demonstrate that the gas-relief system for the annulus is functioning properly
- Sealing test to confirm the integrity of the external sheath and sealing/crimping of the external sheath at the end fitting.

The hydrostatic pressure test is mandatory for all pipes. The other tests apply according to relevance for the specific pipe design.

### B5.2.5 On-board structural integrity test

The on-board structural integrity test (SIT) is required if a pipe is fully retrieved and repaired on-board an installation vessel, and when the structural integrity have been affected. SIT is a pressure test to a specified pressure.

### B5.2.6 Offshore structural integrity test

The offshore structural integrity test (SIT) is required post-installation if the pipe is repaired in-situ and when the structural integrity have been affected, or to re-assess the integrity versus suspected damage/reduced resistance. SIT is a pressure test to a specified pressure.

### B5.2.7 Materials testing

A wide range of materials are used to build a flexible pipe cross section; stainless steel, carbon steel, extruded polymers, polymer tape, composite fibre tape. In operation the materials are subjected to a complex range of loadings; static and dynamic stress, aggressive environment, thermal cycles and abrasive action. Documentation of the material properties is therefore important.

In [API 17J, 2008] is listed a large number of tests for characterisation of materials (approximately 65 normative standards, plus a large number of informative references). These are in most cases standardised tests from a number of organisations:

- American Petroleum Institute (API)
- American Society for Testing and Materials (ASTM)
- American Society of Mechanical Engineers (ASME)
- Det Norske Veritas (DNV)
- European Committee for Standardization (CEN)
- International Organisation for Standardization (ISO)
- Lloyds Register (LR)

- National Association of Corrosion Engineers (NACE)

It is outside the scope of this handbook to give a discussion of these test methods, except giving some very brief comments on two tests of specific significance for flexible pipe applications.

One specific test of metallic components stands out as particularly important, the NACE test for resistance to sulphide stress cracking and stress corrosion cracking in H<sub>2</sub>S environments, NACE TM 01-77. The distinction between sweet and sour service armour wire is essentially based on this test.

Polymer materials for liners are to be tested extensively with respect to mechanical, chemical, thermal and abrasive resistance. The [API 17TR2, 2003] specification for testing of ageing of polyamide PA-11 was specifically developed for riser applications. Polyamides at elevated temperature and with presence of water are susceptible to hydrolysis. Over time the polymeric structure breaks down and the material starts cracking. Under acidic conditions the aging will be accelerating. The [API 17TR2, 2003] gives criteria for the service life of polyamide liners.

## B5.3 Corrosion fatigue testing

As discussed in Chapter B4 the annulus of a flexible pipe in many cases may be subjected to a range of corrosive environments. The fatigue strength may be significantly affected by the environment and fatigue design should be based on empirical SN-curves from component testing in the relevant environments.

### B5.3.1 Test protocol

Corrosion testing is non-standard, and a test protocol has been worked out, [Berge, 2007]Berge (2007). The protocol provides detailed description on test procedures and parameters. Recommendations are given on:

- specifications for the environment
- specimen preparation
- fatigue loading procedure
- data processing, assessment of design SN-curves

Methods and procedures for corrosion fatigue testing of armour wire are presented and discussed in several papers, [Berge et al., 2003], [Berge et al., 2008], [Rubin and Gudme, 2009], [Santos et al., 2011]) and [Clements et al., 2012]. A brief review is given here, mainly based on the test protocol, [Berge, 2007].

### B5.3.2 Specifications for the environment

Two different aqueous environments are specified, ASTM sea water and distilled water with 1000 ppm of chloride (to simulate the industrial environment of pipe manufacture). Use of inhibitor is case dependent, and needs to be specified for each case. Buffers should not be

added, such that the environment is allowed to stabilise at a natural level of pH. The pH level should be monitored during testing.

Three mixtures could be used, of high purity gas, with composition defined by the respective partial pressures:

- CO<sub>2</sub> (+ N<sub>2</sub>)
- H<sub>2</sub>S (+ CO<sub>2</sub>)
- H<sub>2</sub>S + CO<sub>2</sub> (+N<sub>2</sub>)

Test conditions are assumed to simulate environmental conditions in an annulus, with a large ratio of steel area relative to liquid volume. It is recommended to use steel wool or steel chips to create a large surface area. The steel wool/chips should not be in galvanic contact with the specimens. In the case of testing in CO<sub>2</sub> environment a pre-conditioning time of 2 days is advised for establishing super-saturation of iron in the solution. In H<sub>2</sub>S environment the conditioning is extended to 4 days, in compliance with procedures of [[NACE TM 01-77, 1996](#)].

Unless close to a leak in the outer sheath the annulus environment is anaerobic. If even small amounts of oxygen are allowed into the test chamber, test conditions could become significantly more onerous. For this reason great care must be taken in equipment design and test procedures to prevent oxygen ingress. It is recommended that the test cell and piping, unless all metal, is double wall with annulus either purged with gas (pure N<sub>2</sub>) or flushed with oxygen free water which has been purged with N<sub>2</sub>. Oxygen levels need to be monitored, and a general requirement is that oxygen concentration in the electrolyte is below 5 ppb at all times, preferably below 1 ppb.

A generic problem is that due to the number of parameters a test matrix to cover all possible design cases becomes very large. Test parameters investigated in a single test programme and discussed by [[Berge et al., 2008](#)] are listed below:

#### **Aqueous environment**

- None (air)
- Sea water
  - aerated
  - anaerobic
- Condensed water
  - ionic content

#### **Cathodic protection**

- Yes
- No

#### **Gas diffusion**

- H<sub>2</sub>S (balanced with CO<sub>2</sub>)
- CO<sub>2</sub> (balanced with N<sub>2</sub>)
- H<sub>2</sub>S + CO<sub>2</sub> (balanced with N<sub>2</sub>)

**Partial pressures of H<sub>2</sub>S (plus combinations balanced with N<sub>2</sub>)**

- 0.1 mbara
- 1.0 mbara
- 10.0 mbara

**Partial pressures of CO<sub>2</sub> (plus combinations balanced with N<sub>2</sub>)**

- 0.1 bara
- 0.5 bara
- 1.0 bara
- 2.0 bara
- 3.0 bara

**Temperature**

- Room temperature
- Elevated temperatures
  - 60 °C
  - 90 °C

**Loading parameters**

- Loading frequency
- R-ratio/mean stress

**Additional requirements**

- Testing in aqueous environments with H<sub>2</sub>S and/or CO<sub>2</sub> requires conditioning (pre-charging) before loading is applied.
- For anaerobic conditions the requirement is O<sub>2</sub> < 5 ppb, preferably O<sub>2</sub> < 1 ppb.
- Super-saturation of Fe<sup>++</sup> in aqueous environments.

In addition, grade of armour material is an essential parameter, with a rough distinction between sweet service and sour service steels.

### B5.3.3 Specimen preparation and fatigue loading

Specimens should be taken from a pipe, to include technological factors from the production process, i.e. plastic deformation and possible deterioration of the surface condition. Testing should always be on specimens with the original surface, with no machining or surface preparation that could affect fatigue life. Straightening of the wire should be carried out by hand rolling or similar process, with minimum plastic deformation. A test area representing minimum 50 mm length of wire is advised.

Axial and bending loading is considered to be equivalent. With axial loading alignment must be controlled to avoid secondary bending. Bending loading may be applied as three- or four-point bending, or cantilever bending. Bending tests must be calibrated against strain gauge measurements. Specific guidance is given on the design of bend test fixtures and procedures for displacement controlled bending tests to avoid effects of shake-down of residual stresses.

Constant amplitude loading is recommended, at constant R-ratio or constant mean stress. The parameters should correspond to in-service stress conditions for armour wire. R-ratio  $R = 0.1$  or a mean stress in the range 250 - 300 MPa are typical values. Testing to obtain design criteria for deep water risers may require higher mean stress. Models are available for assessment of the effect of mean stress or R-ratio, on fatigue strength, the Goodman or Gerber model. For tests carried out at a constant R-ratio the recommended values are suitable reference points for application of these models.

For assessment of a fatigue design curve, testing should be carried out in the high cycle region, generally at  $N \geq 10^5$  cycles. Tests that lead to plastic deformation of the armour wire are non-valid. The main contribution to the fatigue damage for typical riser applications is for stress ranges  $50 < \Delta S < 350$  MPa, corresponding to fatigue life in the range  $N > 10^6$  cycles. As a general rule, SN-data at the high cycle end are the most relevant ones for assessment of design curves.

The choice of loading frequency is a vexing point in corrosion fatigue testing. Corrosion fatigue is a time-dependent process, involving chemical reactions at the metal surface, transport of reaction products in the electrolyte, and hydrogen permeation into the metal. It is well known that if the loading frequency in a fatigue test is too high, the effect of the corrosive environment on fatigue strength may become reduced and in the limit eliminated.

[API 17B, 2008] recommends a maximum loading frequency of 0.5 Hz for corrosion fatigue testing. At this frequency the testing time to  $10^7$  cycles is 230 days. This is prohibitively long for a testing program involving a large number of test cases. The consequence of the API recommendation is that test data will be limited to a range below approximately  $2 \cdot 10^6$  cycles, and extrapolation of SN curves to the  $10^7$  range (which is the range that in most design cases gives the major contribution to the fatigue damage) becomes very uncertain, cf. Figure B5.1.

Fortunately, data indicate that the frequency effect in corrosion fatigue of armour wire is small, [Berge et al., 2008]. A number of pilot tests were reported for several environments, showing no significant frequency effect in the band 0.2-2.0 Hz. For this reason testing has been carried out at 2.0 Hz to fatigue lives into the  $10^7$  cycles range, apparently with realistic results.

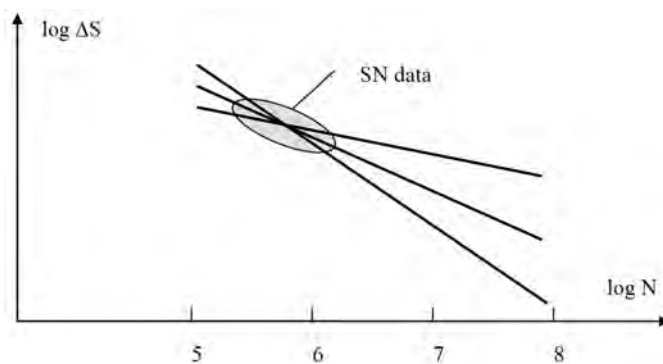


Figure B5.1: Uncertainty in extrapolation of SN curve to long lives (schematic).

#### B5.3.4 Assessment of design criteria from SN-data

Assessment of fatigue design criteria from a given sample of SN-data may be carried out following the procedure that was applied for development of the current fatigue design criteria for steel structures, Gurney and Maddox (1973). The method is often referred to as the 'mean minus two standard deviations' procedure, giving an SN-curve with a notional 2.3 % probability of failure. More refined statistical procedures are also available, e.g. from ASTM E739 (2004) [[ASTM E 739, 2004](#)].

Assessment of design criteria from SN-data is not straight forward. As evidenced by the number of test parameters the statistical population of SN-data is highly multivariate. The test results may be affected by hidden parameters, and the data samples tend to be small and exhibit large scatter. The dominating problem is that no quantitative models for prediction of fatigue strength, or effect of the various parameters, are available - the analysis and the interpretation of the data are empirical.

A particular challenge due to the small sample sizes is to distinguish between sample-to-sample variations (within the same statistical population) and variations that are caused by change in parameters and have a physical origin. For this reason statistical analysis of the data in most cases must be coupled with engineering judgement.

### B5.4 Fatigue testing of pressure armour

Fatigue is strongly influenced by component properties. For pressure armour, local geometry (stress concentration factor) and technological factors (surface condition, residual stress, texture) may significantly affect fatigue strength. Testing of fully machined material specimens, e. g. hour-glass specimens, may give unrealistic results.

Fatigue failures of pressure armour have been reported from full scale tests, caused by fatigue cracks growing in the hoop direction (longitudinal to the wires). The cause of the failures was apparently dynamic stress in the cross-wire direction. To simulate this, a bi-axial test fixture was developed, Figure B5.2, [[Berge et al., 2001](#)]. The methodology for fatigue assessment is as follows:

- Fatigue life data is recorded from the tests in terms of load range per unit length of wire (N/m).

- By finite element modelling the geometry, loading and boundary condition of the test specimen is simulated, to give an SN curve in terms of hot spot stress range.
- Using the same finite element model for the wire geometry, the loading and boundary conditions of a wire in a pipe is simulated, for assessment of hot spot stress.

In this way, the difference in boundary conditions for the wire between the test condition and in a full scale pipe is compensated. The test thus simulates real life conditions with regard to the following factors: Full scale armour profile and notch effects, as-fabricated surface, residual stress from fabrication, contact pressure, and direction of stress.

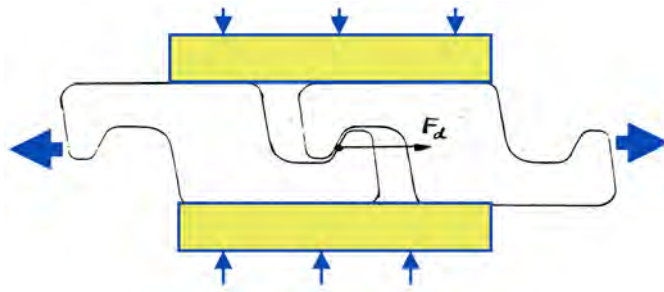


Figure B5.2: Fixture for cross-wire fatigue testing of pressure armour. Here are shown Zeta profiles, the same principle applies to testing of C-clip and Theta profiles. Dynamic loading is applied horizontally, static contact pressure (vertical) is provided by proving ring.

The procedure has been used for assessment of fatigue design criteria for various profile geometries for pressure armour.

# **Part C**

# **Operation**



## **Chapter C1**

# **Integrity Management**

*Author: 4Subsea*

## C1.1 Introduction

The purpose of this chapter is to provide guidance and recommendation for practical in-service integrity management (IM) for flexible pipes. The intention is to comply with and provide guidance that is supplementary to, the framework for integrity management in [API 17B, 2008], [DNV-RP-206, 2008] (Riser Integrity Management), and [DNV-RP-F116, 2009] (Integrity Management of Submarine Pipeline Systems). In particular this Chapter C1 of the Handbook presents recommendations on the development and execution of Integrity Management Programs and on the evaluation of the activities performed therein.

The IM-program shall provide documentation of the flexible pipe's integrity status, and verify and document acceptable integrity throughout the pipe's (design) lifetime. Unacceptable integrity level or operation outside design requires a lifetime assessment to be performed to determine conditions for continued operation of the pipe. Details are given in Chapter C2 Lifetime assessment.

Integrity management strategies adopted in today's standards and guidelines are in general risk based. The need for follow-up and monitoring of the pipe over its entire lifetime is acknowledged and becoming universally accepted.

The main motivation for comprehensive integrity management of flexible pipes is to ensure safe and cost effective operation of flexible pipes. Replacement of a pipe is costly, and failure of a flexible pipe may potentially be catastrophic with large economic impact.

This excerpt from Section 5.3.3 of the publication *Risk level in Norwegian petroleum industry* by PSA-Norway [PSA Norway, 2013b] is illustrative of the current industry status (Official translation by PSA-Norway):

"It is an invariable regulatory requirement (Section 57 of the Facilities Regulations concerning pipelines) that '**for flexible pipeline systems and pipeline systems of other materials than steel, utilisation factors and any load/action and material factors shall be stipulated so that the safety level for such systems is not lower than for steel pipelines and steel risers**'. Looking at the incident frequency for flexible risers, one could question whether this requirement has been met and whether the complexity of safely operating flexible risers has been adequately communicated in the organizations. There are also grounds for questioning whether the industry does a good enough job in handling the challenges associated with operating existing flexible risers and pipelines that are continuously ageing, in addition to designing and installing new ones. The industry needs to address the following improvement areas:

- Updating standards with the most recent experience
- integrity management of flexible risers with continuous monitoring and systems for documenting operations history, which are actively used in follow-up
- ensure good training and expertise throughout the organization responsible for following up integrity
- clear and unambiguous responsibilities for safe operation and integrity management
- the industry must do a better job at sharing information between companies in order to ensure continuous improvement throughout the sector

- the industry must actively commit to research and development in order to increase knowledge about flexible risers
- quick and precise incident reporting associated with pipelines, risers and subsea facilities"

## C1.2 Key aspects of integrity management

### C1.2.1 Standards and Guidelines for Integrity Management

#### C1.2.1.1 Introduction

A framework for integrity management of flexible pipes is found in [API 17B, 2008], [DNV-RP-F116, 2009] and [DNV-RP-206, 2008]. In particular the latter recommended practice presents guidance on the development and execution of an Integrity Management Program for flexible pipes and on the evaluation of the activities performed therein. The methodology in the three references is considered mutually consistent. The methodology for Risk Based Integrity Management as described in Chapter B2 Risk Analysis Methodology in the present handbook and in [DNV-RP-206, 2008] has been adopted.

Integrity of a pipe is established in design. The choices made in the design phase should be taken with due consideration of the requirements for in-service Integrity Management including access for in-service inspection and facilities for testing and monitoring activities. Learning should be taken from previous and ongoing integrity management activities. The importance of a lifecycle perspective is emphasized, even from the early design stage, when planning for integrity management: the operational conditions over the pipe's entire lifetime should be taken into account, both through use during a part of its lifetime and planned future use (potential re-use).

#### C1.2.1.2 In-service Integrity Management Process

An overview of the in-service (flexible pipe) integrity management process is provided in terms of the key steps shown in Figure C1.1.



Figure C1.1: Overview of the Integrity Management Process (Ref: Figure 2-1 in [DNV-RP-206, 2008])

The foundation for developing an IM-program is identification and assessment of potential failure causes and damage scenarios. The probability of failure (PoF) and consequence of failure (CoF) must be determined to establish risk rating for comparison against the risk acceptance criteria.

An Integrity Management Plan consisting of inspection, testing and monitoring activities should be developed based on the risk assessment. Details on the process of hazard evaluation, risk assessment and development of an IM-Plan are given in Section [C1.3](#).

Implementation and execution of the Integrity Management Plan comprises:

- Perform the defined activities (testing, inspection and monitoring as required)
- Review and evaluate the results from each activity
- Perform regular integrity review to assess the pipe's integrity

Detailed guidance on the practical Integrity Management is given in Section [C1.4](#).

DNV RP-F206 [[DNV-RP-206, 2008](#)] recommends periodic loopbacks to include new learning and improvements into the Integrity Management system. The learning and improvements should include review of the present integrity management system, its effectiveness, suitability and possible improvements. It should also include new experiences in the company and in the industry. Further details are given in Section [C1.4.7](#).

### **C1.2.2 Governmental requirements and Company specific requirements**

There are global and regional variations in legislation and governmental requirements to integrity management for pipes used in offshore petroleum production and transportation. Additionally, there are variations in the extent and content of Company specific requirements.

With reference to the legislation in Norway and the United Kingdom, the intent of these requirements is foremost to ensure safe operation. The requirements are typically expressed in general terms, as opposed to the specific guidance found in standards and guidelines. In the legislation, the operator is required to assess and evaluate the potential risks and to implement plans and actions the operator considers to be reasonable and necessary.

### **C1.2.3 Information Handling**

There should be a document register and database providing overview and containing all relevant information for a specific flexible pipe: documents, line data, historical information, test and inspection data and reports and monitoring data, reference is given to [[DNV-RP-206, 2008](#)] section 3 for details. The time series containing monitoring data should include essential information, such as source item instrument, time of disconnected/off-line instrument, and any modification from the original files due to identified errors. The document register should enable both version control and tracking of documents.

## **C1.3 Risk Based Integrity Management for Flexible Pipes**

### **C1.3.1 Pipe system boundaries and system components definition**

In the present chapter, the pipe system boundaries are the *pipe end-fitting flanges*. All ancillary devices *clamped* or *connected* to the pipe are included in the pipe system.

The proposed assessment strategy is a layer-by-layer approach, referring to the layers in the pipe cross section. Ancillaries are presented component-by-component: bend stiffeners, buoyancy modules, tether clamps, tethers, etc. Further, for each layer, relevant failure causes are identified.

### C1.3.2 Classification and grouping of pipes

In order to facilitate efficient development of an Integrity Management for a field or installation with multiple flexible pipes, it is common to classify or group pipes with similar properties and operational characteristics and develop an integrity management plan intended for an entire group of pipes, rather than making specific plans for each pipe. However, there are varying experiences with this approach. Although the idea may look promising at a first glance, there may still be sufficient variations across the pipes that the approach may not be suitable.

### C1.3.3 Hazard identification and probability of pipe failure

#### C1.3.3.1 Evaluation of failure modes and probability of pipe failure

A list of failures and failure causes categorized by layer is given in Chapter [A3 Failure Modes](#) and detailed evaluations are presented for selected failure causes. When establishing an IM-program, all failure causes should be subject to evaluation according to the tables in Section [A3.2](#) and Section [A3.3](#) in Chapter [A3 Failure Modes](#).

The evaluation shall include an assessment of probability of the ultimate pipe failures (loss of pipe function) and consequences of these failures. Hence, the probability of ultimate pipe failure as function of time shall be assessed, being the combined probability of the layer failure (a single failure mode) and the probability of development of a layer failure into a pipe failure. The definition of ultimate pipe failure is given in Chapter [A3 Failure Modes](#) and the parameters affecting the consequences are described in Section [C1.3.3.2.1](#). The risk for each layer failure is defined as the product of probability of ultimate pipe failure and consequence of ultimate pipe failure.

The probability of failure should ideally be quantified in terms of yearly probability. This could in principle be calculated from extensive field experience. However, for flexible pipes many of the failure modes are associated with specific pipe designs, certain operating conditions and use regimes that will limit the number of relevant cases making it meaningless to determine adequately precise failure statistics. There is a high risk of including non-relevant applications in the statistics.

For some layer failures it may be possible to define yearly probability of failure based on extensive laboratory testing such as some cases of fatigue of steel wires. For others it is necessary to make qualitative estimates of the probability of failure based on knowledge of the degradation mechanisms, qualification, laboratory testing and field experience for comparable applications.

A typical approach is to estimate the range of the expected remaining service life and determine a qualitative probability of failure for next year. The criteria for classification of PoF

can be related to whether defined time limits are exceeded. However, it is essential to take uncertainties duly into consideration in such an approach.

### C1.3.3.2 Defects from fabrication and installation

**C1.3.3.2.1 Known defects** Defects or initiation of failure may occur during fabrication or installation. All non-conformances from original design shall be documented, including any anomaly or event. A Design Fabrication Installation (DFI) resume should be established, and reference is given to [DNV-OS-F101, 2007] Dynamic Risers (sec. 12 H200) for details on the required content of the DFI resume. Prior to bringing the pipe into service, all anomalies and non-conformances should be checked and accepted. In case of acceptance of minor faults or the initiation of a specific failure, the impact on the probability of pipe failure shall be evaluated. These known defects should be managed as described in the section above, Section C1.3.3.1.

**C1.3.3.2.2 Unknown (latent) defects** Unknown (not detected) and latent defects from fabrication and installation represent uncertainties which result in an elevated probability of pipe failure compared to what is expected from the evaluation of failure causes, refer to Section C1.3.3.1, which is performed under the assumption that the pipe is in accordance with design specifications. This uncertainty should be addressed in terms of an increased effort in the IM-program with more inspection, testing and monitoring than predicted by an isolated risk assessment of an intact pipe, ref section 3.3.1. A typical basic IM-program is presented in Table C1.1 (in Section C1.3.6). As safety precaution, to detect incipient pipe failures resulting from undetected failure mechanisms, operators should consider putting in place increased monitoring efforts to that could detect precursors to pipe failures such as: wire rupture, pipe twist and increased vent rates.

### C1.3.3.3 New technology

Flexible pipes used in offshore oil and gas production were developed in the 1960ies and taken into use in the 1970ties. Compared to the use of steel pipes the flexible pipe technology is still very young. Applications have become more challenging with time in terms of harsher environments, increasing water depths and production conditions. Flexible pipes are complex multilayer structures with challenging combinations of steel and polymers with a potential multitude of degradation mechanisms and failure modes.

As with all new technology for offshore, new designs have to undergo extensive qualification programs. This is required in [API 17J, 2008] / [ISO 13628-2, 2006] and should ideally ensure detection of all performance and integrity issues but evidently qualification testing has not detected all. The qualification programs, including accelerated tests for instance, are in general not able to properly reproduce the actual conditions experienced by the pipe to such an extent that all failures can be properly evaluated and ruled out.

Integrity issues that were discovered early in the use of flexible pipes have been solved adequately by the industry either by design modifications or tighter use envelops. However, published statistics shows an increasing number of reported failures. New issues have been

discovered over recent years and it would not be surprising if yet more appear over coming years. The industry has to be prepared to deal with these and hopefully detect well before pipes fail and preferably early enough to initiate cost effective mitigating actions.

The challenge is to implement integrity management programs that could facilitate detection of new degradation mechanisms. This requires methods and techniques that provide screening and monitoring of overall performance and features that could reveal anomalies. As a minimum, the complete list of basic inspection, testing and monitoring methods listed in Table C1.1 (in Section C1.3.6) should be incorporated in an IM-program when employing new technology to a flexible pipe. All relevant continuous monitoring methods is recommended used as the experience with new technology is occurrence of new or unexpected failure modes.

#### C1.3.4 Consequence of pipe failure

The operator must identify the consequences and the parameters influencing the consequences of potential pipe failure. The consequence categories should reflect the risk categories described in Section C1.3.5. Reference is given to Chapter B2 Risk Analysis Methodology.

A few aspects to consider are described in the following. The consequences of a pipe failure are dependent on the type of ultimate failure, on the location of the damage and on specific conditions for the pipe and installation - and in particular the combination of these aspects.

Consequences to be considered should include impact on:

- Personnel (health and safety)
- Asset (in addition to the pipe itself)
- Environment
- Economy (for the operator; loss of production, claims and liability)
- Reputation
- Other

As described in Chapter A3 Failure Modes, there are two main types of ultimate pipe failure (i.e. loss of function):

- Blockage or restriction of the flow path caused by failure of a pipe layer or by the bore medium & bore conditions
- Loss of containment - full pipe rupture or leakage limited by intact steel layers

*The consequences of a flow restriction* will in general have low impact on personnel, asset, environment and reputation. The economic consequence will to a large extent depend on the operation and type of pipe. Depending on the cause, the blockage may have the potential to be removed (e.g. removal of hydrates or wax). The possible consequence on pipe integrity involved with removing a pipe blockage should be considered.

The consequence of loss of containment will depend on the pipe content (e.g. water, oil, pressurized hydrocarbon gas), the leakage rate (i.e. differential pressure and leakage path; small hole or full pipe rupture), location of the leakage and the potential exposure to personnel.

- A full pipe rupture leakage from a high pressure gas riser inside or just under a turret can lead to dramatic scenarios with fatalities and loss of key facilities
- A leakage of a production flowline, with a high water cut, close to a step out well away from manned installations will lead to some oil spillage to the sea with a magnitude depending on how early it is discovered

### C1.3.5 Risk assessment

In the process to identify the level of integrity and needs for mitigating measures the operator of a flexible pipe system should perform a risk assessment for all identified potential layer failures and failure causes. Risk is defined as probability of failure (PoF) multiplied by consequence of failure (CoF). The resulting risks should be associated with ultimate pipe failure before mitigating actions. Details on the risk analysis methodology are given in Chapter B2.

Many operators will have defined their own procedures for quantification and assessment of risks often developed for other types of equipment. These procedures may have to be tailored for application to flexible pipes in particular in relation to categorization of PoF and CoF.

An example of a risk matrix is given in Figure C1.2 reproduced from [DNV-RP-F116, 2009].

	Safety	Environment	Cost (million Euro)	Very low	Low	Medium	High	Very high
Consequence				Failure is not expected	Never heard of in the industry	An accident has occurred in the industry	Has been experienced by most operators	Occurs several times per year
Multiple fatalities	Massive effect Large damage area >100 BBL	>10	M	H	VH	VH	VH	
Single fatality or permanent disability	Major effect Significant spill response <100 BBL	1-10	L	M	H	VH	VH	
Major injury, long term absence	Localized effect Spill response <50 BBL	0.1-1	VL	L	M	H	VH	
Slight injury, a few lost days	Minor effect Non-compliance <5 BBL	0.01-0.1	VL	VL	L	M	H	
	No or superficial injuries	Slight effect on the environment <1 BBL	<0.01	VL	VL	VL	L	M

Legend: Risk and risk acceptance criterion

Very low Acceptable	Low Acceptable	Medium Acceptable	High Unacceptable	Very high Unacceptable
---------------------	----------------	-------------------	-------------------	------------------------

Figure C1.2: Example of a risk matrix ([DNV-RP-F116, 2009], Table 4-1

There are additional risks due to the potential hazards described in Section [C1.3.3.2.1](#), Section [C1.3.3.2.2](#) and Section [C1.3.3.3](#):

- Known defects (from fabrication and installation): In case of such defects resulting in an increased probability of pipe failure, this should be accounted for in the risk assessment for known failure modes as outlined in the above.
- Unknown defects (from fabrication and installation): The risk is expected to be larger at an early stage.
- New technology. There is an increased risk due to the increased probability of failure associated with new technology.

When performing the risk assessment, attention should be given to how the governing risk may change over time. Time dependent processes (e.g. fatigue and polymer degradation) may be a low risk (low annual probability of failure) in the early life of the pipe and increasing risk towards the end of the pipe life, while unknown (latent) defects may be a high risk in the early life and decreasing risk over time when building confidence.

### **C1.3.6 Risk mitigation and development of an Integrity Management Program**

When the risk assessment identifies unacceptable risk levels, possible mitigating actions (or measures) that can reduce the risk rating should be identified. This shall be incorporated in an Integrity Management Plan [[DNV-RP-206, 2008](#)].

Mitigating actions including intervals for inspection, testing and monitoring should be evaluated for all failure causes based on the resulting risk rating (Section [C1.3.5](#)).

A new risk assessment should be performed after selection of mitigating actions for all failure causes. Any risks above the acceptance criteria should be reassessed in terms of alternative mitigations. This process should be repeated until all risks are below the risk acceptance criteria. It should be noted that mitigations in terms of inspection, testing and monitoring will not in themselves reduce identified risks but the findings (after assessment of data) may facilitate reduction in the risk rating.

All identified mitigating actions or measures must be combined into an Integrity Management Plan including detailed written procedures. Recommendations for the execution of the activities are provided in Section [C1.4](#).

From experience a typical minimum scope of activities are employed in an IM-program to any flexible pipe irrespective of risk considerations. However, there are reasons to differentiate between dynamic risers and static flowlines. The risk based approach described herein may then provide other mitigation actions *in addition* to these basic activities. The basic inspection, testing and monitoring activities frequently used in IM-plans for any flexible pipe are listed in Table [C1.1](#) along with *typical* intervals for inspection, testing and data review. Note that the listed intervals and sampling frequencies should be interpreted as guidance, and the actual intervals and frequencies shall be based on a specific risk assessment.

Table C1.1: IM:Basic inspection, testing and monitoring activties and intervals (months)

<b>Inspection, testing and monitoring activities</b>	<b>Inspection /testing intervals [month]</b>	
	<b>Flowlines</b>	<b>Risers</b>
<b>Inspection</b>		
External visual inspection (Above sea )	NA	1
External visual inspection (Subsea )	24	24
Internal visual inspection	R	R
Cathodic protection survey	24	24
Sonar / pipe tracker	12 - 48	NA
<b>Testing</b>		
Annulus volume test	NA	12
Annulus ventilation test	NA	12 *
Annulus vent rate test (for comparison:diffusion)	R	12
Annulus gas sampling	R	12
Polymer coupon sampling	36	36
Bore fluid characteristics measurements	NA	R
Pressure test	R	R
<b>Monitoring</b>		
Operational temperature monitoring (including valve position: open/closed)		
6* (Typical sampling rate: 1hour mean)		6 (Typical rate: 1 hour mean)
Operational pressure monitoring (including valve position: open/closed)		
6* (Typical sampling rate: 1min)		6 (Typical sampling rate: 1min)
Bore flow monitoring /Pressure loss	R	R
Annulus volume monitoring	NA	R**
Annulus vent monitoring	NA	R**

Notes:

R: limited to cases of suspected error or damage

NA: Not applicable

\*: driven by other action - practical to perform simultaneously

\*\*: continuous monitoring of high risk risers

## C1.4 Practical Integrity Management

### C1.4.1 Introduction

Inspections, testing and monitoring are performed to control that the lines are operated within the specified operating envelopes and to detect potential accidental events (e.g. impacts), developing damages or degradation processes. Exceedance of the limits may lead to a shortened service life or line failure. A list of possible methods for inspection and integrity monitoring along with related industry practice is presented in Table C1.2:

Table C1.2: Inspection and integrity monitoring methods and related industry practice

Inspection and monitoring method	Industry Practice
Pressure testing offshore (hydro test) <ul style="list-style-type: none"> <li>- Offshore leak test (OLT as defined in [API 17J, 2008])</li> <li>- Structural integrity test (SIT as defined in [API 17J, 2008])</li> </ul>	Common: Used to demonstrate no leak or structural integrity (mostly after installation)
Internal pressure and temperature monitoring	Common
Bore fluid characteristics including sand detection/monitoring	Common. Sand detection / monitoring commonly used on subsea production systems where sand erosion is an issue
External Visual inspection: General visual inspection (GVI) and close visual inspection (CVI). Including cathodic protection survey	Widely used
In-line coupon monitoring	Widely adopted in new systems
Annulus volume test	Widely adopted
Annulus ventilation test	Widely adopted
Annulus vent monitoring	Widely adopted
Annulus gas sampling (including on site gas measurement)	Widely adopted
Sonar	Common for long distance flexible flowlines. Not applicable to short jumpers and risers.
Internal gauging	Often used during commissioning
Radiography	Above sea only. Used in several applications with variable success rate from inconclusive to excellent pictures. Digital processing is recommended. Subsea equipment under development.
Curvature monitoring	Standard system exists. Not commonly used for flexible pipe systems
Internal visual inspection	Limited to cases of potential/suspected internal damage
Fiber optic tensile wire strain monitoring within flexible pipes	Limited. Qualified and in use offshore in Brazil for monitoring of tensile wire rupture
Eddy current methods	Limited
Laser leak testing	Limited
Annulus temperature monitoring	Limited (installed offshore, but limited operational experience)
Ultrasonic inspection	Limited. In development
X-ray based tomography	Successfully used in R&D but no known offshore experience
Torsion monitoring	Used in Brazil
Acoustic emission (for detection of tensile wire or carcass failure)	Limited offshore experience
Non-intrusive stress monitoring (sensors based on changes in the magnetic properties of armour wires in response to applied stress)	Campaign based inspection
Online vent gas analysis	In development

Note: Indirect riser monitoring methods like top end excursion, sonar based systems, tension measurements, and H<sub>2</sub>S measurements etc. are not included in the table.

The present report concentrates on basic inspection, testing and monitoring methods included in an integrity management system. For completeness, other common or widely adopted

methods are included although they are usually not performed regularly. Attention is given to the following methods:

#### Inspection

- External visual inspection
- Internal visual inspection (usually not performed regularly)
- Cathodic protection survey
- Sonar

#### Testing

- Annulus volume test, annulus ventilation test, annulus gas sampling
- Polymer coupon sampling
- Bore fluid characteristics measurements
- Pressure test (usually not performed regularly)

#### Monitoring

- Operational temperature monitoring (including valve position: open/closed)
- Operational pressure monitoring (including valve position: open/closed)
- Bore flow monitoring
- Annulus vent monitoring

The present report describes how to perform these activities and implement this into an integrity management system including data review, evaluation and reporting. The Sureflex JIP and the Sureflex Guidance Note ([MCS Kenny State of the Art, 2010] [MCS Kenny Guidance Note, 2010]) are recognized as providing descriptions of these methods. However, the Guidance Note needs additional explanation. The present report emphasizes guidance and recommendations for review and evaluation of these activities.

Note that the recommendations for test or inspection intervals or sampling frequencies should be interpreted as guidance, and the actual intervals and frequencies shall be based on specific risk assessment.

Further, it is also of importance to have strict procedures and reporting tools in place to facilitate swift and proper actions in the event of line anomalies, as well as consistent handling of anomalies.

The inspections, testing and monitoring records shall be reviewed by technical experts on a regular basis. This is proposed to be done during a regularly issued status report. The status assessment shall reflect the asset's capability for safe and reliable operation. Critical findings that are revealed through the status assessment shall be mitigated through a dedicated action task list with deadlines and responsibilities.

### C1.4.2 Inspections

#### C1.4.2.1 External visual inspection

**C1.4.2.1.1 Purpose** General visual inspection (GVI) is performed to detect gross damages to the flexible pipe and its ancillaries. The survey should preferably cover the entire pipe length. Close visual inspection should be performed at critical areas both subsea and above sea level.

**C1.4.2.1.2 Description** Subsea inspections are normally performed by use of ROV. General visual inspections have limited capabilities in detecting smaller damages; this is particularly the case for pipes with marine growth or with large dynamic motions. Inspections may further be restricted by bend stiffeners, guide tubes and difficult access near interface to an installation or vessel, or by trenching and rock dumping. Subsea inspections of flexible pipes will in general only detect failure modes that have already developed into a gross component failure (e.g. sliding clamp) or pipe failure (leak). Several failure modes progress from the internal pipe structure and are thereby not visible before they result in loss of bore containment in one way or another. Still, leaks can occur without being detected by topside instrumentation such as flow- and pressure monitoring. Regular subsea line GVI is therefore important in the context of detecting smaller line leaks that has not (yet) developed into a full loss of containment.

Based on experience and pipe configuration, some areas may be selected for close visual inspection. Examples are given below.

**C1.4.2.1.3 Recommendations** An external visual inspection survey should comprise the following:

- **Surface inspection of the external sheath** to identify wear/abrasion or damaged external sheath. Bubbles and/or liquid escaping from the external sheath may indicate a damaged external sheath or loss of containment (micro leaks)
- **Assess the pipe lay-out configuration** and as a minimum identify the depth and location of touch down point, hog and sag bends (for risers in wave or S-configurations)
- **Assess the condition of ancillaries** and verify that ancillaries are in position, a few examples:
  - Buoyancy modules: verify the number, location and spacing of modules
  - Mid-water arch: look for wear and surface defects (dropped objects), assess marine growth and anodes
  - Tether clamp: look for corrosion products, scratches, dents or buckles in the outer sheath near the clamp, inspect the connection between clamp and tether
  - Tether: Verify tension and angle of tether, verify configuration of the tether arrangement, verify intact outer hose on tether (look for wear and signs of degradation), inspect connections to clamp and gravity base (look for wear in pad-eye), look for wear and corrosion products
  - Gravity base: Verify location and orientation of gravity base, look for signs of movement of the gravity base (sand dunes or local depressions/scour in the ground near the gravity base)

- **Inspection of previous repairs** (clamps, polymer welds) and previously reported anomalies (to capture development/progress of a possible failure).
- **Inspection of end fitting** to reveal any excessive corrosion on the steel surface, coating degradation, cracks or end fitting seal failures. For the end-fittings that are inside housing or covered in insulation, the inspection shall seek to inspect the housing or insulation while the inspection objectives remain the same.
- **Inspection of bend restrictors and guide tube ducts** to look for excessive corrosion or restrictor malfunction such as component unlocking. A bend restrictor anomaly may be an indication of a problem that is developing and the anomaly must be assessed by expert personnel.
- **Inspection of rock dumped** sections to check for rock dump coverage, bubbles and detect and inspect the external sheath at exposed sections, emerging buckling (prior to exposure of the pipe), change in shape of rock dump.
- **Inspection of all gas relief valves (GRV)**, for pipes equipped with such, to reveal any anomalies that may indicate insufficient venting capacity. Excessive marine growth or any other obstruction that may limit venting capacity shall be removed. Note that the GRVs are fragile and may be damaged by ROV intervention. Bubbles escaping from GRVs are normal behavior for a line in production, but any observations shall still be reported and reviewed, also the absence of bubbles shall be reported.
- **Perform anode potential reading** where possible; details are given in Section [C1.4.2.3](#).
- **Look for protruding surfaces or excessive marine growth** that may lead to external sheath damage, particularly near bending restrictors, end of rock dump and at guide tube exits

Unburied / exposed sections shall be continuously evaluated with respect to risk of trawl, anchor or dropped object damage.

Evidence of upheaval buckling may sometimes be difficult to locate unless the pipe is lying uncovered in a trench or clearly protrudes above the seabed/rock berm. For covered pipes, sonar techniques could be applicable, see Section [C1.4.2.4](#). Occasionally, pipes can lose cover through upheaval creep that is a gradual lifting of sections of the pipe, without any effect on pipe integrity (i.e. no bend radius problems etc.). In such cases, visual inspection shall seek to identify the unburied sections, any spans or damage and comparison between periodic GVI records should be used to determine if upheaval is gradually increasing or presenting a risk of trawl, anchor or dropped object damage.

Topside GVI should include inspection of end-fitting and pipe hang-off arrangement to assess the structural integrity and to identify any ongoing excessive corrosion process. Evidence of hang-off movement must be reported. The inspection in its most simple form may be performed on the daily area inspection. Further, the annulus vent system should be subject to topside CVI to reveal any anomalies related to corrosion, routing or operational errors (valves etc.). The CVI of the topside annulus vent system includes a surface inspection of the most central parts of the ventilation system to verify that the system is intact, that no unreported modifications have been performed and that no damage to the tubing has occurred. All valves on the system shall be checked to be in the correct position.

General data at the time of survey should be obtained and reported, including vessel draught, location and orientation, pipe operational condition and pipe content density, sea level (water depth) including tide and environmental conditions such as current and wave.

General visual inspections are recommended at regular intervals; annually for hydrocarbon-carrying or critical risers or flowlines and at least biannually for pipes not containing hydrocarbons. If other testing or monitoring data indicates line rupture or leakage, the line should as soon as possible be subject to an external general visual inspection along the entire length, in addition close visual inspection should be performed at selected areas.

**C1.4.2.1.4 Evaluation of inspection results** Any anomalies shall be documented systematically with video and reviewed by expert personnel. Close visual inspection should be performed where specific issues or defects are identified. Results from the inspection should be compared to those from previous inspections and the as-installed survey. Non-conformances and deviations reported and accepted during previous inspections and as-installed surveys should always be included in report appendix. The external sheath GVI should be coupled with a dropped-objects reporting protocol in order to ensure that visual inspections of the pipe are conducted after any incident considered likely to have resulted in a dropped object falling on or close to the pipe or its ancillary equipment. The same applies to critical work being conducted near a flexible pipe.

#### **C1.4.2.2 Internal visual inspection**

**C1.4.2.2.1 Purpose** Internal visual inspection is usually *not* performed regularly as part of an IM-program. This inspection is often limited to cases of potential or suspected internal damage. The internal visual inspection is used to identify bore flow obstacles and to assess the condition of the carcass (or pressure sheath in smooth bore pipes), in addition to its historical use for assessment of pressure sheath crimping in end-fitting.

**C1.4.2.2.2 Description** Internal visual inspection requires shut-down of the pipe, and the inspection will often require preceding flushing or cleaning of the pipe's internal. Access to bore for the internal inspection camera is often obtained by disconnecting topside process piping close to the end of the flexible pipe. In addition to the pure visual inspection, the inspection could be combined with different measurement tools, such as carcass profile or ovality measurements.

**C1.4.2.2.3 Recommendations** Internal visual inspection should be performed after incidents with (potential) or suspected internal damage, and when old pipes are checked for potential re-use. After removal of hydrate/wax plugs, the carcass should be inspected both upstream and downstream of the hydrate plug location.

**C1.4.2.2.4 Evaluation of inspection results** No permanent deformation of the carcass is allowed in dynamic sections. For static sections, fit for purpose analysis shall be done. No significant axial movement inside end-fittings is allowed. In cases where carcass axial

overload is a concern, the carcass pitch (e.g. fully extended) should be evaluated to assess the utilization of the carcass capacity.

#### C1.4.2.3 Cathodic protection survey

**C1.4.2.3.1 Purpose** The purpose is to assess the functionality of the cathodic protection and to assess the anode consumption; extensive anode consumption indicating an ongoing corrosion process.

**C1.4.2.3.2 Description** The cathodic protection potential is measured by the use of probes measuring the electric continuity and anode potential. Anode consumption is assessed by an estimate from visual inspection of the anode system. The visual inspection is inaccurate also due to the anode properties; the outer part of anodes may become fluffy and porous such that the solid part of the remaining anode may be significantly smaller than what appears from a visual inspection.

**C1.4.2.3.3 Recommendations** When measuring anode potential, direct contact with bare metal should be ensured. If in doubt of contact with metal, it is advised to make a scratch in the metal coating. The exact location of test/measurement should be documented to allow for repeatability of the test.

Observed or reported significant anode consumption should lead to a check of the anode design report. In response to confirmed significant anode consumption, there should be actions to investigate the cause in addition to replacement of depleted anodes. Potential causes include electric connection to surrounding structures. Reduced cathodic protection (reduced amount of anodes and an increased rate of anode consumption) make the pipe more vulnerable to outer sheath damages.

**C1.4.2.3.4 Evaluation of inspection results** Assessing the anode consumption is difficult and dependent on experience, although fresh anodes (close to 100%) and anodes almost depleted (<10%) are more easily identified. Be aware that reported values from a survey may be misleading.

Requirements and acceptance criteria for cathodic protection of subsea pipelines are provided in [[NORSOK M-503, 1997](#)] (NORSOK Cathodic protection) and the references herein. For further details on cathodic protection, reference is given to [[DNV-RP-B401, 2010](#)] (Cathodic Protection Design) and [[DNV-RP-F103, 2010](#)] (Cathodic Protection of Submarine Pipelines)

---

#### C1.4.2.4 Sonar

**C1.4.2.4.1 Purpose** Sonar is applicable to long distance flexible flowlines, not for short jumpers and risers. The purpose is to assess the pipeline's configuration and detect deviations, e.g. upheaval buckling of the pipe, loss of cover, burial depth, free spans, etc. Sonars may also be mounted near the topside end (below a turret) for topside monitoring

of riser configuration (movement and angles/declination) and bend stiffeners; primarily to verify that structures are in place. Permanent monitoring could be considered near interfaces/connections to provide an early warning for pollution or leakage by applying sonars capable of leak detection (detection density variations). This is applicable to MEG in seawater and oil in seawater (although this is expected to be detected more directly visually if light is available). Such leak detection is applicable to static sections and more difficult in dynamic sections.

**C1.4.2.4.2 Description** Ship-borne sonar is now widespread for flowline application and is likely the preferred method. The side scan sonar survey may also be performed by a vehicle equipped with sonar which is either towed by a ship, mounted on an AUV (autonomous underwater vehicle), or mounted on a ROV which in turn is connected to a survey vessel. Anyway, the vessel/unit carrying the sonar will be moving along the pipeline to obtain a picture of the pipeline configuration, surrounding seabed topology, dropped objects and structures.

**C1.4.2.4.3 Recommendations** To assess upheaval buckling it is recommended to perform inspections regularly to inspect for change in free span and potential progressing or emerging upheaval buckling. Further, the pipe should be inspected to verify the burial depth, configuration and that expansion covers are in place.

**C1.4.2.4.4 Evaluation of inspection results** The results should be compared to the as-installed and as-laid reports as well as to preceding reports to identify any changes. The inspection should also assess changes to seabed features such as erosion, slides and piles of drill cutting. Any initial leak detection by sonar should be followed by a close visual inspection for further investigation.

## C1.4.3 Testing

### C1.4.3.1 Annulus volume testing

**C1.4.3.1.1 Purpose** The purpose of the annulus free volume test is to evaluate outer sheath integrity and monitor annulus liquid filling/blockage. The riser annulus is expected to stay dry or have a slow liquid filling over time depending on the diffusion through the pressure barrier and condensation, normally calculated by the manufacturer based on operational data. The integrity of the external sheath and presence of permeated liquid is important input to service life assessments. Potential micro leaks from bore may be interpreted as annulus water filling.

**C1.4.3.1.2 Description of the test** The normal annulus free-volume test is recommended to be performed by pressurizing the riser annulus to 3 barg with Nitrogen (or another inert gas) from a bottle with a known volume. Then by measuring the pressure drop in the Nitrogen bottle and the pressure build-up in the riser annulus, the free annulus volume can

be calculated. The calculation should account for the temperatures in the bottle and in the annulus.

There are additional test methods supplementary to the recommended 3barg positive pressure test, these are: vacuum testing, stepwise positive pressure test (1-2-3 barg test) and test by filling a small volume of liquid (e.g. MEG).

Vacuum testing may be an alternative to the normal positive pressure test under certain conditions. This test may be combined with a positive pressure test to obtain a higher differential pressure or in combination with a lower positive pressure than normal in case of limitations in maximum allowable pressure. Vacuum testing may also be used in combination with a 1-2-3-barg test. Vacuum testing could also be used as a standalone test. However, vacuum testing is considered less accurate than the positive pressure test to 3barg.

A stepwise positive pressure test (1-2-3 barg test) may be performed subsequent to a normal annulus test as a check of extraordinary test results and when suspecting breached outer sheath. The test is performed in the same manner as the normal positive pressure test: annulus is pressurized in steps to 1barg, 2barg and 3barg, and for each step the annulus pressure is stabilized and the free volume is calculated.

A test by filling a small volume of liquid (MEG) may be performed subsequent to the normal and stepwise pressure tests in case of unclear results or when suspecting a breached outer sheath. After the regular annulus test, a known amount of liquid (MEG) is injected into the annulus. Subsequently, a new regular annulus test is performed. The resulting free annulus volumes from the two tests are then compared. An intact outer sheath is indicated if the difference between the two calculated free annulus volumes corresponds to the injected amount of liquid.

#### C1.4.3.1.3 Recommendations

Caution should be exercised when applying a positive pressure test on the following pipe systems:

- Smooth bore pipes: Generally, these pipes have less collapse resistance and are vulnerable to pressure differences across the pressure sheath (i.e. between bore and annulus). The test procedure and the applied test pressure should be adjusted to account for the pipe collapse capacity with ample margin. This is of particular importance for conditions with an empty bore or a low bore pressure (or vacuum). Smooth bore pipes may have a polymeric Intermediate sheath terminated at the pipe ends, encapsulating the pressure armour. There is then an inner annulus between the pressure barrier and the intermediate sheath and an outer annulus between the intermediate sheath and outer sheath. Radial forces due to overpressure in the outer annulus are then transferred to the pressure armour and not to the pressure barrier.
- Pipe systems with gas relief valves (GRV): The test procedure and applied test pressure should be adjusted to account for the release pressure on the valves. Unintended opening of the valves will produce a wrong test result. Possible liquid filling height in annulus must be accounted for.
- Risers in wave or S-configurations with large height differences between sag and hog bends: Breach of the outer sheath might be a risk for risers in such configurations with liquid filled annulus where gas pockets may form in sections along the pipe, expected to be located in hog bends. Due to the height differences and the varying internal density (liquid/gas) of the annulus along the pipe, there will be variations

in the differential pressure across the outer sheath. The critical case would be a gas pocket extending from bottom of the sag bend to top of the hog bend. The resulting differential pressure across the outer sheath at the top of the hog bend will then be due to the external water column over the vertical distance of the internal gas pocket and the additional internal test pressure. The outer sheath typically has a capacity to withstand a differential pressure in the order of 7 barg (dependent on temperature, time, manufacturing tolerances, scratches etc).

In any event, care should be taken to avoid the annulus pressure exceeding the capacity of the outer sheath. If there are indications that the exerted pressure results in an annulus pressure above the test pressure, due to a significant pressure drop/increase across the vent port, corrective actions must be taken to avoid exceeding outer sheath capacity, e.g. reduced test pressure and limited test time. Ventilation, in terms of flow out of the vent port, should be verified after the pressurization period.

After having pressurized the annulus, there should be sufficient time to allow for stabilization of the annulus pressure. A constantly decreasing pressure indicates a leakage, either in the test equipment assembly, in the end fitting or in the outer sheath. This is described in more detail below. This is described in more detail below.

The importance of a consistent test methodology for every test of a pipe is emphasized in order to limit the inaccuracies. It is recommended to perform periodic annulus volume tests. The test interval is dependent on the use and operational condition of the pipe: Annual testing is recommended for pipes with no expected anomalies, carrying hydrocarbons at high pressure. The test interval should be set to capture any new damages before they reach a critical level. Frequency of testing is of importance when establishing the time of an outer sheath breach. More frequent testing should be considered in case of nearby activities with probability of damage or known accidental events and for pipes where an outer sheath breach is critical. Corrosion and fatigue is expected to be an increasing problem in the future as the new revision of the [API 17B, 2008] allows for a higher utilization of armoring wires which implies a reduced steel area, and correspondingly reduced margin for corrosion damages.

**C1.4.3.1.4 Evaluation of test results** The resulting annulus test volume is compared to the reference volume and earlier annulus volume test measurements. The reference volume should preferably be the post-installation volume, but can alternatively be either the theoretical free volume or FAT volume.

For a riser in operation, slow filling or blockage of the annulus in the configuration low point is expected due to condensation of gas diffused through the pressure barrier. This can be monitored by performing annulus volume testing at regular intervals. Any sudden changes may be identified and should then be investigated as necessary. Different causes for liquid filling of the annulus are experienced on pipes in operation: liquid filling due to diffused gases through the pressure sheath, ingress of seawater due to outer sheath breach or due to missing vent plug in subsea end-fitting, micro-leakage from bore to annulus through end-fitting and liquid filling through platform vent system (liquid from neighboring risers).

Slow filling of the test medium into the annulus during testing could be encountered in pipes with porous insulation layers in the annulus due to micro channels in these layers which provide narrow passages for the gas and due to the potentially significant volumes in these structures.

A test which is unable to obtain pressure build-up would normally indicate a leakage in the test equipment or in the connection onto the piping, vent port or the flare system. A re-test should then be performed after having verified leak tight test equipment and ensured no leaks in any connections or piping system. A re-test then unable to obtain any pressure build-up indicates a hole in the outer sheath above sea water.

Liquid filling to sea surface is the first indication of a hole in the part of the outer sheath located below the sea level. Due to the communication through a hole, the applied test pressure (3barg) is expected to lower the water column inside the pipe by 10m per 1barg test pressure. Hence, the measured free volume indicating liquid filling to sea surface will be the annulus volume corresponding to the length of the pipe above water and the additional length due to lowering of the water surface (approximately 30m at 3barg). A free volume corresponding to liquid filling to sea level and a stabilizing pressure at 3barg then indicates that the hole is located 30m or further below the sea surface. A free volume corresponding to liquid filling to sea level and a stabilizing pressure less than the feeding pressure (3barg) indicates a hole below the sea surface and above 30m below the sea surface.

In case of an outer sheath breach located below the sea level, the resulting volumes from a stepwise positive pressure test (1-2-3 barg test) should increase fairly linearly as the pressure is gradually increased from 1barg to 2barg and 3barg. For a pipe with intact outer sheath, the calculated volumes should ideally be nearly identical for all three pressures. Further, in case of a riser in wave or S-configuration, compressibility of any gas pocket formed in the hog bend region may lead to results which may be misinterpreted as a breached outer sheath. It should be noted that all testing at small differential pressures as 1barg and 2barg inevitably introduces uncertainties in the test results.

Annulus volume testing has the potential to detect a hole in the outer sheath located above seawater and down to a water depth of approximately 20-30m depending on test pressure, and may have the potential to detect a hole below 30m relying on water filling of the annulus. The capabilities of annulus testing are limited by the pipe configuration. In particular this relates to risers in wave or S-configuration and to pipe segments located on the seafloor with an inclination (due to seabed topology) from the test side (e.g. in a section from TDP to subsea end-fitting).

For pipes with a measured free volume corresponding to a free distance down to the sag bend, limited information can be deduced about the condition of the annulus further down towards the subsea end. Examples are observed where the anticipated liquid in the sag bend (indicated from annulus testing) may have a local extent while the remaining part of the annulus further down could be dry or liquid filled in sections. Despite this limitation, outer sheath breaches are expected to manifest themselves over time in terms of liquid filling to the sea level. For the purpose of differing between ingress of sea water and condensation processes, time span is of importance. This is another argument for annual annulus testing.

### C1.4.3.2 Annulus Ventilation Flow Test

**C1.4.3.2.1 Purpose** For most risers, gas is diffusing through the pressure liner and into the annulus void, and to some extent further out of the external sheath. To avoid pressure build-up in the annulus and subsequent outer sheath breach, the diffused gas has to be ventilated out through the annulus vent ports. Normally, risers have three vent ports and preferably all ports should be connected to a vent system. Over time, the vent port flow

may be restricted and it is thus necessary to perform flow capacity check at regular intervals to enable early detection of any flow restriction. Additionally, a minor hole initiating in the pressure sheath may manifest itself in terms of an increased diffusion rate.

**C1.4.3.2.2 Description** The vent port flow capacity is measured by using a flowmeter.

The flowrate through the individual vent ports are measured after the free volume test is performed, i.e. flow out of annulus with normally 3barg overpressure in riser annulus. If all three riser vent ports are accessible and connected to the vent system, the flow rate should be measured through all three vent ports individually.

**C1.4.3.2.3 Recommendations** Periodic measurement of the annulus vent flow capacity is recommended and the activity is considered an important integrity check of the flexible riser. The recommendations for test intervals are similar to those given for annulus testing in Section [C1.4.3.1.3](#): Annually for pipes with no expected anomalies, carrying hydrocarbons at high pressure. More frequent testing should be considered for pipes with known restricted vent flow.

In any event, care should be taken to avoid the annulus pressure exceeding the capacity of the outer sheath. If there are indications that the exerted pressure results in an annulus pressure above the test pressure, due to a significant pressure drop/increase across the vent port, corrective actions must be taken to avoid exceeding outer sheath capacity, e.g. reduced test pressure and limited test time.

**C1.4.3.2.4 Evaluation of test results** The assessment of vent system functionality should be related to each riser's individual design diffusion rate. The riser design diffusion rate is normally given in the Flexible Pipe Design Report or Operating and Maintenance Manual, or has been documented by a more detailed diffusion analysis elsewhere. The design diffusion rate is the calculated amount of gas flow from riser annulus during riser operation at design parameters, however often omitting the permeation through the outer sheath.

The following definitions to assess the vent system functionality are recommended:

Table C1.3: Assessment of vent system functionality

Functionality Categories	Evaluation Criteria	Description
Ok	<ul style="list-style-type: none"> <li>- Above 4 x riser design diffusion rate</li> <li>AND</li> <li>- practical to perform an annulus volume test</li> <li>AND</li> <li>- Not decreasing trend in vent flow rate since FAT and previous vent flow tests</li> </ul>	Excess vent flow capacity is available; vent flow failure is not expected in the near future.

Functionality Categories	Evaluation Criteria	Description
Restricted	- Above riser design diffusion rate and less than 4 x riser design diffusion rate OR - Decreasing trend in vent flow rate since FAT and previous vent flow tests	Vent system flow is partially blocked, and the flow capacity is reduced. The vent system has enough flow capacity to avoid larger pressure-build up in riser annulus.
Less than design	Less than riser design diffusion rate	The vent flow capacity is less than the diffusion design values and hence not acceptable. Further actions are recommended to increase the flow. When the flow is this low complete blocking of the vent ports are also likely. Until the flow is re-established more frequent testing or monitoring is required if the design values are not reduced. If only a single vent-port is functional, similar consideration may apply due to loss of redundancy
Blocked	Not measurable	No communication to riser annulus through vent ports. Vent system does not have capacity to fulfill its purpose. Pressure build-up in riser annulus is likely, and mitigation actions should be taken immediately.

### C1.4.3.3 Annulus Gas Sample Collection

**C1.4.3.3.1 Purpose** An annulus gas sample is taken to evaluate if the annulus gas contains corrosive gases such as H<sub>2</sub>S, O<sub>2</sub>, CO<sub>2</sub>, or H<sub>2</sub> indicating that a CO<sub>2</sub>-corrosion process is ongoing, and may also provide indication of potential pressure sheath leakage.

**C1.4.3.3.2 Description** One or two annulus gas samples are extracted by using a vacuum pump or by direct filling from a pressurized annulus into a non-diffusing test bag and shipped to a laboratory for analysis of gas composition.

**C1.4.3.3.3 Recommendations** Continuous monitoring of the annulus gas composition allows for a more direct surveillance of a suspected ongoing corrosion process and may also provide an early warning of an emerging breach in the pressure sheath, or an end fitting seal problem.

**C1.4.3.3.4 Evaluation of test results** The annulus gas samples are analyzed to establish the composition and amount (fraction) of different compounds and the development over time (trends). Light hydrocarbons are expected to diffuse through the pressure barrier while heavy hydrocarbons are expected to be kept in the bore. Hence, the presence of heavy hydrocarbons in the annulus gas may indicate a possible bore leakage (permanent or minor at start up and shut down). The presence of both H<sub>2</sub> and CO<sub>2</sub> may indicate an ongoing corrosion process in the annulus (of tensile or pressure wires).

#### C1.4.3.4 On Site Gas Measurement

**C1.4.3.4.1 Purpose** On site gas measurements are normally performed to detect the presence of H<sub>2</sub>S. Online gas measurements may also be integrated in the annulus gas vent monitoring unit.

**C1.4.3.4.2 Description** The gas sample measurement can be performed by using indicator tubes, where annulus gas is drawn through.

**C1.4.3.4.3 Recommendation** The testing for H<sub>2</sub>S may be performed on pipes where its presence is anticipated to verify conditions according to design: annulus environment, permeation rates and the concentration's development over time (trend).

**C1.4.3.4.4 Evaluation of test results** For a flexible pipe annulus containing water or moisture, the majority of any H<sub>2</sub>S present in the annulus is assumed to react with iron iones in the water, hence limited H<sub>2</sub>S is measured in the vent gas. Thus, it may be difficult to test for H<sub>2</sub>S. For a flexible pipe with a dry annulus (e.g. the upper riser section close to topside end), the presence of H<sub>2</sub>S in annulus is not expected to react with the iron and hence it is expected to be measured in annulus gas.

Sudden increase in concentration should be further investigated including the possibility for a bore leakage.

#### C1.4.3.5 Polymer coupon sampling

**C1.4.3.5.1 Purpose** Polymer coupon sampling is at present relevant for PA-11 only, and is a supplement to ageing calculation as coupons provide a more accurate and direct measurement of the degradation.

**C1.4.3.5.2 Description** The coupons are immersed in the process stream and arranged either in racks or as single discs or samples. Coupons are then sampled over the lifetime of the pipe and the coupons are sent to laboratory for analysis.

**C1.4.3.5.3 Recommendation** Polymer coupons should preferably be located at that end of the pipe most likely exposed to the maximum temperature; predominantly the upstream end of the pipe. Higher temperatures typically promote PA-11 degradation. The subsea well is typically the high temperature end on a production riser. To ease the sampling of coupons from such riser systems, the coupons might be located near the topside end. The results from these coupons must then take into account the temperature difference between the topside and subsea ends. To compensate for the temperature difference, it may also be possible to place the coupons in a test spool with the same process flow at an elevated temperature corresponding to the conditions at the high temperature end.

**C1.4.3.5.4 Evaluation of test results** The coupons may be sampled at regular intervals to obtain a trend line or to verify ageing calculation at the time when the calculated ageing is close to the limit. The typical testing of sampled coupons includes measurement of the Corrected Inherent Viscosity (CIV) and tensile testing if the coupon size permits. The test results should be correlated with records of temperature and temperature degradation analyses. Additional information and guidance on polymer ageing and degradation and polymer coupons are given in Chapter A3 Failure Modes in the present handbook.

#### **C1.4.3.6 Bore fluid characteristics measurements**

**C1.4.3.6.1 Purpose** Bore fluid characteristics measurements are performed to verify operation of the pipe within design limits for corrosive conditions (carcass and annulus environment) and for degradation assessment of pressure barrier and other polymer layers. Sand content is used to assess erosive conditions.

**C1.4.3.6.2 Description** Measurement of bore fluid properties is either assessed by analysis of samples or by online instruments ( $H_2S/CO_2$ ). In any case, bore fluid monitoring is often performed in topside process system.

**C1.4.3.6.3 Recommendations** When interpreting the bore fluid characteristics measurements, it is important to have knowledge and understanding of the specific process lay-out. Dependent on the subsea and topside process lay-out, obtaining representative samples for a specific riser may be difficult. In everyday production several wells/risers are often connected to a common manifold, and the samples collected are a mix from multiple wells. Sampling from a test separator would be beneficial. During well testing, one single well is run through a 'test separator' and samples for that specific well may be collected. Another source for bore fluid characteristics is reservoir models and results from production test during exploratory drilling. This is often the only source for bore fluid characteristics during design of the pipe system. For installations where all wells produce from the same reservoir or the bore fluids are similar across the risers, representative samples are more easily obtained.

Bore fluid characteristics should be measured periodically, upon changes in reservoir zone for production or at least every 5 years.

Ageing issues may be heavily dependent upon information on acidity and pH for crude and water phase. Water samples should be taken by expert personnel according to procedures for the purpose of laboratory testing.

Measuring low levels of  $H_2S$  may require special equipment and procedures.

**C1.4.3.6.4 Evaluation of measurements** The following parameters should be established: Gas/oil ratio (to be seen in relation to type of pipe: GI, WI, OP), water cut, amount and partial pressure of gas components (in particular  $H_2S$  and  $CO_2$ ), TAN, additive chemicals, sand production and bore fluid pH.

### C1.4.3.7 Pressure test

**C1.4.3.7.1 Purpose** Pressure testing is usually not performed regularly as part of an IM-program. A pressure test is usually performed on lines that are recently installed and lines that have been out of service for years. A hydrostatic pressure test is appropriate in determining the immediate general condition of a static flow line or riser because it applies loads in the principal directions of the in-service loads. The pressure test will therefore provide a measure of confidence that the line has a residual life given that the maximum operation pressure is sufficiently below the test pressure. In case of suspected material loss due to corrosion, a pressure test and subsequent de-rating to a lower pressure may be appropriate for continued short term operation.

**C1.4.3.7.2 Description** [API 17B, 2008] distinguish between two types of pressure tests dependent on the applied pressure: a leak test is performed at 1.1 times the design pressure and a structural-integrity test is performed at 1.25 the design pressure. For details, reference is given to [API 17B, 2008].

**C1.4.3.7.3 Recommendations** Latent defects triggered by internal pressure may be detected by a pressure test. Pressure tests are often performed with the pressure and temperature instrumentation isolated from the pipe. Hence, it is important to document pressure tests and ensure test data are properly stored. Pressure tests are often seen as extensive operations and include the change of bore medium (hydrotect). Performing pressure test with hydrocarbons and/or gas in bore requires a separate risk assessment. If possible, perform pressure test at temperatures reasonably close to operational temperatures (recommended due to possibly undesired additional loading from low temperature and high pressure / in case of armour defects, higher temperature during test will provoke failure during pressure test). If possible, monitor pipe twist during testing.

**C1.4.3.7.4 Evaluation of test results** For non-torsionally stable pipes, compare observed twist to design values. For torsionally stable pipes, no torsion should be observed during pressure testing. If possible, check elongation of pipe and check against design values. The test acceptance criteria in terms of pressure and time are given in [API 17B, 2008].

## C1.4.4 Monitoring and monitoring data review

### C1.4.4.1 Temperature and pressure monitoring

**C1.4.4.1.1 Purpose** Temperature and pressure monitoring is used to monitor exceedance of operational limits and records of temperature may be used for polymer ageing calculations while records of pressure may be used to evaluate critical pressure surges and cycles.

**C1.4.4.1.2 Description** The monitoring activity includes evaluation of the maximum and minimum values in addition to time series over the lifetime of the riser. Monitoring of product temperature and bore pressure should be applied to all flexible pipe system.

Maximum temperatures and pressures are most likely to occur at the upstream end of the pipe, while minimum temperature occurs at the end of pressure bleed which could be either upstream or downstream. For a riser used for production, the upstream end would be at the wellhead side and the downstream end at topside end. Opposite for a pipe used for gas injection, the upstream end would then be topside end and downstream end at the wellhead side. (topside end for a riser).

**C1.4.4.1.3 Recommendations** Temperature and pressure monitoring instruments should preferably be located as close as possible to the flexible pipe itself (ideally inside the flexible). In case process equipment (such as cooler or separator) and valves are located between the pipe and the instrument, care must be taken to ensure understanding of the process and what is actually measured: an assessment should be made on temperature and pressure measurement relevance. Preferably the pipe should be instrumented at both the inlet and outlet. In case of one instrument only, the instrument should preferably be located at the upstream end as this is most likely exposed to the most extreme conditions. For pipes missing downstream or upstream instruments, temperature and pressure must be assessed by calculations, flow models or by extrapolation of values. This will clearly introduce uncertainties and prohibit full utilization of the pipe.

Recommended period of sampling is 1 hour average for temperature instruments (Due to heat capacity. Slow variations compared to pressure). Recommended period of sampling is 1 minute for pressure. Records of temperature and pressure history shall be maintained for the lifetime of the structure and assessed on a yearly basis. The temperature assessment shall be coupled with pressure barrier degradation analyses. EV data should also be stored, it is sufficient to have sampling when opened and closed.

#### **C1.4.4.2 Bore flow monitoring**

**C1.4.4.2.1 Purpose** Flow - or flow rate - monitoring is a strategy for detecting both bore flow obstructions and loss of containment as this may be indicated by a sudden drop in flow or changes to bore pressure-flow ratio without other changes in operational conditions.

**C1.4.4.2.2 Description** The flow rate is monitored directly by on-line instrumentation with direct communication to the control room.

**C1.4.4.2.3 Recommendations** Observed irregular events should be immediately investigated by expert personnel. Possible causes of bore flow obstructions are wax deposits, hydrate formation and collapse of carcass and/or pressure sheath, while possible causes for loss of containment are significant leakage or full pipe rupture.

#### **C1.4.4.3 Annulus vent monitoring**

This section should be read in light of Section [C1.4.3.1](#) and Section [C1.4.3.2](#) on annulus volume testing and annulus ventilation flow test, respectively.

**C1.4.4.3.1 Purpose** Continuous annulus vent monitoring is an extension of the periodic annulus volume and ventilation flow tests and is appropriate where additional surveillance is required. As such, the purpose of continuous annulus vent monitoring is primarily to detect any unexpected vent performance in terms of increased annulus pressure and/or flow rate, or a reduced flow indicating restricted (or blocked) vent flow through the vent ports. Available annulus vent monitoring systems also provide monitoring of the free annulus volume. A hole in the outer sheath above sea level may be detected either in terms of a sudden loss of overpressure. Equivalent to standard annulus volume tests, the free annulus volume may also be estimated based on depressurization rates and vent flow: The starting point is then an intentional pressure build up in annulus (e.g. to 3barg). This is then succeeded by flow measurements of vent gas during the depressurization of annulus (e.g. to 1 bar). The free annulus volume may then be calculated from the pressure drop in annulus and the total outflow during the depressurization.

**C1.4.4.3.2 Description** Dependent on the purpose and installation, the monitoring system may be directly connected to the control room and alarms may be set to predefined levels.

**C1.4.4.3.3 Recommendations** Successful implementation of annulus vent monitoring requires accompanying procedures for actions upon significant deviations and extraordinary results. These procedures and the interpretation of the results must take into account changes in flow rate, pressure and free volume due to changes in operational conditions.

#### **C1.4.4.4 Overview of the monitoring data review process**

The monitoring data review process is characterized by the following main tasks which are further described in the next sections:

1. Verify system data and compile input data
2. Assess data quality and coverage
3. Data review:
  - (a) Maximum and minimum values
  - (b) Operational envelope (histogram) and hours above limit
  - (c) Differential pressure along the pipe
  - (d) Pressure and temperature cycles
  - (e) Polymer ageing (applicable for nylon-polymers: PA11/PA12)
  - (f) Thermal fatigue (applicable to PVDF pressure barriers)
  - (g) Check of findings

#### C1.4.4.5 Input Requirements

As part of performing the monitoring data review, field engineers should be conferred to verify if any events related to the flexible lines have occurred in the relevant time period; examples are line hydrostatic pressure tests, EV-tests, system modifications or line relocations between different subsea X-mas trees, crossovers in the process facilities or similar. This check allows for a better understanding of the received data, and thus helps ensure correct interpretation of any findings made.

System P&ID's are necessary to identify the correct instruments, valves and to enable understanding of the system logic and layout. The monitoring review should include a check ensuring that the latest revision is utilized for describing the system layout, i.e. revision control.

Files containing the time stamped data for pressure, temperature, EV and choke position are to be obtained. The following should be specified when making an enquiry for this information:

- Platform or Plant ID
- Riser ID
- Instrument TAG
- Instrument type
- Time period (UTC-format)
- Required output format e.g 01-NOV-10 21:30:54,78
- Required file name format e.g. EV-13-0001.csv
- Sampling rate, typically 1 sample/min (temperature and pressure data)
- Filters assigned to the measurement

Assembling the system layout and checking for any updates since last reporting period should be performed as part of updating the data. Any changes are to be described in the report to allow tracking of the history.

#### C1.4.4.6 Assess Data Quality and Coverage

Typical is to utilize data sampled with 1 minute period to allow short-term variations to be included in the review. Sampling rates at longer intervals than 1min is in general not recommended. In events related to possible pressure surges, due to rapid closure of valves with high flow velocity, sample data interval required is significantly reduced, e.g. as low as < 0.1 seconds.

The data received should, as a general requirement, have coverage above 90%, provided that the missing data are sufficiently distributed. Depending on the type of data missing, e.g. time-spans or single points spread out through the relevant time period lower coverage may be utilized while considering the impact on the analysis and possibly highlighting the deviating quality when reporting. It is important to include incidents where the instruments are not connected, such as leak tests performed directly at flange. Calculation of coverage is not

relevant for time series which only contains samples when changes occur in the measurement values. However, then the instrument should be verified to be 'alive' and online.

Where possible, the instrument representing the most severe service conditions should be used for performing the analysis, i.e. the 'hot-end' or 'high-pressure end'.

Normally the instruments contain redundant sensors, and these should be compared against each other to rule out possible error-sources affecting the quality of the data. Typical errors include a stable offset or high-frequency 'noise' in reported values.

#### **C1.4.4.7 Maximum and minimum values for temperature and pressure, including hours above limits**

The time series shall be checked against the threshold limits defined by the flexible manufacturer or relevant technical recommendations (operator specific). Normally this includes both operational- and design limits. Short periods, typically in the order of 10 hours (1-2% of the time), outside the operational limits are normally not critical for the pipe. If the pipe is operated outside operational limits for longer periods, a new lifetime calculations shall be performed (fatigue and liner ageing). Design limits should not be exceeded at any time.

Both the maximum and minimum value and the accumulated time above the set limit are reported. For smooth bore lines it is emphasized that the minimum pressure shall be checked to identify if the line has experienced vacuum conditions. The minimum temperature shall also be checked, in particular for risers with PVDF pressure liner.

Observed values which are clearly erroneous, e.g. values from pressure testing of valves where the riser bore has been shut-in or instrument failures have occurred, may be omitted in the reporting of found maximum/minimum values, but a note shall be made of the applicable time periods or incidents for later tracking.

#### **C1.4.4.8 Operational envelope**

The operational envelope is developed over time to enable a simple visualization of the flexible service conditions. The histograms in Figure C1.3 and Figure C1.4 show examples of the accumulated time for a given range of pressure and temperature.

#### **C1.4.4.9 Differential pressure along the pipe**

The typical differential pressure, or another relationship, between subsea and topside instruments should be established at normal operation. The pressure time series should then be investigated for abnormal changes in the differential pressure. A sudden change in differential pressure may indicate a collapse of the carcass and/or pressure liner on multi-layer configurations or other flow restrictions due to accumulation of deposits or similar.

The differential pressure is affected by the flow medium, temperature and bore pressure, and no single value can normally be identified, but the check may enable an early detection of progressing failure. This will require continuous monitoring and proper understanding of the underlying process.

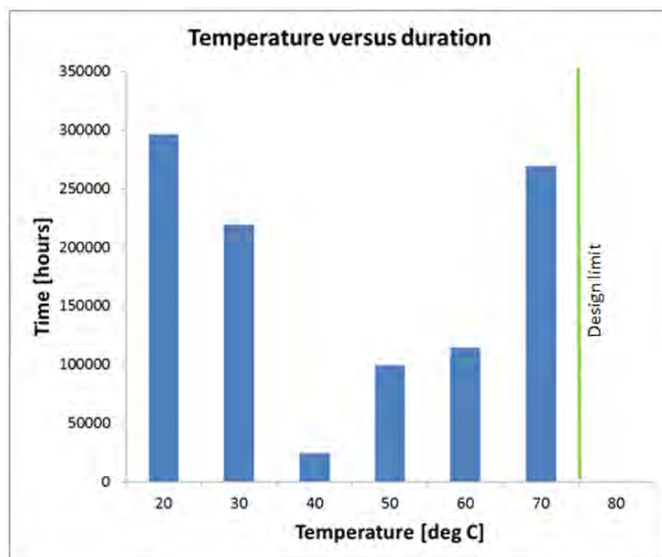


Figure C1.3: Example of operating temperature histogram

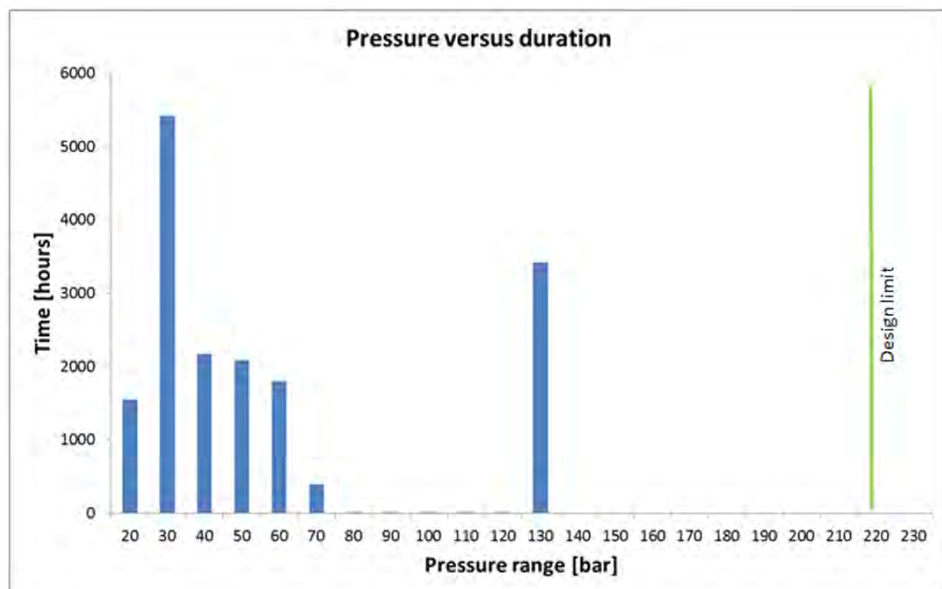


Figure C1.4: Example of operating pressure histogram

A similar check can be made for temperature data, but this is not standard practice at present.

#### C1.4.4.10 Pressure and temperature cycles, rate of decrease and increase

This check is mainly valid for pipes with a multi-layer pressure sheath where rapid and repeated increase or decrease in pressure or temperature can pose a threat to the pipe integrity or lines subject to blistering of pressure sheath. Several failure causes exist: shock loading of the cross section 'slugging' effects or the inability to equilibrate pressure or temperature along the length or through the cross section resulting in abnormal force distributions. For single layer pressure sheaths, extremely rapid depressurization of the bore is in general required

to cause collapse. At present, this check is performed for pressure data only, and not for temperature data. Where fatigue cracks in the pressure barrier (PVDF or aged PA) or PVDF axial termination issues are identified as risks, shutdowns should be recorded in terms of frequency, magnitude of temperature drop and cool down rate.

The flexible manufacturer normally states limits for the pressure and/or temperature rates in the documentation. Alternatively, if no relevant reference information is available, 4Subsea recommends using the following standard values: pressure drop rate should be below 1 Bar/min, and total differential pressure should be below 2/3 of the collapse capacity of the cross section. The pressure increase rate should be held below 5 bar/min. Rapid changes always lead to higher polymer stresses.

The valve and choke position data should be assessed to verify if the measurements really correspond to what is experienced by the flexible pipe. This check is emphasised as many of the findings are erroneous due to operation of valves or shut-in systems where the instruments do not represent the bore conditions at that time instance. This is illustrated by two typical scenarios:

1. EV test is performed by pressurizing the topside end with EV-closed. Pressure is never experienced by the riser.
2. EV is closed and the top side piping is depressurized. A very high depressurization rate is observed, but never experienced by the riser.

Any occurrences outside the defined limits shall be reported.

#### C1.4.4.11 Polymer ageing (PA-11 pressure barriers)

Estimation of ageing effects is performed for flexible lines with PA11 polymer pressure liner. The ageing calculation is performed according to the methodology given in [API 17TR2, 2003]. This method is generally recognized to carry significant uncertainties, though it is emphasized that ageing effects due to chemical incompatibility or other effects are not taken into account. It is therefore important to recognize that the check performed is for screening purposes, and cannot be used directly to validate the integrity for the pipeline. (work is ongoing to update [API 17TR2, 2003])

In the method outlined in [API 17TR2, 2003], full utilization (cumulative ageing of 1.0) corresponds to the acceptance criterion of  $CIV=1.2 \text{ dl/g}$ . The value of 1.0 indicates that the service life is expired. The utilization factor is calculated based on the Miner sum of the contributions from total operational time at each temperature and pH. In this work, the operational envelope (histogram) described in Section C1.4.4.8 may be utilized. The value for pH may be found by calculation based on knowledge about bore fluid composition or review of bore fluid composition monitoring. Due to the inability of the calculation method to accurately represent the actual material degradation, a refined ageing study is advised to be initiated when approaching end of calculated service life. Any large changes in the ageing rate should be further checked; this normally indicates change of operating conditions. To improve the accuracy of the polymer ageing assessment, ageing calculations should be used in combination with coupon sampling/testing and bore fluid composition measurements.

If the input data is of sufficient quality and with a high level of coverage as described in Section C1.4.4.5, the time series can be utilized directly with the relevant corrections between

measurement point and the most critical PA11 liner position. Typically, the time series will still include some erroneous or missing values for some time-instances. At these instances, values should be inserted to the time series. The value should be selected based on either of the two below:

- For time series with **missing point-values or missing short time periods**: utilize a 'typical' maximum value based on the remaining data. If no typical value can be found, or if the typical value is close to the threshold limit, the operational limit value, as defined in the riser DFI, is to be used. This normally produces a conservative result.
- For time series with **missing data for extended time periods**; extrapolating the available data based on the previous or following time period based on engineering judgment. This approach requires a sufficiently stable operational profile and should only be used for limited time spans.

If there is a lower level of coverage or if the data is found to be erroneous or misleading, there will be substantial uncertainties and it will generally not be possible to determine ageing of PA-11 based on operational data.

#### C1.4.4.12 Thermal fatigue of pressure sheaths (PVDF and aged PA)

Thermal fatigue can occur in PVDF and aged PA pressure barriers as a result of stress development during cooling of the pipe, particular due to shut-downs. The number of allowable temperature drops is to be specified by the manufacturer. A temperature drop is defined as a drop from the normal operating temperature over some extent of time; this does not include small temperature fluctuations. Further details on thermal fatigue of the pressure sheath are given in Chapter A3 Failure Modes in the present handbook. Similar considerations should be applied to cases where the PVDF liner termination may be questioned [Fergestad et al., 2017].

#### C1.4.4.13 Check of findings

The findings from the monitoring data review should be subject to a detailed check of the physical realism and the validity of the measurements. This should include

- Check of pressure versus temperature data: The data should be qualitatively evaluated to assess the operational condition at the time of interest; 'operational like' or 'shut-down like'.
- Check for possible instrument errors; sudden spikes very local in time, drifting instrument readings, sudden zero values or other default values indicating instrument errors.
- Check of choke and valve (such as ESV) position at the time of the measured data to verify that the instrument readings are representative for the conditions experienced by pipe. This is dependent on the location of the instrument relative to any choke or valve. As an example, in case of a closed valve located upstream of a topside instrument, the instrument is isolated from the pipe and thus not valid for the pipe. Similarly, the instruments should be checked to have been in service, online and not being by-passed.

### C1.4.5 Integrity Review and Reporting

Integrity review should be performed periodically and should also be triggered by events such as extreme weather or vessel response, accidents or suspected damage and deviating operational conditions. The review should include review of inspection, testing and monitoring activities and additional reports such as dropped objects reporting and survey. Integrity review should be documented by status reporting, recommended to be performed annually. Events or conditions outside design limits should be subjected to an integrity assessment as described in Chapter [C2 Lifetime Assessment](#).

### C1.4.6 When is repair advisable?

Anomalies and non-conformances should in general be subjected to an integrity assessment as described in Chapter [C2 Lifetime Assessment](#) before assessing the need and feasibility for repair. Exceptions are pre-qualified damages and associated pre-qualified repair methods, examples are outer sheath damages during installation which may be repaired by polymer welding. Under such circumstances repair may be performed without performing the regular integrity assessment.

### C1.4.7 Learning and improvement

Periodic loopbacks are strongly recommended in order to include new learning and improvements into the Integrity Management system. The learning and improvements should include review of the present integrity management system and new experiences in the company and in the industry. This should include:

- Incident investigations and new knowledge of failure causes and layer failures
- New methods for inspection, testing, monitoring and repair
- New knowledge of properties related to materials, layers and components
- New analytical methods and tools

There is at present no established practice for this. The operator is encouraged to strive to stay up-to-date and seek advice from the recognized experts in the company and in the industry. Proper experience transfer in the industry is reflected in authority requirements and requires designated arenas and systems for sharing safety critical information in the industry. Today's practice for sharing knowledge in the industry is primarily by development of standards. Amendments to the standards reflect established industry learning, and there will always be a delay from the time where the experience is gained until the implementation in standards.



## **Chapter C2**

# **Lifetime Assessment**

*Author: 4Subsea*

## C2.1 Introduction

### C2.1.1 Objective and Scope

The scope of this chapter is to provide guidance and practical advice for performing a lifetime assessment of flexible pipe systems. Main emphasis is to describe a systematic and practical approach to determine if a flexible pipe can safely operate after sustained damages, anomalies, change of operational conditions or exceeding the original service- or design life.

### C2.1.2 General

Flexible pipe technology may still be considered immature given the relative short time in use for an expanding range of operating conditions. Significant developments in material technology and analysis methods have been made by both suppliers and operators as time has elapsed, resulting in continuous improvements to both the design integrity level and ability to perform the integrity management activities.

There are several positive experiences where successful service life extensions or continued operation based on modified operational criteria has provided a large benefit to the operator. However, the experience shows that the complex interaction occurring in the multi-layer structure of a flexible pipe presents significant challenges to both safe- and cost effective operation of the flexible pipe system. Examples illustrating this are cases where flexible lines have been replaced pre-maturely or where failure has occurred for flexible lines in spite of having been accepted for extended life.

In general, each operator is responsible for maintaining an acceptable safety level. The importance of having a systematic approach towards maintaining the safety level throughout the lifetime of an asset is emphasised. This requires the responsible personnel to actively develop their knowledge and experience when operating flexible pipe systems.

### C2.1.3 Limitations

This chapter on life time assessment of flexible pipes is limited to the flexible pipe body and end-fittings for unbonded flexible pipes.

Ancillary equipment is only briefly covered - see Section [C2.4.5](#). These components may often require a different approach and assessment methodology. For some components, replacement is often the preferable course of action as compared to extensive assessment work.

Government regulations at the location of the asset may determine the formal process and requirements for documenting safe operation of the system. Implications due to national regulations and legislation is not within the scope for this chapter.

Relevant standards or guidelines are referred to in order to avoid re-production of information presented elsewhere. However, when considered necessary for the completeness and readability of this text, some information will be included in full.

### C2.1.4 Contents

Section [C2.2](#) presents a work process for performing a lifetime assessment in a systematic manner, largely based on the information in [[NORSOK Y-002, 2010](#)] Life Extension of Transportation Systems. For lifetime assessment tasks other than expiry of service- or design life, relevant modifications are performed.

Section [C2.3](#) presents reference publications, guidelines and standards relevant for performing lifetime assessment, along with references to other sections of this handbook.

Section [C2.4](#) presents a questionnaire based format to support the engineer performing the lifetime assessment. The checks are relatively general, and may be expanded on a case by case basis. Depending on the nature of the lifetime assessment being performed, additional information sources may be required.

Section [C2.5](#) briefly presents relevant industry references and experiences. This is to illustrate typical key issues, concerns and limitations during a lifetime assessment process. Two examples are presented more in detail; one related to lifetime extension and one to re-qualification of a riser system.

An example of a lifetime assessment process for a realistic case of a flexible riser is presented in Chapter Section [D1 - Case study](#), Chapter [D7](#).

## C2.2 Principles of lifetime assessment

### C2.2.1 General

The term Integrity may be considered in two different perspectives:

1. Structural integrity
2. Operational integrity

Structural integrity of a system is normally defined as the ability of the system to perform its functions, i.e. for a flexible pipe the ability to contain and convey the fluid for the relevant imposed loads. Operational integrity introduces additional requirements, e.g. system availability, time for repairs, availability of spare components. The term *integrity* will for this chapter always refer to structural integrity if not specifically mentioned otherwise.

An integrity acceptance limit is selected based on a confidence level describing the relation between load and response or time and degradation, i.e. what can be interpreted as a safety margin towards flexible pipe failure.

During the design phase, based on the available information for service parameters and known degradation mechanisms, the system is developed to maintain a satisfactory integrity level for the design life. Additional margin is often added due to selection of conservative parameters or analysis methods in determining the degradation rate.

Removing the conservatism between the integrity level at the end of the current service- or design life and the acceptance level threshold, may enable flexible pipe systems to be

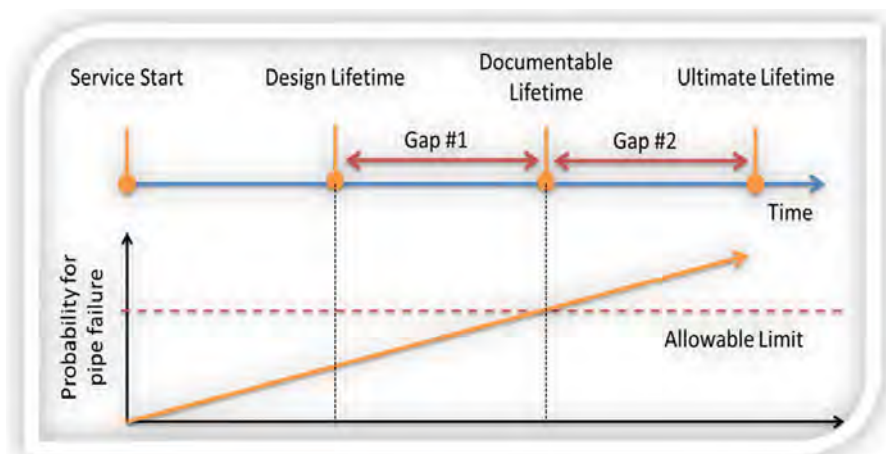


Figure C2.1: Life-time attribution for flexible pipes:

Gap #1 is based on fully utilizing the available knowledge and tools to document a lifetime beyond what was selected as a minimum requirement from field development premises. The documentable lifetime of the flexible pipe may be significantly longer than the overall field service- or design life dependent on service conditions.

Gap #2 is based on the lack of analysis and inspection tools to correctly predict when the line is at the border of failure, and thus includes the necessary safety factors and precautions in managing the flexible pipe integrity.

operated for an extended time period with a significant cost reduction and benefit to the operator.

It is not yet possible to exploit the full integrity life (ultimate lifetime), i.e. take the flexible pipe out of operation at the critical point prior to failure. This is due to the limitations in determining the actual integrity level. Developing more refined inspection techniques and analysis tools as well as gathering knowledge from inspection of decommissioned and recovered systems will help to reduce the uncertainties.

The design integrity level (including the expected, normal subsidence over time (e.g. fatigue, wear)) is to be monitored and maintained through the service life by the Integrity Management System (IMS), as described in Chapter C1 - Integrity Management. The validity of the original design life assessment may be challenged due to important parameters deviating from design phase assumptions or due to randomly occurring incidents or accidents. The threats can be divided into three main categories based on their nature of occurrence:

- Event based (dropped objects, dragged anchor, land slide)
- Condition based (changes in operational parameters, injection fluids)
- Time based (fatigue, wear, polymer degradation, insufficient corrosion protection)

Additionally, updated industry experience or knowledge may also require revising the original design life assessment.

In case of identifying an invalid integrity model, a Lifetime Assessment (LTA) should be initiated to verify that the system is fit for continued operation for the remaining required service life.

### C2.2.2 Process overview and Methodology

The process of performing a lifetime assessment can be described by a flowchart as shown in Figure C2.2. This flowchart is similar to those presented in [ISO/TS 12747, 2011] and [NORSOK Y-002, 2010]. As the latter concern lifetime extension, the flowchart in Figure C2.2 is mildly modified to include the general lifetime assessment process.

The activities presented in Figure C2.2 are described individually in the sections below:

- Assessment Initiator: Section C2.2.3
- Assessment Premise: Section C2.2.4
- Lifetime Assessment:
  - Diagnostic: Section C2.2.5.3
  - Prognostic: Section C2.2.5.4
- Condition Control, Mitigations or Modifications: Section C2.2.6
- Documentation and Implementation: Section C2.2.7

The lifetime assessment process need to conclude on the following two questions:

1. Is the current integrity level above acceptance limit?  
Question answered by a diagnostic process, evaluating the integrity level at the time.
2. Is the predicted integrity level at the end of specified service life above acceptance limit?  
Question answered by a prognostic process, modelling the integrity level at the current time.

The lifetime assessment conclusion may be one of four possible, i.e. to decommission the flexible pipe at:

1. At current time due to unacceptable integrity level
2. At a specific time before original service- or design life
3. At the end of original service- or design life
4. At the end of extended service- or design life

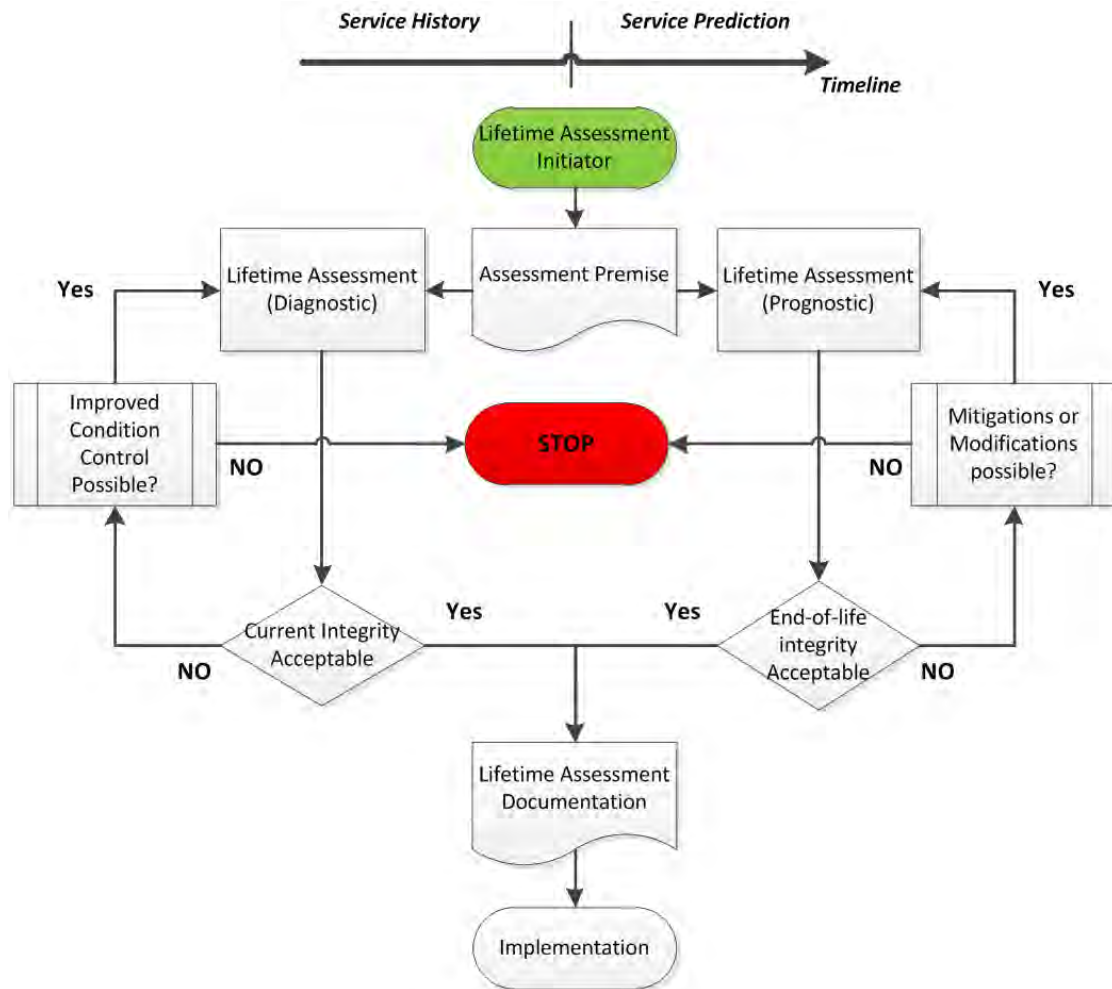


Figure C2.2: Lifetime Assessment Process Overview

The decision is ultimately based on a combination of both technical (including safety), economical and operational aspects.

### C2.2.3 Initiators

The different types of assessment initiators can be divided in six main categories:

1. Change of design code or methodology
2. Change of operational function
3. Change of operational conditions
4. Relocation
5. Damages / anomalies
6. Exceeding service- or design life (lifetime extension)

The initiator typically determines the required detail level and work scope. Initiating due to change of design code may for example require a high level risk assessment. Others,

e.g. a minor change in operational conditions may only require a 'spot-check' of relevant parameters. Finally, e.g. life extension may be subject to authority approval and formal restrictions during the process.

### C2.2.3.1 Change of design code or analysis methodology

The design tools and analysis methodologies are continuously improved, including update of the industry best-practice standards.

Verifying the integrity degradation model based on the updated best practice may be necessary after an initial gap analysis. Depending on the level of probability and consequence, i.e. risk level these gaps should be closed to ensure the continued safe operation.

Relevant experiences are listed below:

- Working stress versus limit state design
- On-bottom stability / upheaval buckling
- Polymer ageing models - e.g. [API 17TR2, 2003], for polyamide materials
- Fatigue calculation methodology

### C2.2.3.2 Change of operational function

Flexible pipes have often been used in new operational functions . This may be relevant for e.g. converting a flexible pipe designed for oil production into a gas injection pipe or vice versa.

It is expected that the original design documentation is found to be invalid for the new conditions, thus a full qualification is normally required covering all aspects considered for a new design and installation. This includes verifying that the polymer and steel materials are compatible with new fluid type and operating conditions, updated or new stress and fatigue calculations and so on. As the materials and cross-sectional design is already pre-determined, work is focused on verifying the integrity degradation model and optimizing the system layout, e.g. global configuration, intervention work where possible etc.

### C2.2.3.3 Change of operational conditions

During field and system design, a multitude of assumptions are made based on the best available data. As operation commences, real life data is gathered. If assumptions made in the design basis are found to be non-conservative or erroneous, a re-qualification should be performed. This should provide an updated integrity degradation model verifying that the flexible pipe system can be operated safely within the intended service life.

Relevant examples are listed below:

- Metocean criteria updates (more severe conditions)
- Reservoir fluid data (deviating from design, souring)
- Temperature / pressure profile (normal operation, shut-in)

#### C2.2.3.4 Relocation

Relocating flexible pipes happens rather infrequently, but is relevant. Relocation has mainly been done for riser systems and for topside- or subsea jumpers. For long flowlines relocation experience is limited. Due to the requirement for extensive intervention work with uncertainty in current condition of the flowline, the overall risk level for such an operation is considered high. Generally, flowline relocation, i.e. full length, should be avoided for trenched or rockdumped sections. However, re-routing of tie in loops, (a limited length at either end of the flowline), involving deburial has been performed several times.

For a flexible pipe to be used for a different, but similar service, (i.e. no changes that affects the design documentation) the re-use is straightforward provided the remaining service life is acceptable. Verification that the new service conditions are similar or less severe than for the previous installation is recommended to be performed with detailed attention. Minor changes may have significant effects in terms of risk level.

For flexible pipes to be relocated and used in new conditions, similar requirements as described in Section [C2.2.3.2](#) and Section [C2.2.3.3](#) apply. Depending on the level of difference, the documentation process may turn out to be similar as for a new installation, i.e. a full qualification of the existing pipe.

For both intra- or inter field relocations, the flexible pipe may be recovered to shore. This enables further detailed inspection, testing, repair or modification work than what is feasible while offshore. This provides an increased level of confidence when assessing the current condition and integrity of the flexible pipe.

Relevant examples are listed below:

- Flexible pipe re-located subsea only to a different well with the same production profile and fluid properties as the previous well
- Flexible pipe recovered from field, inspected and tested onshore and re-qualified for use on a new field

#### C2.2.3.5 Damages / anomalies

The need for a re-qualification after experiencing some type of damage to the flexible pipe is perhaps the most likely and frequent occurrence requiring a lifetime assessment.

Relevant examples of damages and anomalies are listed below; (the list not being exhaustive)

- Installation and handling damages
  - Overbending, twist or kinking
  - Compression in system leading to armour wire bird-caging
  - Tension overloading during pull-in
  - Crushing loads above design limit (from caterpillars)
  - Installation with open vent-ports resulting in seawater flooding annulus volume
  - No vent-system installed leading to outer sheath burst short time after start-up of production

- Outer Sheath damages where armour wires are exposed / flooding of annulus and subsequent fatigue/corrosion issues (lines not designed for flooded annulus)
- Impact damage
  - Dropped objects, Trawl board / anchor snagging or vessel impact leading to
    - \* deformation of armour wire / polymer layers
    - \* compromising MBR
    - \* outer sheath damages and annulus flooding
- Extreme events
  - Weather conditions exceeding the accidental cases from design
  - Vessel motion/excursion exceeding the accidental cases from design
- Operation outside design limitations
  - Temperature - operation (long-term) and design (short-term)
  - Pressure - operation (long-term) and design (short-term), depressurization or loss of pressure incidents or cycling for smooth bore designs
  - Depressurization rate (both multi- and single layer)
  - Bore fluid composition
    - \* H<sub>2</sub>S, CO<sub>2</sub>, Organic acids, injection or treatment chemicals not approved for use, sand production (particle size, flow velocity)
  - Hydrate event - removal using differential pressures
  - Buckling compromising MBR (lateral and upheaval)
  - Marine growth exceeding design criteria leading to change in global configuration and increased hydrodynamic loading
  - Loss of buoyancy elements leading to change in global configuration

Some of the damages and anomalies may be resolved through reviewing documentation alone. For example, design limits for a component may be set based on an overall system philosophy, while the component alone may have surplus capacity and thus not affecting the current integrity level. In other situations, where for example the material qualification limits are exceeded, the assessment may require extensive analytical work or testing of materials in components to conclude on their integrity status.

Damages during installation will, if no critical defects are identified, result in the flexible pipe being considered to have integrity level similar to design. Exemption is typically where a change of condition is resulting, e.g. annulus flooding if not covered by design assumptions. Confidence in the assessment may be higher than otherwise due to availability of detail information for the damage occurrence, thus providing the necessary input data for analysis.

Damages occurring during the operation phase are often more difficult to assess due to difficulties and limitations in obtaining accurate input data. Changes in material properties, development of interlayer effects, 'material memory' or possible uncertainty in key input parameters increase the complexity in the analysis compared to an installation damage. Such assessments may therefore prove significantly more challenging.

It is not possible to give detailed recommendations for all types of damages or anomalies presented in this chapter. Individual flexible pipe applications may differ significantly in terms of layout, operational conditions and cross-section designs. For some anomalies, e.g. outer sheath damage, tether failure or sliding tether clamp, engineering guidance as presented in Chapter A3 - Failure Modes may be referenced. Similarly, where the analytical models exist, these can be utilized in a similar manner as for a design situation to assess the criticality and possible impact on integrity level.

#### C2.2.3.6 Exceeding service- or design life

The number of installed flexible pipes approaching the end of their service and design life is rapidly increasing. Operation beyond original service and design life by safely utilizing remaining capacity may be a major value contributor for the field operators.

The types of re-qualifications discussed in previous chapters are normally performed for only a single or a few flexible pipes at a time. A lifetime extension process is often performed jointly for several flexible pipes across differing applications with differing design characteristics (e.g. production, gas lift/injection, water injection).

A clear set of definitions and nomenclature is essential for assessing a lifetime extension work scope. There is substantial differences in terms and definitions used in the most relevant set of standards and guidelines, which may lead to confusion or wrongful interpretation. For instance [API 17J, 2008] does not define Design Life, but use the term Service Life according to the following definition: 'period of time during which the flexible pipe is designed to fulfil all specified performance requirements.'

In [API 17B, 2008], the term Design Life is not defined, but used extensively within the recommended practice . It is natural to assume that this is to be interpreted as Service Life in line with [API 17J, 2008].

[DNV-RP-F116, 2009] Integrity management of submarine pipeline systems defines both Design Life and Service Life:

**Design life:** The design life is the period for which the integrity of the system is documented in the original design. It is the period for which a structure is to be used for its intended purpose with anticipated maintenance, but without requiring substantial repair.

**Service Life:** The time length the system is intended to operate. The service life is a part of the application toward authorities.

The definitions above are used in this handbook, which is also in agreement with [NORSOK Y-002, 2010].

There are then two main requalification scenarios after exceeding the service life or design life:

1. Service life is expired: however the integrity level of a flexible pipe is not necessarily at the end of the documented integrity time period, i.e. design life, and may have substantial remaining capacity for extended operation. Documenting that the current integrity level is in line with or higher than the design prediction is then the key requirement for extended service life.
2. Design life is expired: at the end of design life, the integrity level is not documented. The flexible pipe may still have remaining integrity life which a lifetime extension process seeks to exploit. The work is normally more comprehensive than for the former

scenario, and may require both extended material testing programs and destructive testing from recovered reference flexible pipes.

Experience shows some main areas that should be given attention:

- Initiating life extension process at an early stage:

Often the life extension process is only started upon reaching end of current service or design life, leaving little or no time to perform the assessment and required additional inspection or testing. As a consequence, the flexible pipe may have to be taken out of service until proper documentation is completed and available.

- The quality of the Integrity Management System (IMS):

The availability and quality of documentation and process or inspection data is a key factor, affecting both the assessment confidence level and the time necessary to perform the work. With a good IMS system the work to assess current integrity may already be completed which reduces the work load during a lifetime extension process.

## C2.2.4 Assessment Premise

### C2.2.4.1 General

An assessment premise should be prepared to document details on background, objective and any requirements for the assessment, e.g. reporting format, communication requirements, and authority or company regulation. The assessment premise should be as detailed as possible. For a lifetime extension this would include a fully updated design premise according to [API 17B, 2008]. Similar for an identified damage, a full description including system layout, high quality photography, video and sketches describing the location, extent of damage and any geometrical parameters should be included. Assumptions made must be clearly stated and should be conservative.

### C2.2.4.2 Design Code or Standard

The selection of design code or standard to be used is important. Typically the following applies:

1. Re-qualification within original design life and minor repair
  - (a) Original design code and revision
  - (b) Possibility to perform a risk assessment to assess consequence of new requirements or design codes changes
2. Extensive repair or modification work
  - (a) Updated design code and revision or a detailed risk assessment showing no significant increased risk level as compared to new design requirements
3. Lifetime extension
  - (a) Updated design code and revision or a detailed risk assessment showing no significant increased risk level as compared to new design requirements

[API 17B, 2008] provides no explicit guidance on this issue.

[NORSOK Y-002, 2010] presents the possibility to use the original design codes or standards (including revisions) in performing either lifetime assessment or life extension. However, it is also recommended to at least perform a gap analysis comparing new or updated codes or standards to identify any possible risks.

[DNV-RP-206, 2008] Riser Integrity Management is more restrictive and states that for re-qualification of risers (including extending design life) that '*The same safety level shall apply for lifetime extension of an existing riser as would apply for the design of a new riser*', explicitly requiring the use of updated design codes and standards. It is difficult to justify anything other than using the best available knowledge. This may reduce the conservatism in early designs at a time of more limited knowledge, or impose new restrictions to maintain the required safety due to identified shortcomings in previous design codes

### C2.2.5 Lifetime Assessment

A systematic approach is required to establish if the integrity level is acceptable, both at the current time and at the end of the required lifetime. A support may be found in the questionnaire in Section C2.4 which presents a review list for the system. The questionnaire should be used in combination with the detailed engineering guidance from Chapter A3 - Failure Modes to establish the current integrity level.

The lifetime assessment is typically performed in a sequence, as presented in the following.

#### C2.2.5.1 Sourcing and Structuring Information

The availability and quality of documentation covering all phases and events from design through installation and operation is a key factor for the outcome of the lifetime assessment. The quality and implementation of the integrity management system is a determining factor as lack of critical information may result in prematurely decommissioning of the system.

The following list shows an example of data required to perform the screening and subsequent detail analysis for a typical life extension process. For several other assessments, a similar list would be relevant with minor exceptions due to specific nature of the assessment being undertaken.

Table C2.1: Information Relevant for Lifetime Assessment - Example listing

Lifecycle Phase	Type	Type(sublevel/comment)
Engineering, Fabrication Installation Phase	Design Documentation	Design premise / basis Design report Pipe data sheets Dynamic analysis report Service life reports (fatigue analysis, polymer ageing, corrosion) Ancillary component design reports (cathodic protection system, buoyancy elements, bending restrictors, bending stiffeners, tether clamps, etc.)

Lifecycle Phase	Type	Type(sublevel/comment)
	Manufacturing Report	Non-conformance report Fabrication data book As-built data
	Operation and Maintenance Manual	
Installation Phase	Installation report	Procedures Non-conformance / deviation report Anomaly reports
	As-built reports and drawings	
Operation Phase	Integrity Assessment or Status Reports	
	Line Connection history	Comment: may be included in status reports / other information management system.
	P&IDs (instruments, coupons, layout)	
	Inspection, Test and Repair (ITR) reports	GVI and CVI (topside, subsea) Global configuration - nominal, as-built and current inspection results CP inspection data (potential measurements, anode depletion) Annulus test data Pressure tests (leak, structural integrity) Coupon samples Repair Reports (outer sheath, vent-system etc.)
	Operational Data	Pressure data Temperature data Flow data Choke/ESV settings (used for interpretation of pressure, temperature data) Bore fluid data - including sand production Injection & treatment chemical type and usage
	Anomaly Record	Comment: typically this should be available through either individual reports or through periodically issued integrity status assessments
	Modification reports	Comment: modifications directly affecting the system; i.e. replacement of components, changes to configuration etc.  Example of major modification: flexible re-termination
	Meteocean data	Comment: mainly relevant for dynamic service flexible pipes; however may be applicable to static service, e.g. considerations related to seabed current velocities
	Vessel motion data (if recorded)	Comment: mainly relevant for dynamic service flexible pipes

The work of sourcing, structuring and reviewing the documentation is a major task in its own. Experience is that this work phase is often time consuming and differ a lot depending on the quality level of the IMS.

### C2.2.5.2 Screening Phase

The screening phase should establish the level of feasibility for performing the lifetime assessment. The objective is to establish confidence level and support decision making for either to carry out or stop the detailed lifetime assessment work.

The key topics to be given attention for the decision to continue or abort a lifetime assessment process are listed below. An equipment review form, similar to [NORSOK Y-002, 2010], Table B.1 may be used as a basis for completing the screening phase. An extended table is presented in Section C2.4.2

### C2.2.5.3 Diagnostic Assessment

The diagnostic integrity assessment is a detailed review of the current status of the flexible pipe system based on the available historical information. The objective is to provide a best possible status at the time of reporting, and thus also establishing a valid baseline as an input for the prognostic assessments.

[NORSOK Y-002, 2010], identifies four main types of condition control which describe how the asset integrity level may be controlled:

Table C2.2: Condition Control Basis

Type	Definition	Comment
Condition unknown	No integrity management system (IMS) established	'Install and forget' approach - experienced, but not common. The quality level of the IMS may be low, de facto rendering the current condition as unknown
Condition by design	Operational parameters monitored to be within design limits	Normally the level of verification performed through the IMS through periodic review or inspection work. If not performed, this is typically the initial review work to be performed to identify any critical anomalies
Condition by operational experience	Operational data available and Structural integrity may be assessed	Where possible, the integrity degradation model from design may be calibrated or verified through analysis tools utilizing real data as compared to assumptions from design phase work - i.e. improved condition control
Condition is quantified through direct measurement	Physical condition of structure measured	In general there is very limited possibility to accomplish this for flexible pipes. For some components or layers, the condition may be measured directly - as for polymer coupons or cathodic protection potential level.

The expressions 'by design' and 'by operational experience' typically indicates the level of control one is confined to, in combination with relevant industry experience for the subject application.

Limited possibilities exists for direct quantification of the flexible pipe condition. The possibility for direct measurements allows for an increased confidence in the assessment carried out, removing possible overly conservative assumptions or in fact identifying severe degradation not previously detected. Examples of such direct measurement methods are polymer coupon sampling, cathodic protection potential measurements, anode depletion, armour wire inspection (after outer sheath damage) and similar.

#### C2.2.5.4 Prognostic Assessment

The prognostic integrity assessment should verify an acceptable integrity level at the end of the required service life. The work is based on the current status defined by the diagnostic integrity assessment. Calculation models, where available, are used to predict the development based on an assumed future operational service profile and relevant time dependent degradation mechanisms, such as:

1. Fatigue analysis (steel armour layers and polymer materials (PVDF))
2. Polymer degradation (applicable to polyamide materials)
3. Anode material consumption (Ancillary system component, however included in this list for completeness)
4. Corrosion due to CO<sub>2</sub> and H<sub>2</sub>S in annulus for steel armour layers or internal carcass
5. Erosion of internal carcass
6. Wear in both metallic layers and polymers.

Relevant calculation models are similar to those used during the design phase, covering global analysis and service life. One of the main issues is that design tools may assume intact pipe cross section as input for the analysis. Damages or local defects often complicate the methodology used for the initial design phase analysis.

The need to perform a new prognostic assessment is often driven by new operating conditions due to annulus flooding, requirement for continuous operation at higher pressures or life extension considerations. For dynamic service systems fatigue is by experience often the driving factor for the analysis work followed by polymer degradation.

Re-analysis of the anode material consumption model may prove necessary for life extensions. This is seldom encountered within the original design life due to the margins added in the design phase.

Corrosion and erosion design rates are normally conservative, providing some margin for changes in operating conditions or life extension. The quantification of the actual degradation is difficult, limiting the exploitation if experiencing less severe degradation than assumed in design.

The requirement for material re-qualifications or prototype testing may be relevant due to e.g. souring of reservoirs or other changes in the produced fluids, increasing temperatures or use of treatment chemicals not covered in the original qualification program. [API 17J, 2008] specifies requirements for material qualification testing or prototype testing

#### C2.2.6 Improved Condition Control, Mitigations and Modifications

The assessment performed for both diagnostic and prognostic integrity level may conclude that the predicted integrity level is not sufficient. Identifying possible improvements in condition control basis, mitigating actions or modifications may be evaluated to reduce conservatism in the diagnostic or the prognostic assessment. If not sufficient or unsuccessful, the possibility of system- or operational modifications may be pursued. Relevant examples for all types are described in the following sections.

The feasibility of the proposed improved condition control method, mitigation or modification must be reviewed and evaluated based on several requirements besides technical integrity, e.g. cost profile, asset availability, timeframe for execution of modification and several other factors. This is not discussed further here.

### C2.2.6.1 Condition controls

If the current integrity level is shown unacceptable, the following methods for improved condition control are normally used:

- Fatigue
  - using actual bore pressure values (historic data) compared to design assumptions
  - using temperature dependent bending stiffness and hysteretic behavior
  - tuning of interlayer friction
  - refinement in finite element modelling, i.e. 3D compared to in-plane
  - response measurements
  - more accurate modeling of dynamic load history (vessel motion historic data)
- Polyamide degradation
  - Refining calculation by [API 17TR2, 2003], using actual temperature data compared to design assumptions
  - Assessing effect of bore fluids compared to normally utilized pH4 curve from [API 17TR2, 2003]
  - Polymer coupons sampling and verification
- General corrosion of armour wires
  - Refining corrosion model based on measured bore fluid composition and / or levels of permeation rate and annulus gas samples
  - Include service profile as long periods of time with flexible pipe depressurized and at low temperature lead to reduced availability of corrosive elements in annulus
- Use of novel inspection techniques
  - Several techniques are available or being developed, e.g. radiography and eddy-current systems allowing mainly localized inspection that may provide data for improved calculations or by direct quantification of condition

### C2.2.6.2 Mitigations and Modifications

Examples of mitigations for improved prognostic assessment if the predicted integrity level is shown unacceptable, are listed below:

- reduce the system loadings or exposure to decrease integrity level degradation rate
  - reduced pressure rating

- reduced temperature through choking or additional coolers
- reduction of aggressive bore fluid components for gas lift or export systems
- installation of monitoring systems that allow sufficient reaction time before the degradation drops below acceptance level, i.e. end operation at the actual threshold level allowing some additional service time
- reduction in required service life, e.g. plan for replacement before the integrity level becomes unacceptable.

Examples of modifications for improved prognostic assessment, if the predicted integrity level is found unacceptable:

- Injection of inhibitor fluid in annulus (flushing, filling)
- intervention work – supporting structures, rock-dump, additional buoyancy
- repair work, e.g. re-termination of riser to remove damaged section or replacement of GRVs – refer to Chapter [B3](#) - Repair Methods for Flexible Pipes, including warnings related to HSE issues on flexible riser re-termination.

### C2.2.7 Documentation and Implementation

The lifetime assessment work should be closed by a documentation and implementation phase. This includes reporting all assessment work according to normal engineering practice, implement any required modifications or changes to the physical system or procedures, and update the integrity management system as applicable.

The outline presented in [[ISO/TS 12747, 2011](#)] may be used for preparing the documentation and reporting. The main topics to cover are listed in Table [C2.3](#).

Table C2.3: Contents of the life extension report. Source: [ISO/TS 12747, 2011], Table 1

Section	Description
Executive Summary	Overview of life extension process
Introduction	Description of pipeline location, history and the purpose of the life extension requirement
Conclusions	The findings of the life extension assessment, including <ul style="list-style-type: none"> <li>- remnant life and associated life extension period</li> <li>- required legislative approvals</li> <li>- deviations from original design basis and non-conformances</li> <li>- deviations from current legislation and codes</li> <li>- corrosion, fatigue and wall thickness assessment results</li> <li>- any residual risks</li> <li>- risk mitigation measures</li> </ul>
Recommendations	Recommendations for remedial measures or further inspection and assessment, necessary to justify life extension
License, permit agreements and organizations	License holder, owner and operator structures and agreements; past, present and future regulatory agreements should also be addressed
Design and construction	Summary of pipeline system design and construction, including <ul style="list-style-type: none"> <li>- original design requirements, codes and specifications</li> <li>- review of original design against current design codes</li> <li>- description of any difficulties or unforeseen events prior to start-up</li> <li>- construction methods (particularly new or non-standard methods)</li> </ul>
Operation	Review of operational history and a summary of future operations
Current Integrity of the pipeline system	Review of the current integrity of the pipeline system, including <ul style="list-style-type: none"> <li>- condition of the pipelines, risers and tie-in spools</li> <li>- condition and functionality of safety critical items such as ESDVs</li> <li>- internal corrosion assessment, accounting for any chemical injection</li> <li>- condition of coatings and CP systems</li> <li>- assessment of the effects of any repairs or modifications</li> <li>- fatigue assessment</li> <li>- assessment of the effects of any changes in land use or settlement</li> <li>- review of identified anomalies</li> </ul>
Life Extension Assessment	Description and findings of the life extension assessment covered by Clause 9 of [ISO/TS 12747, 2011]
Studies	Identification of any specific work or studies (past and future) that may have an impact on the pipeline and its life extension
References	References to all documentation used during the compilation of the report
Appendices	Useful information, such as <ul style="list-style-type: none"> <li>- inspection and monitoring records used to assess pipeline integrity</li> <li>- calculations performed during the life extension assessment</li> </ul>

Table C2.3 is prepared for life extension of rigid pipelines, but may also be used for flexible pipe systems. This also applies for the type of assessment being performed, for e.g. damage assessments or other re-qualification purposes some sections may be omitted partially or in whole.

As a key note, it is important to ensure that the whole system within the defined work scope is fully covered. Interface management towards other parallel assessments, especially applicable for lifetime extension, is important in order to avoid conflicting requirements.

## C2.3 Standards and Guidelines for Lifetime Assessment

### C2.3.1 Overview

Several papers and reports have been published on the topic of flexible pipe integrity management and integrity- or lifetime assessment. SINTEF Technology and Society, on behalf of Petroleum Safety Authority Norway (PSA), published in 2010 an extensive report titled 'Ageing and Life Extension for Offshore Facilities in General and for Specific Systems' [Hokstad et al., 2010].

The report provides an overview of issues related to ageing and management of life extension for offshore facilities. This includes both a description of principle aspects for an assessment process and typical ageing phenomena along with possible challenges, including a specific study for pipelines, risers and subsea systems with focus on physical degradation. The report has served as the main input in terms of current best practice based on the extensive literature review reported.

Performing integrity- or lifetime assessment work can be described by two levels, both requiring their set of available protocols and guidance information:

1. Process guidance
2. Detail engineering guidance

The currently most important flexible pipe standards relevant for such guidance are listed in Table C2.4:

Table C2.4: Flexible Pipe References for Lifetime Assessment

Standard, Design Code or Technical Specification	Title	Comment
[API 17J, 2008] [ISO 13628-2, 2006]	Specification for Unbonded Flexible Pipe	Defines the minimum design integrity level through stating the requirements for service life analysis and minimum requirements to which each layer and material shall perform.
[API 17B, 2008] [ISO 13628-11, 2007]	Recommended Practice for Flexible Pipe	<p>Provides detail guidance related to design, analysis, manufacture, testing, installation and operation.</p> <p>Limited information for flowline and jumper systems as such systems specific requirements and advisory is not included.</p> <p>Provides recommended allowable degradation levels (Table 5) - however difficult to accommodate in practice for some of the components (layers).</p> <p>Limited information on re-qualification as it only covers re-use after recovery to shore (Chapter 12). High-level (low detail) guidance to assess condition is included and may be used for reference.</p>
[API 17TR2, 2003]	The Ageing of PA-11 in Flexible Pipes	Guideline for degradation modeling of polyamide polymer material used in flexible pipes.

Standard, Design Code or Technical Specification	Title	Comment
[NORSOK Y-002, 2010]	Life Extension for Transportation Systems	<p>Part of several guidelines prepared for use on Norwegian controlled assets, see OLF guideline 122 - Norwegian Oil and Gas Association recommended guideline for the Assessment and Documentation of Service Life Extension of Facilities.</p> <p>Provides detailed information for process guidance and may be used to design a lifetime extension process by Company.</p> <p>Includes less detailed engineering guidance: should be supplemented by detail engineering guidance on failure mechanisms and modes.</p>
[DNV-RP-F116, 2009]	Integrity Management of Submarine Pipeline Systems	Report specifically covers rigid submarine pipelines only (not flexible). High-level process guidance is relevant and may be used for reference.
[DNV-RP-206, 2008]	Riser Integrity Management	Report mainly concerns integrity management and initiating events leading up to lifetime assessment. Less detailed engineering guidance relevant for flexible pipes.
[ISO/TS 12747, 2011]	Recommended practice for pipeline life extension	<p>Report covers rigid submarine pipelines only (not flexible). High-level process guidance is relevant and may be used for reference.</p> <p>Similar approach as for [NORSOK Y-002, 2010]</p>

### C2.3.2 Process Guidance

The overall process of performing a lifetime assessment is described similarly in several standards and guidelines:

[NORSOK Y-002, 2010], provides a full overview of the work involved and includes some general engineering guidance. The standard is intended to be used for lifetime extensions, but the guidelines and work methodology is valid for lifetime assessment and lifetime extension.

DNV recommended practices [DNV-RP-F116, 2009], and [DNV-RP-206, 2008], should be regarded as supplementary to [NORSOK Y-002, 2010], as they include guidance relevant for both in-service integrity assessment and life extension. Their main objective and scope is however integrity management guidance. [DNV-RP-F116, 2009] only covers rigid pipelines; however the general principles apply also to flexible pipes.

[API 17B, 2008], mainly Chapter 12.3 Pipe Evaluation, is not regarded to include sufficient detail or guidance for the process of performing a lifetime assessment or lifetime extension.

### C2.3.3 Detail Engineering Guidance

When selecting acceptance limits for pipe integrity assessment, guidance is given in both [API 17J, 2008] and [API 17B, 2008], as these state requirements for material properties

and utilization rates.

[[API 17B, 2008](#)], Chapter 5 Pipe Design Considerations, includes recommendation on permissible levels of degradation in the service life analysis. However the presented criteria are not specific and for some layers / components it is impossible to confirm acceptable status for the flexible pipe while in operation, based on this reference only.

The detail engineering guidance for flexible pipes available in the public domain is limited. This is in contrast to rigid pipeline systems where the industry has developed best practices for assessment of several damages or defects. Refer to the paper 'Pipeline Defect Assessment Manual', [[Cosham and Hopkins, 2002](#)].

Before performing a lifetime assessment, triggered by any of the issues listed in Section [C2.2](#), it is recommended to review the detail engineering guidance provided in Chapter [A3 - Failure Modes](#). This section includes guidance for several experienced failures, suggested acceptance criteria, as well as procedures or models to predict service life or Probability of Failure (PoF).

Where relevant, other standards or guidance notes are referenced. Combined, these form a set of guidelines enabling the responsible engineer to arrive at a conclusion on lifetime assessment in a consistent manner.

[[DNV-RP-F116, 2009](#)], includes an overview of damages/anomalies versus assessment codes for rigid submarine pipeline systems. A similar overview for flexible pipe systems, see Table [C2.5](#), will be further improved when agreements are made for assessment codes for experienced damages, anomalies or degradation processes.

Table C2.5: Damage and Anomaly versus Assessment Code or Guideline

<b>Damage / Anomaly</b>	<b>Code / Guideline</b>	<b>Comment</b>
Metal Loss	Corrosion - not available Wear - not available	Tensile and pressure armour strength may be assessed based on permissible utilization ratios specified in [ <a href="#">API 17J, 2008</a> ]
	Corrosion - not available Wear - not available Erosion [ <a href="#">DNV-RP-O501, 2007</a> ]	Carcass strength may be assessed based on permissible utilization ratios specified in [ <a href="#">API 17J, 2008</a> ]. Carcass erosion may be assessed based on reference code/guideline.
Outer Sheath Damage	Manufacturer guidelines	Manufacturers typically presents basic level of guidance in an 'Operation and Maintenance manual' - no common standard. Different approaches or assessment guidelines may apply between through thickness damages or superficial damages. A minimum pressure capacity sufficient to allow functionality of GRVs and performing annulus testing without affecting the layer integrity may be used as a guidance, e.g. typically minimum 3 bar(g).
Exposure (seabed)	[ <a href="#">DNV-RP-F107, 2010</a> ]	'Risk Assessment Of Pipeline Protection' - provides guidance on a risk based approach to assess criticality of interference with riser and pipelines from accidental events (impact, dropped objects etc.)

<b>Damage / Anomaly</b>	<b>Code / Guideline</b>	<b>Comment</b>
Anode depletion / Protection Potential	[DNV-RP-F103, 2010] / [NORSOK M-503, 1997]	Code / guideline is developed for steel pipes and is developed further by individual flexible pipe suppliers to cover flexible products. Issues related specifically to flexible, e.g. protection potential decay along a continuous length of flexible pipe, is not covered in full and requires assumptions to be made. These may differ between operators and vendors.
Fatigue of steel armours	[API 17B, 2008]	Additionally, fatigue, in a combination with localized metal loss (e.g. pitting corrosion), may require local FE-analysis to determine stress concentration factors to be applied.
Polymer degradation	[API 17B, 2008] / [API 17TR2, 2003]	[API 17B, 2008] specifies allowable degradation, however this requires material testing and possibly destructive testing.  [API 17TR2, 2003] gives guidance for ageing of polyamide materials - no guidelines for ageing of other polymer materials exists in public domain. The use of [API 17TR2, 2003] may produce both conservative and non-conservative results as it does not consider all relevant input parameters (update planned).
Displacement Upheaval Buckling, Free Span	[API 17TR2, 2003] / [DNV-RP-F110, 2007]	Steel pipeline codes or guidelines may provide guidance to some extent applicable to flexible pipe. However, these do not provide the full extent of guidance required. Several individual additional guidelines or procedures have been developed to cover the additional requirements, however not commonly available.
Impact Damage	[DNV-RP-F107, 2010]	Table 5 - Impact capacity and damage classification of flexible pipelines and risers. Special test program may be required to assess actual damages as referenced guideline may be conservative.
Over bending	[API 17J, 2008]	Specified MBR for the actual service to be used as acceptance criteria. Observed bending radius which may un-lock or damage interlocked hoop spiral should be considered an unacceptable damage which require replacement or extensive evaluation/test. Similar consideration may apply to carcass layer based on functional requirements. Polymer strain criteria as in [API 17J, 2008] or special evaluations/tests.

## C2.4 Lifetime Assessment Questionnaire

### C2.4.1 General

A questionnaire based format is used in the following sections to support the assessment of the flexible pipe system integrity. The questionnaire is intended to support the flexible pipe engineer in identifying deviations from the design basis, detecting relevant failure modes or other areas of concern for the flexible pipe integrity. Where available, references to sources for detailed information is included.

The cost associated with performing an extensive lifetime assessment may in some cases high compared with decommissioning and / or replacement. This option needs to be assessed, however, such considerations are not part of the scope for the Handbook.

An overall system screening questionnaire, Table C2.6, may be used in an early phase to assess the confidence and probability of a successful outcome.

The type of condition control available may be evaluated by Table C2.7.

The layer assessment questionnaire is provided in Table C2.8 through Table C2.17. The use of these tables may depend on the initiation of the lifetime assessment process. An assessment due to an identified anomaly may need an evaluation of both system, all layers or only a single layer / component.

### C2.4.2 System Screening

Table C2.6: Screening Questioner

Purpose / System Type	Check Number	Question	Guidance
Doc. Review	Q 1.1	Is Engineering, Fabrication and Installation phase documentation available	Refer to Table C2.1 for example list
	Q 1.2	Is operation phase documentation available	Refer to Table C2.1 for example list
	Q 1.3	Is design premise reviewed and found valid for current and/or future service requirements	The design premise or design basis assumptions is key for verification of validity for current- and future operating conditions If the original design premise is found to be invalid for several key design input parameters, it is to be expected that the lifetime assessment work may require substantial resources.

Purpose / System Type	Check Num-ber	Question	Guidance
	Q 1.4	Is non-conformance record available and been reviewed for continued validity	Non-conformances from design, fabrication and installation phase should always be reviewed. For the intended service- or design life and assumed operational conditions, it may be that non-conformances were acceptable. For extended service or changes in operational conditions it is important to assess if this conclusion is still valid, or if risk level may increase
Integrity Management System Input	Q 1.5	Is operational data reviewed for any deviations from design premise and prescribed limitations?	Operational data includes temperature, pressure, bore fluids etc.  This type review is often performed as part of a period status assessment. If not performed, this needs to be included in full for the lifetime assessment scope of work.
	Q 1.6	Are all previous anomaly assessments reviewed for time restrictions in regards for assessment validity	Similar considerations as for Q 1.4 apply; the previous conclusion may show to be invalid given extended service- or design life or for changes in operational conditions
	Q 1.7	Are existing risk assessments valid	As the risk assessments are key to conclude, these may need to be updated to reflect current knowledge  Updates are typically due to industry experience, change of design codes, findings made during review(s)  This includes an evaluation of identified failure modes to assess if risk assessment should be updated due to improved knowledge or due to new threats
	Q 1.8	Are there any identified anomalies that are not processed or are pending conclusions	The possible impact on the current lifetime assessment needs to be considered as a minimum. Including the anomalies in the current lifetime assessment may be beneficial to ensure consistency and improved decision basis in regards to determining the integrity- and risk level
	Q 1.9	Is a gap analysis between original and current design code performed	The gap analysis may be required dependent on the assessment premise and lifetime assessment initiator (re-qualification or lifetime extensions).  If gap analysis is applicable, the screening phase should include an evaluation of possible impact on integrity- and risk level as a minimum.  The final lifetime assessment documentation should include a detail assessment of impact on integrity- and risk level.

Purpose / System Type	Check Num-ber	Question	Guidance
	Q 1.10	Is Industry experience for similar type of cross section design and/or operational conditions, anomaly or damage reviewed	<p>Public domain publications are important sources of information.</p> <p>The information is normally used as input for determining the risk level. As parameters between the reference set and subject flexible pipe may differ significantly the direct application of data should be treated with caution to maintain conservatism.</p>
Ancillary Equipment and Support Systems	Q 1.11	<p>Are all ancillary and supporting systems checked and verified as fit-for-service per their individual requirements and design codes</p> <ul style="list-style-type: none"> <li>a. Hang-off structure</li> <li>b. Annulus ventilation system</li> <li>c. Bend stiffener</li> <li>d. Clamp (tether, MWA)</li> <li>e. Tether line</li> <li>f. Buoyancy modules</li> <li>g. Anchor/riser base structure</li> <li>h. MWA structure</li> <li>i. Bend restrictors</li> <li>j. Cathodic protection system</li> <li>k. Seabed protection</li> </ul>	<p>The ancillary and supporting systems functionality are key to the flexible pipe performance.</p> <p>For detail engineering guidance refer to [API 17L1, 2013], and [API 17L2, 2013].</p>
Modifications or Repairs	Q 1.12	Are there any previous modifications or repairs performed	<p>Identifying possible deviations from original design documentation is important.</p> <p>The initiating cause, type of modification or repair selected and possible impact on integrity- and risk level should be assessed.</p>
	Q 1.13	Is the modification or repair sufficiently documented	<p>If there are modifications or repairs that are improperly documented, additional inspections or an increase in assessment scope may be required.</p> <p>Typical examples include repairs of outer sheath performed during installation. If no documentation proving the outer sheath integrity being restored after repair, it may be impossible to avoid highly conservative assessment assumptions.</p>
	Q 1.14	Is the modification or repair system documented for current and/or future service requirements	Mainly relevant for lifetime extensions where the repair system itself may require a replacement or lifetime extension.

### C2.4.3 Condition Control Basis

Table C2.7: Condition Control Basis Questionnaire

Purpose/ System	Type	Check Number	Question Guidance
Information Availability for analysis, calibration of calculation models or direct quantification of condition	Q 2.1	Monitoring Data (up-and downstream) a. Pressure b. Temperature c. Choke setting d. Valve position/setting (ESV, PMV, PWV)	<p>Key requirement for assessing both current and predicted integrity level.</p> <p>Sample data with 1 minute intervals required to identify transients and performing pressure- or temperature cycling evaluations. In events related to possible pressure surges, due to rapid closure of valves with high flow velocity, sample data interval required is significantly reduced, i.e. as low as &lt; 0.1 seconds.</p> <p>Valve position settings is used to exclude possible erroneous data, e.g. shut-in while doing pressure build-up tests up- or downstream</p> <p>In the absence of any historical pressure and temperature data, the assessment may be severely limited in regards to determining the integrity level with required confidence level.</p>
	Q 2.2	Bore fluid a. Sand particle size / type b. H <sub>2</sub> S and CO <sub>2</sub> partial pressures c. Total Acid Number (TAN) d. Chlorides concentration e. Water Cut f. Injection chemicals (type, treatment frequency)	<p>Data is important for all assessments of polymer and steel material compatibility as well as determining any possible anomalies or changing production profiles not covered by design premise.</p> <p>In the absence of any historical data for bore fluid composition, the assessment may be severely limited in regards to determining the integrity level with required confidence level.</p>
	Q 2.3	Annulus Environment a. Permeation rate b. Gas Sample composition c. Free volume d. Liquid type (if filled/flooded) e. Injected inhibitor fluids f. Possibility for back-flow from atmosphere or downstream vent system g. Possibility for leakage through GRVs	<p>Annulus environment data is important for all assessments of polymer and steel material compatibility as well as determining any possible anomalies or changing production profiles not covered by design premise. The data is key input for corrosion and fatigue life calculations, i.e. SN-curve to be applied.</p> <p>Annulus environment data is further used for detecting possible defects in pressure containing layers and to verify outer sheath integrity.</p> <p>The data is used in combination with input data from Q 2.2.</p>

Purpose/ System	Type	Check Number	Question Guidance
	Q 2.4	Load and response data a. Wave data b. Vessel motion c. Riser motion	<p>Wave and vessel motion data normally are updated during the service life of a field due to improved statistics and/or vessel/platform modifications or improved calculations</p> <p>The data is highly relevant for global system analysis and fatigue life calculations.</p> <p>It is required to verify, as a minimum, that the original design data remains valid</p>
	Q 2.5	Degradation Coupons d. Polymer coupons e. Corrosion coupons f. Erosion coupons g. Flexible cross-section length from actual / reference flexible pipe system	<p>If available, this data provides a direct quantitative status for applicable materials and layers.</p> <p>The use of data needs to consider any possible impacts of location of coupons compared to critical location in system.</p> <p>The use of destructive testing of flexible pipes may be required if uncertainty in condition control level and thus integrity- and risk level cannot be concluded.</p> <p>The latter approach is typically relevant for lifetime extension where multiple lines are subject for an assessment, and using a single line for testing is overall beneficial</p>
Riser Systems	Q 2.6	Inspection data for riser configuration: a. Hog depth and position along length of riser b. Sag depth and position along length of riser c. Touch-down point position along length of riser d. All support systems present and active	<p>Verify if riser configuration is within envelope from global analysis and in accordance with as-built inspection data.</p> <p>Variations in bore fluid density, marine growth outside design envelope or partial loss of buoyancy are examples of deviations lending the configuration different than design condition</p> <p>In the absence of any inspection data, the assessment may be severely limited in regards to determining the integrity level with required confidence level.</p>
	Q 2.7	Is riser and/or vessel motion data available	<p>Verify if riser motions is within envelope from global system analysis - ref. Q 2.4.</p> <p>Normally direct measurement is not available, however observations by ROV / GVI data may provide some level of verification.</p> <p>Dedicated measurement campaigns using both dry- and subsea sensors may provide valuable input data for fatigue calculations.</p>

<b>Purpose/ System</b>	<b>Type</b>	<b>Check Number</b>	<b>Question Guidance</b>
Flowline/ jumper Systems	Q 2.8	Is flowline/jumper system possible to inspect?	<p>Depending on field location, there may or may not be a requirement for covering the seabed sections for protection purposes. An inspectable system provides substantially better data for any assessment.</p> <p>Emphasis to be placed on location of intermediate connections due to possible sealing/connection related issues. Inspection team must be aware that gas bubbles may emit at GRVs - the rate may be used for assessing if normal range or possible leakage.</p> <p>Note - where several segments are used, some may be altogether covered including both end-fittings, i.e. condition by design at best (for most parameters)</p>
	Q 2.9	Is cover level/depth and/or global configuration (routing) possible to inspect and verify	Used for verifying no upheaval- or lateral buckling as well as comparison with requirements for impact- and/or over trawling protection

## C2.4.4 Layer Assessment

### C2.4.4.1 Carcass

The carcass layer function is maintained if it provides

1. Sufficient resistance against hydrostatic collapse
2. Protects polymer layers from abrasive particles
3. No obstructions - i.e. not collapsed

Layer integrity is thus to be documented by

1. Minimum thickness
2. No discontinuities - i.e. tear off
3. No diameter reduction above acceptance criteria

Table C2.8: Layer Assessment - Carcass

Check Number	Assessment Question	Guidance
Q 3.1	Is flow rate below design assumption	<p>Flow rates impacting integrity level is mostly relevant for production lines where abrasive particles may be present in transported fluids, thus impacting erosion calculations.</p> <p>Flow rates are normally monitored closely; thus data should be available for checking against design assumptions. Flow rates above design assumptions may render the erosion calculations invalid, requiring updating to verify that unacceptable loss of collapse resistance does not occur.</p>
Q 3.2	Is any sand production recorded	<p>Typically only limited time of sand production is allowed for in design (start-up of new wells).</p> <p>Continued sand production combined with high flow rates (see Q 3.1) should trigger an erosion assessment to verify if pipe design provides a sufficiently high integrity level for the required service lifetime.</p> <p>Refer to failure description Carcass Collapse (Chapter <a href="#">A3</a> - Failure Modes).</p>
Q 3.3	Are any hydrate/blockage of bore events recorded	<p>If any events are identified, which may have resulted in high differential pressures across blockage, the historical pressure data should be checked for to determine risk for having exceeded the carcass load capacity.</p> <p>Refer to failure description Carcass Axial Overloading (Chapter <a href="#">A3</a> - Failure Modes)</p>

Check Number	Assessment Question	Guidance
Q 3.4	Are there any internal inspection and/or pigging runs performed	<p>Performed pigging may prove no tear-off, significant collapse or deformations above acceptance criteria (visual inspection pigging, gauge pigging)</p> <p>Visual inspection is valuable for all failure mechanisms related to carcass failure modes.</p> <p>Pigging is however in itself a possible initiator of failure modes; proper procedures and equipment is emphasized for internal inspections.</p>
Q 3.5	Is the cross-section a multi-layer pressure barrier structure	<p>Several failures has occurred where the carcass has collapsed. Initial failure mode has in some events triggered failure modes related to the pressure barrier.</p> <p>For any multi-layer, high pressure application it is recommended to review to failure description Carcass Collapse (Chapter A3 - Failure Modes)</p>
Q 3.6	Has pipe bore been directly exposed to seawater for any significant amount of time, e.g. wet storage, disconnected from subsea connection point or other without sealing cap	<p>Prolonged exposure to seawater is normally not allowed due to risk of gross and local corrosion damages to carcass.</p> <p>Stagnant conditions may also trigger Microbiological corrosion mechanisms depending on bore content other than seawater.</p> <p>Refer to failure description Carcass Collapse and Carcass Axial Overloading (Chapter A3 - Failure Modes)</p>
Q 3.7	Is there any curvatures in the system near limiting MBR, with hydrostatic pressure equal or close to calculated collapse resistance	<p>High curvature combined with possible local reduction in carcass collapse capacity increases risk of failure if outer sheath integrity is lost, transferring the hydrostatic load onto the carcass layer.</p> <p>Refer to failure description Carcass Collapse (Chapter A3 - Failure Modes)</p>
Q 3.8	If possibility of severe carcass degradation - can pressure sheath alone provide sufficient margin towards collapse	<p>In shallow waters the pressure sheath alone may provide collapse resistance sufficient to withstand hydrostatic pressure. Mitigating action may consider including operational procedures ensuring that internal bore pressure is maintained at a level equal to hydrostatic level, thus reduce risk of collapse.</p> <p>For damages which may have separated the carcass profile, the possibility for damages to pressure barrier layer needs to be included. Operation without carcass support is normally not acceptable.</p>

#### C2.4.4.2 Pressure Barrier

The pressure barrier layer function is maintained if it provides

1. Contains conveyed fluid

Layer integrity is thus to be documented by

1. Material properties within requirements for
  - (a) strength
  - (b) toughness
  - (c) ductility
  - (d) creep resistance
  - (e) Permeation (affects annulus environment)
2. Accumulated fatigue below threshold limit - only applicable for specific polymer materials (PVDF)
3. No operation outside design limitations

Table C2.9: Layer Assessment - Pressure Barrier

Check Number	Assessment Question	Guidance
Q 4.1	Is polymer coupons or reference pipe samples with similar exposures available allowing material property testing	<p>Polymer coupons provides important data and should be used for material analysis where significant material degradation is suspected.</p> <p>Flexible pipes with similar exposures that have been recovered, if dissected and inspected, may provide supporting information. The similarity in operational conditions should be evaluated to ensure conservatism.</p> <p>Availability of material samples may show that the material properties are within requirements, verifying layer integrity remains intact from severe time degradation.</p>
Q 4.2	Is any leak test performed in recent times	<p>Leak test may prove that no significant loss of containment is present, however there is a possibility for micro-leakages through end-fitting sealing arrangement or micro-voids in material that are not detected during a leak test.</p>
Q 4.3	Is current permeation rate in-line with or than lower design value Is any increase in permeation rates apparent from test data trending	<p>Online monitoring systems are normally the best available data source - intermittent sampling should be cross referenced for the operational conditions at the time for performing the test. Differences in measuring methods, calibration of equipment and reporting detail may render data inconclusiv.</p> <p>Upon identifying elevated permeation rates, detail assessment should be undertaken due to possible pressure barrier layer defects, i.e. loss of containment.</p> <p>Refer to failure description Pressure Sheath Enbrittlement (Ageing of Polyamides) (Section A3 Chapter A3 - Failure Modes)</p>

Check Number	Assessment Question	Guidance
Q 4.4	Is annulus gas samples checked for non-diffusive/permeating constituents	<p>The presence of such constituents may indicate a direct flow path between bore and annulus.</p> <p>Different polymers have differing diffusion- and permeation characteristics - see Chapter A2- Flexible Pipe Properties and Performance.</p> <p>Upon identifying abnormal annulus gas constituents, detail assessment should be undertaken due to possible pressure barrier layer defects, i.e. loss of containment.</p>
Q 4.5	Are there any events where temperature or pressure is below or above operating- or design limitations, including pressure testing	<p>Sensor location and recording interval is critical for confidence in assessment.</p> <p>Pressure testing is often not recorded in data acquisition system due to valve settings - thus necessary to check individual test reports.</p> <p>Smooth bore pipes are especially vulnerable for minimum bore pressure (vacuum) conditions; this should be included in the check out operational data.</p> <p>Profiling of temperature or pressure decay along length may support assessment if lack of upstream sensors (critical end).</p> <p>Normally, short term excursions above operating pressure- and temperature limits will not present a high-risk for the integrity level.</p> <p>Exceeding design pressure- and temperature limits are considered as severe with possible immediate or long-term effect on integrity level. Detail assessment should be undertaken to assess criticality of event(s), i.e. calculation of armour wire utilization or testing of material degradation for similar loading.</p>
Q 4.6	Are there any events where pressurization or de-pressurization rates is above threshold limits	<p>Operation and Maintenance manuals from the flexible pipe suppliers normally state a limiting pressurization and de-pressurization level.</p> <p>Exceeding of these limits presents risk related to polymer blistering, shock loading and carcass collapse.</p> <p>If no operational data is available, an evaluation of possible maximum rates may be performed, based on system layout and operational procedures.</p> <p>Damages to the carcass may result in triggering failure modes related to the pressure sheath. For any multi-layer, high pressure application it is recommended to review to failure description Carcass Collapse (Chapter A3 - Failure Modes).</p>

Check Number	Assessment Question	Guidance
Q 4.7	Is the bore fluid composition checked and verified against design assumptions	<p>Design assumptions normally includes conservative estimates. The verification of bore fluid composition compared to these estimates is important to validate the design assumptions, and should normally be performed by the integrity management system.</p> <p>Possibility for already occurred or expected changes to transported fluid should be assessed. Some possible reasons for rendering design assumptions invalid are; changes in reservoir characteristics or well completion, modification of topside equipment, change of operational service etc.</p> <p>Accurate data per transportation segment may be difficult to obtain due to comingled flow in some production systems.</p> <p>Reliance on well completion or initial phase test production data may be needed if no updated reservoir fluid testing or modeling has been performed.</p>
Q 4.8	Is the use of injection chemicals (type, concentration) checked and verified against approved types	<p>The operation and maintenance manual provided by flexible pipe supplier normally includes listing of approved chemicals and their concentration.</p> <p>Use of chemicals other than those approved presents a high-risk for possible failure modes related to polymer degradation. Detail assessment and possible material compatibility tests may be evaluated based on the chemical type.</p>
Q 4.9	Are there any non-conformance related to pressure sheath under-thickness from fabrication	<p>The approval of such non-conformances is possible, and may impact lifetime assessment if the reason for approval is currently invalid; e.g. change of operational function.</p>
Q 4.10	Is pressure barrier material a polyamide type If yes - is ageing calculation showing less than 5 years remaining service life	<p>Comparison between calculations and actual condition using polymer coupons, thus establishing confidence in calculation model, is recommended in the initial life phase.</p> <p>Risk of failure due to polymer ageing is increasing over the service life time.</p> <p>Calculations from design is normally performed using the maximum operation temperature; if actual temperature is significantly lower a substantial capacity may remain.</p> <p>Refer to failure description Pressure Sheath Enbrittlement (Ageing of Polyamides) (Chapter A3 - Failure Modes)</p>
Q 4.11	Is pressure barrier material a PVDF type	<p>If polymer material is initially fatigue susceptible, refer to failure description Fatigue cracks in pressure barrier (PVDF, aged PA) (Chapter A3 - Failure Modes)</p>

### C2.4.4.3 Pressure Armour

The pressure armour layer (including back-up spiral) function is maintained if it provides

1. Capacity to support radial loads from bore- and external pressure

Layer integrity is thus to be documented by

1. Utilization level below threshold limits - [API 17J, 2008]
2. Accumulated fatigue below threshold limit
3. Gap size below design value - i.e. no unlocking or significant deformation
4. No significant wear at sliding surfaces

Table C2.10: Layer Assessment - Pressure Armour

Check Number	Assessment Question	Guidance
Q 5.1	Is annulus environment checked and verified against design assumptions a. H <sub>2</sub> S partial pressure b. CO <sub>2</sub> partial pressure c. Liquid filled / dry	To be based either on diffusion and permeation calculations based on bore fluid composition or by direct measurements on annulus gas samples and permeation rate. Known outer sheath damage(s) affects the type of annulus environment to be assumed in evaluation. If higher than assumed values of corrosive elements are identified, material qualification records should be reviewed to identify limiting values - these may be substantially higher than design input.
Q 5.2	Is general corrosion material loss calculation valid based on current/predicted annulus environment	The calculation model utilize a mole balance between corrosive elements and iron. Thus the consumption rate may be calculated based on steady-state annulus conditions.
Q 5.3	Are there known outer sheath damage(s) with loss of external barrier and possibility of localized corrosion	Known outer sheath damages(s) affects the corrosion rate - calculations may be performed based on recommended free corrosion rates in seawater/air available in public domain. If materials susceptible to embrittlement (high strength, low alloy) are used in tensile armours, the consequence of outer sheath breach must include assessment of hydrogen induced stress cracking (HISC) and similar failure mechanisms.
Q 5.4	Is utilization ratio at current and end of required service life within limits in [API 17J, 2008] for all design load cases	Including updated general or localized corrosion calculations.
Q 5.5	Is accumulated fatigue calculations valid	A high level of conservatism may be present due to use of assumed pressure levels during design phase. If significantly lower pressures are recorded, significant reductions in accumulated fatigue may be gained.
Q 5.6	Is predicted remaining fatigue life sufficient for required service life	

Check Num-ber	Assessment Question	Guidance
Q 5.7	If pressure level is at high end of typical range - is there any wear prediction models available or possibility to use radiography in highest utilized area	
Q 5.8	Are there any events in service history related to possible violation of MBR	<p>Installation phase or intervention work is considered as most critical, i.e. accidental events.</p> <p>For flowlines upheaval- or lateral buckling may be relevant. During normal operation sufficient limit between allowable MBR and armour profile locking radius is prescribed by [API 17B, 2008]</p>
Q 5.9	Is any leak test performed in recent times.	<p>Leak test may be used for calculating minimum remaining material based on an assumption that yield and failure will occur at utilization equal to 1.0. In absence of leak tests, the highest operational pressures may possibly be used as a baseline for calculations.</p> <p>Re-calculating allowable pressure based on a maximum utilization per design code can then be performed - normally only with significant reductions in allowable load input.</p> <p>Predicting a material loss rate, the time span from current date to reaching maximum utilization from normal operating conditions can be performed to establish criticality level.</p> <p>Difference between normal operating pressure- and design pressure (is important to determine if reduction in risk level is applicable based on such a calculation).</p> <p>For a scenario where operational pressure is close to the design pressure, there is less margin between the normal, operational loading and thus also the forced loading during a leak test pressure) determines the level of confidence for an integrity assessment purpose. Failure may either in fact be triggered by the leak test, or occur in short time afterwards due to continued degradation.</p>

#### C2.4.4.4 Intermediate Sheath (Anti-Collapse)

The intermediate sheath or anti-collapse layer is normally used only for smooth bore pipes. The layer provides

- Barrier between internal - and external environment

Layer integrity is thus to be documented by

- Material properties within requirements for
  - strength
  - toughness
  - ductility
- No through layer defects

Table C2.11: Layer Assessment - Intermediate Sheath (Anti-Collapse)

Check Number	Assessment Question	Guidance
Q 6.1	Is 'inner annulus' and 'outer annulus' possible to monitor or test either separately or jointly	<p>Some end-fitting designs allow independent testing of the inner- and outer annulus, thus providing positive confirmation of both annulus conditions.</p> <p>Dependent on the reason for having an intermediate sheath there is differing considerations:</p> <ul style="list-style-type: none"> <li>a. For smooth bore risers, the intermediate sheath is normally introduced to transfer the hydrostatic loading onto the pressure armour, in case of loss of outer sheath integrity. Tensile armours may be located both in the inner- and outer annulus.</li> <li>b. For designs where the intermediate sheath is used to divide the steel armour layers from insulation layers.</li> </ul> <p>Depending on the cross section design, it may be of key importance to test either only the inner or both annulus volumes. See Q 6.2</p>
Q 6.2	If no separate test possibility: is annulus free volume tests in line with calculated values for only 'outer annulus' or 'inner annulus'?	<p>Depending on the measured volume, it may be that either the inner or outer annulus is flooded.</p> <p>Outer sheath damages, other than large, abnormal damage, would normally only lead to flooding the outer annulus volume. If inner annulus volume is found to be flooded, based on comparison between measured free volumes and calculations, the loss of anti-collapse function is lost. This is normally only applicable for smooth bore risers; if the pipe design incorporates a carcass this may provide partial or full resistance against collapse from hydrostatic loading.</p> <p>In any event, the reason for flooding of both inner- and outer annulus should be determined (damage to intermediate and/or outer sheath, leakage through end-fitting sealing arrangement, condensed permeated gas). Subsequent possible impact on service life from corrosion or fatigue degradation mechanisms should be evaluated.</p> <p>Operational procedures may be considered to ensure bore pressure remains above the hydrostatic pressure, if the pressure barrier and/or carcass is not sufficiently able to withstand the hydrostatic pressure loading.</p>
Q 6.3	Is annulus free volume tests trend data indicating any abrupt increases in free volume	<p>Any abrupt changes in free volume (increase, decrease) may be used to detect possible loss of function.</p> <p>Dependent on vent-port configuration, and possibility for testing independently or jointly, the results should be compared to either previous test data of calculated annulus free volumes to identify most probable scenario; e.g. loss of intermediate sheath sealing in end-fitting, damage to outer sheath, leakage from bore to inner annulus etc.</p>

Check Number	Assessment Question	Guidance
Q 6.4	Is there a possibility for having operated with 'empty bore' or with vacuum conditions after last confirmation of intact intermediate sheath layer	If the riser is a smooth bore design, the loss of intermediate sheath layer function, and thus anti-collapse protection, combined with low bore pressure increases risk of pressure barrier collapse. Reviewing the operational data, to exclude possible events triggering collapse should be performed. Operational procedures may be considered to ensure bore pressure remains above the hydrostatic pressure, if the pressure barrier and/or carcass is not sufficiently able to withstand the hydrostatic pressure loading.
Q 6.5	Is there any planned internal inspection or other activity which may increase risk of damage to pressure sheath	Pressure sheath damage with subsequent leak into inner annulus will result in large radial gaps in pipe wall and major shortening of the pipe as the intermediate sheath will act as pressure barrier

#### C2.4.4.5 Tensile Armour

The tensile armour layer function is maintained if it provides

- Capacity to support tensile loads
- Torsional stability

Layer integrity is thus to be documented by

- Utilization level below threshold limits - [API 17J, 2008]
- Accumulated fatigue below threshold limit

Table C2.12: Layer Assessment - Tensile Armour

Check Number	Assessment Question	Guidance
Q 7.1	Is annulus environment checked and verified against design assumptions a. H <sub>2</sub> S partial pressure b. CO <sub>2</sub> partial pressure c. Liquid filled / dry	To be based either on diffusion and permeation calculations based on bore fluid composition or by direct measurements on annulus gas samples and permeation rate. Known outer sheath damage(s) affects the type of annulus environment to be assumed in evaluation. If higher than assumed values of corrosive elements are identified, material qualification records should be reviewed to identify limiting values - these may be substantially higher than design input
Q 7.2	Is general corrosion material loss calculation valid based on current/predicted annulus environment	The calculation model utilize a mole balance between corrosive elements and iron. Thus the consumption rate may be calculated based on steady-state annulus conditions

Check Number	Assessment Question	Guidance
Q 7.3	Are there known outer sheath damage(s) with loss of external barrier and possibility of localized corrosion	Known outer sheath damages(s) affects the corrosion rate - calculations may be performed based on recommended free corrosion rates in seawater/air available in public domain If materials susceptible to embrittlement (high strength, low alloy) are used in tensile armours, the consequence of outer sheath breach must include assessment of hydrogen induced stress cracking (HISC) and similar failure mechanisms
Q 7.4	Is utilization ratio at current and end of required service life within limits in [API 17J, 2008] for all design load cases	Calculations should include for general or localised corrosion.
Q 7.5	Is accumulated fatigue calculations valid	A high level of conservatism may be present due to use of assumed bore pressure levels during design phase. If significantly lower pressures are recorded, significant reductions in accumulated fatigue may be gained
Q 7.6	Is predicted remaining fatigue life sufficient for required service life	
Q 7.7	Are there any events in service history related to possible high tension- or compression outside design assumptions a. Overpull during installation b. Vessel motion higher than assumed for design	Differentiate between effective compression and true wall compression as they relate to different failure modes.
Q 7.8	Are there any indications of severe locked-in twist (i.e. torsion) in the pipe, or does it twist when pressurized from ambient	Severe torsion or twist of the pipe, changing with internal bore pressure, may indicate tensile armour wire breakage - resulting in severe torsional imbalance. Depending on pipe design, the rotation angle per length may be calculated to assess if the measured rotation angle is abnormal or within expected range. During leak testing, pipe twist may be monitored to assess any abnormal torsional behavior, [Marinho et al., 2007]

Check Number	Assessment Question	Guidance
Q 7.9	<p>Is any leak test performed in recent times</p> <p>Other high pressure events may also be used - normally though the highest loadings are seen during leak testing</p>	<p>Leak test may be used for calculating minimum remaining material based on an assumption that yield and failure will occur at utilization equal to 1.0. In absence of leak tests, the highest operational pressures may possibly be used as a baseline for calculations.</p> <p>Re-calculating allowable pressure based on a maximum utilization per design code can then be performed - normally only with significant reductions in allowable load input.</p> <p>Predicting a material loss rate, the time span from current date to reaching maximum utilization from normal operating conditions can be performed to establish criticality level.</p> <p>Difference between normal operating- and design pressure is important to determine if reduction in risk level is applicable based on such a calculation.</p> <p>For a scenario where operational pressure is close to the design pressure, there is less margin between the normal, operational loading and the forced loading during a leak test. Failure may either in fact be triggered by the leak test, or occur in short time afterwards due to continued degradation.</p> <p>Pipes with reduced pressure rating must consider all accidental and design pressure events such as shut-in and surge pressures</p>

#### C2.4.4.6 Anti-Wear Protection

The anti-wear layer function is maintained if it provides

- Separation between steel layers

Layer integrity is thus to be documented by

- Material qualifications if outside design assumptions

Table C2.13: Layer Assessment - Anti-Wear Protection

<b>Check Number</b>	<b>Assessment Question</b>	<b>Guidance</b>
Q 8.1	Is annulus environment checked and verified against design assumptions for material used as layer separation	Any use of corrosion inhibitor injected into annulus, or raw seawater exposure should be checked against material qualification
Q 8.2	Is there experience with similar materials and time dependent degradation	If the anti-wear layer is made of polymer materials where a known time dependent degradation model exists, this may be utilized to assess integrity level
Q 8.3	Is the pipe used in dynamic application with possibility for dislocation of separation layer	If tape layers are used to provide the anti-wear protection, the possibility for dislocation of the tape layers should be considered. Several dissections of used pipe shows that there is indeed a possibility for dislocation in local areas, especially if tape layers are laid side-by-side instead of large overlaps or fully extruded layers. For layers fully extruded the possibility of dislocation can be excluded.
Q 8.4	Is the contact pressure levels sufficiently high to introduce wear or fretting as a degradation mechanism	Metal-to-metal wear is highly dependent on the contact pressure between the steel layers, determined by the bore pressure. For high-pressure systems, the risk related to degradation and failure mode triggering upon loss of anti-wear protection layer may be assessed based on calculations models in Chapter B1 - Design Analysis. For low-pressure systems, the risk is significantly reduced, and normally not a significant driver for integrity level degradation.

#### C2.4.4.7 Anti-Buckling Protection

The anti-buckling layer function is maintained if it provides

- Load bearing capacity to restrain tensile armour wires

Layer integrity is thus to be documented by

- Material qualification is outside design assumptions
- Inspection beneath outer sheath (destructive testing)

Anti-Buckling Protection is presented in Table [C2.14](#)

Table C2.14: Anti-Buckling Protection

<b>Check Number</b>	<b>Assessment Question</b>	<b>Guidance</b>
Q 9.1	Is annulus environment checked and verified against design assumptions for material used as anti-buckling protection	Any use of corrosion inhibitor injected into annulus, or raw seawater exposure should be checked against material qualification
Q 9.2	Is there experience with similar materials and time dependent degradation	Several high-temperature risers dissected show that significant degradation of tape layer had occurred. The tape had partially dissolved or melted - leaving the tape ineffective
Q 9.3	Is the pipe exposed to high compression (true wall) during normal operation	Global analysis result may be used to determine if loss of anti-buckling protection introduces an increased risk for tensile armour buckling. If analysis results shown that there is a substantial tension in the armour wires, for all operational conditions, the risk associated with loss of the anti-buckling protection layer may be considered negligible.
Q 9.4	Is there any findings from inspections indicating dislocation of armour wires	High risk area is near touch-down point, as this area is susceptible to compression loads (true wall). Refer to failure description Tensile Wire Axial Compression Failure (Chapter <a href="#">A3</a> - Failure Modes)

#### C2.4.4.8 Insulation Material

The insulation layer function is maintained if it provides

- U-value below requirement
- No significant 'thinning' which may affect ancillaries

Layer integrity is thus to be documented by

- Temperature drop along line within requirements for arrival temperature
- Verifying no movement of ancillary equipment

Table C2.15: Layer Assessment - Insulation Material

Check Number	Assessment Question	Guidance
Q 10.1	Is the measured temperature loss between upstream and downstream end of the flexible pipe system in accordance with design calculations	<p>The loss of insulation may be evident by comparing initial- and current temperature drop, for similar bore fluids and pressure levels, between upstream and downstream temperature sensors. Significant changes may show that the insulation material is degraded.</p> <p>The assessment needs to consider possible seawater flooding of annulus or insulation layer and impact on insulation properties.</p>
Q 10.2	Is arrival temperature sufficient to meet flow assurance requirements	<p>The loss of insulation layer function is mainly associated with flow assurance. Direct consequences for the pipe integrity is not expected.</p>
Q 10.3	Is there any findings from inspections indicating movement of clamped ancillaries (tether or MWA clamps, buoyancy modules, other)	<p>Movement is often identified due to partial/full removal of marine growth in localized areas at ancillary attachments</p> <p>Refer to failure description Sliding Tether Clamp and Altered Buoyancy (Chapter A3 - Failure Modes)</p>
Q 10.4	Are any ancillary devices clamped on.	<p>Clamping of ancillaries on insulated flexible pipe is difficult and possible damages to the pipe as well as malfunction of the clamped on device must be checked - e.g. close visual inspection</p>

#### C2.4.4.9 Outer Sheath

The outer sheath (and intermediate) layer function is maintained if it provides

- Barrier between internal- and external environment

Layer integrity is thus to be documented by

- Material properties within requirements for
  1. strength
  2. toughness

### 3. ductility

- No through layer defects

Table C2.16: Layer Assessment - Outer Sheath

Check Number	Assessment Question	Guidance
Q 11.1	<p>Is annulus possible to monitor or test:</p> <ul style="list-style-type: none"> <li>a. Is annulus free volume tests in line with calculated values or FAT values</li> <li>b. Is annulus free volume tests trend data indicating any abrupt decreases or increases in free volume</li> <li>c. Is refined testing using stepwise pressure increases or injection of known amount of fluid to verify no breach</li> <li>d. Are GRVs possible to inspect and monitor to verify function</li> </ul>	<p>For any loss of outer sheath integrity, refer to failure description Impact, wear and pressure induced rupture creating hole in the outer sheath (Chapter A3 - Failure Modes)</p>
Q 11.2	<p>Are there any findings from inspections showing local damages, continuous abrasion or interference with other structures/components</p>	<p>Relates to risk of experiencing loss of layer integrity in future due to ongoing degradation or latent defect that may be triggered in normal operation.</p> <p>For buried flowlines/jumpers it is not possible to visually inspect for anomalies resulting in a lower confidence in layer integrity if no other inspection method is available</p>
Q 11.3	<p>Are there any findings from inspections indicating movement of clamped ancillaries (tether or MWA clamps, buoyancy modules, other)</p>	<p>Movement is often identified due to partial/full removal of marine growth in localized areas at ancillary attachments. Refer to failure description Sliding Tether Clamp and Altered Buoyancy (Chapter A3 - Failure Modes).</p>
Q 11.4	<p>Are there any previous repairs performed</p>	<p>Repairs should be regarded to restore layer integrity if proven sealing capacity.</p> <p>Previous clamp-on repairs should be given attention as they present a higher risk for loss of barrier towards external environment.</p>
Q 11.5	<p>Are there any areas resulting in high insulation and possible temperature driven degradation modes</p>	<p>This is normally only regarded as relevant for high-temperature systems. Higher risk areas are beneath</p> <ul style="list-style-type: none"> <li>a. Bend stiffeners</li> <li>b. Buoyancy modules</li> <li>c. Clamps (tether and MWA)</li> <li>d. Bend-restrictors</li> <li>e. Buried sections</li> </ul> <p>Failure is expected to manifest at high-strain areas, i.e. high curvature.</p> <p>Refer to failure description Outer Sheath Embrittlement (Chapter A3 - Failure Modes)</p>

Check Number	Assessment Question	Guidance
Q 11.6	Is the outer sheath exposed to UV-radiation	No known defects have occurred attributed to UV exposure, and is considered low risk. Additionally such areas of the system are normally inspectable or possibly even available to extract a material sample. Failure is expected to manifest at high-strain areas, i.e. high curvature.

#### C2.4.4.10 End Fitting

The end-fitting function is maintained if it provides

1. Anchoring of all loading bearing layers
2. Sealing integrity between terminated layers
3. Structural capacity to withstand all design loads

Layer integrity is thus to be documented by

1. No dislocation or pull-out of layers
2. No dislocation of sealing components
3. No significant material loss (external and internal)

Table C2.17: Layer Assessment - End Fitting

Check Number	Assessment Question	Guidance
Q 12.1	Is the surface coating intact	End-fittings which are accessible, can be inspected and controlled directly. Where the end-fitting is inaccessible (located inside closed guide-tube, buried etc.) the condition of cathodic protection system is critical to limit corrosion.
Q 12.2	Are there any observations of significant corrosion on end-fitting body or fasteners (bolts, nuts or studs)	Similar considerations as in Q 12.1 applies.
Q 12.3	Is electrical discontinuity between riser and/or hang-off and remaining structure verified	Some cathodic protection systems require a discontinuity between the flexible pipe and adjacent structure. The discontinuity may be verified through direct measurements if end-fitting is accessible.

Check Number	Assessment Question	Guidance
Q 12.4	Are the jumper wires between bracelet anodes and end-fitting verified to be intact	Applicable to subsea end of risers or flowlines, where the end-fitting is accessible. Especially important for intermediate connections where there is a significant distance to other structures that could have, in event of damage to jumper wire, provided the required cathodic protection
Q 12.5	Are there any observations of oily fluids in ventilation system	If oily fluids have been observed in the vent-system, this may indicate minor leaks in internal sealing arrangement. This inspection is normally only possible for the topside end-fitting, with the connection point for annulus testing near the end-fitting.
Q 12.6	Is pressure barrier material expected to swell or loose volume exposed to bore fluids	Loss of volume may affect sealing integrity due to reduction in effective compression fit. Coupons may be used for reference to assess relevance of failure mechanism
Q 12.7	Are there any indications of possible loss of layer anchoring or pull-out of layers	Early PVDF end-fitting termination designs are high-risk due to a number of experienced failures If suspected failure related to anchoring of tensile wires or other internal steel components, radiography may be evaluated to document status For fluid integrity the use of permeation rate and annulus testing may be used to document status
Q 12.8	Is the seal arrangement towards downstream/upstream piping system evaluated for time dependent degradation mechanisms	Included to alleviate interface management. Dependent on sealing material (steel, polymer, elastomer) time dependent degradation mechanisms may be applicable.
Q 12.9	Are there indications of leakage from bore into annulus through end-fitting sealing arrangement	Annulus vent gas should be checked for traces of bore fluids and excessive vent rates. Leakage in end-fitting seals will influence annulus vent rates and annulus gas composition. Annulus monitoring may be used if such failure modes are suspected.

## C2.4.5 Ancillary Components

Ancillary components are important for the performance and integrity of a flexible pipe. As part of a lifetime assessment, the functionality and integrity level of such components may be of key importance to conclude on the flexible pipe integrity. The ancillary components should be included for any lifetime assessment of the overall system, e.g. especially relevant for lifetime extension.

Components to be evaluated include amongst several others:

- Bend stiffener

- Buoyancy elements
- MWA, support towers or anchor bases (structures)
- Clamps (tether or MWA)
- Tether (steel or fibre materials)
- Bend restrictors
- Hang-off structure
- Connection clamps between flexible pipe sections, topside- or subsea structure interface
- Cathodic protection (CP) system

Main reference for flexible pipe ancillary equipment are [[API 17L1, 2013](#)] and [[API 17L2, 2013](#)].

[[API 17L1, 2013](#)], and [[API 17L2, 2013](#)], presents specifications and recommendations for flexible pipe ancillary equipment, respectively. The latter contains a section on integrity management (including relevant failure modes) for each system component.

[[NORSOK U-009, 2011](#)] Life extension for subsea systems, includes specific guidance for some ancillary components. In Annex H guidance is given for tether and buoyancy components, which may be used in addition to [[API 17L1, 2013](#)] and [[API 17L2, 2013](#)].

The standards provide a good overview of important functional requirements and design parameters , valuable upon undertaking a lifetime assessment.

## C2.5 Industry References and Experiences

### C2.5.1 General

A list of experiences is shown in Table C2.18 to highlight key topics related to lifetime assessments. Two examples are presented in more detail for the illustration of common issues or concerns during re-qualification.

Table C2.18: Industry References and Experiences List

System and Assessment Initiator	Assessment	Comment
Riser to single satellite well, failure of carcass in topside end-fitting	Possible to repair through re-termination; updated global- and fatigue analysis due to shortening of catenary length	Failed due to excessive carcass axial force, without proper design for this load.
Relocation of risers between fields utilizing same vessel (FPSO moved)	Onshore repair and inspection, including re-termination. Re-analysis of fatigue due to flooded annulus. PA11 investigations,	Performed in line with guidance from [API 17B, 2008] requirements for flexible pipe reuse in similar conditions.
Gas-lift riser system lifetime extension	During lifetime assessment, the riser system was found to have an integrity level below acceptance limits due to PA11 degradation.	Analysis based on [API 17TR2, 2003] showed sufficient remaining lifetime, however coupons were more degraded than calculated. Further investigations required destructive testing of the riser identified as most critical.  Coupons had not been sampled regularly - likely to have been detected at an earlier stage
Production flowline system lifetime extension	Not possible to confirm condition and remaining service lifetime due to inaccessible CP system components	Not possible to confirm outer sheath integrity or any damages occurring during installation/operation, thus reliance on CP system was found to be critical.
Production flowline lifetime extension	Predicted souring of reservoirs leading to increased H <sub>2</sub> S levels in bore fluids.  Diffusion and permeation assessment concluded that operation at design limits was not within material qualification limits, thus decommissioned at end of design life	Utilizing actual pressure and temperature data the qualification limit could be adhered to. Combined uncertainty due to other corrosion processes resulted in an overall too high risk level

System and Assessment Initiator	Assessment	Comment
Gas export riser system	Extended lifetime after extensive re-analysis of global configuration and fatigue life due to non-conservative original design parameters compared to current best practice	Initiation of lifetime extension work was done at a too late stage, rendering the system unfit for service due to lacking documentation. Integrity Management system was not effective, i.e. unsuccessful in documenting history of operational parameters
Over bending, i.e. violation of MBR limit, of gas export riser during installation	Extensive testing of reference cross section proved that no significant damage was likely to have occurred, and with subsequent successful pressure testing line was re-qualified to be within design conditions	The availability of a sample pipe section from the actual production run enabled the testing to be performed with minimum conservative assumptions on as-built profiles and details.
Re-qualification of gas-lift riser after outer sheath damage.	Annulus test program detected damage in splash-zone - exposure time approximately 2 years, i.e. time since last positive annulus test. Re-qualified based on updated fatigue analysis showing large remaining fatigue life.	Possible stress concentrations or stress re-distribution due to localized damages not investigated in detail. In retrospect close visual inspection using divers should probably have been performed.
Re-qualification of gas-lift riser after outer sheath damage.	Damage identified initially in submerged part of riser, later in splash zone due to vessel draft change.  During re-qualification, the most severe fatigue concentration spot was found to be not at outer sheath damage location, but at bend-stiffener end.	Fatigue analysis method by today's best practice compared to original design process may reveal other critical failure mechanisms than the initiator of the analysis/assessment.
Gas lift flow line suffering impact damage - caused by dragged anchor line	Re-qualification aborted due to uncertainty in impact energy, time for exposure of armour wires and associated high risk if failure in operation	Impact damages are typically difficult to successfully re-qualify. Limited accuracy of input data often results in highly conservative evaluations with negative outcome.
Gas export flow line system pressure increase	Re-qualification should initially not be required as system design included the higher pressure level as part of the load cases. However, project execution approved a non-conformance of less cover depth than required for the higher pressures levels to restrain upheaval buckling.	Project showed the importance of assessing all previous non-conformances and challenge the conclusion based on current or future predicted situation.

System and Assessment Initiator	Assessment	Comment
Production riser decommissioned due to fatigue life expiry	Investigations of recovered pipe showed that a key integrity concern, not included in the lifetime assessment, was local corrosion on tensile armour wires reducing the layer capacity and creating fatigue hot-spots	Project showed the importance of developing knowledge related to annulus corrosion and implementation of additional condition control mechanisms.

## C2.5.2 Flowlines Life Extension Example

### C2.5.2.1 General

An operator commissioned work to assess and execute a lifetime extension study for a single flexible pipe system. Work was performed according to the approach described in [NORSOK Y-002, 2010] Lifetime Extension of Transportation Systems guideline.

### C2.5.2.2 System Description

The system consisted of a static riser segment and several flowline segments. All were of similar cross sections with minor additional re-enforcing layers in the riser cross section (double outer sheath and increased armour wire thickness). A simplified system layout is shown in Figure C2.3:

### C2.5.2.3 System Screening

The systems had been thoroughly reviewed few years earlier while establishing an integrity management program. This included a test and inspection, assessment of threats, risk level, necessary short- and long term modifications and an integrity management plan.

The system review is summarized by the following notes:

1. Documentation had been sourced and organized during the IM work. Some key information was missing, such as modification and repair reports from the installation phase
2. System review had recently been carried out, and there were no non-closed anomalies or findings that needed to be assessed during the lifetime extension work
3. Current design premise and risk assessments were found to be valid for the required extended time period
4. Gap analysis was performed with the conclusion that original design criteria were more conservative than current revisions. One exception was identified for the cathodic protection system where current requirements for anode mass is based on a significantly higher exposed steel surface area
5. Industry experience for flexible pipes having been a similar time in service was limited. There were no identified industry concerns for similar applications or service history.

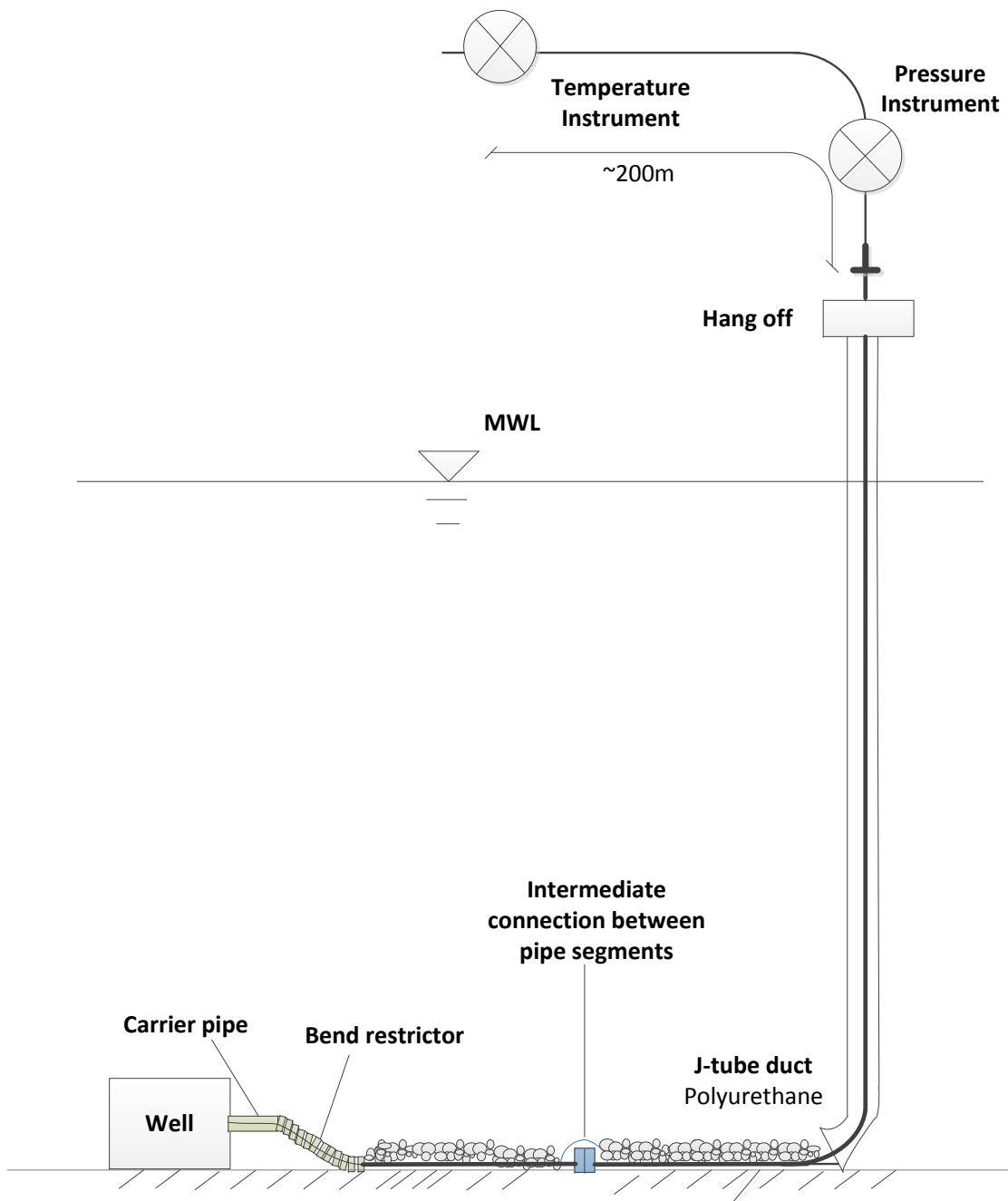


Figure C2.3: Riser and flowline system schematic

#### C2.5.2.4 Condition Control Tools

Condition control tools were assessed to identify possible areas of concern. The following was observed:

1. Direct quantification of ageing of pressure barrier possible due to presence of coupons in topside process piping
2. Operational experience could be gathered for pressure, temperature, and annulus gas and bore fluid sampling. The data for pressure and temperature was however in-

complete as data for initial years was not possible to retrieve, requiring conservative assumptions to be used for this time interval

3. No information was available from visual inspections due to the riser being inside guide-tube, while the flowlines was covered due to protection and upheaval buckling requirements. Only topside end-fitting was accessible.

#### C2.5.2.5 Layer Assessment

A layer assessment was performed with no findings except two areas of concern:

1. Pressure barrier condition due to calculated remaining lifetime less than 5 years
2. Armour wire condition due to uncertainty in flowline annulus condition (dry, condensed liquid from permeation or flooded with seawater. The riser annulus condition was possible to test, providing verification of current annulus condition. )

#### C2.5.2.6 Pressure Barrier Condition

The evaluation was undertaken based on [API 17TR2, 2003]. A modelling of the polymer degradation can then be performed in a quantitative manner. Temperature data was unavailable for the first approximately 8 years of service time, requiring a conservative temperature to be used for this period. From that time on accurate data was available for calculations.

Resulting values indicated that time for reaching the degradation acceptance level for the polymer material was imminent for all possible temperature scenarios (50, 55 or 60°C) - see Figure C2.5. Calculations were performed by the pH 4 curve as a common conservative approach due to partially incomplete bore fluid and chemical usage data.

To verify the calculated results, polymer coupons was extracted from the topside piping for material analysis. A typical coupon setup is shown in Figure C2.4. The spool piece contains 5 individual coupons allowing several samplings during the lifetime. The coupon includes both the carcass and the polymer pressure barrier layer similar to the flexible pipe, but not the remaining layers.



Figure C2.4: Left: Coupon Spool Piece. Right: retrieved coupon sample

The results from actual material testing see Figure C2.5 for comparison toward calculations, showed that sufficient integrity level was present for the required extended service life. Some

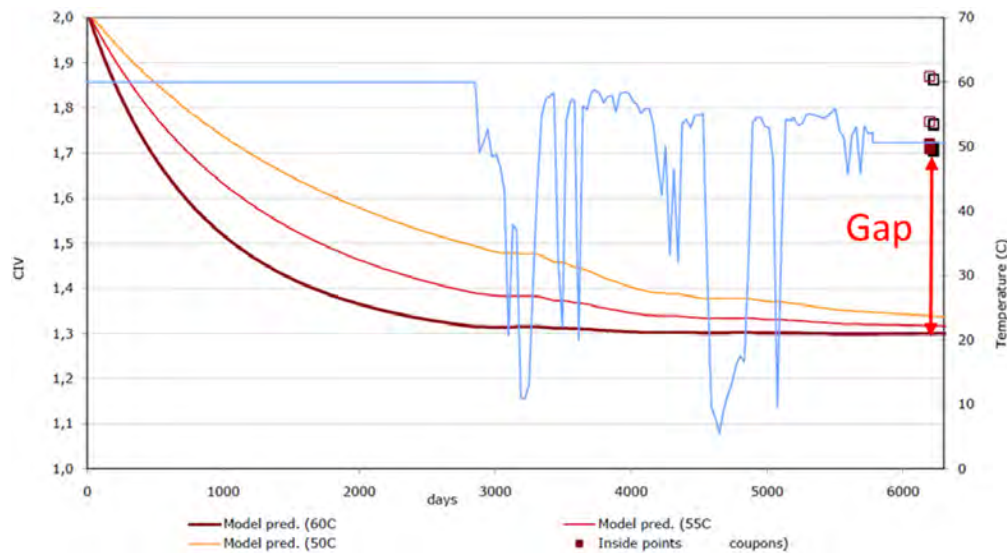


Figure C2.5: Polyamide degradation based on [API 17TR2, 2003]. Figure shows reduction of Corrected inherent viscosity (CIV), an indirect measure of molecular weight and material ductility, as function of time in operation. Gap indicates difference between lowest calculated CIV value and lowest measurement from coupons. Blue line represents the temperature profile (historical data) - horizontal section in left part represents time where assumption has to be made due to unavailability of measurement data. Different assumptions were used - only one temperature profile line is shown however.

uncertainty is inherent as the coupons are located topside, while the high-temperature end may have a higher degradation rate.

A lesson learnt was that further confidence could be obtained if the integrity management program had performed periodic coupon retrieval, thus allowing trending data and possibly calibrating the calculation model at an earlier stage.

### C2.5.2.7 Armour Wire Condition

Annulus conditions for the flow-lines were thoroughly assessed. Based on:

- experiences with outer sheath damages during installation,
- risk of outer sheath burst if GRVs had failed in closed position
- risk of GRVs failing in open position

It was concluded that a flooded annulus should be assumed. Liquid filling in itself did not present a problem; however any direct exposure of armour wires to surrounding fluids results in requirement for verifying CP system condition.

Due to the fact that neither the protection potential nor anode mass could be inspected and verified, general armour wire corrosion needed to be considered.

Calculating the acceptable armour wire corrosion based on a damage during installation and malfunctioning CP system showed that within 22 years the maximum allowable utilization during operation would be exceeded.

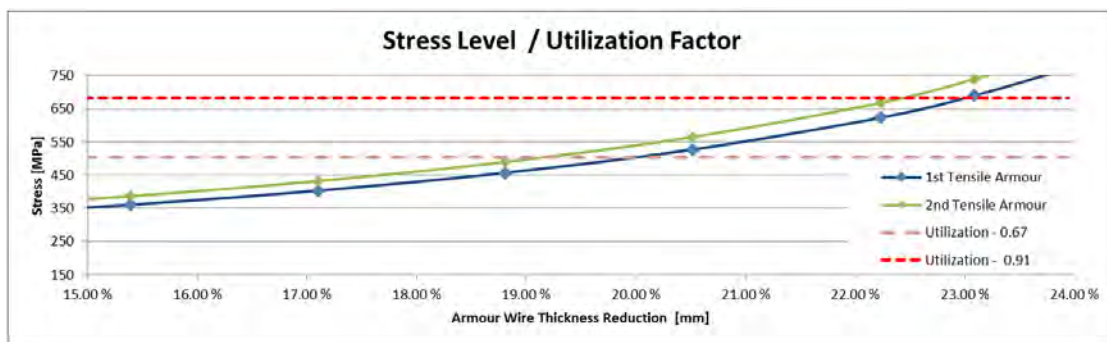


Figure C2.6: Tensile armour wire stress level as function of thickness reduction

With the estimated thickness reduction over 22 years of operation a maximum pressure of 95 bars was found. This was concluded unacceptable as the well shut-in pressure was significantly higher.

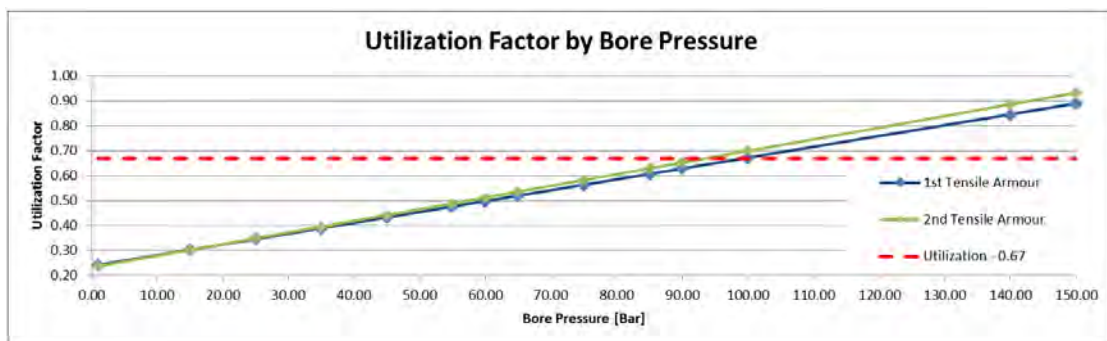


Figure C2.7: Tensile armour utilization factor as function of bore pressure at determined minimum wire thickness level

### C2.5.2.8 Conclusion

Based on the armour wire corrosion scenarios evaluated, it was found required to verify the cathodic protection system condition. As the whole length of the flowline segments were covered (due to requirements for impact- and trawling protection), this was not feasible. In addition this would entail intervention work of high risk for causing damage to the flexible pipe as well as high cost.

Final conclusion was that the flexible pipe system should be decommissioned at the end of current design life.

Lesson learnt is that to provide solutions for inspection and monitoring during the design and development phase needs to be pursued. Inspection possibilities may have provided an acceptance of lifetime assessment, thus allowing an extended service life. Integrity management within the design life would also have benefitted from such possibilities through providing inspection data confirming the design integrity.

### C2.5.3 Re-qualification example after outer sheath damage and annulus flooding

Several older design premises only considered dry annulus as input to fatigue calculations. Several of these systems have experienced outer sheath damages resulting in annulus flooding with seawater.

Annulus testing indicated the presences of an outer sheath loss of integrity in the upper riser section, i.e. above 30m water depth. Upon performing ROV inspections, the damage was located and confirmed, see example in Figure C2.8.

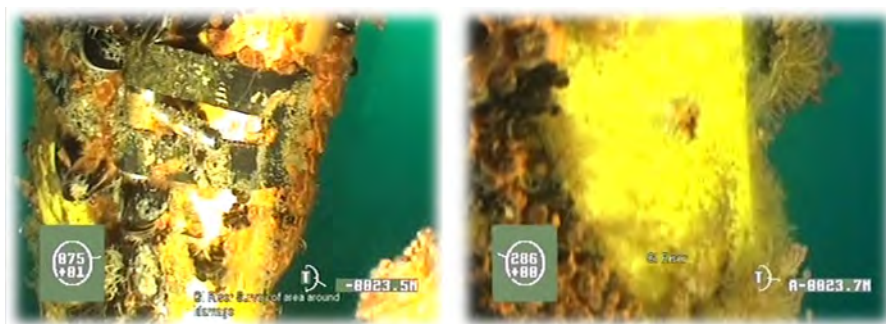


Figure C2.8: Outer sheath damage due to interference with neighboring riser bundle

The time from the last annulus test provided a timeframe for the exposure time, i.e. 1.5 years. This timeframe is typically based on an annual inspection plan. General corrosion and material loss for the maximum exposure time was not found to be critical, refer to Figure C2.9. Conservative assumptions applied for both corrosion rates and exposed area. Short-term integrity was thus found to be acceptable, and repair work was successfully undertaken to restore the outer sheath integrity as soon as possible to limit further exposure of the armour wires.

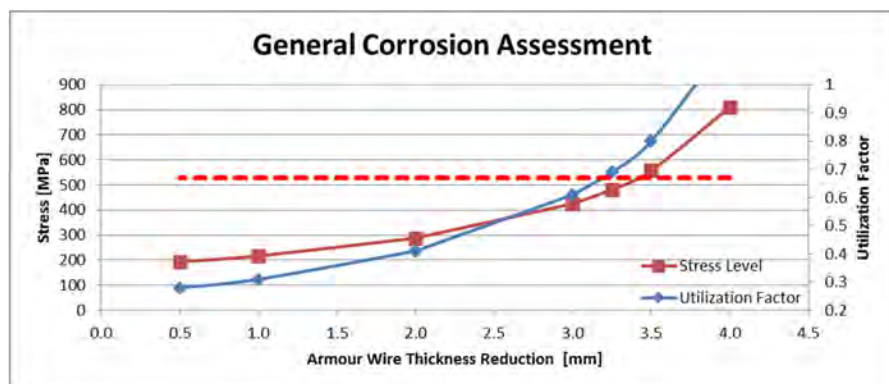


Figure C2.9: General corrosion assessment in regards to remaining service life. Remaining service life > 5 years from damage initiation

Establishing the long-term integrity and allowable service life was undertaken in parallel with the repair work. The design premise was found to only consider dry annulus, thus the service life was not documented in the current condition, where the possibility for accelerated fatigue due to a more aggressive annulus environment was present.

Fatigue calculations were performed according to a similar process and best practices as for the design phase works. The key challenges identified were the following:

1. Accurately quantify accumulated fatigue damage up to the event of outer sheath integrity loss due to missing operational bore pressure data
2. Accurately quantify future fatigue damage due to unavailability of SN curves for the current annulus environment

Challenge 1 resulted in the necessity to utilize bore pressure at the operational maximum limit as a conservative approach. Actual bore pressure values were expected to be in the order 80% of this, which could have gained approximately doubling of the fatigue life, see Figure C2.10. Reduction of available remaining service life is thus directly related to insufficient monitoring data handling.

Challenge 2 resulted in the necessity to utilize SN curves for higher concentrations of corrosive elements, i.e. SN curve #3 (see Figure C2.10), than actual expected values as shown in SN curve #2. A reduction in the order of 1/4 of the more probable lifetime was experienced. Developing accurate SN curves are both time consuming and costly, however this parameter is perhaps the most single most significant input with very large impact on the new total allowable service life.

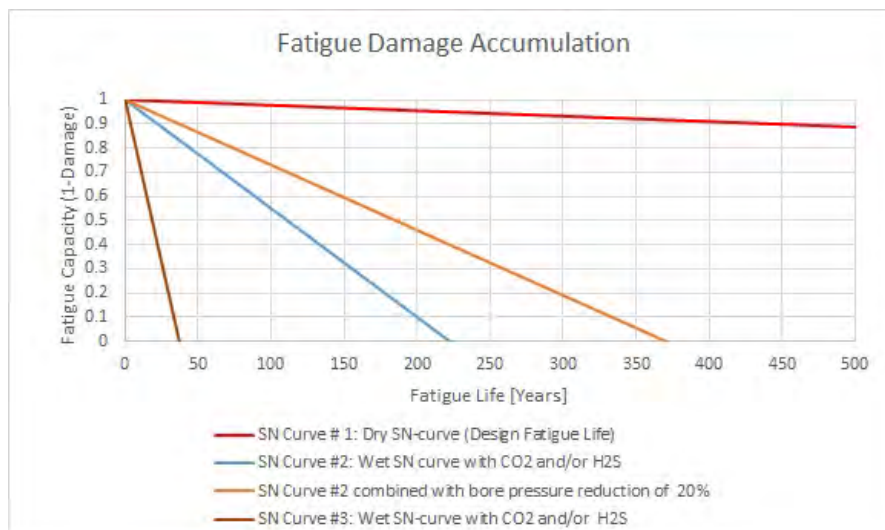


Figure C2.10: Fatigue service life sensitivity for different input parameters. Fatigue capacity is 1 if no damage ( $D$ ) has been accumulated. At a value of 0 no remaining capacity exists, i.e. end of service life. NOTE: Fatigue Life is Fatigue Service Life  $\times$  SF = 10



## **Chapter C3**

# **Repair Methods**

*Author: 4Subsea*

## C3.1 Introduction

This chapter addresses repair methods for flexible pipe including end-fitting. Ancillary devices to flexible pipes such as bend stiffeners, buoyancy modules and friction clamps are omitted.

Historical data of failure and damage to flexible pipes are described in Chapter [A3 Failure Modes](#).

A list of possible methods for inspection and integrity monitoring along with related industry practice is presented in Chapter [C1 Integrity Management](#). The feasibility and actual use of the inspection methods are presented as part of Table [C3.1](#).

The outline of this chapter is as follows:

Section [C3.2](#) gives an overview of repair methods status for a wide range of known failure modes.

Section [C3.1](#) describes the process of planning for repair from detection of the damage to continued operation of the pipe after repair.

Section [C3.4](#) describes repair methods for outer sheath damages.

Section [C3.5](#) describes repair methods to re-establish annulus vent for flexible pipes with restricted annulus vent flow.

Section [C3.6](#) presents an overview of re-termination of end-fitting as a repair method. This repair method can be suitable for a variety of damages near the pipe ends. Re-termination could also be applied to a segment along the pipe: by cutting the pipe, re-terminate both ends and insert a short flexible jumper or spool piece connecting the two re-terminated ends.

## C3.2 Repair method status

### C3.2.1 Overview of failure modes

This section presents a list of known failure modes for flexible risers based on tables 30-31 in [API 17B, 2008] and a report from PSA Norway on flexible pipes [Muren, 2008]. Related methods known to 4Subsea for inspection and repair are listed for each failure mode where applicable.

Table C3.1: Failure modes, inspection methods and repair methods for flexible risers - [API 17B, 2008]. Column 'Defect ref.' refers to relevant section in [API 17B, 2008].

Pipe layer	Defect ref.	Defect	Inspection methods	Repair method	Comment
Carcass	1.1	Hole, crevice, pitting or thinning	Internal visual inspection	None *	Careful internal inspection over full pipe length recommended
	1.2	Unlocking deformation	Internal visual inspection Digital X-ray	None *	Acoustic methods in pilot applications offshore
	1.3	Collapse or ovalization	Collapse: Internal visual inspection, and digital X-ray Ovalization: Internal measurements and inspection (intelligent or gauge pigging)	None *	Collapse: Replacement of riser
	1.4	Circumferential cracking / wear	Internal visual inspection	None *	
		Carcass fatigue cracks	Internal visual inspection	None *	Careful internal inspection in all dynamic areas recommended
		Carcass erosion	Internal visual inspection	None	Likely to be spread out over riser length, most significant in curves / bends
		High frequency vibrations due to vortex shedding at carcass cavities (in gas pipes)	Audible noise Vibration measurement Spectral analysis	Components attached to connected pipe work may be removed, or strengthened	No experienced carcass or riser damages due to vibrations
Internal pressure sheath	2.1	Crack or hole	None (Internal inspection in smooth bore pipes)	None *	Breach in the pressure sheath will eventually lead to leak.

Pipe layer	Defect ref.	Defect	Inspection methods	Repair method	Comment
	2.2	Rupture	None (Internal inspection in smooth bore pipes)	None *	
	2.3	Collapse	Internal visual inspection	None	
	2.4	Ageing embrittlement (PA11, PVDF, HDPE)	Coupon sampling and analysis	None *	Re-termination of a riser with pressure sheath ageing localized to the end successfully performed
	2.5	Excess creep (extrusion) of polymer into metallic layer	None	None	
	2.6	Blistering	None	None	
	2.7	Rupture (due to fatigue)	None	None *	
	2.8	Wear / nibbing	None (Internal inspection in smooth bore pipes)	None *	
	3.1	Individual or multiple wire rupture (static lines)	X-ray	None	Successfully used to detect wire fracture and unlocking. Used onshore and offshore above waterline.
	3.2	Unlocking	X-ray	None	
	3.3	Collapse or ovalization	External inspection Internal inspection (due to interaction with layers inside pressure armour)	None *	Gross errors are possible to identify from external and/or internal inspection
	3.4	Corrosion	None	None	
	3.5	Individual or multiple wire rupture (Dynamic lines)	See 3.1	See 3.1	See 3.1
	3.6	Longitudinal wire crack (hoop direction)	None	None	Should be possible to detect by X-ray tomography. (Currently used in laboratory, no offshore experience)

Pipe layer	Defect ref.	Defect	Inspection methods	Repair method	Comment
Back-up pressure armour layer	4.1	Rupture (single wire or all wires)	X-ray	None	
	4.2	Ovality	External inspection Internal inspection (due to interaction with layers inside pressure armour)	None *	Gross errors are possible to identify from external and/or internal inspection
	4.3	Clustering	X-ray	None	
	4.4	Corrosion	None	None	
	4.5	Individual or multiple wire crack	None	None	
Tensile armour layers	5.1	Multiple-wire rupture (static line)	Eddy current, Digital X-ray External inspection related to outer sheath rupture Torsion measurements Fiber optics measurement	None	Fractures identified on outermost armour layers. Used in positions with identified anomaly. Promising development based on acoustic methods
	5.2	Bird-caging or clustering	Eddy current or X-ray for clustering External inspection for bird-caging	None	Successful X-ray inspection performed
	5.3	Kinking	X-ray External inspection	None	External inspection frequently performed
	5.4	Corrosion	X-ray, eddy current, ultrasonic inspection	None	X-ray successfully used to detect gross corrosion damage
	5.5	Individual-wire rupture (dynamic line)	See 5.1	See 5.1	See 5.1
		Hydrogen induced stress cracking (HIC)			For wire rupture due to HIC see 5.1
		Wear between steel armor layers and other layers	None	None	

Pipe layer	Defect ref.	Defect	Inspection methods	Repair method	Comment
		Buckling of the pipe	External inspection permanent buckling (e.g. upheaval buckling)	None	Frequently used for flow lines
Annulus		H <sub>2</sub> S or CO <sub>2</sub> diffusion: Acid annulus	Bore fluid monitoring, H <sub>2</sub> S-measurements in annulus test, annulus vent monitoring	Change operational condition / bore fluid	H <sub>2</sub> S-measurements performed on annulus vent gas may be inconclusive due to absorption of H <sub>2</sub> S in steel and volatile gas
		Flooded annulus	Annulus volume test	Consider injection of inhibitor all dependent upon cause for flooding	Annulus volume test is not able to distinguish between oil, condensed water or minor leak to sea. Liquid pockets in low points may disturb inspection accuracy Re-assessment of riser permissible service life required if not considered in design.
Anti-wear layer	6.1	Wear, cracking	None	None	
	6.2	Clustering	None	None	
Insulation layer	7.1	Crushed layer	External visual inspection	Retrofit additional external insulation Repair or replace whole or part of insulation layer	Repair must consider clamp-on devices where relevant
	7.2	Flooded layer	Monitoring of temperature (temperature drop) and bore condition. Temperature reading on optical fibers	Not required	Flooded layer shall be considered during design [API 17J, 2008]

Pipe layer	Defect ref.	Defect	Inspection methods	Repair method	Comment
	7.3	Pipe clogging (bore)	Flow monitoring (bore) Internal inspection	Internal pigging Chemical injection Flushing Retrofit additional external insulation Repair or replace whole or part of insulation layer	Pigging and chemical injection are frequently used Hydrate removal may damage carcass
Outer sheath	8.1	Hole, tear, rupture or crack	Annulus volume test External visual inspection Annulus vent monitoring	Repair methods for outer sheath damage (see Section C3.4 )	
	8.2	Ingress of seawater	Annulus volume test Ultrasonic external tool	If hole in outer sheath located near subsea end: Flushing of annulus with MEG and repair of outer sheath damage (see Section C3.4 )	
	8.3	Wear, tear	External visual inspection	Repair methods for outer sheath damage (see Section C3.4 )	Repair or additional protection may be adequate for wear damages
		Ageing and degradation	External visual inspection	None	For local repair see Section C3.4
End fitting	9.1	Internal pressure sheath pull-out	X-ray for pressure sheaths with platinum markers Annulus vent monitoring Major leak when fully pulled out	Re-termination	May result in failure of riser.
	9.2	Tensile-armour pull-out (all wires)	None, major leak when fully pulled out	None	Expected to result in failure of riser.
	9.3	Outer sheath pull-out	Annulus vent monitoring or annulus volume test Visual inspection	Re-termination	

Pipe layer	Defect ref.	Defect	Inspection methods	Repair method	Comment
	9.4	Vent-valve blockage	Annulus volume test / Annulus vent flow test Annulus vent monitoring	Repair methods to re-establish annulus vent (see Section C3.6)	Restore annulus vent. Test for permanent damages to outer sheath.
	9.5	Vent-valve leakage	Subsea: Purge gas or detectable liquid through annulus Topside: Gas leakage test	Replace valves (replacement of subsea vent plugs have been performed successfully)	Asses impact of the leakage on remaining service life.
	9.6	Individual tensile-armour pull-out	None	None	
	9.7	Failure of sealing system (sealing rings, etc.)	None	None	
	9.8	Crack or rupture of pressure armour or back-up pressure armour	None	None	
	9.9	Crack or rupture of tensile armour	None	None	
	9.10	Structural failure of end fitting body or flange	None	None	Pipe burst / catastrophic failure. Replacement of riser
	9.11	Cracking of pressure sheath	None	None	Pipe burst / catastrophic failure. Replacement of riser

\* Note: Re-termination if defect is confirmed to be close to end only

### C3.2.2 Market screening

In categorising proven repair techniques and commercial products for flexible pipes the market has been screened for known designs and vendors. This included a dialog with different parties involved in the flexible pipe market from flexible pipe manufacturers and offshore installation companies to consultancy groups and inspection companies.

The market for commercial products associated to repair of flexible pipe is fairly narrow and is more related to stand alone products designed for a specific project. Different solutions exist at a development level still to be tested and are not at present commercially available.

Hence, detailed description of these products is not presented.

The available and proven methods are grouped into three main categories:

- Repair methods covered by flexible pipe manufacturer
- Commercially available repair methods
- Stand-alone repair methods

Polymer welding of the outer sheath is the most common repair method covered by the pipe supplier, a service most often provided during installation of the pipes.

A limited number of commercial products are identified which includes the products 'FlexGel' and 'Armadillo' both developed and supplied by Flexlife and 'Armawrap' supplied by NICC.

Several special designed repair methods exist and have been used on various locations for temporary or permanent use. Most common methods comprise sealing of outer sheath rupture by soft or steel clamps and re-establishment of end-fitting vent system by installation of annulus vent clamps.

The different repair methods are described in Section [C3.4](#), Section [C3.5](#) and Section [C3.6](#).

### **C3.2.3 Evaluation of repair methods and general guidance on repair possibilities**

On the basis of the preceding sections, there are a limited number of failure defects which are possible to detect, and even fewer which are possible and beneficial to repair.

The repair methods covered in this report are limited to failure modes which are both possible to detect and possible to repair. Common for the identified repair methods is that both the products available on the market and the stand alone designs used on specific projects all relate to:

- Outer sheath damages
- Restricted or blocked annulus vent

4Subsea is aware of in total 4 re-terminations of flexible pipe end-fittings conducted offshore by the pipemanufacturers; of these at least two have been described as unsuccessful. Note also the separate hazard warning for re-termination in Section [C3.6.2.1](#). Re-termination of flexible pipe end fittings should always be performed in cooperation with the flexible pipe manufacturer. This will be covered separately in Section [C3.6](#).

From 4Subsea experience it is generally possible to repair damages limited to the outer sheath or to restricted (blocked) annulus vent. Any structural damage needs careful consideration and is never straight forward to repair.

### **C3.2.4 Qualification of new inspection methods and repair methods**

New methods and technologies are continuously developed and there is a need for qualification to ensure that the new technology meets the specified requirements. Qualification

of a repair method is a part of the complete process of planning for repair as described in Section [C3.3](#). For qualification of new inspection methods and new repair methods, guidance may be found in standards and reference documents. Reference is here given to DNV's recommended practice (RP) on Qualification of New Technology [[DNV-RP-A203, 2012](#)]. The general methodology in the DNV RP is briefly described in the following.

The recommended practice is based on a system approach, in which an initial screening of the system should be performed to identify novel elements. The failure mechanisms associated with the use of these novel elements will in turn be the main focus in the qualification process. The elements which are not novel should be verified separately as for proven technologies. The qualification is an iterative process to detect and correct for deviations on material, components and assembly levels. Possible failure modes for the system should be identified and the qualification must include appropriate margins for each failure mechanism associated with the failure modes. Thus, larger uncertainties will require larger margins to meet the requirements.

### C3.3 Planning for repair

The process of planning and executing a repair is illustrated in a flow chart in Figure C3.1. The flow chart covers the entire process from detection of damage to continued operation of the pipe. For a damage which is possible to repair, there are 4 main steps in the process:

1. Damage assessment
2. Design and qualification of repair method
3. Execution of repair and verification of pipe integrity
4. Continued operation of the flexible pipe and update of the integrity management program

These steps are described in the following with reference to Figure C3.1.

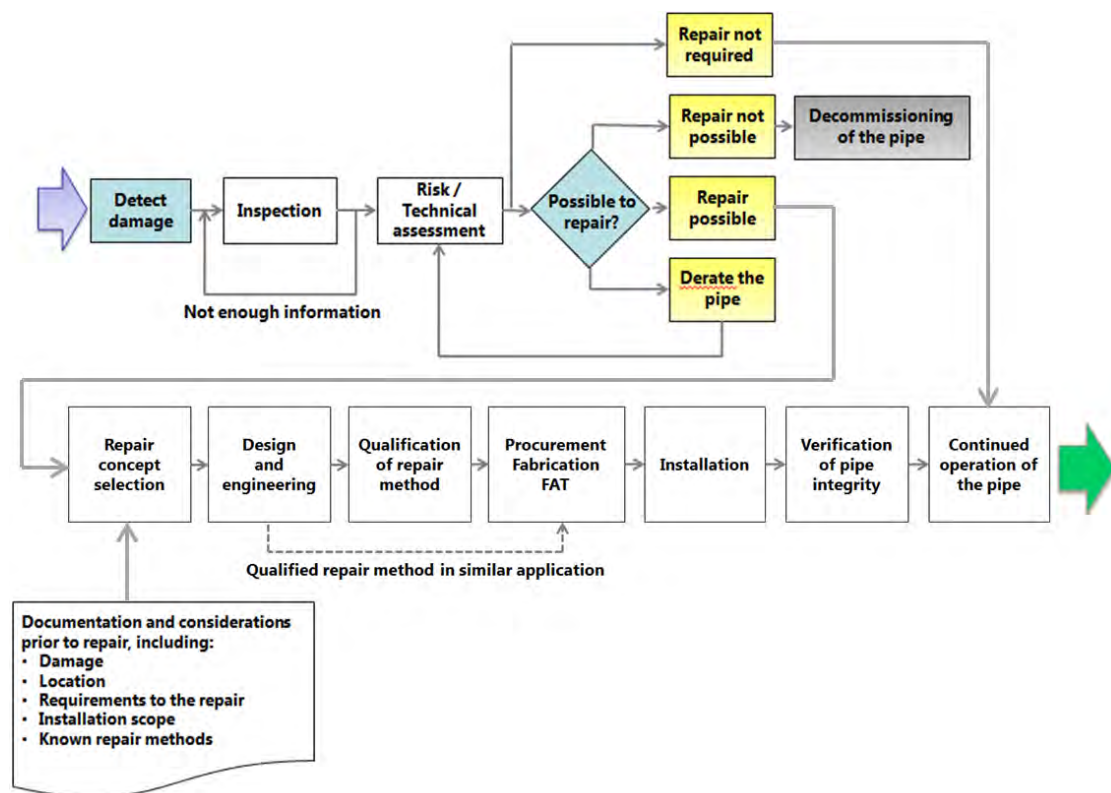


Figure C3.1: Flow Chart for the process of repair execution

#### C3.3.1 Damage assessment

The obvious starting point for a repair process is detection of the damage. This is followed by an inspection of the damage in order to provide input for a technical assessment of the damage. The inspection should address the following: pictures and extent of the damage, type of damage and possibly the cause. If the current information from inspection proves insufficient, there will be a loopback to perform additional inspections before continuing on the technical assessment.

The technical assessment covers the following:

- structural integrity of the pipe
- risk level
- remaining service life
- feasibility for repair
- updated integrity management system

Additional or more detailed inspections may be necessary as part of the technical assessment.

The technical assessment should eventually result in a conclusive answer to the following question: 'Is it required and possible to repair the damage?' There are generally four alternative answers:

- Repair is not required: The pipe is ready for continued operation, update of integrity management program may be required e.g. frequent inspections
- Repair is not possible: The pipe should be decommissioned
- Repair is possible and required: Continue the process of planning and executing a repair
- Derate the pipe: This should be considered for pipes where repair initially is considered not possible for the existing service/operational conditions. Derating the pipe will change the input for the technical assessment and hence result in a loopback to a new technical assessment.

### C3.3.2 Design and qualification of repair method

There is a need for a broad range of input to establish functional requirements for the repair as part of the repair concept selection. The list of necessary documentation and considerations to this process includes:

- Key properties of the pipe
  - Datasheet, structural composition
  - Riser configuration lay-out
  - Operating pressure, temperature, bore content and injection chemical history
  - Possible deviations during manufacturing of the pipe
  - Any previous repair history of the pipe
- Key features of the damage, including pictures
  - Extent of damage
  - Type of damage
  - Cause of damage
- Location of damage
  - Water depth

- Dynamics and curvature of the pipe at the location of the damage
  - Interference with surrounding structures
  - Access to the damage
- Requirements to the repair
    - Structural integrity
    - Durability
    - Outer environment (sea water, hydrocarbons, riser dynamics, adjacent structures, etc.)
    - Material properties and degradation mechanisms (corrosion, ageing, creep, etc.)
  - Installation scope
    - Access to the damage, consider the feasibility for use of ROV, divers or rope access
    - Time
    - Cost
  - Known repair methods
    - Review previous repairs for similar applications

The repair concept design and engineering includes description of concept, selection of materials, calculations, drawings, installation method, and maintenance issues.

The repair method is subject to a qualification run including verification testing to ensure that the resulting repair method meets the specifications and fulfill its objective. The type of test is to be agreed with the pipe owner. Qualification process includes FMECA of failure modes and mechanisms associated with the loads determined for the specific application, and identification of tests on material, components and assembly levels that have not been previously performed or whose outcome cannot be confidently inferred by using predictive tools validated with prior test data.

When a previously qualified repair method is applied to an equivalent damage, the design and verification process may be simplified. However, it is emphasized that a previously qualified repair method should undergo a new qualification when used in a different application.

### C3.3.3 Execution of repair and verification of pipe integrity

The final repair solution is prepared, including procurement of the necessary components and fabrication of the repair solution itself. A factory acceptance test (FAT) is usually performed to verify the final repair solution and its accompanying components prior to installation. Reference is given to the details on hydrostatic pressure test (leak test and structural integrity test) provided in [API 17B, 2008]

Installation is usually performed by ROV or divers in subsea application. For outer sheath damages located above sea level, access for installation may be obtained by rope access or scaffolding. Direct access to the topside end-fitting (as for repair methods to re-establish annulus vent) is often facilitated at the hang-off location. Further details on installation are

given for each repair method in the following Section [C3.4](#), Section [C3.5](#) and Section [C3.6](#).

Documentation of the installation usually includes installation summary, as-built documentation and test report.

The repair and pipe integrity is verified after repair; normally pipe integrity is verified as follows:

- An annulus test is performed to confirm a successful repair after a repair of outer sheath damage or re-establishment of annulus vent.
- A pressure test is performed to confirm structural integrity of the pipe and end fitting after re-termination.

A successful repair is followed by continued operation of the pipe and update of the integrity management program for the flexible pipe. Generally, there are also requirements for periodic inspection and maintenance of the repair. Details on these requirements are presented for each repair method in the following sections ( Section [C3.4](#), Section [C3.5](#) and Section [C3.6](#) ).

## C3.4 Repair methods for outer sheath damages

Outer sheath damages include wear, tear, holes and breaches. Damages which are not penetrating through the outer sheath shall not be cut through or be handled so as to cause a hole. These damages should be reinforced if required with one of the methods described in this section.

### C3.4.1 Injection of inhibitor liquid in annulus

#### C3.4.1.1 Objective and application

In the case of an outer sheath leakage, injection of a corrosion inhibitor may constitute a mitigating action. The objective is to top-off riser annulus with the inhibitor in order to both displace already ingressed seawater as well as limiting further ingress, thus avoiding seawater containing oxygen from circulating the armour wires.

For the purpose of displacing seawater, the use of an inhibitor – such as Mono Ethylene Glycol (MEG) – with density somewhat higher than seawater is beneficial. Injection of MEG, combined with tracer dye, could additionally be used for leakage test to localize the outer sheath damage. Injection of inhibitor is preferably used in combination with one of the other repair methods for outer sheath damages described in the following sections in order to seal off the damage from a corrosive environment.

The strategy of using an inhibitor fluid, e.g. Mono Ethylene Glycol (MEG), to limit further corrosion has been performed by operators in the North Sea [[Taylor et al., 2002](#)], [[Picksley et al., 2002](#)]. The methodology is not standardized, but shown viable for the riser in question. It should be ensured that no related material degradation effects are enhanced.

#### C3.4.1.2 Description of the use and injection setup for an inhibitor liquid

An example of a MEG injection system assembly is schematically depicted in Figure C3.2. An air driven pump injects MEG from a storage tank in to the riser annulus. The pump air inlet pressure is controlled by a pressure regulator. Pressure safety valves (PSV) are used as extra precaution to avoid pressure surges in the system. The applied feeding pressure depends on the capacity of the outer sheath and the riser configuration for the actual flexible pipe in question. Gravity feeding of the inhibitor fluid is an alternative for injecting the fluid into riser annulus – though limited flow rates experienced shows this to be more viable for topping-up than initial filling.

It is difficult to verify successful protection of the armour wires by this method. In this context, the importance of having control of the injected volume, riser annulus volume, applied feed pressure and riser configuration is emphasized. Prior to the injection, the annulus volume should be estimated and used to establish criteria for the necessary injected volume. Throughout the injection of the inhibitor, the injected volume and volume rate should be continuously monitored to provide a basis for a subsequent evaluation of the repair. Dye added to the injected inhibitor and simultaneous monitoring of the location of the outer sheath damage may provide additional information on the flow of inhibitor and the effect of the injected inhibitor.

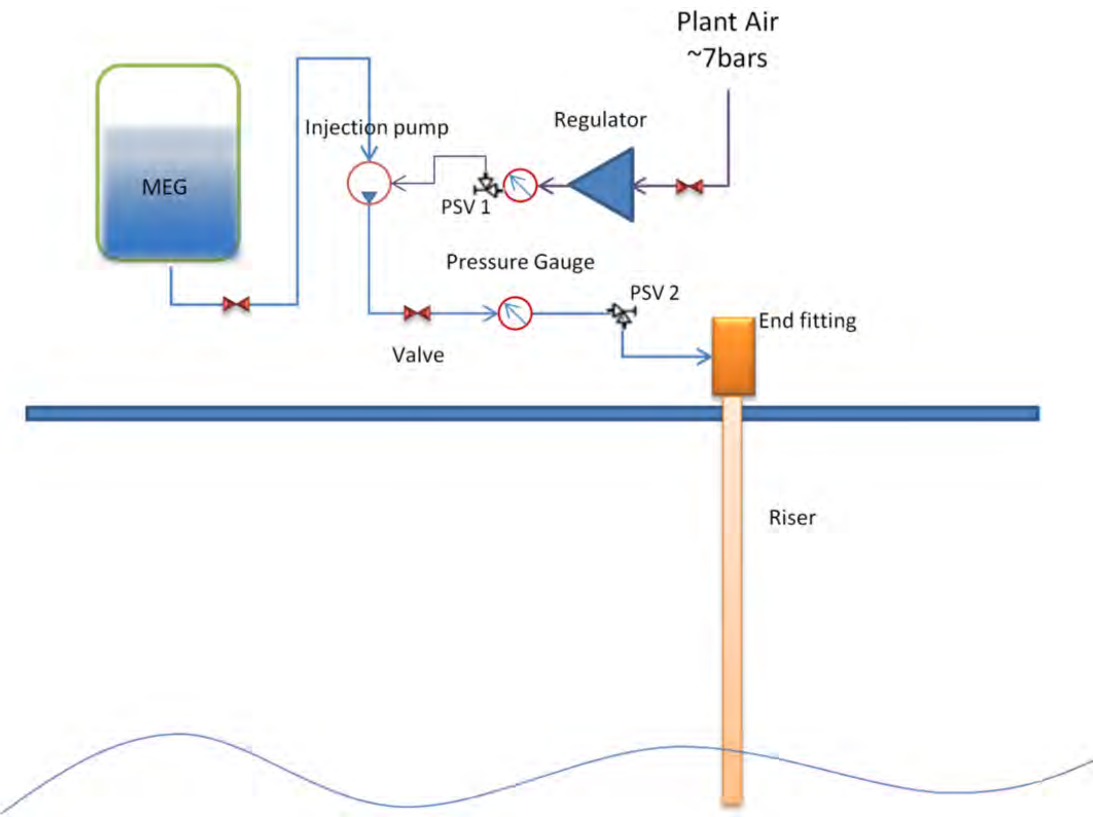


Figure C3.2: MEG injection setup

#### C3.4.1.3 Subsequent inspection and maintenance

Subsequent to the injection of inhibitor, the outer sheath damage may be repaired by one of the methods presented in the following sections or alternatively more MEG may be added periodically to top off riser annulus and thereby prevent ingress of seawater. For a permanent repair, periodically gas sampling is advised in order to monitor the annulus condition, in particular with respect to possible corrosion processes.

#### C3.4.1.4 Advantages and drawbacks, including aspects to consider before injection

One of the advantages of this method is that it does not require any direct access to the repair area.

The injection of an inhibitor liquid in annulus is either used as a mitigating action until a permanent repair is installed sealing off the outer sheath damage or to control corrosion in a wet annulus. There are additional concerns and limitations related to this method:

- Requires acceptable flow rates through the vent parts and end-fitting
- The allowable feeding pressure is limited by the capacity of the outer sheath
- Dependent on the riser configuration, there may be local elevation differences along the riser length, i.e. between sag and hog bends. A large elevation difference here may cause entrapment of permeated gases in annulus resulting in a local pressure build up and possibly burst of outer sheath. There are known examples of installing a vent

clamp with a relief valve at the hog bend to prevent the local pressure build up. Such vent clamps may prevent the injection of inhibitor liquid.

- It is difficult to verify successful protection of the armour wires by this method. However, having ensured the ability to inject MEG along the full riser length, a single point of leakage (a hole in the outer sheath or an open vent port) located near the subsea end could ensure proper evacuation of seawater and thus improve control of the inhibitor's effect.
- Some concerns have been raised on the long term effect of MEG in regards to souring and subsequent polymer and steel material degradation. The properties of the applied inhibitor and its interaction with polymers, armor wires and annulus fluids should be assessed before initiating this repair. The inhibitor's exposure to temperature and possible reactions with permeated gases from bore fluid should also be part of this evaluation.
- The application of this method to displace seawater involves discharge of the inhibitor liquid to sea. Local legislation and regulations concerning discharge of the inhibitor liquid to sea should be considered upon choice of inhibitor.

## C3.4.2 Soft repair clamp

### C3.4.2.1 Objective and application

The soft repair clamp is typically suitable for subsea areas of the flexible riser with minor damages of the outer sheath, such as a hole or a tear. It is not suitable to repair structural damages such as damages to the armor wires. The repair clamp can be specifically designed to seal around small protruding parts of the outer sheath next to the damage.

The purpose of this repair clamp is to seal off the damage and thereby avoid seawater containing oxygen from circulating the steel armour.

There are no known limitations to the structural dimensions of the flexible pipe to be repaired, as the soft clamp is custom made for the repair area. Examples of successful repairs:

- Riser with OD 204 mm, damage with approximate dimensions: area 50 mm x 50 mm
- Dynamic umbilical with OD 204 mm, damage with approximate dimensions: area 80 mm x 40 mm and height of protruding part 40 mm

### C3.4.2.2 Description of the repair clamp and installation method

The damaged area and the surrounding area of the outer sheath are cleaned prior to clamp installation. The clamp is illustrated in Figure C3.3 . The main component of the clamp is the polyester strop which provides constant radial pressure on the damaged area through hoop tension. The polyester band has slings at each side with a tension rod inside. One tension rod is equipped with two bolts and the other is equipped with two nut receptacles. The repair clamp is installed using a work-class ROV (WROV) and a hydraulic clamp installation tool, illustrated in Figure C3.4. The WROV places the clamp over the damaged area and closes the tool hydraulically around the riser. Then, the bolts are flipped over to enter the

receptacles and the bolts are tightened to the specified torque. A rubber pad mounted inside of the repair clamp is designed to seal around the damage in the outer sheath.

The repair is verified by performing an annulus volume test in order to check that the clamp is pressure tight as intended.

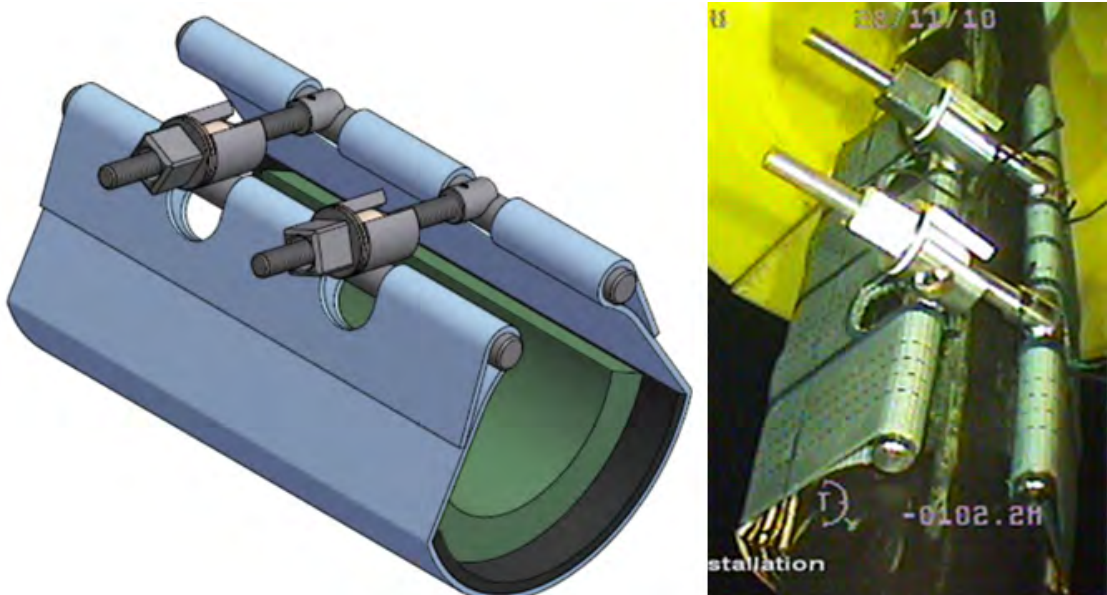


Figure C3.3: Soft clamp



Figure C3.4: Soft clamp: ROV installation tool and soft clamp

#### C3.4.2.3 Subsequent inspection and maintenance

Dependent on the installed clamp and flexible pipe properties, retightening of bolts may be required. Further, periodic annulus volume tests should be performed in order to verify outer sheath integrity and annulus condition. Additionally, the repair clamp should periodically be subject to visual inspection to check the condition of the clamp, e.g. check for interference with neighboring structures, corrosion and general condition of the clamp and its components.

Table C3.2: Design issues for a soft repair clamp

Component	Main Function	Design issue
Polyester band	Transfer bolt-tension to radial pressure onto pipe body (load bearing)	Creep
Tension rod, bolts, nuts and nut receptacles	Tensioning of the clamp	Corrosion Thread damage (galling of threads)
Tension rod, bolts, nuts and nut receptacles	Tensioning of the clamp	Poor fit or buckling of the rubber liner Sealing Durability

Marking of the as installed position on the riser should be made and the clamp should be periodically verified to stay in position. The choice of inspection method, either general visual inspection (GVI) or close visual inspection (CVI) is dependent on the purpose of inspection and environmental conditions such as marine growth and visibility.

#### C3.4.2.4 Advantages and drawbacks

An advantage is that this is a proven repair method with several successful repairs. The clamps are considered as low-cost. The clamp is customized for a perfect fit with the dimensions of the damage and the diameter of the flexible pipe. However, there are some drawbacks for the subsea soft-clamp:

- Difficulties are experienced related to pressure sealing capabilities; the outer sheath surface around the damage must be clean and smooth in order to get a tight seal.
- Protruding bolts from the clamp will be present after the installation. The risk of interference and damage on neighboring structures must be considered. Mitigations are for example proper orientation of clamp, cutting surplus protruding bolt length and applying a soft protection.
- Small dynamic motions of the flexible pipe and WROV are required at the location of the damage (may yield weather restrictions on installation)
- An experienced WROV pilot is required in order to install the clamp correctly at the location of the damage
- Sufficient spacing to the neighboring risers must be present for the WROV to get access.

#### C3.4.2.5 Design aspects

The main components of the soft repair clamp are listed in Table C3.2 along with their main function and particular issues which should be considered in design. In addition to these particular design issues, there are general issues to consider as presented in Section C3.3.2.

The design issues listed in Table C3.2 are described in more detail below:

- **Creep**  
Dependent on the applied pretension, creep in the strop may cause reduced radial pressure and possibly poor sealing of the damage.
- **Corrosion**  
Metallic parts may be fabricated in material resistant to corrosion.
- **Thread damage**  
Coating may be used to ensure the nuts can be torqued to the set level without thread damage occurring (galling of threads). Plastic spacer may be used between the nuts and clamp body to control friction and surface damage.
- **Poor fit or buckling of the rubber liner**  
In order to prevent buckling of the rubber liner and to ensure constant radial tension, the rubber liner should match the actual OD of the flexible pipe and fit the damaged area. Further, the rubber surface may be lubricated in order to reduce friction between the rubber liner and the outer sheath of the flexible pipe.
- **Sealing**  
In order to improve the sealing capabilities of the rubber liner, sealing tape or mastic may be filled into the rubber liner window and acting as a sealing putty.
- **Durability**  
The material selection for the rubber liner should take into account ageing of the materials and the exposure to the environment; such as hydrocarbons, annulus compounds, seawater, chemicals and sunlight.

### C3.4.3 Rigid clamp

#### C3.4.3.1 Objective and application

This method is applicable to outer sheath damages. The purpose of this repair is to restore the outer sheath integrity and avoid exposure of steel armour wires to environmental exposure. This clamp may also be modified to allow for future re-establishment of annulus vent as described in Section [C3.5.1](#). Numerous successful repairs are performed with clamps of this kind. The clamp is not suitable to repair structural damages, e.g. broken armour wires.

#### C3.4.3.2 Description of the rigid clamp and installation method

The clamp is manufactured in stainless or duplex steel of a desired quality and often made up of two half shells. A typical clamp for illustrative purposes is shown in Figure [C3.5](#)

The damaged area and the surrounding area of the outer sheath are cleaned prior to clamp installation. The clamp is then assembled onto the riser. The as-installed position is marked onto the outer sheath for future reference. The repair integrity is verified by performing an annulus volume test in order to check that the clamp is pressure sealing to set test pressure level.

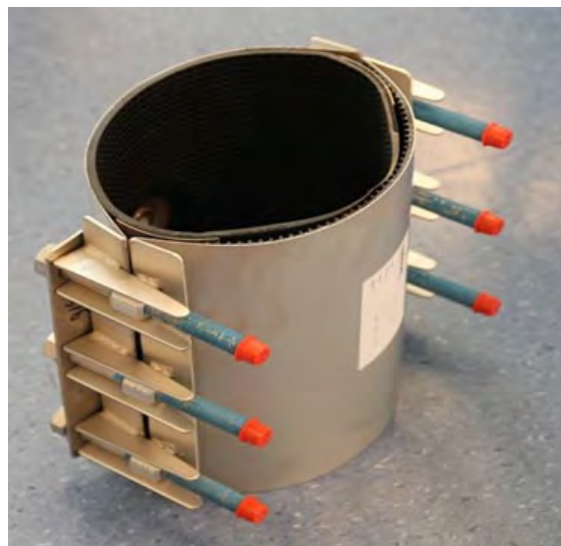


Figure C3.5: Rigid clamp

#### C3.4.3.3 Subsequent inspection and maintenance

Re-torqueing of bolts may be required due to cross-section and rubber liner creep. Further, periodic annulus volume tests should be performed in order to verify outer sheath integrity and annulus condition. The clamp should be verified to stay in position with no slippage. Additionally, the repair clamp should periodically be subject to visual inspection to check the condition of the clamp, e.g. check for interference with neighboring structures, corrosion and general condition of the clamp and its components. The choice of inspection method, either general visual inspection or close visual inspection, is dependent on the purpose of inspection and environmental conditions such as marine growth and visibility.

#### C3.4.3.4 Advantages and drawback

This method is proven successful in several repairs and the repair is relatively easy to perform. The same limitations apply to this clamp as to the clamp modified for re-establishing annulus vent (Section [C3.5.1](#)):

- The clamp should preferably be attached to a straight part of the pipe, away from the splash zone and with no or limited dynamics
- Interference between the clamp and adjacent risers or structure is not permitted
- Availability for installation, inspection and bolt torqueing.
- The repair method requires direct access to the outer sheath. The location must be without any guide tube or other structure surrounding the flexible pipe. For a riser located in a guide tube with an outer sheath damage located close to the topside end-fitting, then dependent on hang-off and topside layout, it may be possible to pull up the riser and end-fitting a few meters to get access to the outer sheath and perform the repair.

Table C3.3: Design issues for a rigid repair clamp

Component	Main Function	Design issue
Metallic clamp	Transfer bolt-tension to radial pressure onto pipe body (load bearing)	Corrosion
Tension bolts, nuts and nut receptacles	Tensioning of the clamp	Corrosion Thread damage (galling of threads)
Rubber liner	Sealing of the damage	Poor fit or buckling of the rubber liner Durability

### C3.4.3.5 Design Aspects

The main components of the rigid repair clamp are listed in Table C3.3 along with their main function and particular issues which should be considered in design. In addition to these particular design issues, there are general issues to consider as presented in Section C3.3.2

The design issues listed in Table C3.3 are described in more detail below:

- **Corrosion**  
Metallic parts may be fabricated in material resistant to corrosion or protected with coating and anodes.
- **Thread damage**  
Coating may be used to ensure the nuts can be torqued to the set level without thread damage occurring (galling of threads). Plastic spacer may be used between the nuts and clamp body to control friction and surface damage.
- **Poor fit or buckling of the rubber liner**  
In order to prevent buckling of the rubber liner and to ensure constant radial tension, the rubber liner should match the actual OD of the flexible pipe and fit the damaged area.
- **Durability**  
The material selection for the rubber liner should take into account ageing of the materials and the exposure to the environment; such as hydrocarbons, annulus compounds, seawater, chemicals and sunlight.

### C3.4.4 Structural repair clamp

#### C3.4.4.1 Objective and application

This method is applicable to damages with a damaged outer sheath and a limited number of broken armour wires. 4Subsea is only aware of one dynamic riser with broken wires that has been repaired: The structural repair clamp was then applied to a 3" gas lift riser with damaged outer sheath and where 1 or 2 armour wires appeared to be broken.

The purpose of the structural repair clamp is:

- Seal off the damage and thereby avoid seawater containing oxygen from circulating the steel armour wires.

- Immobilize the tensile armour wires in the damaged region and thereby provide a structural repair.

#### C3.4.4.2 Description of the structural repair clamp and installation method

For the one known repair, installation was performed by divers. The damaged part of the outer sheath is cut away prior to installation of the repair clamp. The removed volume is then replaced by rubber filler and covered with a thin sheet of adhesive rubber. Then the clamp is closed over the repaired area to seal off the damage.

The clamp itself consists of two main parts: the inner clamp and the outer clamp, both depicted in Figure C3.6. The inner clamp is a steel structure which clamp tightly in the center of the clamp. The length of the inner clamp is sufficient to transfer the loads and lock the dynamic stresses in the armour wires at the damage area.

An external plastic clamp with bellmouth shaped inside is mounted outside the central steel clamp to ensure controlled bending near the inner steel clamp. The length of the external clamp is sufficient to avoid local riser bending at the exit of the clamp.

The holding capacity of the clamp was tested as part of the design verification. Assembly testing was done prior to shipment.

The structural repair clamp as installed is depicted in Figure C3.7. The outer sheath repair integrity is verified by performing an annulus pressure test in order to check that the clamp is pressure sealing to the set test pressure level.

#### C3.4.4.3 Subsequent inspection and maintenance

Periodic annulus pressure and volume tests should be performed in order to verify outer sheath integrity and annulus condition. Additionally, the repair clamp should periodically be subject to visual inspection to check the condition of the clamp, e.g. check that the clamp is in position, and check for interference with neighboring structures, corrosion and general condition of the clamp and its components. The choice of inspection method, either general visual inspection (GVA) or close visual inspection (CVA) is dependent on the purpose of inspection and environmental conditions such as marine growth and visibility.

#### C3.4.4.4 Advantages and drawbacks

The main advantage of this clamp is that it provides repair method for combined outer sheath damage and broken armour wires. However, there are several limitations and challenges to be considered for this clamp:

- The dynamics, curvature and fatigue calculations for the flexible pipe at the location of the clamp must be evaluated prior to repair.
- The possibility for interference between the clamp and adjacent risers or structure and the associated consequences of interference should be evaluated prior to repair.
- Access for installation, inspection and bolt torqueing.

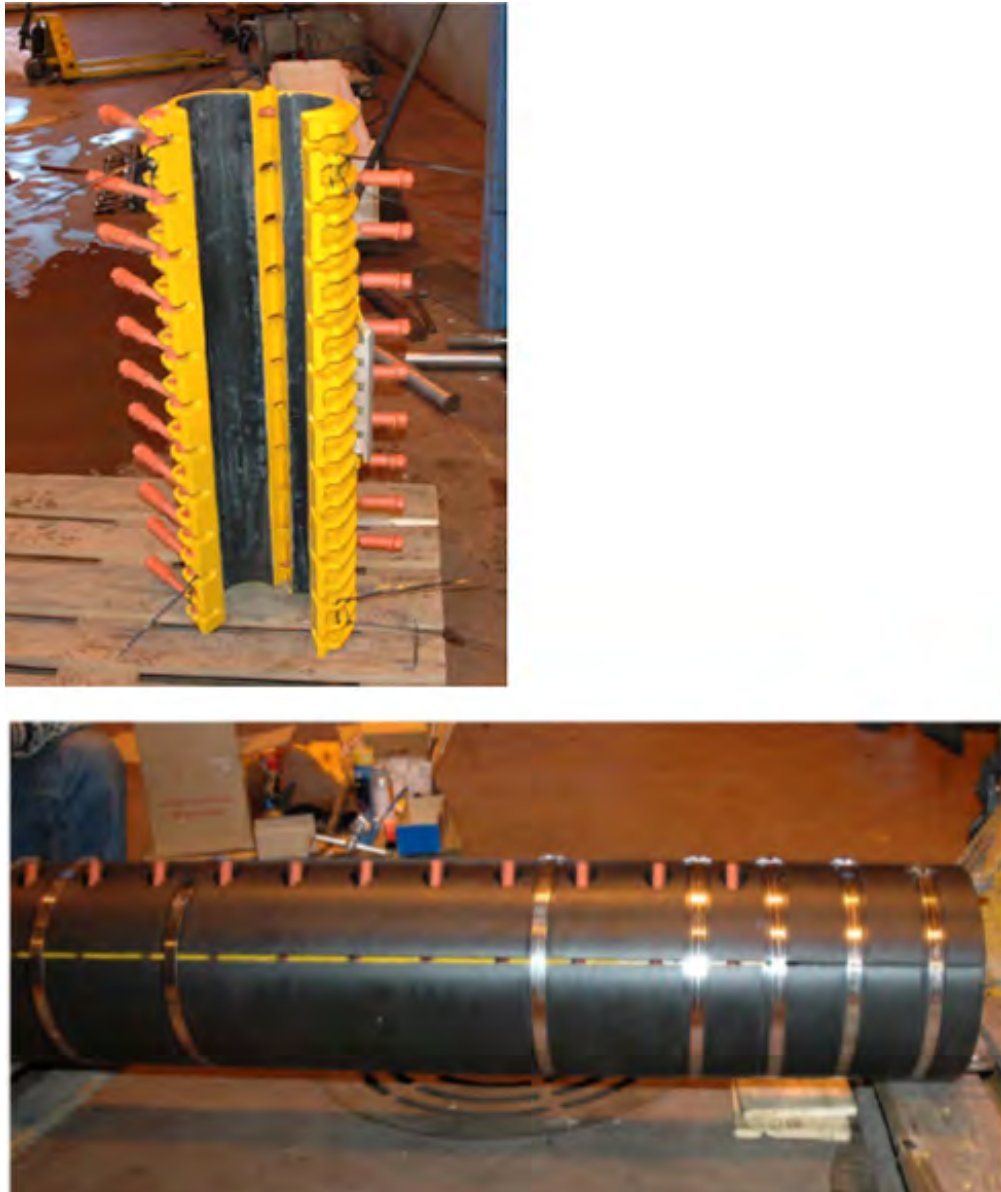


Figure C3.6: Structural repair clamp: Upper picture: Inner clamp in open position. Bottom picture: Outer clamp in closed position with inner clamp inside

- The repair method requires direct access to the outer sheath. The location must be without any guide tube or other structure surrounding the flexible pipe.
- The structural integrity of the repair cannot be directly verified after the repair. Hence, this matter requires a proper qualification and test program prior to installation

Generally, for repair of a riser with one or more broken armour wires a lifetime assessment is required prior to repair.

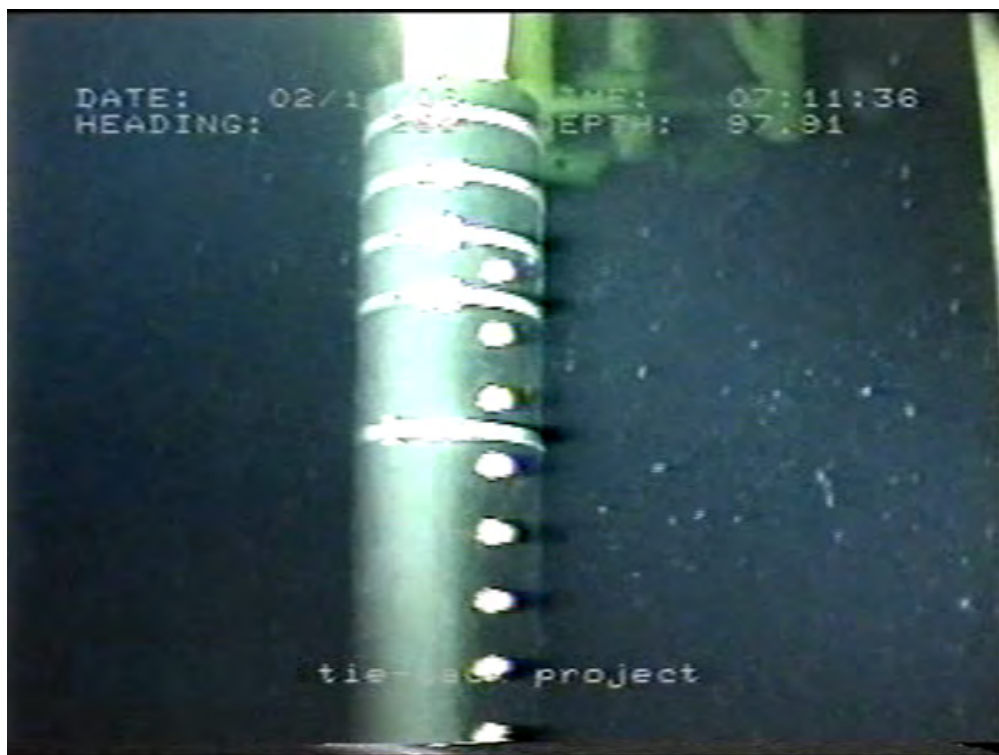


Figure C3.7: Structural repair clamp as-installed

### C3.4.5 Design aspects

The main components of the structural repair clamp are listed in Table C3.4 along with their main function and particular issues which should be considered in design. In addition to these particular design issues, there are general issues to consider as presented in Section C3.3.2.

Table C3.4: Design issues for a structural repair clamp

Component	Main Function	Design issue
Rubber fill and sheet	Sealing of the damage	- Poor fit - Durability
Inner clamp	Transfer bolt-tension to radial pressure onto pipe body (load bearing) immobilizing the tensile wires	- Structural capacity and sufficient radial pressure to immobilize the tensile wires
Tension bolts, nuts and nut receptacles	Tensioning of the inner clamp	- Corrosion - Thread damage (galling of threads)
Outer clamp	Limit bending of the riser	- Structural capacity - Durability
Tension bands	Tensioning of the outer clamp	- Corrosion

The design issues listed in Table C3.4 are described in more detail below:

- **Poor fit of the rubber fill and sheet.**

In order to obtain a good seal and to ensure constant radial tension, the damaged area should be considered to be removed (cut away) and replaced by rubber fill. The surface of the rubber fill and outer sheath should then be prepared and smoothed before attaching the rubber sheet. The inner diameter of the inner clamp should match the actual OD of the flexible pipe and fit the damaged area.

- **Durability.**

The material selection should take into account ageing of the materials and the exposure to the environment, such as hydrocarbons, annulus compounds, seawater, chemicals and sunlight.

- **Structural capacity and sufficient radial pressure to immobilize the tensile wires.**

The clamp geometry and stiffness, and the applied torque of tension bolts are of importance to obtain sufficient radial support and to transfer the riser loadings across the inner clamp. For this particular clamp, the purpose is to immobilize the tensile wires. The structural capacity of the clamp must also be sufficient to limit bending of the riser near the center of the inner clamp.

- **Corrosion.**

Metallic parts may be fabricated in material resistant to corrosion or protected with coating and anodes.

- **Thread damage.**

Coating may be used to ensure the nuts can be torqued to the set level without thread damage occurring (galling of threads). Plastic spacer may be used between the nuts and clamp body to control friction and surface damage.

## C3.4.6 Casting repair

### C3.4.6.1 Objective and application

This method is applicable to outer sheath damages located above sea level and where an ordinary clamp is inadequate, such as for static sections where the pipe has a bend (large curvature) or where the external sheath has a variation in its outer diameter. This repair is applicable for repair in areas where hot-work permission is limited; e.g. polymer welding (described in Section C3.4.7) is unacceptable.

The purpose of this repair is to restore the outer sheath integrity and avoid exposure of steel armour wires to environmental exposure.

This repair method has been applied once: to a flexible riser with OD 109mm, and the damage having the following approximate dimensions: 300mm x 150mm. However, the repair was only partially successful as a not discovered blockage in the annulus vent system caused a weak area and very small leakage path through the cast before the material could fully cure. The cast repair is still considered to give a good degree of protection for the armour layers from the surrounding corrosive environment.

### C3.4.6.2 Description of the casting repair and installation method

The damaged area and the surrounding area of the outer sheath to be covered by the cast are cleaned and abraded in order to prepare the surface and increase bonding. A PVC mould is mounted enclosing the damaged area. The mould can be fixed to the pipe by clamps at both ends. This is illustrated in Figure C3.8. The cast itself is made from a polymer (e.g. polyurethane) and the liquid casting material is poured into a fill port in the mold. The cast is then allowed to cure before the mold and clamps are removed. The final cast repair is depicted in Figure C3.9 .

The repair is verified by performing an annulus pressure test in order to check that the clamp is pressure sealing to the set test pressure level.

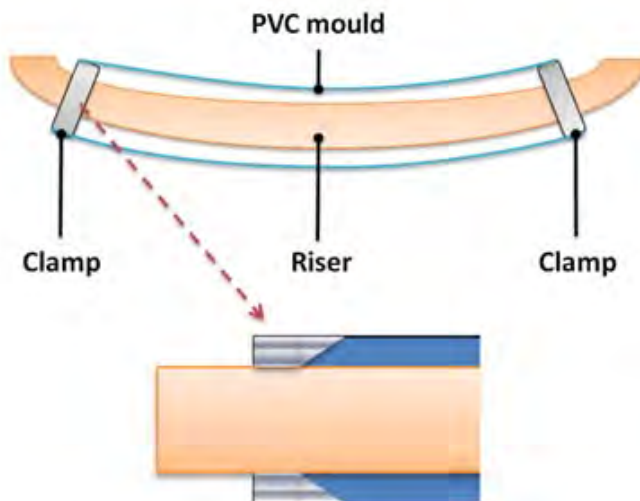


Figure C3.8: Cast repair: Schematic of repair. Top: general view. Bottom: detail of outer clamp

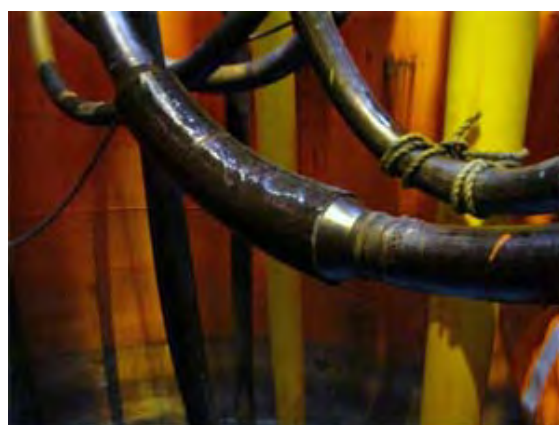


Figure C3.9: Cast repair: Permanent solution

### C3.4.6.3 Subsequent inspection and maintenance requirements

The need for further inspection and maintenance is dependent on the initial success of the casting repair. If the casting repair initially is found not to be pressure tight, further modifications may be required. A first attempt to improve a repair with a micro leakage may be to set a new cast partially or fully covering the initial repair cast.

Further, periodic annulus pressure and volume tests should be performed in order to verify outer sheath integrity and annulus condition. Additionally, the repair should periodically be subject to visual inspection to check the condition of the cast, e.g. check for interference with neighboring structures. The choice of inspection method, either general visual inspection or close visual inspection, is dependent on the purpose of inspection and environmental conditions such as marine growth and visibility.

### C3.4.6.4 Advantages and drawbacks, including design aspects

When successful, this repair method provides a solution to damages where an ordinary clamp is inadequate as described in Section [C3.4.6.1](#). The main drawback is the challenge in obtaining a pressure tight repair with satisfactory bonding between the casting material and the outer sheath.

The main components of the casting repair are listed in Table [C3.5](#) along with the main function and particular issues which should be considered in design. In addition to these particular design issues, there are general issues to consider as presented in Section [C3.3.2](#).

Table C3.5: Design issues for a casting repair

Component	Main Function	Design issue
Mould and clamp	Encapsulate and support the casting material while curing	- Sliding clamp / mould - Mould leakage - Poor fit of mould
Casting material	Sealing the outer sheath: - Keep internal annulus pressure - Prevent ingress of air, seawater or moist	- Bonding to the outer sheath / leakage - Durability

The design issues in Table [C3.5](#) are described in more detail below:

- **Sliding clamp/mould**

The mould and clamp should be fixed at the intended location. Hence, the clamp and mould should be properly connected and clamped to the pipe with sufficient radial tension.

- **Mould leakage**

All ends and joints of the mould should be properly sealed and the opening where the casting material is poured in should be located so that the potential for leakage is minimized.

- **Poor fit of mould**

It could be challenging to make the mould fit a pipe with high curvature or irregular outer sheath. Hence, careful preparation of the mould is recommended, and the mould

should preferably be made of a somewhat flexible material to allow for adjustments on site.

- **Bonding to the outer sheath / leakage**

Dependent on the casting material and outer sheath material it has proven challenging to obtain satisfactory bonding. Hence leakage in the cast and interface layer is an issue to be addressed. Before applying the casting, it could be considered to temporarily seal off the damage to avoid annulus fluids emerging into the casting material.

- **Durability**

The choice of casting material should be taken with due consideration of the cast's durability and its exposure to temperature, pH and annulus fluids. Water and moisture present at the location for casting may cause a poor and porous cast.

### C3.4.7 Polymer welding of outer sheath

#### C3.4.7.1 Objective and application

This is a solution mainly applied for installation damages to the outer sheath. The purpose is to restore an intact outer sheath. Successful repair require that the work is performed under dry conditions and according to strict procedure.

#### C3.4.7.2 Description of polymer welding of outer sheath

The successive steps in polymer welding are:

- Drying the outer sheath
- Welding
- Grinding the weld

Polymer welding will often require permit for hot work.

The repair is verified by performing an annulus pressure test in order to check that the clamp is pressure sealing to the set test pressure level.

#### C3.4.7.3 Subsequent inspection and maintenance

No additional inspection or maintenance is required for polymer welding of outer sheath. However, when performing periodic visual inspection of the pipe, the location of the outer sheath weld should be subject to close visual inspection, looking for possible defects and corrosion products. Periodic annulus volume testing is also recommended.

#### C3.4.7.4 Advantages and drawbacks

A successful polymer welding will result in an intact outer sheath, and as stated above, no particular inspection or maintenance is required subsequent to the repair.

However, problems of porosity and cracking are observed, resulting in unsuccessful repairs. A qualified weld procedure is required. Performing a successful repair includes requirements

on the external environmental conditions, including dry condition, the ambient temperature and sufficient time for the work. As a consequence, a habitat is often necessary.

Polymer welding on aged materials is often challenging and may involve conditioning of the aged material and complex welding procedures to obtain reliable welds. The procedures will be material dependent.

### C3.4.8 Examples of commercially available products for outer sheath repair

#### C3.4.8.1 Flexlife - FlexGel

FlexGel is a commercial product from Flexlife and is an example of an inhibition to mitigate annulus corrosion. The description in this section is based on the data sheet for FlexGel [Flexlife, 2012b] provided by Flexlife. The repair method is applicable to outer sheath damages in the splash zone for flexible pipes located within guide tubes. The purpose is to mitigate the effect of splash zone environment and prevent ingress of seawater or air. The gel is deployed into the guide tube, filling the area around the damage and displacing the sea water. FlexGel is depicted in Figure C3.10.

Due to limited information about this product, the product cannot be properly evaluated. Also, there is an unknown need for periodically inspection and maintenance subsequent to installation.



Figure C3.10: FlexGel. Picture from FlexGel data sheet provided by Flexlife [Flexlife, 2012b]

#### C3.4.8.2 Flexlife - Armadillo

Armadillo is a commercial product from Flexlife and an example of a casting / clamp repair. The description in this section is based on the data sheet for Armadillo [Flexlife, 2012a] provided by Flexlife. The purpose of the repair is to encapsulate and seal the outer sheath damage in order to prevent ingress of seawater containing oxygen. The repair is applicable to flexible pipes with OD of 2"-24" and is customized to fit the length of the damage and to fit each pipe.

The Armadillo repair system is modular and consists of two half shells which are clamped around the flexible pipe. The Armadillo is filled with a sealing fluid. The repair gel cures

during 24 hours to form an elastic solid which allows the flexible pipe to bend as normal and simultaneously prevents ingress of seawater. The Armadillo is installed by ROV or by diver. Armadillo is depicted in Figure C3.11.

The repair is verified by performing an annulus pressure test in order to check that the clamp is pressure sealing to the set test pressure level.

Due to limited information about this product, the product cannot be properly evaluated. Also, there is an unknown need for periodically inspection and maintenance subsequent to installation.

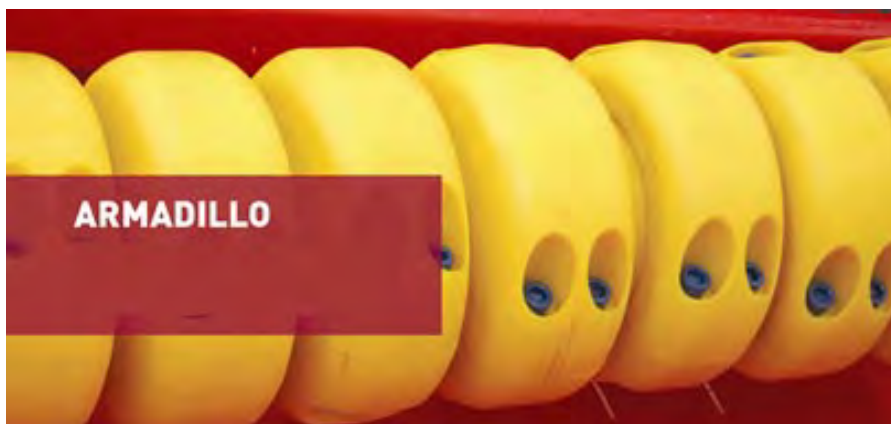


Figure C3.11: Armadillo. Picture from Armadillo data sheet provided by Flexlife [Flexlife, 2012a]

### C3.4.8.3 NICC - Armawrap

Armawrap is a commercial product from NICC. It is noted that Armawrap in principle is a particular design of a soft clamp. Hence, this description of Armawrap is to be seen in the context of Section C3.4.2 presenting the soft clamp in detail. The description in this section is based on the product description, [NICC Systems, 2012b] and [NICC Systems, 2012a] provided by NICC.

**C3.4.8.3.1 Objective and application** The purpose of the repair is to encapsulate and seal the outer sheath damage in order to prevent ingress of seawater containing oxygen. According to NICC, Armawrap is applicable to damages located subsea, above water or in the splash zone.

**C3.4.8.3.2 Description of Armawrap and installation method** Armawrap is made up of an elastomer and is clamped around the flexible pipe. A gel and corrosion inhibitor is applied on the inside of Armawrap in order to seal off the damage. According to NICC, the Armawrap can easily be removed and replaced for inspection. Armawrap is depicted in Figure C3.12. Installation of Armawrap can be performed by divers or by rope access, dependent on the location of the damage.

The repair is verified by performing an annulus pressure test in order to check that the clamp is pressure sealing to the set test pressure level.

**C3.4.8.3.3 Evaluating Armawrap** Due to limited information about this product, the product cannot be properly evaluated; neither can its advantages and drawbacks. Also, there is an unknown need for periodically inspection and maintenance subsequent to installation.

According to NICC, Armawrap has been used for repair of outer sheath damages on several flexible risers, including the following customers [[Stewart, 2012](#)]:

- GOT/Enquest
- Apache
- Addax Petroleum
- Shell
- Wellstream



Figure C3.12: Armawrap. Picture from NICC web page [[NICC systems, 2012](#)]

## C3.5 Repair methods to re-establish annulus vent

### C3.5.1 Installation of annulus vent clamp and drilling through outer sheath

#### C3.5.1.1 Objective and application

Installation of annulus vent clamp and drilling through the outer sheath is the most common known method to re-establish annulus vent for risers. This is performed if the vent flow cannot be restored through the existing vent ports. 4Subsea has experience with numerous successful repairs performed with installation of vent clamps. The installation of vent clamp can be applied as a repair method for outer sheath as described in Section [C3.4.3](#)

#### C3.5.1.2 Description of the vent clamp, drilling and installation method

The clamp is manufactured in stainless steel of a desired quality and often made up of two half shell. A vent port is welded onto one of these half shells. In order to increase the redundancy, an additional vent port can be added either above the first vent port (this will increase the length of the clamp) or on the second half shell of the clamp. The clamp area and the surrounding area of the outer sheath are cleaned prior to clamp installation. The clamp is then assembled onto the riser. A typical annulus vent clamp is illustrated in Figure [C3.13](#).

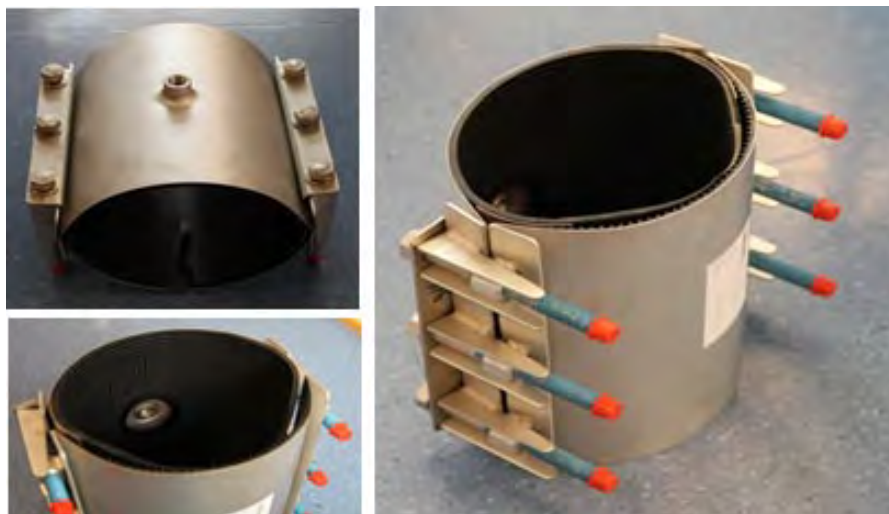


Figure C3.13: Typical annulus vent clamp

In order to establish new vent ports, it is required to drill through the outer sheath. The drilling is performed through the vent ports on the installed clamp. The drilling operation must take into consideration that the annulus is pressurized with hydrocarbons and that the drilling operation should not scratch or damage the outer tensile armor wires. Scratching the tensile armor wires can possibly cause fatigue or high-stress hot-spots. To reduce the probability of scratching the tensile armor wires, a drill with a soft material tip could be considered. The hardness of the tip should be significantly lower than the hardness of the armoring wires to minimize the risk of scratching the armour wires. Prior to performing the

repair, the applied drill(s) should be subject to thorough testing to ensure no scratching of the tensile wires.

The drilling tool is designed to divert overpressure in the riser annulus, to ensure a safe and controlled operation. In order to obtain good ventilation through the ventilation port, the hole is wider than one tensile armor wires, such that ventilation is obtained through the gaps / space between three neighboring wires.

After drilling, the annulus is depressurized and annulus volume test is performed to verify the repair. A permanent hose or piping is connected to the vent port(s) and the hose is secured along the riser and finally connected at the location where the original vent piping is/was connected. The annulus vent gas may be directed to the same vent system as originally intended.

#### **C3.5.1.3 Subsequent inspection and maintenance**

Dependent on the installed clamp, retightening of bolts may be required. Further, periodic annulus volume tests should be performed in order to verify satisfactory vent flow. The clamp should be verified to stay in position with no slippage. Additionally, the repair clamp should periodically be subject to visual inspection to check the condition of the clamp, e.g. check for interference with neighboring structures, corrosion and general condition of the clamp and its components.

The vent port flow capability should be significantly larger than the design diffusion rate of the pipe. Vent flow capability less than the design diffusion rate is not acceptable as complete blocking of the vent ports then will be likely. Further actions are recommended to increase the flow. Until the flow is re-established, annulus volume tests should be performed more frequently to ensure pipe integrity.

#### **C3.5.1.4 Advantages and drawbacks**

This method is proven successful in several repairs and the vent clamp allows for direct communication with annulus. Offshore field experience also include successful submerged installations of vent clamps with ventilation topside. The following limitations should be considered when the clamp location is chosen:

- The clamp should be located close to the topside end fitting.
- The clamp should preferably be attached to a part of the riser that is straight, away from the splash zone and with no or limited dynamics.
- Interference between the clamp and adjacent risers or structure is not permitted.
- Access for installation, inspection and bolt torqueing.
- The repair method requires direct access to the outer sheath. The location must be without any guide tube or other structure surrounding the flexible pipe. For a riser located in a guide tube, then dependent on hang-off and topside layout, it may be possible to pull up the riser and end-fitting a few meters to get access to the outer sheath and perform the repair.

### C3.5.1.5 Design aspects

The main components of the annulus vent clamp are listed in Table C3.6 along with their main function and particular issues which should be considered in design. In addition to these particular design issues, there are general issues to consider as presented in Section C3.3.2.

Table C3.6: Design issues for annulus vent clamp and drilling through outer sheath

Component	Main Function	Design issue
Drilling tools	Drilling through the outer sheath and establish communication to annulus	Appropriate for the outer sheath material and the tensile wires
Metallic clamp	Provides constant radial pressure	Corrosion
Tension bolts, nuts and nut receptables	Tensioning of the clamp	Corrosion
Rubber liner	Sealing of the damage	Poor fit or buckling of the rubber liner Durability
Hose / piping	Communication between annulus and platform vent system	Durability

The design issues listed in Table C3.6 are described in more detail below:

- **Drilling tools appropriate for outer sheath material and tensile wires**

The drilling tool should be tested for the relevant outer sheath material. The possibility for unintentional rupture of the outer sheath should also be considered. The drill should be designed to avoid damaging the tensile wires as scratches and dents in tensile wires can initiate crack growth and provide hotspots for fatigue. The size of the hole should also ensure satisfactory communication with annulus.

- **Corrosion**

Metallic parts may be fabricated in material resistant to corrosion or protected with coating and anodes.

- **Poor fit or buckling of the rubber liner**

In order to prevent buckling of the rubber liner and to ensure constant radial tension, the rubber liner should match the actual OD of the flexible pipe. Further, the rubber surface may be lubricated in order to reduce friction between the rubber liner and the outer sheath of the flexible pipe.

- **Durability**

The material selection for the hose / piping and for the rubber liner should take into account ageing of the materials and the exposure to the environment; such as hydrocarbons, annulus compounds, seawater, chemicals and sunlight.

### C3.5.2 Establish new vent ports for a pipe located inside a guide tube

#### C3.5.2.1 Objective and application

This is a method to re-establish annulus vent for risers with restricted vent flow and where the vent flow cannot be restored through the existing vent ports. This method can be applied where the more common method described in Section [C3.5.1](#) is not possible, if access to the outer sheath of the flexible pipe is prevented due to surrounding guide tubing. There are restrictions to how small the outer diameter of the riser can be, but no known upper limitation to the outer diameter of the riser. Naturally, the internal diameter of the guide tube limits the outer diameter of the riser. 4Subsea has performed one successful repair with this method of drilling new vent ports. That repair was performed on a flexible pipe with OD 352mm.

#### C3.5.2.2 Description of the drilling and installation method

In order to establish new vent ports, it is required to drill through the outer sheath. Access to the outer sheath could preferably be obtained through an existing opening in the riser guide tube such as nitrogen filling line or an inspection hatch. Where no such openings exist, access to the riser outer sheath may be obtained by drilling through the guide tube wall. Prior to the repair, the guide tube must be depressurized. A sketch of the resulting arrangement with new vent port and new vent hose to flare is depicted in Figure [C3.14](#).

The drilling operation must take into consideration that the annulus is pressurized with hydrocarbons and that the drilling operation should not scratch or damage the outer tensile armor wires. Scratching the tensile armor wires can possibly cause fatigue or high-stress hot-spots. To reduce the probability of scratching the tensile armor wires, a drill with a soft material tip could be considered. The hardness of the tip should be significantly lower than the hardness of the armoring wires to minimize the risk of scratching the armour wires. Prior to performing the repair, the applied drill(s) should be subject to thorough testing to ensure no scratching of the tensile wires.

The drilling tool is designed to divert overpressure in the riser annulus, to ensure a safe and controlled operation. In order to obtain good ventilation through the ventilation port, the hole is wider than two tensile armor wires, such that ventilation is obtained through the gaps/space between three neighboring wires.

A specifically designed fitting is attached to the drilled hole in the outer sheath after the riser annulus is confirmed to be depressurized. A flexible hose is connected to the fitting in order to permanently lead annulus vent gas back to the existing vent system.

The repair integrity is verified by performing an annulus volume test in order to check that the clamp is pressure sealing to set test pressure level.

#### C3.5.2.3 Subsequent inspection and maintenance

Periodic annulus volume tests should be performed in order to verify satisfactory vent flow. As the repair is located inside the guide tube, periodical visual inspection is generally not feasible. Hence, inspection of the repair itself is to be performed only when suspecting a

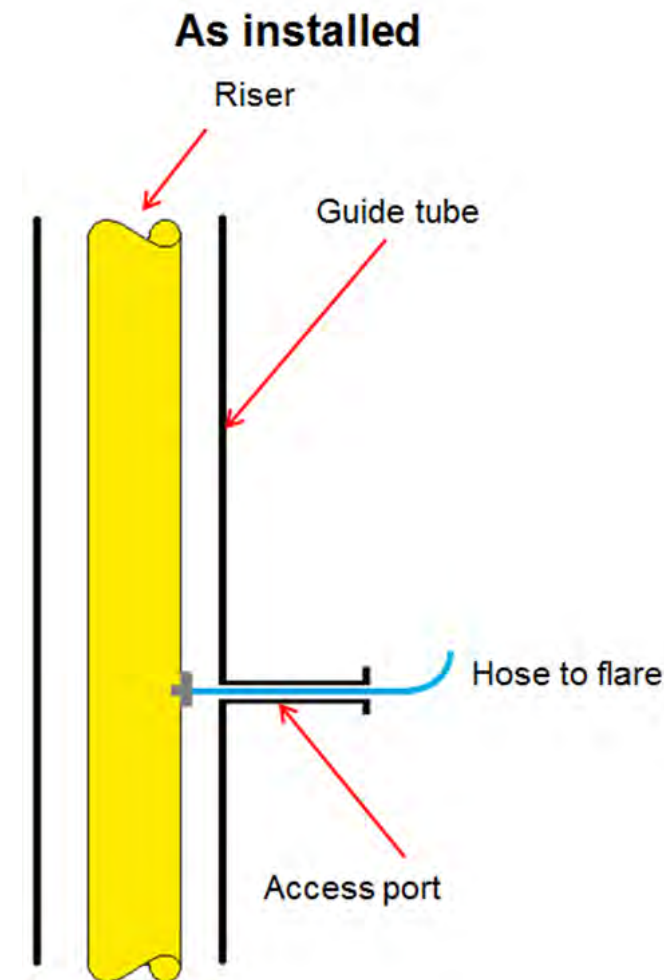


Figure C3.14: Establish new vent ports for a pipe located inside a guide tube

leakage or anomaly. The parts of the repair located outside the guide tube, should periodically be subject to visual inspection to check the condition of vent piping and connections.

As the riser is located inside a guide tube pressurized with nitrogen, the pressure and nitrogen consumption in the guide tube should be monitored in order to detect a possible increased consumption caused by leakage from the guide tube through the vent system to flare.

The vent port flow capability should be significantly larger than the design diffusion rate of the pipe. Vent flow capability less than the design diffusion rate are generally not acceptable over longer periods of time. When the flow is this low complete blocking of the vent ports are also likely. Further actions are recommended to increase the flow. Until the flow is re-established, annulus volume tests should be performed more frequently to ensure pipe integrity.

#### C3.5.2.4 Advantages and drawbacks

The main advantage of this repair method is that it provides annulus vent for flexible pipes located inside guide tubes. Any uncertainties to the location and extent of the blockage

Table C3.7: Design issues for establishing new vent for a pipe located inside a guide tube

Component	Main Function	Design issue
Drilling tools	Drilling through the outer sheath and establish communication to annulus	- Appropriate for the outer sheath material and the tensile wire. - Contain and divert annulus pressure in a safe and controlled manner
Nipples	Pressure tight connection between annulus and hose	- Corrosion - Holding capacity
Hose	Communication between annulus and platform vent system	- Durability

within the end fitting are irrelevant, as the repair creates a vent flow path bypassing the end-fitting. Having performed one repair, 4Subsea's experience is that repair is durable and holds tight for several years. This method is however more challenging than the method described in Section [C3.5.1](#) due to the following:

- Could be challenging to get access with tools inside the guide tube.
- Depressurizing of the guide tube is required.
- The guide tube opening must be modified to allow for the vent flow hose / tubing to pass through.
- The repair requires the dynamic displacements of the flexible pipe inside the guide tube to be relatively small.

### C3.5.2.5 Design aspects

The main components for establishing a new vent port are listed in Table [C3.7](#) along with their main function and particular issues which should be considered in design. In addition to these particular design issues, there are general issues to consider as presented in Section [C3.3.2](#).

The design issues listed in Table [C3.7](#) are described in more detail below:

- **Drilling tools appropriate for outer sheath material and tensile wires**  
The drilling tool should be tested for the relevant outer sheath material. A concern when drilling in the outer sheath is that the shape of hole may not be as intended and hence it may be difficult to attach the nipple. The possibility for rupture of the outer sheath should also be considered.  
The drill should be designed and tested to avoid damaging the tensile wires as scratches and dents in tensile wires will initiate crack growth and provide hotspots for fatigue. The size of the hole should also ensure satisfactory communication with annulus.
- **Contain and divert annulus pressure in a safe and controlled manner**  
The drilling operation must take into consideration that the annulus is pressurized with hydrocarbons. The drilling tool should be designed to contain and divert overpressure

in the riser annulus, to ensure a safe and controlled operation. The tool's pressure capacity should have appropriate margins to the potential annulus pressure

- **Corrosion**

Possibility for corrosion due to contact between nipple and tensile wires should be considered and mitigated.

- **Holding capacity**

Threading and glue could be the method for fixation of the nipple. The holding capacity is an important issue because this connection should also be leak tight. Threading after drilling the hole must be considered for the relevant outer sheath material and should be performed without risk of damaging the tensile wires. The properties of the glue and its interaction with tensile wires, polymers and annulus compounds should be assessed.

- **Durability**

The material selection for the hose should take into account the exposure to the environment; such as hydrocarbons, annulus compounds, seawater, chemicals and sunlight.

There are also risks to assess prior to depressurization of the guide tube. These risks are related to the possibility of burst of outer sheath, release of hydrocarbons, suffocation from N2-release and seawater being pushed up to the working area through the guide tube.

### C3.5.3 Cyclic vacuum and nitrogen pressure

#### C3.5.3.1 Objective and Application

The purpose of this method is to restore annulus vent through the existing vent ports. However, some attempts with this method have proven limited success, as the driving force from the limited overpressure is small (to avoid eventual damages on the riser).

#### C3.5.3.2 Description of the repair method

The method is applied to one vent port at a time while the other vent ports are capped. Cyclic vacuum and overpressure is applied through the vent ports. Vacuum can be applied with a vacuum pump driven by compressed air available on site. The overpressure is applied by feeding nitrogen into the vent port. As an alternative to cyclic pressure, a constant overpressure could be applied for some time, e.g. 2–12 hours. The setup of the equipment is sketched in Figure C3.15. The applied feeding pressure depends on the capacity of the outer sheath for the actual flexible pipe. After completion of the repair, an annulus vent flow test is performed to verify that the vent port is successfully opened.

#### C3.5.3.3 Subsequent inspection and maintenance

Periodic annulus volume tests should be performed in order to verify satisfactory vent flow. The vent port flow capability should be significantly larger than the design diffusion rate of the pipe. Vent flow capability less than the design diffusion rate is not acceptable. When the flow is this low complete blocking of the vent ports are also likely. Further actions are recommended to increase the flow. Until the flow is re-established, vent-port flow capacity test should be performed more frequently to ensure pipe integrity.

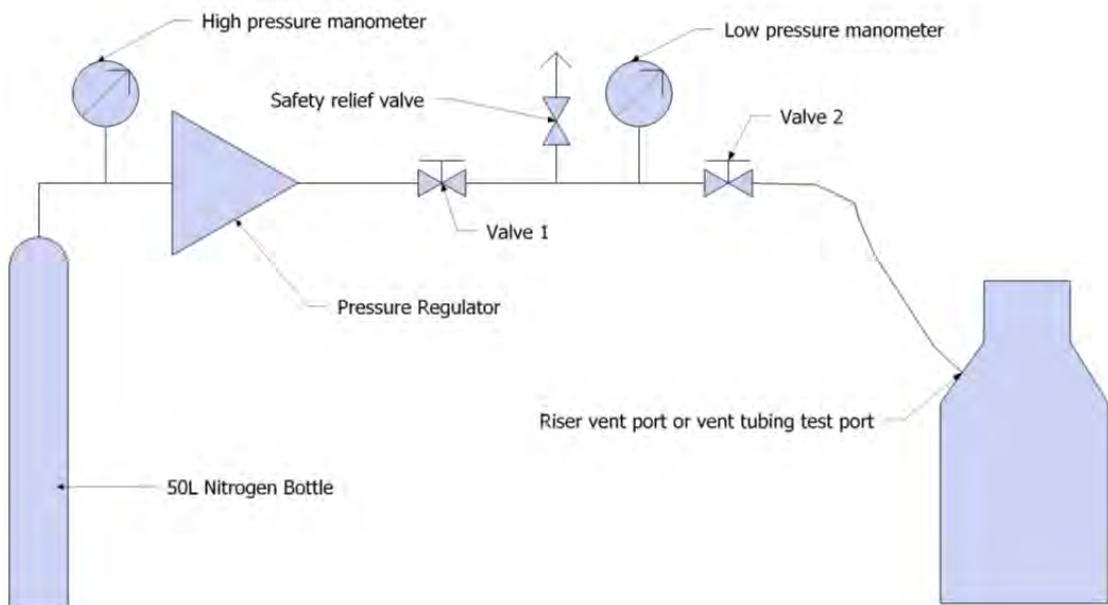


Figure C3.15: Sketch of setup for nitrogen feeding

#### C3.5.3.4 Advantages and drawbacks

This method is a simple and less intrusive method than the repair methods described in Section C3.5.1, Section C3.5.2 and Section C3.5.4. However, only limited success has been achieved with this method.

### C3.5.4 Hydraulic pressurization of vent port

#### C3.5.4.1 Objective and Application

The purpose of this method is to restore annulus vent through the existing vent ports using a hydraulic pressure. The liquid has the benefit of being incompressible, and is hence regarded safer to apply than an overpressure of nitrogen. The properties of the applied liquid and its interaction with polymers (i.e. outer sheath) and armor wires should be assessed before initiating this repair. This method can be applied subsequently to the repair method described in Section C3.5.3.

#### C3.5.4.2 Description of the repair method

Liquid is injected into one of the vent ports at a time while the other vent ports are capped. The setup for injection of oil into the vent port is schematically sketched in Figure C3.16. The setup of the system ensures that any gas evacuating from the annulus vent system is routed to the external vent system.

Liquid is injected into the vent ports by the use of a hand pump and the pressure applied is limited to a pre-determined level. The exact pressure depends on the capacity of the

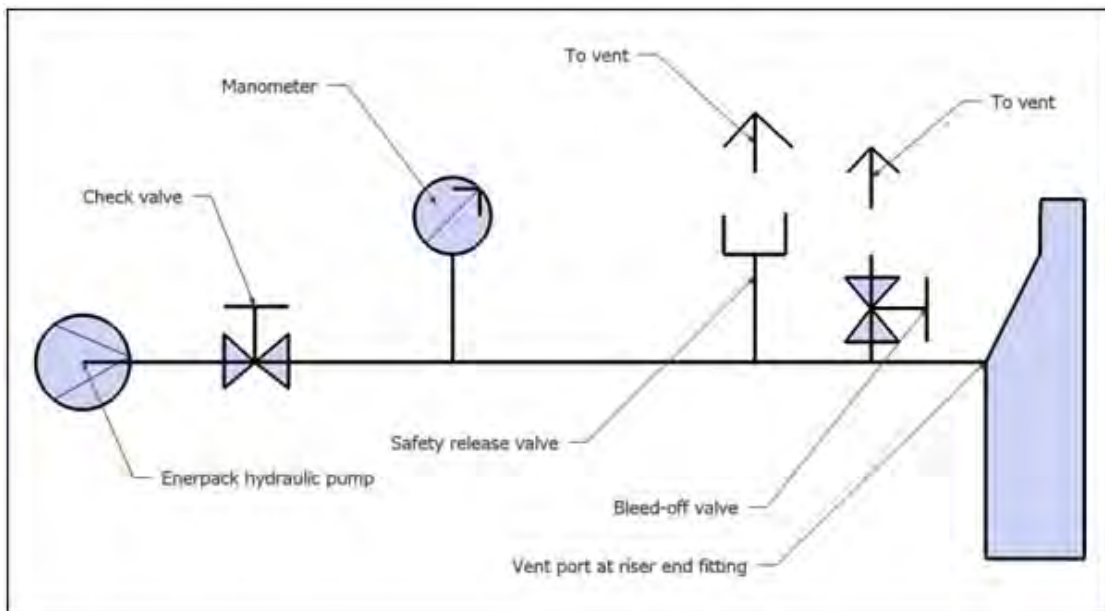


Figure C3.16: Sketch of setup for injection of oil into vent port

outer sheath for the actual flexible pipe. If the flexible pipe is located in a pressurized guide tube, this can allow for injection at a higher pressure. After applying the desired pressure, a pressure drop is anticipated. Then, if subsequent attempts to build up pressure do not succeed, the vent port is assumed to be open. However, if no immediate pressure drop occurs, the vent port is sealed off to keep it pressurized for 2-12 hours. Finally, an annulus vent flow test is performed to verify that the vent port is successfully opened.

#### C3.5.4.3 Subsequent inspection and maintenance

Periodic annulus volume tests should be performed in order to verify satisfactory vent flow. The vent port flow capability should be significantly larger than the design diffusion rate of the pipe. Vent flow capability less than the design diffusion rate is not acceptable. When the flow is this low complete blocking of the vent ports are also likely. Further actions are recommended to increase the flow. Until the flow is re-established, annulus volume tests should be performed more frequently to ensure pipe integrity.

#### C3.5.4.4 Advantages and drawbacks

The method described in the present section is simpler than the repair methods described in Section C3.5.1 and Section C3.5.2. However, no successful repairs are known.

### **C3.5.5 Drilling a new vent port through the end-fitting**

#### **C3.5.5.1 Objective and Application**

This method has been applied successfully where no access to the riser outer sheath is possible due to a surrounding guide tube, and where an existing epoxy-filling port on the end fitting made this convenient. A similar application would be to drill through the outer body of the end fitting, if an epoxy filling port is not available.

#### **C3.5.5.2 Description of the repair method**

Communication to riser annulus is established by drilling through the steel body of the riser end-fitting, and in to the epoxy cast that is terminating the steel armour layers. The epoxy is likely containing 'micro-cracks' or small voids along the steel surfaces which becomes canals for transporting annulus vent gas inside the end fitting to the new vent port consisting of the old epoxy filling port.

#### **C3.5.5.3 Subsequent inspection and maintenance**

Periodic annulus volume tests should be performed in order to verify satisfactory vent flow. The vent port flow capability should be significantly larger than the design diffusion rate of the pipe. Vent flow capability less than the design diffusion rate is not acceptable. When the flow is this low complete blocking of the vent ports are also likely. Further actions are recommended to increase the flow. Until the flow is re-established, annulus volume tests should be performed more frequently to ensure pipe integrity.

#### **C3.5.5.4 Advantages and drawbacks**

The advantage of this method is that it allows for re-establishment of ventilation without access to the riser outer sheath. There is however a large uncertainty to the presence of the voids and micro-cracks in the internal epoxy, and its ability to transport gas from the riser annulus through the internal of the end fitting and out to the newly drilled port. There is also uncertainty related to if the micro-cracks in the epoxy can become blocked by the same mechanism as the original vent ports in the end fitting.

## C3.6 Re-termination of end-fitting as a repair method

### C3.6.1 Objective and application

The repair involves cutting off the damaged section and terminate the new end. Re-termination of end-fitting is applicable for repairs to a variety of damages on flexible pipes located near one of the pipe ends. Re-termination could also be applied to a segment along the pipe: by cutting the pipe, re-terminate both ends and insert a short flexible jumper or steel spool piece connecting the two re-terminated ends. The relevant damages include:

- Outer sheath damages
- Polymer ageing (PA11) under bend stiffener
- Leakage in the end-fitting
- Carcass damages, e.g. carcass tear-off
- Restricted annulus vent

Carcass collapse could be an application for this repair. However, when identifying a collapse it may prove difficult to inspect and assess the carcass below the collapse. Hence, it may be uncertain whether a repair is beneficial or not. Re-termination is then likely to be discarded for this type of failure.

There are also other applications to be considered. The outer sheath is often subject to wear due to interaction with a bell mouth. Re-termination of the pipe will then change the wear zone on the pipe.

The upper part of the flexible pipe is often most exposed/vulnerable to fatigue. Re-termination of the pipe will alter the distribution of loading such that another part of the pipe – which possibly has previously been less exposed – will be exposed to fatigue. In this way, re-termination could possibly increase the ultimate fatigue life of the flexible pipe. It is noted that this consideration perhaps is more of theoretical interest.

The applicability and feasibility of performing a re-termination should be assessed with due consideration of the space required on board the installation, changes to the configuration of the flexible pipe during the re-termination (e.g. pulled up, bent, suspended from a vessel) and loadings imposed on the pipe (e.g. a free hanging flowline for static application subject to dynamic motion of an installation vessel for 5 days).

### C3.6.2 Re-termination

Re-termination of the subsea end requires an installation vessel to recover the subsea end and to facilitate the re-termination aboard the vessel. Re-termination of the topside end could be performed on the installation (platform) dependent on the available space and layout on the installation. Hence, an installation vessel may be required also in this case. A complete production stop on the installation is required when performing the re-termination on the installation. The repair is performed by the manufacturer of the flexible pipe and must be performed under controlled environmental conditions, i.e. a habitat. A pressure test (structural-integrity test as described in [API 17B, 2008]) is performed to confirm pressure tight end fitting after re-termination.

### C3.6.2.1 Hazard warning: Exposure to hydrocarbon gases, NORM, etc.

In general the flexible pipe suppliers have significant reservations on performing re-termination on flexible risers which have been in operation due to risk level and HSE issues

*Hydrocarbon gases:* The method involves risk with reference to performing hot work (i.e. welding) on a flexible pipe which has been used in operation where gas is trapped in annulus or bore - with the potential of ignition of those gases. Preventive measures should be taken to reduce the risk. Although having taken preventive measures, there is still considered to be a high risk of hydrocarbon gases being present or migrating through the annulus or bore to the work site at the pipe end.

*NORM (Naturally occurring radioactive material):* On a flexible pipe which has been used in operation, scale containing NORM may be present in the pipe. These deposits of radioactive material are usually low specific activity scale, meaning that the main hazard is related to inhalation or swallowing - in particular being exposed to dust or small particles. Hence, measurements for NORM should be performed both prior to and during the work. Preventive measures should be taken.

*Other compounds:* The work involves the potential for exposure to other compounds and elements in residuals of the bore flow such as injection chemicals and heavy metals (e.g. mercury, lead).

### C3.6.3 Subsequent inspection and maintenance

No additional inspection or maintenance is required for the new end-fitting after a successful re-termination.

### C3.6.4 Advantages and drawbacks

The repair provides a solution to a wide range of damages and provides a brand new end fitting – although an end fitting made on site will never be as good as a factory made end fitting fabricated at ideal conditions.

There are some limitations and drawbacks for this repair method:

- The repair is generally limited to damages located near the ends of the flexible pipe. As the repair involves a shortening of the pipe length, the resulting total (dynamic) length after the repair should be evaluated.
- The method is costly due to hire of an installation vessel and/or the required production stop in addition to the costs of the end-fitting itself and the man hours for re-termination.
- The method involves risk with reference to performing hot work (i.e. welding) on a flexible pipe which has been used in operation where gas is trapped in annulus or bore.
- The method involves the potential of exposure to NORM and other compounds (details are given above).
- The method is time consuming (in the order of 4 days).

## C3.7 Summary

This chapter addresses repair methods for flexible pipes including end-fitting. Ancillary devices to flexible pipes such as bend stiffeners, buoyancy modules and friction clamps are omitted.

An overview of flexible pipe failure modes with evaluation of service experience, available inspection methods and repair methods is presented. The overview shows that only a limited number of the failure modes are possible to detect and repair. The failure statistics and available inspection and repair methods advocate the importance of repair methods for the failure modes reviewed in this chapter:

- Outer sheath damage
- Restricted annulus vent flow

Additionally, re-termination of end fitting is applicable as a repair method for damages located near the pipe ends. Re-termination of flexible risers normally requires that flexible manufacture provide new end-fittings and is responsible for the repair.

The chapter also presents a flowchart of the repair process from detection of damage to, if proven viable, continued operation of the flexible pipe after repair.

The available repair methods for outer sheath damages are summarized in Table [C3.8](#).

The available repair methods for restricted annulus vent flow are summarized in Table [C3.9](#).

The following experienced flexible pipe body defects have no reported repair method:

- Carcass (collapse, fatigue, erosion, termination failure and tensile rupture have been experienced)
- Pressure liner (collapse, fatigue, termination failure, polymer degradation have been experienced)
- Pressure armour layers (fatigue and unlocking has been experienced)
- Tensile armour layers (fatigue and corrosion and severe handling induced damage have been experienced). Structural repair clamp may be feasible for minor damages.

However, for damages near end-fittings re-termination has been used successfully for a limited number of the above failures.

Table C3.8: Summary of repair methods for outer sheath damage

<b>Repair method</b>	<b>Application</b>	<b>Track record</b>	<b>Comment</b>
Injection of inhibitor liquid in annulus	Subsea and above sea level Temporary action before a permanent repair	Several applications, usually combined with another repair for outer sheath damage	Normally used to control corrosion. Limited by temperature and annulus condition
Soft repair clamp	Subsea and above sea level	Numerous successful repairs	Only for outer sheath damages
Rigid clamp	Subsea and above sea level	Numerous successful repairs	Only for outer sheath damages
Structural repair clamp	Subsea and above sea level Structural damages: tensile wire	One known installation	Require extensive engineering including post-repair service life assessment
Casting repair	Above sea level. Straight sections Sections with curvature and variable OD	One known installation	Only for outer sheath damages
Polymer welding of outer sheath	Subsea (to be performed above sea e.g. on an installation vessel) and above sea Applies mainly during installation or re-use of flexible pipes	Well proven method	Only for outer sheath damages Requires dry conditions during welding. Strict weld procedure required to avoid defects.

Table C3.9: Summary of repair methods for annulus vent

<b>Repair method</b>	<b>Extent of use</b>	<b>Strengths</b>	<b>Limitations</b>
Annulus vent clamp	Numerous successful repairs	Allows for direct communication with annulus	Require direct access to the outer sheath, most frequently used near topside end-fitting.
Drilling new vent port for a pipe located inside a guide tube	One known application.	Allows for direct communication with annulus	Require access to the flexible pipe
Cyclic vacuum and nitrogen pressure	Often tried as a first attempt to recover annulus vent	Easy to apply and the least intrusive repair method	Limited success. Outer sheath burst capacity must be considered when defining test pressure.
Hydraulic pressurization of vent port	Tried as an initial attempt to recover annulus vent.	Easy to apply and less intrusive than annulus vent clamp and drilling of new vent ports.	No successful repairs known. Potential for pressure build up in the annulus must be considered when defining test pressure.
Drilling new vent port through the end-fitting	One known application	Applicable to a pipe with access to end-fitting and where the outer sheath is inaccessible (e.g. pipe located inside a guide tube)	Uncertainty of success: Dependent on annulus vent through micro cracks in the internal epoxy in end-fitting. Often more complex than other alternatives

### C3.7.1 Track record for repair methods

Table C3.10: Track record for repair methods

Repair method	Track record
<b>Repair methods for outer sheath damages</b>	
Injection of inhibitor liquid in annulus	Several known applications, usually in combination with one of the other repair methods for outer sheath damage
Soft repair clamp	Numerous successful applications
Rigid clamp	Numerous successful applications
Structural repair clamp	One successful application (One known installation)
Casting repair	One known installation
Flexlife – FlexGel	Unknown
Flexlife – Armadillo	Unknown
NICC – Armawrap	Numerous successful applications, see Section <a href="#">C3.4.8.3.3</a>
Polymer welding of outer sheath	Standard procedure work by flexible pipe suppliers
<b>Repair methods to re-establish annulus vent</b>	
Installation of annulus vent clamp and drilling new vent ports	Numerous successful applications
Establish new vent ports for a pipe located inside a guide tube	One known installation
Cyclic vacuum and nitrogen pressure	Often tried as a first attempt
Hydraulic pressurization of vent ports	Tried as a first attempt. No successful repairs are known
Drilling a new vent port through the end-fitting	One known installation
<b>Re-termination of end-fitting as a repair method</b>	Standard procedure work by flexible pipe suppliers – dependent on site layout and conditions

The method involves the potential of exposure to NORM and other compounds (details are given above).

## **Part D**

# **Case Study**



## **Chapter D1**

### **Introduction**

## D1.1 Introduction

The Case Study is made to illustrate some steps to be taken and evaluations to be made should certain damage occur during operation of a given riser for a given situation. The damage described and the operational scenario selected is believed to be sufficiently typical in order to serve as an illustrating example. Emphasis is made toward corrosion damaged flexible pipes.

The purpose of the Case Study is also to highlight implementation of methods and methodologies described in the Handbook Chapters from [A2](#) to [C3](#).

The current Case Study will not fully meet the hopes of illustrating all sections of the Handbook, but should serve as a good starting point for further extensions in a later edition.

The Case Study is generally based on the riser case 'North Sea Riser'. However, during the JIP project some studies are performed by using the 4" (ID) riser from the Balmoral field as a case: fatigue testing of armour wire in air, evaluation of corroded armour wire surfaces by scanning and application of in-air SN-curve for reliability evaluation. Access to the riser data is given by an agreement with the JIP - Riser End of Life, performed by Flexlife. The results from the studies based on the Balmoral riser are included where relevant in supplementing the results from the North Sea Riser.

After describing the riser structures, necessary aspects of operational life are defined - along with selected alternative scenario, Chapter [D2](#).

Chapter [D3](#) describes the fatigue testing performed for the retrieved armour wire samples - a mean to obtain important the remaining fatigue life of the armour wire.

The study of the corroded armour wire samples continue in Chapter [D4](#) Chapter [D4](#) by investigating the corroded surfaces with the aim of obtaining yet more helpful data in understanding the effect of corrosion damage and how to measure the corrosion damage.

In Chapter [D5](#) some structural aspects of tension armour wire failure due to corrosion is studied. The described numerical analysis serves to illustrate a methodology in how to account for wire failures in the integrity assessment analysis.

Integrity Management and Lifetime Assessment evaluations of the North Sea Riser are presented in Chapter [D6](#) and Chapter [D7](#), applying the Methodologies described in Chapters [C1](#) and [C2](#).

In Chapter [D8](#) probabilistic models and reliability analysis are illustrated for the Case along with assessment of the remaining lifetime for different comparable scenario during operation.

## D1.2 Case Description

### D1.2.1 North Sea Riser

The riser section shown in Figure [D1.1](#) has been used in the North Sea for 11 years connected to a semisubmersible type of floater. The tension armour wires are subjected to fatigue testing. However, the riser properties and operational information used in this Case Study is only partially in agreement with this physical sample. The data basis for the Study is

gathered from different sources in a way which should be fairly representative for North Sea conditions, but otherwise not true.

The armour wire samples are taken from the static part of the same riser, one section from a corroded part and one non-corroded section serving as a reference.

A representative North Sea flexible riser configuration at a water depth of 300m is considered. The riser pipe has an internal diameter of 6" and its build-up is illustrated in Figure D1.1 and Table D1.1.



Figure D1.1: A sample section of the North Sea flexible riser after 11 years of operation.

Table D1.1: North Sea Riser structure

No.	Layer description	Numerical model
1	INTERLOCKED CARCASS	
2	PVD LAYER	
3	PRESSURE ARMOUR	
4	SPIRAL	
5	POLYAMID ANTI-WEAR TAPE	
6	FIRST ARMOUR LAY	
7	POLYAMID ANTI-WEAR TAPE	
8	SECOND ARMOUR LAY	
9	OUTER SHEATH	

The Case Study riser is intended for sweet service and conveys oil at an initial operating pressure of around 300 bar, which is decreasing with time.

Due to confidentiality clauses, the specifications for the flexible pipe and the armour wire cannot be released in full. Below are given some essential parameters.

**Specifications of pipe:**

Sweet service.

Design pressure 420 bar.

Design temperature 105°C.

Internal diameter of pipe 6 inches.

**Specifications of armour wire:**

Ultimate tensile strength 1400 MPa.

Cross section 3 x 12 mm<sup>2</sup>.

The riser is connected to a floater of the semisubmersible type. Damage in the outer sheath has caused the riser to be flooded, the exact period of time not known.

### D1.2.2 Balmoral Riser

The 4" Gas lift riser, here denoted Balmoral riser, was replaced on the Balmoral FPV (owned by Premier Oil) after 23 years of service.

The Balmoral riser is a 4" ID gas lift sweet service riser with a design pressure of 190 bar (2700 psi). The armour wires of steel FI 41 have an ultimate tensile strength of 1400 MPa and a cross-section of 3 x 6 mm<sup>2</sup>. The Balmoral riser was used for 23 years before being retrieved. The last part of service life the riser was subjected to wet annulus conditions (exact time or gas/fluid content are not known). Also wire from a spare sample stored on-shore for 23 years was available.



(1) Balmoral riser - used (23 years) wire.



(2) Balmoral riser - stored on shore.

Figure D1.2: Sample sections of the Balmoral riser - both used and stored (courtesy Flexlife).



## **Chapter D2**

### **Data Basis**

## D2.1 Introduction

The data basis for the Case Study includes data predominantly from the North Sea Riser, but supplemented by data from the Balmoral riser. **The operational data used for the Case Study are partly real, partly fictitious or assumed.**

## D2.2 Temperature and pressure records (operation pressure)

The operating pressure is characterized by a decreasing trend. The average pressure during the last 8 years in operation has been around 85 bar. In the following, it is assumed that the operating pressure varies linearly from 300 to 85 bar during the first three years in operation. Subsequently the operating pressure is assumed to be constant and equal to 85 bar.

The average temperature during the last six years in operation is around 70°C. It is assumed that this value also applies to the first five years in operation.

## D2.3 Annulus pressure tests

A sequence of annulus pressure tests are performed, starting during the second year in operation. Based on the observed free volume in the riser, leakage of the outer sheath at the upper part of the riser was suspected during the fifth year in operation. This was confirmed by ROV inspection.

### D2.3.1 Annulus gas sampling

Measurement of annulus gas composition is performed during the two last years that the riser was in operation. In addition, a measurement was performed within one year after the replacement riser was put in operation (i.e. after 11 years).

It is observed that the CO<sub>2</sub> content in the annulus of the new riser is at the same level as was observed for the decommissioned riser after the first year in operation. The same applies to the hydrogen level in the annulus. This implies that the saturation of CO<sub>2</sub> takes place quite rapidly. This is also likely to hold for the associated CO<sub>2</sub>-induced corrosion which leads to an increase of the hydrogen level, indicating presence of permeated water in the annulus.

The H<sub>2</sub>S level in the annulus was found to be negligible throughout the lifetime of the riser.

## D2.4 Stress cycle distribution

Global dynamic analysis is performed to establish the long-term distribution of the cross-section forces. These are applied in a local FEM analysis to calculate stress ranges for the relevant pipe cross section by means of cycle-counting procedures. The long-term stress cycle distribution forms the basis for computation of fatigue damage by application of the relevant SN-curve. The effect of possible stress concentrations also needs to be taken into account by proper magnification of the stress range.

By combining the damage contribution for all the cycle range classes based on the number of cycles per class obtained from rainflow counting, the annual fatigue damage for the critical cross-section is found.

The base case stress-range distribution for the relevant cross-section is shown in Figure D2.1.

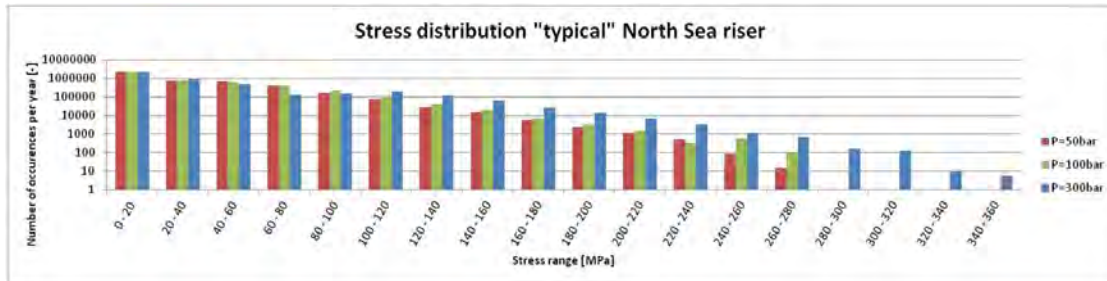


Figure D2.1: Stress range distribution for relevant cross-section (Corrected for the effect of mean-stress based on the Gerber approach).

## D2.5 Sheath and corrosion damage

The sheath damage is located just below the guide tube at the top end of the riser. The damage is very localized as shown for a similar type of damage in Figure D2.21 (left part). After the damage the annulus is filled with sea-water. After the period of 1-year with sea-water exposure, a limited amount of corrosion products are observed at the riser surface. This indicates localized corrosion without any serious damage to single or multiple wires.

After 1 year the damage is repaired by a clamp which is indicated by a clamp of a similar type in the right part of Figure D2.22. This seals the sheath and stops oxygen-driven corrosion. An inhibitor fluid is also applied at the time of repair in order to prevent further corrosion.

A second scenario is also considered where the damage is located inside the guide tube such that access is difficult and repair is not performed. This implies that the corrosion process will be continuously on-going once the sheath damage has occurred.



(1) Type of sheath damage



(2) Type of riser clamp

Figure D2.2: Type of sheath damage (left, [Muren, 2008]) and type of riser clamp (right)

## D2.6 SN-curves

For the in-air condition, the SN-curve obtained from the tests of wires from the stored and unused samples of the Balmoral riser, is applied (based on the results for the stored samples), see Figure D2.3. The fatigue design curve is expressed on the following form:

$$\log_{10}N = \log_{10}\bar{a} - m\log_{10}\Delta S \Rightarrow \log_{10}\Delta S = -\frac{1}{m}(\log_{10}\bar{a} - \log_{10}N) \quad (\text{D2.1})$$

where  $\Delta S$  is the stress range,  $N$  is the number of cycles to fatigue failure,  $m$  is the exponent of the SN-relationship and  $\bar{a}$  is the intercept along the horizontal axis.

The slope of the left part of the SN-curve is  $1/m = 1/6$ , and the associated value of  $\log_{10}(a_{Design})$  is around 20.5. A design fatigue limit is also applied. This limit is observed to be just higher than the uppermost stress cycle (load effect) for the present riser, as given in Figure D2.1 above. This implies that all the stress cycles fall below the fatigue limit. However, in the present calculations the fatigue limit is removed such that an SN-curve with a single slope is applied.

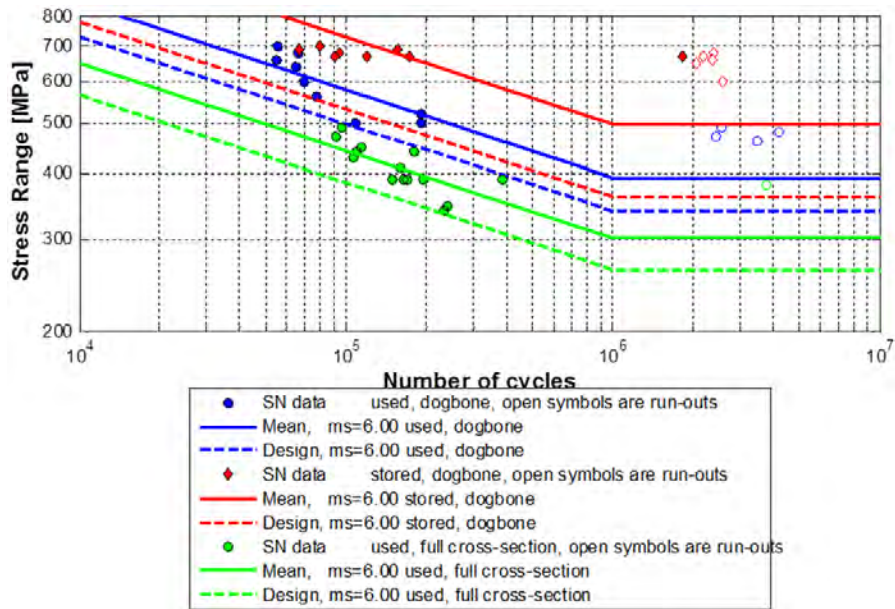


Figure D2.3: In-air fatigue design curve (red dashed line), obtained from [Wang and Berge, 2012].

An issue in the calculations will be the relative effects on the SN-curve due to presence of CO<sub>2</sub> (in addition to condensed water or sea-water). The SN-curve in Figure D2.4 is obtained from [Charlesworth et al., 2011]. The tests correspond to conditions with both CO<sub>2</sub> (0.67 bara) and seawater(4%) / inhibitor(96%) being present. It is assumed in the following that this curve applies for the phase before the outer sheath is broken, i.e. before the damage occurs (even if no inhibitor and seawater in reality may be present for that case, but instead CO<sub>2</sub> and condensed water without inhibitor).

Based on the results from the annulus sampling, it seems reasonable to assume that the transition from 'in-air' conditions to the SN-curve with CO<sub>2</sub> being present takes place within the first year of operation.

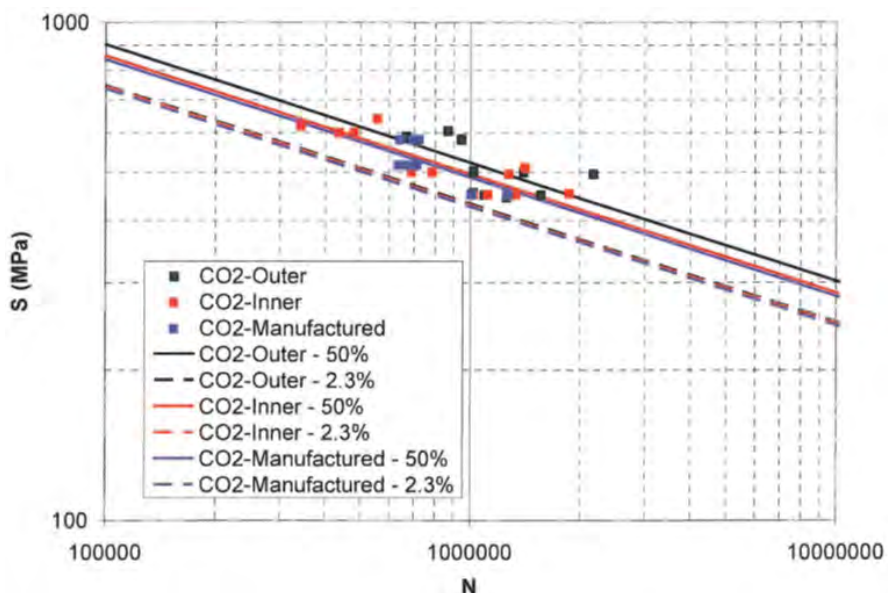
Figure 12: CO<sub>2</sub> Testing Results

Figure D2.4: SN-curve based on [Charlesworth et al., 2011]

Based on the dashed design curve in Figure D2.4, the m-exponent was estimated to be around 4.1, and  $\bar{a}_{Des}$  around 16.8.

The effect of aerated sea-water being present (without any inhibitor) due to damage of the outer sheath can be represented by increasing the slope of the SN-curve in Figure D2.4 slightly. The intersection point with the vertical axis is taken to be constant. This also implies that the value of  $\bar{a}_{Des}$  is reduced somewhat.

After the clamp has been installed and the inhibitor fluid has been injected, the same design SN-curve as that given in the Figure D2.4 is applied.

In order to mimic a situation without access to a sufficient amount of relevant test data, the standard deviation associated with the fatigue test data is increased significantly while keeping the design curve constant. This implies that the mean SN-curve is lifted. As part of the reliability assessment, the mean curve and standard deviation represent the input to the statistical modeling. As more test data becomes available, the variability reflected in terms of the standard deviation is updated accordingly.

## D2.7 Parameter variations

With respect to the internal pressure, the stress cycle distribution has been computed for three different pressure levels as described above (i.e. 50 bar, 100 bar and 300 bar). The normalized fatigue damage corresponding to the SN-curve given above is shown in Figure D2.5 as a function of normalized pressure (with 100 bar applied as the normalization value).

The effect of moving the floater (semi-submersible) to a different position due to workover at a particular well will be quantified in relation to the associated long-term cycle distribution at the critical cross-section. The relative durations of the floater being located at the two relevant positions (quantified as percentage of time) will be estimated.

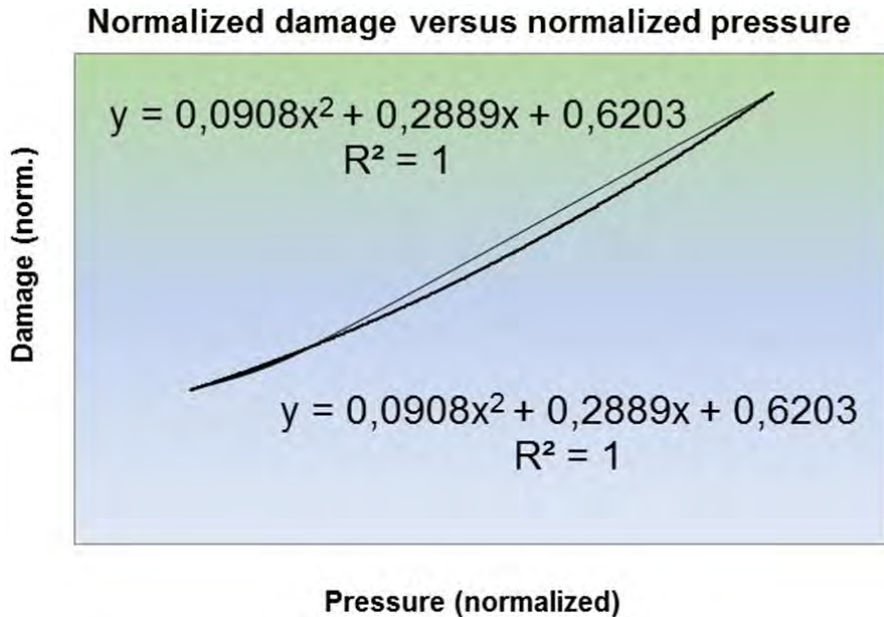


Figure D2.5: Normalized fatigue damage versus pressure level. (Fatigue damage is normalized by the value corresponding to 100 bar. Pressure is normalized by 100 bar)

Parameter studies will also be performed with respect to the following additional quantities:

- Drag coefficient
- Floater motion amplitudes
- Riser internal friction coefficients

The results of the parametric studies are given in terms of variation of the normalized fatigue damage versus the normalized values of the parameters.

## D2.8 Available floater motion and position data

Additional floater motion and position data will allow a more precise statistical modelling of the input to the riser fatigue analysis.

## **Chapter D3**

### **Testing**

## D3.1 Introduction

Armour wire from two risers (Balmoral riser and North Sea riser) that had been in service for several years, were available for investigation. Both risers had been subjected to wet annulus conditions during the last part of their service life. The tensile armour wires were visibly corroded, however, with no significant loss of cross section. Reference wire from non corroded sections was also available for testing.

## D3.2 Data provided by testing

Fatigue testing of corroded wire and reference wire (non corroded) was performed in air with constant amplitude axial loading to obtain fatigue test data. The results were analysed to evaluate the effect of the corrosion damage on the wires in terms of reduction of fatigue strength and of fatigue life. The fatigue strength of the corroded wire was found to be strongly degraded relative to the reference wire.

## D3.3 Small scale testing in air

### D3.3.1 Fatigue testing - general

The specimens were taken from the pipe sample and were straightened by hand rolling prior to testing. The inside of the armour wire was marked on each specimen, to identify the inside vs. the outside of the wires. The inside was subjected to tensile plastic strain during the straightening process.

Two different geometries of the specimens were used in this study. The non-corroded (reference) wire was tested with dog-bone shaped specimens Figure D3.1, to avoid failures initiated by the grips. The corroded specimens were tested both with dogbone and with full cross section, Figure D3.2.

The dog-bone specimens of the reference wire had a test section of 90 mm. The machined surfaces were polished with grit paper and the edges were rounded to a radius of approximately 0.5 mm. The purpose of this treatment was to ensure that fatigue failures would be initiated from the faces of the wires that had not been prepared in any way and thus represented the original state of the wire.

The geometry of the full cross-section specimens of corroded wire is shown in Figure D3.2. Specimens that failed from the grip area were not included in the analysis of test data (non-valid).

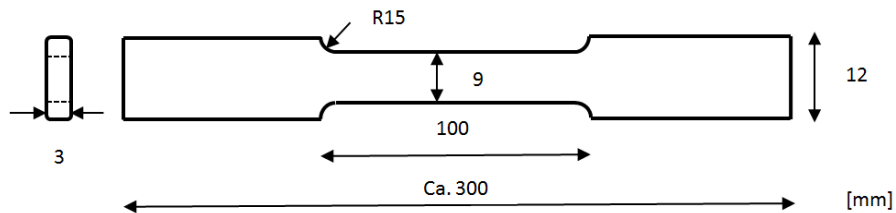


Figure D3.1: Geometry of the dog-bone shaped specimen

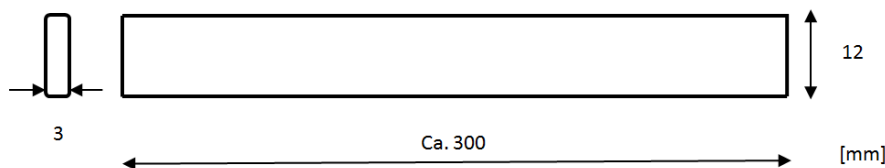


Figure D3.2: Geometry of full cross-section specimens

It is generally recommended to have at least 12 specimens to establish a design SN curve for one series (one material in one condition) [[ASTM E 739, 2004](#)]. Some tests turned out to be invalid for various reasons. Specimens surviving 2 million cycles were considered run outs.

### D3.3.2 Test procedure

Testing was carried out in conformance with MARINTEK test procedures [[Berge, 2012](#)], [[Berge et al., 2003](#)]. A state-of-art digital servo-hydraulic test frame was used, with capacity 100 kN. Axial load was applied by a servo-hydraulic actuator in load control. The test rig and test set-up are shown in Figure D3.3. The loading was axial tension-tension with stress ratio  $R = 0.1$ , sinusoidal with frequency 10 Hz.

Stress range was calculated from the load cell reading and the cross section of the specimens. The load cell had a nominal accuracy of 0.5%. The cross section of each specimen was measured with a digital caliper with resolution 0.01 mm.

Clamping of the specimens was provided by mechanical wedge grips, Figure D3.3. A common problem in axial fatigue testing, in particular when testing high strength armour wire, is fatigue failure initiated by fretting contact with the grips. For this reason the non-corroded specimens were machined to a dog-bone shape, Figure D3.1.

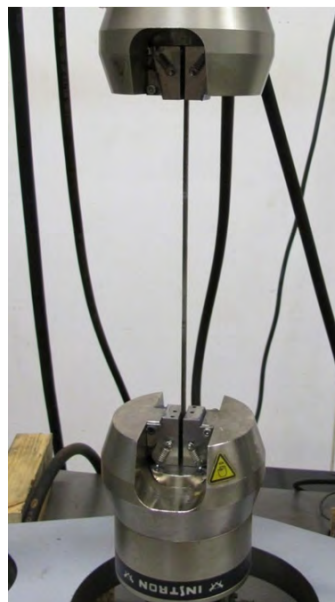


Figure D3.3: Test rig for axial loading

Fatigue strength of non-notched components tends to be governed by the condition of the

surface. With the dog-bone specimens two types of surfaces were present on the test section, the original surface of the armour wire, and the machined / polished surface. The purpose of polishing was to create a surface with fatigue strength better than that of the original surface. If this could be proved to be successful, the fatigue strength of a specimen would be representative of the fatigue strength of the original armour wire. After testing all fracture surfaces were inspected visually and the location of fatigue initiation was identified. Only test specimens with failure initiating from the original surface (face) were considered to be valid. Specimens with failures that were suspected to be influenced by the machining or by the grips were discarded. The SN data are therefore assumed to be representative for the fatigue strength of armour wire in the as-laid condition in a pipe.

Positions of fatigue initiation are indicated according to Figure D3.4.

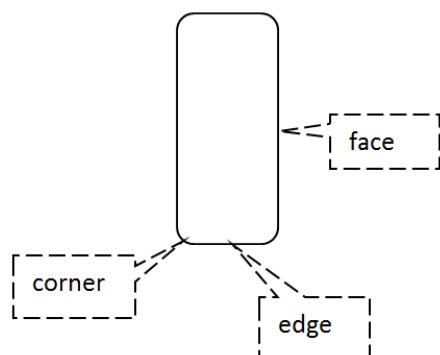


Figure D3.4: Positions on the specimen cross section.

Specimens surviving 2 million cycles were considered as run outs.

### D3.3.3 Armour wire from North Sea riser tested in air

#### D3.3.3.1 Introduction

A flexible riser herein termed 'North Sea Riser' was taken out of service after 11 years. It is known that the annulus of the riser had been flooded by sea water for the last six years of service. Tensile armour wire was taken from a section of the riser that had been subjected to essentially static loads. The wires were visibly corroded, but with no significant loss of cross section. Armour wire was also taken from a static section far from the point of water ingress, believed not to have been affected by sea water. These wires were tested as reference. The armour wire was a high strength sweet service grade with ultimate tensile strength 1400 MPa. Wires from both samples were fatigue tested in air with constant amplitude axial loading. For the reference wires dog-bone specimens were used, to avoid failures being initiated by the grips. The corroded specimens were tested with the full cross section.

Wires from both samples were fatigue tested in air with constant amplitude axial loading. The results were analyzed to evaluate the effect of the corrosion damage on the wires in terms of reduction of fatigue strength and of fatigue life.



Figure D3.5: Sample of North Sea riser reference armour wire. Wire is taken from a non-corroded section of the riser.

### D3.3.3.2 Fatigue testing

Two samples of wire were tested. The reference sample was taken from a static section of the pipe at a location far from the point of sea water ingress, where it is believed that no sea water had been present during the service life of the pipe. The armour wire had a bright appearance, with no sign of corrosion attack, see Figure D3.5. These specimens were tested with the dog-bone geometry.

### D3.3.3.3 Discussion of the results from the reference specimens

The data are shown in Figure D3.6, with regression lines. The appearance of the SN plot for these specimens is typical of SN data for new armour wire tested in air, with a narrow scatter-band and a tendency for specimens surviving 1 million cycles to go to run-out. The slope parameter coming out of the regression analysis  $mr = 25$  is a very high value. Further discussion on the slope parameter is given in [Berge, 2012].

Three specimens failed from the inside face of the wire (relative to pipe axis), four specimens failed from the outside face. As described above, the helical wires coming off the pipe were straightened by hand rolling prior to testing. The plastic deformation (tensile for the inside face, compressive for the outside face) and corresponding residual stress thus had no apparent effect on the fatigue strength.

### D3.3.3.4 Discussion of the results from corroded specimens

The corroded sample was also from a static section of the pipe, where sea water had been present during the period of water ingress (6 years). The wire was visibly corroded with a layer of rust and some shallow pitting, Figure D3.7 and Figure D3.8. However, the cross section was not significantly reduced. These specimens were tested with full cross-section.

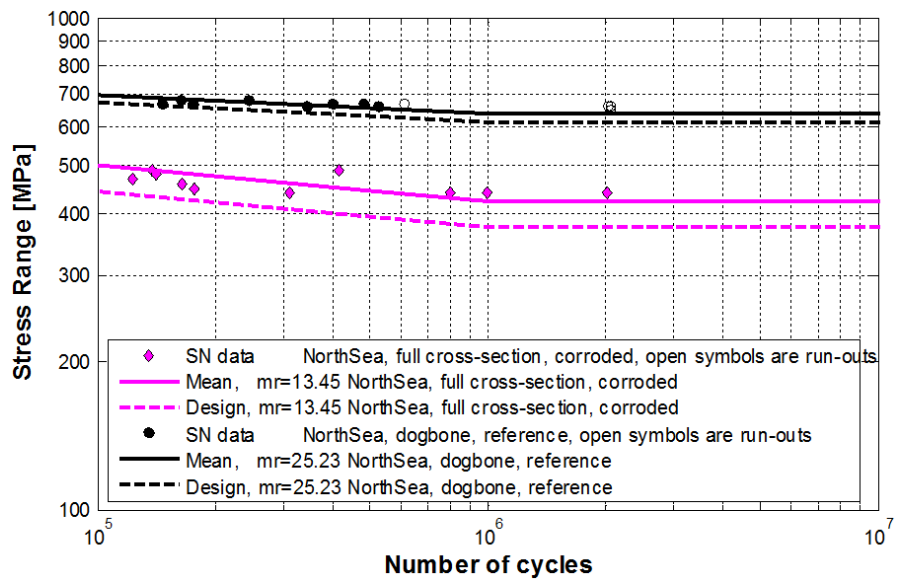


Figure D3.6: North Sea riser SN data points and regression lines



Figure D3.7: Corroded North Sea armour wire prior to being dissected and cleaned before testing takes place.

The test matrix and number of valid tests in the two series are shown in Table D3.1.

Table D3.1: Test series and sample numbers

Test series specimen type	Number of valid specimens
Non-corroded (reference), dog-bone	12
Corroded, full cross-section	10

The data are shown in Figure D3.9, with regression lines.

The SN data for the corroded specimens are significantly different from the data from the reference wire. The fatigue strength is much lower. Inspection of specimens shows that 50% of the specimens failed from the edge/corner, cf. Figure D3.4. This could indicate that the corrosion damage had no preference with respect to position on the wires.



Figure D3.8: Corroded North Sea armour wire prior to testing.

#### D3.3.3.5 Comparison of SN data from reference and from corroded wire

As discussed in [Berge, 2012] regression analysis of small samples of SN data, in particular if the data samples cover only a narrow range of fatigue lives, could give very misleading results, in particular regarding the slope parameter  $m$ . In [Berge, 2012] it is argued that in-air fatigue data for tensile armour should be analysed with a fixed slope parameter, and  $m = 6$  is advised unless there is evidence to assume some other value. For corroded specimens it is not possible to give general recommendations on a slope parameter, because of a different initiation mechanism due to corrosion damage.

For illustration, the two samples were analysed with a fixed slope parameter  $m = 6$ , as shown in Figure D3.9. As shown, the corroded specimens had a significantly lower fatigue strength compared to the reference wire. The reduction in strength (mean life curves) was 30 %, and the residual life of the corroded specimens (assuming  $m = 6$ ) was 10 %.

On the basis of the assumed design SN curves the reduction in strength/life is even larger. However, due to the small size of the samples and relatively large scatter a comparison of the design SN curves becomes very uncertain.

#### D3.3.3.6 Summary and conclusions for North Sea riser

Armour wire taken from a used flexible riser was fatigue tested in air. Two samples of wire were tested, both were taken from static parts of the riser. One sample was from a section of the pipe that had been flooded by sea water for approximately six years. The wire was visibly corroded, but with no significant loss of cross section. The other sample was taken from a section far from the point of sea water ingress, and was believed to have not been subjected to sea water corrosion. The pipe had been in operation for a total of 11 years.

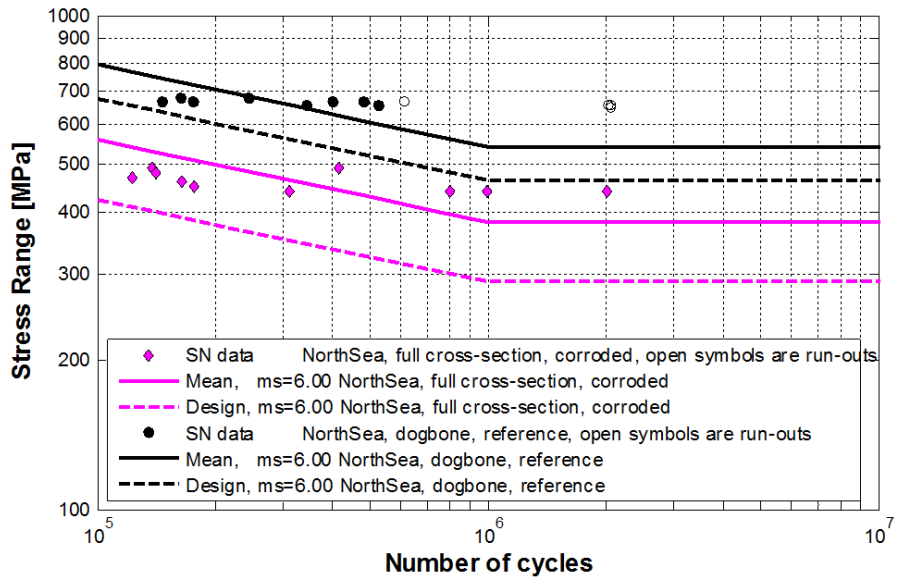


Figure D3.9: S-N data from North Sea riser, both reference tensile wire and corroded tensile armour. Regression analysis with fixed slope parameter  $m_s = 6$ .

The reference wires had no visible corrosion damage. The S-N data are believed to be representative of new (unused) wire.

Wires from the flooded section of the riser had visible corrosion damage in the form of a layer of rust and shallow pits. The reduction in cross section area was not significant. The fatigue strength was significantly lower than that of the reference wire. The reduction in fatigue strength (mean life curves with forced slope parameter  $m = 6$ ) relative to the reference wire was approximately 30 %. The remaining fatigue life was approximately 10 %.

The data samples are very small, and the conclusions are indicative only.

### D3.3.4 Armour Wire from Balmoral riser tested in air

#### D3.3.4.1 Introduction

Flexlife has obtained sections of two risers from the same production with the same specifications. One riser has been stored for 23 years. The conditions of the storage are not known. The other one has been in service for the full period, subjected to wet annulus conditions for the last part of the service life. An exact period for wet conditions is not known, neither gas mixture nor fluids in the annulus for the wet condition. The wires from this riser had general corrosion damage in the form of shallow pits. However, the cross section was not significantly reduced.

#### D3.3.4.2 Fatigue testing

The tested armour wire was grade FI 41 material, with a nominal ultimate tensile strength of 1400 MPa.

Three series of samples were tested in the current project. The first series samples are from wires taken out of service (used) with the test section machined to a dog-bone shape. The second series are from the stored riser (stored) with a machined (dog bone) test section. The third series samples are from the used wires with full cross-section.

The test matrix and specimen numbers in each of the three series are provided in Table D3.2.

Table D3.2: Test series and sample numbers, Balmoral riser

Test series / specimen type	Number of specimens
Used and machined test section (dog bone)	16
Stored and machined test section (dog bone)	19
Used and full cross-section	13

#### D3.3.4.3 Discussion of the test results from reference wire, dog bone shaped specimens

The data are shown in Figure D3.10. Two specimens failed outside of the 90 mm test section, with initiation from the edge. The initiation was not caused by the clamping. For these two specimens the stress range was calculated on the basis of the original cross section, i.e. the cross section at the location of the failure. By inspection these two specimens were found to be significantly corroded, and the fatigue failures had been initiated from the corroded section, Figure D3.11. As stated above, no information was available on the condition of the storage of this pipe. Apparently some corrosion had taken place in parts of the pipe, Figure D3.11.

The remaining specimens had no significant corrosion damage, judged from visual inspection. The appearance of the SN plot for these specimens is typical of SN data for new armour wire tested in air, with a narrow scatter-band and a tendency for specimens surviving 1 million cycles to go to run-out.

Based on these observations the data sample, excluding specimens 3 and 19, were taken as representative of unused armour wire, Figure D3.12.

Regression analysis of the data sample will give a very uncertain estimate (large confidence interval) of the slope parameter  $m$ . MARINTEK has adopted a standard slope  $m = 6$  for armour wires in air (fixed slope regression analysis), with a fatigue limit at  $N = 10^6$ .

Assuming the same slope for the SN curve ( $m = 6$ ) a regression analysis was carried out. The resulting mean life and design life SN curves are shown in Figure D3.12. The curves are shown for demonstration only, due to the very small sample size.

#### D3.3.4.4 Discussion of the test results for corroded, dog bone shaped specimens

The data are shown in Figure D3.10. The resulting mean life and design life SN curves are shown in Figure D3.12.

The SN data for used (dog bone) specimens are very different from the data for the stored (dog bone) specimens, with much lower fatigue strength. Two specimens had failed from fatigue initiation outside of the test section, and not being affected by the grips. For these two specimens the stress range was calculated on the basis of the original cross section, i.e. the cross section at the location of the failure.

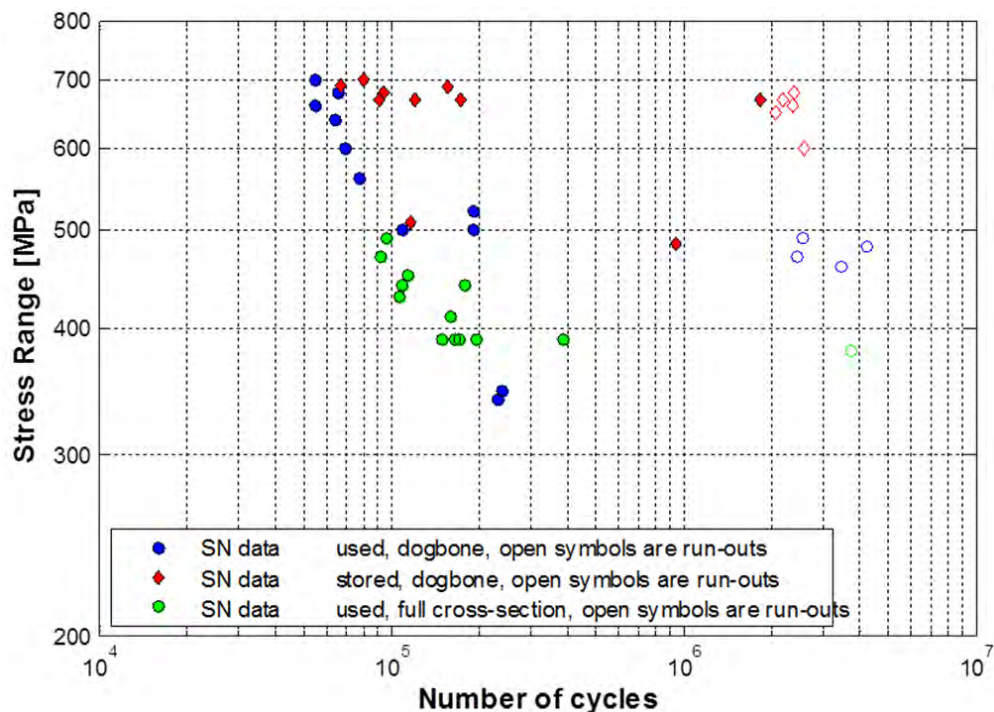


Figure D3.10: SN data points for Balmoral riser tested in air



Figure D3.11: Photo of stored dog bone specimens that failed from corroded area outside of test section.

The appearance of the data may lead to a conclusion that the SN curve for used wire is very steep, with a low value of the slope parameter  $m$ . However, this is most probably fortuitous, due to the random choice of stress range for each specimen, in this case leading by chance to an apparent systematic behaviour. The appearance of the SN data is most probably linked to the random nature of corrosion damage, as discussed in Section D3.3.4.5.

#### D3.3.4.5 Discussion for the corroded full cross-section specimens

The data are shown in Figure D3.10. For regression analysis (Figure D3.12) the two dog bone specimens of the used wire that had failed in the full cross section, were included the same

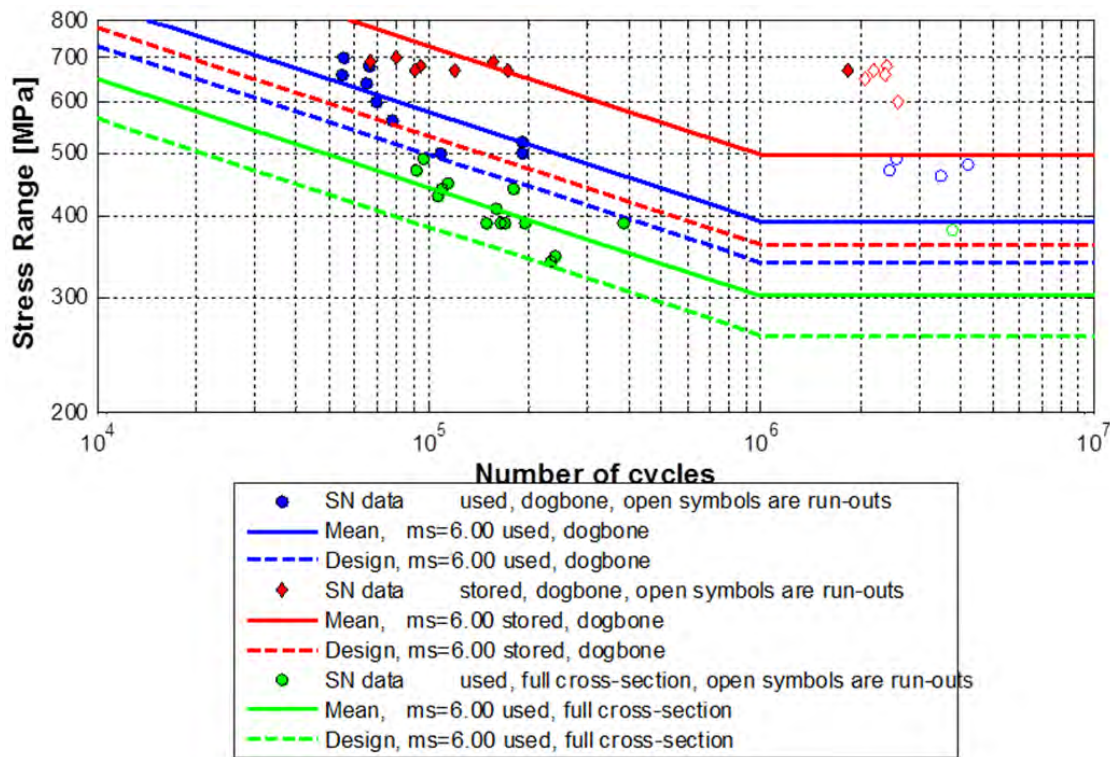


Figure D3.12: Valid SN data points and regression lines with assumed fatigue limit for Balmoral riser testen in air.

sample. The resulting mean life and design life SN curves are shown in Figure D3.12. It can be seen that the mean life SN curve of these data is significantly lower than for the used, dog bone specimens, and that the two scatterbands (based on two standard deviations) are hardly overlapping. This indicates that the two samples (dog bone and unmachined specimens) are statistically different.

It is observed that for this test series 11 out of 15 specimens failed from the corner or edge, i.e. from the part that was machined off for the dog bone specimens. This could indicate that the corrosion damage had some preference for the corner/edge, and the dog bone specimens in this case giving unconservative results.

Fatigue of tensile armour is a weakest link process, starting from the location on the surface where the combination of microstructure, residual stress, surface condition and in this case corrosion damage is most severe. Comparing the used and the stored samples, and assuming that corrosion exposure is the main difference, it is apparent that the corrosion damage has a significant effect on the fatigue strength of used wire. In each test 90 mm section of wire is tested, and the probability of testing a 'lower bound' defect is relatively small. In the dynamically loaded section of a flexible pipe several 10's of meters are fatigue loaded. Hence, the design must be based on 'lower bound' data, conventionally taken to be the mean life curve minus two standard deviations. Assuming that the full cross section specimens give the most realistic data for used wire, the reduction in strength (mean life curve) in relation to stored wire is approximately 40 %. The remaining fatigue life is approximately 5%.

Due to the small size of the samples and relatively large scatter a comparison of the design SN curves becomes very uncertain.



Figure D3.13: The fractured used, full cross-section specimens, Balmoral riser

#### D3.3.4.6 Summary and conclusions for Balmoral riser

Armour wires taken from two flexible risers were fatigue tested in air. The two rises were from the same production, with identical specifications. One riser has been stored for 23 years. The other one has been in service for the same period.

Totally three series of the wires were tested. One series were wires for the used riser with machined test section (dog bone shaped). Another series were wires from the stored riser with machined test section (dog bone shaped). The last series were wires from the used riser with full cross-section.

Wires from the stored pipe showed some corrosion damage which is related to storage conditions. Samples from these corroded sections were excluded from the analysis of this test series. The main part of the sample that was tested showed fatigue strength characteristics typical of new wire.

Wires from the used pipe had significant corrosion damage in the form of shallow pits on the surfaces. The reduction in cross section area was not significant. The fatigue strength was significantly lower than that of stored wire. Comparison of data from dog bone shaped specimens with the edges machined off in the test section, and specimens that were tested with full cross section, showed a significant difference in fatigue strength. The full cross section specimens had lower fatigue strength. By inspection it was found that nearly all full cross section specimens failed from the unmachined corner or edge, indicating preferential corrosion damage at these locations.

Based on the data from the full cross section specimens the reduction in fatigue strength (mean life curves) relative to wire from the stored pipe was approximately 40%. The re-

maining fatigue life was approximately 5%.

The data samples are very small, and the conclusions are indicative only.

#### D3.3.4.7 Further use of test results for Balmoral riser

The SN curves for the stored (unused) armour wire are also presented in Section [D2.6](#) for the in-air conditions. The fatigue limit is removed such that an SN curve with a single slope is applied in the calculations presented in Chapter [D8](#).

### D3.4 Concluding remarks

The following observations and concluding remarks are based on the data presented for the testing of the North Sea riser:

- Testing in air of non-corroded wire gave results that are typical of high strength armour wire, a very flat SN-curve that is essentially a fatigue limit.
- Testing in air of wire taken from a corroded section of the same riser gave results indicating a significant fatigue notch. The reduction in fatigue strength was a factor of approximately (1/1.4). The reduction in fatigue life (assuming a slope parameter  $m = 6$ ) was a factor 1/10.
- The corrosion damage was superficial, with no significant loss of cross section.



## **Chapter D4**

# **Evaluation of specimen surface of tension armour samples from two different risers**

## D4.1 Introduction

Sections from two risers (the Balmoral and North Sea risers) that had been in service for several years, were available for investigation. Both risers had been subjected to wet annulus conditions during the last part of their service life. The tensile armour wires were visibly corroded, however, with no significant loss of cross section.

Tensile armour wires from both risers were tested with cyclic axial loading in air conditions as described in Section [D3.3](#). The fatigue strength was found to be strongly degraded relative to reference wire. The degradation of fatigue strength appeared to be related to the corrosion damage of the surface of the wires.

### D4.1.1 Balmoral riser

The Balmoral riser had been in service for 23 years, subjected to wet annulus conditions for the last part of the service life. An exact period for wet conditions is not known, neither gas mixture nor fluids in the annulus for the wet condition. The grade of wire was FI 41, a high strength wire for sweet service with dimensions 6 x 3 (mm).

The wires from this riser had general corrosion damage in the form of shallow pits, [[ASTM G 46, 2005](#)]. However, the cross section was not significantly reduced. A photo of a typical sample is shown in Figure [D4.1](#).



Figure D4.1: Photo of tensile armour wire from Balmoral riser, after 23 years of service. Period of flooded condition is not known.

### D4.1.2 North Sea riser

The North Sea riser had been taken out of service after 11 years. It is known that the annulus of the riser had been flooded by sea water for the last six years of service. The tensile wire was high strength wire for sweet service with ultimate tensile strength 1400 MPa.

Tensile armour wire was taken from sections of the riser that had been subjected to essentially static loads. The wires were visibly corroded, but apparently to a lesser extent compared to the Balmoral riser. The degradation of fatigue strength was also less as described in Section D3.3. There was no significant loss of cross section. A photo of a typical sample is shown in Figure D4.2.



Figure D4.2: Photo of tensile armour wire from North Sea Riser after 11 years of service, six years in flooded condition.

#### D4.1.3 Material samples

The samples were taken from specimens that had undergone fatigue testing. The specimens were cleaned according to [ASTM G 1, 2005]. The cleaning solution was 500 ml of concentrated HCl and 3.5 g hexamethylene mixed to 1000 ml with distilled water. The specimens were soaked in this solution for 10 min. at room temperature, then rinsed carefully with tap water, washed in ethanol and dried.

Positions on the respective specimens are identified as shown in Figure D4.3.

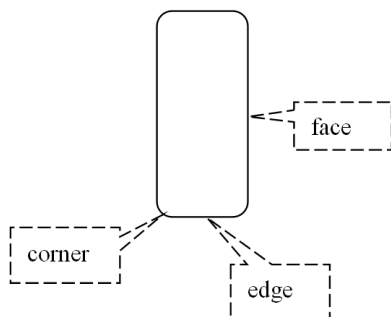


Figure D4.3: Positions on specimens.

## D4.2 Surface characterization of fatigue specimens

Surface characterization of the wires using an optical microscopy technique termed optical 3D surface metrology is performed for both the North Sea and Balmoral risers. Surface profiles of selected samples were obtained, and cross-sectional dimensions of corrosion pits were measured. Examples of the work are presented in this section.

### D4.2.1 Microscopy

The microscopy was carried out by SINTEF Tribology Group. The microscope utilizes a technique termed infinite focus for optical 3D surface metrology. Its operating principle combines the small depth of focus of an optical system with vertical scanning to provide topographical and color information from the variation of focus. Vertical resolution can be as low as 10 nm making the instrument ideal for surface study of both homogeneous and compound materials.

The microscope is able to sample only a small area for each scan. Fatigue is a weakest link process, a fatigue crack will initiate at the surface defect producing the largest notch effect. In this case it was not possible to scan the defect that actually had caused the fatigue failure in the respective specimens. The strategy was thus to select an area on the specimen surface that could represent a worst case with regard to corrosion damage.

### D4.2.2 Procedure for investigation

The procedure for the investigation was as follows:

- Area for scanning on each specimen was selected based on visual inspection. The intention was to investigate an area which appeared to have the most severe corrosion damage.
- Images and measurements were taken in the following sequence:
  - x2.5 objective, 45x magnification:
    - \* Optical image
    - \* Colour image
    - \* Line profile of surface
  - x20 objective, 355x magnification
    - \* Optical image
    - \* Colour image
    - \* Line profile of surface
    - \* Measurements of surface roughness parameters

The most meaningful information was provided by the colour image and the surface profile at 25x magnification, enabling measurement of cross section of the deepest pit within the sample length. Selected results for the North Sea riser is presented in Section [D4.2.3](#).

### D4.2.3 North Sea Riser

The following specimens for the North Sea Riser with the respective fatigue test parameters were investigated:

Table D4.1: Specimens from the North Sea Riser.

Specimen	ID	$\Delta S$ (MPa)	N(cycles)	Comments
3	NC-O-42-5	490	137 863	Failure from face corner
4	NC-O-46-2	480	140 990	Failure from edge corner
5	NC-O-43-7	470	123 320	Failure from face
6	NC-O-4-4	460	164 189	Failure from edge

From visual inspection the corrosion damage on the North Sea Riser material was much less and of a different nature compared to the Balmoral riser. The pitting was more uniform, and with shallower pits.

#### D4.2.3.1 North Sea Riser Specimen 3

A microscope colour image of specimen 3 is shown in Figure D4.4.

A line profile for the line indicated in Figure D4.4 is shown in Figure D4.5.

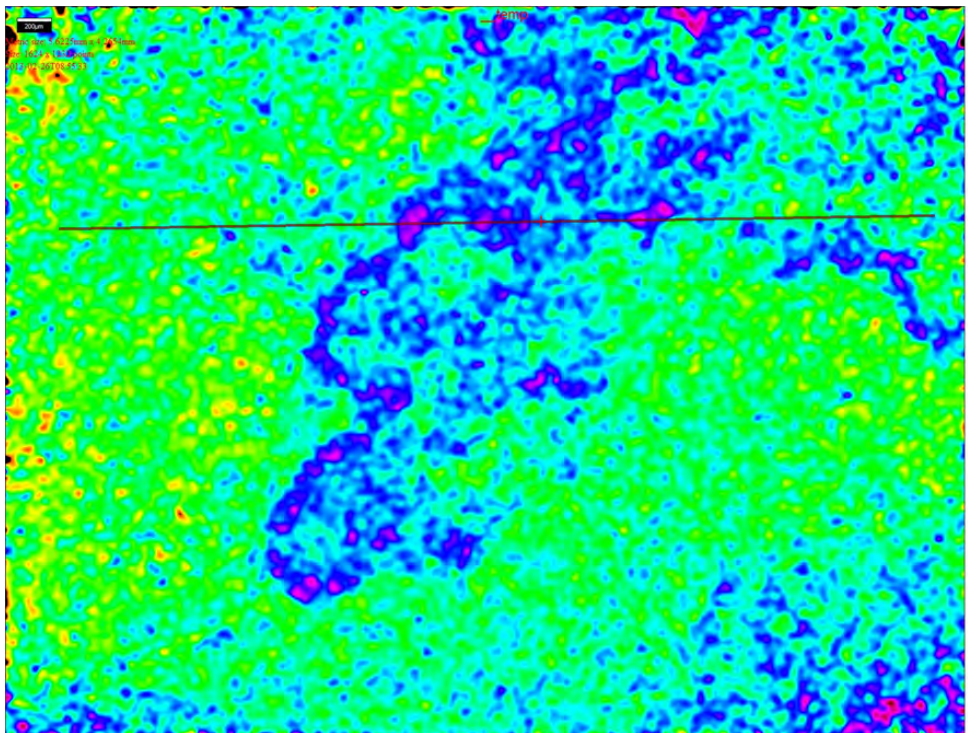


Figure D4.4: Colour image of Specimen 3. The size of the area is 5.6 x 4.3 mm. The range of depth scale is 0μm (light green) to -40μmm (deep purple).

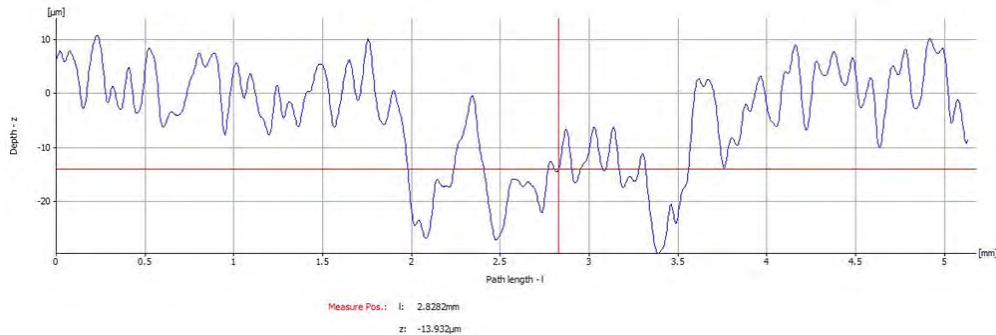


Figure D4.5: Line profile from Figure D4.4. Dimension of deepest pit (approximately) 25  $\mu\text{m}$  depth, 500  $\mu\text{m}$  width

#### D4.2.3.2 North Sea Riser Specimen 4

A microscope colour image of specimen 4 is shown in Figure D4.6.

A line profile for the line indicated in Figure D4.6 is shown in Figure D4.7.

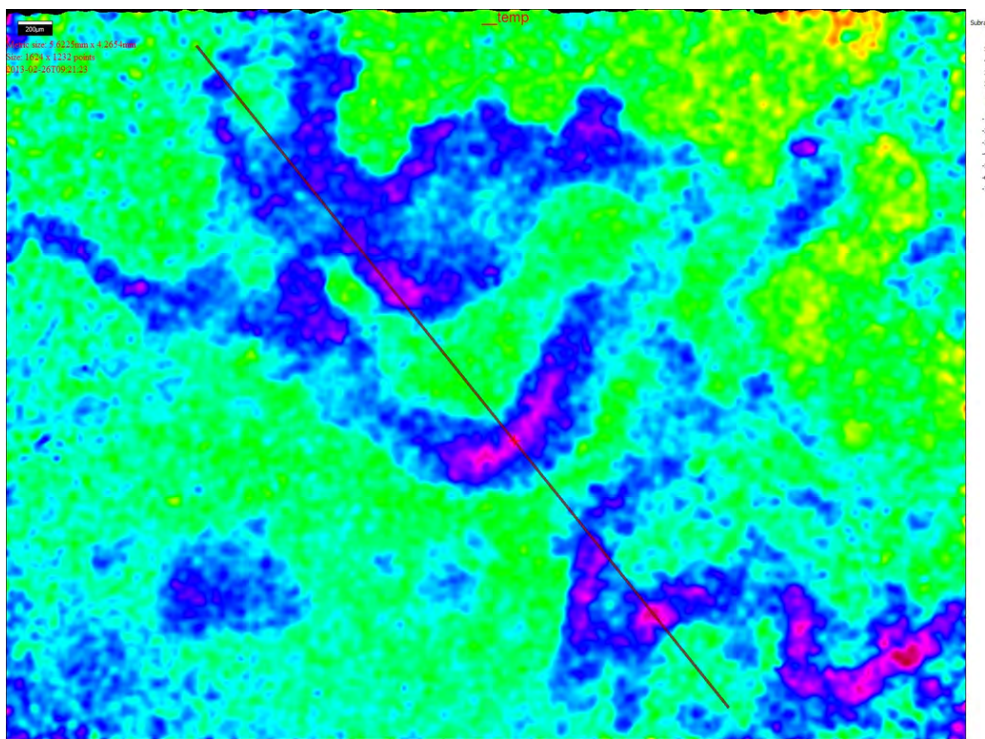


Figure D4.6: Colour image of Specimen 4. The size of the area is 5.6 x 4.3 mm. The range of depth scale is 0  $\mu\text{m}$  (light green) to -70  $\mu\text{m}$  (deep purple).

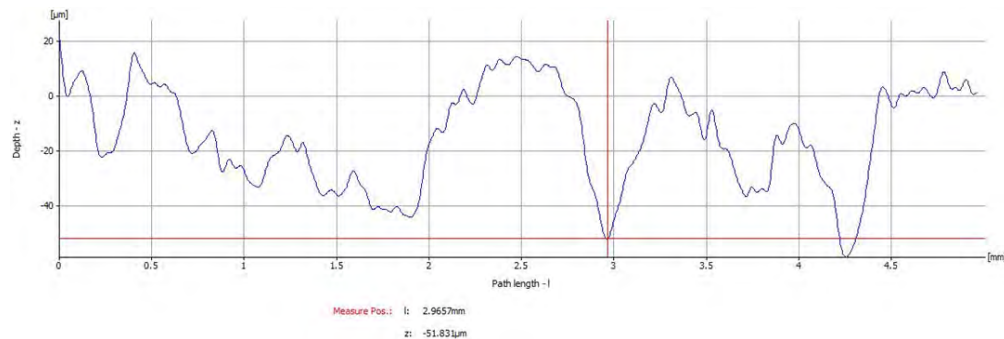


Figure D4.7: Line profile from Figure D4.6. The deepest pit has dimensions (approximately)  $60\mu\text{m}$  depth and  $500\mu\text{m}$  width.

#### D4.2.3.3 North Sea Riser Specimen 5

A microscope colour image of specimen 5 is shown in Figure D4.8.

A line profile for the line indicated in Figure D4.8 is shown in Figure D4.9.

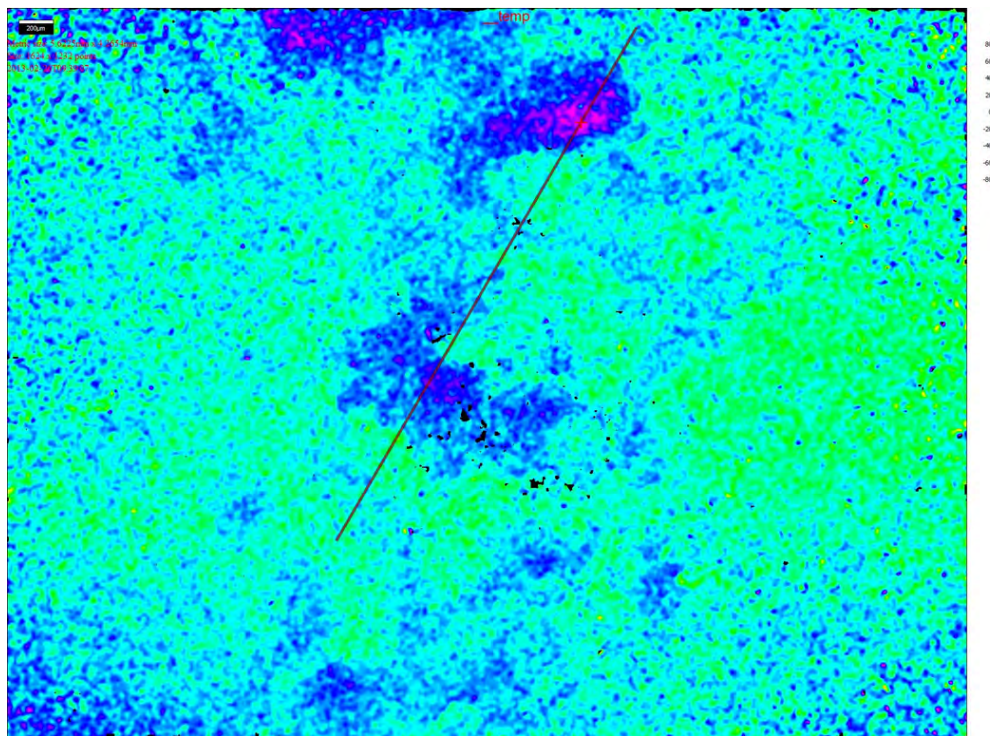


Figure D4.8: Colour image of Specimen 5. The size of the area is  $5.6 \times 4.3\text{ mm}$ . The range of depth scale is  $0\mu\text{m}$  (light green) to  $-80\mu\text{m}$  (deep purple).

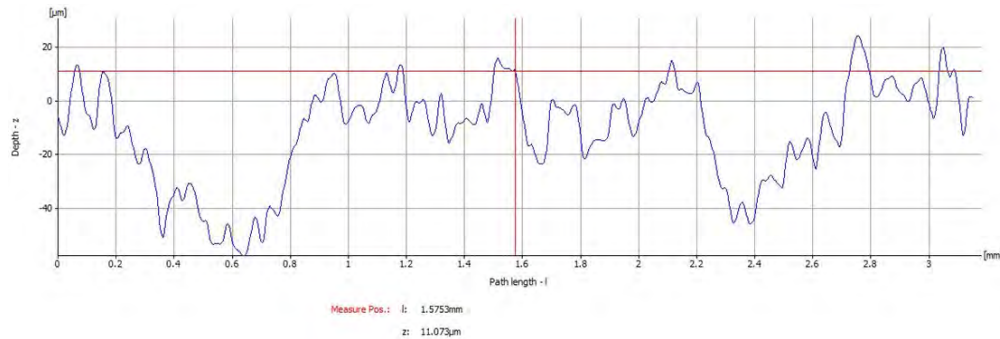


Figure D4.9: Line profile from Figure D4.8. The deepest pit has dimensions (approximately)  $60\mu\text{m}$  depth and  $700\mu\text{m}$  width.

#### D4.2.3.4 North Sea Riser Specimen 6a and 6b

Specimen 6 showed very different corrosion patterns on the respective faces. On face 6a relatively wide and isolated pits were found. On face 6b a pattern of corrosion stripes was observed, possibly from anti-wear tape. Both sides were scanned.

Colour image of Specimen 6a is shown in Figure D4.10.

A line profile for the line indicated in Figure D4.10 is shown in Figure D4.11.

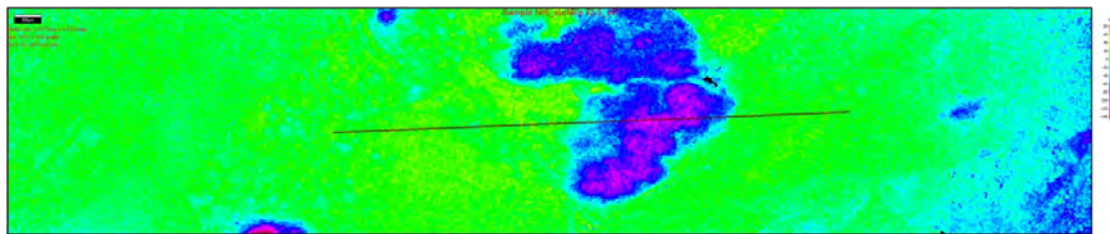


Figure D4.10: Colour image of Specimen 6a. The size of the area is  $20.0 \times 4.3$  mm. The range of depth scale is  $0\mu\text{m}$  (light green) to  $-140\mu\text{m}$  (deep purple).

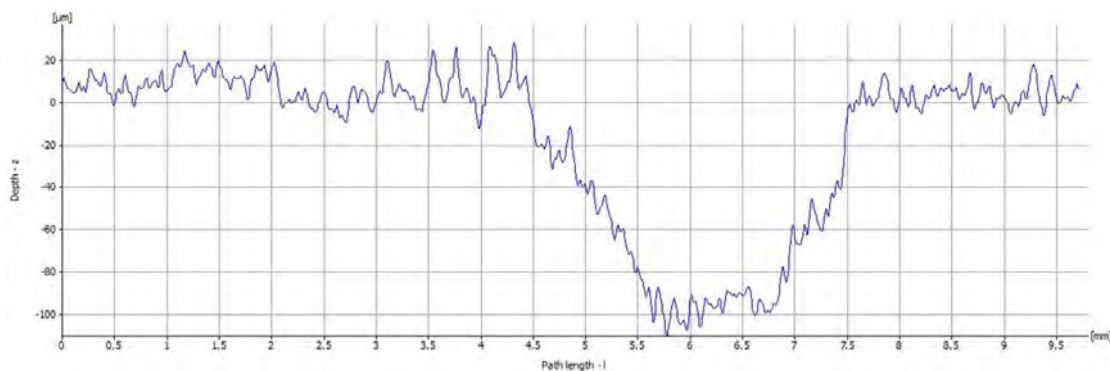


Figure D4.11: Line profile from Figure D4.11. The deepest pit has dimensions (approximately)  $110\mu\text{m}$  depth and  $3\text{ mm}$  width.

Colour image of Specimen 6b is shown in Figure D4.12.

A line profile for the line indicated in Figure D4.12 is shown in Figure D4.13.

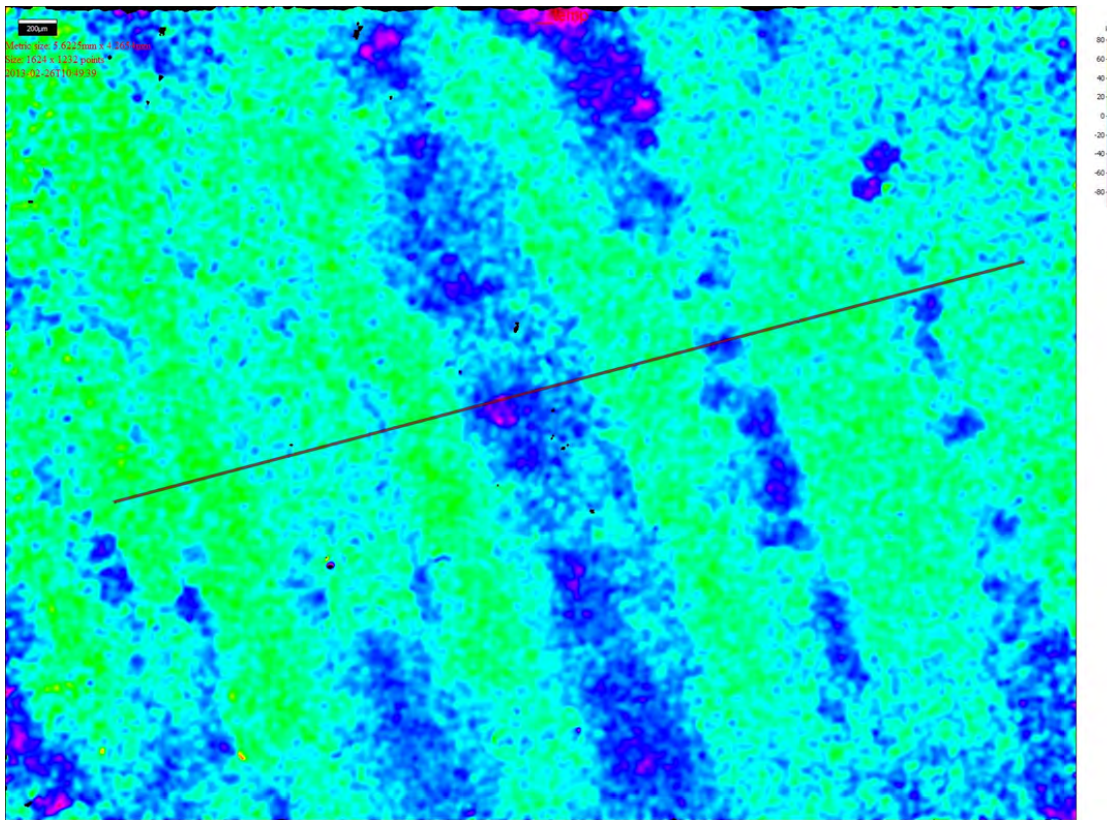


Figure D4.12: Colour image of Specimen 6b. A pattern possibly due to the tape is apparent. The size of the area is 5.6 x 4.3 mm. The range of depth scale is 0  $\mu\text{m}$  (light green) to -90  $\mu\text{m}$  (deep purple).

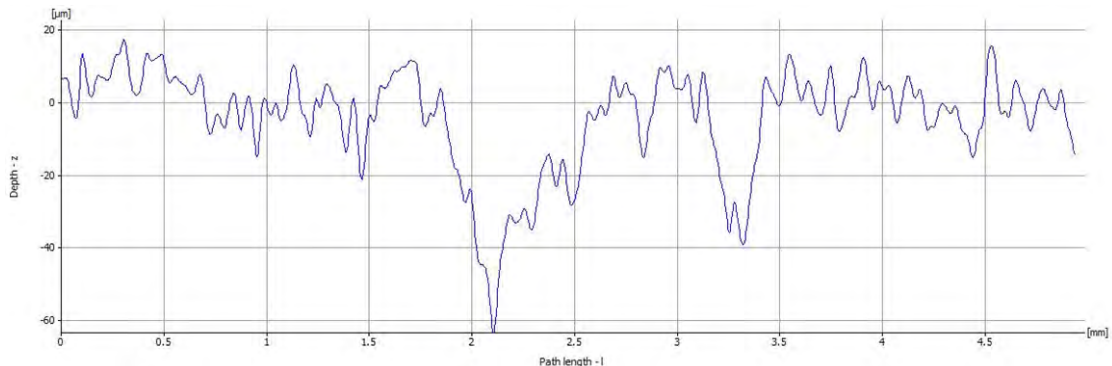


Figure D4.13: Line profile from Figure D4.12. The deepest pit has dimensions (approximately) 65  $\mu\text{m}$  depth and 500  $\mu\text{m}$  width.

#### D4.2.4 Discussion and summary

The line profile with x2.5 objective (35x magnification) gave the most useful results in terms of surface properties related to fatigue strength. In Table D4.2 the cross sectional dimensions of the largest pits for each specimen are summarized.

The aspect ratio is defined as the ratio Depth/Width of the pits. The aspect ratio is a measure of the acuity of a pit in terms of stress concentration factor. Measurements of pit

dimensions for both North Sea Riser and Balmoral riser are presented in Table [D4.2](#).

Table D4.2: Summary of the measurements of pit dimensions.

Riser	Specimen	Depth(μm)	Width(μm)	Aspect ratio
Balmoral	21	200	2000	0.10
	22	150	300	0.50
	26	200	1300	0.15
	26	150	1500	0.10
	<b>Mean</b>	<b>175</b>	<b>1275</b>	<b>0.21</b>
North Sea	3	25	500	0.05
	4	60	500	0.12
	5	60	700	0.09
	6a	110	3000	0.04
	6b	65	500	0.13
	<b>Mean</b>	<b>64</b>	<b>1040</b>	<b>0.09</b>

### Observations:

Armour wire material was taken from two risers that had been subjected to flooded annulus conditions. Specimens that had been fatigue tested to failure were investigated for pitting corrosion damage. What appeared to be worst case pits from visual investigation of each specimen were scanned. The following observations were made:

- The depth of the pitting on the Balmoral wire was significantly larger than on the North Sea Riser.
- With one exception, the aspect ratio was in the range  $< 0.15$  for pits on both samples of wire.
- One pit on Balmoral wire had an aspect ratio of 0.5.
- The overall results are in agreement with the fatigue strength data.

## D4.3 Scanning electron microscopy of fatigue fracture surfaces of tensile armour

### D4.3.1 Microscopy

The investigation was carried out at the Metallurgical Laboratory of SINTEF. The defects were characterized using the nomenclature of [[ASTM G 46, 2005](#)].

### D4.3.2 Specimen description

Specimens from both North Sea and Balmoral risers were investigated.

An overview of the North Sea riser specimens with the respective fatigue test parameters is presented in Table [D4.3](#).

Table D4.3: Specimens from the North Sea Riser.

Specimen	ID	$\Delta S$ (MPa)	N(cycles)	Comments
3	NC-O-42-5	490	137 863	Failure from face corner
4	NC-O-46-2	480	140 990	Failure from edge corner
5	NC-O-43-7	470	123 320	Failure from face
6	NC-O-4-4	460	164 189	Failure from edge
7	NC-O-2-3	450	176 951	Failure from corner
13	NC-O-31-13	440	310 848	Failure from edge

#### D4.3.2.1 Example - North Sea Riser specimen No.3

Fatigue initiation location and initial defect are shown in Figure D4.14 and Figure D4.15.

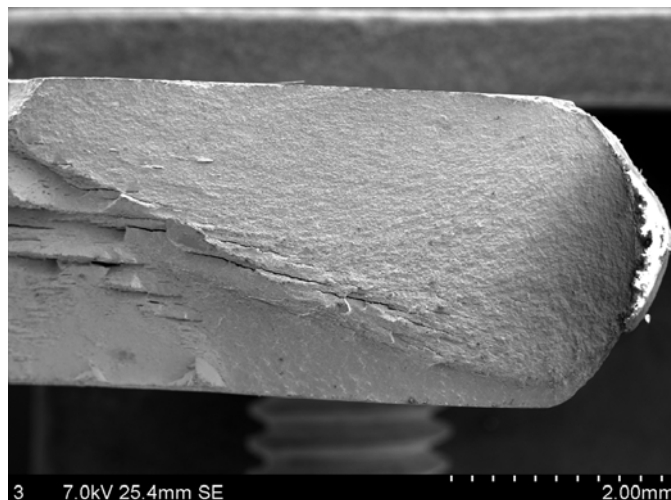


Figure D4.14: Fatigue initiation from upper right hand corner, North Sea riser specimen no. 3.

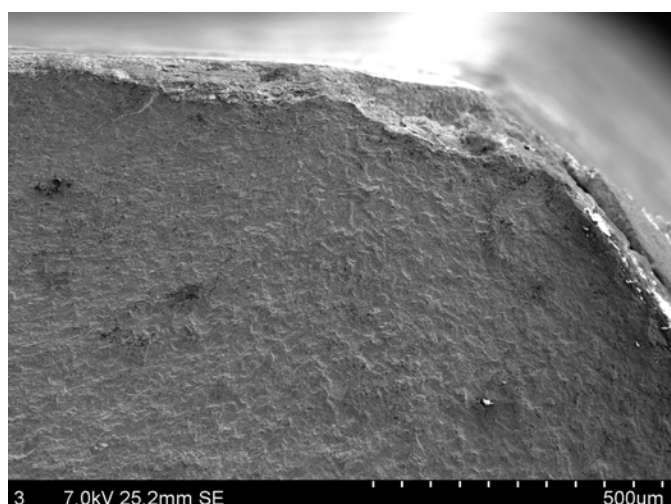


Figure D4.15: Initial defect, specimen no. 3: Wide, shallow pit. Dimensions  $110 \mu\text{m}$  (depth)  $\times 730 \mu\text{m}$  (width).

### D4.3.3 Discussion and summary

Summary of the measurements of pit dimensions.

In the below the cross sectional dimensions of the pits for each specimen are summarized. The aspect ratio is defined as the ratio Depth/Width of the pits. In this case the dimensions of the respective pits are measured in the crack plane. The cross-sectional dimension in the direction of the principal stress is not known. Thus, there is no information on the acuity of the defects in terms of stress concentration factor.

Table D4.4: Summary of the measurements of pit dimensions.

Riser	Specimen	Depth ( $\mu\text{m}$ )	Width ( $\mu\text{m}$ )	Aspect ratio	Comment
Balmoral	21	170	475	0.36	
	22	115	320	0.36	
	25	250	NA	NA	
	26	90	900	0.10	
	27	250	640	0.39	
	31	80	200	0.40	
		150	500	0.30	Not an initiation site
North Sea	3	110	730	0.15	
	4	120	500	0.24	
	5	130	800	0.16	
	6	85	375	0.23	
		40	450	0.09	Not an initiation site
	7	65	800	0.08	
		50	240	0.21	Not an initiation site, possibly a fabrication defect
	13	85	470	0.18	

For fatigue crack initiation the *depth* dimension is the most important. The average of initiation defects (not counting the defects that were judged not to have initiated fatigue cracks) is presented in Table D4.5.

Table D4.5: Average depth of initiation defects.

Riser	Average depth ( $\mu\text{m}$ )	Average width ( $\mu\text{m}$ )	Average aspect ratio
Balmoral	159	507	0.32
North Sea	99	612	0.17

The initial defects on the Balmoral wire were significantly larger than the defects on the North Sea wire. This is consistent with the findings from optical surface scanning of the respective wires. It is also consistent with the finding that the Balmoral wire was more affected by corrosion damage than the North Sea wire in terms of fatigue strength reduction.

The aspect ratio of the pits appears to be significantly different for the two armour materials. The aspect ratio of the pits on the Balmoral wire is nearly twice as large as the aspect ratio of the pits on the North Sea riser. This could indicate a somewhat different corrosion mechanism in the two cases, pitting corrosion on the Balmoral being more localized. It could also be an indirect result of the fact that on the Balmoral wires the corrosion had reached a more advanced stage. The average width of the pits is nearly the same for the two cases. If

it may be assumed that further pitting corrosion on the North Sea riser takes place primarily in the depth direction, the pit shapes would end up like in the Balmoral case.

**Observations:** Armour wire material was taken from two risers that had been subjected to flooded annulus conditions. The fracture surfaces of specimens that had been fatigue tested to failure were investigated by scanning electron microscopy. The following observations were made:

- In all the cases fatigue cracks had been initiated at corrosion pits.
- The initial defects (pits) on the Balmoral wire were significantly larger than the defects on the North Sea wire.
- The aspect ratio of the pits was significantly different for the two types of material. The interpretation of this observation is unclear.
- The overall results are in agreement with the fatigue strength data.



## **Chapter D5**

# **Numerical evaluation of some integrity problems for flexible pipe cross-sections**

## D5.1 Introduction

Two integrity problems are addressed in this section of the Case Study:

- Integrity assessment of damaged flexible pipe cross-section
- Lateral buckling analysis of tension armour wire of a flexible riser

The first problem addresses consequences for the flexible pipe cross-section when tensile wires fails, specifically when 2, 4 or 6 neighbouring wires of the inner tensile layer fails. The cross-section of the North Sea riser is applied for the study.

The second problem addresses the development of rational procedures for evaluating long term armour buckling behaviour in flexible pipes. The study objects are a 6" riser, a 14" jumper and a 8" riser cross-sections. None of the study objects are related to the North Sea riser since the numerical estimates are compared towards laboratory tests performed by Nils Højen Østergaard (PhD thesis, [[Østergaard, 2012a](#)])

## D5.2 Integrity assessment of damaged flexible pipe cross-sections

### D5.2.1 Introduction

The main axial load-carrying layer of the flexible pipe is the tensile armour layer(s). The failure of the tensile armour layer to carry the tensile loads will cause pipe failure. The tensile armour layer consists of a significant number of tensile armour wires, and for a layer failure to occur a certain number of wires need to fail. The failure of individual wires may happen due to exceeding the ultimate or fatigue capacity excessive loads or reduced resistance (f.inst. corrosion)

A FE analysis of a section of the North Sea Riser is applied as a basis for an integrity assessment of a damaged flexible pipe cross-section. The studied scenario is the integrity of the cross-section when either 2, 4 or 6 neighbouring inner tensile armour wires fails.

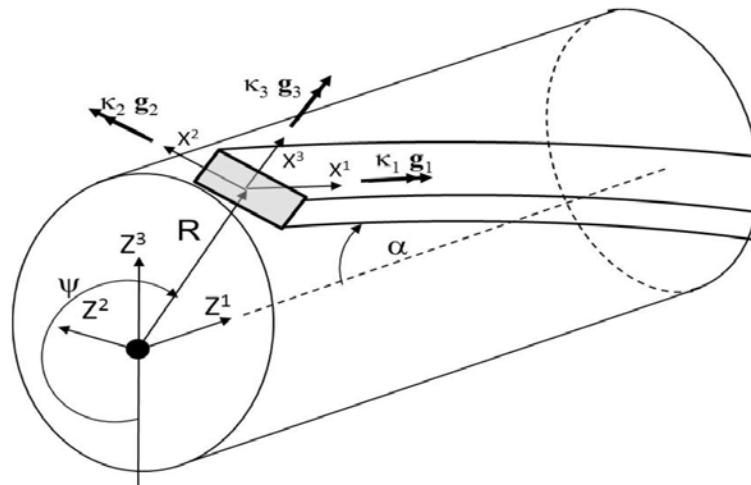
Most of the results presented here are based on the scenario of 6 broken wires. However, in tabulated analysis results, the cases of 2 and 4 broken wires are included as well.

### D5.2.2 Stresses and stress component

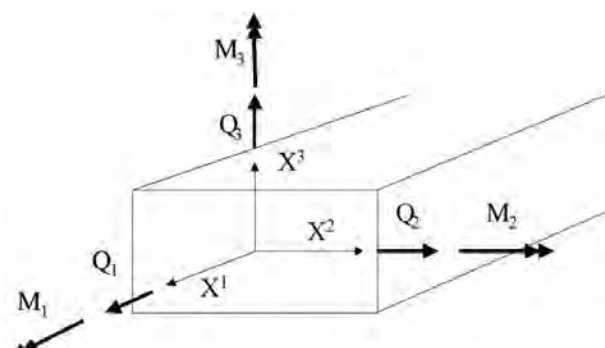
For the tensile armor wire the stresses are related to the governing force resultants defined in Figure D5.12 and the load scenario, which can be divided into:

- Axisymmetric loads that only change the length and diameter of the straight pipe cylinder and with small relative deformations between wires. This includes tension, torsion, internal and external pressure loads, the latter assuming that no local buckling or collapse effects occur.
- Bending loads where the straight pipe cylinder is bent into a torus and where significant relative deformations will occur between the wires.

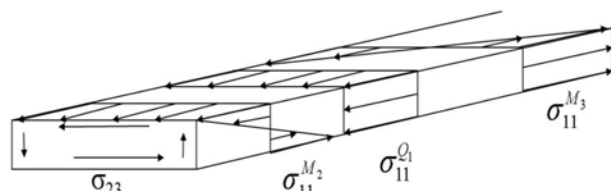
The significant stress components are shown in Figure D5.13 which includes components from axial force (basis for strength calculation), torsion moment and bidirectional bending.



(1) Initial torsion and curvature quantities



(2) Wire force resultants



(3) Stress components in armour wires

Figure D5.1: Definition of wire coordinate axes and mechanical quantities

A flexible riser hanging from a floater will be exposed to cyclic loads from top motions and hydrodynamic effects resulting in cyclic riser motions and global responses in terms of tension and curvature variations.

The static reference stress level in the tensile armor is given by the mean static effective tension and associated internal and external pressures. This gives a mean axial stress and associated contact pressures that govern the friction moment. In a flexible riser the tension and external pressure will vary along its length, hence the friction moment will also change along the riser. Because of the differences in contact pressure between layers, the response in terms of dynamic stresses due to bending (induced by floater motion and hydrodynamic loads) will be different between layers. Hence, the nature of dynamic stresses will be characterized by variations both between layers and along the length of a flexible riser.

The dynamic stresses will consist of an axial friction stress associated to the slip between layers, axial stresses from dynamic tension, local torsion and bending stresses resulting from the components of global curvature along each wire. This results in dynamic longitudinal and shear stresses in the tensile armor where the longitudinal stress represents the most important contribution with respect to fatigue. The longitudinal stress and associated mean stress being input to the fatigue calculation consist of different contributions. For the tensile armour these are:

$$\Delta\sigma_{11} = \Delta\sigma_{11}^{Q_1,T} + \Delta\sigma_{11}^{Q_1,F} + \Delta\sigma_{11}^{M_2} + \Delta\sigma_{11}^{M_3} \quad (\text{D5.1})$$

Where

- $\Delta\sigma_{11}$  = the tensile armour longitudinal stress range
- $\Delta\sigma_{11}^{Q_1,T}$  = the stress range from dynamic tension variation,
- $\Delta\sigma_{11}^{Q_1,F}$  = the dynamic stress range from friction effects,
- $\Delta\sigma_{11}^{M_2}$  = the dynamic stress from bending about the wire weak axis
- $\Delta\sigma_{11}^{M_3}$  =the stress range from bending about the wire strong axis.

Considering one load cycle, the stress response at one point in the wire cross-section exposed to curvature cycle at constant tension and pressure will typically look like the one in Figure D5.2. The steep part of the curve is primarily governed by the stick regime where the armor behaves as a stiff pipe until the layer friction is exceeded and the stress increase from that point will be governed by local bending of the wire. Since the rate of stress increase in the stick regime is much higher than for local elastic bending of the wire, small curvature ranges often governs the fatigue life. This is especially the case for corrosion fatigue calculations where no cut-off is applied in the fatigue curve (all stress ranges counts in the Miner sum).

### D5.2.3 FE analysis procedure

The methodology applied to perform an integrity assessment of damaged flexible pipe cross-sections is described as follows:

- Establish a lower bound estimate for the SN curve and perform fatigue analysis in the traditional way. Obtain stress distribution based on intact pipe properties and updated parameters based on operational history

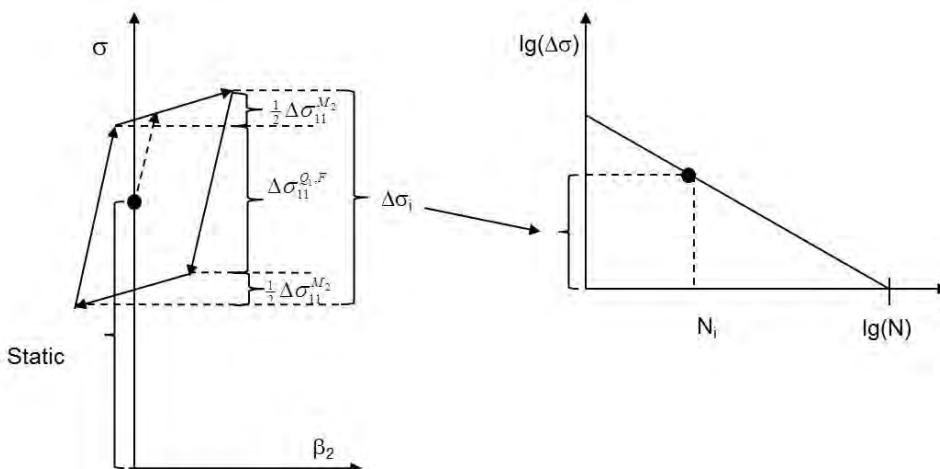


Figure D5.2: Typical stress history and fatigue calculation procedure

- Perform robustness checks using FE analysis to find how many tensile armor wires can fail
- In order to possibly obtain an estimate for the number of wire failures, evaluate:
  - if it is possible to use the numerical model to monitor multiple tensile armor failures before the pressure spiral fails?
  - if sufficient robustness of the riser can be verified by applying elevated pressure?
- If the answer to the two questions above is yes, then establish Stress Concentration Factors (SCFs) for the stress components in the armor wires (due to failure of some tensile armor wires) with respect to Mean stress and Dynamic stress:
  1. Establish FE model
  2. Apply tension and operating internal pressure
  3. Increase pressure to design pressure
  4. Vary the number of tensile wire failures (inner layer) and measure:
    - Rotation per length
    - Stress distribution in tensile and pressure armor
    - Static SCF
  5. Apply dynamic curvature and measure dynamic SCF
- The stress concentration factor (SCF) in this case is defined as the ratio of corresponding mean and dynamic stresses between the analyses of intact and damaged (wire failure) model conditions
- Apply the SCF's in analytical formulas:
  - for longitudinal mean stress:

*un-damaged cross-section:*

$$\sigma_{11} = \frac{Q_1}{A} + \frac{M_2}{W_2} + \frac{M_3}{W_3} = \sigma_{11-Q1} + \sigma_{11-M2} + \sigma_{11-M3}$$

*damaged cross-section:*

$$\sigma_{11}^* = SCF_{11-Q1} \cdot \sigma_{11-Q1} + SCF_{11-M2} \cdot \sigma_{11-M2} + SCF_{11-M3} \cdot \sigma_{11-M3}$$

- for dynamic stress, longitudinal direction:

*damaged cross-section:*

$$\Delta\sigma_{11}^* = \Delta SCF_{11-Q1} \cdot \Delta\sigma_{11-Q1} + \Delta SCF_{11-M2} \cdot \Delta\sigma_{11-M2} + \Delta SCF_{11-M3} \cdot \Delta\sigma_{11-M3}$$

- Perform fatigue analysis with mean and dynamic stress accounting for SCF's along with sensitivity analysis with respect to number of failed wires.

### D5.2.4 FE analysis of North Sea Riser section

The following is a summary of the model applied and the results obtained for a finite element analysis of a section of the North Sea Riser. The general finite element code MARC<sup>®</sup> is used for the analysis.

#### D5.2.4.1 Flexible Pipe Model Data, 6" Pipe

Pipe and model layers are illustrated in Table D5.1. The FE model with applied tension is shown in Figure D5.3

Table D5.1: North Sea Riser structure

No.	Layer description
1	INTERLOCKED CARCASS
2	PVD LAYER
3	PRESSURE ARMOUR
4	SPIRAL
5	POLYAMID ANTI-WEAR TAPE
6	FIRST ARMOUR LAY
7	POLYAMID ANTI-WEAR TAPE
8	SECOND ARMOUR LAY
9	OUTER SHEATH

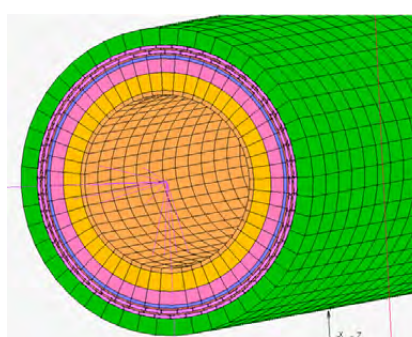
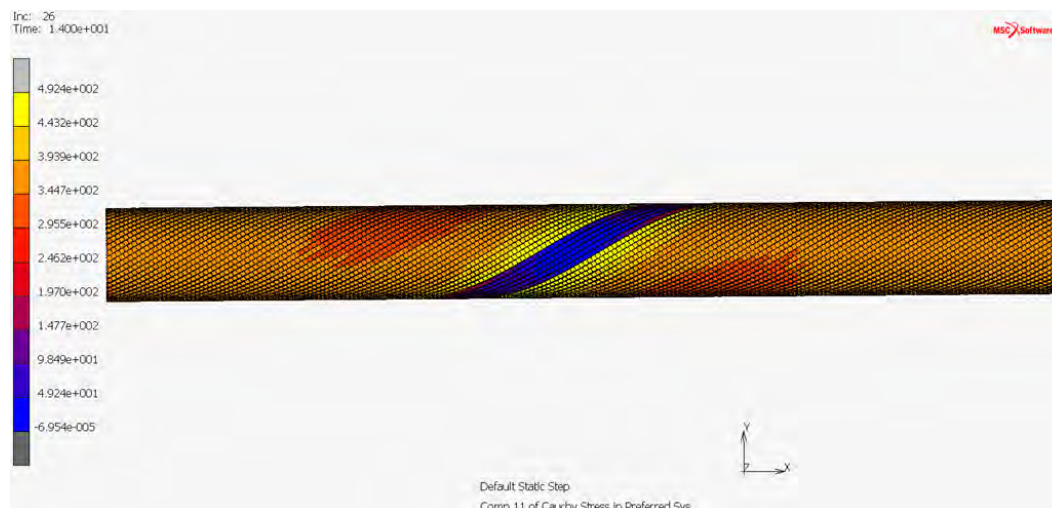



Figure D5.3: FE model for a section of the North Sea Riser

The individual layers shown in Table D5.1 are modelled separately and combined into the final model, Figure D5.3. Layer models are described in the following.

**Carcass model, Figure D5.4:**

- Modeled in a simplified manner using 8-node brick elements, 1 element across the thickness.
- An orthotropic material model was used to give the correct stiffness in the radial, circumferential and longitudinal direction.
- Example: The Young's modulus in the longitudinal direction is set to be a very small value as the axial stiffness of the carcass is negligible

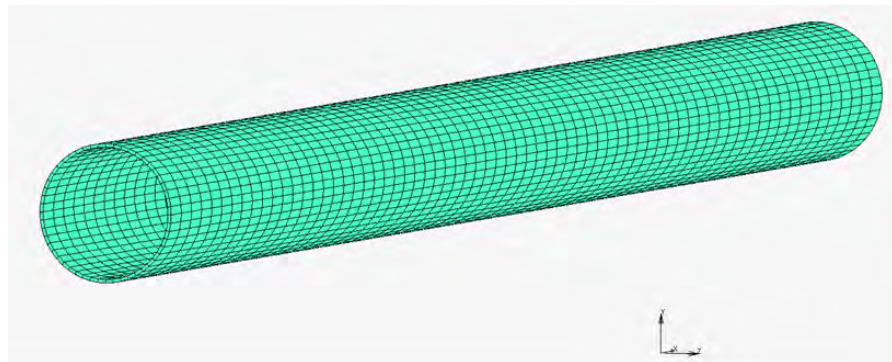


Figure D5.4: Carcass model

**PVD layer model, Figure D5.5:**

- Modeled using 8-node brick elements, 1 element across the thickness.
- The Young's modulus was reduced from 350 MPa to 210 MPa to ensure correct bending stiffness of the pipe

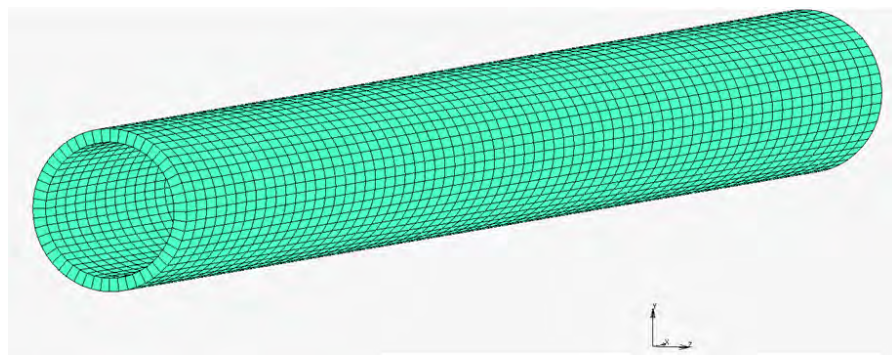


Figure D5.5: PVD layer model

**Pressure armor model, Figure D5.6:**

- Modeled in a simplified manner using 8-node brick elements (1 element across the thickness), but adding a rebar element model in order to obtain the same stiffness properties (w.r.t. local bending of cross-section and pressure) as for the physical pressure armour
- Orthotropic material model with tuned material properties for correct stiffness
- Two types of elements are used in the analysis

- 8 node solid element
- Special element (rebar), only takes membrane forces, located in neutral axis

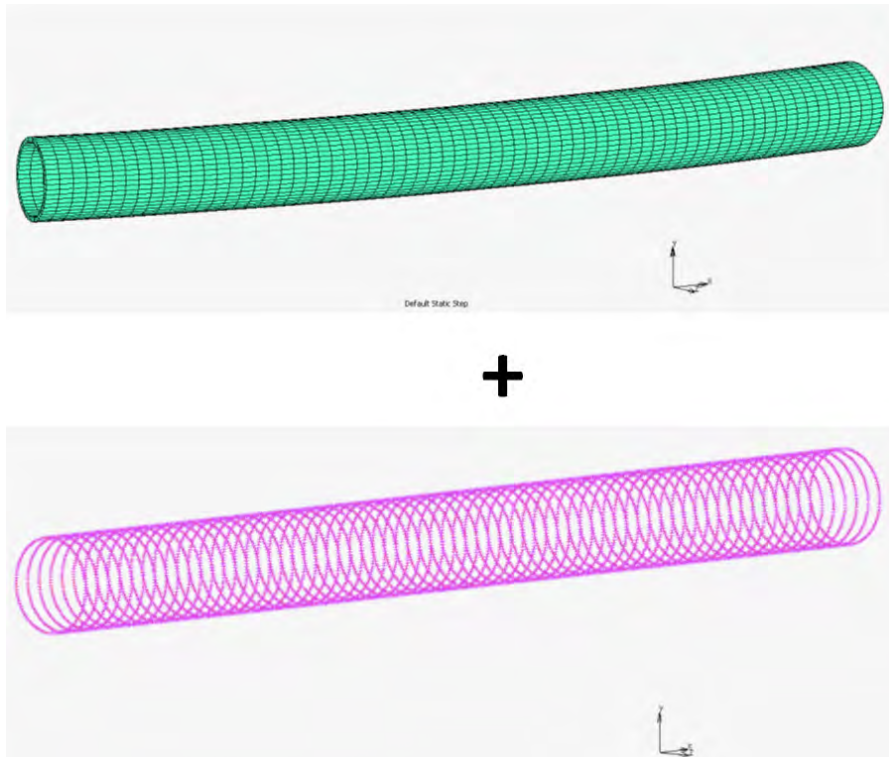


Figure D5.6: Pressure armour model

**Spiral model, Figure D5.7:**

- Modeled in a simplified manner using 8-node brick elements, 1 element across the thickness
- An orthotropic material model was used to give the correct stiffness in the radial, circumferential and longitudinal direction.
- Example: The Young's modulus in the longitudinal direction is set to be a very small value as the axial stiffness of the spiral is negligible

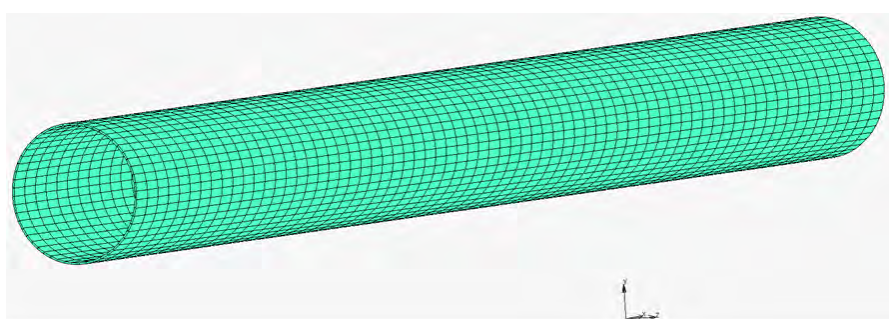


Figure D5.7: Spiral model

**Anti-wear tape model, Figure D5.8:**

- Insignificant structural stiffness contribution
- Included for improved convergence with respect to contact and friction

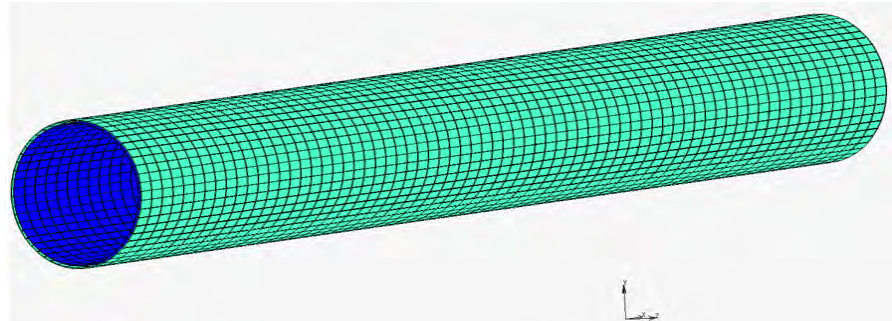


Figure D5.8: Anti-wear tape model

**Tensile armor layers model, Figure D5.9:**

- Rectangular steel wires of dimension 3 mm x 9mm
- Modeled using 8 node solid element
  - one element across the thickness
  - one element in width
- One contact body, including self contact (the deformation of wire may cause contact between different wire locations of the same wire) and friction

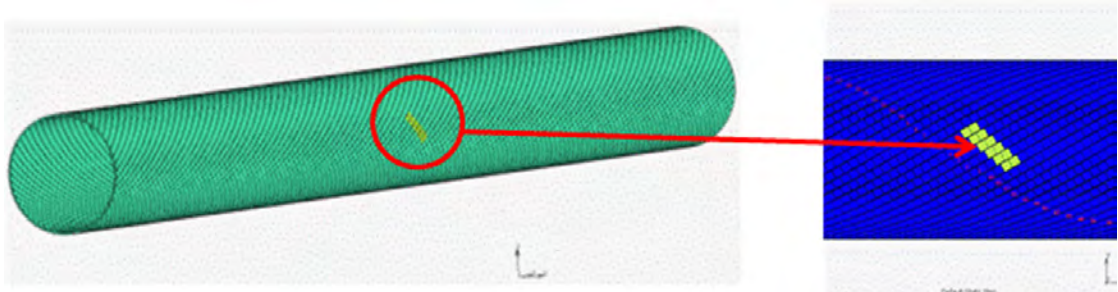
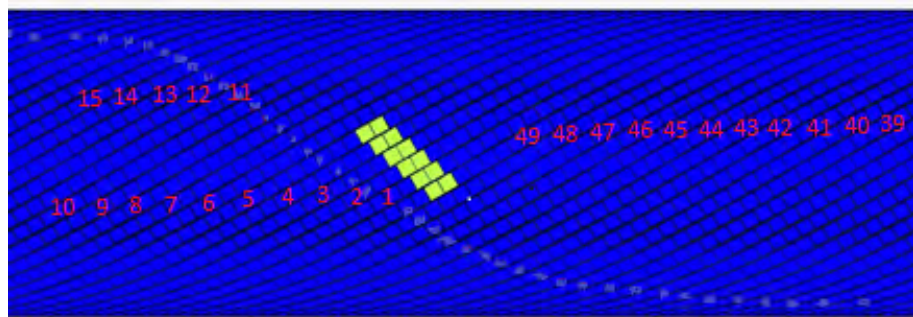
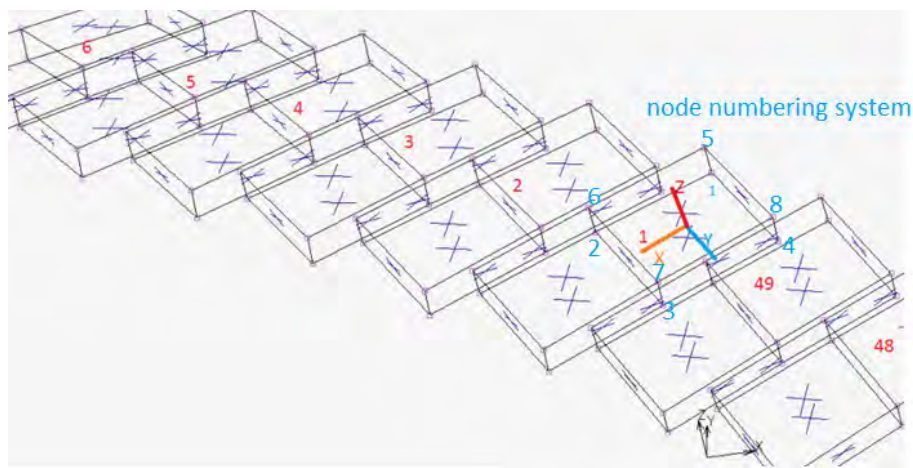


Figure D5.9: Tensile armour layer model. For the inner tensile armour layer: yellow pairs of elements modelled such that separation is obtained for the scenario of broken wires.

Modelling and numbering of the inner tensile armour layer, including the elements for simulating armour failure, are shown in Figure D5.10



(1) Pairs of glued elements for the simulation of wire failures



(2) Model numbering of a selected section of the inner tensile armour layer

Figure D5.10: Numbering and modeling of the first (inner) tensile armour layer

**Outer sheath model, Figure D5.11**

- Modeled using 8-node brick elements
- Isotropic material properties
- The Young's modulus was reduced to 132 MPa to ensure correct bending stiffness of the pipe

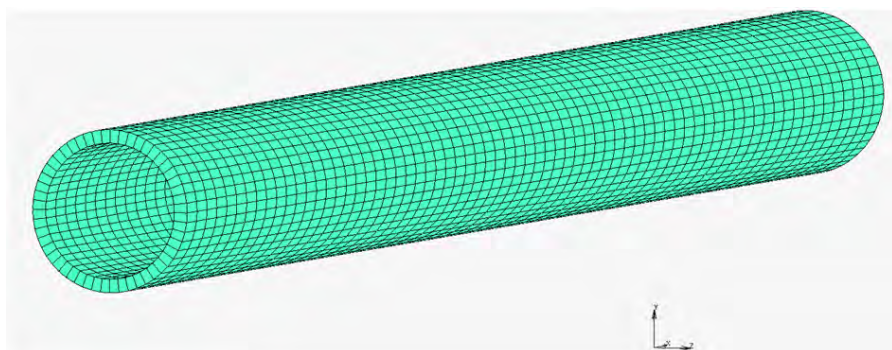


Figure D5.11: Outer sheath model

### Boundary conditions, Figure D5.12

- Boundary conditions applied to each end
  - Constraints assuming plane sections to remaining plane
  - Bending (i.e. enforced rotation) Dynamic curvature ( $\pm 2^\circ$ ) applied, see Figure D5.13.



Figure D5.12: Bending of model  $2^\circ$ (enforced rotation)

#### D5.2.4.2 Load cases

##### Definition of Loads:

- Case A (no bending)
  - Fix all translations and rotations at the ends
  - Step 1: gradually increase tension to design tension
  - Step 2:
    - \* External pressure: increase to 1 MPa
    - \* Internal pressure: increase to operating pressure
    - \* Tension: increase to 375 kN, also accounting for end cap
  - Step 3:
    - \* Internal pressure: increase to design pressure
    - \* Tension: increase to 986 kN, also accounting for end cap
- Case B (bending)
  - Fix all translations and 2 out of 3 rotations at the ends
  - Step 1 and 2 as for Case A
  - Step 3:
    - \* Internal pressure: keep at operating pressure
    - \* Tension: keep tension at 375 kN
    - \* Rotation of ends: gradually apply bending to  $\pm 2^\circ$  at each end while keeping tension constant

##### Model variation to account for wire failures in the inner tension armour layer:

A total of 4 models were analyzed, see also Figure D5.13:

- Model 1: All wires intact (no failures)

- Model 2: 2 broken wires (in the inner tension armour layer)
- Model 3: 4 broken wires (in the inner tension armour layer)
- Model 4: 6 broken wires (in the inner tension armour layer)

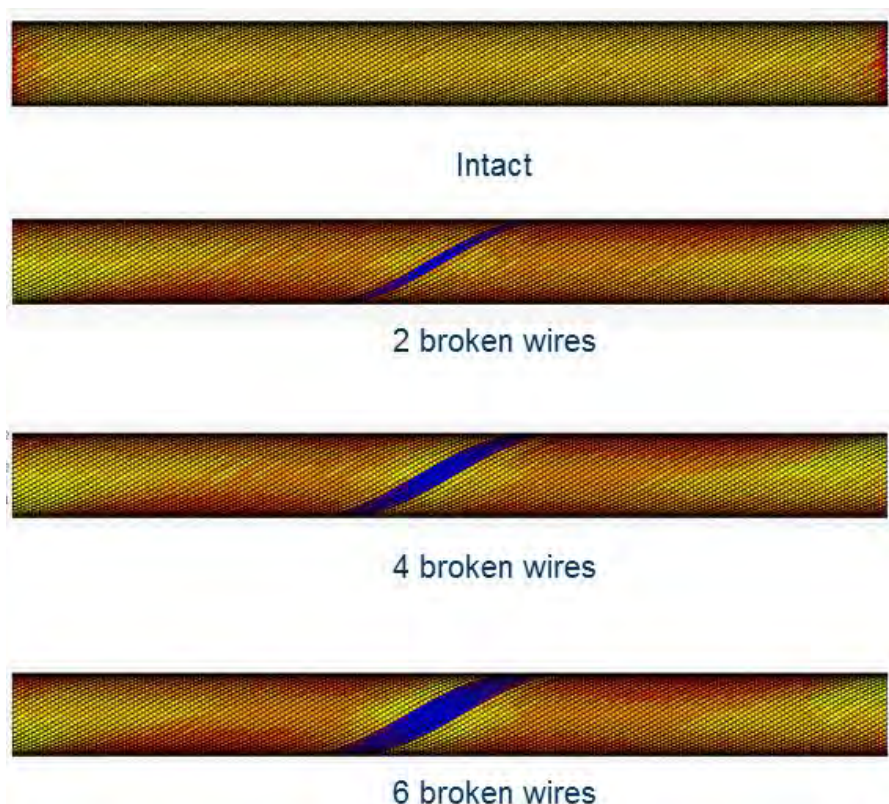


Figure D5.13: FE models applied for the study

### D5.2.5 FE analysis results

#### D5.2.5.1 Response values

6 SCF's are of interest for each model:

- Mean stress:

$$SCF_{11-Q1}, SCF_{11-M2}, SCF_{11-M3}$$

- Dynamic stress:

$$\Delta SCF_{11-Q1}, \Delta SCF_{11-M2}, \Delta SCF_{11-M3}$$

The **mean stress SCF's** were found by comparing analysis results from Model 2, 3 and 4 to Model 1 (intact) for **Case A** (no bending)

The **dynamic SCF's** were found by comparing analysis results from Model 2, 3 and 4 to Model 1 (intact) for **Case B** (bending)

Responses evaluated for both the inner (first) tension armour layer and for the pressure armour layer. The tensile armour layers also represent added resistance for the pressure armour to withstand the internal pressure. A reduction of the tensile armour resistance due to wire failures will influence the resulting stresses in the pressure armour. A quantification of this influence is valuable for the evaluation of a possible failure of the pressure spiral prior to a loss of function of the tensile armour layers.

The notations used for stress in the results are shown in Table D5.2. The definition of stress concentration factor for inner tensile armour wires are described in Table D5.3.

Note: Superscript indexes **t**, **b**, **d** denotes

- **t** *tension*; combined tension and pressure loading
- **b** *bending*; combined tension, pressure and bending
- **d** *damaged*; wire failures in inner tensile armour layer

Table D5.2: Stress notation used, see also Figure D5.1 for definitions.

Condition		Intact		Damaged	
Total longitudinal stress		$\sigma_{11}^t$	$\sigma_{11}^b$	$\sigma_{11}^{t,d}$	$\sigma_{11}^{b,d}$
Stress component	Axial stress	$\sigma_{11-Q1}^t$	$\sigma_{11-Q1}^b$	$\sigma_{11-Q1}^{t,d}$	$\sigma_{11-Q1}^{b,d}$
	Bending stress about y-axis	$\sigma_{11-M2}^t$	$\sigma_{11-M2}^b$	$\sigma_{11-M2}^{t,d}$	$\sigma_{11-M2}^{b,d}$
	Bending stress about z-axis	$\sigma_{11-M3}^t$	$\sigma_{11-M3}^b$	$\sigma_{11-M3}^{t,d}$	$\sigma_{11-M3}^{b,d}$

Table D5.3: The definition of stress concentration factor (SCF) for inner tensile armour wires

Stress	Stress concentration factor (SCF)	
Mean stress	$SCF_{11-Q1}$	$\sigma_{11-Q1}^{t,d} / \sigma_{11-Q1}^t$
Dynamic stress	$\Delta SCF_{11-Q1}$	$(\sigma_{11-Q1}^{b,d} - \sigma_{11-Q1}^{t,d}) / (\sigma_{11-Q1}^b - \sigma_{11-Q1}^t)$
	$\Delta SCF_{11-M2}$	$(\sigma_{11-M2}^{b,d} - \sigma_{11-M2}^{t,d}) / (\sigma_{11-M2}^b - \sigma_{11-M2}^t)$
	$\Delta SCF_{11-M3}$	$(\sigma_{11-M3}^{b,d} - \sigma_{11-M3}^{t,d}) / (\sigma_{11-M3}^b - \sigma_{11-M3}^t)$

### D5.2.5.2 Results Case A; SCF of mean longitudinal stress for inner tensile armour layer

The load case is defined by:

Tension and pressure only (no bending). The resulting SCFs for mean stress are shown in Table D5.4, and response patterns for the 4 different models are shown in Figure D5.14.

Table D5.4: SCFs for inner tensile armour due to wire failures in inner tensile armour layer, applied tension and pressure only.

Model	Response (inner tensile armour layer)		
	$SCF_{11-Q1}$ (mean stress)	$SCF_{11-M2}$	$SCF_{11-M3}$
2 wire failures	1.15		<b>Not relevant (NR),</b> see discussion below
4 wire failures	1.29		
6 wire failures	1.43		

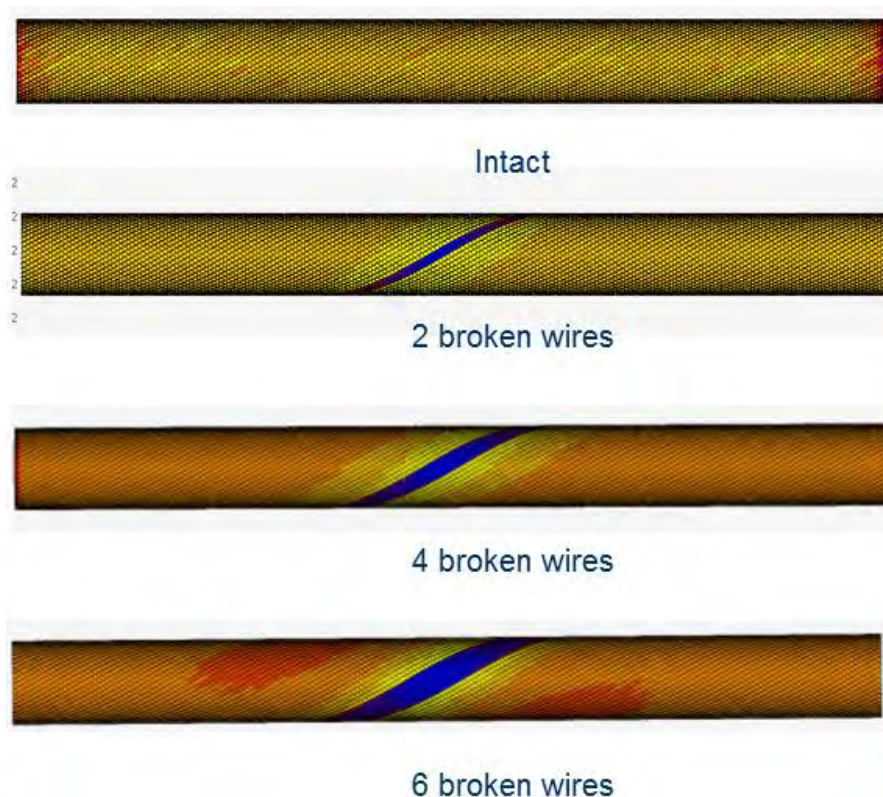


Figure D5.14: Indicated response patterns for the 4 different models during load case A (tension and pressure only)

The axial stresses  $\sigma_{11-Q1}^t$  and the total longitudinal stresses  $\sigma_{11}^t$  ( $\sigma_{11}^t = \sigma_{11-Q1}^t + \sigma_{11-M2}^t + \sigma_{11-M3}^t$ ) in the inner tensile armour layer are shown in Figure D5.15 for the intact model. For this load condition the bending stress  $\sigma_{11-M2}^t$  is insignificant and the bending stress  $\sigma_{11-M3}^t$  is zero.

The corresponding stresses  $\sigma_{11-Q1}^{t,d}$  and  $\sigma_{11}^{t,d}$  ( $\sigma_{11}^{t,d} = \sigma_{11-Q1}^{t,d} + \sigma_{11-M2}^{t,d} + \sigma_{11-M3}^{t,d}$ ) for the damaged condition with six broken tensile wires are shown in Figure D5.16. The maximum value of  $\sigma_{11-Q1}^{t,d}$  and  $\sigma_{11}^{t,d}$  is about 188.5MPa and 193.9 MPa, as indicated by Figure D5.16.

There is only a small difference in the maximum values, which means that the stress component  $\sigma_{11-M2}^{t,d}$  and  $\sigma_{11-M3}^{t,d}$  from introduced bending moments due to wire failure, is small and insignificant for this load condition. The dominant effect of wire failures on the mean stress is seen for the axial stress  $\sigma_{11-Q1}^{t,d}$ . The SCFs for  $\sigma_{11-M2}^t$  and  $\sigma_{11-M3}^t$  are then considered irrelevant.

The ratio of axial stress between  $\sigma_{11-Q1}^{t,d}$  (damaged condition) and  $\sigma_{11-Q1}^t$  (intact condition), are presented in Figure D5.17 - Figure D5.19. In Figure D5.17 the axial stress ratio is shown for the broken wires only, and in Figure D5.18 and Figure D5.19 the ratio is shown for the ten wires adjacent on either side of the broken wires. A reduction in SCF from 1.43 to 1.03 is noticed for the wire furthest away (wire no.15 and 39) from the broken tensile wires.

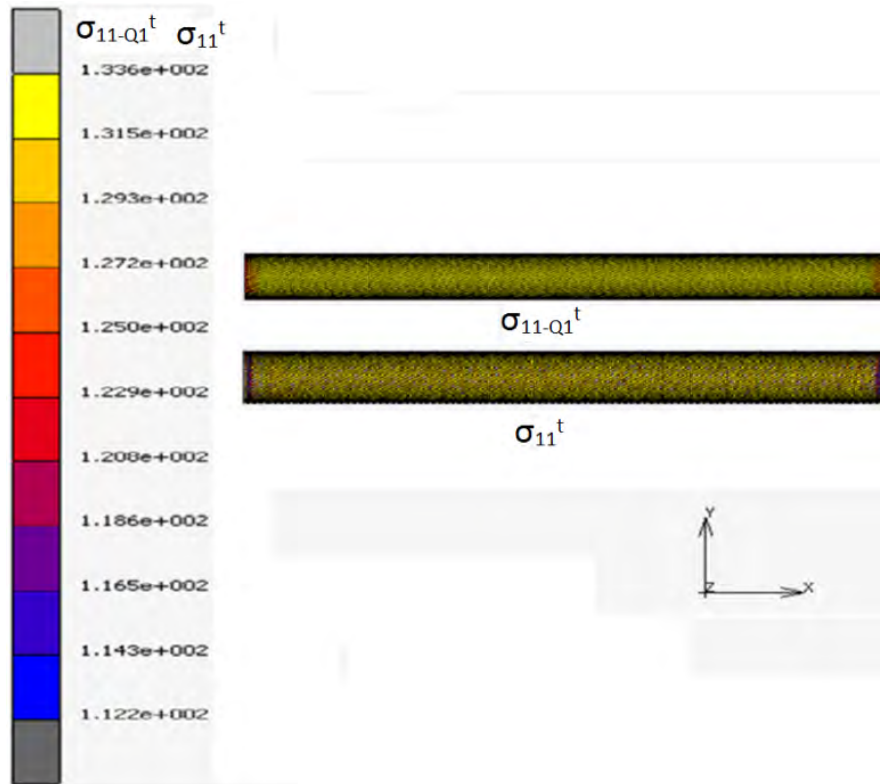


Figure D5.15: Axial stress  $\sigma_{11-Q1}^t$  and total longitudinal stress  $\sigma_{11}^t$  in inner tensile armour layer (intact condition)

The SCF for the longitudinal axial stress  $\sigma_{11-Q1}$  for the inner tensile armor wires is presented in Figure D5.20 and Table D5.4. The analysis results show that the SCF increase linearly with increasing number of failed wires, see Figure D5.20. A SCF of 1.36 is noticed for five broken inner tensile armour wires.

[De Sousa et al., 2011] performed a test of a 6" riser to measure strain concentration factors between damaged (five tensile armour wires broken in outer layer) and intact condition under pure tension load. Strain concentration factors of 1.64 and 1.32 were found for the outer and inner tensile wires, respectively. The broken inner tensile armour wires are still constrained by the outer tensile armour wires. It is then reasonable that the SCF is smaller for the broken inner tensile wire layer than for the layer outside. A good correspondence is seen between the results from De Sousa and the results obtained in the North Sea riser analysis.

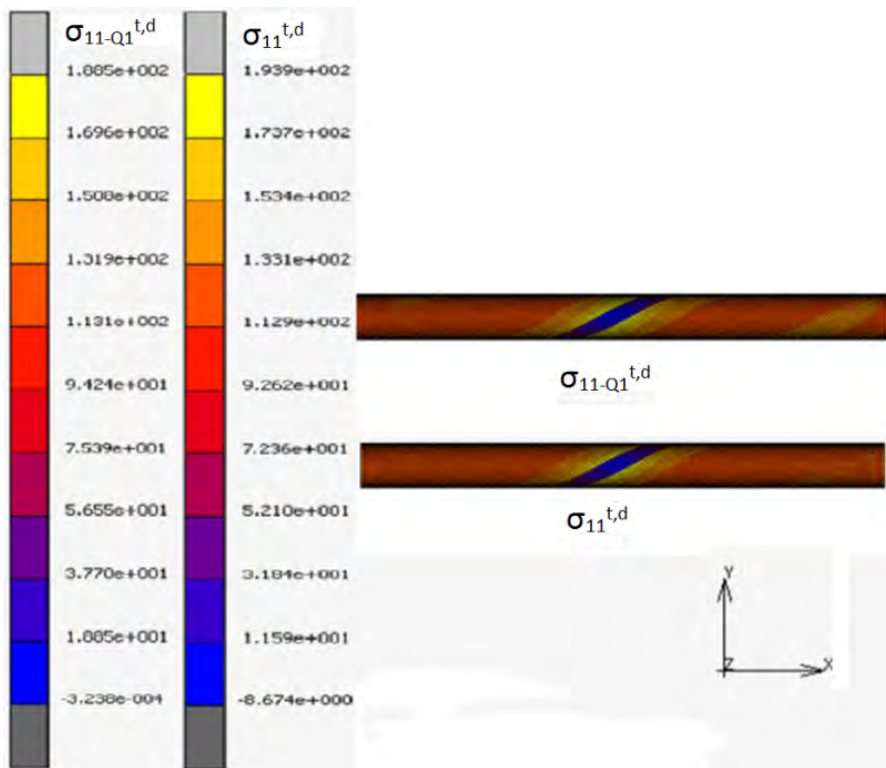


Figure D5.16: Axial stress  $\sigma_{11-Q_1}^{t,d}$  and total longitudinal stress  $\sigma_{11}^{t,d}$  in the inner tensile armor layer (damaged condition, 6 broken wires)

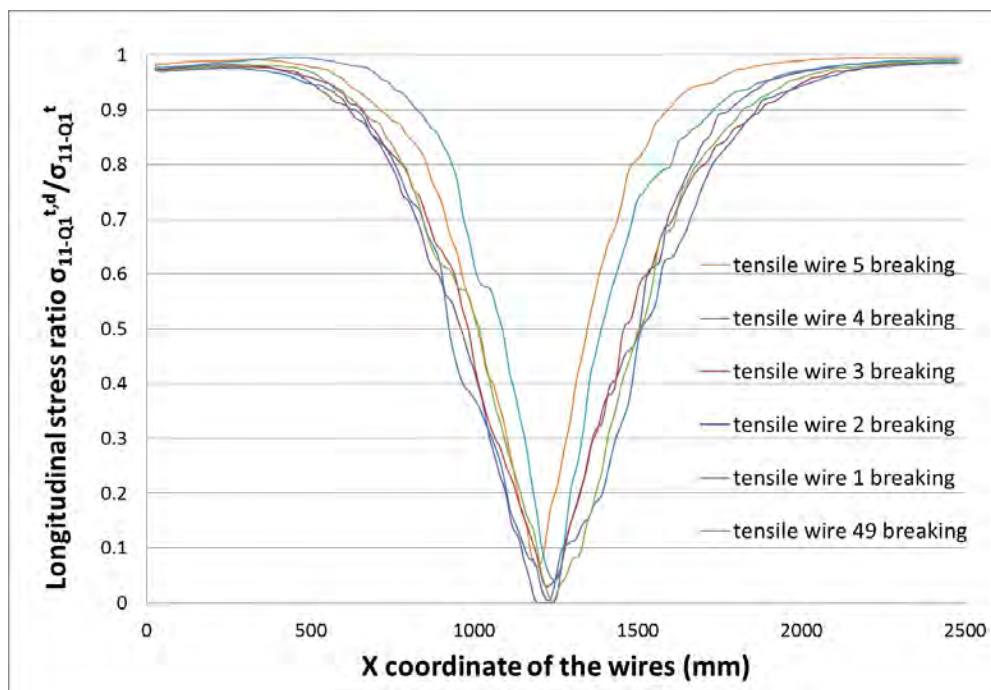


Figure D5.17: Axial stress ratio  $\sigma_{11-Q_1}^{t,d} / \sigma_{11-Q_1}^t$  for 6 broken wires in the inner tensile armour layer.

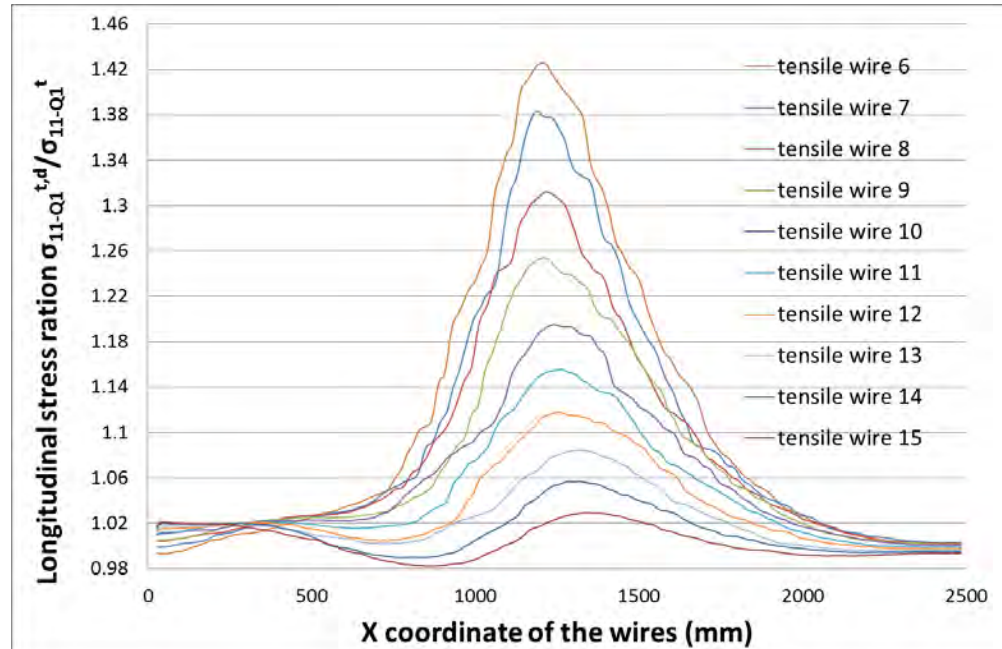


Figure D5.18: Axial stress ratio  $\sigma_{11-Q1}^{t,d} / \sigma_{11-Q1}^t$  in wire number 6 to 15

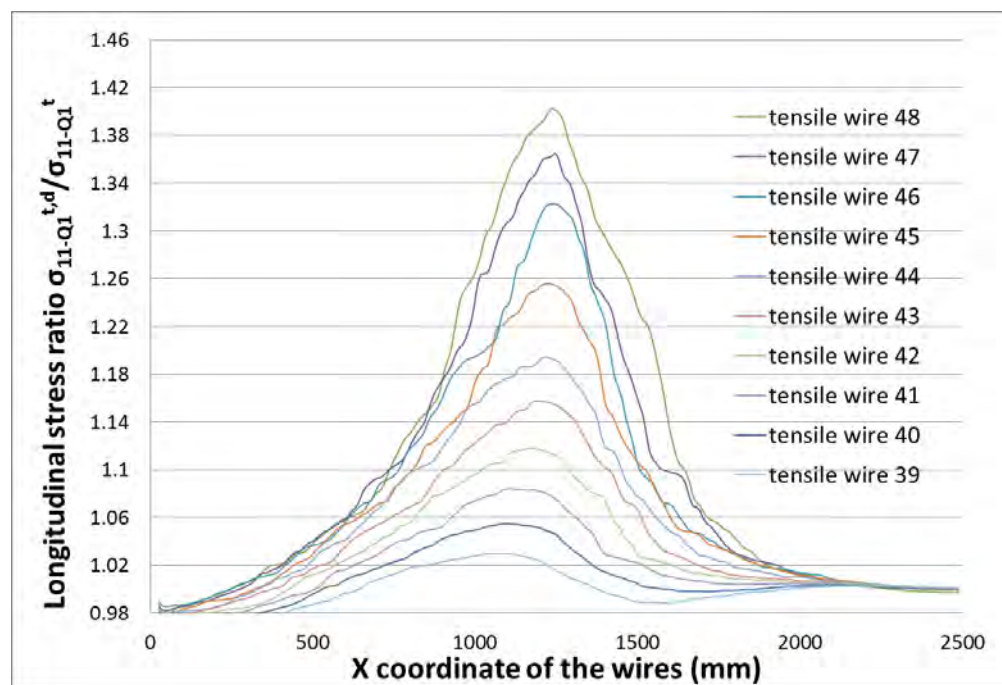


Figure D5.19: Axial stress ratio  $\sigma_{11-Q1}^{t,d} / \sigma_{11-Q1}^t$  in wire number 39 to 48.

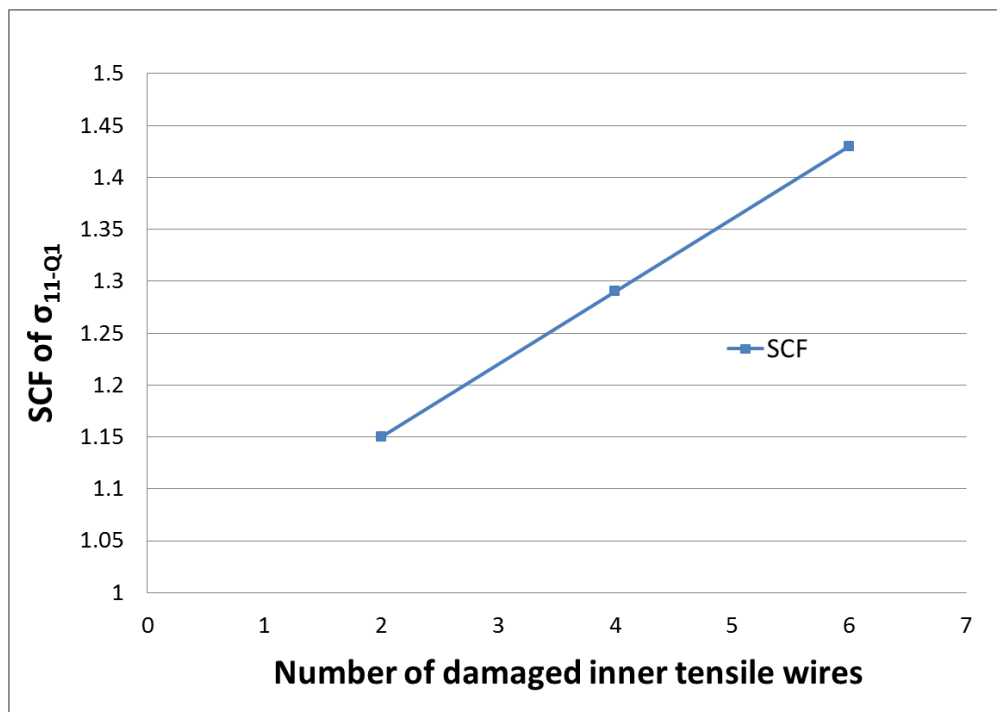


Figure D5.20: SCF for  $\sigma_{11-Q1}$  with 2, 4 and 6 broken inner tensile armour wires

### D5.2.5.3 Results Case B (bending); SCF of dynamic stress for inner tensile armor layer

The load case is defined by: Tension and pressure applied, followed by bending.

The SCF of dynamic stress for the inner tensile armour wire is presented in Table D5.4, and response patterns for the 4 different models are shown in Figure D5.23

The longitudinal axial stresses  $\sigma_{11-Q1}^b$  and the total longitudinal stress  $\sigma_{11}^b$  in the inner tensile armor layer for the intact condition with combined tension, pressure and bending loads are shown in Figure D5.22. The stresses  $\sigma_{11-Q1}^{b,d}$  and  $\sigma_{11}^{b,d}$  for the damaged condition with six broken tensile wires are shown in Figure D5.23

Table D5.5: SCFs for inner tensile armour layer under applied tension, pressure and bending and due to 2, 4 and 6 wire failures in the inner tensile armour layer.

Model	Response (inner tensile armour layer)		
	$\Delta SCF_{11-Q1}$ (mean stress)	$\Delta SCF_{11-M2}$	$\Delta SCF_{11-M3}$
2 wire failures	1.12	<b>Not relevant (NR),</b> see discussion below	
4 wire failures	1.18		
6 wire failures	1.20		

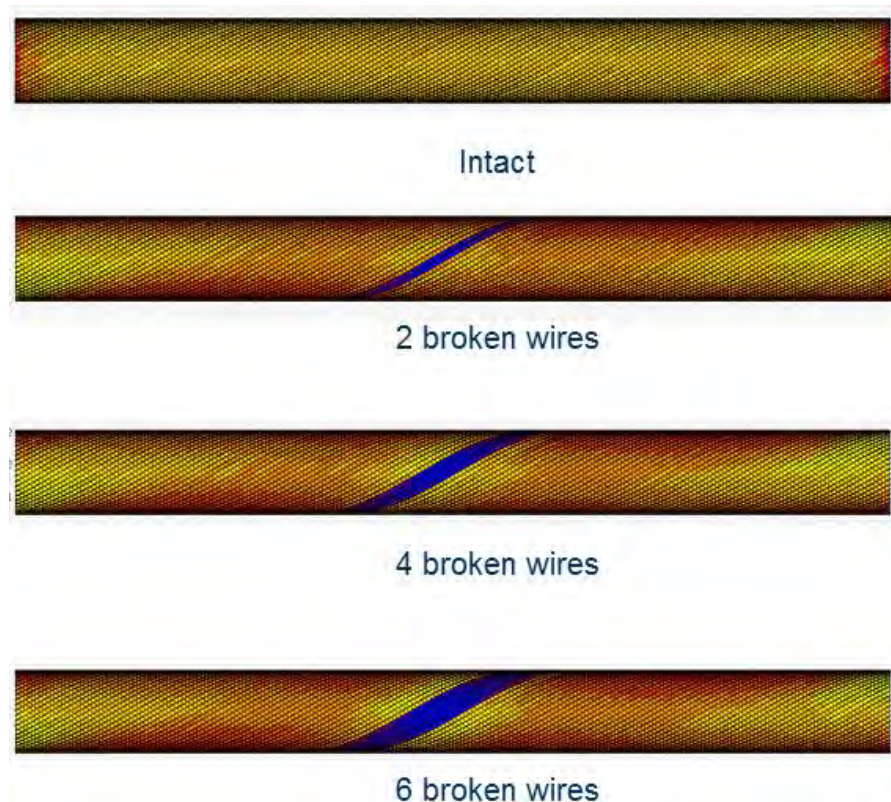


Figure D5.21: Indicated response patterns for the 4 different models during load case B (tension, pressure and bending)

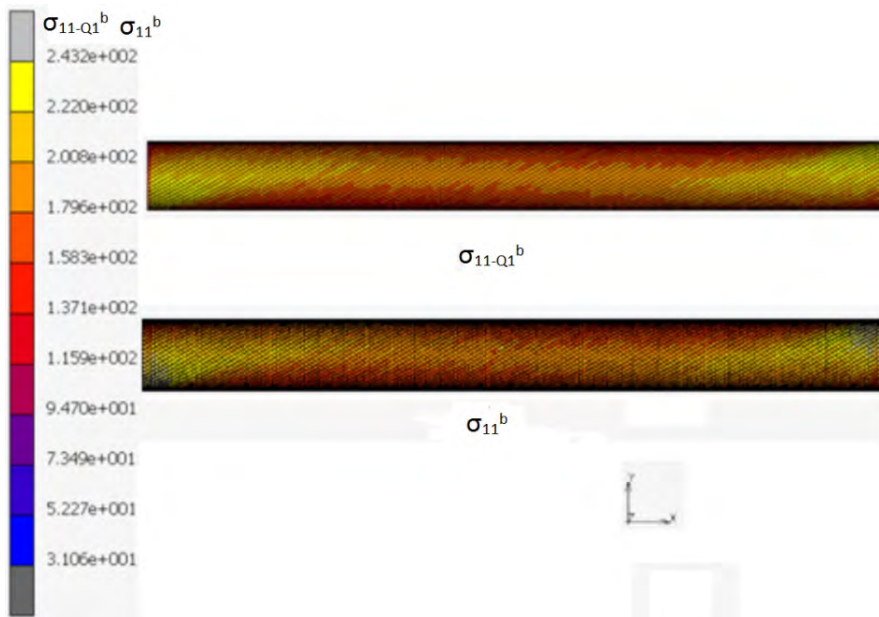


Figure D5.22: Axial stress in the inner tensile armour layer (intact condition)

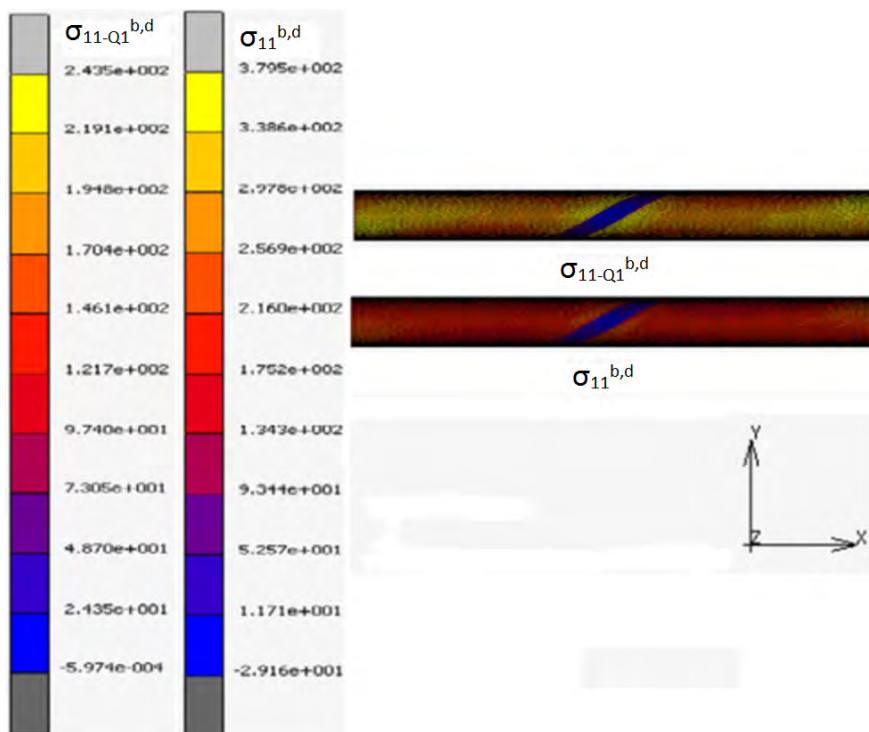


Figure D5.23: Axial stress in the inner tensile armour layer (damaged condition; 6 broken wires)

The effect of bending on the longitudinal axial stress  $\sigma_{11-Q1}$  along tensile wire no.48 and 47 is shown in Figure D5.24 for the intact and damaged conditions with 6 broken wires. Wire no.49 has failed along with the five adjacent ones (wires no.1-5), see Figure D5.10. It is observed (dotted lines) that the increase in longitudinal axial stress ( $\sigma_{11-Q1}^{b,d} - \sigma_{11-Q1}^{t,d}$ ) for wire no.48 (next to the damages wires) in damaged condition is less than the increase

in longitudinal axial stress ( $\sigma_{11-Q1}^b - \sigma_{11-Q1}^t$ ) in intact condition. At the same time for wire no.47 there is a larger increase in axial stress for the damaged condition than for the intact condition. The SCF is calculated at the location with the maximum longitudinal axial stress  $\sigma_{11-Q1}^{b,d}$  for the damaged condition.

The maximum bending stress about local  $X_2$  axis occurs at 12 o'clock location when the global bending moment is applied about Y axis (see Figure D5.25). The 12 o'clock location is approximately the location where the wires failed. The concentration factor about the  $X_2$  axis ( $\Delta SCF_{11-M2}$ ) is evaluated at this location. Due to the small wire thickness and the 30.0° lay angle of the inner tensile armour wire, the increase of the stress component induced by the bending about  $X_2$  axis ( $\sigma_{11-M2}^{b,d} - \sigma_{11-M2}^{t,d}$  and  $\sigma_{11-M2}^b - \sigma_{11-M2}^t$ ) at this location is in the range of 2-3 MPa. The contribution to the increase of longitudinal stress range for the fatigue analysis is insignificant and  $\Delta SCF_{11-M2}$  is then neglected (not relevant) for the current case.

The minimum bending stress about local  $X_3$  axis occurs at 12 o'clock location when the global bending moment is applied about Y axis (see Figure D5.25). The contribution to the increase of longitudinal stress range for the fatigue analysis is insignificant and  $\Delta SCF_{11-M3}$  is thus not relevant for the current case.

#### D5.2.5.4 Results; SCF of mean circumferential stress of pressure armor

The circumferential stresses in the spiral layer for intact and damaged condition with combined tension and pressure loads are shown in Figure D5.26. The SCF of mean circumferential stress for pressure armor layer is presented in Table D5.6.

For the pressure armor layer, cylindrical coordinates are adopted in the analysis. SCF of circumferential stress are evaluated by comparing between corresponding analysis steps of the damaged and the intact conditions.

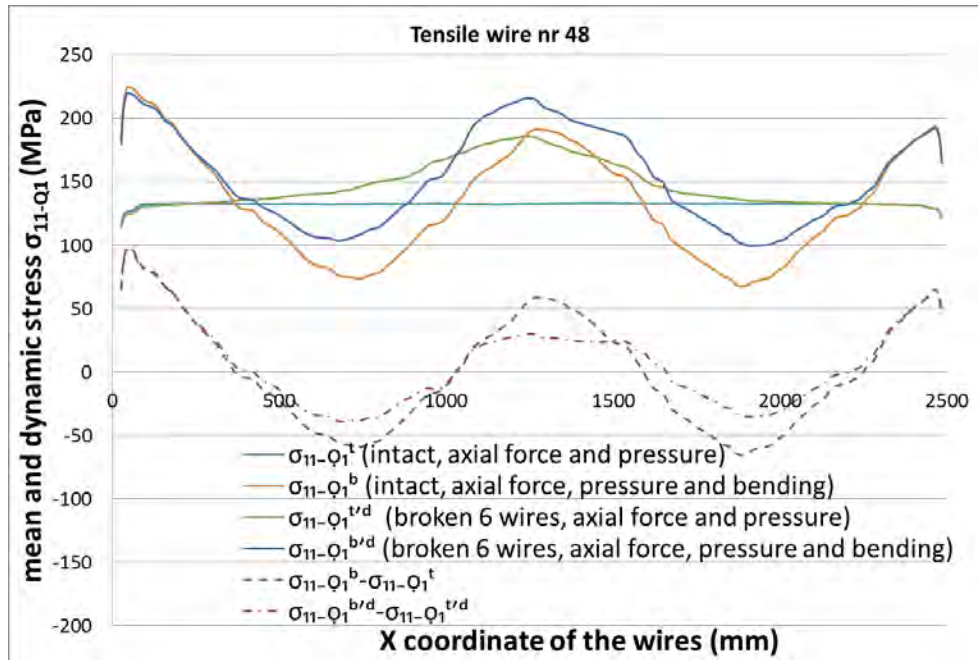
Bending responses in pressure armour are 'not applicable' (NA) due to using an orthotropic material model which is not suitable for describing the stress concentrations sufficiently.

Table D5.6: SCF of pressure armor layer

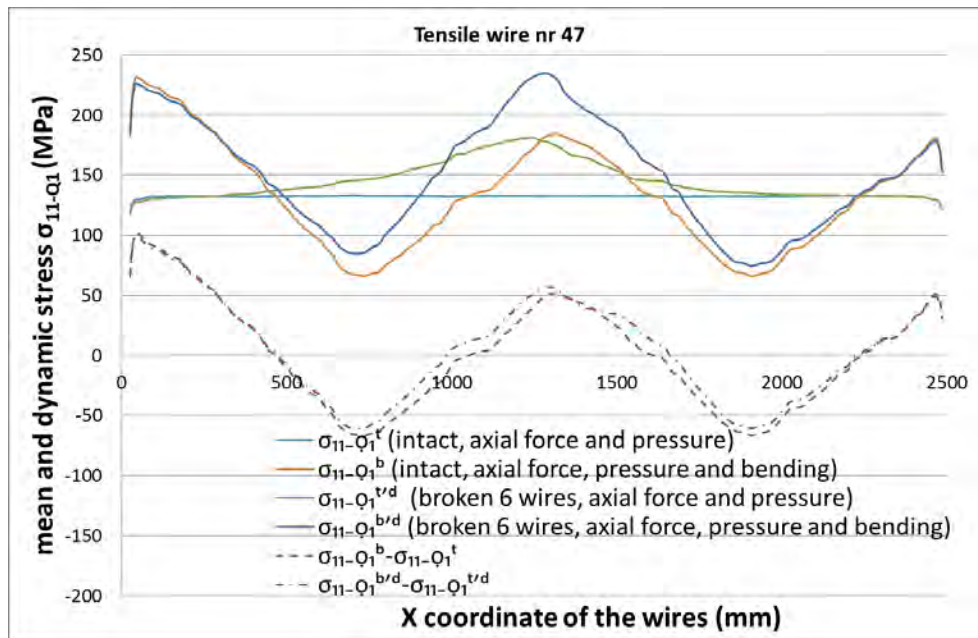
Model	SCF of mean circumferential stress
2 broken wires	1.05
4 broken wires	1.10
6 broken wires	1.13

#### D5.2.5.5 Influence of broken inner tensile wire on the curvature of the riser

The curvatures along the length of the riser model under bending load of  $\pm 2^\circ$  at each end for intact and damaged conditions are shown in Figure D5.27. The curvature will increase slightly when the number of broken inner tensile wires is increasing. The curvature increases from 0.02595 to 0.02631 when the 6 inner tensile wires are broken.



(1) Tensile wire nr. 48



(2) Tensile wire nr. 47

Figure D5.24: The axial stress  $\sigma_{11-Q_1}$  and the increase of the axial stress  $\Delta\sigma_{11-Q_1}$  in inner tensile armour layer due to bending (6 broken wires)

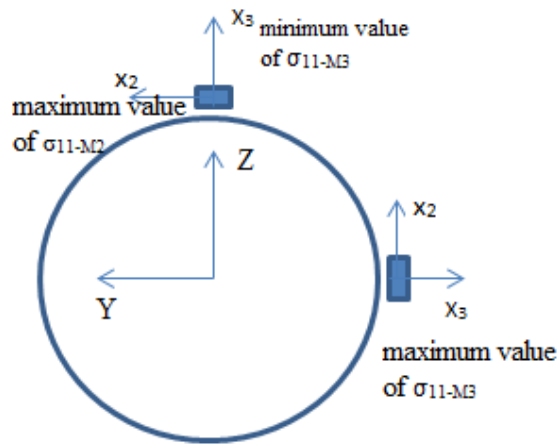


Figure D5.25: The circumferential stress at spiral layer.

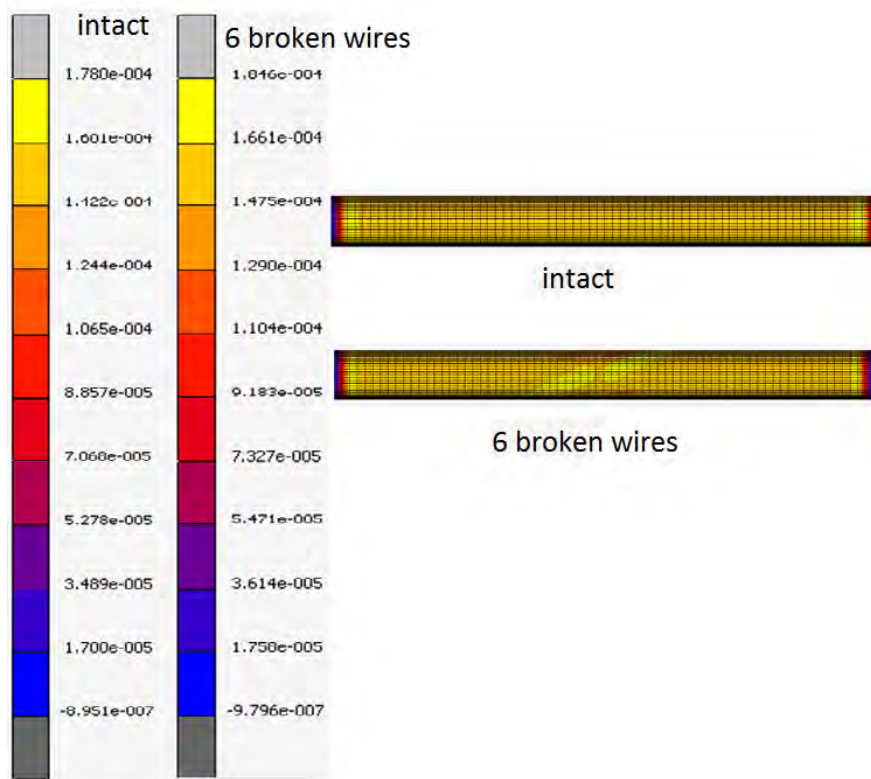


Figure D5.26: The circumferential stress at spiral layer.

#### D5.2.5.6 Summary of results from FE analysis of North Sea riser section

A summary table of the obtained stress concentration factor between a damaged 6" riser cross-section by a selected number of armour wire failures and an intact cross-section is shown in Table D5.7.

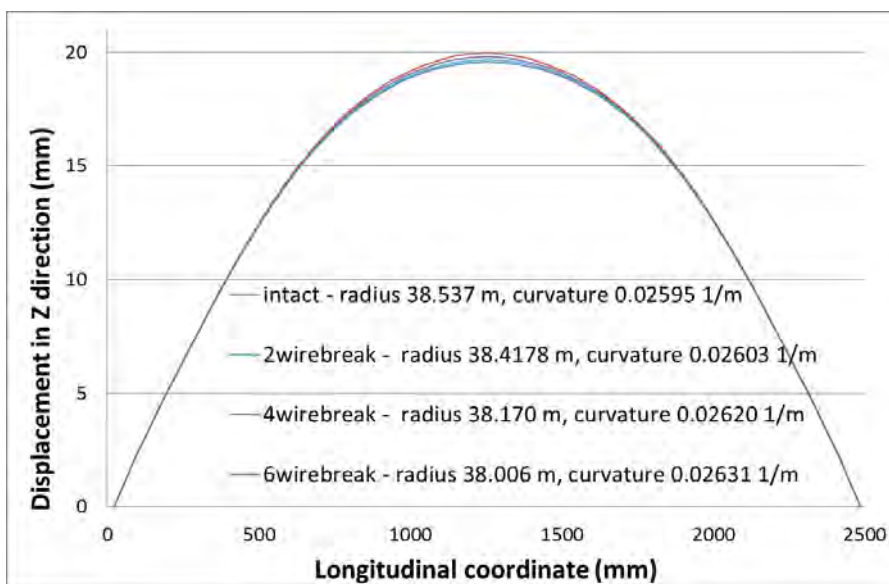


Figure D5.27: The curvature of riser under bending load of  $\pm 2^\circ$  at each end.

Table D5.7: Summary of results from FE analysis of North Sea riser Case Study

No. of wire failures in Tensile 1 layer	Response layer	$SCF_{11-Q1}$	$SCF_{11-M2}$	$SCF_{11-M3}$	$\Delta SCF_{11-Q1}$	$\Delta SCF_{11-M2}$	$\Delta SCF_{11-M3}$
2	Tensile 1	1.15	NR	NR	1.12	NR	NR
	Pressure	1.05	NA	NA	NA	NA	NA
4	Tensile 1	1.29	NR	NR	1.18	NR	NR
	Pressure	1.10	NA	NA	NA	NA	NA
6	Tensile 1	1.43	NR	NR	1.20	NR	NR
	Pressure	1.13	NA	NA	NA	NA	NA

NR - not relevant due to small values

NA - not applicable for the pressure armour layer due to the material modelling

**Discussion of results:****Stress increase by 6 failed wires; effect on fatigue life:**

## a) Mean stress:

An increase in mean stress by a factor (SCF) of 1.43 will affect (increase) the stress range applied for the fatigue calculation according to the mean stress correction predicted by Goodman or Gerber.

As an example, assuming:

$$\sigma_m = 300 \text{ MPa} \text{ assumed mean stress level}$$

$$\sigma_u = 1200 \text{ MPa} \text{ assumed ultimate stress}$$

$$\Delta\sigma_0 = \text{constant} = \text{stress range at zero mean stress}$$

$$\Delta\sigma = \text{increase in stress range}$$

$$\text{Goodman: } \Delta\sigma = \frac{(\Delta\sigma_0)}{\left(1 - \left(\frac{(\sigma_m \cdot SCF)}{\sigma_u}\right)\right)}$$

$$\text{For intact condition (SCF} = 1) : \Delta\sigma = 1.33 \cdot \Delta\sigma_0$$

$$\text{For damaged condition (6 failed wires, SCF} = 1.43) : \Delta\sigma = 1.56 \cdot \Delta\sigma_0$$

$$\text{Increase in stress range: } \Delta\sigma_{SCF} = 1.56/1.33 = 1.17$$

An increase in stress range will (as an estimate) reduce the fatigue life by a factor of:

$$(\Delta\sigma_{SCF})^3 = (1.17)^3 = 1.6$$

## b) Dynamic stress:

$$\text{An increase in dynamic stress (stress range) by a factor (SCF) of 1.2}$$

An increase in stress range will (as an estimate) reduce the fatigue life by a factor of:

$$(SCF)^3 = (1.2)^3 = 1.73$$

$$\text{Estimated total factor of fatigue life reduction: } 1.6 \cdot 1.73 = 2.76$$

**Hole in the outer seal scenario:**

A common cause for corrosion damage of tensile armour wires is a penetration of the outer seal allowing seawater to fill the annulus. Normally the outer tensile armour layer will be damaged first. Based on this scenario a numerical model with failures in the outer tensile armour layer will be more realistic.

**Numerical analysis and selection of wire failure in the inner tensile armour layer:**

By selecting wire failures to occur in the inner tensile armour layer, the influence on the pressure armour layer inside may be studied. The inner tensile armour layer offer support to the pressure armour layer. Failures in inner tensile wires reduces the support to the pressure armour and more load needs to be carried by the pressure armour. This increases the stresses in these wires, which eventually may cause failure of the pressure armour layer.

The outer tension armour layer offers support to the inner layer and will thus limit the increase in stress in the inner layer for increasing number of wire failures.

## D5.3 Lateral buckling analysis of flexible riser tensile armour wire

### D5.3.1 Background

During deep water flexible pipe installation, the pipe is normally free hanging from the installation vessel to the seabed in empty condition. This will introduce large hydrostatic forces to the pipe causing true wall compression. In addition, the pipe will be exposed to cyclic bending caused by waves and vessel motion. The combination of true wall axial compression and cyclic bending may lead to tensile armor instability in both lateral and radial directions. If the anti-buckling tape is assumed to be strong enough, the inner tensile armor will lose its lateral stability first due to the gap that may occur between the inner tensile armor and the pipe core, hence restricting the available friction restraint forces. These may further be reduced by cyclic motions that act to create slip between the layers, hence introducing lateral buckling of the tensile armor, with associated severe global torsion deformation of the pipe, ultimately causing the pipe to lose its integrity.

The anti-buckling tape is designed to prevent the radial buckling behavior, however, its effect on lateral buckling has not yet been documented in available literature. In the following, the effect of the winding direction of the anti-buckling tape on the twist of the cross section is studied, including comparisons with available test data from literature.

### D5.3.2 Introduction

The tensile armor is a key strength component of flexible pipes providing resistance to pressure, gravity loads and cyclic bending caused by environmental loads. It normally consists of an even number of layers which are cross wound by a number of flat rectangular wires with a lay angle of 30 to 55 degrees. For deep water applications, the coupled effect from cyclic bending and external pressure may lead to lateral and radial instability of tensile armors during pipe installation and operation.

Any failure of the tensile armor wires may cause loss of pipe integrity and such failures are therefore not permitted by design standards. Ultimate and fatigue strength have been extensively studied in recent years, while quite little effort has been devoted to address the mechanism of the lateral and radial buckling of the tensile armor wires. Figure D5.28 and Figure D5.29 illustrates two types of tensile armor instability scenarios: the radial buckling and lateral buckling. It can be seen that the integrity of the flexible pipe may be completely destroyed once these failure modes occur.

The anti-buckling tape is usually used to prevent radial instability of the tensile armor, however it will also influence the lateral buckling process. Lateral buckling was first introduced and described by [Braga and Kaleff, ] based on experimental results. Further experiments to study the lateral buckling behavior were carried out by Secher, Bectare and Felix-Henry [Secher et al., 2011], studying flexible pipe behavior at 3000m water depth, however, details were not given.

Lateral buckling under net annulus condition due to the cyclic bending was studied by Østergaard, Lyckegaard and Andreasen [Østergaard, 2012b]. The work included both experimental tests and formulation of a theoretical model under the assumption of no friction

[Østergaard et al., 2011], [Østergaard, 2012a] and [Østergaard et al., 2012]. The experiments were carried out in 2012 for three risers with different size and material under same load conditions and is used as a benchmark in the work reported here [Østergaard, 2012a].

An analytical model for evaluating the tensile armour buckling capacity was presented in [Sævik and Ji, 2014] based on formulating the linearized differential equation describing the transverse stability of a thin curved wire under no friction. This was followed by a numerical study based on FE analyses to evaluate the extra capacity from friction during cyclic bending behavior, applying first yield of the wires as failure criteria. The results were then compared to the test data by Østergaard, and a design criteria for transverse tensile armour buckling proposed. Excellent correlation with test data was found with respect to failure / no failure. However, the study did not include the effect of the anti-buckling tape in terms of torque coupling. In the present work, which is partly based on [Zhou et al., 2015], both the tape torque and friction effects are included, yielding slightly more conservative results than obtained in [Sævik and Ji, 2014].



Figure D5.28: Radial buckling failure mode



Figure D5.29: Lateral buckling failure mode

### D5.3.3 Theoretical background

#### D5.3.3.1 Theoretical model

The axial stress from axisymmetric loads, including tension, torsion, internal and external pressure loads, is the primary stress component in the tensile armor. In addition secondary stresses will occur due to local bending and friction due to bending.

The basis for the modelling applied here was partly presented by Sævik and Thorsen [Sævik et al., 2012] including tensile armor and core contact elements (HSHEAR353 and HCONT453). However, since then two more elements have been developed for application in the present study, [Sævik, 2015], revised as per 2015 and [Zhou et al., 2015]. These are:

- The HSHEAR363 element that enables to model the tape, pressure spiral and sheath layers
- The HCONT463 element that enables to model contact between the tensile armor and the tape, sheath and pressure spiral layers.

HSHEAR363 is a 13 degree of freedom (DOF) beam element which includes the standard 12 beam DOF's plus one extra to capture radial motion, see Figure D5.30. The element applies thin shell theory for the sheath, whereas the longitudinal helix strain is used for the armor wire. In both cases, the strain is expressed in terms of the radial DOF and the beam axial strain and torsion quantities. It is noted that this represents a simplification that excludes considering the full 3D stress state (neglecting stress in the thickness direction), however, this is justified by axial membrane action being the primary variable in this case.

The HCONT463 element describes contact and friction between a supporting cylindrical layer and the tensile armor as shown in Figure D5.31.

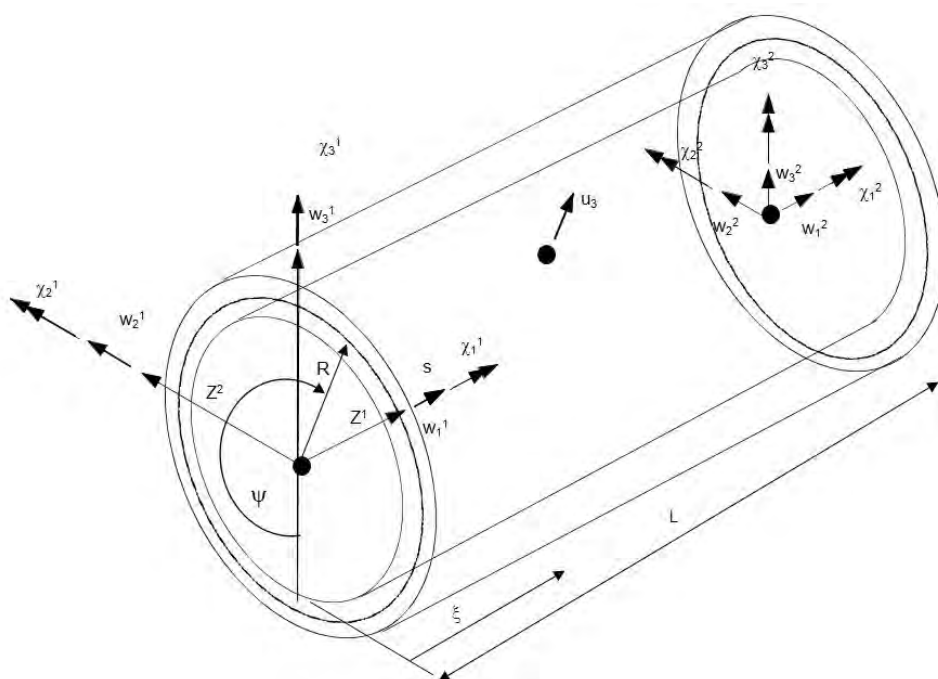


Figure D5.30: HSHEAR363 ELEMENT

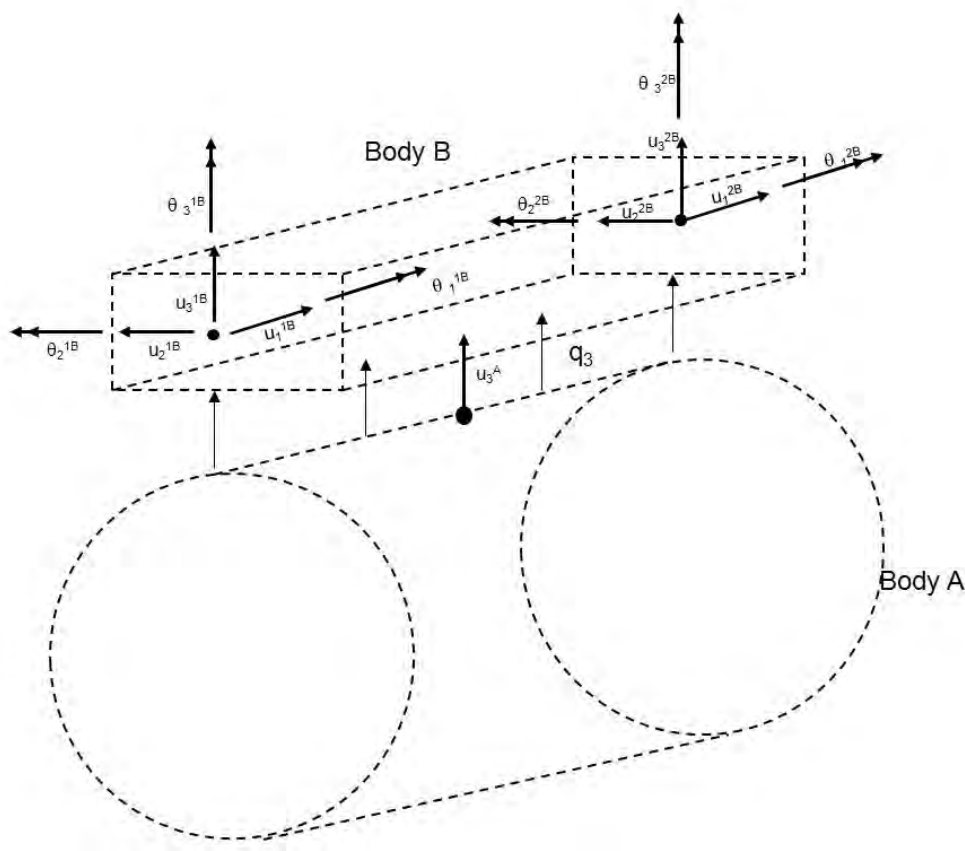


Figure D5.31: HCONT463 ELEMENT

### D5.3.3.2 Failure Mechanism

The process of lateral buckling is initiated from the end cap force, where the two tensile layers will be squeezed against the anti-buckling tape. Under wet annulus conditions, as assumed here, a gap will develop between the inner tensile armor layer and the pressure armor. By assuming that the anti-buckling tape is strong enough, the tensile layer will only be able to slide in the lateral direction. The inner tensile armor layer will have the smallest friction resistance and begin to lose its capacity first. In order to keep the torsion balance in the cross-section, a loss in axial compression is necessary for the outer layer, associated with pipe twist in its helix direction.

Then the pipe will rotate and follow the lay angle direction of the outer tensile layer. If the pipe is exposed to cyclic bending, a certain rotation will take place during each cycle until the torsion failure of the cross-section is reached.

The mechanism can be understood by looking at the expected buckling behaviour of each wire. Considering the tensile wire restrained by friction, bent to a certain curvature and then exposed to a gradually increasing axial load, the expected force displacement characteristic is visualised in Figure D5.32. The capacity is limited by the asymptotes of the Euler buckling force,  $P_E$ , and the yield force,  $\sigma_y A$ . Due to the restraint from friction, the capacity is larger than the theoretical Euler buckling load even if the imperfection introduced by curvature is large, leading to snap buckling. However, when exposed to cyclic curvature, every cycle will lead to a reduction of the lateral transverse friction resistance, thus reducing the lateral

buckling capacity of each wire until the capacity reaches the Euler buckling load.

### Axial load

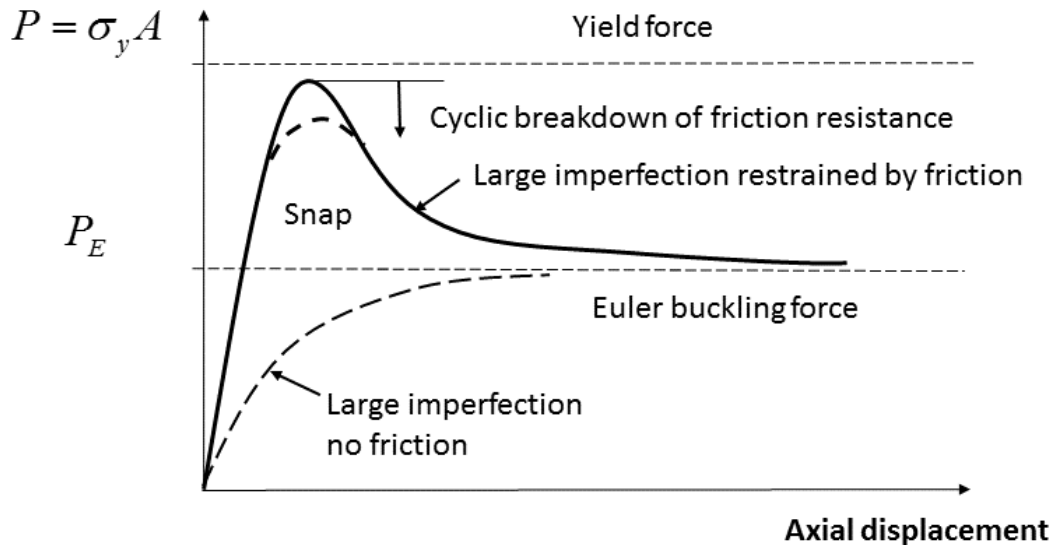


Figure D5.32: Axial force versus axial displacement for a wire restrained by friction

#### D5.3.3.3 Analytical Method

Under the assumption of no friction, a conservative estimate of the axial buckling force contribution from each wire can be achieved from the curve beam differential equation [Sævik and Ji, 2014] as:

$$P = \cos \alpha \left[ \frac{\pi^2 EI_3}{l^2} + GI_1(\kappa_2^2 - \kappa_t \kappa_2) + 4EI_2\kappa_1^2 + EI_3\kappa_1^2 \right] \quad (\text{D5.2})$$

where  $l$  is the unknown buckling length,  $E$  is the Young's modulus and  $G$  is the shear modulus.  $\kappa_1$  is the initial torsion,  $\kappa_2$  is the initial normal curvature and  $\kappa_t$  is the cylinder curvature in the tendon lateral transverse direction being expressed as:

$$\kappa_1 = \frac{\sin \alpha \cos \alpha}{R} \quad (\text{D5.3})$$

$$\kappa_2 = \frac{\sin^2 \alpha}{R} \quad (\text{D5.4})$$

$$\kappa_t = \frac{\cos^2 \alpha}{R} \quad (\text{D5.5})$$

where  $\alpha$  is the lay angle and  $R$  is the helix radius. The inertial moments corresponding to the three wire axes are listed below, where  $b$  is the width and  $t$  is the thickness of the tendon cross-section.

$$I_1 \simeq \frac{1}{3}bt^3 \quad (\text{D5.6})$$

$$I_2 = \frac{1}{12}bt^3 \quad (\text{D5.7})$$

$$I_3 = \frac{1}{12}tb^3 \quad (\text{D5.8})$$

As the buckling length increases towards infinite, the first term of Eq. D5.2 will be very small and can be neglected. Then the axial force capacity contribution from each wire specializes into the following lower bound estimate:

$$P = \cos \alpha [GI_1(\kappa_2^2 - \kappa_t \kappa_2 + 4EI_2\kappa_1^2 + EI_3\kappa_1^2)] \quad (\text{D5.9})$$

#### D5.3.4 Analysis tools

The analyses were performed by the finite element software BFLEX, which is developed by SINTEF Ocean, [Sævik, 2015]. BFLEX is based on the principle of virtual displacement, and a co-rotational formulation is applied to solve the non-linear equilibrium equations. The first release of the software was made in 1990s for stress and fatigue analysis of tensile armor wire in the flexible risers. It has been under continuous development since then by adding new functionalities, see [Sævik, 2015].

#### D5.3.5 Model description

The model set-up applied in the laboratory test tests reported by [Østergaard, 2012a] and used to benchmark the present model, is shown in Figure D5.33. Each test pipe was equipped with a smaller pipe on the inside which was pretensioned to obtain the desired true wall compression level. Then the test specimen was exposed to one sided cyclic bending (zero curvature - maximum curvature - zero curvature) until failure occurred.

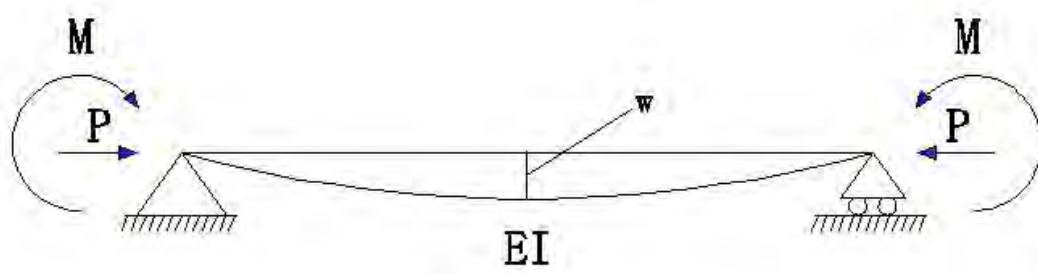


Figure D5.33: Buckling model

The flexible pipes studied are the same as reported by Østergaard in 2012 [Østergaard, 2012a]. Tests were carried out for three flexible risers with the inner diameter of 6 inch, 8 inch and 14 inch. The details are listed in Table D5.8 [Østergaard, 2012a].

Table D5.8: Pipes design and material properties

Pipe layer / pipe design		6" Riser *1)	8" Riser *2)	14" Jumper *2)
Inner layer of tensile armour wires	Outer diameter (m)	0.201	0.276	0.442
	Pitch length, $L_{pitch}$ (m)	1.263	1.474	2.247
	Pitch angle, $\Phi_{hel}$ (deg)	26.2	30	31.5
	Wire size, (height x width) (mm)	3x10	5x12.5	4x15
	Number of wires	52	54	70
Outer layer of tensile armour wires	Outer diameter (m)	0.209	0.289	0.452
	Pitch length, $L_{pitch}$ (m)	1.318	1.525	2.345
	Pitch angle, $\Phi_{hel}$ (deg)	-26.2	-30.3	-31.0
	Wire size, (height x width) (mm)	3x10	5x12.5	4x15
	Number of wires	54	56	72
High strength anti-birdcaging tape *3)	Yield strength (MPa)	650	1350	1350
	Pitch length, $L_{pitch}$ (m)	0.075	0.025	0.140
	Pitch angle, $\Phi_{hel}$ (deg)	83.5	88.4	-84.4
	Tape size, (height x width) (mm)	1x60	1.8x1.3	1x60
	Number of windings	1	8	2
Outer sheath *4)	Outer diameter (m)	0.225	0.314	0.477
	Thickness (mm)	6.0	10.0	10.0
Pipe sample	Number of inner layer pitches in pipe sample (including end fittings)	3.96	3.39	3.34
*1) A basic grade steel used for wires with yield strength of approximately 650 MPa, elastic modulus 210 GPa, Poisson's ratio 0.3				
*2) A high strength grade steel used for wires with yield strength of approximately 1350MPa, elastic modulus 210GPa, Poisson's ratio 0.3				
*3) Tape material properties chosen are: elastic modulus 27GPa. Poisson's ratio 0.4				
*4) Sheath material properties chosen are: elastic modulus 400MPa, Poisson's ratio 0.4				

The full model shown in Figure D5.35 includes two cores, two tensile layers, one structural tape layer between the two tensile layers, one anti-buckling layer and one sheath layer. One core was modelled by elastic pipe elements to introduce true wall compression by pretension as applied in the test. The other core was used to support the inner tensile layer and was modelled by HSHEAR363 elements. The inner and outer tensile layers were modelled by helix element HSHEAR353. Each tensile layer was represented by four helix tendons. The structural tape, anti-buckling tape and the sheath were all modeled by HELIX363 elements. The friction between layers was included by means of the HCONT363 contact element. Since the contact between the anti-buckling tape and the sheath will not influence a lot, the two element groups shared the same radial node, which means that there were only four contact layers. The cross section is shown in Figure D5.36. The friction coefficient between layers was set to 0.15 and the pipe length applied in the analyses corresponded to approximately five pitches of the inner tensile armour layer.

There were two loading conditions: cyclic bending and compression. The analysis of the first 10 seconds was by static analysis and included prescribing a tensile axial strain to the inner core to obtain the desired true wall compression in the tensile armour. Then the next 2460 seconds included cyclic bending by prescribed end rotations. Each bending cycle lasted 20 seconds and the applied time increment was 0.005s. Dynamic analysis was applied in this sequence to ensure numerical stability.

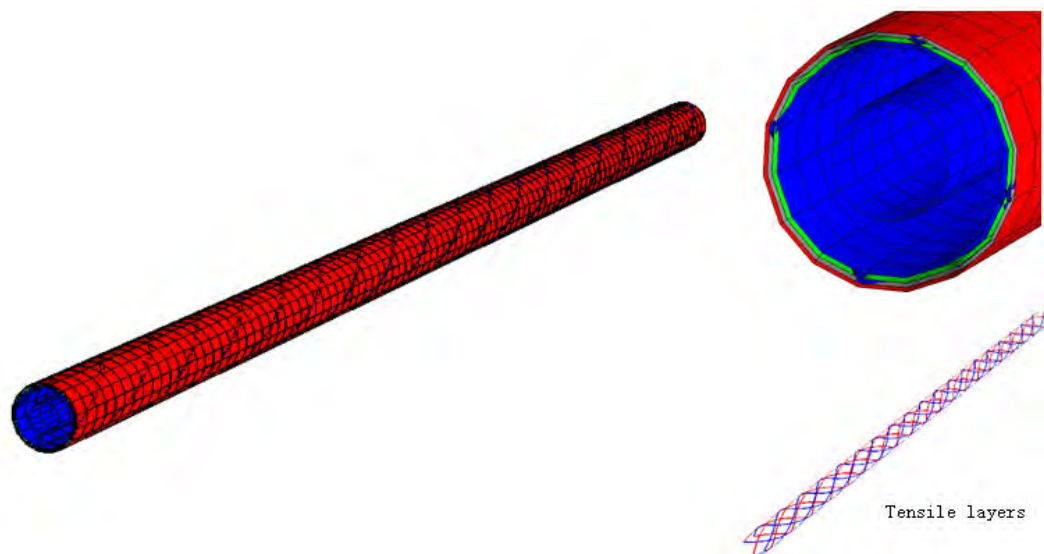


Figure D5.34: Model in BFLEX

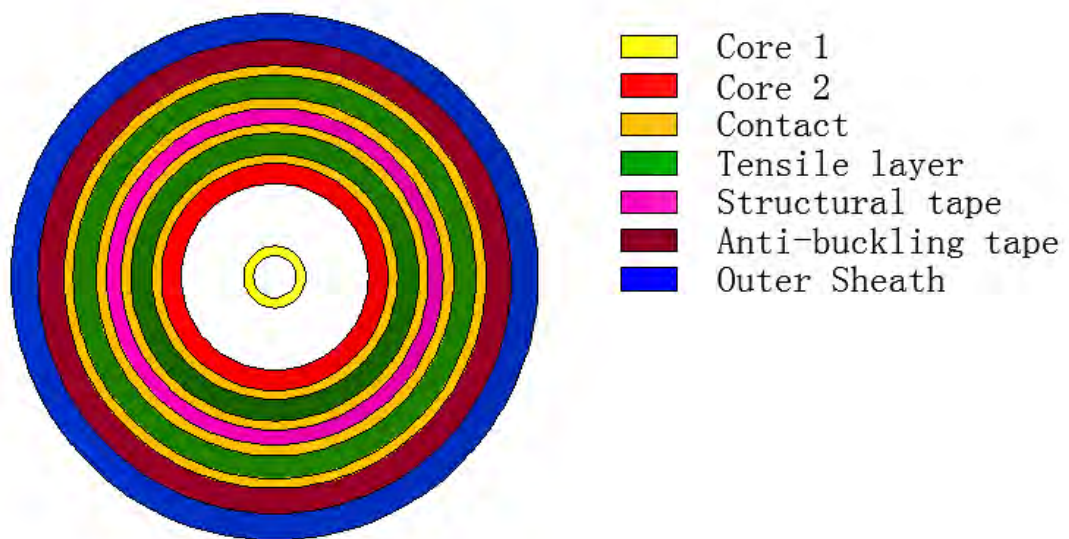


Figure D5.35: Model cross section

## D5.3.6 Analysis and results

### D5.3.6.1 Case Overview

Twelve cases were carried out to study the lateral buckling behavior due to cyclic bending, consistent with the experimental input data sheet shown in Table D5.8. The loading conditions for the 12 cases are shown in Table D5.9.

Table D5.9: Test loading conditions

Pipe ID	Case Number	Applied compression (kN)	Bending radius (m)
6 inch riser, L = 5 m	2	265	11
	3	80	11
	4	210	11
	5	160	11
	6	265	8
14 inch jumper, L = 7.5 m	7	277	21
	8	269	8
	9	411	10
	10	950	12
8 inch riser, L = 5 m	11	300	12
	12	400	12
	13	700	12

### D5.3.6.2 Analysis Process

The applied failure criterion was when the outer fibre of the steel wire reached the yield stress. If there were no failures, the torsion and rotation will be small and increase slowly.

Case 2 is studied as an example of a test leading to failure as shown in Figure D5.36. To avoid the influence of the boundary conditions, the middle part of the pipe was chosen. The red part of the tendon indicates the section of the pipe where the wire stress exceeded the yield stress.

Having identified yield stress exceedance during the applied cycles, the corresponding end rotation was found as shown in Figure D5.37. Since the inner tensile layer fails first, in order to keep the torsion balance, the outer tensile layer rotates following the direction of outer layer lay angle which results in torsion rotation of the whole pipe. For the test pipes, the lay angle is negative, so the end rotation will be negative as well.

Figure D5.38 demonstrates the longitudinal stress as a function of time for one critical element. The yield stress of 650MPa is exceeded after approximately 34 cycles.

Case 3 is studied as an example of a no failure case as shown in Figure D5.39. The rotation is very small and buckling will not occur. The element with the maximum longitudinal stress is shown in Figure D5.40. The longitudinal stress does not exceed the yield stress of 650MPa, which means there is no failure in the tensile layer.

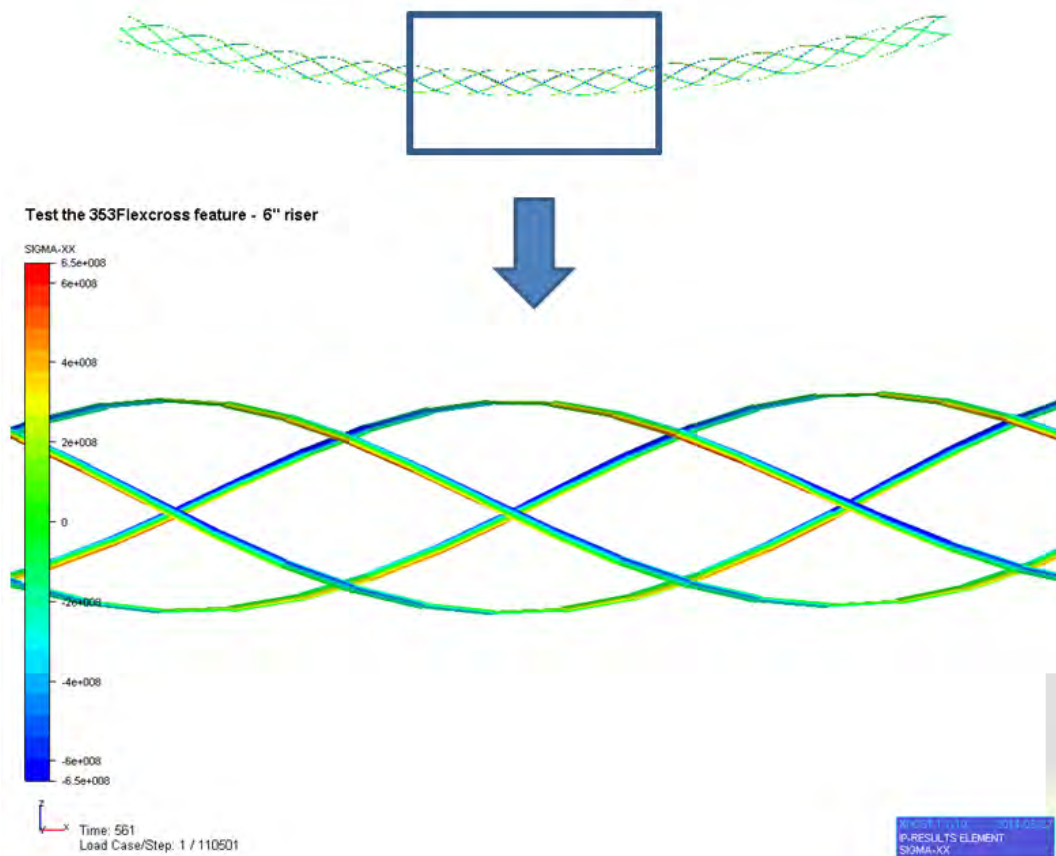


Figure D5.36: Example of failure - Case 2- identification of failure location

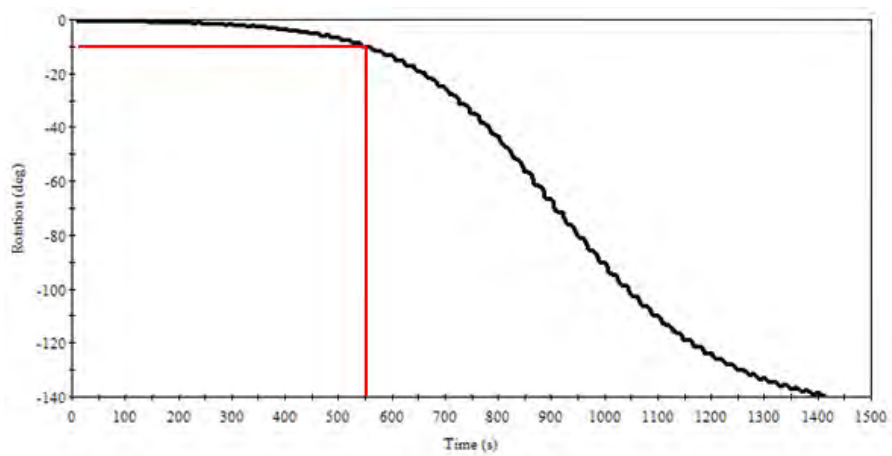


Figure D5.37: Example of failure - Case 2 - end rotation as a function of time

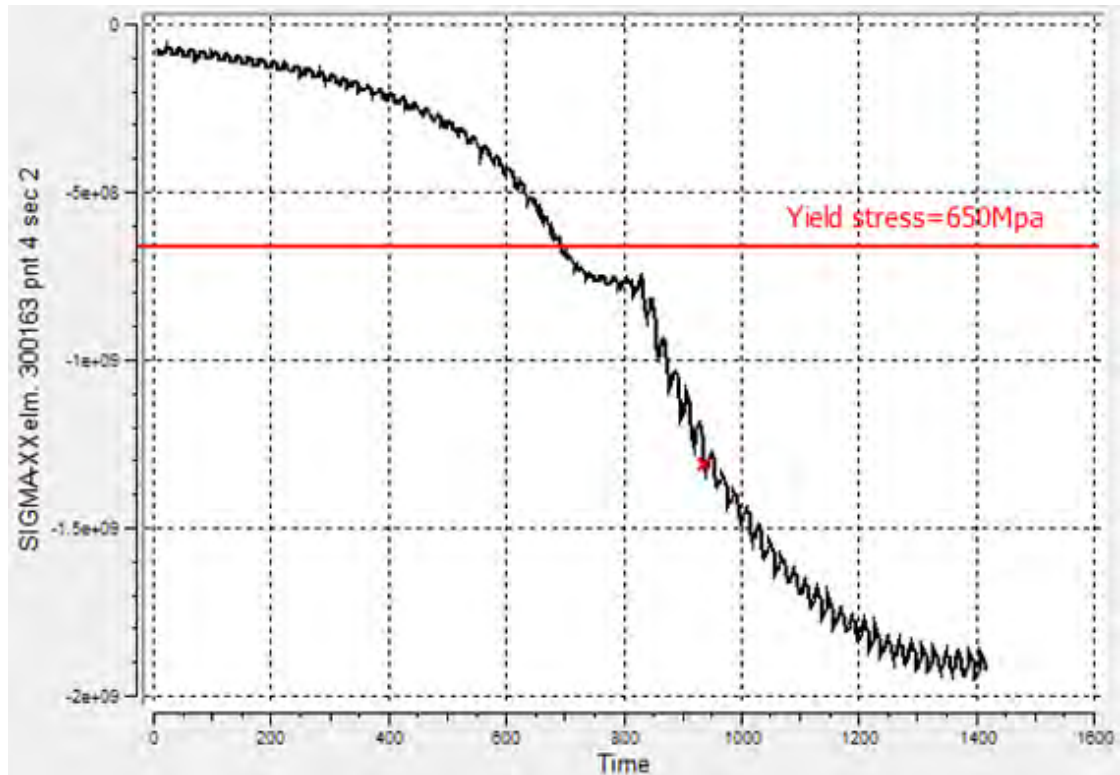


Figure D5.38: Longitudinal stress  $\sigma_{xx}$  history during failure - Case 2

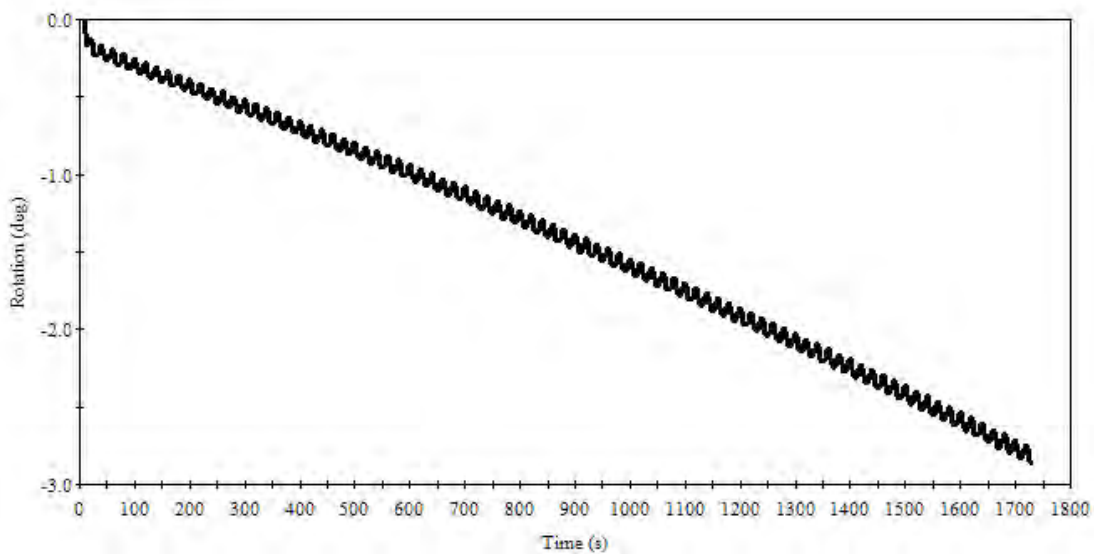
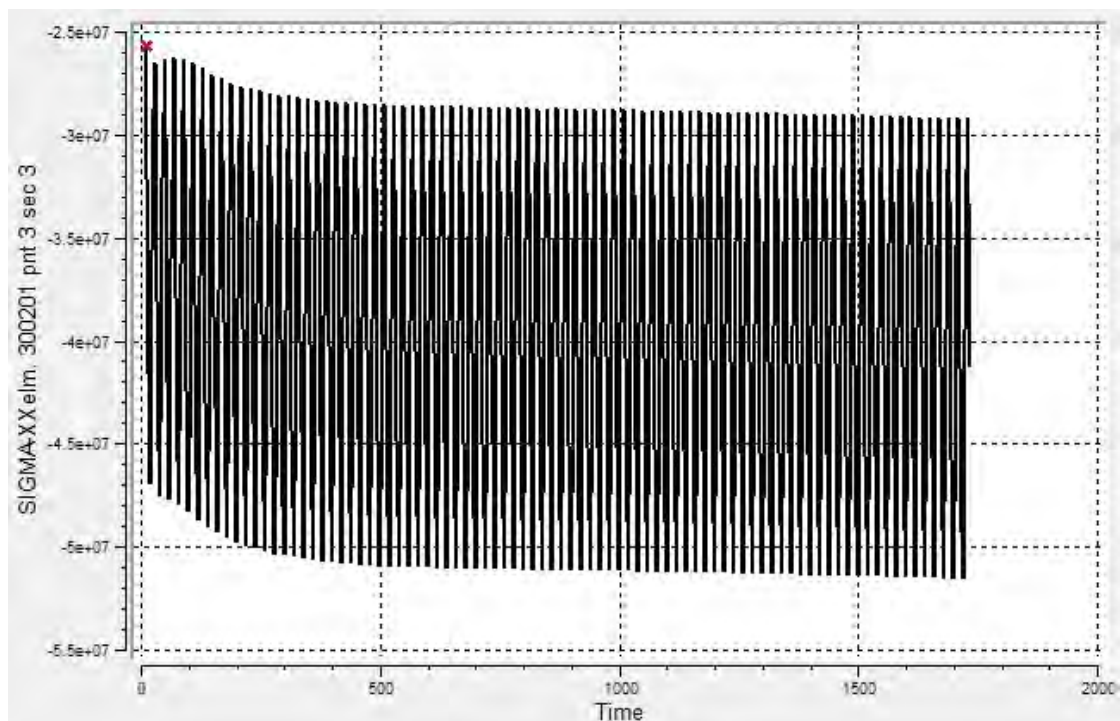


Figure D5.39: Example of no failure - Case 3

Figure D5.40: Longitudinal stress  $\sigma_{xx}$  for Case 3

### D5.3.6.3 Results in terms of failure and end rotation

The comparison of end rotation and failure/no failure between BFLEX simulation and measured values are shown in Table D5.10

Table D5.10: Results of pipe failure due to cyclic bending

Pipe ID	Case Number	Applied compression (kN)	Bending radius (m)	Results in experiment	Pipe twist before unloading (deg)	Results in Bflex	Bflex twist before failure (deg)
6 inch	2	265	11	Failure	45 (increasing)	Failure	10 (increasing)
	3	80	11	No failure	<1 (stable)	No failure	3 (slowly increasing)
	4	210	11	Failure	45 (increasing)	Failure	11 (slowly increasing)
	5	160	11	No failure	3 (slowly increasing)	Failure	3 (increasing)
	6	265	9	Failure	45 (slowly increasing)	Failure	10 (increasing)
14 inch	7	277	21	No failure	<1 (stable)	No failure	5 (slowly increasing)
	8	269	8	No failure	6.5 (increasing)	Failure	17 (increasing)
	9	411	10	Failure	27	Failure	27 (rapidly increasing)
	10	950	12	Failure	10 (rapidly increasing)	Failure	11 (rapidly increasing)
8 inch	11	700	12	Failure	27 (slowly increasing)	Failure	21 (increasing)
	12	300	12	No failure	1	No failure	2.8 (slowly increasing)
	13	400	12	No failure	15 (slowly increasing)	Failure	18 (increasing)

For the 6 inch riser, BFLEX predicts failure for Case 5 whereas no failure was observed in the test. However, for case 4 with 50 kN more compression, failure was obtained both numerically and experimentally.

For the 14 inch jumper, the torsion end rotations of the failure cases agree quite well with the experimental results. However, the collapse for Case 8 was not obtained in the test, whereas the model predicted failure.

For the 8 inch riser, the result from Cases 11 (failure) and 12 (no failure) fit well with the experimental results. However, for Case 13, BFLEX predicts failure whereas no failure was observed in the test.

Hence, for the cases investigated the proposed model demonstrates some conservatism when applying the proposed first yield as failure criterion. The study reported in [Sævik and Ji, 2014] concluded with exact correlation in terms of failure or no failure for the same experimental tests and by application of same failure criterion. However, the model was based on excluding the effect of the antibuckling tape torque which may lead to small differences in contact pressure and friction. This may explain the differences seen by applying the two modelling approaches.

The advantage of including the anti-buckling tape as in the procedure reported here is that the strengthening effect from the anti-buckling tape can be documented as elaborated on in the following.

### D5.3.7 Effect of anti-buckling tape

The effect of the anti-buckling tape on the lateral buckling behavior of the tensile armor was studied including sensitivity analysis of the effect of the lay direction, lay angle of anti-buckling tape and the friction coefficient between layers.

#### D5.3.7.1 Influence of anti-buckling tape

The effect of anti-buckling tape was studied by comparing a case without anti-buckling tape with the same case including the anti-buckling tape. The results are shown in Figure D5.41, which reveals clearly the effect of anti-buckling tape on the lateral buckling behavior. It indicates that the anti-buckling tape can slow down the buckling process significantly. By simply linearizing the curves in the figure, the end rotation rate of the pipe without anti-buckling tape is almost 20 times higher than for the case with anti-buckling tape.

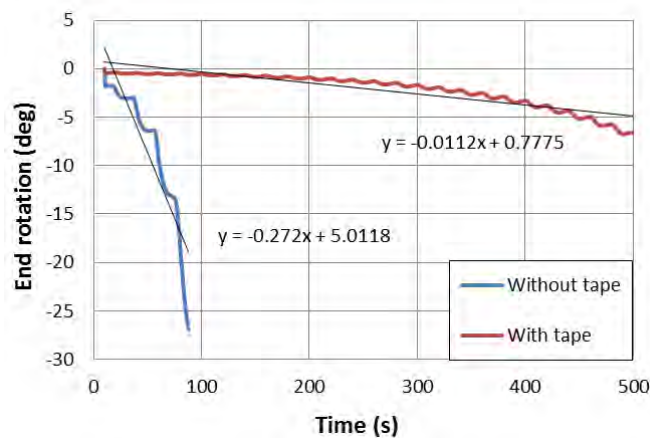


Figure D5.41: Comparison between the riser with and without anti-buckling tape

#### D5.3.7.2 Influence of Lay Direction of Anti-buckling Tape

The anti-buckling tape is helically wound, often with a steep angle close to 90 degrees. Its lay angle may influence the buckling behavior of the tensile armors. A sensitivity study based on Case 8 was performed to study this effect. The direction of the lay angle of anti-buckling tape in Case 8 was changed from -84.4 to +84.4.

Figure D5.42 and Figure D5.43 show the effect of lay direction on the end rotation of the cross section. Since the lay angle of the outer tensile layer is negative, the negative anti-buckling tape lay angle means that it is in the same direction as the outer tensile layer. A positive lay angle means that it is in the opposite direction. It is seen that the negative lay angle direction will slow down the buckling process. In addition, for the negative lay angle

case, the pipe have a stronger tendency of twisting in the opposite direction after failure, contributing to limit the end rotation.

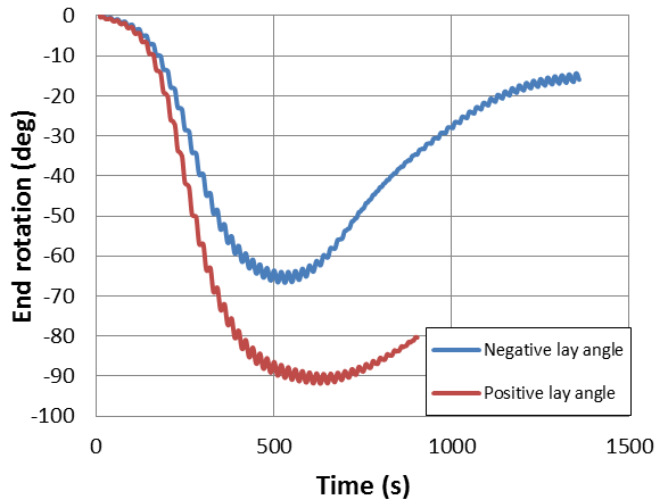


Figure D5.42: Influence of lay direction of anti-buckling tape

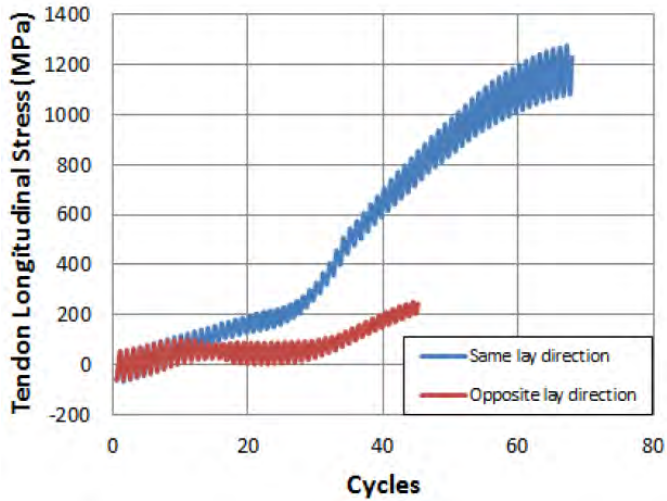


Figure D5.43: Influence of lay direction of anti-buckling tape 2

The longitudinal stress in the anti-buckling tape is shown as a function of time in Figure D5.44 for both cases. When the anti-buckling tape has the same lay direction as the outer tensile layer, the tape will slow down the torsion end rotation process by mobilising more stress as the process goes on. For the opposite case, the rotation of the outer layer will give a corresponding reduction in the stress mobilised in the tape layer. This means reduced capability of reducing the end rotation.

### D5.3.7.3 Influence of the Lay Angle applied for the Anti-buckling Tape

The lay angle applied for the anti-buckling tape may also influence the lateral buckling capacity. The lay angle was therefore changed between -76 to -88 degree and the results in

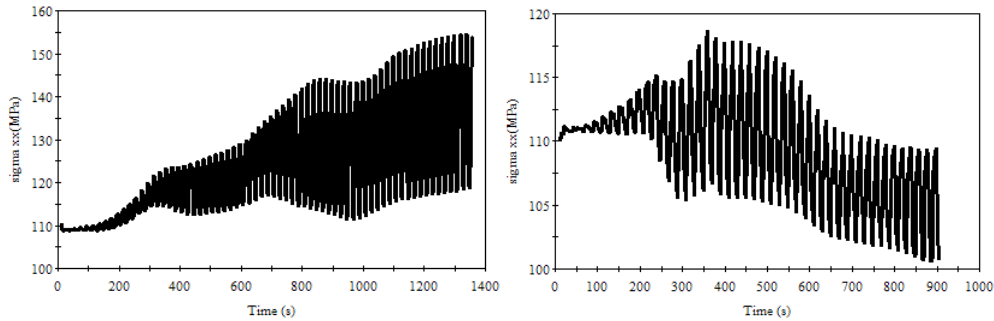


Figure D5.44: Longitudinal stress in anti-buckling tape comparison by changing lay directions

terms of end rotation are shown in Figure D5.45.

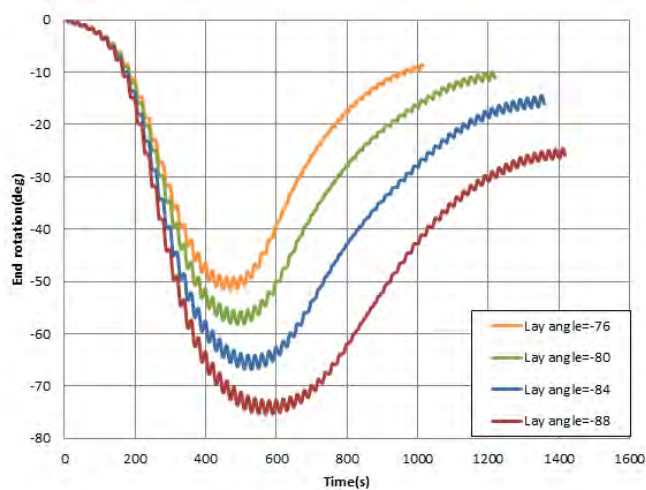


Figure D5.45: Influence of lay angle of anti-buckling tape

The anti-buckling tape with smaller lay angle will have a better capability to prevent the end rotation. The component of longitudinal stress on the global x-axis direction is larger due to the smaller lay angle, which will provide more resistance when the tape is squeezed towards the pipe centre due to the end rotation behavior.

#### D5.3.7.4 Influence of friction coefficient

In order to study the effect of the friction coefficient on the end rotation during cyclic bending, the friction coefficient between all the layers was changed from 0.15 to 0.2. The results are shown in Figure D5.46.

A larger coefficient will provide more friction resistance between layers and reduce the slip between layers during the lateral buckling process, which results in a smaller end rotation.

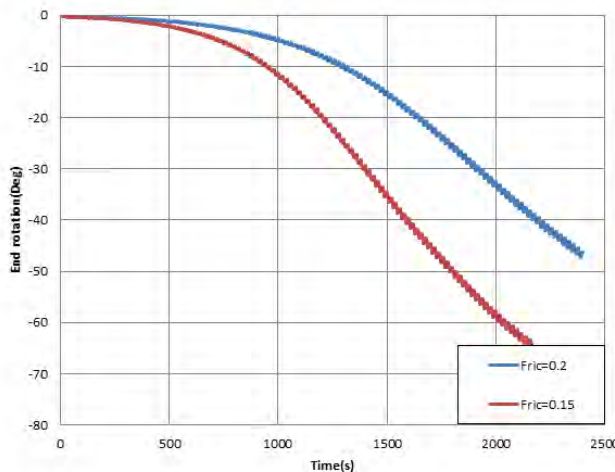


Figure D5.46: influence of friction coefficient

### D5.3.8 Conclusions

The following conclusions can be drawn from the study:

- True wall compression due to external pressure in combination with cyclic bending during pipe installation and operation may lead to lateral buckling failure of the armour wires. This is particularly the case under wet annulus conditions.
- Pipe failure can be observed as severe torsion deformation of the cross-section. In laboratory tests this can be observed as severe end rotation.
- End rotation predicted by BFLEX agrees well with most of the measured values from laboratory tests.
- In all cases studied the proposed failure criterion based on exceeding the yield stress demonstrated conservatism with regard to the tests
- Anti-buckling tape will have a great influence on the lateral buckling process.
- The same lay direction between the outer tensile layer and anti-buckling tape will perform better than the opposite lay direction. The effect is to resist end rotation.
- Smaller lay angle of the antibuckling tape will have better performance than higher lay angle. However, it is important to notice that the end rotation phenomenon studied here is based on the assumption that the anti-buckling tape is strong enough, and that the tensile layer will fail by lateral buckling, i.e radial buckling is assumed to not occur. A smaller lay angle of anti-buckling tape will provide more resistance to lateral buckling, however, the radial buckling capacity will be reduced. So it is necessary to consider both effects for an optimized design.
- Larger friction coefficient between layers will result in smaller end rotation, i.e. increasing the capacity against lateral wire buckling.
- The elastic buckling value provides a conservative estimate. For all cases the axial compressive load observed in the tests was a factor 1.6-1.9 above the elastic buckling load found from analytical theory.



## **Chapter D6**

# **Integrity Management of North Sea Riser**

## D6.1 Introduction

The basis for the integrity management (IM) planning is the Handbook Chapters [B2 Risk Analysis Methodology](#), [A3 Failure Modes](#) and [C1 Integrity Management](#). This case study section suggests a working methodology to transform the presented information tools into an actual integrity management plan for the case study riser, 'North Sea riser'. The method can be graphically represented by the below figure:

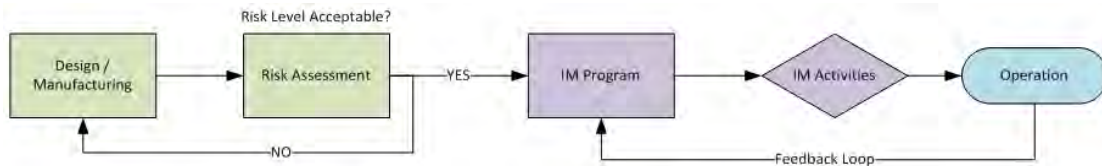


Figure D6.1: Integrity Management Plan Development

For a field development it will normally be distinctive 'families' of flexible pipes, based on the pipe design, physical location, operational function or operational parameters. Being aware of both the similarities and dissimilarities are important to ensure that the final risk level in fact reflects the actual situation. Oil production risers may be effective to plan as a group, however important differences arise if one riser for instance is a high pressure, high temperature service while others may be at the other end of the scale.

Planning an integrity management program requires good and updated knowledge on flexible pipe failure modes, layer failure mechanisms and the many, interconnected pathways possible from initiation to ultimate pipe failure. Reviewing the Chapter [A3 Failure Modes](#) is highly recommended in advance of reading the case study presented below.

## D6.2 Methodology

Initially the pipeline design for the given operational conditions assumed in the design premise is reviewed for all presently known failure modes as presented in Chapter [A3 Failure Modes](#), Section [A3.3](#). In sequence the review is performed according to the following outline:

- Step 1: Determine if failure mode is applicable for the system being reviewed (materials, structural layout, global configuration etc.)
- Step 2: Assess relevant field experience: essentially determine if failure mode is theoretical, experienced previously or a frequent occurrence
- Step 3: Identify if conditions promoting degradation are present for system being reviewed
- Step 4: Identify for which operational or environmental conditions the ultimate loss of layer function is expected to occur
- Step 5: Identify if the layer failure may trigger other failure modes
- Step 6: Identify if layer failure may trigger ultimate pipe failure and identify the time scale for progression of failure

- Step 7: Assess risk level: probability, consequence and risk without any mitigations implemented and if control mechanisms are required
- Step 8: Identify relevant risk reducing control mechanisms: preventive, monitoring, inspection or testing.
- Step 9: Re-assess risk level considering successful implementation of suggested control mechanisms

## D6.3 Review of Selected Failure Modes

For a limited number of failure modes, the below sections contains a review according to methodology presented in Chapter [D6](#). The review is an illustrative text presenting how to utilize the information from Chapter [A3](#) Failure Modes with the actual conditions assumed for the North Sea riser. The text is not exhaustive and is only to be considered for information.

### D6.3.1 Carcass Collapse

#### D6.3.1.1 Step 1: Applicability of Failure Mode

Failure mechanism related to gas absorption and release in polymer is not applicable for single layer pressure sheath designs. It is only valid for extremely rapid depressurisations which are not considered realistic in an oil production riser.

Severe bending of pipe may occur due to accidental damage during installation or in extreme environmental conditions more severe than design premise.

Hydrate melting is considered as not applicable due to low gas content of transported fluid, i.e. factors enabling hydrate formation is not present.

#### D6.3.1.2 Step 2: Field Experience

Field experience is that failure mode is only experienced in testing for single layer pressure sheath pipes. Failure mode is thus not to be considered as a risk factor for the subject riser.

#### D6.3.1.3 Step 3: Degradation Promoters

High operational bore pressures (300 bar) in early service life (condition based).

Extended time with sand production and high flow rates (condition based).

#### D6.3.1.4 Step 4: Occurrence of Layer Failure

At event of severe bending significantly below MBR; highest probability expected during installation/intervention (event based).

Subsequent to outer sheath loss of layer function allowing hydrostatic pressure to act directly onto carcass through pressure sheath (event based, time based).

**D6.3.1.5 Step 5: Trigger for other failure modes**

Carcass collapse can trigger pressure sheath layer failure.

**D6.3.1.6 Step 6: Ultimate Pipe Failure and Time Scale**

Partial or complete or partial bore obstruction occurs immediately after carcass collapse.

The time scale to loss of containment is medium to long term after triggering pressure sheath layer failure and subsequently outer sheath layer failure. Failure mechanism: cyclic deformations of pressure sheath lacking internal support.

**D6.3.1.7 Step 7: Risk Level (Un-Mitigated)**

Probability (Failure Mode): Very Low.

Probability (Ultimate Pipe Failure): Very Low.

**Consequence:**

1. Safety: No or superficial injuries (loss of containment expected only due to high hydrostatic pressure (seabed)).
2. Environment: Massive effect, large damage area, > 100 barrel oil (BBL) (loss of containment).
3. Cost: > 10 mill. (EUR) - replacement riser.

Risk: Medium.

Requirement for IM actions: No.

**D6.3.1.8 Step 8: Control Mechanisms**

Installation phase is considered as main risk driver. Through performing post-installation gauge pigging it is verified that no deformations are present.

Residual probability of occurrence exists due to possibility for extreme environmental conditions resulting in severe dynamic motions. Post-event verification of global motion compared to design basis may be performed to validate design integrity if anomalies are identified.

Combination of time- and event based factors may increase probability of occurrence in late service life. Reduction of the initial carcass collapse capacity due to material loss (erosion, corrosion) combined with outer sheath damage. Periodic review of monitoring data, bore fluid data and annulus test data provide information and is considered satisfactory.

Table D6.1

Control Mechanism	Periodic	Event based
Gauge Pigging		X
Pressure Monitoring		X
Status assessment	X	
Annulus Free Volume Measurement		X

## Procedures

Anomaly reporting from post-event extreme weather conditions outside design premises.

### Monitoring:

Operational data review to assess differential pressure topside / subsea versus flow rates and experienced bore depressurization rates.

### Inspection:

Internal inspection: gauge pigging post-installation.

### Testing:

Verification of outer sheath integrity through annulus free volume testing.

**D6.3.1.8.1 Step 9: Risk Level (Mitigated)** Ultimate pipe failure is expected to be controlled through selected IM activities. Remaining consequence are economic due to loss of operational integrity.

Probability (Failure Mode): Very Low.

Probability (Ultimate Pipe Failure): Very Low .

### Consequence:

1. Safety: No or superficial injuries.
2. Environment: Slight effect on the environment, <1 BBL due to failure occurring before operation.
3. Cost: > 10 mill. EUR - replacement riser.

Risk: Medium.

## D6.3.2 Carcass Axial Overloading

### D6.3.2.1 Step 1: Applicability of Failure Mode

Pipe Blockage and large differential pressure across blockage through either of the below occurrences:

- a Wax plug - not applicable based on fluid properties; flow assurance calculations.
- b Hydrate plug - not applicable based on fluid properties; flow assurance calculations.

- c Slug - not applicable based on fluid properties; flow assurance calculations.
- d Pig - applicable; gauge pigging after installation.

From flow assurance calculations and produced fluid properties, wax and hydrate plugging and slugging is considered to be not applicable. Remaining initiator is if pig becomes stuck and attempts to release through increasing differential pressure.

Loss of radial contact between the inner layers is considered not applicable for single layer pressure sheath of polyamide material.

#### **D6.3.2.2 Step 2: Field Experience**

Failure mechanism a, b and d of Step 1 are experienced.

#### **D6.3.2.3 Step 3: Degradation Promoters**

Main degradation promoters relate to manufacturing anomalies, i.e.

1. fully extended carcass: checked and verified during Factory Acceptance Test (FAT) - not applicable.
2. insufficient anchoring of the carcass in the end-fitting: design integrity.

Loss of radial contact in cross section is considered not applicable, refer to Step 1.

#### **D6.3.2.4 Step 4: Occurrence of Layer Failure**

On the assumption of only pigging can trigger layer failure, occurrence is related pre-operation commissioning operations.

#### **D6.3.2.5 Step 5: Trigger for other failure modes**

Occurrence of failure mode triggers 'Carcass Collapse' failure mode through loss of radial support of pressure sheath.

#### **D6.3.2.6 Step 6: Ultimate Pipe Failure and Time Scale**

If failure mode is triggered there are two scenarios, both resulting in loss of containment:

1. Worst case; pull-out of pressure sheath and pressure armour. Occurs immediately.
2. Best Case: through indirect mechanism, i.e. damage to pressure sheath developing finally through thickness. Expected to be long-term as polyamide pressure sheath is less notch- and fatigue sensitive than PVDF.

### D6.3.2.7 Step 7: Risk Level (Un-Mitigated)

Probability (Failure Mode): Very Low.

Probability (Ultimate Pipe Failure): Very Low.

#### **Consequence:**

1. Safety: No or superficial injuries
2. Environment: Slight effect on the environment, <1 BBL due to failure occurring before operation.
3. Cost: > 10 mill. EUR - replacement riser.

Risk: Medium.

Requirement for preventive actions: Yes.

Requirement for IM actions: No.

### D6.3.2.8 Step 8: Control Mechanisms, see Table D6.2

Table D6.2

Control Mechanism	Periodic	Event based
Anomaly Reporting		X

#### **Preventive**

Avoid failure mode through commissioning procedure; control and verification of differential pressure across pig during execution. Ensure compliance to pipe supplier recommendations to pig specification.

Upon entering operations phase it is assumed that failure mode is negligible.

#### **Procedures**

None

#### **Monitoring:**

None

#### **Inspection:**

None

#### **Testing:**

None

### D6.3.2.9 Step 9: Risk Level (Mitigated)

Ultimate pipe failure is expected to be controlled through selected IM activities. Remaining consequence relates to economic due to loss of operational integrity.

Probability (Failure Mode): Very Low.

Probability (Ultimate Pipe Failure): Very Low.

**Consequence:**

- Safety: No or superficial injuries.
- Environment: Slight effect on the environment, <1 BBL due to failure occurring before operation.
- Cost: > 10 mill. EUR - replacement riser.

Risk: Medium.

### **D6.3.3 Pressure Sheath Embrittlement (Ageing of Polyamides)**

#### **D6.3.3.1 Step 1: Applicability of Failure Mode**

Brittle rupture or crack growth through thickness.

#### **D6.3.3.2 Step 2: Field Experience**

Several reported failures believed to be due to methanol batch treatment or high Total Acid Number (TAN).

Uncertainty in prediction model; both less and more severe degradation due to factors not presently in the ageing models.

#### **D6.3.3.3 Step 3: Degradation Promoters**

1. High temperature.
2. High concentration of acidic species / alkalinity of the produced water.
3. Oxygen (from chemical treatment or leakages).

#### **D6.3.3.4 Step 4: Occurrence of Layer Failure**

Direct: Cool-down / cold conditions due to reduction of ductility with temperature. If simultaneous handling (e.g. bending) is experienced this may initiate layer failure.

Indirect: None.

#### **D6.3.3.5 Step 5: Trigger for other failure modes**

#### **D6.3.3.6 Step 6: Ultimate Pipe Failure and Time Scale**

Direct: loss of containment: fluids leaking to annulus.

Indirect: outer sheath burst, fluids leaking to environment.

Ultimate failure: loss of containment.

Time frame for ultimate failure after layer failure is very short.

### D6.3.3.7 Step 7: Risk Level (Un-Mitigated)

Probability (Failure Mode): Medium.

Probability (Ultimate Pipe Failure): Medium.

#### **Consequence:**

1. Safety: Multiple fatalities.
2. Environment: Massive effect, large damage area, > 100 BBL (loss of containment).
3. Cost: > 10 mill. EUR - replacement riser.

Risk: Very High.

Requirement for preventive actions: Yes.

Requirement for IM actions: Yes.

### D6.3.3.8 Step 8: Control Mechanisms, see Table D6.3

Table D6.3

Control Mechanism	Periodic	Event based
Status assessment	X	
Temperature Monitoring	X	
Annulus Vent Flow Monitoring		X
Sampling of Bore Fluid	X	
Pressure Barrier Coupon Sampling	X	

#### **Preventive**

Minimize batch methanol treatment.

Temperature minimisation cannot be performed - reservoir characteristics are fixed. Flow restrictions are not desired, i.e. lowered production rates.

#### **Procedures**

None.

#### **Monitoring:**

Monitoring data for temperature and shut-downs.

Annulus vent monitoring for detection of ultimate pipe failure (may be installed upon accumulating critical levels for ageing end-of-life).

#### **Inspection:**

None.

#### **Testing:**

Polymer coupons exposed to flow environment: not possible to install subsea (hot end).

### D6.3.3.9 Step 9: Risk Level (Mitigated)

Probability (Failure Mode): Medium.

Probability (Ultimate Pipe Failure): Very Low.

#### Consequence:

1. Safety: Multiple fatalities.
2. Environment: Massive effect, large damage area, > 100 BBL (loss of containment).
3. Cost: > 10 mill. EUR - replacement riser.

Risk: Medium.

## D6.3.4 Tensile Armour Wire Fatigue

### D6.3.4.1 Step 1: Applicability of Failure Mode

Failure mode is applicable for any dynamic service flexible pipe through two degradation mechanisms:

1. Corrosion fatigue (corrosive environment in annulus).
2. Fatigue (dry annulus).

### D6.3.4.2 Step 2: Field Experience

Experienced - i.e. failure mode had led to accidents.

### D6.3.4.3 Step 3: Degradation Promoters

High internal pressure; this is valid as riser is expected to operate at 300 bar in initial phase. This is however accounted for in design calculations. Continued higher internal pressures than accounted for in design premise may invalidate fatigue calculations, i.e. condition based degradation.

Increased bending: global dynamics controlled through design. Events with extreme environmental conditions are short-term and not expected to contribute to gross fatigue damage.

Wear of the anti-wear tape: cannot be inspected, however only a concern in late phase of life cycle, i.e. time based degradation.

Unfavourable local design of bending stiffener or bellmouth: riser is supported by bellmouth, limiting riser curvature at bellmouth exit, i.e. curvature is controlled through design.

Corrosion: annulus condition if hole in outer sheath and/or H<sub>2</sub>S or CO<sub>2</sub> in produced bore fluids and/or condensed water. Outer sheath damage may occur during whole life cycle, i.e. event based degradation. Riser is designed for sweet service, thus any change of bore fluid composition may invalidate design assumptions, i.e. condition based.

#### D6.3.4.4 Step 4: Occurrence of Layer Failure

Inner tensile wires more susceptible to fatigue. If outer sheath damages local corrosion may result in outer wires becoming dominant failure area.

Torsional imbalance and twisting of the pipe.

Loss of support for pressure armour resulting in unfavorable loading and possible fatigue/overloading.

Full pipe rupture.

#### D6.3.4.5 Step 5: Trigger for other failure modes

Pressure sheath extrusion.

Pressure armour fatigue and unlocking.

#### D6.3.4.6 Step 6: Ultimate Pipe Failure and Time Scale

Leakage from pressure sheath, possible outer sheath failure. Loss of containment; either partial or worst case full pipe rupture.

#### D6.3.4.7 Step 7: Risk Level (Un-Mitigated)

Probability (Failure Mode): Medium.

Probability (Ultimate Pipe Failure): Low.

##### Consequence:

- Safety: Multiple fatalities. Service life predictions estimate highest fatigue in upper part of riser near manned installation, thus loss of containment with ignition imposes significant safety consequences.
- Environment: Massive effect, large damage area, > 100 BBL (loss of containment).
- Cost: > 10 mill. EUR - replacement riser.

Risk: High.

Requirement for preventive actions: Yes.

Requirement for IM actions: Yes

#### D6.3.4.8 Step 8: Control Mechanisms, see Table D6.4

Table D6.4

Control Mechanism	Periodic	Event based
Anomaly Reporting		X
Status assessment	X	
Pressure Monitoring	X	
Annulus Free Volume Measurement	X	
Sampling of Bore Fluid	X	
Annulus Gas Sampling	X	

**Preventive**

Design robustness and safety factors for fatigue calculations provide margin against failure.

**Procedures****Monitoring:**

Pressure monitoring to enable review of operational data.

**Inspection:**

None.

**Testing:**

Bore fluid sampling to verify produced fluid composition.

**D6.3.4.9 Step 9: Risk Level (Mitigated)**

Example of reliability considerations for tensile wire fatigue may be found in Chapter [D8](#)

Probability (Failure Mode): Medium.

Probability (Ultimate Pipe Failure): Very Low.

**Consequence:**

- Safety: Multiple fatalities. Service life predictions estimate highest fatigue in upper part of riser near manned installation, thus loss of containment with ignition imposes significant safety consequences.
- Environment: Massive effect, large damage area, > 100 BBL (loss of containment).
- Cost: > 10 mill. EUR - replacement riser.

Risk: Medium.

**D6.3.5 Outer Sheath: hole in the outer sheath****D6.3.5.1 Step 1: Applicability of Failure Mode**

Applicable to any riser system due to several initiators; accidental impacts, blocked annulus, abrasion, handling/installation or manufacturing defects, i.e. mainly event based but also time based.

Applicable to all outer sheath materials.

**D6.3.5.2 Step 2: Field Experience**

Frequent failure mode; detection and repair possible. Critical if layer failure is located in splash zone or in sections of significant dynamic loading.

### D6.3.5.3 Step 3: Degradation Promoters

#### Events:

- a falling objects - applicable.
- b impact from fishing equipment/lines - not applicable due to exclusion zone.
- c broken mooring lines - applicable, will be detected.
- d installation - procedures should avoid layer failure to occur, however not possible to exclude.
- e improper operation of annulus vent system, i.e. shut-in.

#### Time:

- f restricted annulus vent - applicable based on experience; diffusion rate and annulus free volume determines time scale for layer failure to occur.
- g abrasion from attachments to neighbouring structures, guide-tube, seabed etc. - applicable, however clashing between riser/structure not identified in design. Abrasion from guide-tube or seabed possible.

### D6.3.5.4 Step 4: Occurrence of Layer Failure

Mainly related to events, i.e. randomly during both installation and through life.

Some time-based degradation promoters; thus increased probability for occurring in late life phase (abrasion, restricted annulus vent).

### D6.3.5.5 Step 5: Trigger for other failure modes

Corrosion of steel armours in annulus (pressure armour, tensile armour).

Tensile armour fatigue.

Pressure armour fatigue.

### D6.3.5.6 Step 6: Ultimate Pipe Failure and Time Scale

Gradual loss of pressure- and tensile armour capacity in terms of strength and fatigue life. If reaching critical level full pipe rupture is possible.

Time scale dependent on location of damage, utilization rate of armours, design fatigue life and design service condition (sweet). Indication of failure in a few years, i.e. short- to medium term.

### D6.3.5.7 Step 7: Risk Level (Un-Mitigated)

Probability (Failure Mode): High.

Probability (Ultimate Pipe Failure): High.

**Consequence:**

1. Safety: Multiple fatalities. Service life predictions estimate highest utilization (fatigue, strength) in upper part of riser near manned installation, thus loss of containment with ignition imposes significant safety consequences.
2. Environment: Massive effect, large damage area, > 100 BBL (loss of containment).
3. Cost: > 10 mill. EUR - replacement riser.

Risk: Very High

Requirement for preventive actions: Yes.

Requirement for IM actions: Yes.

**D6.3.5.8 Step 8: Control Mechanisms, see Table D6.5**

Table D6.5

Control Mechanism	Periodic	Event based
Anomaly Reporting		X
Status assessment	X	
Dropped Object Reporting and Survey		X
Annulus Free Volume Measurement	X	X
Annulus Flow Measurement	X	
Topside GVI	X	X
Subsea GVI	X	X

**Preventive**

Accidental event prevention through procedures.

**Procedures**

Annulus vent system operation.

**Monitoring:**

None.

**Inspection:**

Topside General Visual Inspection (GVI) (gross anomalies, improper operation of vent-system).

Subsea GVI (gross anomalies, dropped objects, trawl board impacts etc.).

**Testing:**

Annulus Free Volume Measurement.

Annulus Flow Measurement (confirm vent capacity).

Testing is to be performed both periodic and post-events presenting increased probability for outer sheath damage. This could be for instance installation work on neighbouring systems or other intervention works, detection of clashing towards mooring lines or similar.

#### D6.3.5.9 Step 9: Risk Level (Mitigated)

Probability (Failure Mode): High (event driven, no significant probability reduction).

Probability (Ultimate Pipe Failure): Very Low.

##### Consequence:

- Safety: Multiple fatalities. Service life predictions estimate highest utilization (fatigue, strength) in upper part of riser near manned installation, thus loss of containment with ignition imposes significant safety consequences.
- Environment: Massive effect, large damage area, > 100 BBL (loss of containment).
- Cost: > 10 mill. EUR - replacement riser.

Risk: Medium.

## D6.4 Summary

A summary of the integrity management plan for the North Sea riser is presented in the following sections.

### D6.4.1 Failure Event Tree

Failure modes and their applicable failure causes and following events or mechanisms leading to ultimate pipe failure can be analysed through a failure event tree to identify the relationships and interactions, see Figure D6.2.

The failure causes are shown in blue, the resulting failure mode in green and subsequent pathway to ultimate pipe failure in purple. Ultimate pipe failure is shown in red.

The failure event tree can be used as a tool; e.g. detection of outer sheath damage often leads to a review and assessment of corrosion and fatigue issues. However, as can be seen in the below chart, also the carcass collapse failure mode may be triggered, which may lead to ultimate pipe failure directly or through pressure sheath failure. The result should be that also this failure mode is taken into account when assessing the new risk level subsequent to the outer sheath damage.

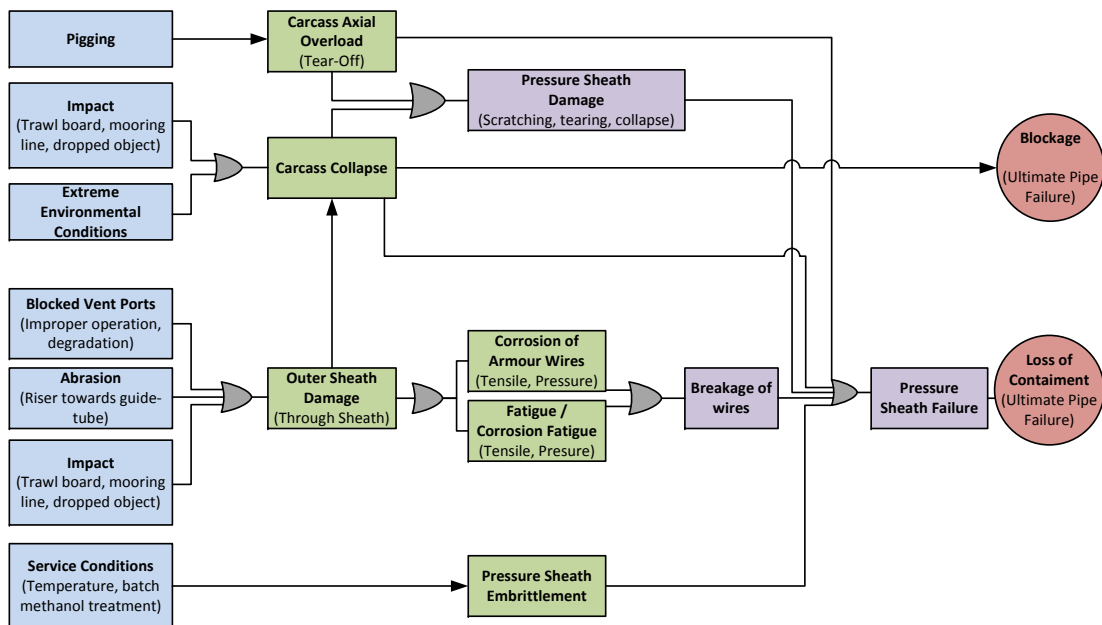


Figure D6.2: Failure Event Tree for Selected Failure Modes

### D6.4.2 Unmitigated Risk Level

Risk level associated with no implemented control mechanisms are shown in Table D6.6 - i.e. summary of above sections.

Table D6.6: Risk Level - Unmitigated

Failure Mode	Probability (Failure Mode)	Probability (Ultimate Pipe Failure)	Safety	Environment	Cost (million EUR)	Risk Level
Carcass Collapse	Very low	Very Low	No or superficial injuries	Massive effect, Large damage area, >100 BBL	>10	M
Carcass Axial Overload	Very low	Very Low	No or superficial injuries	Slight effect on the environment, <1 BBL,	>10	M
Pressure Sheath Embrittlement	Medium	Medium	Multiple fatalities	Massive effect, Large damage area, >100 BBL	>10	VH
Tensile Armour Wire Fatigue	Medium	Low	Multiple fatalities	Massive effect, Large damage area, >100 BBL	>10	H
Outer Sheath Damage	High	High	Multiple fatalities	Massive effect, Large damage area, >100 BBL	>10	VH

Three failure modes are presenting unacceptable high risk level due to probability for ultimate pipe failure to occur. It is required to implement control mechanisms - as suggested in previous sections.

### D6.4.3 Mitigated Risk Level

The mitigated risk level is shown in Table D6.7; note that the probability for the failure mode to occur is static. The probability for ultimate pipe failure is however reduced due to the implementation of control mechanisms.

Table D6.7: Risk Level - Mitigated

Failure Mode	Probability (Failure Mode)	Probability (Ultimate Pipe Failure)	Safety	Environment	Cost (million EUR)	Risk Level
Carcass Collapse	Very low	Very low	No or superficial injuries	Slight effect on the environment, <1 BBL,	>10	M
Carcass Axial Overload	Very low	Very low	No or superficial injuries	Slight effect on the environment, <1 BBL,	>10	M
Pressure Sheath Embrittlement	Medium	Very Low	Multiple fatalities	Massive effect, large damage area, > 100 BBL (loss of containment)	>10	M
Tensile Armour Wire Fatigue	Medium	Very Low	Multiple fatalities	Massive effect, large damage area, > 100 BBL (loss of containment)	>10	M
Outer Sheath Damage	High	Very Low	Multiple fatalities	Massive effect, large damage area, > 100 BBL (loss of containment)	>10	M

An important note is that the risk level is no less than Medium. The fact that cost of replacement is high drives the risk level. Cost effectiveness is therefore driven by avoiding premature replacement of riser system, to be further improved through an optimization in regards to cost of control mechanism implementation.

### D6.4.4 Control Mechanisms

Table D6.8 summarizes the identified control mechanisms to be implemented based on the performed review. There are separate tables for periodic activities and event-based activities.

Table D6.8: Integrity Management Plan - Event Based Control Mechanisms

Control Mechanism / Failure Mode Reference	Carcass Collapse	Carcass Axial Overload	Pressure Sheath Embrittlement	Tensile Armour Wire Fatigue	Outer Sheath Damage
Annulus Vent Flow Monitoring			X		
Annulus Free Volume Measurement	X				X
Anomaly Reporting		X		X	X
Dropped Object Reporting and Survey					X
Gauge Pigging	X				
Pressure Monitoring	X				

The installation phase is critical towards elevated failure probability. However the methods implemented are assumed to be able to detect critical and initiated defects - mainly through verification of an intact outer sheath and through the gauge pigging. The main safeguard is in any event installation procedures and the strict adherence to those.

Following any events that may impact the riser system integrity, an important safeguard is anomaly reporting. This is to ensure that any anomaly is properly assessed and addressed. This is valid for both installation-, commissioning- and operation phase of the system service life.

Annulus vent flow monitoring is not an initially required control mechanism, however may be utilized if damages are suspected or if high-risk degradation levels of the pressure sheath are reached.

The periodic control mechanisms are implemented both to have a solid data foundation and to detect those event, condition or time-based degradation modes not immediately discovered in day to day operation. Status assessments provide an important safeguard by ensuring that there is an active follow-up of the riser system, both detection of new anomalies, proper follow up of existing ones and tracking of historical data and events.

Table D6.9: Integrity Management Plan - Periodic Control Mechanisms

Control Mechanism / Failure Mode Reference	Carcass Collapse	Pressure Sheath Embrittlement	Tensile Armour Wire Fatigue	Outer Sheath Damage
Annulus Flow Measurement				X
Annulus Free Volume Measurement			X	X
Annulus Gas Sampling			X	
Pressure Barrier Coupon Sampling		X		
Pressure Monitoring			X	
Sampling of Bore Fluid		X	X	
Status assessment	X	X		
Status assessment			X	X
Subsea GVI				X
Temperature Monitoring		X		
Topside GVI				X

#### D6.4.5 Implementation

Periodic activities are to be performed according to planned intervals. The time scale is dependent on the period of time from initial layer failure to ultimate loss of pipe function and also on practical considerations. None of the reviewed failure modes relevant for operation, are expected to progress immediately from initial damage to loss of containment.

Necessary time for being added to detect progressing degradation or non-reported events dictates typically semi-annual or annual reviews, testing and inspection in the initial life phase of the life cycle. This is to ensure that the design premises are valid based on operational experience.

In the mid-life phase a decrease in control mechanism scope or increased intervals may be justified based on the provided historical data, e.g. bore fluid composition, coupon sampling, if it can be verified that design premises are conservative.

In the late-life phase typically the risk level will increase due to higher uncertainty in the actual pipe condition compared to design predictions. Additional control mechanisms or detail studies, related to time based degradation modes, may be introduced to ensure that the risk level remains acceptable. Typically this would be a fatigue re-analysis with actual operational parameters (internal pressure, environmental conditions).

## **Chapter D7**

# **Lifetime Assessment of North Sea Riser**

## D7.1 Introduction

The basis for case study lifetime assessment is the handbook Chapters C2 Lifetime Assessment and A3 Failure Modes. This case study section presents a worked example of a lifetime assessment for the North Sea riser according to the workflow presented in referenced chapters.

The basis for the lifetime assessment is an anomaly reported by the Integrity Management (IM) system after being in operation for 5 years. The anomaly relates to suspected outer sheath breach, detected by annulus free volume testing. This triggered a subsea General Visual Inspection (GVI) inspection, confirming outer sheath damage located just below guide-tube exit.

The fundamental basis for performing the lifetime assessment is the below flowchart in Figure D7.1, also presented in Chapter C2 Lifetime Assessment.

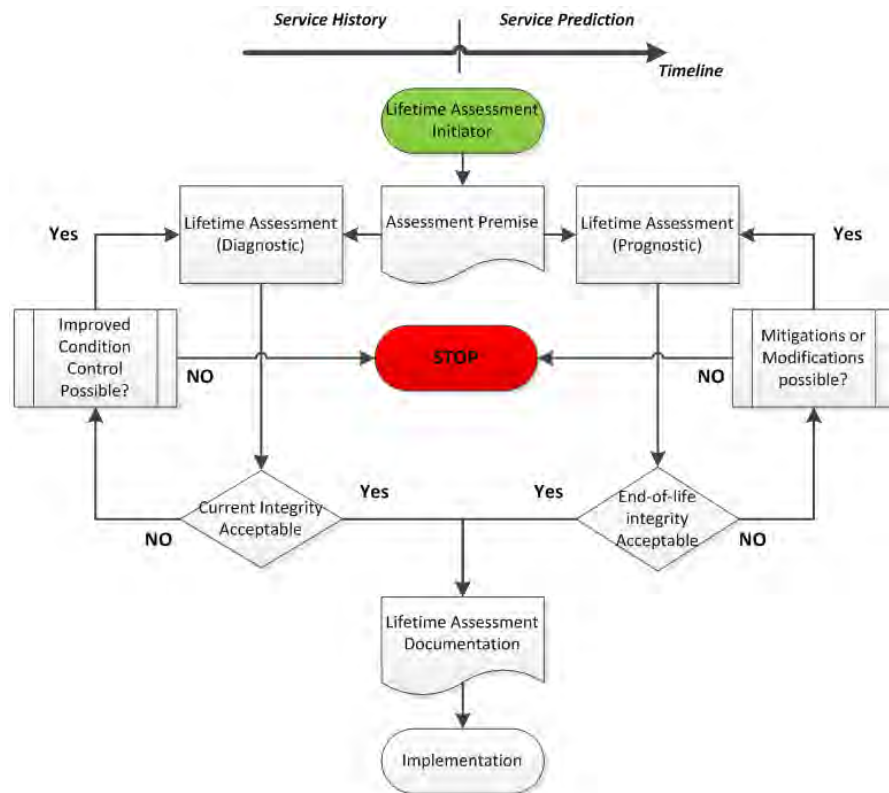


Figure D7.1: Flowchart for lifetime assessment (LTA) process

The review will consider the main steps, (from Figure D7.1), in sequence to verify if the riser can be safely kept in service for the required service life, essentially conclude on the following two questions:

1. Is the current integrity level above acceptance limit?
2. Is the predicted integrity level at end of specified service life, above acceptance limit?

## D7.2 Lifetime Assessment - North Sea Riser Case Study

### D7.2.1 Lifetime Assessment Initiator

The initiator is an anomaly confirmed by subsea GVI. The riser has been annulus tested regularly as required by the IM program, however last test did detect an abnormal changes in annulus free volume.

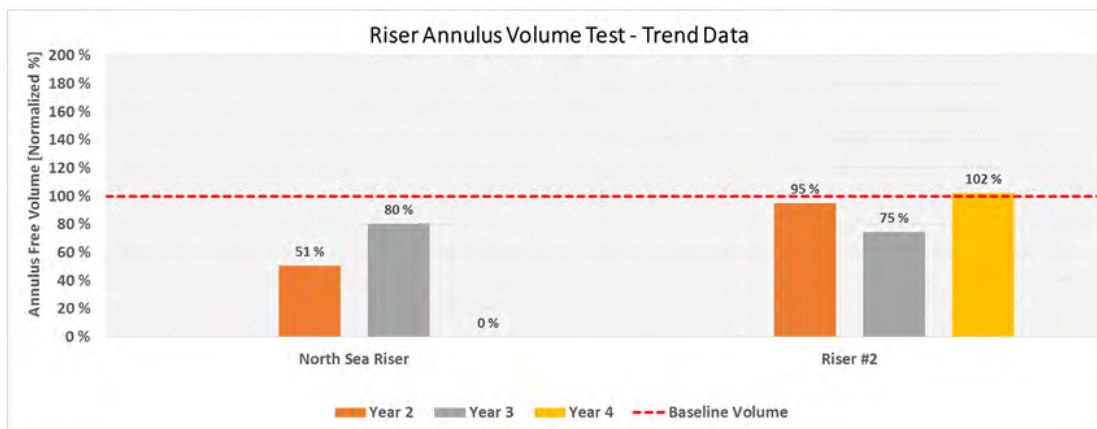


Figure D7.2: North Sea Riser - Annulus Test history (Riser #2 included for illustration purposes - i.e. normal trend data)

The initial test, Year 2, showed approximately 50% free volume compared to theoretical volume. The following year, annulus free volume was found significantly higher at 80%. In the fourth year, annulus pressure could not stabilize during test, i.e. suspected loss of outer sheath integrity - subsequent confirmed by subsea GVI.

This implies that at time of test in Year 3, the outer sheath was intact, while at test in Year 4 it was breached. This information is important for the estimation of a timeframe between damaging event and time for detection. In this example, the period of time between the tests was 401 days or 1.1 years - slightly above the annual period.

Damage details are further investigated by subsea GVI. The damage is characterized by the following:

1. Type: linear, narrow cut damage at 45° towards pipe main axis.
2. Exposure size: minor breach, no directly exposed wires. Approximately 10cm length.
3. Failure Causes: assumed accidental damage by external object.

### D7.2.2 Lifetime Assessment Premise

The assessment premise for the current riser in simplest form consist of the following information:

1. Background Information.
2. Objective Statement.

3. Requirements Statement.
4. Detail Information.
  - (a) Annulus Test reports (all years).
  - (b) Subsea GVI report.
  - (c) Sketch of system / damage location / relevant features.

**Background information** is essentially the compilation of contents in Section [D7.2.1](#)

**Objective statement** could for this case be:

1. Verify if riser system is safe to operate within the required service life of 15 years from year 5.
2. Identify any mitigating actions or modifications to allow operation within required service life.

**Requirements Statement** should include reference to applicable design standard, company guidelines and reporting format. For the current case, normally the original design standard would be utilized. Reporting format is company specific, however should as a minimum include the information required to update risk- and failure event tree charts and IM program.

**Detail Information** is not further included here. This type of information should be available through the IM information management systems.

### D7.2.3 Lifetime Assessment

Initially, the determination of possible failure modes and their relationship is required to proceed with both the diagnostic and prognostic assessment. To ensure that the full line system is analysed, the questioners from Chapter [C2](#), Lifetime Assessment, Section [C2.4](#) are reviewed. Objective is to identify deviations from the original design basis and assumptions, other possible threats to the riser integrity. Given that there is a specific initiator for the assessment, the questions are used as screening tools as compared to what would be the case for a full lifetime extension type assessment.

#### Layer Assessment - Outer Sheath

From Chapter [C2](#), Section [C2.4.4.9](#) 'Outer Sheath' it is evident that layer function is lost, i.e. not providing a barrier towards external environment. This presents a change compared to design assumptions.

Q11.1 presents the following guidance note: 'For any loss of outer sheath integrity, refer to failure description Impact, wear and pressure induced rupture creating hole in the outer sheath (Chapter [A3](#) - Failure Modes)'

Q11.2 'Are there any findings from inspections showing local damages, continuous abrasion or interference with other structures/components' relates to determining the cause of the outer sheath damage to avoid further degradation. By the Remote Operating Vessel (ROV) inspection performed, no interfacing objects, sharp edges or protruding objects were identified. It is thus assumed that the initial assessment of accidental damage from either installation that has progressed into through sheath thickness.

Action: verify requirement for restoring layer function by repairing outer sheath. Note that this is normally a general requirement from flexible pipe vendors in case of outer sheath damages.

#### **Layer Assessment - Insulation Material**

Through questions Q10.1 'Is the measured temperature loss between upstream and downstream end of the flexible pipe system in accordance with design calculations' and Q10.2 'Is arrival temperature sufficient to meet flow assurance requirements' it is verified using temperature monitoring data that there has been no significant change to temperature drop from subsea to topside interface points, and that arrival temperature still meets the requirements. Essentially no impact to existing design assumptions.

#### **Layer Assessment - Anti-Buckling Protection**

The anti-buckling protection is vital if the riser can experience compression. However in the damage area, even if the anti-buckling protection tape was damaged, the riser is only experiencing tension. Essentially no impact to existing design assumptions based on the questionnaire.

#### **Layer Assessment - Anti-Wear Protection**

No remark for the anti-wear protection layers.

#### **Layer Assessment - Tensile Armour**

Q 7.1 'Is annulus environment checked and verified against design assumptions' is negative; the current annulus environment is outside the design specification being flooded. Implications of this needs to be considered and applicable reports updated.

Q 7.2 'Is general corrosion material loss calculation valid based on current/predicted annulus environment': the design premises stated that with dry annulus, any corrosion processes were negligible. With the introduction of liquid filled annulus, re-calculations needs to be performed taking into account sweet corrosion. Sour corrosion is not valid given the negligible amounts of H<sub>2</sub>S reported from both bore fluid sampling and annulus gas sampling.

Q 7.3 'Are there known outer sheath damage(s) with loss of external barrier and possibility of localized corrosion' is detailed in Section [D7.2.3.2](#) in regards to localized corrosion and possible reduction of cross section capacity.

Q 7.4 'Is utilization ratio at current and end of required service life within limits in [API 17J, 2008] for all design load cases': this needs to be verified as current design premise is invalid.

Q 7.5 'Is accumulated fatigue calculations valid' and Q 7.6 'Is predicted remaining fatigue life sufficient for required service life': this needs to be verified as current design premise is invalid.

Remaining questions are possible to close out as they are either not applicable or can be ruled out.

#### **Layer Assessment - Pressure Armour**

Similar considerations as for the tensile armour wire is applicable.

Action: Corrosion and material loss calculations. See Section [D7.2.3.2](#) and Section [D7.2.3.3](#)

#### **Layer Assessment - Pressure Barrier**

Questions can be closed out as not applicable.

### Layer Assessment - Carcass

Q 3.1 'Is flow rate below design assumption' and Q 3.2 'Is any sand production recorded' needs to be considered due to possible reduction in carcass collapse capacity due to erosion.

Q 3.4 'Are there any internal inspection and/or pigging runs performed' presents the option of performing a pigging run to verify no deformation of the carcass. This must be seen in relationship with most probable damage cause, and thus not selected in this case as pressure monitoring data provides no signals of significant blockage.

#### D7.2.3.1 Failure Event Tree

Finally, reviewing the failure event tree from Section [D6.4.1](#), it can be seen that there are additional triggered failure modes due to an initial outer sheath failure, see Figure [D7.3](#).

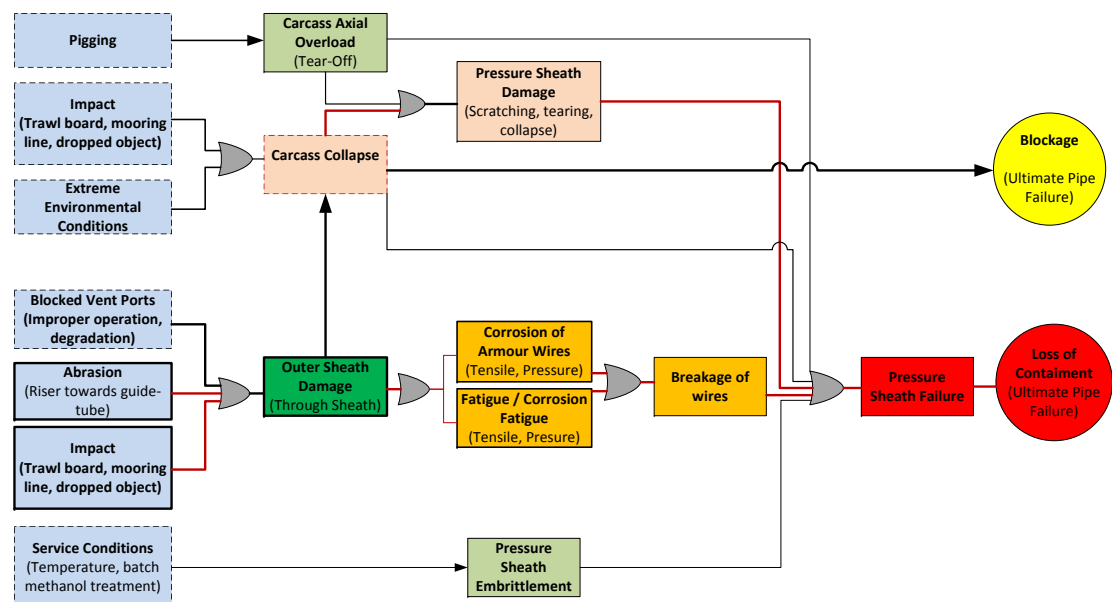


Figure D7.3: Failure Event Tree after outer sheath damage: Red-line indicates pathways to and from experienced failure causes- and modes (full black outline)

These failure modes, in addition to the outer sheath damage failure mode, needs to be considered and reviewed additionally.

#### Summary Actions

1. Verify requirement outer sheath repair
2. Utilization ratios of steel armours due to corrosion (sweet, oxygen)
3. Fatigue service life
4. Review based on failure modes from Chapter [A3](#) Failure Modes
  - (a) Carcass collapse (Verify no reduction in carcass collapse capacity)
  - (b) Corrosion of armour wires
  - (c) Corrosion fatigue / fatigue of armour wires

### D7.2.3.2 Diagnostic

**Carcass Collapse:** Utilizing the monitoring strategies for this failure mode, reviewing data for differential pressures between topside- and subsea sensors versus flow rates/choke settings is performed. There are no identified anomalies, i.e. changes from initial operation phase. The probability for a collapse to have occurred can be considered negligible.

**Corrosion of armour wires:** Corrosion rates depends on several parameters. A key issue for this event is if the cathodic protection system can be considered effective, thus preventing corrosion. Reviewing previous subsea GVI inspection reports provide information on anode status and protection potential - and for the subject riser there are no findings indicating that the CP system is rendered ineffective.

Conservative data may be used to determine consequence of an ineffective CP system for comparison. Corrosion rates are available in several published papers, ranging from near 0.5 mm/year to more generally accepted level of approximately 0.1 mm/year [Clements, 2003].

Using the latter, the current exposure of 1.1 years provide a total corrosion of 0.11 mm from any surface. To perform a calculation of current increase in stress levels the following is assumed:

1. Armour wires only adjacent to damage is corroding - i.e. maximum of 1/4 of total wires.
2. Armour wires subject to corrosion have material loss on both sides, but not at the edges.

Assumption 2 is considered sufficiently conservative when determining reduction of load bearing area, seeFigure D7.4.



Figure D7.4: Tensile Armour Wire - Corrosion Scenarios to assess conservatism in calculation

Figure D7.5 shows results from an axi-symmetric model; design stress levels can thus be compared with worst-case current stress levels:

Only a modest increase in stress level from design state to year 1.1 occurs: a 9 MPa increase. The conclusion is that at current time being, the conservative corrosion scenario does not

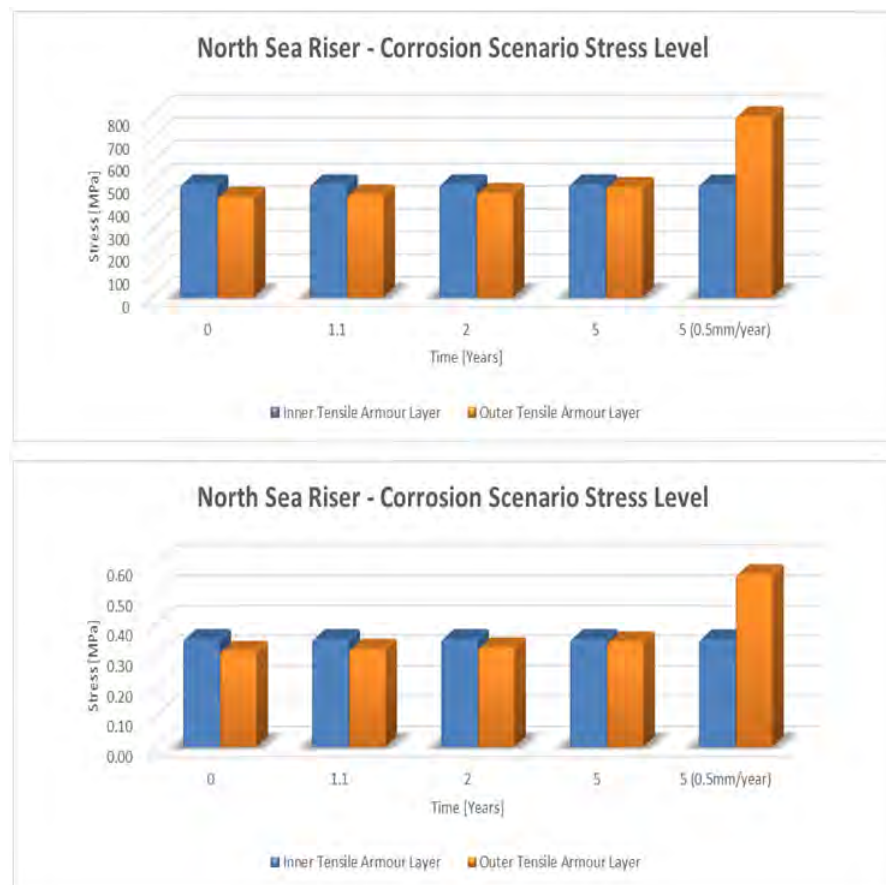


Figure D7.5: North Sea riser: Stress Levels and Utilization Rate versus time. 0.1mm/year corrosion for 1/4 of the tensile armour wires in outermost layer.

impose any threats to the riser cross section, even at design pressures. As the current operational pressure is significantly lower, approximately 85 bar compared to design pressure of 420 bar, the margin towards unacceptable utilization rates is significant - using 0.5 mm/year corrosion rate it is evident that only after year #5 one is nearing the limiting utilization ratio of 0.67.

Note that this is only considerations based on static stress values to assess the criticality of current exposure time. The conclusion is that the outer sheath damage does not impose an immediate risk to continued operation, given the surplus capacity of the cross section.

**Corrosion fatigue / fatigue of armour wires:** Corrosion fatigue or pure fatigue damage accumulation is a time-based degradation mode. The failure mode is always present for dynamic risers. For a riser where the original fatigue service life was calculated based on a dry annulus environment, the presence of an outer sheath breach, with subsequent both annulus flooding and possible direct oxygen corrosion, accelerates the fatigue damage accumulation due to a more severe SN-curves that needs to be considered.

The original design fatigue calculations showed a considerable surplus fatigue life capacity. Figure D7.6 can be used to assess the criticality of the new annulus conditions.

From Figure D7.6, it is evident that if the CP system is ineffective, only 7 years of fatigue life is available. Taking into consideration that standards prescribe a safety factor of 10 as

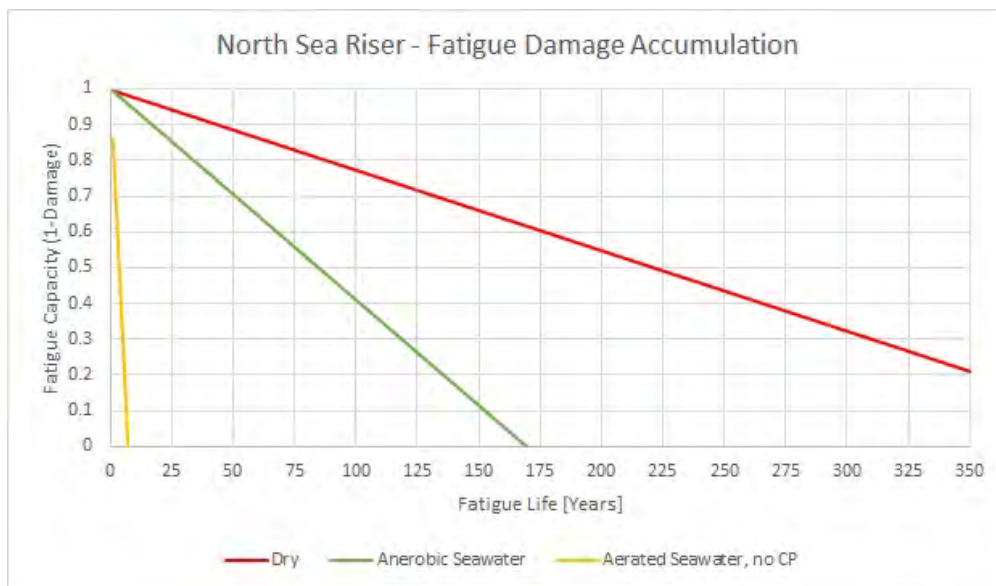


Figure D7.6: North Sea riser: Fatigue damage accumulation versus time. NOTE: Fatigue Life is Fatigue Service Life  $\times$  SF=10

the steel armours are not inspectable, only 0.7 years of service life would be available.

Given that the CP system is shown to be functioning, it is evident that a significant gain is to be expected. Given the damage type, the uncertainty of CP system effectiveness some distance away from the actual damage, using the anaerobic seawater curve is the selected curve. This conservative assumption shows expectations of close to 17 years of fatigue service life.

A gain in service life is expected by the fact that the riser has been operating at a significantly lower pressure than assumed in design premises. Combined, the conclusion is that the outer sheath breach does not impose an immediate threat to the riser integrity given the short exposure time.

#### D7.2.3.3 Prognostic

**Carcass collapse:** There is no identified change to risk level over the whole service life due to

1. Design integrity provides margin between hydrostatic pressure and collapse resistance of carcass.
2. There is no recorded active time dependent degradation promoters, i.e. sand production resulting in erosion or other corrosive processes, which both could be reducing the load capacity of the carcass layer.

As such the failure mode is considered to have no impact on the service life of the riser - based on no change from current operational parameters, refer to Section D6.3.1.8. I.e. the failure mode is considered negligible also for the future service lifetime of the riser.

**Corrosion of armour wires:** From Figure D7.5 it is evident that repair will be necessary to avoid reaching limiting utilization ratios due to general corrosion. There is time to perform

the repair within the indicated timeframe of 1 year from discovery, without any significant further accumulation of damage. The increase in stress level is 17 MPa or a corresponding increase in utilization ratio of 0.01.

From the layer assessment there is an additional requirement to verify if other corrosion processes, considered negligible in the design due to dry annulus, now will present a future integrity risk. Performing material loss calculations based on public domain or vendor specific methodology should be performed. For the current riser this relates to sweet corrosion processes due to CO<sub>2</sub> present in bore gas, permeating into annulus. Sour corrosion is considered negligible. Through this analysis it is found that sweet corrosion is acceptable, if current design levels of CO<sub>2</sub> in transported oil remains stable.

**Corrosion fatigue / fatigue of armour wires:** Provided that a repair is performed, the fatigue life chart in Figure D7.6 shows that approximately 17 years of service life may be available. To properly verify the remaining service life, fatigue re-analysis might be required to be performed. This can take into account actual historic operating pressures, time with annulus in dry condition, exposed to seawater due to outer sheath breach and flooded annulus but with outer sheath integrity restored and expected future service conditions, i.e. operating pressure.

For the current riser, increased stress levels due to material loss (sweet corrosion) is expected, requiring a re-analysis. This is discussed in Chapter D8 of this Case Study. It is assumed a successful outcome - providing the minimum required additional 15 years of service life.

#### D7.2.4 Lifetime Assessment Conclusion

The lifetime assessment conclusion is that:

1. The current integrity level is acceptable, allowing continued operation while repair is performed
2. The end-of life integrity level is acceptable, without need for major modifications or repair

This is only valid if performing the outer sheath repair to restore the outer sheath integrity. The option of postponing or avoiding repair may be interpreted as possible based on the above chapters. However, considering that there are possibilities for severe local corrosion and armour wire pitting, with subsequent introduction of higher SCFs, the option is not viable given the lack of accurate inspection tools.

Documentation of the lifetime assessment should include a final report, based on Chapter C2 - Lifetime Assessment, Section C2.2.7.

This would, for this limited assessment:

1. Anomaly close-out report.
  - (a) Description of assessment initiator and assessment premise.
  - (b) Conclusions on lifetime assessment:
    - i. Acceptable integrity level at current time and for required service life.
  - (c) Recommendations to Integrity Management program.

- i. Repair of outer sheath within 1 year from damage occurrence.
  - ii. Include new control mechanism: sampling of annulus gas.
  - iii. Update of information management system.
    - A. Integrity Management Plan (risk assessments, failure event tree).
    - B. References to reports provided by the lifetime assessment (below).
2. Updated riser service life report(s).
    - (a) utilization rate calculations for steel armours due to material loss.
    - (b) fatigue service life of steel armours for flooded annulus condition.



## **Chapter D8**

### **Reliability**

In the following, the basis for reliability analyses related to fatigue lifetime of specific flexible riser configurations is elaborated. Initial reliability calculations are also performed. Focus is on the tensile helix. The fatigue damage due to the combination of wave action and dynamic floater motion is considered.

An 'imaginary case' without repair being performed is also considered for the purpose of comparison. The applied failure criterion corresponds to fatigue failure of a single wire in the tensile helix.

## D8.1 Probabilistic Models and Reliability analysis

### D8.1.1 Introduction

In general, design criteria related to the different types of limit states need to be considered. These apply to the Serviceability, Ultimate, Fatigue and Accidental Limit States.

In the following, the possibility of fatigue failure for the tensile armour is focused upon since this is critical in relation to assessment of remaining lifetime.

### D8.1.2 Relevant failure functions

The failure function corresponding to fatigue accumulation for constant annulus conditions is first considered. The effect of experiencing changing conditions after a certain time in operation (e.g. stepwise change of corrosive environment) will subsequently be addressed. Designating the randomized Miner sum at failure by  $X_1 = X_{Fail}$  and the accumulated damage at time  $T$  by  $D(T; X_2, X_3 \dots X_N)$ , the failure function  $g(X_1, X_2, \dots, X_N)$  is expressed as:

$$g(T; X_1, X_2 \dots X_N) = g(T; X) = X_1 - D(T; X_2, X_3 \dots X_N) \quad (\text{D8.1})$$

Failure occurs if this function becomes negative, i.e. when the accumulated damage is larger than the Miner sum which corresponds to failure.

The probability of failure for a specified time in operation is then obtained as the probability that the failure function becomes negative, i.e.:

$$p_f(T) = P(g(T; X_1, X_2 \dots X_N) < 0) = P[\{X_1 - D(T; X_2, X_3 \dots X_N)\} < 0] \quad (\text{D8.2})$$

This probability can then be computed for a sequence of increasing values of the time in operation, i.e.  $T_{op} = T = k \cdot \Delta T$  where  $k$  is a positive integer and  $\Delta T$  is a specified time increment.

In the case that a change of the annulus conditions occur (e.g. due to fluid diffusion, sheath damage or clamp repair), the cumulative probability distribution of the accumulated damage at the given point in time when the change occurs (e.g.  $t_{c,0}$ ) needs to be found. This can be obtained by application of the following expression:

$$F_D(d; t_{c,0}) = P(D(t_{c,0}; X_1, X_2 \dots X_N) < d) = P[\{D(t_{c,0}; X_2, X_3 \dots X_N) - d\} < 0] \quad (D8.3)$$

The corresponding density function  $f_D(d; t_{c,0})$  is then obtained by differentiation.

For the time period following  $t_{c,0}$ , the failure probability can be obtained by conditioning on the probability for a specific value of the damage at  $t_{c,0}$  to be present, and by subsequently integrating over all possible such values:

$$\begin{aligned} p_f(T) &= P(g(T; X_1, X_2 \dots X_N) < 0) \\ &= \int_{0 \leq v=D(t_{c,0}) \leq 1} P(\{X_1 - D(T; X_2, X_3 \dots X_N)\} < 0 | D(t_{c,0}) = v) \cdot f_D(v; t_{c,0}) dv \end{aligned} \quad (D8.4)$$

For the case with a damaged sheath followed by repair with a clamp, this expression needs to be applied twice: First for the time interval after damage up to the repair is performed, and secondly for the time period after the clamp is installed.

### D8.1.3 Random variables and probabilistic models

Initially, only the variability related to the Miner sum and the relevant SN-curve is considered. The former variability is modeled by representing the Miner sum as a Lognormal variable with a mean value of 1.0 and a coefficient of variation equal to 0.3. The SN-capacity is given on the form  $N(\Delta S)^m = C$  where  $N$  is the number of cycles until failure;  $m$  and  $C$  are material constants and  $\Delta S$  is the stress range. On logarithmic form this relationship can be written as follows:

$$\log_{10} \Delta S = -\frac{1}{m} (\log_{10} N - \log_{10} C) \quad (D8.5)$$

The SN-curve uncertainty is modeled by representing the SN-curve intercept (i.e.  $\log_{10} C$ ) as a Gaussian random variable. The mean value of the intercept corresponds to the mean SN-curve. The design curve (which corresponds to the case that  $C = \bar{a}$  as given above) is hence obtained by applying the mean value minus two standard deviations (i.e. a parallel shift of the SN-curve in Log-Log-scale).

The randomness associated with the  $CO_2$  condition is somewhat increased as compared to that implied by Figure D2.4. This is modelled by keeping the design curve constant and 'lifting' the mean curve. The reason for this increase of variability is to be more aligned with the 'in-air' uncertainty representation.

For both annulus conditions, three different levels of randomness (SN-curve 'uncertainty') are applied. The term 'Base Case' refers to the middle level of variability. The 'high level' corresponds to an increase of the standard deviation (i.e. which is associated with the intercept as just explained) for the Base Case by a factor of 2.0. The 'low level' corresponds to a decrease of the standard deviation by applying a factor of 0.5.

#### D8.1.4 Analysis method

The probability of failure is computed by application of the so-called First Order Reliability Method (FORM). This approach consists of two main steps: (i) Transformation of the basic variables and the failure function into standard Gaussian variables (ii) Computation of the minimum distance from the origin to the failure surface (i.e. the surface corresponding to the failure function being equal to zero). This distance is then directly applied for estimation of the failure probability. Further details of this procedure are given e.g. in [Madsen et al., 1986] and [Thoft-Christensen and Baker, 1982].

#### D8.1.5 Acceptance criteria

Relevant target reliability levels for metallic risers are given e.g. in [DNV-OS-F201, 2010]. It is reasonable to apply the same target values also for flexible risers if a single type of potential failure mode dominates for a given cross-section. Regarding the target failure probability levels, these can be determined by means of a risk assessment approach. The requirements related to the target probability level in the above-mentioned document depend on the applicable Safety Class which varies from 'Low' through 'Normal' to 'High'. The categorization into class is made based on the type of fluid which is conveyed by the riser and assessment of consequences. The probabilities are given as 'probability of failure per year per riser'. For the three Safety Classes the values are  $10^{-3}$ ,  $10^{-4}$  and  $10^{-5}$ . Here, these values are assumed to correspond to the failure probability per year for the most critical location and the most critical layer, which presently is the tensile armour. For the upper part of the present riser it appears that Safety Class High is relevant due to the conveyed fluid being gas under high-pressure.

### D8.2 Assessment of remaining SN-lifetime

#### D8.2.1 Introduction

Different scenarios are now considered in relation to estimation of fatigue lifetime for the present riser. These correspond to the following cases:

Table D8.1: Summary of scenarios for estimation of fatigue lifetime of tensile armour.

	<b>Scenario</b>	<b>Variables</b>	<b>Annulus condition</b>	<b>Average pressure</b>
A	Undamaged, benign conditions	SN-Curve*	In-air	Operation pressure 300 bar
B	Undamaged, corrosive	SN-Curve	Corrosive with CO <sub>2</sub>	Operation pressure 300 bar
C	Undamaged, monitored pressure	SN-Curve	Corrosive with CO <sub>2</sub>	Recorded pressure, avrg = 115 bar
D	Damaged, repaired	SN-Curve	Seawater w/ inhibitor	Recorded pressure = 85 bar (at time of damage)
E	Damaged, un-repaired	SN-Curve	Corrosive with seawater	Recorded pressure = 85 bar (at time of damage)
F	Undamaged, monitored pressure	Multiple**	Corrosive with CO <sub>2</sub>	Recorded pressure, avrg = 115 bar

	Scenario	Variables	Annulus condition	Average pressure
G	Damaged, repaired	Multiple	Seawater w/ inhibitor	Recorded pressure = 85 bar (at time of damage)
H	Damaged, un-repaired	Multiple	Corrosive with seawater	Recorded pressure = 85 bar (at time of damage)

\* SN-Curve variables correspond to Miner sum uncertainty and intercept of SN-curve variability

\*\* The applied variables are given for the different cases in the relevant sections below

For each of the scenarios the effect of increasing and decreasing the variability associated with the applied SN-curve is also considered.

### D8.2.2 Scenario A: Initial assessment: In-air one-slope SN-curve

The case of the in-air curve without any fatigue limit (i.e. the one-slope curve with  $m = 6$ ) is first considered. This is SN curve for the Balmoral riser, as presented in Section D3.3.4, also described in Section D2.6. The cumulative probability of failure versus time in operation is shown in Figure D8.1, where the middle curve corresponds to the base case. Note that presently only SN-related sources of variability are included. (Incremental probability per year is not shown since this value is very low throughout the considered time period)

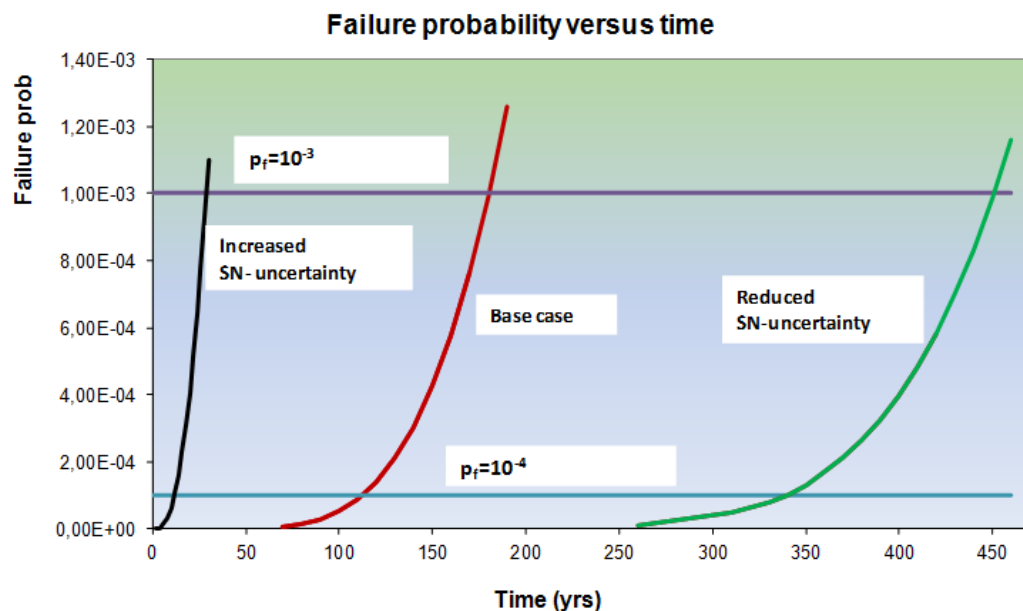


Figure D8.1: Failure probability versus time based on one-slope in-air SN-curve without fatigue limit. Only SN-related variability is included. Middle curve is base case, rightmost curve corresponds to reduced SN-variability, leftmost curve corresponds to increased SN-variability (Operation pressure is 300bar)

The effect of reducing the uncertainty related to the applied SN-curve (e.g. due to testing of a large number of homogeneous test samples) is next investigated by increasing the associated

standard deviation. The mean SN-curve is kept constant while the standard deviation is half of the base case value. This implies that the design curve moves significantly upwards. The corresponding probability of failure versus time is shown as the rightmost curve in Figure D8.1.

The effect of increasing the uncertainty related to the SN-curve is also investigated. The mean SN-curve is still the same, while the standard deviation is now twice the base case value. The resulting probability of failure versus time is shown as the leftmost curve in Figure D8.1.

A summary of the results is given in Table D8.2 for the three different levels of variability associated with the SN-data. (The 'engineering design' procedure for the present base case SN design curve gives a estimated fatigue life of 461 years without any safety factor included.)

Table D8.2: Summary of time in operation until transition between different safety levels occurs corresponding to results in Figure D8.1

<b>SN-data</b>	<b>Years in operation</b>	
	<b>From <math>10^{-5}</math> to <math>10^{-4}</math></b>	<b>From <math>10^{-4}</math> to <math>10^{-3}</math></b>
Half variability	340	450
Base case	75	180
Double variability	12	30

### D8.2.3 Scenario B: Initial assessment: SN-curve for corrosive environment with full operation pressure

It is next assumed that the SN-curve which corresponds to presence of CO<sub>2</sub> applies (i.e. the curve which was shown in Section D2.6, Figure D2.4). The failure probability as a function of time is shown in Figure D8.2. Also for this case only SN-related variability is included. Transition from safety class high to safety class normal occurs at around 70 years. Safety class low is predicted to occur at around 100 years for the present basis of analysis.

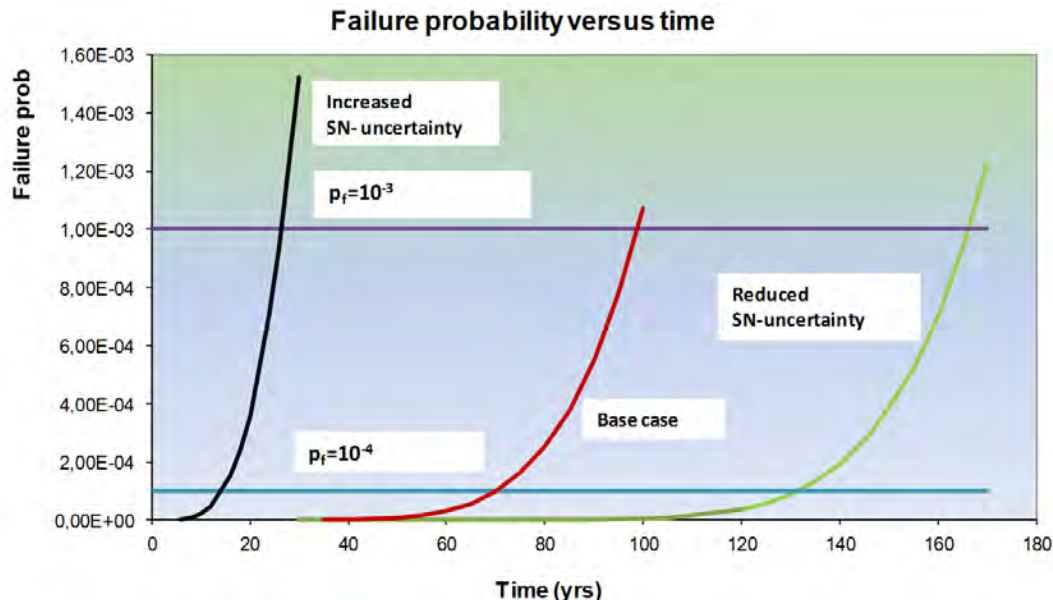


Figure D8.2: Failure probability versus time based on SN-curve for CO<sub>2</sub>-corrosive environment. Only SN-related variability is included. Middle curve is base case, rightmost curve is reduced SN-variability, leftmost curve is increased SN-variability (Operation pressure is 300bar)

The effect of both increasing and reducing the variability related to the applied SN-curve is investigated also for this case by increasing/decreasing the standard deviation. The results are given in Figure D8.2 corresponding to the leftmost and rightmost curves, respectively. A summary of the results is given in Table D8.3 for the three different levels of variability associated with the SN-data. (The 'engineering design' procedure for the present base case SN design curve gives an estimated fatigue life of 210 years without any safety factor included.)

Table D8.3: Summary of time in operation until transition between different safety levels occurs corresponding to results in Figure D8.2

SN-data	Years in operation	
	From 10 <sup>-5</sup> to 10 <sup>-4</sup>	From 10 <sup>-4</sup> to 10 <sup>-3</sup>
Half variability	132	167
Base case	70	100
Double variability	12	30

### D8.2.4 Scenario C: Lifetime estimation based on monitored data (i.e.pressure reduction)

As described above, the variation of the operation pressure and the annulus gas content with time has been measured. The average operation pressure is computed as 115 bar based on the available information. This implies that the stress cycle distribution and SN-curve can be updated accordingly. The resulting probability of failure versus time in operation is shown in Figure D8.3 .

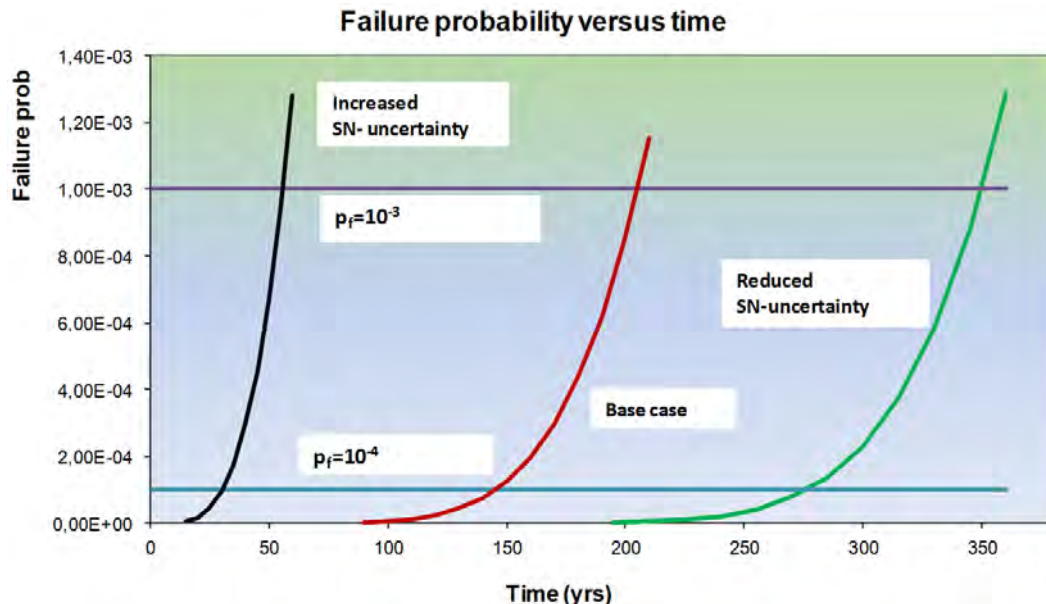


Figure D8.3: Failure probability versus time based on SN-curve for CO<sub>2</sub>-corrosive environment. Only SN-related variability is included. Middle curve is base case, rightmost curve corresponds to reduced SN-variability, leftmost curve corresponds to increased SN-variability (Average operation pressure is 115 bar)

The effect of both increasing and reducing the uncertainty related to the applied SN-curve is again investigated. The results are given in Figure D8.3 in terms of the leftmost and rightmost curves, respectively. The results are summarized in Table D8.4 for the three different levels of variability of SN-data. (The 'engineering design' procedure for the present base case SN design curve gives a estimated fatigue life of 440 years without any safety factor included.)

Table D8.4: Summary of time in operation until transition between different safety levels occurs corresponding to results in Figure D8.3. (CO<sub>2</sub> environment, pressure reduction is accounted for)

SN-data	Years in operation	
	From 10 <sup>-5</sup> to 10 <sup>-4</sup>	From 10 <sup>-4</sup> to 10 <sup>-3</sup>
Half variability	277	350
Base case	145	208
Double variability	31	56

### D8.2.5 Comparison of results for cases without sheath damage - Scenario A - C

A summary of the results for the three cases which correspond to an intact sheath is provided by Table D8.5. It is observed that the case with CO<sub>2</sub> conditions and pressure reduction gives the highest estimated values of the time in operation. The in-air condition (with full operation pressure of 300 bar) gives intermediate values for the same cases, while the CO<sub>2</sub> condition with full operation pressure of 300 bar gives the lowest values.

Table D8.5: Summary of time in operation until transition between different safety levels for different conditions (without sheath damage).

SN-data	Years in operation					
	From 10 <sup>-5</sup> to 10 <sup>-4</sup>			From 10 <sup>-4</sup> to 10 <sup>-3</sup>		
	In air	CO <sub>2</sub>	P-rd/CO <sub>2</sub>	In air	CO <sub>2</sub>	P-rd/CO <sub>2</sub>
Half variability	340	132	277	450	167	350
Base case	75	70	145	180	100	208
Double variability	12	12y	31	30	27	56

It should be noted that the results for the In-air and CO<sub>2</sub> conditions are not directly comparable as the inherent scatter of the SN-curves are different. If the scatter associated with the In-air condition is instead taken to be the same as for the CO<sub>2</sub> condition, the following comparison will result for the Base case (by keeping the mean curve for the In-air condition constant and hence modifying the design curve accordingly):

- (i) Transition from 10<sup>-5</sup> to 10<sup>-4</sup> occurs at 240 years for In-air versus 70 years for CO<sub>2</sub> conditions (i.e. the latter value is the same as before)
- (ii) Transition from 10<sup>-4</sup> to 10<sup>-3</sup> occurs at 340 years for In-air versus 100 years for CO<sub>2</sub> conditions (i.e. the latter value is the same as before).

### D8.2.6 Scenario D: Sheath damage with repair

The contribution to accumulated damage due to the one year period where seawater is present will dominate at the time when the clamp is installed. The expected damage after this one-year period with sea-water (i.e. at  $t = 6$  years) is computed as 0.25. The probability of failure as a function of the time elapsed after the clamp repair has been performed can be computed by application of the expressions given above.

The results are shown in Figure D8.4. The middle curve corresponds to the base case value of the SN-curve scatter, while the leftmost and rightmost curves correspond to increased and decreased values of this scatter, respectively.

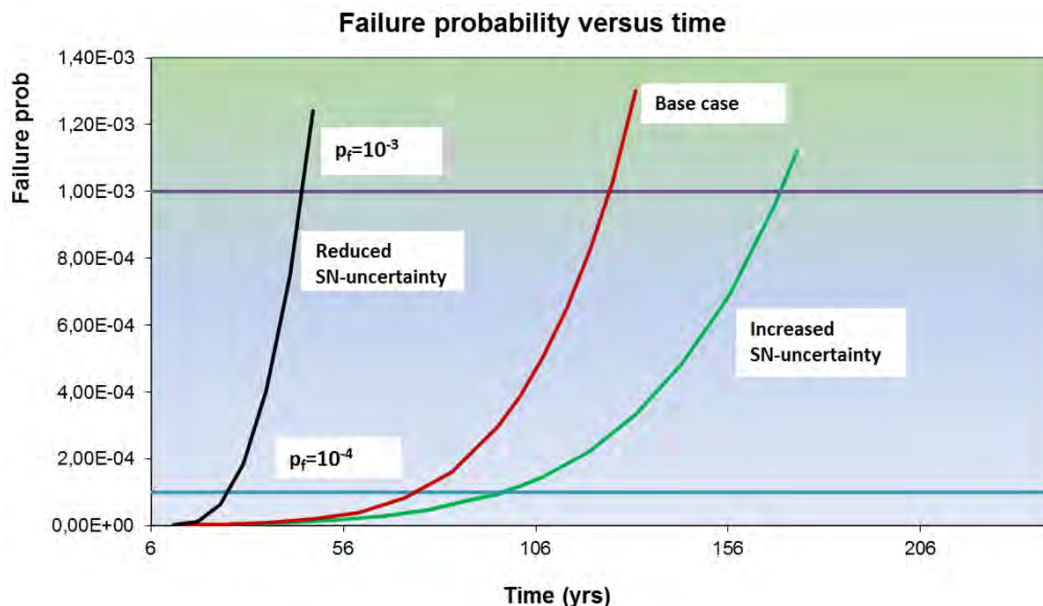


Figure D8.4: Failure probability versus time. Sheath damage occurs at  $t = 5$  years followed by a clamp repair at  $t = 6$  years.

### D8.2.7 Scenario E: Sheath damage without repair

For the case without repair, the expected value of the initial damage at  $t = 5$  years is computed as 0.01 (corresponding to the Base case with CO<sub>2</sub> being present and pressure reduction taken into account) which is negligible. Subsequently, there is a transition to the new SN-curve which reflects that seawater is present. Note that at present the direct effect of corrosion in terms of possible increase of stress concentration is neglected.

The resulting failure probability versus time is shown in Figure D8.5. Corresponding results for the cases with increased and decreased scatter associated with the available SN-data are also shown.

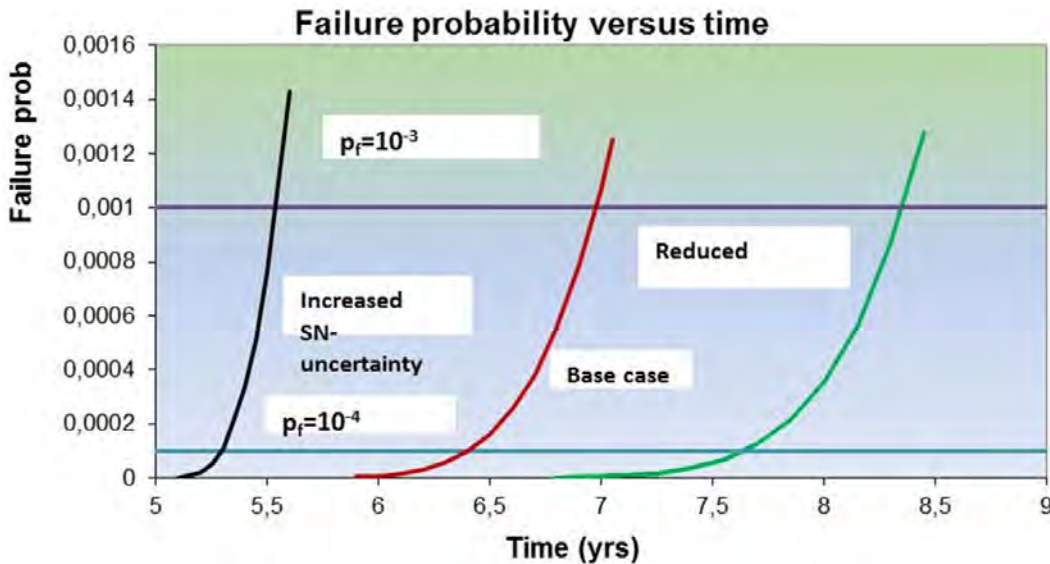


Figure D8.5: Sheath damage at  $t=5$  years without any repair.

A summary of the results is given in Table D8.6 for the three different levels of variability of SN-data. It is observed that for the case without clamp repair, the anticipated residual lifetime is significantly reduced.

Table D8.6: Summary of time in operation until transition between different safety levels for different conditions (with and without repair after sheath damage at  $t = 5$  years).

SN-data	Years in operation			
	From $10^{-5}$ to $10^{-4}$		From $10^{-4}$ to $10^{-3}$	
	With rep.	Without rep.	With rep.	Without rep.
Half variability	97	7.65	170	8.35
Base case	75	6.40	126	6.95
Double variability	26	5.30	45	5.55

### D8.2.8 Comparison of base case results for all scenarios A - E.

A comparison of the curves which show the variation of the failure probability versus time for the different scenarios is provided by Figure D8.6 for the case with solely SN-related variability included. As observed, the scatter of the predicted lifetime increases for increasing probability levels.

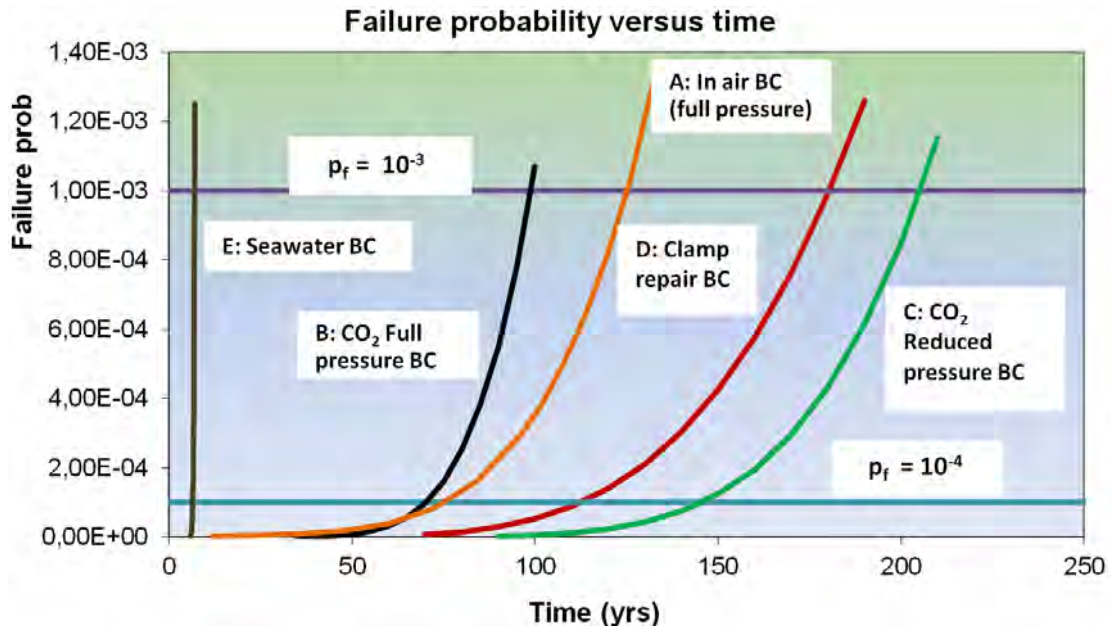


Figure D8.6: Comparison of failure probability as a function of time for the various base case conditions.

### D8.2.9 Scenario F: Carbon dioxide with reduced pressure: Multiple sources of variability.

The effect of including additional sources of variability in the calculations is next considered. This is performed for the following three cases which were considered above:

- CO<sub>2</sub> conditions with reduced pressure
- Sheath damage with repair
- Sheath damage without repair

For all of these three conditions, an identical set of additional random variables are included. These are summarized in Table [D8.7](#).

Table D8.7: Summary of additional random variables for reliability assessment of Case Study.

Variable	Distribution	Base case	Mean value	St.dev.
Drag coefficient	Lognormal	1.0	1.0	0.20
Surface floater surge amplitude, X <sub>s</sub>	Lognormal	1.0	1.0	0.05
Surface floater pitch amplitude, X <sub>p</sub>	Lognormal	1.0	1.0	0.05
Friction coefficient	Lognormal	1.0	1.0	0.10
Internal pressure	Lognormal	1.0	1.0	0.05
Three-dimensional effects load and response effects, X3D**	Normal	1.0	1.0	0.05
Analysis method, global analysis	Normal	1.0	1.0	0.05
Analysis method, local analysis	Normal	1.0	0.9	0.15
Environmental description** <sup>1</sup>	Lognormal	1.0	1.0	0.05

A further description of the methods which are applied for reliability analysis is found in Chapters [B2](#) and [B3](#) of the Handbook. For the five first variables in Table [D8.7](#), parametric variations are first performed such that the fatigue damage is computed for several 'levels' of the relevant quantity (e.g. drag coefficient and surge amplitude). Response surface polynomials are subsequently established based on the computed values of the fatigue damage. These are polynomials are next given as input to the reliability analysis. The four last variables in Table [D8.7](#) are applied in a more direct manner as model uncertainty factors which are multiplied with the computed fatigue damage.

The computed failure probability versus time with these additional variables being included is compared to the base case (i.e. for the case that solely variables which are related to the fatigue capacity parameters are taken into account). This comparison is provided by the leftmost and middle curve in Figure [D8.7](#). It is seen that the transition between the high and normal safety classes now occur at around 92 years (versus 145 years for the base case). The transition between safety class normal and safety class low occurs for 142 years with the additional variables being included (versus 208 years for the base case).

The effect of introducing a certain degree of reserve margin in the description of the external loading is next considered (which leads to more optimistic predictions of remaining lifetime). It has been observed that so-called 3D effects (i.e. lack of colinearity and homogeneity of the physical processes which correspond to the current, wave, wind and floater motion). These

<sup>1</sup>\*\*The variables representing uncertainty related to analysis method and environmental description are assumed to apply for the stress range rather than the fatigue damage. This variable is hence elevated to a power equal to the m-exponent of the SN-curve in the reliability calculations

effects are not captured by the numerical calculation models due to simplifications, and will typically lead to over-estimation of the external loading and the associated riser response. This is taken into account by decreasing the mean value of the computed stresses (i.e. by introducing a bias factor with a value of 0.80 instead of 1.0).

The resulting failure probability versus time is shown by the rightmost curve in Figure D8.7. The transition between safety class high and normal now takes place at around 225 years, and the transition between safety class normal and low occurs at around 345 years.

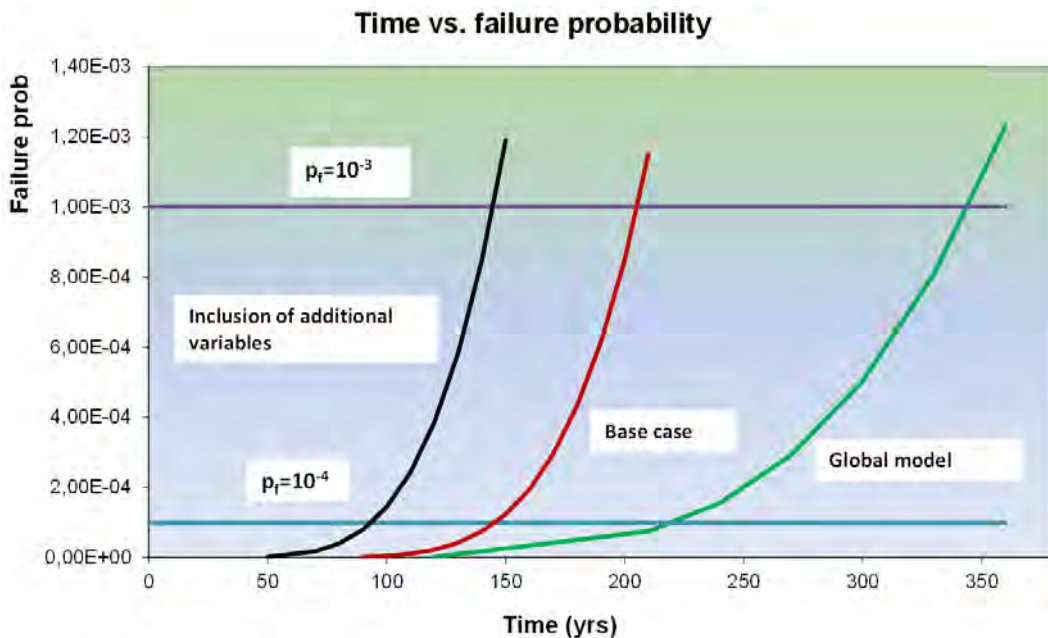


Figure D8.7: CO<sub>2</sub> environment with reduced operation pressure. Results for multiple random variables as compared to solely SN-curve uncertainty (base case). Effect of possible conservatism inherent in global computation model is shown by rightmost curve.

The relative influence of the various random variables on the computed failure probability is measured by the so-called Importance Factors which sum up to a total value of 1.0 (or 100%). For the leftmost curve (and failure probability levels of 10<sup>-3</sup>), the SN-curve uncertainty variable contributes by 48 % and the Miner sum uncertainty by 19 %. The environmental description and the 3D load and response effects each contributes by 9 %. The remaining variables accordingly together contribute by a total of 15%.

For the case with the bias factor of 0.80, the relative importance of the variables is slightly shifted. The SN-curve uncertainty variable now contributes by 46% and the Miner sum uncertainty by 19%. The environmental description contributes by 9% and the 3D load and response effects by 13%. The remaining variables sum up to a contribution of 14%.

The estimated transition times for the three cases shown in Figure D8.7 are summarized in Table D8.8 below.

Table D8.8: Summary of time in operation until transition between different safety levels for different conditions (for the case with CO<sub>2</sub> environment and monitored pressure level).

SN-data	Years in operation	
	From 10 <sup>-5</sup> to 10 <sup>-4</sup>	From 10 <sup>-4</sup> to 10 <sup>-3</sup>
Additional variability	92	142
Base case	145	208
Global model conserv.	225	345

### D8.2.10 Scenario G: Sheath damage with repair: Multiple sources of variability

A corresponding analysis is performed by introducing the additional sources of variability for the case where the sheath has been damaged and with a subsequent clamp repair (with the repair being assumed to have no flaws or defects). The resulting probability of failure versus time is shown by the leftmost curve in Figure D8.8, where also the base case curve is included as the middle curve. Transition from safety class high to safety class normal takes place at around 19 years. Further transition from safety class normal to safety class low occurs at 46 years (The base case values are respectively 36 years and 58 years).

The rightmost curve in Figure D8.8 represents the case where possible conservatism associated with the global calculation model is taken into account. The transition between safety class high and normal is observed at around 63 years, and the transition between safety class normal and low at around 103 years.

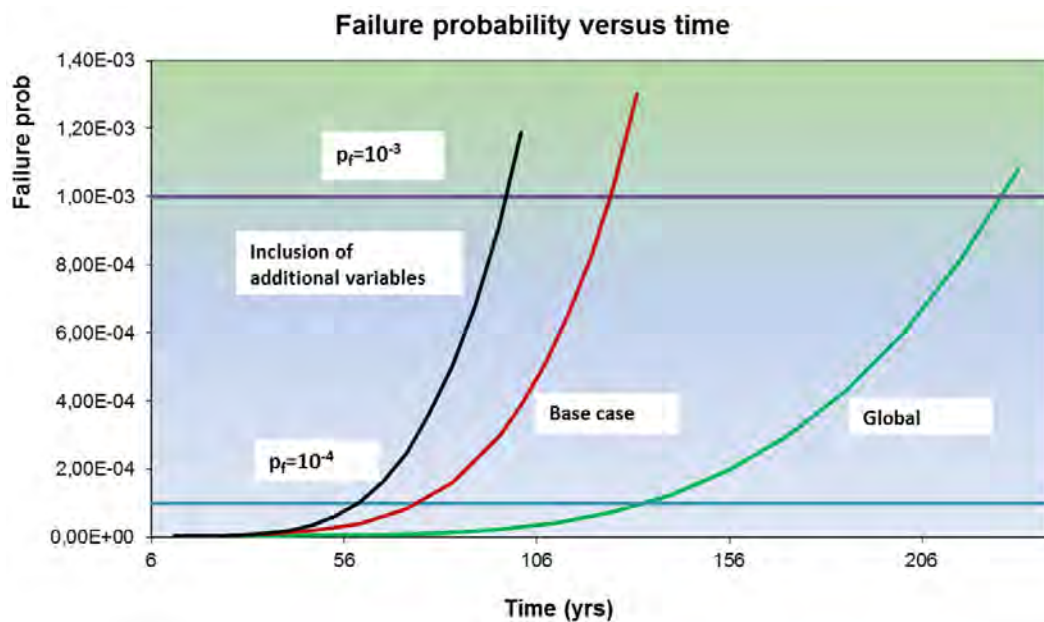


Figure D8.8: Sheath damage with repair. Results for multiple random variables as compared to solely SN-curve uncertainty (base case). Effect of possible conservatism inherent in global computation model is shown by rightmost curve.

The relative importance of the variables is a little modified compared to the previous case (i.e. for a probability level of 10<sup>-3</sup>). The SN-curve uncertainty variable contributes by 35% and the Miner sum variability now accounts for 41%. The environmental description amounts

to 7% and 3D load and response effects to 6%. Hence, the remaining variables give a total of 11%.

For the case with the bias factor of 0.80, the SN-curve uncertainty variable now contributes by 32% and the Miner sum uncertainty by 41%. The environmental description variability amounts to 6% and the 3D load and response effects to 9%. This implies that the remaining variables sum up to a contribution of 12%.

The results for the three cases presented in Figure D8.8 are summarized in Table D8.9 below.

Table D8.9: Summary of time in operation until transition between different safety levels for different cases (for the case with sheath damage followed by clamp repair).

<b>SN-data</b>	<b>Years in operation</b>	
	<b>From <math>10^{-5}</math> to <math>10^{-4}</math></b>	<b>From <math>10^{-4}</math> to <math>10^{-3}</math></b>
Additional variability	60	98
Base case	75	126
Global model conserv.	129	230

### D8.2.11 Scenario H: Sheath damage without repair: Multiple sources of variability

The effect of including the additional random variables is next studied for the case without repair of the external sheath, i.e. with sea-water corrosion. The resulting failure probability versus time is shown by the leftmost curve in Figure D8.9 . Corresponding results for the base case (i.e. by including solely variables associated with the SN-uncertainty) are shown by the middle curve in the figure. The rightmost curve also now provides results when taking into account possible conservatism associated with the global analysis model.

The resulting transition times between the different safety classes are summarized in Table D8.10 for the different cases. It is observed that the values span the range from around 5.9 to around 7.9 years.

The relative ranking of the random variables also now gives results along the same lines as for the previous cases. The SN-curve variability represents % of the total, and the Miner sum contributes by %.

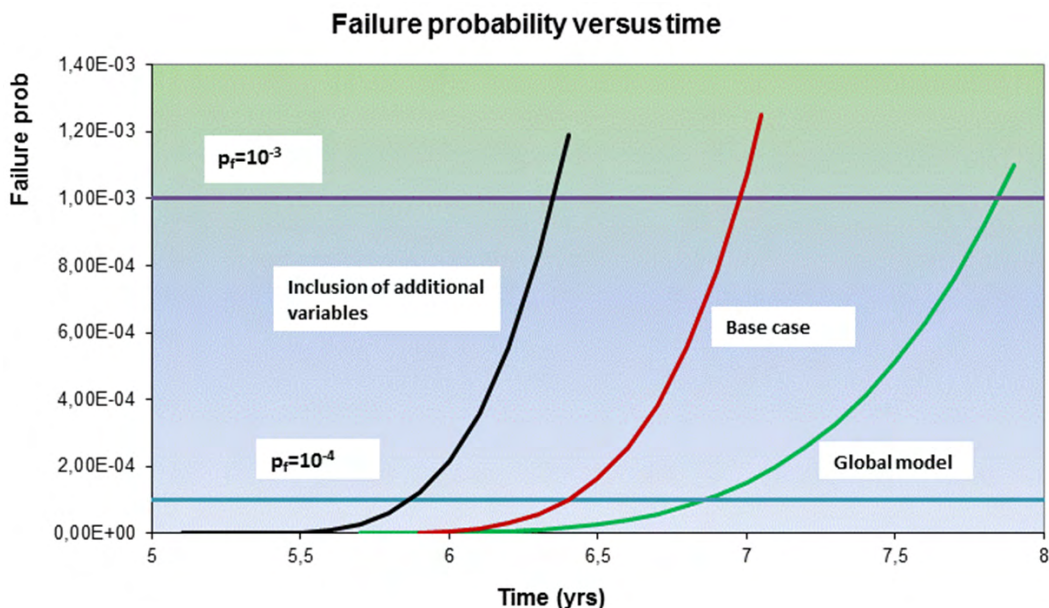


Figure D8.9: Sheath damage at t=5 years without any repair. Results for multiple random variables as compared to SN-curve uncertainty (base case). Effect of possible conservatism inherent in global computation model is shown by rightmost curve.

Table D8.10: Summary of time in operation until transition between different safety levels for different cases (for the case with sheath damage followed by clamp repair).

SN-data	Years in operation	
	From 10 <sup>-5</sup> to 10 <sup>-4</sup>	From 10 <sup>-4</sup> to 10 <sup>-3</sup>
Additional variability	5.9	6.4
Base case	6.4	7
Global model conserv.	6.9	7.9

## D8.3 Consideration of successive wire failures

### D8.3.1 General

If the external sheath which is damaged after 5 years in operation remains unrepaired, the consequence will be a sequence of individual wire failures until failure of the whole cross-section occurs. It is hence highly relevant to estimate the time from seawater ingress until failure of a specific number of wires which corresponds to cross-section failure.

The following analysis is based on application of the results which were obtained from the numerical analysis of a damaged pipe. These results are found in Appendix D9 Section ???. From the analysis it is observed that after failure of the sixth wire, the load-carrying capacity of the cross-section is mainly lost. Accordingly, this is considered to be the failure criterion in the present assessment.

As a result of the successive wire failures, there will be an increase of the stress levels in the remaining wires. This is presently modeled by introducing a stress concentration factor which increases after each wire failure. Based on the numerical study referred to above, a linear increase is presently applied. Following the first wire failure, the stress concentration factor is set to 1.075. Following the second failure, the value is 1.15. After that, the values are 1.225, 1.3 and 1.375, respectively.

### D8.3.2 Correlation properties between pairs of failure events

For analysis of multiple wire failures, the pairwise correlation between the different failure events will play an important role. This correlation depends on variability associated with the load effect versus that of the resistance. This is first demonstrated based on fairly general considerations.

Schematically, the safety margin with respect to fatigue failure for each wire (indicated by the subscript i) can be written on the following form:

$$M_i = D_{Ri} - D_{Si} \quad (\text{D8.6})$$

where the first term is a function of the fatigue capacity variables and the second term is a function of the variables related to the load effect. The safety margin will generally decrease with time, and failure occurs as soon as this margin transits from positive to negative values (i.e. when it becomes zero). If the two terms on the right-hand side are assumed to be independent from each other, the variance of the safety margin is obtained as

$$\text{Var}[M_i] = \text{Var}[D_{Ri}] + \text{Var}[D_{Si}] \quad (\text{D8.7})$$

since the expected value of the cross term, i.e.  $E[\{D_{Ri} - E[D_{Ri}]\} \cdot \{D_{Si} - E[D_{Si}]\}]$ , is zero due to independence. Introducing a safety margin of the same type for a second wire with subscript j, we similarly obtain

$$\text{Var}[M_j] = \text{Var}[D_{Rj}] + \text{Var}[D_{Sj}] \quad (\text{D8.8})$$

The covariance between the two safety margins is next obtained as (by still assuming independence between the resistance and load effect terms):

$$Covar[M_i, M_j] = Covar[D_{Ri}, D_{Rj}] + Covar[D_{Si}, D_{Sj}] \quad (D8.9)$$

The correlation coefficient between the two safety margins is next expressed as

$$\rho_{M_i M_j} = \frac{Covar[M_i, M_j]}{\sqrt{Var[M_i]Var[M_j]}} = \frac{Covar[D_{Ri}, D_{Rj}] + Covar[D_{Si}, D_{Sj}]}{\sqrt{Var[M_i]Var[M_j]}} \quad (\text{D8.10})$$

For the case that the load effect dominates a high value of the correlation coefficient between failure events will be observed since the stress levels in the different wires will be highly correlated (i.e. the first term in the numerator will be large). For the case that the resistance term dominates a low value of the correlation coefficient will result. This is based on the assumption that the resistances of the different wires are uncorrelated and accordingly both terms in the numerator will be small relative to variances in the denominator.

For the present case with a damaged external sheath a quite localized corrosion process is likely to occur. The relevant wires which are most likely to fail due to strength reduction will hence be located in the vicinity of the sheath damage. The corrosion process which takes place in each individual wire is further assumed to be very differentiated. This implies that there will be a low correlation between the remaining strength properties of the different wires.

### D8.3.3 Consideration of possible failure sequences

In the general case, after failure of each wire, there will be a number of wires which are candidates for being the next one to fail. The likelihood for each of the candidates to be the one that really breaks depends on a number of factors such as the initial value of the accumulated damage when the previous wire failed, the future stress level in the particular wire being considered, possible cross-section reduction of the wire and fatigue resistance. A fairly general illustration of the sequence of possible failure events is shown in the Figure D8.10.

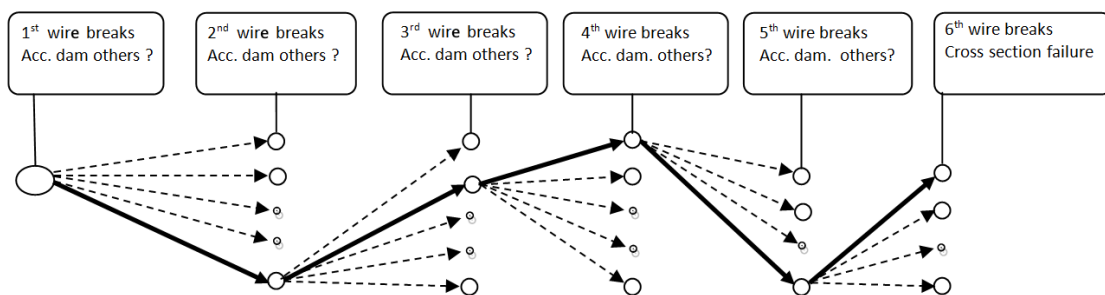


Figure D8.10: Illustration of sequence of individual wire failures.

A simplified failure sequence will result if there is only one possible candidate for the next wire failure after each wire failure event. This is illustrated in Figure D8.11. Accordingly, it is assumed that there is a corrosion process which is progressing from one wire to the next (somewhat depending on the extension of the damage to the outer sheath). For this case, it

is also assumed that the initial magnitude of the accumulated damage (due to cyclic stresses) in the other unbroken wires at the time of failure of one specific wire is of somewhat limited magnitude. Such a sequence is more relevant for the present case where there is a localized damage to the outer sheath of the flexible pipe.

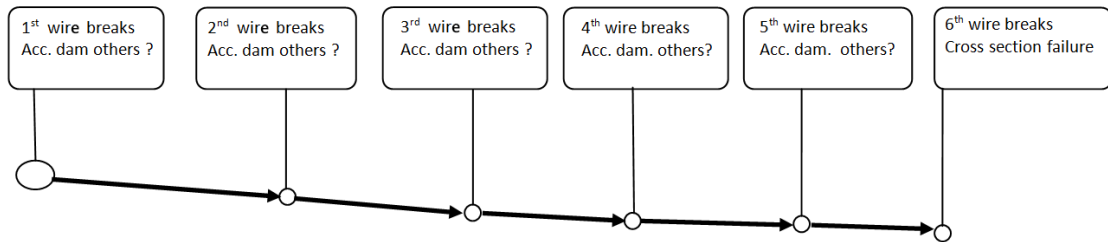


Figure D8.11: Simplified failure sequence with only one potential candidate at each step.

#### D8.3.4 Failure of first wire

By application of the design SN-curve which corresponds to seawater conditions, the time elapsed from seawater ingress until failure of the first wire (which is not necessarily the one with highest stresses) is computed as 4.3 years.

By representing the SN-curve intercept parameter as a random variable instead of as a fixed 'design value', the time until breakage of the first wire also becomes a random variable. The corresponding cumulative distribution is shown in Figure D8.12, where also the Miner sum uncertainty has been included (see Section D8.1.3).

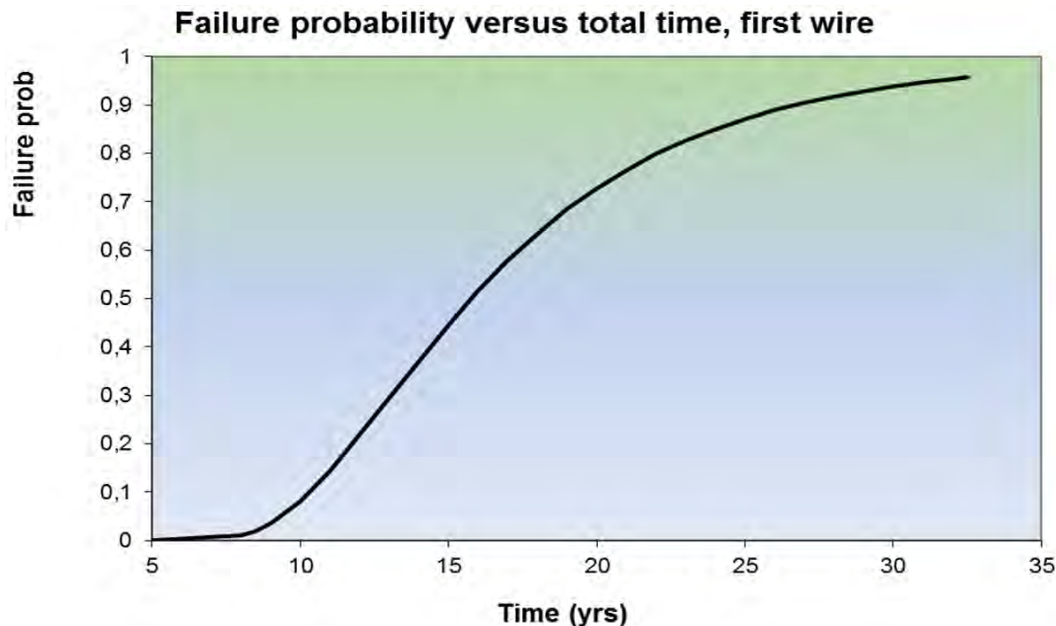


Figure D8.12: Probability distribution of (total elapsed) time until breakage of first wire. Solely SN-curve variability (base case) and Miner sum uncertainty are included. Cumulative distribution is well fitted by lognormal model with mean value of 17 years and standard deviation of 6 years.

From the distribution function it is seen that there is a probability of only around 5% for the time until wire breakage to be less than  $(5 + 4.3)$  years = 9.3 years. In order for this probability to reach 50%, it is seen that the corresponding elapsed time needs to be  $(5+11)$  years = 16 years. It is found that the distribution function is quite well approximated by a lognormal model with a mean value of 17 years and a standard deviation of 6 years.

Clearly, by including additional relevant sources of uncertainty (which are related e.g. to the calculation of stresses in the wires) the probability distribution function for the time period will typically be 'wider' than that shown in Figure D8.12.

### D8.3.5 Failure of second wire

By application of the same design SN-curve as before but now combined with a stress concentration factor of 1.075, the time until failure of the second wire (as measured from the time of failure of the first wire) is computed as 2.2 years. It is noted that this estimate is based on the assumption that the initial accumulated fatigue damage in the second wire at the time of failure of the first wire is equal to zero.

Given that the first wire has failed, the cumulative distribution function for the time until the second wire fails can be computed in a similar manner as for the first wire. However, for the present analysis an initial damage is assumed for the second wire at the time of breakage of the first wire. The defect-driven scenario as discussed above is considered where the correlation between the accumulated damage in the different wires is very low. As a representative example, a value of  $D_{Init} = 0.3$  is applied. The resulting cumulative distribution function is shown in Figure D8.13. It is found that for the present case the distribution function is quite well approximated by a lognormal model with a mean value of 4.5 years and a standard deviation of 2.5 years.

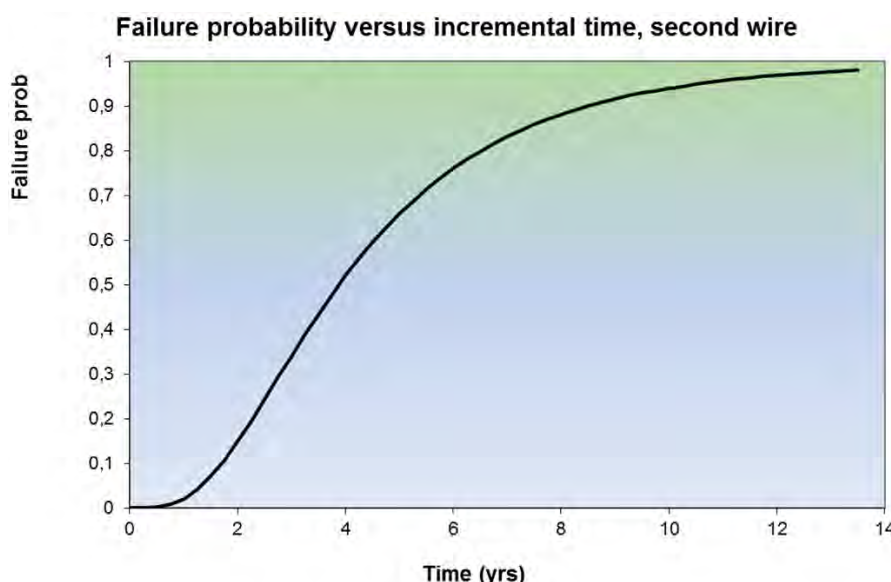


Figure D8.13: Probability distribution of time from breakage of first wire until breakage of second wire, solely SN-curve variability (i.e. the base case level) and Miner sum uncertainty are included.

A cumulative probability of 0.5 is now reached after an elapsed time (with  $t=0$  at the time

of breakage for the first wire) equal to 3.9 years.

The total time (counted from start of operation) until failure of the second wire is found by means of the following expression:

$$\begin{aligned}
 P((T_{b2} = T_1 + T_2) < t_{b2}) &= F_{Tb2}(t_{b2}) \\
 &= \sum_{\text{All } t_1} P(T_2 \leq t_{b2} - t_1 | T_1 = t_1) \cdot P(T_1 = t_1) \\
 &= \int_0^{t_{b2}} P(T_2 \leq t_{b2} - t_1 | T_1 = t_1) \cdot f_{T_1}(T_1 = t_1) dt_1 \\
 &= \int_0^{t_{b2}} F_{T_2}(t_{b2} - t_1 | T_1 = t_1) \cdot f_{T_1}(T_1 = t_1) dt_1
 \end{aligned} \tag{D8.11}$$

where  $t_1$  designates (a specific value of) the time at failure of the first wire and  $t_2$  refers to (a specific value of) the additional time elapsed until breakage of the second wire (i.e. corresponding to the cumulative distribution function in Figure D8.13).

The resulting cumulative distribution function is shown in Figure D8.14. It is seen that the 'width' of the distribution function is somewhat larger than for the distribution functions both in Figure D8.12 and in Figure D8.13. The new mean value and standard deviation of the fitted lognormal distribution are equal to 21.5 years and 6.5 years, respectively.

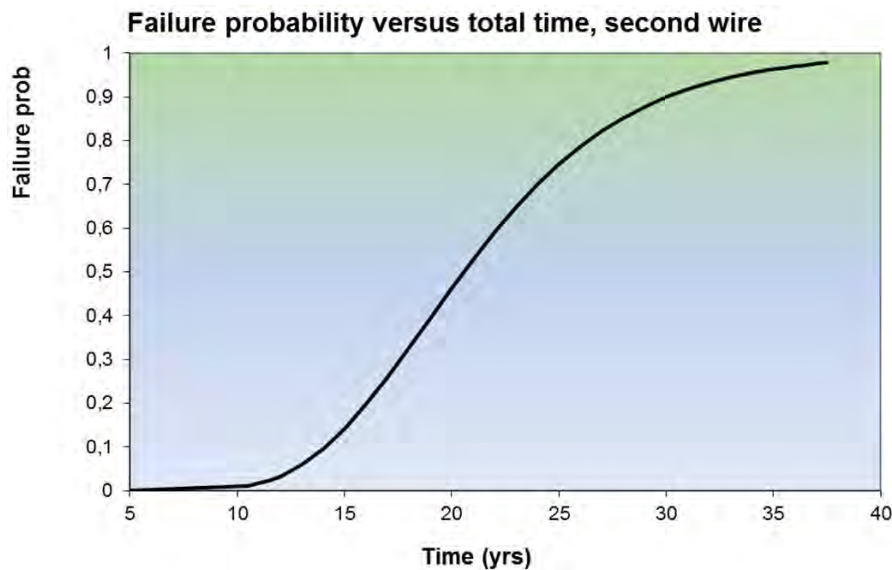


Figure D8.14: Probability distribution of (total elapsed) time until breakage of second wire. Solely SN-curve variability (base case) and Miner sum uncertainty are included. Initial damage in second wire at time of failure of first wire is 0.3. Cumulative distribution is well fitted by lognormal model with mean value of 21.5 years and standard deviation of 6.5 years.

### D8.3.6 Failure of third wire

By application of the design SN-curve for seawater conditions but now combined with a stress concentration factor of 1.15, the time until failure of the third wire (as measured from the time of failure of the second wire) is computed as 1.8 years. This estimate is also based

on the assumption that the initial accumulated fatigue damage in the third wire at the time of failure of the second wire is equal to zero.

By introducing the same random variables and the same initial damage (i.e. 0.3) as for the second wire, the resulting cumulative distribution function which is shown in Figure D8.15 is obtained. It is found that for the present case the distribution function is quite well approximated by a lognormal model with a mean value of 3.7 years and a standard deviation of 2.5 years.

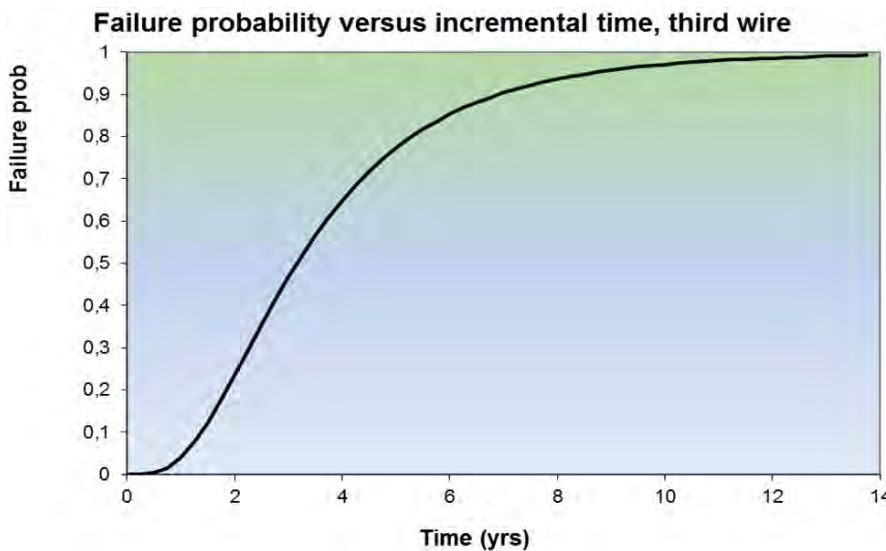


Figure D8.15: Probability distribution of time until failure of third wire, given failure of second wire (assuming that the initial damage in third wire at the time of failure in second wire is 0.3). This distribution is well fitted by a lognormal model with mean value of 3.7 years and standard deviation of 2.5 years.

The cumulative distribution function for the total elapsed time until failure of the third wire (See Figure D8.16 ) is given by an expression of the same type as before:

$$\begin{aligned}
 P((T_{b3} = T_1 + T_2 + T_3) < t_{b3}) &= F_{T_{b3}}(t_{b3}) \\
 &= \sum_{\text{All } t_{b2}} P(T_3 \leq t_{b3} - t_{b2} | T_{b2} = t_{b2}) \cdot P(T_{b2} = t_{b2}) \\
 &= \int_0^{t_{b3}} P(T_3 \leq t_{b3} - t_{b2} | T_{b2} = t_{b2}) \cdot f_{T_{b2}}(T_{b2} = t_{b2}) dt_{b2} \\
 &= \int_0^{t_{b3}} F_{T_3}(t_{b3} - t_{b2} | T_{b2} = t_{b2}) \cdot f_{T_{b2}}(T_{b2} = t_{b2}) dt_{b2}
 \end{aligned} \tag{D8.12}$$

where the second factor is the probability density function for the time until failure of the second wire (which can be obtained by differentiation of the cumulative distribution function that is shown in Figure D8.14).

### D8.3.7 Failure of fourth wire

The stress concentration factor is now increased to 1.225 and the corresponding time until failure of the fourth wire (as measured from the time of failure of the third wire) is computed

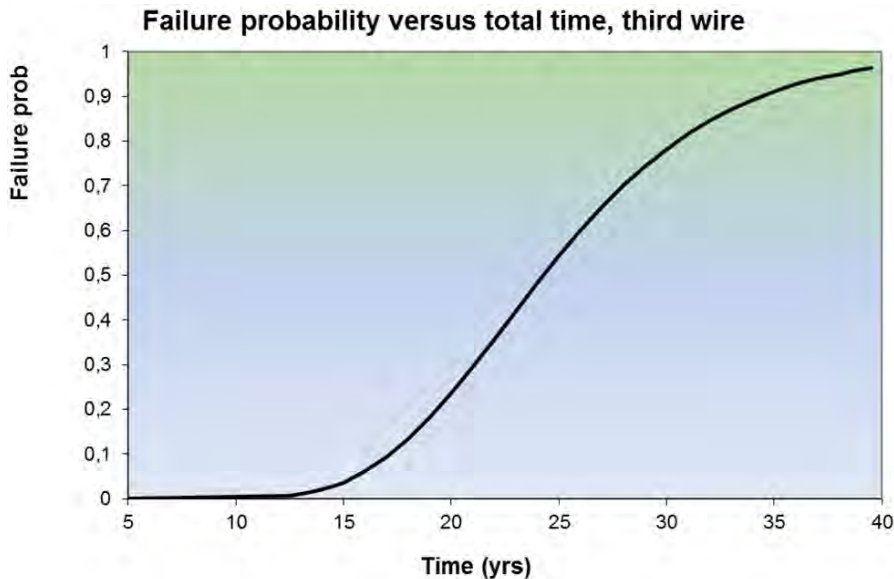


Figure D8.16: Resulting cumulative distribution for time until failure of third wire. Cumulative distribution is well approximated by lognormal model with mean value 25.2 years and standard deviation 7.0 years.

as 1.5 years. This estimate is still based on the assumption that the initial accumulated fatigue damage in the third wire at the time of failure of the second wire is equal to zero.

The same random variables as before are next introduced, while the initial damage is increased to 0.4 (i.e. the damage in the fourth wire at time of failure of the third wire). The resulting cumulative distribution function is shown in Figure D8.17. It is found that for the present case the distribution function is quite well approximated by a lognormal model with a mean value of 2.8 years and a standard deviation of 2.1 years.

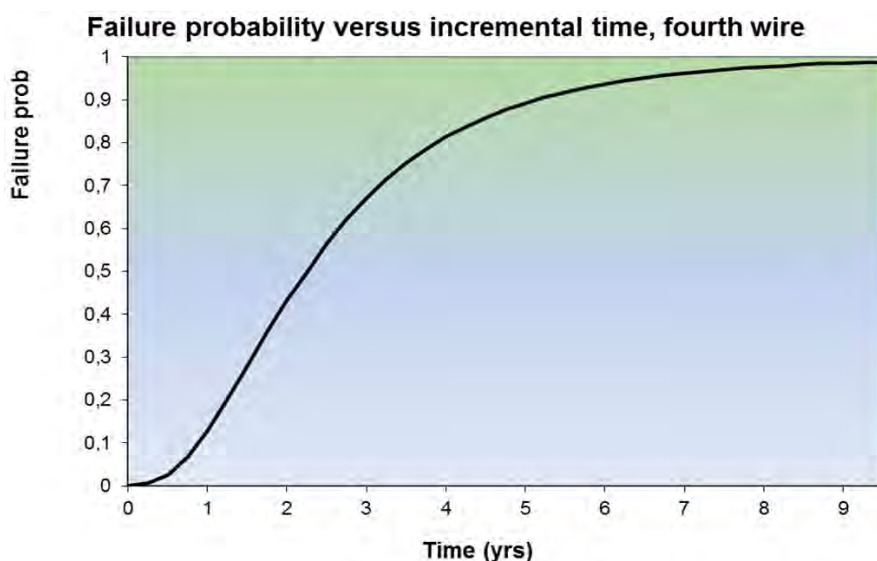


Figure D8.17: Probability distribution of time until breakage of fourth wire, given breakage of third wire. Cumulative distribution function is well fitted by lognormal model with mean value of 2.8 years and standard deviation of 2.1 years.

The cumulative distribution for the total elapsed time until failure is obtained in the same way as before by application of the probability density function for the time until failure of the third wire. Considering the expression for the cumulative distribution of the time until failure of the third wire, all the relevant indices are just incremented by 1 (e.g b2 to b3 and b3 to b4).

The resulting distribution function is shown in Figure D8.18. It is found to be well fitted by a lognormal model with a mean value of 28 years and a standard deviation of 7.3 years.

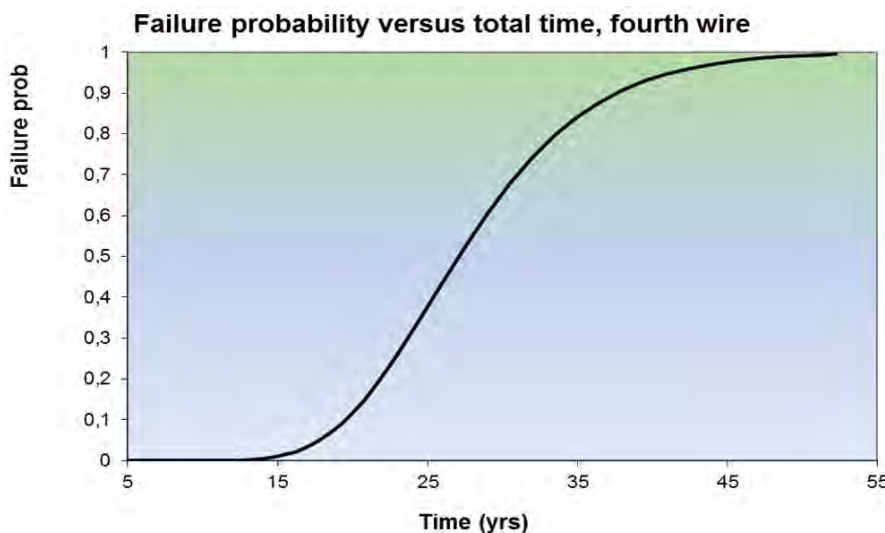


Figure D8.18: Resulting cumulative distribution for time until failure of fourth wire. Cumulative distribution is well approximated by lognormal model with a mean value of 28.0 years and a standard deviation of 7.3 years.

### D8.3.8 Failure of fifth wire

The stress concentration factor is next increased to 1.3 and the corresponding time until failure of the fifth wire (as measured from the time of failure of the fourth wire) is computed as 1.2 years (based on the assumption that the initial accumulated fatigue damage in the fifth wire at the time of failure of the fourth wire is equal to zero).

The same random variables as before are next introduced, while the initial damage is also now equal to 0.4 as for the fourth wire (i.e. the damage in the fifth wire at time of failure of the fourth wire). The resulting cumulative distribution function is shown in Figure D8.19. It is found that for the present case the distribution function is quite well approximated by a lognormal model with a mean value of 2.4 years and a standard deviation of 1.8 years.

The cumulative distribution for the total time until failure is obtained in the same way as before by application of the probability density function for the time until failure of the fourth wire in combination with the cumulative distribution function in Figure D8.19 .

The resulting distribution function is shown in Figure D8.20. This distribution is found to be well fitted by a lognormal model with a mean value of 30.4 years and a standard deviation of 7.5 years.

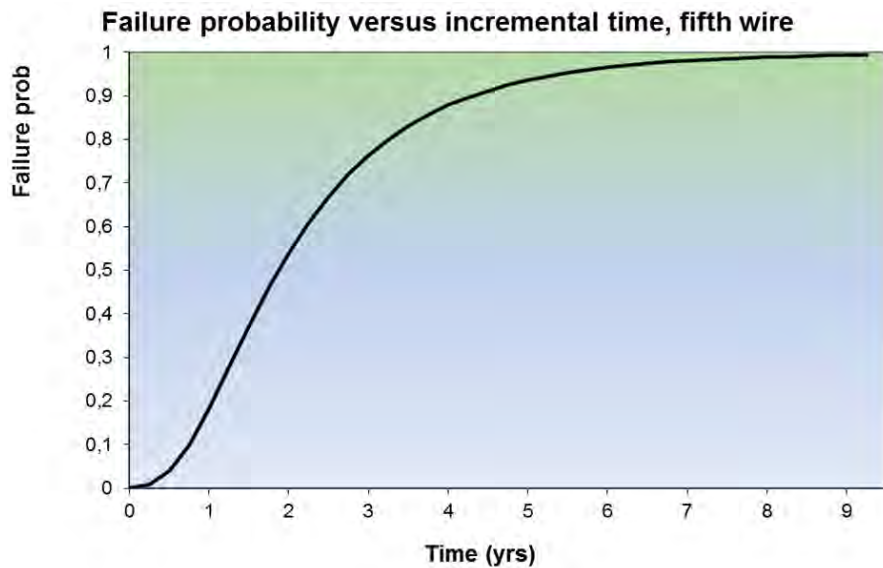


Figure D8.19: Probability distribution of time until failure of fifth wire after failure of fourth wire. Cumulative distribution is quite well fitted by a lognormal model with a mean value of 2.4 years and a standard deviation of 1.8 years.

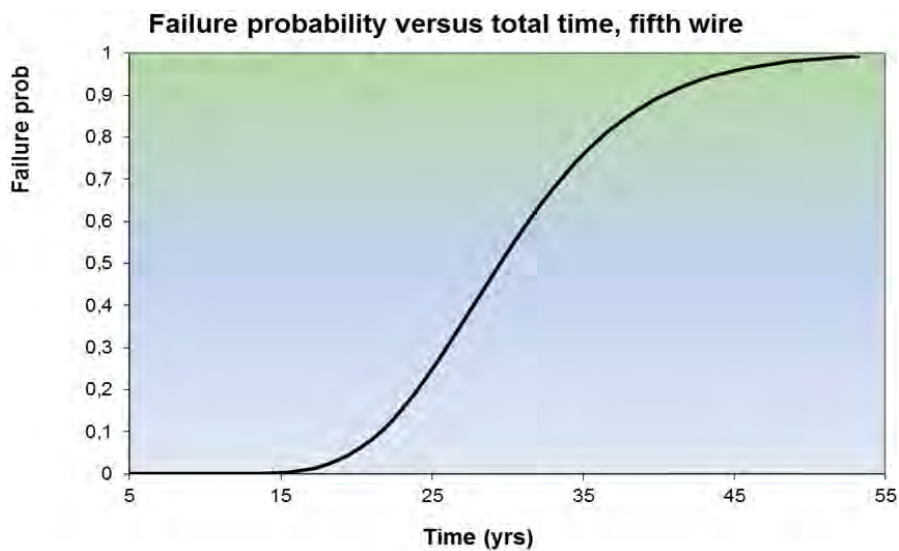


Figure D8.20: Resulting cumulative distribution for time until failure of fifth wire. Cumulative distribution is well approximated by lognormal model with a mean value of 30.4 years and a standard deviation of 7.5 years.

### D8.3.9 Failure of sixth wire

The stress concentration factor is next increased to 1.375 and the corresponding time until failure of the sixth wire (as measured from the time of failure of the fifth wire) is found to be 1.05 years (based on an initial accumulated fatigue damage in the sixth wire equal to zero at the time of failure of the fifth wire).

The same random variables as before are next introduced combined with an initial damage of 0.4 as for the fifth wire. The resulting cumulative distribution function is shown in Figure

[D8.21](#). The distribution function is now quite well approximated by a lognormal model with a mean value of 2.0 years and a standard deviation of 1.7 years.

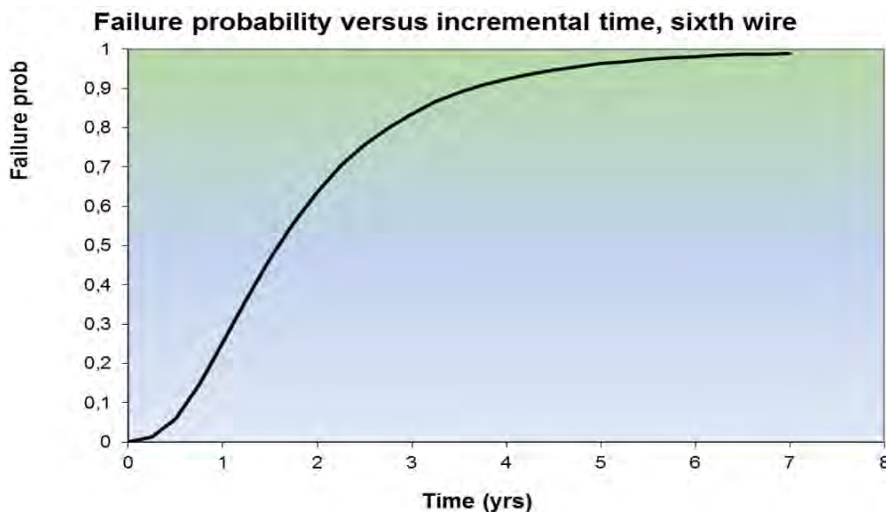


Figure D8.21: Probability distribution of time until failure of sixth wire, given failure of fifth wire. Distribution function is well fitted by lognormal model with mean value of 2.0 years and standard deviation of 1.7 years. (Initial damage in sixth wire at time of failure of fifth wire is assumed to be 0.4)

The cumulative distribution for the total time until failure is obtained in the same way as before by application of the probability density function for the time until failure of the fifth wire in combination with the cumulative distribution function in Figure [D8.21](#).

The resulting distribution function is shown in Figure [D8.22](#). This distribution is found to be well fitted by a lognormal model with a mean value of 30.4 years and a standard deviation of 7.7 years.

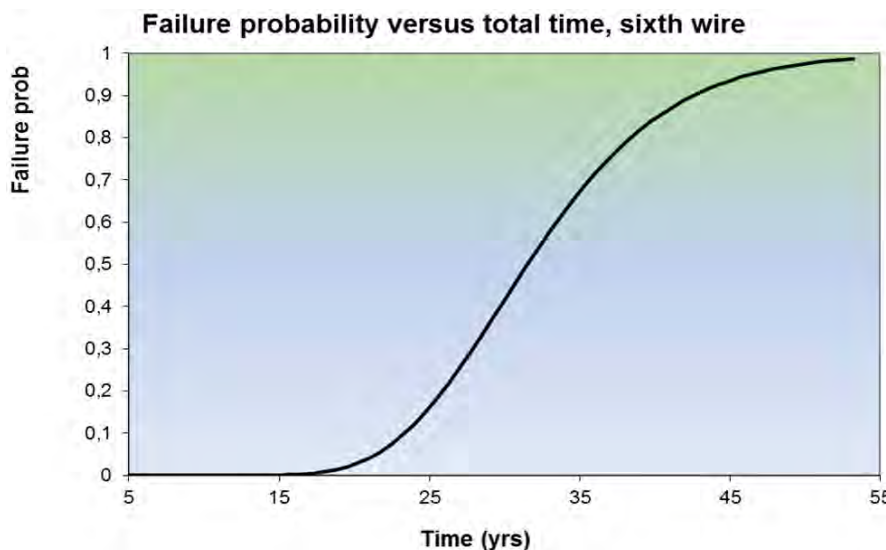


Figure D8.22: Resulting cumulative distribution for time until failure of sixth wire. Cumulative distribution is well approximated by lognormal model with a mean value of 32.4 years and a standard deviation of 7.7 years.

### D8.3.10 Summary of results for sequential wire failure

A summary of the properties of the sequence of cumulative distribution functions for the time until the first, second, third, fourth, fifth and sixth wire failures are given in Table D8.11 below.

Table D8.11: Properties of cumulative distribution functions for total time until sequence of wire failures

Failure in wire number	Mean value [years]	Standard deviation [years]
1	17.0	6.0
2	21.5	6.5
3	25.2	7.0
4	28.0	7.3
5	30.4	7.5
6	32.4	7.7

It is furthermore worthwhile to consider the time until the three probability levels which correspond to safety class high, normal and low are reached for the sequence of wire failures (i.e.  $10^{-5}$ ,  $10^{-4}$  and  $10^{-3}$ ). These values can be directly identified from the sequence of cumulative distribution functions for  $T_{b1}$ ,  $T_{b2}$ ,  $T_{b3}$  and up to  $T_{b6}$ . The results are given in Table D8.12 below. For the purpose of comparison, the corresponding accumulated values based on application of the design SN-curve (also assuming the initial damage in the individual wires to be identical to zero) are also shown in the rightmost column of the table. The resulting factored values which are obtained by application of a safety factor of 10 is also shown in the same column.

An estimate of the time until failure of the sixth wire based on application of the design SN-curve and the given stress distribution (including successively increasing stress concentration factors) is accordingly obtained as  $(4.3+2.2+1.8+1.5+1.2+1.05)$  years = 12.15 years. This exceeds the estimated time until failure for the first wire (i.e. 4.3 years) by almost a factor of 3 (Note: These values do not include the time until sea water ingress occurs, i.e. 5 years).

It is noted that this estimate is based on the assumption of complete independence between the failure events (i.e. breakage) for the individual wires. Accordingly this estimate is based on one conservative assumption (the design SN-curve which represents a lower fractile) and one assumption which is likely to be unconservative (i.e. related to independent failure events). It is further observed that dividing the estimated fatigue lifetimes by a factor of 10 gives a negligible design value of the corresponding residual lifetime of 1.2 years.

Table D8.12: Time until safety levels are reached versus design values

Wire number	Safety level high transition [years]	Safety level normal transition [years]	Safety level low transition [years]	Design SN-curve Factored/unfactored (Note that the common starting point for all time values is at t=5 years)
1	5.8	6.4	7.0	$[(5+0.43)=5.4]/[(5+4.3)=9.3]$
2	6.0	6.8	8.3	$[(5+0.65)=5.7]/[(5+6.5)=11.5]$
3	7.6	9.0	10.5	$[(5+0.83)=5.8]/[(5+8.3)=13.3]$
4	9.2	10.5	12.2	$[(5+0.98)=6.0]/[(5+9.8)=14.8]$
5	10.5	12.0	14.0	$[(5+1.1)=6.1]/[(5+11.0))=16.0]$
6	11.6	13.2	15.5	$[(5+1.2)=6.2]/[(5+12.1)=17.1]$

## D8.4 Concluding remarks

For the Case Study riser configuration reliability analyses are performed for the two cases corresponding to conditions with an intact outer sheath versus a damaged one. In the latter case sea-water is present in the annulus, and conditions corresponding to clamp repair as well as no repair are analysed.

Three different SN-curves which correspond to environments with different corrosive properties are considered. These correspond respectively to in-air conditions, CO<sub>2</sub> conditions without sea-water and subsequently with seawater being present. For the case with CO<sub>2</sub> being present in the annulus, the effect of applying the monitored operation pressure instead of the initial pressure is quantified. This is found to have a strong influence on the predicted remaining lifetime of the riser.

Statistical scatter associated solely with available SN-data is first taken into account. The effect of including additional sources of uncertainty is subsequently investigated. The time until transition between the different safety levels is found to decrease significantly, although the variability related to SN-related uncertainty still dominates the picture.

An assessment of the probabilistic characteristics for the time from seawater ingress until possible cross-section failure is performed based on consideration of a sequence of multiple wire failures. For the case that there is low correlation between the individual wire failures (e.g. due to a defect-driven failure process) it is found that there is a significant effect related to single versus multiple wire failure events.

Statistical scatter associated solely with available SN-data is first taken into account. The effect of including additional sources of uncertainty is subsequently investigated. The time until transition between the different safety levels is found to decrease significantly, although the variability related to SN-related uncertainty still dominates.



## **Part E**

# **Abbreviations, Units and Constants**



## **Chapter E1**

## **Abbreviations**

*Author: 4Subsea, SINTEF Ocean, NTNU*

## Abbreviations

Table E1.1: Abbreviations

AISI 304	Stainless steel grade
AISI 316	Stainless steel grade
API	American Petroleum Institute
APL	Advanced Production and Loading, the company is now part of National Oilwell Varco
A&R	Abandon and Recover
ASME	American Society of Mechanical Engineers
AUV	Autonomous underwater vehicle
CALM	Catenary Anchor Leg Mooring
CAPEX	Capital Expenditures
CIV	Corrected Inherent Viscosity
CoF	Consequence of failure
CoG	Centre of gravity
CP	Cathodic Protection
CRA	Corrosion Resistant Alloy
CVI	Close visual inspection
DEH	Direct Electrical Heating
DFI	Design, Fabrication and Installation
DNV	Det Norske Veritas
EPIC	Engineering Procurement Installation and Commissioning
ESC	Environmental Stress Cracking
ESV	Emergency shutdown valve
EV	Emergency valve
FAT	Factory Acceptance Test
FE FEM	Final Element Method (computational analysis type)
FPSO	Floating Production Storage and Offloading
GI	Gas injection
GRP	Glass Reinforced Polyester
GRV	Gas Relieve Valve
GVI	General visual inspection
HDPE	High Density PolyEthylene
Hs	Significant Wave Height
ID	Inner Diameter
IM	Integrity Management
IMR	Inspection Maintenance and Repair
IMS	Integrity Management System
ISO	International Organization for Standardization
IPB	Integrated Production Bundle
ISU	Integrated Service Umbilical
ITR	Inspection, Test and Repair
JIP	Joint Industry Project
Kp	Kilometer position
LPP	Length between perpendiculars (vessel length measurement)

LTA	Lifetime Assessment
LTE	Life Time Extension
MBR	Minimum Bending Radius
MEG	Mono Ethylene glycol
MWA	Mid Water Arch
NACE	National Association of Corrosive Engineers
NORSOK	Norwegian Standards for the Oil Industry
OD	Outer Diameter
OLF	The Norwegian Oil Industry Association
OOS	Out-Of Straightness
OP	Oil production
OPEX	Operational Expenditure
P&ID	Piping and Instrumentation Diagram Process and Instrumentation Diagram
PA	Polyamide
PA	11 Polyamide 11
PE	PolyEthylene
PLEM	PipeLine End Manifold
PLET	PipeLine End Termination
PMV	Production Master Valve (subsea production trees/manifolds)
PoF	Probability of failure
PSA	Petroleum Safety Authority Norway
PU	PolyUrethane
PVDF	Polyvinylidene fluoride
PWV	Production Wing Valve (subsea production trees/manifolds)
QA	Quality assurance
RAO	Response Amplitude Operator
RFO	Ready For Operation
ROV	Remotely Operated Vehicle
RP	Recommend Practice (used by DNV)
SBM	Single Buoy Mooring, company
SN	Stress range versus number of cycles to failure
SSIV	Subsea Isolation Valve
TAN	Total acid number
TDP	Touchdown Point
TFL	Through Flow Line
TLP	Tension Leg Platform
UHB	Upheaval Buckling
UV	Ultraviolet (radiation)
VDF	Vinylidene Fluoride
WI	Water injection
WL	Water level
WROV	Work- ROV
XLPE	Cross linked Polyethylene
$\gamma_{UR}$	Utilisation related to Upheaval Buckling based on displacement needed to mobilise peak upward resistance
$\gamma_{UF}$	Utilisation related to force required to initiate Upheaval Buckling



## **Chapter E2**

# **Units and Constants**

*Author: 4Subsea, SINTEF Ocean, NTNU*

## Units and Constants

SI units are used for calculations and reporting. However, for the purpose of clarity some imperial units may be used. If not noted otherwise, all units are SI or units derived thereof.

Table E2.1: Units and Constants

Units used	
Length	meter [m]
Force	Newton [N]
Pressure	bar ( $105 \times [N/m^2]$ or 0.1 [Pa])
Mass	kilogram [kg]
Stress	Pascal [Pa] and [MPa] ( $10^6 \times [Pa]$ )
Temperature	[°C]
Viscosity	[mPa· s] (= 1 centipoise [cp])
<b>Constants</b>	
Acceleration due to gravity	9.81 [m/s <sup>2</sup> ]
Density of seawater	1025 [kg/m <sup>3</sup> ], unless otherwise specified.
Density of steel	7850 [kg/m <sup>3</sup> ]
Steel modulus of elasticity	$2.06 \times 10^5$ [MPa], unless otherwise specified.
Poisson's ratio	0.3 [-]

# Bibliography

- [4Subsea, 2013] 4Subsea (2013). Un-bonded flexible risers - recent field experience and actions for increased robustness. Technical report, 4Subsea.
- [A. Engseth, 1988] A. Engseth, A. B. a. M. L. (1988). Efficient method for analysis of flexible risers. *BOSS '88 : proceedings of the International Conference on Behavior of Offshore Structures*, pages 1357–1371.
- [Aage et al., 1999] Aage, C., Bernitasa, M., Choi, H., Crudu, L., Hirata, K., Incecik, A., T. Kinoshita, S. M., and Murray, J. (1999). 22nd ittc report, the specialist committee on deep water mooring.
- [AIChE, 1985] AIChE (1985). American institute of chemical engineers, guidelines for hazard evaluation procedures.
- [Airy, 1845] Airy, G. (1845). Tides and waves. *Encyclopaedia Metropolitana*.
- [Andersen et al., 2001] Andersen, M., Berg, A., and Sævik, S. (2001). Development of an optical monitoring system for flexible risers. In *OTC2001, Houston*.
- [Anderson et al., 2007] Anderson, K., MacLeod, I., and O'Keeffe, B. (2007). In-service repair of flexible riser damage experience with the north sea galley field. In *OMAE*.
- [API 17B, 2008] API 17B (2008). Recommended practice for flexible pipe. Technical Report 4th ed., American Petroleum Institute (API).
- [API 17C, 2010] API 17C (2010). Recommended practice on through flowline (tfl) systems. Technical report, American Petroleum Institute (API).
- [API 17E, 2010] API 17E (2010). Specification for subsea umbilicals. Technical report, American Petroleum Institute (API).
- [API 17J, 2008] API 17J (2008). Specifications for unbonded flexible pipe. Technical report, American Petroleum Institute (API).
- [API 17K, 2005] API 17K (2005). Specification for bonded flexible pipe. Technical report, American Petroleum Institute (API).
- [API 17L1, 2013] API 17L1 (2013). Specification for flexible pipe ancillary equipment. Technical Report 1st ed., American Petroleum Institute (API).
- [API 17L2, 2013] API 17L2 (2013). Recommended practice for flexible pipe ancillary components. Technical Report 1st ed., American Petroleum Institute (API).

- [API 17TR1, 2003] API 17TR1 (2003). Evaluation standard for internal pressure sheath polymers for high temperature flexible pipes. Technical report, American Petroleum Institute (API).
- [API 17TR2, 2003] API 17TR2 (2003). The aging of pa-11 in flexible pipes. Technical report, American Petroleum Institute (API).
- [ASTM D 638, 1977] ASTM D 638 (1977). 10 standard test method for tensile properties of plastics.
- [ASTM E 739, 2004] ASTM E 739 (2004). Statistical analysis of linear or linearized stress-life ( $s-n$ ) and strain-life ( $\epsilon -n$ ) fatigue data.
- [ASTM G 1, 2005] ASTM G 1 (2005). Examination and evaluation of pitting corrosion,.
- [ASTM G 46, 2005] ASTM G 46 (2005). Examination and evaluation of pitting corrosion.
- [Aven, 1992] Aven, T. (1992). *Reliability and Risk Analysis*. Elsevier Science, New York.
- [Back-Pedersen, 1991] Back-Pedersen, A. (1991). *Analysis of slender marine structures*. PhD thesis, The Technical University of Denmark, DTH, Lyngby, Denmark.
- [Bardal, 1994] Bardal, E. (1994). *Korrosjon og Korrosjonsvern, 2dn edition*. Tapir, Trondheim.
- [Bectarte and Coutarel, 2004] Bectarte, F. and Coutarel, A. (2004). Instability of tensile armour layers of flexible pipes. In *Proc. of OMAE'2004*.
- [Berge, 2007] Berge, S. (2007). Test protocol: Corrosion fatigue testing of armour wire for flexible risers. Report 700120.00.01, MARINTEK, Trondheim, Norway.
- [Berge, 2012] Berge, S. (2012). Assessment of sn design curves for tensile armour for flexible risers. Memo 2012-10-01, MARINTEK, Trondheim, Norway.
- [Berge et al., 2003] Berge, S., Bendiksen, E., Gudme, J., and Clements, R. (2003). Corrosion fatigue testing of flexible riser armour – procedures for testing and assessment of design criteria. In *Int. Conf. Offshore Mechanics and Arctic Engineering OMAE, Cancun, Mexico, June 2003*. ASME. OMAE2003-37327.
- [Berge et al., 1992] Berge, S., Engseth, A., Fylling, I., Larsen, C., Leira, B., Nygaard, I., and Olufsen, A. (1992). Handbook on design and operation of flexible pipes. Technical report, SINTEF – Structures and Concrete. ISBN 82-595-7266-4.
- [Berge and Glomsaker, 2004] Berge, S. and Glomsaker, T. (2004). Robust material selection (rms) in the offshore industry – flexible risers. Report MT70 A04–048, MARINTEK, Trondheim, Norway.
- [Berge et al., 2008] Berge, S., Langhelle, N., and Eggen, T. (2008). Environmental effects on fatigue strength of armour wire for flexible risers. In *Int. Conf. Offshore Mechanics and Arctic Engineering*. OMAE2008-57132.
- [Berge and Sævik, 1993] Berge, S. and Sævik, S. (1993). Correlation between theoretical prediction and testing of two 4-inch flexible pipes. In *Proc. Energy-Sources Technology Conference (ETCE), American Society of Mechanical Engineers (ASME)*, Houston, Texas, USA.

- [Berge et al., 2001] Berge, S., Sævik, S., Langhelle, N., Holmås, T., and Eide, O. (2001). Recent developments in qualification and design of flexible risers. In *Proc. of OMAE'2001*, ISBN: 0-7918-3529-4, Rio de Janeiro, Rio de Janeiro, Brazil. ASME.
- [Berger et al., 2011] Berger, J., Franosch, J., Schuett, C., and Dowe, A. (2011). The ageing of offshore polyamides under service conditions in subsea applications. In *OTC Brazil, Rio de Janeiro, Paper 22613*.
- [Binet et al., 2003] Binet, E., Tuset, P., and Mjøen, S. (2003). Monitoring of offshore pipes. In *Proc. OTC, Houston. Paper 15163*.
- [Blevins, 1990] Blevins, R. (1990). *Flow-induced Vibration*. Van Nostrand Reinhold, New York.
- [Bourguet et al., 2011] Bourguet, R., Karniadakis, G., and Triantafyllou, M. (2011). Vortex-induced vibrations of a long flexible cylinder in shear flow. *Journal of Fluid Mechanics*, 90.
- [Brack et al., 2005] Brack, A., Troina, L., and Sousa, J. (2005). Flexible riser resistance against combined axial compression, bending and torsion in ultra-deep water depths. In *Proc. of OMAE'2005*.
- [Braga and Kaleff, ] Braga, M. and Kaleff, P.
- [Breitung, 1984] Breitung, K. (1984). Asymptotic approximations for multinormal integrals. *ASCE, J. Eng. Mech. Div.*, 110:357–366.
- [BS 5760-5, 1991] BS 5760-5 (1991). British standard: Reliability of systems, equipments and components. part 5. guide to failure modes, effects and criticality analysis (fmea and fmeca). Technical report, British Standards Institution, London.
- [Buchner et al., 2007] Buchner, S., Baron, C., Sheldrake, T., and Tullmann, R. (2007). Pa12 for flexible flowlines and risers. In *OMAE 2007, Paper 29615*.
- [Charlesworth et al., 2011] Charlesworth, D., D'All, B., Zimmerlin, C., Remita, E., Langhelle, N., and Wang, T. (2011). Operational experience of the fatigue performance of a flexible riser with a flooded annulus. In *OTC Brasil, 2011, Paper 22398*.
- [Chen et al., 1992] Chen, B., Nielsen, R., and Colquhoun, R. (1992). Theoretical models for prediction of burst and collapse and their verification by testing. In *Flexible pipe technology, Int. seminar on Research and Development 18-20 February, NTH*.
- [Chollet and Do, 2013] Chollet, C. and Do, A. (2013). Qualification of new polyamide for flexible flowlines and risers at elevated pressure and temperature. In *OTC2013, Paper 24019*.
- [Clements, 2003] Clements, A. R. (2003). Corrosion testing of armour wire in simulated annulus environments of flexible pipeline - and update. In *OMAE 2003*, pages OMAE-37473. ASME.
- [Clements, 2008] Clements, R. (2008). Corrosion assessment prediction for a confined flexible pipe annulus. In *EUROCORR*. EUROCORR.
- [Clements et al., 2012] Clements, R., Pires, F., and Gallon, N. (2012). An analysis of the effect of frequency, environment, materials variation and test modes in corrosion fatigue testing of flexible pipe armour wires. In *EUROCORR*. Int. Conf. National Association of Corrosion Engineers (NACE) 2012.

- [Clough and Penzien, 1975] Clough, R. and Penzien, J. (1975). *Dynamics of structures*. McGraw-Hill, New York.
- [Colquhoun et al., 1981] Colquhoun, R., Hill, R., and Nielsen, R. (1981). Principle of normal tail approximation. *ASCE, J. Eng. Mech. Div.*, 107:1191–1208.
- [Colquhoun et al., 1990] Colquhoun, R., Hill, R., and Nielsen, R. (1990). Design and materials considerations for high pressure flexible flowlines. *Advances in Subsea Pipeline Engineering and Technology, Society for Underwater Technology, C.P. Ellinas (ed.)*, 24:357–366.
- [Cook et al., 1975] Cook, R., Malkus, D., Plesha, M., and Witt, R. (1975). *Concepts and Applications of Finite Element Analysis*. John Wiley & Sons, Hoboken, New Jersey, 4 edition.
- [Cornell, 1969] Cornell, C. (1969). A probability-based structural code. *Journal of the American Concrete Institute* 60(12): 974:985., 60(12):974–985.
- [Cosham and Hopkins, 2002] Cosham, A. and Hopkins, P. (2002). The pipeline defect assessment manual. Technical report, Penspen Integrity.
- [Custodio and Vaz, 2002] Custodio, A. and Vaz, M. (2002). A nonlinear formulation for the axisymmetric response of umbilical cables and flexible pipes. *J. of Applied Ocean Research*, 24:21–29.
- [Désamais et al., 2007] Désamais, N., Félix-Henry, A., Taravel-Condat, C., and s, A. D. (2007). Use of high strength steel wires for flexible pipe in low sour service conditions: Impact on deep water applications. In *Proc. International Offshore and Polar Engineering Conference (ISOPE)*, Lisbon, Portugal.
- [Désamais and Taravel-Condat, 2006] Désamais, N. and Taravel-Condat, C. (2006). Full scale corrosion fatigue testing of a flexible pipe in co<sub>2</sub>/h<sub>2</sub>s environment. In *EUROCORR*.
- [Désamais and Taravel-Condat, 2009] Désamais, N. and Taravel-Condat, C. (2009). On the beneficial influence of a very low supply of h<sub>2</sub>s on the hydrogen embrittlement resistance of carbon steel wires in flexible pipe annulus. In *OTC*, Houston.
- [Dawans et al., 1998] Dawans, F., Jarrin, J., and Hardy, J. (1998). Improved thermoplastic materials for offshore flexible pipes. SPE Production Engineering.
- [De Sousa et al., 2011] De Sousa, J., Campello, G., Bueno, A., Vardaro, E., Ellwanger, G., and Strohaecker, T. (2011). On the structural response of a flexible pipe with damaged tensile armor wires. In *OMAE2011, Rotterdam, Netherlands Paper 50113*.
- [de Sousa et al., 2012] de Sousa, J., Viero, P., Magluta, C., and Roitman, N. (2012). An experimental and numerical study on the axial compression response of flexible pipes. *J. of Offshore Mechanics and Arctic Engineering*, 134.
- [de Vecchi et al., 2009] de Vecchi, A., Sherwin, S., and Graham, J. (2009). Wake dynamics past a curved body of circular cross-section under forced cross-flow vibration. *Journal of Fluid and Structures*, 25(ISSN:0889–9746):721–730.
- [Dean, 1965] Dean, R. G. (1965). Stream function representation of nonlinear ocean waves. *J. Geophys. Res.*, 70(18):4561–4572.
- [Dean and Dalrymple, 1984] Dean, R. G. and Dalrymple, R. A. (1984). *Water Wave Mechanics for Engineers and Scientists*. Prentice-Hall, New Jersey.

- [Dixon and Rutledge, 1968] Dixon, D. and Rutledge, D. (1968). Stiffened catenary calculations in pipeline laying problem. *Journal of Engineering for the Industry*.
- [DNV-DSS-401, 2012] DNV-DSS-401 (2012). Service specification: Technology qualification management. Technical report, DNV, Det norske Veritas.
- [DNV-OS-501, 2009] DNV-OS-501 (2009). Composite components. Offshore Standard DNV-OS-501, Det Norske Veritas, Oslo, Norway.
- [DNV-OS-F101, 2007] DNV-OS-F101 (2007). Offshore standard: Submarine pipeline system. Technical report, DNV, Det norske Veritas.
- [DNV-OS-F201, 2010] DNV-OS-F201 (2010). Offshore standard: Dynamic risers. Technical report, DNV, Det norske Veritas.
- [DNV-RP-206, 2008] DNV-RP-206 (2008). Recommended practice: Riser integrity management. Technical report, DNV, Det norske Veritas.
- [DNV-RP-A203, 2012] DNV-RP-A203 (2012). Recommended practice: Qualification of new technology. Technical report, DNV, Det norske Veritas.
- [DNV-RP-B401, 2010] DNV-RP-B401 (2010). Recommended practice: Cathodic protection design. Technical report, DNV, Det norske Veritas.
- [DNV-RP-F103, 2010] DNV-RP-F103 (2010). Recommended practice: Cathodic protection of submarine pipelines. Technical report, DNV, Det norske Veritas.
- [DNV-RP-F107, 2010] DNV-RP-F107 (2010). Dnv recommended practice: Risk assessment of pipeline protection. Technical report, DNV, Det norske Veritas.
- [DNV-RP-F110, 2007] DNV-RP-F110 (2007). Dnv recommended practice: Global buckling of submarine pipelines. Technical report, DNV, Det norske Veritas.
- [DNV-RP-F116, 2009] DNV-RP-F116 (2009). Recommended practice: Integrity management of submarine pipeline systems. Technical report, DNV, Det norske Veritas.
- [DNV-RP-O501, 2007] DNV-RP-O501 (2007). Recommended practice: Erosive wear in piping systems. Technical report, DNV, Det norske Veritas.
- [Do et al., 2013] Do, A.-T., Bernard, G., and Hanonge, D. (2013). Carbon fibre armours applied to presalt flexible pipe developments. In *OTC 24036, Offshore Technology Conference, Houston, USA*.
- [Do and Lambert, 2012] Do, A.-T. and Lambert, A. (2012). Qualification of unbonded dynamic flexible riser with carbon fibre composite armors. In *OTC 23281, Offshore Technology Conference, Houston, USA*.
- [Dugstad, 2006] Dugstad, A. (2006). Fundamental aspects of co2 metal loss corrosion - part i: Mechanism. In *NACE – International Corrosion Conference Series, 2006*.
- [Dugstad, 2013] Dugstad, A. (2013). Private communication with a. dugstad - ?, ife, september 2013.
- [Dupoiron and Taravel-Condat, 2003] Dupoiron, F. and Taravel-Condat, C. (2003). High strength metallic materials for flexible pipes specific environments and corrosion behaviour. In *NACE – International Corrosion Conference Series, 2003*.

- [Ethridge and Cayard, 1997] Ethridge, A. and Cayard, M. (1997). Application of standard ssc test methods for evaluating metallic components of non-bonded flexible pipe. In *NACE – International Corrosion Conference Series, 1997*.
- [Evangelinos et al., 2000] Evangelinos, C., Lucor, C., and Karniadakis, G. (2000). Dns-derived force distribution on flexible cylinders subjected to vortex-induced vibration. *Journal of Fluid and Structures*, 14:429–440.
- [Félix-Henry, 2007] Félix-Henry, A. (2007). Prevention and monitoring of fatigue-corrosion of flexible risers' steel reinforcements. In *OMAE*.
- [Farnes et al., 2013] Farnes, K.-A., Kristensen, C., Kristoffersen, S., Muren, J., and Sødahl, N. (2013). Carcass failures in multilayer pvdf risers. In *OMAE2013*. ASME 10210.
- [Feret et al., 1986a] Feret, J., Bournazel, C., and Rigaud, J. (1986a). Calculation of stresses and slip in structural layers of unbonded flexible pipes. In *Proc. of OMAE'86, New Orleans, USA*.
- [Feret et al., 1986b] Feret, J., Bournazel, C., and Rigaud, J. (1986b). Evaluation of flexible pipes' life expectancy under dynamic conditions. In *OTC5230, Houston, USA*. OTC.
- [Feret and Momplot, 1989] Feret, J. and Momplot, G. (1989). *CAFLEX, Computer program for capacity analysis of flexible pipes, Theory Manual*. SINTEF and IFP, Trondheim, Norway.
- [Fergestad et al., 2017] Fergestad, D., Klæbo, F., Muren, J., Hylland, P., Grøv, T., Lange, H., Gjøsteen, J., Gjendal, A., Melve, B., and Kristensen, C. (2017). An experimental and numerical investigation of the effect of axial thermal gradients in flexible pipes. In *Proc. of OMAE'2017, Trondheim, Norway*.
- [Fergestad et al., 2014] Fergestad, D., Løtveit, S., Berge, S., Sævik, S., Larsen, C., and Leira, B. (2014). Handbook on design and operation of flexible pipes. Technical report, MARINTEK. ISBN 978-82-7174-265-2.
- [Festy et al., 2004] Festy, D., Choqueuse, D., and Leflour, D. (2004). Cathodic protection beneath thick external coating on flexible pipeline. In *EUROCORR., 2004*.
- [Flexlife, 2012a] Flexlife (2012a). Data Sheet for Armadillo EDM.
- [Flexlife, 2012b] Flexlife (2012b). Data Sheet for FlexGel EDM.
- [Fylling et al., 1995] Fylling, I., Larsen, C., Sødahl, N., Ormberg, H., Engseth, A., Passano, E., and Holthe, K. (1995). *RIFLEX Theory Manual*. SINTEF Structural Engineering, Trondheim, Norway.
- [Fylling et al., 1988] Fylling, I., Sødahl, N., and Bech, A. (1988). On the effect of slug flow on the dynamic response of flexible risers and submerged hoses. In *4th International Conference on Floating Production Systems, IBC Technical Services*, London.
- [Garret, 2005] Garret, D. (2005). Coupled analysis of floating production systems. *Ocean Engineering*, 32:802–816.
- [Gudme and Steen Nielsen, 2009] Gudme, J. and Steen Nielsen, T. (2009). Qualification of lean duplex grade lkx 2101 (uns32101) for carcass material in flexible pipes. In *Paper No. 09075, NACE - International Corrosion Conference Series, 2009*.

- [Gumbel, 1958] Gumbel, E. (1958). *Statistics of Extremes*. Columbia University Press, New York.
- [Gurney and Maddox, 1973] Gurney, T. and Maddox, S. (1973). A re-analysis of fatigue data for welded joints in steel. *Welding Research International*, 3(4):1–54.
- [Halse, 1997] Halse, K. (1997). *On vortex shedding and prediction of vortex-induced vibrations of circular cylinders*. PhD thesis, Department of marine structures, NTNU, Trondheim, Norway.
- [Hansen et al., 1988] Hansen, T., Skomedal, N., and Vada, T. (1988). A method for computation of integrated vortex induced fluid loading and response interaction of marine risers in waves and current. In *Proceedings of the International Conference on Behaviour of Offshore Structures (BOSS)*, Trondheim.
- [Hanson et al., 1994] Hanson, T., Otteren, A., and Sødahl, N. (1994). Response calculation using an enhanced model for structural damping in flexible risers compared with full scale measurements. In *International Conference on Hydroelasticity in Marine Technology Trondheim, Norway*.
- [Hasofer and Lind, 1974] Hasofer, A. and Lind, N. (1974). Exact and invariant second moment code format. *ASCE, J. Eng. Mech. Div*, 100:111–121.
- [Haver and Kleiven, 2004] Haver, S. and Kleiven, G. (2004). Environmental contour lines for design purposes – why and when? In *Proc. of OMAE'2004*, pages OMAE2004–51157, Vancouver.
- [Heutier et al., 2001] Heutier, J., Buhan, P. L., Fonatine, E., Cunff, C. L., Biolley, F., and Berhault, C. (2001). Coupled dynamic response of moored fpo with risers. In *Proceedings of the 11th International Offshore and Polar Engineering Conference, Stavanger, Norway*, page 1. ISOPE.
- [Hoerner, 1965] Hoerner, D. S. F. (1965). *Fluid-Dynamic Drag*. Hoerner Fluid Dynamics, Bricktown New Jersey.
- [Hohenbichler and Rackwitz, 1981] Hohenbichler, M. and Rackwitz, R. (1981). Non-normal dependent vectors in structural safety. *ASCE, J. Eng. Mech. Div.*, 107:1227–1258.
- [Hohenbichler and Rackwitz, 1983] Hohenbichler, M. and Rackwitz, R. (1983). First-order concepts in system reliability, structural safety. *Structural Safety*, 1:177–188.
- [Hokstad et al., 2010] Hokstad, P., Håbrekke, S., Johnsen, R., Sigbjørn Sangesland, S. S., Berge, S., B.Skallerud, Eide, O., and Olufsen, A. (2010). Ageing and life extension for offshore facilities in general and for specific systems. Technical report, SINTEF.
- [Huse and Reitan, 1990] Huse, E. and Reitan, O. E. (1990). Handbook for hydrodynamic coefficients of flexible risers. Technical report, MARINTEK, Trondheim, Norway.
- [IEC 60812, 1985] IEC 60812 (1985). Analysis techniques for system reliability – procedures for failure mode and effect analysis (fmea). Technical report, IEC, International Electrotechnical Commission, Geneva.
- [IEEE Standard, 2010] IEEE Standard (2010). Ieee standard for modelling and simulation (m&s) high level architecture.
- [IMO MSC 645, 1994] IMO MSC 645 (1994). Guidelines for vessels with dynamic positioning systems. Technical report, International Maritime Organization.

- [ISO 13628-10, 2005] ISO 13628-10 (2005). Petroleum and natural gas industries – design and operation of subsea production systems – part 10: Specification for bonded flexible pipe.
- [ISO 13628-11, 2007] ISO 13628-11 (2007). Petroleum and natural gas industries – design and operation of subsea production systems – part 11: Flexible pipe systems for subsea and marine applications.
- [ISO 13628-2, 2006] ISO 13628-2 (2006). Petroleum and natural gas industries - design and operation of subsea production systems -part 2: Unbonded flexible pipe systems for subsea and marine applications.
- [ISO/TS 12747, 2011] ISO/TS 12747 (2011). Pipeline life extension.
- [j. Al-Maslamani, 1996] j. Al-Maslamani, M. (1996). Experience with flexible pipe in sour service environment: A case study (the arabian gulf). In *OTC1996*.
- [Ji, 2012] Ji, G. (June 2012). North sea riser-finite element analysis in marc, draft marintek memo.
- [Joel, 2009] Joel, J. (2009). Reinforcing wire corrosion in flexible pipe.
- [Kiureghian and Liu, 1986] Kiureghian, A. D. and Liu, P. (1986). Structural reliability under incomplete probability information. *ASCE, J. Eng. Mech. Div.*, 112(1):85–104.
- [Klust et al., 2011] Klust, A., Vervaecke, F., and Smet, A. D. (2011). Co<sub>2</sub> corrosion resistance of steel cord reinforced thermoplastic materials for flexible pipe systems. In *NACE – International Corrosion Conference Series, 2011*.
- [Korteweg and Vries, 1895] Korteweg, D. and Vries, G. (1895). On the change of form of long waves advancing in a rectangular channel, and on a new type of long stationary waves. *Philos. Magazine*, 39:422–443.
- [Kristiansen et al., 2011] Kristiansen, U., Mattei, P.-O., Pinhde, C., and Amielh, M. (2011). Measurements on tones generated in a corrugated flow pipe with special attention to the influence of a low frequency oscillation. In *34th Scandinavian Symposium on Physical Acoustics*, Geilo, Norway.
- [Krolikowski and Gay, 1980] Krolikowski, P. and Gay, T. (1980). An improved linearization technique for frequency domain analysis. In *Offshore Technology Conference*, Houston.
- [Larsen, 1976] Larsen, C. (1976). *Static and dynamic analysis of offshore pipelines during installation*. PhD thesis, Norwegian Institue of Technology, NTH, Trondheim, Norway.
- [Larsen, 1991] Larsen, C. (1991). Flexible riser analysis, comparison of results from computer programs. *Marine Structures, Elsevier Applied Science*.
- [Larsen, 1992] Larsen, C. (1992). Flexible riser analysis - comparison of results from computer programs. *Marine Structures*, pages 103–119.
- [Larsen and Passano, 1987] Larsen, C. and Passano, E. (1987). Fatigue life analysis of production riser. In *Offshore Technology Conference*, Houston.
- [Larsen and Olufsen, 1992] Larsen, C. M. and Olufsen, A. (1992). Extreme response estimation of flexible risers by use of long term statistics. In *Proc. of ISOPE'92*, pages 202–211, San Fransisco, USA.

- [Larsen and Passano, 1990] Larsen, C. M. and Passano, E. (1990). Extreme response estimation for marine risers. In *Proc. of OMAE'90*, pages 361–369. ASME.
- [Last et al., 2002] Last, S., Groves, S., Rigaud, J., Taravel-Condat, C., Wedel-Heinen, J., Clements, R., and Buchner, S. (2002). Comparison of models to predict the annulus conditions of flexible pipe. In *Offshore Technology Conference (OTC)*, Houston. OTC 14065.
- [Leira and Olufsen, 1992] Leira, B. and Olufsen, A. (1992). Prediction of flexible riser response by the frequency domain method. In *Proc. of the International Offshore and Engineering Conference*, San Francisco, USA. ISOPE.
- [Leira and Remseth, 1985] Leira, B. and Remseth, S. (1985). A comparison of linear and non-linear methods for dynamic analysis of marine risers. In *Behaviour of offshore structures, BOSS*, Delft.
- [Leira, 2009] Leira, B. J. (2009). Assessment of reliability and residual lifetime of flexible risers subjected to time-varying corrosive environments. In *Proc. ESREL2009*, Prague.
- [Leira et al., 2005] Leira, B. J., Igland, R., Baarholm, G., Farnes, K., Nedreliid, K., and Percy, D. (2005). Fatigue safety factors for flexible risers based on case specific reliability analysis. In *Proc. 2005 OMAE*, Halkidiki, Greece.
- [Leira and Mathiesen, 1995] Leira, B. J. and Mathiesen, J. (1995). Reliability-based safety factors for flexible risers. In *OMAE1995*, Copenhagen.
- [Lemos et al., 2008] Lemos, C., Sousa, F., and Sousa, J. (2008). Reliability-based safety factors for flexible risers. In *OMAE2008 Paper 57817*, Estoril, Portugal.
- [Lienhard, 1966] Lienhard, J. (1966). Synopsis of lift, drag, and vortex frequency data for rigid circular cylinders. Technical report, Washington State University.
- [Lienhard, 2010] Lienhard, J. (2010). Dnv-os-f201 dynamic risers. Technical report, Det Norske Veritas, Oslo, Norway.
- [Livesley, 1964] Livesley, P. (1964). *Matrix methods of structural engineering*. Pergamon Press, London.
- [Løtveit and Often, 1990] Løtveit, S. and Often, O. (1990). Limit state design approach for flexible pipes. In *Proc. of NIF Symposium*, NTH, Trondheim. NIF.
- [Madsen et al., 1986] Madsen, H., Krenk, S., and Lind, N. (1986). *Methods of Structural Safety*. Prentice-Hall International, Inc., New Jersey.
- [Marinho et al., 2007] Marinho, M., Camerini, C., dos Santos, J., and Pires, G. (2007). Surface monitoring techniques for a continuous flexible riser integrity assessment. In *OTC2007*. OTC 18946.
- [Mathisen, 1990] Mathisen, K. M. (1990). *Large Displacement Analysis of Flexible and Rigid Systems Consdiering Displacement-Dependent Loads and Non-Linear Constraints*. PhD thesis, Norwegian Institute of Technology, Trondheim, Norway.
- [McNamara and Harte, 1989] McNamara, J. and Harte, A. (1989). Three dimensional analytic simulation of flexible pipe wall structure. In *Proc. of OMAE'89*.
- [MCS Kenny, 2001] MCS Kenny (2001). State of art – flexible riser integrity issues. Report Study report prepared for UKOOA, MCS Kenny.

- [MCS Kenny, 2006] MCS Kenny (2006). Fatigue analysis methodology guidelines. Report Real life JIP, MCS Kenny.
- [MCS Kenny Guidance Note, 2010] MCS Kenny Guidance Note (2010). Guidance note on monitoring methods and integrity assurance for unbonded flexible pipes. Sureflex JIP.
- [MCS Kenny State of the Art, 2010] MCS Kenny State of the Art (2010). State of the art report on flexible pipe technology. Sureflex JIP.
- [Mei, 1983] Mei, C. (1983). *The Applied Dynamics of Ocean Surface Waves*. World Scientific, Singapore.
- [Melchers, 1987] Melchers, R. (1987). *Structural Reliability – Analysis and Prediction*. Ellis-Horwood Ltd., Chichester.
- [Melve, 2001] Melve, B. (2001). Principles for life time estimation of pvdf pressure barriers in high temperature flexible pipes based on fracture mechanics. In *Proc. OMAE 2001*, page Paper 3575, Rio de Janeiro.
- [MIL-ST-1629A, 1980] MIL-ST-1629A (1980). Procedures for performing a failure mode, effects and criticality analysis. Technical report, U.S. Department of Defense, U.S. Department of Defense, Washington, DC.
- [Moan et al., 1980] Moan, T., Spidsøe, N., and Haver, S. (1980). 80011 analyse av usikkerhet. Trondheim, Norway. In Norwegian.
- [Munk, 1949] Munk, W. (1949). The solitary wave theory and its applications to surf problems. *Ann. N.Y. Acad. Sci*, 51:376–424.
- [Muren, 2008] Muren, J. (2008). Flexible pipes - failure modes, inspection, testing and monitoring.
- [Muren and Gjendal, 2011] Muren, J. and Gjendal, A. (2011). Presentation: Flexible risers - weak or strong link? PSA-seminar on rigid and flexible pipelines and risers, Stavanger. 2011-10-19.
- [Myrhaug and Lian, 2009] Myrhaug, D. and Lian, W. (2009). Marine Dynamics, Lecture Notes. The Norwegian University of Technology, Department of Marine Technology, Trondheim, Norway.
- [NACE TM 01-77, 1996] NACE TM 01-77 (1996). Laboratory testing of metals for resistance to sulfide stress cracking and stress corrosion cracking in h<sub>2</sub>s environments. Technical report, National Association of Corrosion Engineers (NACE).
- [Næss and Moan, 2013] Næss, A. and Moan, T. (2013). *Stochastic Dynamics of Marine Structures*. Cambridge University Press, New York.
- [Nestegård et al., 2004] Nestegård, A., Hagatun, K., Haver, S., Kalleklev, A., Wu, Y., and Lehn, E. (2004). Resonant vibrations of riser guide tubes due to wave impact. In *Proc. of OMAE2004 Vancouver, Canada*.
- [NICC Systems, 2012a] NICC Systems (2012a). Armawrap brochure. NICC Limited Corrosion Coating Engineers.
- [NICC Systems, 2012b] NICC Systems (2012b). Corrosion - Corrosion Protection. <http://www.armawrap.com/corrosion.htm> (Accessed 2012-02-28).

- [NICC systems, 2012] NICC systems (2012). Corrosion - Corrosion Protection. <http://www.armawrap.com/corrosion.htm> (Accessed 2012-02-28).
- [Nielsen et al., 1990] Nielsen, R., Colquhoun, R., and McCone, A. (1990). Tools for predicting service life of dynamic flexible pipes. In *Proc. of European Offshore Mechanics Symposium, NTH, Trondheim*.
- [Nordsve, 2007] Nordsve, N. T. (2007). Flexible pipelines and risers, flexible risers at kristin.
- [NORSOK M-503, 1997] NORSOK M-503 (1997). Cathodic protection. NORSOK STANDARD M-503.
- [NORSOK U-009, 2011] NORSOK U-009 (2011). Life extension for subsea systems. NORSOK STANDARD U-009.
- [NORSOK Y-002, 2010] NORSOK Y-002 (2010). Life extension for transportation systems. NORSOK STANDARD Y-002.
- [Nydal, 2010] Nydal, O. (2010). Multiphase transport – tep4250.
- [Nygaard and Mathiesen, 2008] Nygaard, E. and Mathiesen, K. (2008). Hywind metocean design basis. Technical Report MBM-MGE-RA32, 2008-12-01, Statoil, Norway.
- [Offshore Magazine Mustang Engineering, 2011] Offshore Magazine Mustang Engineering (2011). 2011 worldwide survey of semi-fpss and fpus.
- [Often and Løtveit, 1990] Often, O. and Løtveit, S. (1990). A common theoretical formulation for bonded and non-bonded flexible pipes under axisymmetric loads. In *Proc. from kursdagene at the Norwegian Institute of Technology, NTH*. NTH.
- [Olsen and Rongved, 2002] Olsen, G. and Rongved, P. (2002). Operators experience with flexible risers. In *Proc. OMAE 2002*, page Paper 28122, Oslo.
- [Ormberg et al., 1997] Ormberg, H., Fylling, I., Larsen, K., and Sødahl, N. (1997). Coupled analysis of vessel motions and mooring and riser system dynamics. In *Proceedings of the 16th International Conference on Offshore Mechanics and Arctic Engineering, OMAE'97, Yokohama, Japan*. ASME. Yokohama, Japan.
- [Ormberg and Larsen, 1998] Ormberg, H. and Larsen, K. (1998). Coupled analysis of floater motion and mooring dynamics for a turret-moored ship. *Applied Ocean Research*, 20:55–67.
- [Ormberg et al., 1998] Ormberg, H., Sødahl, N., and Steinkjer, O. (1998). Efficient analysis of mooring systems using de-coupled and coupled analysis. In *OMAE98-0351, Proceedings of the 17th International Conference on Offshore Mechanics and Arctic Engineering, OMAE'98*. ASME. Lisbon, Portugal.
- [Ortega et al., 2013] Ortega, A., Rivera, A., and Larsen, C. (2013). Flexible riser response induced by slug flow and wave loads. In *International Conference on Ocean, Offshore and Arctic Engineering*, Nantes, France.
- [Ortega et al., 2012] Ortega, A., Rivera, A., Nydal, O., and Larsen, C. (2012). On the dynamic response of flexible risers caused by internal slug flow. In *International Conference on Ocean, Offshore and Arctic Engineering*, Rio de Janeiro, Brazil.
- [Østergaard, 2012a] Østergaard, N. (2012a). *On Lateral Buckling of Armouring Wires in Flexible Pipes*. PhD thesis, Aalborg University, Aalborg, Denmark.

- [Østergaard et al., 2012] Østergaard, N., Lyckegaard, A., and Andreasen, J. (2012). Simplified approaches to modeling of lateral wire buckling in the tensile armor of flexible pipes. In *OMAE 2012*.
- [Østergaard et al., 2011] Østergaard, N., Lyckeggard, A., and Andreasen, J. (2011). On lateral buckling failure of armour wires in flexible pipes. In *Proc. of OMAE'2011 OMAE2011-49358*.
- [Østergaard, 2012b] Østergaard, N. H. (2012b). *On lateral buckling of armoring wires in flexible pipes*. PhD thesis, Aalborg University NKT-Flexibles, Denmark.
- [Otteren and Hanson, 1990] Otteren, A. and Hanson, T. (1990). Full scale measurement of curvature and motions on a flexibel riser and comparison with computer simulations. In *OMAE Houston Texas, February 18-23 1990*, Houston, Texas. OMAE. February 18-23 1990.
- [Ottøy et al., 2001] Ottøy, M., Finstad, H., Mathiesen, M., Moursund, B., and Nakken, T. (2001). Field experience on rilsan–ageing compared to data from ageing model. In *Int. Conf. Offshore Mechanics and Arctic Engineering (OMAE), Rio de Janeiro, Brazil*.
- [Out, 2010] Out, J. H. (2010). How to live with flexible pipe, happily ever after? Presentation at Klvl Engineering Society lecture, 2010-12-16.
- [Passano, 1994] Passano, E. (1994). *Efficient Analysis of Nonlinear Slender Marine Structures*. PhD thesis, Norwegian Institue of Technology, NTNU, Trondheim, Norway.
- [Patel and Seyed, 1989] Patel, M. and Seyed, F. (1989). Internal flow induced behaviour of flexible risers. *Engineering Structures*, 11:266–280.
- [Pickands, 1952] Pickands, J. (1952). Statistical inference using extreme order statistics. *Ann. Math. Stat.*, 23:470–472.
- [Picksley et al., 2002] Picksley, J., Kavanagh, K., Garnham, S., and Turner, D. (2002). Managing the integrity of flexible pipe field systems: Industry guideline and their application. In *Proc. of OTC'2002*.
- [Plunkett, 1967] Plunkett, R. (1967). Static bending stresses in catenary drill strings. *Journal of Engineering for the Industry*.
- [Procida and Nielsen, 2007] Procida, I.-M. and Nielsen, N.-J. R. (2007). In-line ir-cured xlpe technology for flexible pipes. In *OTC2007, Paper 18791*.
- [PSA Norway, 2009] PSA Norway (2009). State of the art bonded flexible pipes. 2008-4SUB-0189 - PSA Study on bonded flexible pipes.
- [PSA Norway, 2013a] PSA Norway (2013a). Damages to flexibles pipes – failures and incidents from psa norway codam database 1995–2012.
- [PSA Norway, 2013b] PSA Norway (2013b). Risk level in norwegian petroleum industry.
- [Rausand and Høyland, 2004] Rausand, M. and Høyland, A. (2004). *System Reliability Theory. Models, Statistical Methods and Applications, Second Edition*. John Wiley & sons, Hoboken, New Jersey.
- [Reinen, 2008] Reinen, T. (2008). Singing risers experimental work. summary of results and conclusions. Technical report, SINTEF, Trondheim, Norway. F8829.

- [Remita et al., 2008a] Remita, E., Ropital, F., and Kittel, J. (2008a). Experimental and theoretical investigation of the uniform corrosion in the annulus of offshore flexible pipelines. In *NACE conference*.
- [Remita et al., 2007] Remita, E., Tribollet, B., and Sutter, E. (2007). A kinetic model of co<sub>2</sub> corrosion in the confined environment of flexible pipe annulus. In *EUROCORR., 2007*.
- [Remita et al., 2008b] Remita, E., Tribollet, B., and Sutter, E. (2008b). A kinetic model for co<sub>2</sub> corrosion of steel in confined aqueous environments. *Journal of The Electrochemical Society*, 155(1):C41–C45.
- [Ropital et al., 2000] Ropital, F., Taravel-Condat, C., and Saas, J. (2000). Methodology to study the general corrosion of steel armours in simulated conditions of flexible pipe annulus influence of confinement and evaluation of the ph. In *EUROCORR., 2000*.
- [Rubin and Gudme, 2006] Rubin, A. and Gudme, J. (2006). Qualification of steel wire for flexible pipes. In *Paper no. 06149, NACE – International Corrosion Conference Series, 2006*.
- [Rubin and Gudme, 2009] Rubin, A. and Gudme, J. (2009). Test method for corrosion fatigue testing of cold rolled steel wire in sour and sweet environment based on deflection controlled four point bending. In *Paper no. 09103, NACE – International Corrosion Conference Series, 2009*.
- [Rytter and Nielsen, 2002] Rytter, J. and Nielsen, N.-J. R. (2002). A novel compression armour concept for unbonded flexible pipes. In *OTC 14059, Offshore Technology Conference, Houston, USA*.
- [SAE-ARP 5580, 2001] SAE-ARP 5580 (2001). Recommended failure modes and effects analysis (fmea) practices for non-automobile applications. Technical report, American Institute of Chemical Engineers, The Society for Advancing Mobility Land, Sea, Air and Space, 400 Commonwealth Drive, Warrendale, PA 15096-00001, USA.
- [Sævik, 1992] Sævik, S. (1992). *On Stresses and Fatigue in Flexible Pipes*. PhD thesis, NTH, Trondheim, Norway.
- [Sævik, 1993] Sævik, S. (1993). A finite element model for predicting stresses and slip in flexible pipe armouring tendons at bending gradients. *Computer and Structures*, 46(2).
- [Sævik, 1999] Sævik, S. (1999). A finite element model for predicting longitudinal stresses in nonbonded pipe pressure armours. In *Proc. of MARINFLEX ISBN 1-87461-229-3, London, UK*.
- [Sævik, 2011] Sævik, S. (2011). Theoretical and experimental studies of stresses in flexible pipes. *Computers and Structures* 89, 89:2273 – 2291.
- [Sævik, 2014] Sævik, S. (2014). *BFLEX - Theory Manual*, Marintek report no. 22L074.00.04. MARINTEK, Trondheim, Norway.
- [Sævik, 2015] Sævik, S. (2015). *BFLEX2010 - Theory Manual*. MARINTEK, Trondheim, Norway.
- [Sævik et al., 1992a] Sævik, S., Berge, S., B.Skallerud, Eide, O., and Bech, A. (1992a). Fatigue test and analysis of a coflexip 4inch flexible pipe. Draft report Sintef Report STF71 F92xxx, SINTEF.

- [Sævik et al., 1992b] Sævik, S., Berge, S., B.Skallerud, Eide, O., and Olufsen, A. (1992b). Fatigue test and analysis of a 4inch flexible pipe. Final report Sintef Report STF71 F92192, SINTEF.
- [Sævik and Ekeberg, 2002] Sævik, S. and Ekeberg, K. I. (2002). Non-linear stress analysis of complex umbilicals. In *Proc. of OMAE'2002*, Oslo, Norway. ASME. OMAE 2002-28126.
- [Sævik et al., 2001] Sævik, S., Gray, L. J., and Phan, A. (2001). A method for calculating residual and transverse stress effects in flexible pipe pressure spirals. In *Proc. of OMAE'2001*, Rio de Janeiro, Brasil. ASME.
- [Sævik and Ji, 2014] Sævik, S. and Ji, G. (2014). Differential equation for evaluating transverse buckling behaviour of tensile armour wires. In *Proceedings of the 33rd International Conference on Ocean Mechanics and Arctic Engineering*, San Francisco, USA. OMAE2014-24158.
- [Sævik and Li, 2013] Sævik, S. and Li, H. (2013). Shear interaction and transverse buckling of tensile armours in flexible pipes. In *Proc. of OMAE'2013, OMAE2013-10130, Nantes, France*.
- [Sævik et al., 2012] Sævik, S., Thorsen, S., and M.J (2012). Techniques for predicting tensile armour buckling and fatigue in deep water flexible pipes, proceedings of the 31th international conference on ocean, offshore and arctic engineering. In *Proceedings of the 31th International Conference on Ocean, Offshore and Arctic Engineering*, London, UK. OMAE2012-83563.
- [Santos et al., 2011] Santos, F., Pires, F., Clements, R., Clevelario, J., Sheldrake, T., Souza, L., and Kenedi, P. (2011). Evaluation of the effects of co<sub>2</sub> partial pressure on the corrosion fatigue behaviours of flexible pipe tensile armour wire. In *Offshore Technology Conference (OTC), Houston, USA*. OTC 21262.
- [Sarpkaya and Isacson, 1981] Sarpkaya, T. and Isacson, M. (1981). Mechanics of wave forces on offshore structures.
- [Schmitt and Horstemeier, 2006] Schmitt, G. and Horstemeier, M. (2006). Fundamental aspects of co<sub>2</sub> metal loss corrosion - part ii: Influence of different parameters on co<sub>2</sub> corrosion mechanisms. In *NACE conference*.
- [Secher et al., 2011] Secher, P., Bescarte, F., and Felix-Henry, A. (2011). Lateral buckling of armor wires in flexible pipes: reaching 3000 m water depth. In *Proc. of OMAE'2011*.
- [SESAM PA11, 2008] SESAM PA11 (2008). Service life models for pa11 pressure sheaths in flexible pipes under use of methanol, ethanol and small organic acids. Technical report, Noble Denton, Noble Denton.
- [Sharp et al., 1993] Sharp, J., Kam, J., and Birkinshaw, M. (1993). Review of criteria for inspection and maintenance of north sea structures. In *OMAE93, Vol. 2, Safety and Reliability*, page 8. OMAE1993.
- [Shen et al., 2011] Shen, Y., J.Zhao, and Tan, Z. (2011). Influence of bore pressure on the creep behavior of polymer barrier layer inside and unbonded flexible pipe. In *Proc. OMAE 2011*, page Paper 49392, Rotterdam. OMAE2011.
- [Sines and Waisman, 1959] Sines, G. and Waisman, J. (1959). *Metal Fatigue*. McGraw–Hill Book Company, Inc., New Yourk.

- [Skallerud, 1991a] Skallerud, B. (1991a). Damping models and structural damping in a non-bonded pipe. Final report Sintef Report STF71 F91-018, SINTEF.
- [Skallerud, 1991b] Skallerud, B. (1991b). Structural damping in a wellstream pipe. Final report Sintef Report STF71 F91-059, SINTEF.
- [Skeie et al., 2013] Skeie, G., Skjerve, H., Pettersen, S., Axelsson, G., Engh, B., and Vethe, S. (2013). Carcass axial capacity in flexible risers. In *Rio Pipeline Conference & Exposition*.
- [Skeie et al., 2012] Skeie, G., Sødahl, N., and Steinkjer, O. (2012). Efficient fatigue analysis of helix elements in umbilicals and flexible risers: Theory and applications. *Journal of Applied Mathematics*.
- [Skjelbreia and Henderson, 1961] Skjelbreia, L. and Henderson, J. (1961). Fifth order gravity wave theory. In *Proc. 7th Conf. Coastal Eng.*, pages 184–196. ASCE.
- [Sødahl, 1991] Sødahl, N. (1991). *Methods for Design and Analysis of Flexible Risers*. PhD thesis, Norwegian University of Science and Technology, Trondheim, Norway.
- [Sødahl et al., 2011] Sødahl, N., Steinkjer, O., Gjølmesli, E., and Hansen-Zahl, K. (2011). Consistent viv fatigue analysis methodology of umbilicals. In *Proc. of OMAE2011, Rotterdam, Netherlands*. ASME.
- [Søreide, 1985] Søreide, T. (1985). *Ultimate Load Analysis of Marine Structures*. Tapir, Trondheim, Norway.
- [Sparks, 1984] Sparks, C. P. (1984). The influence of tension, pressure and weight on pipe and riser deformations and stresses. *Journal of Energy Resources Technology*, 106.
- [Østergaard et al., 2012] Østergaard, N., Lyckegaard, A., and Andreasen, J. (2012). A method for prediction of the equilibrium state of a long and slender wire on a frictionless toroid applied for analysis of flexible pipe structures. *Engineering Structures*, 34:391–399.
- [Stewart, 2012] Stewart, M. (2012). Repair solutions. e-mail 21.08.2012.
- [Stewart and Melchers, 1997] Stewart, M. and Melchers, R. (1997). *Probabilistic Risk Assessment for Engineering Systems*. Chapman & Hall, London.
- [Stokes, 1847] Stokes, G. (1847). On the theory of oscillatory waves. *Trans. Camb. Philos. Soc.*, 8:441–455.
- [Sun and Nesic, 2007] Sun, W. and Nesic, S. (2007). A mechanistic model of h<sub>2</sub>s corrosion of mild steel. In *NACE Corrosion 2007*, NACE2007-07655.
- [Talisman Energy Norge AS, 2005] Talisman Energy Norge AS (2005). Presentation 2005-09-09.
- [Tan et al., 2006] Tan, Z., Loper, C., Sheldrake, T., and Karabelas, G. (2006). Behavior of tensile wires in unbonded flexible pipe under compression and design optimization for prevention. In *Proc. of OMAE'2006*.
- [Taravel-Condat and Désamais, 2006a] Taravel-Condat, C. and Désamais, N. (2006a). Qualification of high strength carbon steel wires for use in specific annulus environment of flexible pipes containing co<sub>2</sub> and h<sub>2</sub>s. In *OMAE2006*, Hamburg.
- [Taravel-Condat and Désamais, 2006b] Taravel-Condat, C. and Désamais, N. (2006b). Qualification of very high strength carbon steel wires for use in flexible pipes containing small amount of h<sub>2</sub>s. In *EUROCORR.*, 2006.

- [Tavares et al., 2010] Tavares, S., Scandian, C., Pardal, J., Luz, T., and da Silva, F. (2010). Failure analysis of duplex stainless steel weld used in flexible pipes in off shore production. *Engineering Failure Analysis*, 17:1500–1506.
- [Taylor et al., 2002] Taylor, T., Joosten, M., and Smith, F. (2002). Technical solutions applied for the treatment of damaged dynamic risers. In *Proc. of OMAE'2002*, Oslo. ASME. OMAE2002-28371.
- [the Hazop Study Guide, 1977] the Hazop Study Guide (1977). Chemical industry safety and health council, london, guide to hazard and operability studies (the hazop study guide).
- [Thoft-Christensen and Baker, 1982] Thoft-Christensen, P. and Baker, M. (1982). *Structural Reliability Theory and its Applications*. Springer-Verlag.
- [Thorsen, 2011] Thorsen, M. (2011). Capacity of deep water flexible risers. Master thesis, NTNU – Department of Marine Technology.
- [Timoshenko and Gere, 1963] Timoshenko, S. and Gere, J. (1963). *Theory of Elastic Stability*. McGraw-Hill.
- [Tucker et al., 1984] Tucker, M. J., Challenor, P. G., and Carter, D. J. T. (1984). Numerical simulation of a random sea: a common error and its effect upon wave group statistics. *J. of Applied Ocean Research*, 6(2):118–122.
- [Tvedt, 1987] Tvedt, L. (1987). Second order reliability by an exact integral. Technical Report 3, Springer Verlag.
- [Underwood, 2002] Underwood, N. (2002). Corrosion testing of reinforcement in simulated annulus environments of flexible pipelines. In *Proc. of OMAE'2002*, Oslo. ASME. OMAE2002.
- [Vaz and Rizzo, 2011] Vaz, M. and Rizzo, N. (2011). A finite element model for flexible armor wire instability. *Marine Structures*, 24:275–291.
- [Vinnem, 1999] Vinnem, J. (1999). *Offshore Risk Assessment*. Kluwer Academic Publishers, Dordrecht.
- [Wang and Berge, 2012] Wang, T. and Berge, S. (April 2012). Fatigue testing of tensile armour wires from in-service and stored risers including full cross-section specimens marintek report no. Technical report, MARINTEK, Trondheim.
- [W.C.Young and Budynas, 2002] W.C.Young and Budynas, R. (2002). *Roark's Formulas for Stress and Strain*. McGraw-Hill.
- [Wheeler, 1970] Wheeler, J. (1970). Methods for calculating forces produced on piles in irregular waves. *Journal of Petroleum Technology*.
- [Winterstein et al., 1993] Winterstein, S. R., Ude, T. C., Cornell, C. A., Bjerager, P., and Haver, S. (1993). Environmental parameters for extreme response: Inverse form with omission factors. In Schueller, G. I., Shinozuka, M., and Yao, J. T. P., editors, *Proc. of IOSSAR'93, Rotterdam*, pages 77–84. A. A. Balkema.
- [Zhou et al., 2015] Zhou, C., Sævik, S., Ye, N., and Ji, G. (2015). Effect of lay angle of anti-buckling tape on lateral buckling behavior of tensile armors. In *Proc. of OMAE'2015*.
- [Zienkiewicz, 1971] Zienkiewicz, O. (1971). *The finite element method in engineering Science*. McGraw-Hill, London.

